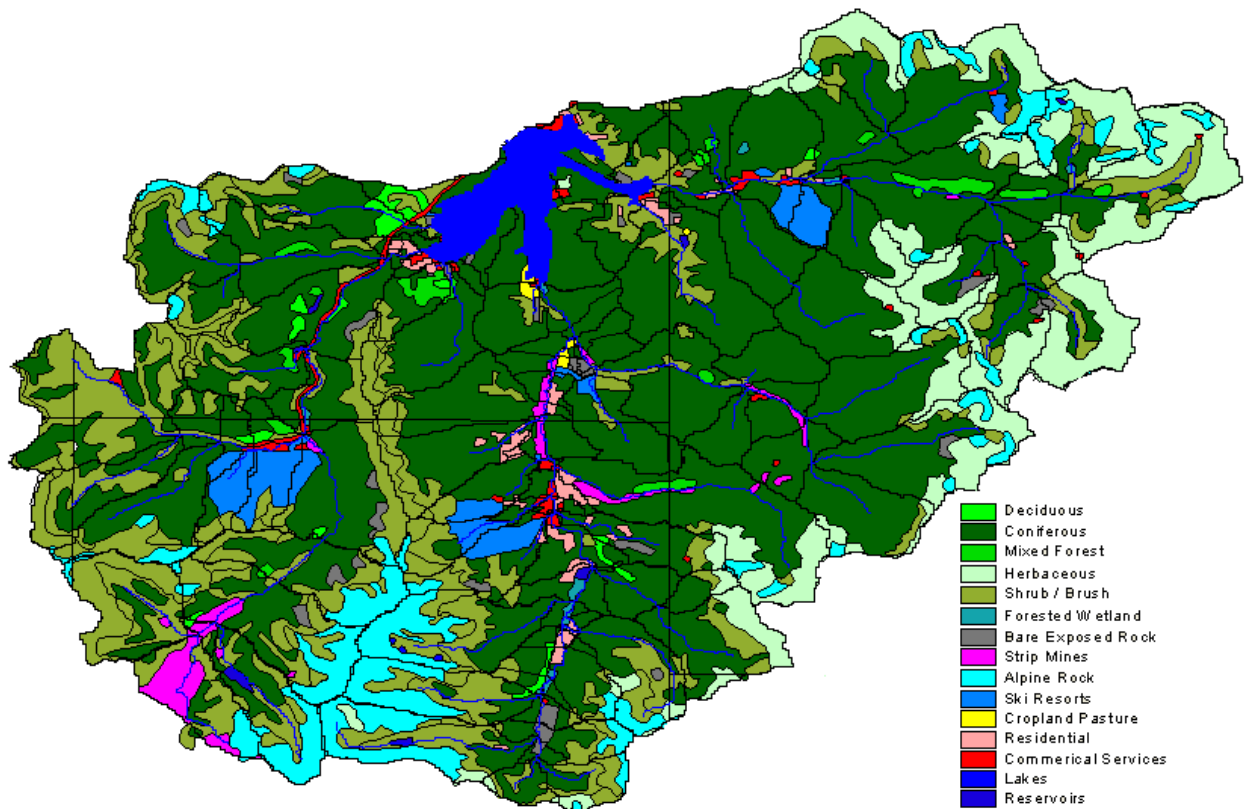




National Decentralized Water Resources Capacity Development Project



Quantifying Site-Scale Processes and Watershed-Scale Cumulative Effects of Decentralized Wastewater Systems

Colorado School of Mines

January 2005

Quantifying Site-Scale Processes and Watershed-Scale Cumulative Effects of Decentralized Wastewater Systems

Submitted by the Colorado School of Mines

Golden, Colorado

NDWRCDP Project Number: WU-HT-00-27

National Decentralized Water Resources Capacity Development Project
(NDWRCDP) Research Project

Final Report, January 2005

DISCLAIMER

This work was supported by the National Decentralized Water Resources Capacity Development Project (NDWRCDP) with funding provided by the U.S. Environmental Protection Agency through a Cooperative Agreement (EPA No. CR827881-01-0) with Washington University in St. Louis. This report has not been reviewed by the U.S. Environmental Protection Agency. This report has been reviewed by a panel of experts selected by the NDWRCDP. The contents of this report do not necessarily reflect the views and policies of the NDWRCDP, Washington University, or the U.S. Environmental Protection Agency, nor does the mention of trade names or commercial products constitute endorsement or recommendation for use.



CITATIONS

This report is based on research completed by a team of investigators including:

Colorado School of Mines, Golden, CO

Dr. Robert L. Siegrist

Dr. John McCray

Ms. Kathryn Lowe, M.S.

Dr. Sheila Van Cuyk

Ms. Jennifer Bagdol, M.S.

Ms. Shiloh Kirkland, M.S.

Ms. Paula Jo Lemonds, M.S.

Ms. Heather Smith, M.S.

Electric Power Research Institute, Palo Alto, CA

Dr. Robert Goldstein

Systech Engineering, Inc., San Ramon, CA

Dr. Carl Chen

Ms. Laura Weintraub, M.S.

Summit County Environmental Health, Frisco, CO

Mr. Jim Rada

The research described in this report was sponsored in large part by the National Decentralized Water Resources Capacity Development Project. Some elements of the research were enabled by supplementary funding provided through grants and student scholarships received from the National Science Foundation, Department of Education, Infiltrator Systems, Inc., and others.

The final report was edited and produced by ProWrite Inc., Reynoldsburg, OH.

This report is available online at www.ndwrcdp.org. This report is also available through the

National Small Flows Clearinghouse
P.O. Box 6064
Morgantown, WV 26506-6065
Tel: (800) 624-8301
WWCDRE45

This report should be cited in the following manner:

Siegrist, R. L., J. McCray, L. Weintraub, C. Chen, J. Bagdol, P. Lemonds, S. Van Cuyk, K. Lowe, R. Goldstein, and J. Rada. 2005. *Quantifying Site-Scale Processes and Watershed-Scale Cumulative Effects of Decentralized Wastewater Systems*. Project No. WU-HT-00-27. Prepared for the National Decentralized Water Resources Capacity Development Project, Washington University, St. Louis, MO, by the Colorado School of Mines, Golden, CO.



ACKNOWLEDGEMENTS

Appreciation is extended to the following individuals for assistance in the preparation of this report:

Colorado School of Mines

Robert L. Siegrist
John McCray
Jennifer Bagdol
Sheila Van Cuyk
Kathryn Lowe
Paula Jo Lemonds
Heather Smith

Electric Power Research Institute

Robert Goldstein

Systech Engineering, Inc.

Carl Chen
Laura Weintraub

Summit County Environmental Health Department

Jim Rada

Acknowledgments are given to Dr. Ron Harvey and his colleagues at the United States Geological Survey (USGS) in Boulder, CO for assistance with the experimentation regarding virus transport and fate.

Dr. Tissa Illangasekare, Colorado School of Mines, is acknowledged for coordination of the independent peer review, which was completed near the end of the project. The members of the peer review panel included: Drs. Arturo Keller, University of California-Santa Barbara, Dr. Jayantha Obeysekera, South Florida Water Management District, Dr. Robert Prucha, Integrated Hydro Systems, LLC, and Mr. Russell Clayshulte, RNC Consulting. Kent Glover, Colorado School of Mines is also acknowledged for his participation in the peer review and assistance with coordination of the peer review report.

Acknowledgements are given to Greg O'Neill and staff of the USGS District Office in Lakewood, Colorado and the USGS National Water Quality Laboratory in Arvada, Colorado for their collaboration on the water quality monitoring facets of the research described herein.

Mark Mumby and Kayenta Consulting, Inc. are acknowledged for their efforts during the drilling activities in support of subsurface exploration and monitoring well installation.

The University of Rhode Island is acknowledged for providing and supporting the watershed modeling using MANAGE.

The residents and owners of property in the Dillon Reservoir watershed who allowed site access in support of the environmental characterization are acknowledged for their cooperation and support of the project.

Appreciation is also expressed to the NDWRCDP for their support of this work:

Principal Investigator

Jay R. Turner, D.Sc., Washington University

Project Coordinator

Andrea L. Shephard, Ph.D.

NDWRCDP Project Steering Committee:

Coalition for Alternative Wastewater Treatment

Valerie I. Nelson, Ph.D.

Consortium of Institutes for Decentralized Wastewater Treatment

Ted L. Loudon, Ph.D., P.E.

Electric Power Research Institute

Raymond A. Ehrhard, P.E.

Tom E. Yeager, P.E.

National Onsite Wastewater Recycling Association

Jean Caudill, R.S.

National Rural Electric Cooperative Association

Steven P. Lindenberg

Scott Drake, P.E.

Water Environment Research Foundation

Jeff C. Moeller, P.E.

Members-At-Large:

James F. Kreissl

Richard J. Otis, Ph.D., P.E.

Jerry Stonebridge



ABSTRACT

The research described in this report was undertaken to enhance the quantitative understanding of site-scale processes affecting the performance of onsite wastewater systems (OWS) and to develop modeling tools that can describe and predict individual system performance and the cumulative effects of multiple systems on water quality within a watershed. To accomplish this goal, the project was designed and carried out in two phases by a collaborative team involving the Colorado School of Mines, Electric Power Research Institute, Systech Engineering, Inc., United States Geological Survey, and the Summit County Environmental Health Department including participation by a stakeholder group from the study area.

The project scope included:

- Literature review and analysis
- Laboratory experimentation and field monitoring
- Development and refinement of mathematical models
- Completion of site-scale and watershed-scale model simulations

Analysis of literature data was used to develop cumulative frequency distributions of pollutant concentrations in domestic septic tank effluent and the rate and capacity parameters governing their transport/fate in a soil and groundwater environment.

Laboratory and field experimentation enhanced the understanding of biozone genesis and the transport/fate of microbes and chemicals in soil-based OWS.

Modeling of individual OWS was completed using an existing numerical model, HYDRUS 2-D, and a new analytical model, the Biozone Algorithm. Literature data and experimental results enabled single site-scale model formulation, calibration, and testing. The OWS site-scale source/transport/fate expressions have been incorporated into an existing watershed model, the Watershed Analysis Risk Management Framework model (WARMF) that can be used for simulating the effects of OWS relative to other pollutant sources on water quality in a watershed or sub-watershed.

The WARMF model as well as the Better Assessment Science Integrating Point and Nonpoint Sources (BASINS)/Soil and Water Assessment Tool (SWAT) and Method for Assessment, Nutrient-loading, and Geographic Evaluation (MANAGE) models were setup for the Dillon Reservoir watershed in Summit County, Colorado. In this watershed there are approximately 1,500 OWS as well as other nonpoint and point sources of pollution, and more than 600 onsite drinking water wells along with community wells and surface water supplies.

Dillon Reservoir supports varied recreation uses and also provides 25% of the drinking water supply for the City of Denver. After setup and calibration, model simulations were completed to examine current wastewater management scenarios and the simulation results were compared to field monitoring data. Examination of future wastewater management scenarios was also completed through watershed-scale model simulations (for example, abandonment of OWS and connection to a centralized publicly owned treatment works [POTW]). An independent peer review of the research was completed near the end of the project period.



EXECUTIVE SUMMARY

Wastewater management in the US includes millions of individual onsite wastewater systems (OWS), which are relied on to effectively treat and dispose of wastewater generated by 25% of the country's population. In the past, OWS have often been viewed as a temporary approach to wastewater management and acceptable for use only until a centralized approach could be implemented. Yet there are many situations within the US (and more so in developing countries) where centralized systems are neither cost-effective nor sustainable due to a variety of factors (such as low-density development, rugged topography, limited water and energy supplies, and lack of skilled labor).

Onsite and decentralized systems are characterized by collection distances that are short or negligible, with tank-based pretreatment followed by soil absorption to provide advanced treatment as the water percolates toward groundwater. These wastewater soil absorption systems can function as porous media biofilters. Soil porous media biofilters have the potential to achieve high treatment efficiencies over a long service life at low cost, and be protective of public health and environmental quality. These facts have been well-established (US EPA 1978; Jenssen and Siegrist 1990; Siegrist *et al.* 2001; and US EPA 2002).

Favorable results from lab and field studies as well as an absence of documented adverse effects are consistent with an assessment that the performance of common OWS serving individual households is generally satisfactory. However, the quantitative understanding of and ability to predict the performance of household OWS as a function of design, installation/operation, and environmental factors have not been fully elucidated (Siegrist 2001; Siegrist *et al.* 2001). These gaps in knowledge are present for some facets of design and performance for OWS serving individual homes in low-density applications (for example, one OWS per hectare), while the knowledge gaps are even greater for OWS serving nonresidential establishments (such as fast-food restaurants, nursing homes, or veterinarian clinics). As a result, the current state of knowledge and standard-of-practice have gaps that can preclude rational design of individual OWS to predictably and reliably achieve performance goals for a specific OWS application. Moreover, for higher density applications of OWS (for example, five OWS per hectare) or applications of large numbers of individual OWS within a watershed-scale framework, the quantitative analysis of long-term treatment efficacy, including assessment of cumulative effects and establishment of total maximum daily loads (TMDLs), is quite difficult.

The goal of this National Decentralized Water Resources Capacity Development Project (NDWRCDP) project, (*Quantifying Site-Scale Processes and Watershed-Scale Cumulative Effects of Decentralized Wastewater Systems*) was to develop understanding and modeling tools that can help quantify site-scale system processes and watershed-scale cumulative effects of OWS. A second major goal was to enhance the understanding of the potential watershed-scale effects of a broad-scale application of OWS, incorporating project results on the dynamic quantification of site-scale processes during the refinement, application, and evaluation of watershed modeling tools. To accomplish these goals, the project was designed and carried out by a collaborative team involving the Colorado School of Mines (CSM), Electric Power Research Institute (EPRI), Systech Engineering, Inc., United States Geological Survey (USGS), and the Summit County Environmental Health Department. The project scope included:

- Literature review and analysis
- Laboratory and field experimentation
- Development and refinement of mathematical models
- Completion of site-scale and watershed-scale model simulations
- Field monitoring in a study watershed

An independent peer review of the research was completed near the end of the project period.

For the common soil-based OWS at the single-system scale, quantitative understanding of hydraulic and purification processes has been improved and site-scale models and decision-support tools have been developed and tested in this project. Based on literature data, cumulative frequency distributions were developed for concentrations of key characteristics of domestic septic tank effluent (STE) and for the transport/fate parameters that describe the treatment of nutrients in soil and groundwater systems (Kirkland 2001 and McCray *et al.* 2005). Experimental studies were completed involving STE treatment in a soil-based OWS to test a new experimental design methodology based on life-cycle acceleration and to provide a dataset for site-scale modeling (Siegrist *et al.* 2002). Through a series of experimental studies, fundamental understanding of bacteria and virus transport/fate in soil-based OWS was enhanced (Van Cuyk 2003). At the Mines Park Test Site on the CSM campus, test cells representing a segment of an in situ porous media biofilter were established to examine hydraulic and purification processes as affected by hydraulic loading rate and infiltrative surface architecture in sandy-loam soils (Lowe and Siegrist 2002 and Tackett *et al.* 2004). An existing numerical model, HYDRUS 2-D, was set up to simulate a soil-based OWS and enable site-scale scenario analyses regarding hydraulic and purification performance (Beach and McCray 2003). A new site-scale model, referred to as the Biozone Algorithm, was formulated by Systech Engineering to describe the biozone development in a soil-based OWS and the hydraulic and purification performance of that OWS (Weintraub *et al.* 2002). This biozone model was tested against CSM experimental datasets.

A major facet of this project involved the refinement, application, and testing of an existing watershed-scale model, Watershed Analysis Risk Management Framework (WARMF) for the Dillon Reservoir watershed in Summit County, Colorado. There are about 1,500 OWS in this watershed as well as other nonpoint and point sources of pollution, and more than 600 onsite drinking water wells along with community wells and surface water supplies. In addition, Dillon Reservoir provides 25% of the drinking water supply for the City of Denver. In this project, WARMF has been modified to include explicit representation of OWS of different performance features, an integrated Biozone Algorithm, and cumulative frequency distribution curves for source concentrations and transport/fate parameters. As demonstrated in this project for the Blue River basin of the Dillon Reservoir watershed, the water quality effects of OWS were simulated using WARMF and compared to a water quality dataset generated during the project. Simulations were also completed to assess realistic decision-making scenarios concerning wastewater infrastructure in the watershed and to determine the comparative effects on water quality.

WARMF as well as two other models, the Better Assessment Science Integrating Point and Nonpoint Sources (BASINS)/Soil and Water Assessment Tool (SWAT) and Method for Assessment, Nutrient-loading, and Geographic Evaluation (MANAGE) models, were set up, calibrated, and applied to the Dillon Reservoir watershed. Compared to WARMF, the BASINS/SWAT model does not explicitly account for OWS, is less efficient in running scenario analyses, and does not include modules for TMDL analysis and stakeholder consensus building. In terms of setup and application to a given watershed, both models will require considerable resources either in the form of the upfront purchase price for a setup and calibrated model (such as WARMF) or for the consultant or in-house labor costs to setup, calibrate, and run a public-domain model (such as BASINS/SWAT). MANAGE is a comparatively simple geographic information system (GIS)-based vulnerability mapping tool to identify potential hotspots and is similar in many respects to mass balance calculation approaches that could be formulated and applied to a particular potential problem area. After setup and calibration, model simulations were completed to examine current wastewater management scenarios and the simulation results were compared to field monitoring data. Examination of future wastewater management scenarios was also completed through watershed-scale model simulations (such as simulation of the abandonment of OWS and connection of homes to a centralized wastewater treatment plant [WWTP]).

The environmental monitoring and subsurface characterization efforts of this project were focused on developing sufficient understanding of the Dillon Reservoir watershed to enable model setup and initial calibration. The water quality monitoring was focused on surface water flow and quality at up to 20 monitoring locations in the watershed. Quality data include routine water quality parameters, wastewater-related pollutants, and some chemical and biological tracers. In performing the characterization work an attempt was made to use limited and potentially uncertain data and to assess the reliability of that approach. At the watershed-scale in the Dillon Reservoir watershed, compared to urbanized development and WWTP discharges, OWS are not a principal source of water pollutants as evidenced by source load mass balance calculations, WARMF and BASINS/SWAT model simulation results, and water quality monitoring and analysis of spatial and temporal trends.

Application of a watershed-scale decision-support tool such as WARMF can enable analysis of wastewater management scenarios and provide critical insight into the water quality benefits of one management option compared to another. Based on WARMF simulations of different wastewater management scenarios in the Blue River basin, extending central sewers and conversion of OWS to a central WWTP appears to offer little or no benefit in terms of surface water quality protection, and in some cases may lead to surface water quality degradation.

While the research completed during this project has advanced the science and engineering of OWS, there are still some gaps in understanding that further research should attempt to fill. In general, there continues to be a need for quantitative understanding to enable proper OWS design to yield a desired performance level. Such understanding also enables the design and implementation of monitoring devices and methodologies for process control and performance assurance.

The methodology and tools developed in this project are recommended for application in support of decision-making in Summit County, Colorado, and the benefits gained from this decision support should be documented and used to assess the benefit/cost of quantitative decision support such as reported herein. In addition, the methods and tools developed in this project should be applied and tested for other situations and environmental conditions to determine the extent of extrapolation possible. Considering the scope of the research completed in this project, those components of the work that would be most valuable to enabling application to another geographic region of the US for watershed-scale management would include WARMF (and a comparative model) model refinement, setup, calibration, and simulations along with necessary and appropriate environmental characterization and watershed monitoring. Depending on the goals of the research during a similar project in another region of the US, additional site-scale testing and experimentation (to generate site-specific input data and algorithms for modeling) might also be warranted.



TABLE OF CONTENTS

1	INTRODUCTION	1-1
	Project Background and Motivation	1-1
	Project Objectives.....	1-6
	Project Approach	1-6
	Report Organization.....	1-8
 2	 STUDY WATERSHED ENVIRONMENTAL SETTING	 2-1
	Introduction to the Study Area	2-1
	Water Quality Monitoring	2-3
	Focus Areas	2-3
	Geology and Soils.....	2-6
	Geology	2-6
	Soils	2-7
	Water Quality	2-9
	Surface Water: Introduction.....	2-9
	Surface Water: Nutrient Results	2-10
	Surface Water: Supporting Parameter Results	2-12
	Surface Water: Discussion	2-13
	Surface Water: Conclusions	2-15
	Groundwater: Introduction	2-16
	Groundwater: Nutrient Results	2-16
	Groundwater: Supporting Parameter Results.....	2-17
	Groundwater: Conclusions	2-19
	Hydrogeology	2-20
	Implications To This Study.....	2-26

3 INTRODUCTION TO THE WATERSHED ANALYSIS RISK MANAGEMENT

FRAMEWORK (WARMF) MODEL	3-1
Mass Balance Methods	3-1
GIS-Mapping-Based Methods	3-1
Mathematical Models	3-2
WARMF Model Overview	3-3
Model Description	3-4
WARMF Applications	3-8
Modifications for OWS: Biozone Algorithm	3-8
Necessary Input Parameters	3-9

4 BIOZONE ALGORITHM

Description of the Biozone	4-1
Motivation	4-1
Theory and Formulation of Biozone Algorithm	4-2
Buildup of Biomass	4-3
Buildup of Plaque	4-4
Impacts of Field Capacity, Saturated Moisture, and Hydraulic Conductivity	4-5
Transformation and Decay Reactions	4-6
Phosphorus Adsorption	4-7
Discharge to Soil Layers	4-7
Other Assumptions	4-8
Calibration and Testing	4-9
Column Study Data	4-9
Model Coefficients	4-10
Simulations Results	4-11
Simulation of Field Scale OWS	4-38
Implementation in WARMF	4-40
Summary	4-42

5 APPLICATION OF WARMF IN THE DILLON RESERVOIR WATERSHED.....5-1

Introduction	5-1
General Input Data	5-1
Study Focus Areas	5-9
OWS Characterization	5-13
Private Drinking Water Well Withdrawals	5-16
Subsurface Characterization	5-17
Hydrology Calibration	5-17
Calibration Parameters	5-17
Model Results	5-17
Water Balance	5-29
Water Quality Calibration	5-30
Calibration Parameters	5-30
Model Results	5-30
Verification	5-54
Hydrology Verification	5-54
Water Quality Verification	5-63
Discussion	5-66
Management Scenarios	5-66
Scenario 1: No OWS in the Watershed	5-67
Scenario 2: Convert Blue River Estates to Centralized Sewers	5-71
Summary	5-78

6 ADDITIONAL MODELS APPLIED6-1

Site-Scale Models	6-1
HYDRUS-2D	6-1
Virus Fate and Transport	6-4
Watershed-Scale Models and Comparisons	6-9
Purpose	6-9
Soil Water Assessment Tool (SWAT)	6-9

Method for Assessment, Nutrient-loading, and Geographic Evaluation (MANAGE)	6-9
Comparison of Model Theoretical Basis	6-10
Model Capabilities	6-10
Calibration Comparison	6-11
Model Availability	6-14
Resource Requirements	6-14
Comparative Model Summary	6-14
 7 STAKEHOLDER AND USER PERSPECTIVES	7-1
WARMF Has Stakeholder Appeal	7-1
Officials Desire a Better Understanding of Water-Quality Impacts	7-2
 8 SUMMARY, CONCLUSIONS, AND RECOMMENDATIONS	8-1
Summary and Conclusions	8-1
Recommendations	8-3
 9 REFERENCES	9-1
 10 ACRONYMS, ABBREVIATIONS, AND SYMBOLS	10-1
Acronyms and Abbreviations	10-1
Symbols	10-4

A	INPUT PARAMETERS FOR MODELING FLOW AND TRANSPORT IN ONSITE WASTEWATER SYSTEMS.....	A-1
	Overview	A-1
	Effluent Concentrations From OWS	A-1
	Bacteria and Virus Concentrations.....	A-3
	Nutrient Concentrations and Transport Parameters.....	A-4
	Methodology	A-5
	Nitrogen Concentrations and Transport Parameters.....	A-6
	Phosphorus Concentrations and Transport Parameters	A-11
	Wastewater Flow.....	A-17
	Summary	A-20
	References	A-21
B	PATHOGEN TRANSPORT-FATE STUDIES.....	B-1
	Purification of Bacteria and Virus in WSASs: One-Dimensional Column Study.....	B-1
	Materials and Methods	B-2
	Results and Discussion	B-7
	Summary and Conclusions.....	B-20
	Fate of Viruses in WSASs: Mini-Column Studies.....	B-22
	Materials and Methods	B-24
	Results and Discussion	B-30
	Summary and Conclusions.....	B-47
	Experimental Data Analysis and Discussion	B-48
	Issue of Scale	B-48
	Modeling Virus Transport-Fate	B-49
	Conclusions	B-54
	References	B-54

C BIOZONE DEVELOPMENT AND WSAS PERFORMANCE: COLUMN STUDIES C-1

Overview	C-1
Methods	C-5
Experimental Apparatus	C-6
Monitoring.....	C-8
Results and Discussion.....	C-13
Hydraulic Performance	C-13
Treatment Performance.....	C-18
Multicomponent Surrogate and Tracer Tests	C-19
Conclusions.....	C-21
References	C-22

D BIOZONE GENESIS AND WSAS PERFORMANCE: FIELD 3-D TEST CELLS D-1

Materials and Methods	D-2
Site Selection and Evaluation.....	D-3
In Situ Test Cell Installation and Setup.....	D-3
Monitoring.....	D-6
Results and Discussion.....	D-8
Field Site Characteristics.....	D-8
Baseline Characterization.....	D-12
Performance	D-14
Summary	D-14
References	D-15

E WATER QUALITY MONITORING..... E-1

Background	E-1
OWS and Watershed Water Quality	E-1
Description of the Study Area.....	E-4
Study Approach.....	E-9
Mass Balance Calculations	E-9

Monitoring Program Design	E-18
Phases I and II Sampling Efforts	E-25
Quality Assurance	E-26
Results	E-26
Flow Measurements	E-26
Field Parameters	E-28
Inorganics	E-33
Other Parameters	E-45
Water Quality Assessment	E-46
Trends in Space and Time	E-49
Comparison to Criteria and Standards	E-71
Discussion of Trends and Assessment of Impact.....	E-74
Summary and Conclusions	E-86
References	E-88

F SITE-SCALE MODELING USING HYDRUS 2-D.....F-1

Background	F-1
Methodology	F-2
Conceptual Model.....	F-2
Mathematical Model	F-3
Results and Discussion	F-9
Unsaturated Water Flow	F-9
Ammonium Transport.....	F-12
Phosphate Transport	F-14
Conclusions.....	F-16
References	F-17

G WATERSHED MODELING USING BASINS/SWAT G-1

Introduction	G-2
Watershed-Scale Modeling Methodology.....	G-4
Approach	G-4
Description of BASINS	G-4
SWAT Setup.....	G-9

Simulation Setup	G-18
SWAT Calibration to Streamflow	G-19
Calibration Procedure	G-20
Sensitivity Study	G-31
Approach	G-31
Sensitivity Study Results	G-35
Model Performance	G-42
Summary and Conclusions	G-44
References	G-47
Supplemental Information: Theoretical Formulation of SWAT	G-55
Model Formulation for Hydrology	G-55
Model Formulation for Phosphorus Transport and Fate	G-65

H WATERSHED MODELING USING MANAGE..... H-1

Background	H-1
Description of MANAGE	H-2
Water Quality Indicator Analysis	H-2
Nutrient Loading Analysis	H-4
GIS Analysis	H-6
Summary	H-6
MANAGE Setup	H-7
GIS Setup	H-7
Setup of MANAGE Excel File	H-8
Fine Tuning MANAGE	H-10
Results of MANAGE Applied to the Dillon Reservoir Watershed	H-12
Watershed Features	H-12
Watershed Indicators	H-13
Nutrient Loading	H-18
GIS Analysis	H-23
Discussion	H-28
Watershed Indicators	H-29
Nutrient Loading	H-30
GIS Analysis	H-31
References	H-33



LIST OF FIGURES

Figure 1-1 Classic Onsite Wastewater System and the Local Site-Scale Setting.....	1-3
Figure 1-2 Site-Scale Processes Affecting the Performance of a Common Soil-Based OWS.....	1-3
Figure 1-3 Watershed-Scale Framework Within Which Large Numbers of Individual OWS Can Occur	1-4
Figure 1-4 Relationships of NDWRCDP Project Tasks	1-7
Figure 1-5 Illustration of Related CSM Research That Supported Completion of the NDWRCDP Project	1-8
Figure 2-1 Location of the Dillon Reservoir Watershed in Summit County, Colorado (Guelfo 2003)	2-1
Figure 2-2 Important Geographic Features of the Study Area (Monitoring Location Identification Includes BR for Blue River, FT for Frisco Terrace, GG for Gold Run Gulch, MW for Monitoring Well, and SR for Swan River).....	2-2
Figure 2-3 Nitrogen Mass Fluxes in the Blue River: A) Select Months of Phase I Nitrate Mass Flow Trends in the Blue River, and B) Upstream Organic Nitrate Trends in July 2002—Part of Phase II Sampling	2-11
Figure 2-4 Up- to Down-Stream Mass Flow of Chloride in the Blue River	2-12
Figure 2-5 Up- to Down-Stream Mass Flow of Sulfur in the Blue River	2-13
Figure 2-6 Nitrate Trends in Groundwater of the Dillon Reservoir Watershed.....	2-16
Figure 2-7 Chloride Trends in Groundwater Within the Dillon Reservoir Watershed.....	2-17
Figure 2-8 Scholler Plot of the Mean Concentrations for Water Chemistry Groups 1 Through 3 and STE	2-18
Figure 2-9 Hydraulic Head for Groundwater and Surface Water in the Frisco Terrace Focus Area.....	2-23
Figure 2-10 Hydraulic Head for Groundwater and Surface Water in the Blue River Estates Focus Area.....	2-23
Figure 2-11 Cross Sectional Conceptual Model of the Groundwater System at Blue River Estates Focus Area.....	2-25
Figure 3-1 The Five Modules of WARMF	3-3
Figure 3-2 Consensus Module Road Map in WARMF	3-4
Figure 3-3 Definition Sketch of Land Catchment for WARMF	3-5
Figure 3-4 Map Showing Locations of WARMF Watershed Applications	3-8
Figure 4-1 Schematic Showing the Biozone Location in an OWS	4-2
Figure 4-2 Schematic Showing of Pathways of Subsurface Flow in WARMF	4-8

Figure 4-3 Simulated Bacteria Biomass in the Biozone for Columns 1, 2, 3, and 4	4-12
Figure 4-4 Simulated Field Capacity (ThetaFC) and Saturate Moisture Content (ThetaS) of Column Experiments	4-13
Figure 4-5 Simulated and Observed Flow for Column 1. $R^2 = 0.72$ (1A), $R^2 = 0.59$ (1B)	4-14
Figure 4-6 Simulated and Observed Flow for Column 2. $R^2 = 0.62$ (2A), $R^2 = 0.54$ (2B)	4-14
Figure 4-7 Simulated and Observed Flow for Column 3. $R^2 = 0.36$ (3A), $R^2 = 0.78$ (3B)	4-15
Figure 4-8 Simulated and Observed Flow for Column 4. $R^2 = 0.06$ (4A), $R^2 = 0.02$ (4B)	4-15
Figure 4-9 Simulated and Observed Ammonia for Column 1	4-16
Figure 4-10 Simulated and Observed Ammonia for Column 2	4-17
Figure 4-11 Simulated and Observed Ammonia for Column 3	4-17
Figure 4-12 Simulated and Observed Ammonia for Column 4	4-18
Figure 4-13 Simulated and Observed Nitrate for Column 1	4-19
Figure 4-14 Simulated and Observed Nitrate for Column 2	4-19
Figure 4-15 Simulated and Observed Nitrate for Column 3	4-20
Figure 4-16 Simulated and Observed Nitrate for Column 4	4-20
Figure 4-17 Simulated and Observed Fecal Coliform Bacteria for Column 1	4-21
Figure 4-18 Simulated and Observed Fecal Coliform Bacteria for Column 2	4-21
Figure 4-19 Simulated and Observed Fecal Coliform Bacteria for Column 3	4-22
Figure 4-20 Simulated and Observed Fecal Coliform Bacteria for Column 4	4-22
Figure 4-21 Simulated and Observed BOD for Column 1	4-23
Figure 4-22 Simulated and Observed BOD for Column 2	4-23
Figure 4-23 Simulated and Observed BOD for Column 3	4-24
Figure 4-24 Simulated and Observed BOD for Column 4	4-24
Figure 4-25 Simulated and Observed Total Phosphorus for Column 1	4-25
Figure 4-26 Simulated and Observed Total Phosphorus for Column 2	4-25
Figure 4-27 Simulated and Observed Total Phosphorus for Column 3	4-26
Figure 4-28 Simulated and Observed Total Phosphorus for Column 4	4-26
Figure 4-29 Simulated and Observed Total Nitrogen for Column 1	4-27
Figure 4-30 Simulated and Observed Total Nitrogen for Column 2	4-27
Figure 4-31 Simulated and Observed Total Nitrogen for Column 3	4-28
Figure 4-32 Simulated and Observed Total Nitrogen for Column 4	4-28
Figure 4-33 Simulated and Observed Alkalinity for Column 1	4-29
Figure 4-34 Simulated and Observed Alkalinity for Column 2	4-29
Figure 4-35 Simulated and Observed Alkalinity for Column 3	4-30
Figure 4-36 Simulated and Observed Alkalinity for Column 4	4-30
Figure 4-37 Simulated and Observed pH for Column 1	4-31
Figure 4-38 Simulated and Observed pH for Column 2	4-31
Figure 4-39 Simulated and Observed pH for Column 3	4-32

Figure 4-40 Simulated and Observed pH for Column 4	4-32
Figure 4-41 R ² Values for Each Parameter and Column	4-33
Figure 4-42 Simulated Mean Biozone Flow Compared to Mean Measured Flow for Each Column	4-34
Figure 4-43 Simulated Mean Biozone Ammonia Compared to Mean Measured Ammonia for Each Column	4-34
Figure 4-44 Simulated Mean Biozone Nitrate Compared to Mean Measured Nitrate for Each Column.....	4-35
Figure 4-45 Simulated Mean Biozone Fecal Coliform Bacteria Compared to Mean Measured Fecal Coliform Bacteria for Each Column	4-35
Figure 4-46 Simulated Mean Biozone BOD Compared to Mean Measured BOD for Each Column.....	4-36
Figure 4-47 Simulated Mean Biozone Total Phosphorus Compared to Mean Measured Total Phosphorus for Each Column	4-36
Figure 4-48 Simulated Mean Biozone Total Nitrogen Compared to Mean Measured Total Nitrogen for Each Column	4-37
Figure 4-49 Simulated Mean Biozone Alkalinity Compared to Mean Measured Alkalinity for Each Column	4-37
Figure 4-50 Simulated Mean Biozone Ph Compared to Mean Measured Ph for Each Column.....	4-38
Figure 4-51 Frequency Distribution of Time to Failure for OWS Simulated with the Biozone Algorithm	4-40
Figure 4-52 WARMF Input Dialog for Biozone Reaction Rates	4-41
Figure 4-53 WARMF Input Dialog for OWS and Biozone Coefficients	4-42
Figure 5-1 WARMF Map of the Dillon Reservoir Watershed	5-2
Figure 5-2 Land Use Map of the Dillon Reservoir Watershed.....	5-5
Figure 5-3 Focus Areas of Dillon Reservoir Watershed Study.....	5-10
Figure 5-4 Catchment Delineation in the Blue River Estates Focus Area.....	5-12
Figure 5-5 Catchment Flow Paths for the Blue River Estates Focus Area	5-13
Figure 5-6 Septic System Input for a Catchment in WARMF.....	5-14
Figure 5-7 STE Input Data	5-15
Figure 5-8 Simulated and Observed Stream Flow for French Gulch	5-18
Figure 5-9 Statistical Output and Scatter Plot for French Gulch	5-19
Figure 5-10 Frequency Distribution Plot for French Gulch.....	5-19
Figure 5-11 Cumulative Quantity Plot for French Gulch	5-20
Figure 5-12 Simulated and Observed Flow for the Blue River at Blue River, CO.....	5-21
Figure 5-13 Statistical Output and Scatter Plot for the Blue River at Blue River, CO	5-21
Figure 5-14 Frequency Distribution Plot for the Blue River at Blue River, CO.....	5-22
Figure 5-15 Cumulative Quantity Plot for the Blue River at Blue River, CO	5-22

Figure 5-16 Simulated and Observed Flow for the Blue River Above Dillon Reservoir	5-23
Figure 5-17 Statistical Output and Scatter Plot for the Blue River Above Dillon Reservoir.....	5-24
Figure 5-18 Frequency Distribution Plot for the Blue River Above Dillon Reservoir	5-24
Figure 5-19 Cumulative Quantity Plot for the Blue River Above Dillon Reservoir.....	5-25
Figure 5-20 Simulated and Observed Flow for Tenmile Creek.....	5-25
Figure 5-21 Statistical Output and Scatter Plot for Tenmile Creek	5-26
Figure 5-22 Frequency Distribution Plot for Tenmile Creek.....	5-26
Figure 5-23 Cumulative Quantity Plot for Tenmile Creek	5-27
Figure 5-24 Simulated and Observed Flow for the Snake River Above N. Fork.....	5-27
Figure 5-25 Statistical Output and Scatter Plot for the Snake River Above N. Fork	5-28
Figure 5-26 Frequency Distribution Plot for the Snake River Above N. Fork.....	5-28
Figure 5-27 Cumulative Quantity Plot for the Snake River Above N. Fork	5-29
Figure 5-28 Calculated Water Balance Volumes for Each Water Year	5-29
Figure 5-29 Simulated and Observed Temperature at BR3	5-31
Figure 5-30 Simulated and Observed Temperature at PC2	5-31
Figure 5-31 Simulated and Observed Temperature at BR4	5-32
Figure 5-32 Simulated and Observed Temperature at SR3	5-32
Figure 5-33 Simulated and Observed Temperature at BR10	5-33
Figure 5-34 Simulated and Observed Ammonia (as $\text{NH}_4\text{-N}$) at BR3	5-34
Figure 5-35 Simulated and Observed Ammonia (as $\text{NH}_4\text{-N}$) at PC2	5-34
Figure 5-36 Simulated and Observed Ammonia (as $\text{NH}_4\text{-N}$) at BR4	5-35
Figure 5-37 Simulated and Observed Ammonia (as $\text{NH}_4\text{-N}$) at SR3	5-35
Figure 5-38 Simulated and Observed Ammonia (as $\text{NH}_4\text{-N}$) at BR10	5-36
Figure 5-39 Simulated and Observed Nitrate (as $\text{NO}_3\text{-N}$) at BR3.....	5-37
Figure 5-40 Simulated and Observed Nitrate (as $\text{NO}_3\text{-N}$) at PC2.....	5-37
Figure 5-41 Simulated and Observed Nitrate (as $\text{NO}_3\text{-N}$) at BR4.....	5-38
Figure 5-42 Simulated and Observed Nitrate (as $\text{NO}_3\text{-N}$) at SR3.....	5-38
Figure 5-43 Simulated and Observed Nitrate (as $\text{NO}_3\text{-N}$) at BR10.....	5-39
Figure 5-44 Simulated and Observed Total Nitrogen at BR3	5-40
Figure 5-45 Simulated and Observed Total Nitrogen at PC2	5-40
Figure 5-46 Simulated and Observed Total Nitrogen at BR4	5-41
Figure 5-47 Simulated and Observed Total Nitrogen at SR3	5-41
Figure 5-48 Simulated and Observed Total Nitrogen at BR10	5-42
Figure 5-49 Simulated and Observed Phosphate (as $\text{PO}_4\text{-P}$) at BR3.....	5-43
Figure 5-50 Simulated and Observed Phosphate (as $\text{PO}_4\text{-P}$) at PC2.....	5-43
Figure 5-51 Simulated and Observed Phosphate (as $\text{PO}_4\text{-P}$) at BR4.....	5-44
Figure 5-52 Simulated and Observed Phosphate (as $\text{PO}_4\text{-P}$) at SR3.....	5-44

Figure 5-53 Simulated and Observed Phosphate (as $\text{PO}_4\text{-P}$) at BR10.....	5-45
Figure 5-54 Simulated and Observed Total Phosphorus at PC2.....	5-46
Figure 5-55 Simulated and Observed Total Phosphorus at BR4.....	5-46
Figure 5-56 Simulated and Observed Total Phosphorus at BR3.....	5-47
Figure 5-57 Simulated and Observed Total Phosphorus at SR3.....	5-47
Figure 5-58 Simulated and Observed Total Phosphorus at BR10.....	5-48
Figure 5-59 Simulated and Observed Fecal Coliform Bacteria at BR3.....	5-49
Figure 5-60 Simulated and Observed Fecal Coliform Bacteria at PC2.....	5-49
Figure 5-61 Simulated and Observed Fecal Coliform Bacteria at BR4.....	5-50
Figure 5-62 Simulated and Observed Fecal Coliform Bacteria at SR3.....	5-50
Figure 5-63 Simulated and Observed Fecal Coliform Bacteria at BR10.....	5-51
Figure 5-64 Simulated and Observed Dissolved Oxygen at BR3.....	5-52
Figure 5-65 Simulated and Observed Dissolved Oxygen at PC2.....	5-52
Figure 5-66 Simulated and Observed Dissolved Oxygen at BR4.....	5-53
Figure 5-67 Simulated and Observed Dissolved Oxygen at SR3.....	5-53
Figure 5-68 Simulated and Observed Dissolved Oxygen at BR10.....	5-54
Figure 5-69 Simulated and Observed Flow for Blue River at Blue River, CO.....	5-55
Figure 5-70 Statistical Output and Scatter Plot for Blue River at Blue River, CO.....	5-55
Figure 5-71 Frequency Distribution Plot for Blue River at Blue River, CO.....	5-56
Figure 5-72 Cumulative Quantity Plot for Blue River at Blue River, CO.....	5-56
Figure 5-73 Simulated and Observed Flow for Blue River Above Dillon Reservoir.....	5-57
Figure 5-74 Statistical Output and Scatter Plot for Blue River Above Dillon Reservoir.....	5-57
Figure 5-75 Frequency Distribution Plot for Blue River Above Dillon Reservoir.....	5-58
Figure 5-76 Cumulative quantity plot for Blue River above Dillon Reservoir.....	5-58
Figure 5-77 Simulated and Observed Flow for Tenmile Creek at USGS Gage.....	5-59
Figure 5-78 Statistical Output and Scatter Plot for Tenmile Creek at USGS Gage.....	5-59
Figure 5-79 Frequency Distribution Plot for Tenmile Creek at USGS Gage.....	5-60
Figure 5-80 Cumulative Quantity Plot for Tenmile Creek at USGS Gage.....	5-60
Figure 5-81 Simulated and Observed Flow for Snake River Above North Fork.....	5-61
Figure 5-82 Statistical Output and Scatter Plot for Snake River Above North Fork.....	5-61
Figure 5-83 Frequency Distribution Plot for Snake River Above North Fork.....	5-62
Figure 5-84 Cumulative Quantity Plot for Snake River Above North Fork.....	5-62
Figure 5-85 Simulated and Observed Nitrate for Blue River Above Dillon Reservoir.....	5-63
Figure 5-86 Simulated and Observed Nitrate For Tenmile Creek Above Dillon Reservoir.....	5-64
Figure 5-87 Simulated and Observed Nitrate for Snake River Above Dillon Reservoir.....	5-64
Figure 5-88 Simulated and Observed Total Phosphorus for Blue River Above Dillon Reservoir.....	5-65
Figure 5-89 Simulated and Observed Total Phosphorus for Tenmile Creek Above Dillon Reservoir (Verification 1990–1995).....	5-65

Figure 5-90 Simulated and Observed Total Phosphorus for Snake River Above Dillon Reservoir	5-66
Figure 5-91 Simulated Nitrate at BR-2 With and Without OWS	5-67
Figure 5-92 Total Phosphorus Loading to Dillon Reservoir With and Without OWS	5-68
Figure 5-93 Closeup of Total Phosphorus Loading to Dillon Reservoir With and Without OWS.....	5-69
Figure 5-94 Total Nitrogen Loading to Dillon Reservoir With and Without OWS	5-70
Figure 5-95 Closeup of Total Nitrogen Loading to Dillon Reservoir With and Without OWS.....	5-70
Figure 5-96 A Schematic of the Proposed Management Scenario to Convert Blue River Estates OWS to a Centralized Sewer System	5-71
Figure 5-97 Simulated Nitrate Concentration in a Local Catchment for Blue River Estates Without OWS (ConvPennCr) Compared With OWS (Base060403)	5-72
Figure 5-98 Simulated Total Phosphorus Concentration in a Local Catchment for Blue River Estates Without OWS (ConvPennCr) Compared With OWS (Base060403)	5-73
Figure 5-99 Simulated Nitrate in the Blue River Below SBRWWTP and Goose Pasture Tarn (BR-6) Comparing With OWS (Base060403) and Without OWS (ConvPennCr).....	5-74
Figure 5-100 Simulated Total Phosphorus in the Blue River Below SBRWWTP and Goose Pasture Tarn (BR-6) Comparing With OWS (Base060403) and Without OWS (ConvPennCr).....	5-74
Figure 5-101 Total Phosphorus Loading Output for With OWS (Base060403) Compared to Without OWS (ConvPennCr)	5-75
Figure 5-102 Closeup of Total Phosphorus Loading Output With OWS (Base060403) Compared to Without OWS (ConvPennCr).....	5-76
Figure 5-103 Total Nitrogen Loading Output With OWS (Base060403) Compared to Without OWS (ConvPennCr)	5-77
Figure 5-104 Closeup of Total Nitrogen Loading Output With OWS (Base060403) Compared to Without OWS (ConvPennCr).....	5-78
Figure 6-1 Steady-State Water Contents for a WSAS System	6-2
Figure 6-2 Steady-State Phosphate Concentrations in the WSAS (mg/mL) for a Mature (Biozone Present) System	6-3
Figure 6-3 Virus Removal Simulation Assuming First Order Removal With Respect to Concentration With Increasing Time of Operation	6-7
Figure 6-4 Virus Removal Simulation Assuming First Order Removal With Respect to Concentration With Increasing Time of Operation	6-8
Figure 6-5 WARMF Simulated and Observed Stream Flow for Blue River Above Dillon Reservoir	6-12
Figure 6-6 SWAT Simulated and Observed Stream Flow for Blue River Above Dillon Reservoir	6-12
Figure 6-7 SWAT Simulated and Observed Phosphate at Blue River Above Dillon Reservoir	6-13
Figure 6-8 Comparison of WARMF and SWAT Phosphate Concentrations for the Blue River Above Dillon Reservoir	6-13

Figure A-1 Cumulative Frequency Distribution for $\text{NH}_4\text{-N}$ Concentrations in Domestic STE.....	A-8
Figure A-2 Cumulative Frequency Distribution for First-Order Nitrification Rate	A-10
Figure A-3 Cumulative Frequency Distribution for First-Order Denitrification Rate	A-10
Figure A-4 Cumulative Frequency Distribution for $\text{PO}_4\text{-P}$ Concentrations in STE	A-11
Figure A-5 Cumulative Frequency Distribution for Linear Sorption Isotherm Constants in Soil and Groundwater Sediments	A-16
Figure A-6 Cumulative Frequency Distribution of Mean Residential Indoor Water Use	A-19
Figure B-1 Schematic of 1-D Column Apparatus.....	B-3
Figure B-2 Percent Removal of Fecal Coliform	B-8
Figure B-3 Comparison of 50% Bromide Breakthrough During Tracer Tests 1, 2, and 3 In All Loading Regimes	B-9
Figure B-4 PRD-1 and MS-2 Breakthrough During Clean-Water Tracer Test (Week 0).....	B-11
Figure B-5 Breakthrough Curves for MS-2 and PRD-1 for LR1–LR4	B-12
Figure B-6 Average Percent Removal of MS-2 and PRD-1 During the Week 1 Tracer Test	B-13
Figure B-7 Estimated Cumulative Loading of Constituents in Applied Effluent to LR3, LR4, and LR5 Columns Just Prior to the Start of the Week 1 Tracer Test.....	B-14
Figure B-8 Bromide Breakthrough Curves for Columns 5A and 5B at Week 0, 1, and 6 Tracer Tests	B-15
Figure B-9 PRD-1 and MS-2 Breakthrough in Columns 5A and 5B at the Week 0, 1, and 6 Tracer Tests	B-16
Figure B-10 Water Content and Total Carbon Values for Soil Samples Collected From Cored Columns	B-18
Figure B-11 Fecal Coliform Levels From Extracted Soil Samples at the Infiltrative Surface and at Three Intervals Below	B-19
Figure B-12 MS-2 and PRD-1 Found in Soil Samples Taken From Extracted Soil Samples at the Infiltrative Surface and at Three Intervals Below.....	B-20
Figure B-13 General Schematic Showing Components of a Soil-Based Treatment System	B-23
Figure B-14 Static Mini-Column Assembly Used for Saturated Conditions Experiments	B-24
Figure B-15 Unsaturated Mini-Column Apparatus	B-29
Figure B-16 MS-2 and PRD-1 Inactivation in Soil-Free Columns at 6 °C at pH 5, 7, and 9 in Artificial Groundwater	B-31
Figure B-17 MS-2 and PRD-1 Inactivation in Soil-Free Columns at 23 °C at pH 5, 7, and 9	B-32
Figure B-18 Time to 1- or 4-Log Removal of Virus Calculated Using a Range of Inactivation Rate (K_i) Values	B-34
Figure B-19 Percent Attachment of MS-2 and PRD-1 in Static Mini-Columns Filled With Medium Sand and Run at pH values 5, 7, and 9	B-35
Figure B-20 Concentration of Fecal Coliform Bacteria in Percolate From Columns Dosed With STE	B-37
Figure B-21 Pore Volumes of Effluent Received by Each Loading Regime for Each Run	B-38

Figure B-22 Percent Removal of MS-2 and PRD-1 at TT1 and TT2 in All Columns for Run 2.....	B-39
Figure B-23 Percent Removal From Columns in Runs 3 and 4 for MS-2 and PRD-1 at TT1 and TT2	B-39
Figure B-24 Three Important Factors in the Removal of Viruses in Unsaturated Mini-Columns: (a) Effluent Applied, (b) Hydraulic Loading Rate, and (c) Soil Type.....	B-41
Figure B-25 Total Amount of Effluent Applied to Columns in Runs 1–4	B-42
Figure B-26 Water Content (% dry weight) Measured in Columns at Time of Dismantling	B-43
Figure B-27 Importance of Soil Type on Measured Level of Water Content (% dry weight) at the Time of Column Dismantling	B-43
Figure B-28 Total Organic Carbon (ppm dry weight) Measured in Soil Samples From Dismantled Columns	B-44
Figure B-29 Values for FC bacteria and HPC Measured in Soil Sample Extracts.....	B-45
Figure B-30 Values for MS-2 and PRD-1 Measured in Extracted Soil Columns.....	B-46
Figure B-31 Virus Removal Simulation With Increasing Time of Operation	B-52
Figure B-32 Virus Removal Simulation With Increasing Time of Operation	B-53
Figure C-1 Schematic of Column Set-Up.....	C-4
Figure C-2 Schematic of Column Set-Up.....	C-6
Figure C-3 TDR Derived Volumetric Water Contents for Column 1A and 4C.....	C-14
Figure C-4 Daily Throughput Rates for All Loading Regimes	C-16
Figure C-5 Representative Nitrogen Series, Columns 2B and 4A	C-19
Figure C-6 Bromide Breakthrough Curves During Tracer Tests 1, 2, and 3 From LR2	C-20
Figure D-1 Phase 1 Septic Tank and Effluent Vault at Mines Park	D-1
Figure D-2 Schematic Detail of Experimental Layout.	D-5
Figure D-3 Cross-Section View of Trench With WSAS Test Cells.....	D-6
Figure D-4 Soil Test Locations.....	D-9
Figure D-5 Baseline Infiltration Rates Measured by Constant-Head Permeameter.....	D-12
Figure D-6 Clean-Water Bromide Tracer Test	D-13
Figure E-1 Location of Frisco and Breckenridge.....	E-6
Figure E-2 Schematic of the Mass Balance Used to Predict Nutrient Levels in the Study Area.....	E-10
Figure E-3 Predicted Nitrogen Concentrations in Pennsylvania Creek Based on OWS Input Scenarios	E-16
Figure E-4 Predicted Phosphate Levels in the Blue River	E-17
Figure E-5 Main Map of Sample Sites and Detailed Maps of the Pennsylvania Creek and Swan River Focus Areas.....	E-19
Figure E-6 Flow Values for the Majority of Sites in the Study Area	E-27
Figure E-7 Specific Conductance Values Measured During This Study	E-29
Figure E-8 DO Values Measured During Phase I (September 2001–March 2002) of This Study	E-30
Figure E-9 All pH Values Measured in This Study.....	E-32

Figure E-10 Temperature Values Measured During Both Phases of This Study.....	E-33
Figure E-11 Explanation to Interpret Piper Diagrams Shown in Figure E-12 and Figure E-13.....	E-35
Figure E-12 Piper Diagram for Phase I Major Ions	E-36
Figure E-13 Piper Diagrams for Phase II Major Ions	E-37
Figure E-14 Box-Whisker Plot of Nitrate Measurements From Phase I.....	E-41
Figure E-15 Box-Whisker Plots of Phosphate Measurements From Phase I	E-41
Figure E-16 Box-Whisker Plots of Nitrogen Results for the Blue River During Phase II Analyses.....	E-43
Figure E-17 Box-Whisker Plots of Nitrogen Results for Pennsylvania Creek During Phase II Analyses	E-43
Figure E-18 Box-Whisker Plots of All Blue River Phosphorous Analyses Conducted in Phase II	E-44
Figure E-19 Box-Whisker Plots of All Pennsylvania Creek Phosphorous Analyses Conducted in Phase II.....	E-45
Figure E-20 Map of All Sample Sites Chosen for This Study	E-48
Figure E-21 Important Geographical Features in the Study Area.....	E-48
Figure E-22 Graph of Seasonal Flow Variation at Two Sites in the Study Area	E-50
Figure E-23 Mean Monthly Flow Collected at Two Gaging Stations in the Study Area	E-50
Figure E-24 Flow Values Measured Along the Blue River.....	E-51
Figure E-25 Seasonal Temperature Trends at Select Blue River Sites.....	E-52
Figure E-26 DO Trends Typical of Sites in the Study Area.....	E-52
Figure E-27 Graph of Temperature Trends Typical of Those Seen in Sites BR7, BR8, and BR9	E-53
Figure E-28 Three months of Upstream to Downstream pH Trends Measured in the Blue River.....	E-53
Figure E-29 Specific Conductance Values Measured in Swan River	E-54
Figure E-30 Specific Conductance Measurements in Tenmile Creek Compared to the Study Average.....	E-54
Figure E-31 Limited Months of Blue River Specific Conductance Data.....	E-55
Figure E-32 DO Trends in the Blue River for Select Months	E-56
Figure E-33 Seasonal Variations in Nitrate Concentrations Measured in Pennsylvania Creek.....	E-57
Figure E-34 Nitrate Loading in Tenmile Creek Sites as Measured During Phase I Sampling	E-58
Figure E-35 Seasonal Nitrate Trends in BR1 Through BR6 for the Entire Study Period	E-58
Figure E-36 Seasonal Nitrate Mass Flow Rate Trends in BR7 Through BR10 for the Entire Study Period	E-59
Figure E-37 Nitrate Mass Flow Rate Trends Observed Between Sites FT1 and FT2.	E-60
Figure E-38 Nitrate and Organic Mass Flow Trends Typical of Pennsylvania Creek	E-60
Figure E-39 Select Months of Phase I Nitrate Mass Flow Trends in the Blue River.....	E-61
Figure E-40 Upstream Organic Nitrogen and Nitrate Trends in the Blue River, July 2002.....	E-62

Figure E-41 Downstream Organic Nitrogen and Nitrate Trends in the Blue River, July 2002	E-62
Figure E-42 Seasonal Phosphate Trends Observed in Sites BR1 Through BR5	E-63
Figure E-43 Upstream to Downstream Mass Flow Trends for (a) Dissolved and (b) Total Phosphorous in Pennsylvania Creek, Phase II	E-64
Figure E-44 Total Phosphate Mass Flow Rate Trends Observed in Tenmile Creek, Phase I	E-65
Figure E-45 Upstream Total Phosphorous Trends in Space	E-65
Figure E-46 Total (a) and Dissolved (b) Phosphorous Mass Flow Trends Observed in the Blue River, Phase II	E-66
Figure E-47 Seasonal Total Solids Mass Flow Rate Trends Measured in the Blue River	E-67
Figure E-48 Upstream to Downstream Solids Mass Flow Measured in the Blue River	E-68
Figure E-49 COD Mass Flow Trends for September 2002 in the Blue River	E-68
Figure E-50 Sulfur Mass Flow Trends for the Blue River: (a) Seasonal and (b) Upstream to Downstream	E-69
Figure E-51 Chloride Mass Flow Trends for the Blue River: (a) Seasonal and (b) Upstream to Downstream	E-70
Figure E-52 Boron Mass Flow Trends for the Blue River	E-71
Figure E-53 Sites that Exceeded the Manganese Standard and the Number of Times It Was Exceeded	E-73
Figure E-54 Specific Conductance Values Plotted Versus Flow for Site BR10	E-75
Figure E-55 Upstream Site Nitrate Levels in the Blue River From the Entire Study Period and From Spring Through Summer Only	E-78
Figure F-1 Conceptual Model of a WSAS	F-2
Figure F-2 Sorption Isotherms From the Literature	F-8
Figure F-3 Steady-State Water Velocities	F-10
Figure F-4 Steady-State Water Contents	F-11
Figure F-5 Steady-State Ammonium Concentrations	F-13
Figure F-6 Steady-State Phosphate Concentrations	F-15
Figure F-7 Steady-State Phosphate Concentrations in the WSAS (mg/mL) for a Mature (Biozone Present) System	F-16
Figure G-1 The Dillon Reservoir Watershed	G-1
Figure G-2 Distribution of Weather Stations Within the Dillon Reservoir Watershed	G-12
Figure G-3 Location of Point-Source Discharges Incorporated Into the SWAT Model	G-14
Figure G-4 Distribution of OWS Along the Blue River	G-16
Figure G-5 Subbasins Where Fertilizer Application Was Used to Simulate OWS Inputs for SWAT Modeling	G-17
Figure G-6 Location of the Two USGS Gaging Stations Used in the Streamflow Calibration of the Model	G-20
Figure G-7 Annually Averaged Streamflow Data for the Blue River Just Upstream of Dillon Reservoir Versus Simulated Values	G-21
Figure G-8 Dillon Reservoir Watershed Mean Annual Temperature Versus Elevation	G-24

Figure G-9 Dillon Reservoir Watershed Mean Annual Precipitation Versus Elevation	G-25
Figure G-10 Annually Averaged Streamflow Data for the Blue River Just Upstream of Dillon Reservoir Versus Simulated Values After Incorporation of Lapse Rates and Elevation Bands	G-27
Figure G-11 Monthly Streamflow Results for Blue River Just Upstream of Dillon Reservoir Before and After Incorporation of Elevation Bands.....	G-28
Figure G-12 Final Monthly Streamflow Results for the Blue River Just Upstream of Dillon Reservoir After Model Adjustment	G-30
Figure G-13 Sensitivity to P Soil Partitioning Coefficient, $k_{d,surf}$	G-36
Figure G-14 Sensitivity to P Availability Index, pai	G-37
Figure G-15 Observed P Values and the Best-Fitting Model to Observed P Data Plotted Versus Time	G-43
Figure G-16 Schematic Diagram Showing the Physical Processes in the Hydrologic Cycle That SWAT Can Simulate	G-57
Figure G-17 SWAT Soil Phosphorus Forms (Pools) and the Processes That Contribute to the Movement and Fate of Phosphorus	G-65
Figure H-1 Percent of Land Use That Is Forest and Wetland and Indicator Ranking Scale ...	H-16
Figure H-2 Percent of Riparian Forest and Wetland and Indicator Ranking	H-16
Figure H-3 Source of Nitrogen in Groundwater Recharge	H-19
Figure H-4 Sources of Nitrogen Loading to Surface Runoff	H-21
Figure H-5 Relative Sources of Phosphorous Loading to Surface Waters	H-22
Figure H-6 Land-Use Map of the Dillon Reservoir Watershed Generated by MANAGE	H-23
Figure H-7 Soil Map of the Dillon Reservoir Watershed Generated by MANAGE	H-24
Figure H-8 Locations of High- and Very-High-Risk Land Uses.....	H-25
Figure H-9 Groundwater Hotspots in the Dillon Reservoir Watershed as Generated by MANAGE.....	H-26
Figure H-10 Surface Water Hotspots in the Dillon Reservoir Watershed as Generated by MANAGE.....	H-27
Figure H-11 Riparian Zone Hotspots in a Portion of the Dillon Reservoir Watershed as Generated by MANAGE	H-28



LIST OF TABLES

Table 1-1 Example Questions That Quantitative Understanding and Modeling Tools Can Help Answer.....	1-4
Table 1-2 Reader's Guide for Supporting Information Given in Appendices to the Report.....	1-9
Table 2-1 Description of Focus Areas and Pertinent Management Questions	2-4
Table 2-2 Physical Characteristics of the Shallow Subsurface in the Dillon Reservoir Watershed Based on Soil Core Analyses During CSM Drilling Activities (Fall 2001)	2-7
Table 2-3 Chemical Characteristics of the Shallow Subsurface in the Dillon Reservoir Watershed Based on Soil Core Analyses During CSM Drilling Activities (Fall 2001)	2-8
Table 2-4 Estimates of Pennsylvania Creek Mass Flow Contributions to the Blue River	2-14
Table 2-5 Comparisons of WWTP Mass Flow Estimates to BR7–BR8 Observed Increases.....	2-15
Table 2-6 Transmissivity Estimated From Equation 2-1 Using CSEO Well Log Information	2-21
Table 2-7 Hydraulic Conductivity Estimates From Equation 2-2 and CSEO Well Log Information	2-21
Table 2-8 Hydraulic Conductivity as Estimated From Grain Size Analysis Data by Three Methods	2-22
Table 3-1 OWS-Related Data Required by WARMF	3-9
Table 4-1 Experimental Dosing Rates	4-9
Table 4-2 Water Quality of STE Used for Simulation Runs	4-10
Table 4-3 Calibrated Coefficients of the Biozone Module	4-11
Table 4-4 Low, Medium, and High Values of Dosing Rates and BOD Concentrations.....	4-39
Table 5-1 Meteorology Stations for WARMF Application of Blue River Watershed.....	5-3
Table 5-2 Point Source Dischargers in Dillon Reservoir Watershed.....	5-4
Table 5-3 Managed Flow in the Dillon Reservoir Watershed.....	5-6
Table 5-4 Observed Stream Flow Stations in Dillon Reservoir Watershed.....	5-6
Table 5-5 Observed Water Quality Stations in Dillon Reservoir Watershed	5-7
Table 5-6 Comparison of Well Sampling Data and WARMF Predicted Soil Solution Concentrations for Blue River Estates	5-9
Table 5-7 50 th -Percentile Values for STE (Kirkland 2001)	5-15
Table 5-8 STE Quality for Various OWS Types	5-16
Table 6-1 Calculated Inactivation Rates ($-k_i$) for Viruses Observed Here and Reported by Other Investigators Under Various Conditions	6-4
Table 6-2 Summary of Model Attributes	6-15

Table 6-3 Summary of Model Features	6-16
Table 6-4 Summary of Model Selection Criteria	6-16
Table A-1 Expected OWS Performance for Various System Types	A-2
Table A-2 Human Viruses Potentially Present in Untreated Domestic Wastewater	A-4
Table A-3 Summary of N and P Concentrations in STE ^{a,b,c}	A-7
Table A-4 Summary of Nitrification and Denitrification Rates Reported in Literature Sources ^a	A-9
Table A-5 Summary of Maximum P Sorption Capacities by Soil Type From Literature ^a	A-14
Table A-6 Summary of Linear Sorption Isotherm Constants (K_D) for P From the Literature ^a	A-15
Table A-7 Residential Wastewater Flows	A-18
Table A-8 Average Daily Wastewater Flows Based on Indoor Water Use Monitoring ^a	A-19
Table B-1 Experimental Conditions for the Column Operation	B-4
Table B-2 Approximate Time (Hours) to 10% and 50% Breakthrough During Clean- Water Tracer Test (Week 0)	B-11
Table B-3 Composition of Effluent Applied to LR5 Columns (5A and 5B)	B-14
Table B-4 Time (Hours) to BT ₁₀ and BT ₅₀ During Tracer Tests Conducted in Columns 5A and 5B at Week 0, 1, and 6 of Column Operation	B-17
Table B-5 Soil Physical and Chemical Properties	B-25
Table B-6 Properties of Septic Tank Effluent and Artificial Groundwater Used in Mini- Column Studies	B-26
Table B-7 Replicated 2 ⁴ Full Factorial Design of Flow-Through Unsaturated Mini-Column Experiments	B-28
Table B-8 Calculated Inactivation Rates ($-k_i$) for Viruses Observed in This Study and Reported by Other Investigators Under Various Conditions	B-32
Table B-9 Overall Average Removal of MS-2 and PRD-1 in Unsaturated Mini-Column Runs 1–4	B-48
Table B-10 Input for Virus Removal Simulation	B-50
Table C-1 Loading Regimes That Can Occur Within the Space-Time Framework of a WSAS	C-2
Table C-2 Experimental Conditions for the Column Operation	C-5
Table C-3 Calculated Effective Saturated Hydraulic Conductivities of Infiltrative-Surface Zone Throughout Column Operation	C-15
Table D-1 Effluent Composition of Mines Park Septic Tank Effluent. ¹	D-2
Table D-2 Experimental Conditions for the Test Cell Operation	D-4
Table D-3 Summary of Soil Properties	D-11
Table E-1 Summary of Previous Water Quality Research Done in the Study Area	E-7
Table E-2 Example of Spreadsheet Used to Predict Nutrient Levels in the Focus Areas	E-11
Table E-3 Summary of Base Conditions Used in Mass Balance Calculations	E-13
Table E-4 Example of Spreadsheet Used to Predict Nutrient Levels in the Blue River	E-15

Table E-5 Summary of Mass Balance Calculation Results.....	E-18
Table E-6 Summary of Monitoring Parameters and CSM Analytical Methods.....	E-21
Table E-7 Methods Used and Detection Limits Obtained by the NWQL for Nutrient Analysis.....	E-23
Table E-8 Equipment Original to Phase II Sampling.....	E-24
Table E-9 Synopsis of Trace Metal Analyses Relevant to This Study	E-38
Table E-10 Summary of Results From Remaining Parameters for the Entire Study Area.....	E-46
Table E-11 Example Water Quality Impacts and Associated Monitoring Parameters	E-47
Table E-12 Summary of Results of Water Quality Monitoring Results to Colorado Standards.....	E-72
Table E-13 Computed Versus Measured Temperature Values for the Blue River Downstream of the Iowa Hill WWTP	E-76
Table E-14 Estimated N Mass Flow From Iowa Hill WWTP Versus Nitrate Mass Flow Increases Seen in the Blue River	E-80
Table E-15 Estimated Chloride Mass Flow From the Iowa Hill WWTP Versus Chloride Mass Flow Increases Seen in the Blue River.....	E-84
Table E-16 Summary of Comparison Results Quantifying the Portion of the BR3 to BR4 Increase for Which Pennsylvania Creek Could Be Responsible.....	E-85
Table E-17 Summary of Results Comparing Rural and Urban Development and Wastewater Constituent Mass Flow to Dillon Reservoir.....	E-86
Table F-1 Hydraulic Parameters	F-6
Table F-2 Solute-Transport Parameters	F-7
Table G-1 Summary of Models Reviewed and Their Capabilities	G-3
Table G-2 Soil Properties and Groundwater Parameters That Are Used by SWAT	G-22
Table G-3 Elevation Bands Used in the SWAT Model of the Dillon Reservoir Watershed.....	G-26
Table G-4 Snowmelt/Snow Formation Parameters Used in Model Calibration	G-29
Table G-5 SWAT Parameters Tested in the Sensitivity Study	G-32
Table G-6 Sensitivity Study Base-Case Values, Values Tested, and Justification of Values	G-34
Table G-7 Summary of Average Daily Loading of P by Varying P Soil Partitioning Coefficient, $k_{d,surf}$	G-36
Table G-8 Summary of Average Daily Loading of P by Varying P Availability Index.....	G-37
Table G-9 Summary of Average Daily Loading of P by Varying the Soil Bulk Density, ρ_b	G-38
Table G-10 The Dillon Reservoir Watershed Soil Order Descriptions and Typical Values of Organic Carbon Content, $orgC_{ly}$, in the Upper 15 cm for Each Soil Order.....	G-39
Table G-11 Summary of Average Daily Loading of P by Varying the Amount of Soil Organic Carbon, $orgC_{ly}$	G-39
Table G-12 Summary of Average Daily Loading of P by Varying the Initial Soluble P Soil Concentrations	G-40
Table G-13 Summary of Average Daily Loading of P by Varying the Concentration of P in the OWS Effluent.....	G-41

Table G-14 Percent Change in P Loading Using Parameter Ranges Shown in Table G-6 and Table G-13	G-41
Table G-15 SWAT Parameter Value Changes That Produced the Best-Fit Model to Observed Data	G-42
Table G-16 Data Requirements of the Three Methods Available in SWAT for Computing PET	G-59
Table G-17 SWAT Input Variables for Initialization of Soil P Levels	G-67
Table G-18 SWAT Input Variable for P Mineralization of Humus	G-68
Table G-19 SWAT Input Variable for Decomposition and Mineralization of Residue	G-70
Table G-20 SWAT Input Variable for Sorption of Inorganic P	G-71
Table G-21 SWAT Input Variables for Leaching	G-71
Table G-22 SWAT Input Variables for Movement of Soluble P	G-72
Table G-23 SWAT Input Variables for Organic and Mineral P Attached to Sediment in Surface Runoff	G-73
Table G-24 SWAT Input Variables for P Lag in Surface Runoff and Lateral Flow	G-74
Table G-25 Summary of the Transport Pathways Available to Each of the Six Pools of P in SWAT	G-75
Table H-1 A List of Indicators and Their Associated Rating Scales Used by MANAGE	H-4
Table H-2 GIS Coverages Obtained for This Project	H-7
Table H-3 Input Table 1 From MANAGE	H-9
Table H-4 Study Area Characteristics by Watershed and by Sub-Watershed	H-13
Table H-5 Summary of Results of Watershed Indicator Analysis	H-14
Table H-6 Summary of Water Budget Estimates Generated by MANAGE	H-18
Table H-7 Summary of Nitrogen Contributions to Surface Water and Groundwater	H-20
Table H-8 Summary of Phosphorous Loading to Surface Water	H-22
Table H-9 Estimated Runoff Increase Due to Development in the Study Area	H-30



1 INTRODUCTION

Wastewater infrastructure includes a continuum of approaches that range from highly centralized systems serving densely populated urban areas to decentralized onsite systems serving sparsely populated rural areas. Centralized systems serve about 75% of the US population and are generally characterized by gravity piping networks that convey wastewaters from remote generation to centralized treatment plants where engineered, tank-based biological processes are supported by physicochemical processes, and the effluent is disinfected and discharged to a receiving surface water near the plant location.

Onsite and decentralized systems serve about 25% of the US population and are characterized by collection distances that are short or negligible, with tank-based pretreatment followed by natural systems for advanced treatment before discharge to the land with recharge to groundwater.

Project Background and Motivation

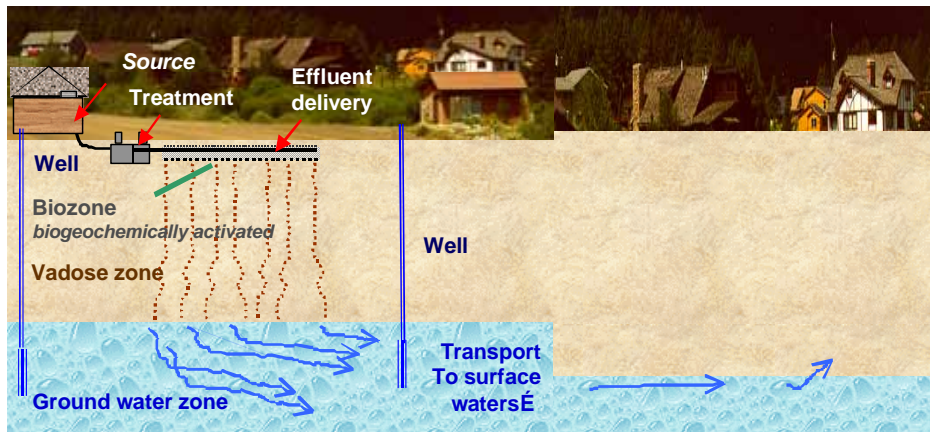
In the past, onsite systems have often been viewed as a temporary approach to wastewater management and acceptable for use only until a centralized approach could be implemented. Yet there are many situations within the US (and more so in developing countries) where centralized systems are neither cost-effective nor sustainable due to a variety of factors (such as, low-density development, rugged topography, limited water and energy supplies, lack of skilled labor). In these situations, decentralized systems can and should be considered as long-term solutions (US EPA 1997).

Decentralized approaches to wastewater infrastructure are based on the use of onsite wastewater systems (OWS). These have evolved greatly during the 20th century from early cesspool and seepage pit designs that were focused simply on waste disposal to contemporary OWS designs that include unit operations to achieve advanced treatment as well as disposal and, in some cases, beneficial reuse. OWS can now be designed from a rapidly increasing array of options that include engineered tank and packed-bed reactors as well as natural system treatment operations. System designs can be tailored for a given application to yield high treatment efficiencies over a long service life at low cost and be protective of public health and environmental quality. Today, there is a considerable knowledge base regarding OWS design, implementation, and performance that enables many commonly used systems to be implemented by experienced practitioners (Crites and Tchobanoglous 1998, Siegrist *et al.* 2001, and US EPA 2002).

While much is known through research and field experiences (US EPA 1997; EPRI 2001; and US EPA 2002), the current state of knowledge does not fully support rational system design to predictably and reliably achieve specific performance goals. As a result, scientists or engineers unfamiliar with the field of OWS often find it difficult to understand how systems are identified, evaluated, designed, and implemented for an expected service life of 10 to 20 years or more. Moreover, when discriminating between optional OWS approaches for a single site (at the site scale) or decentralized versus centralized approaches for a larger development (at the watershed scale) it is often difficult, if not impossible, to ensure that decision-making will lead to a cost-effective solution for reducing wastewater related impacts and risks to an acceptable level. Due to a lack of complete understanding of OWS, the technology may not be exploited fully and/or inappropriate and even harmful applications may occur.

The state of knowledge and practice for onsite wastewater treatment in the US has been summarized in several recent reports and publications (US EPA 1997; Crites and Tchobanoglous 1998; EPRI 2001; and US EPA 2002). A national conference, “National Research Needs Conference: Risk-Based Decision Making for Onsite Wastewater Treatment,” was convened at Washington University in St. Louis in May 2000 with sponsorship by the National Decentralized Water Resources Capacity Development Project (NDWRCDP), United States Environmental Protection Agency (US EPA), and Electric Power Research Institute (EPRI) (EPRI 2001). As described in a white paper prepared by Siegrist *et al.* (2001) and presented at that conference, the primary system for onsite and decentralized wastewater treatment in the US includes septic tank pretreatment followed by subsurface infiltration and percolation through the vadose zone prior to recharge of the underlying groundwater (Figure 1-1). These wastewater soil absorption systems (WSAS) can function as porous media biofilters (Figure 1-2) and have the inherent capability to achieve high treatment efficiencies over a long service life at low cost while being protective of public health and environmental quality. Favorable results from lab and field studies over the years as well as an absence of documented adverse effects suggest that system design and performance are generally satisfactory. However, in contrast, OWS are often reported to be a primary cause of groundwater contamination and even infectious disease transmission in the US (Powelson and Gerba 1994). In addition, as increasing numbers of OWS are located in a geographic area at higher densities, the cumulative effects on water quality in a sub-watershed or watershed can become of concern. In these settings, the effects of older and contemporary OWS need to be considered in light of other sources of pollutant loading to the environment (such as municipal wastewater treatment plant (WWTP) discharges, agricultural runoff, storm water runoff, atmospheric deposition) (Figure 1-3).

The classic onsite system and local setting



An increasing array of options...



Figure 1-1
Classic Onsite Wastewater System and the Local Site-Scale Setting

Site-scale processes

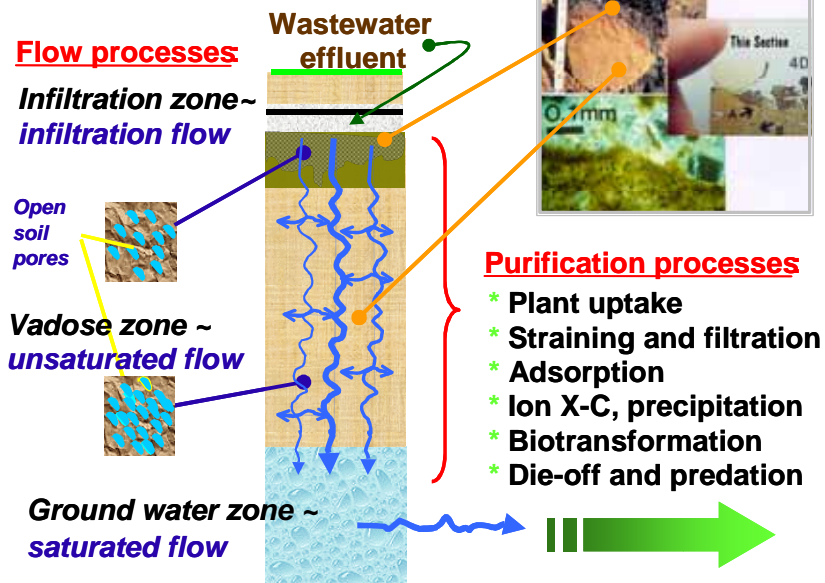


Figure 1-2
Site-Scale Processes Affecting the Performance of a Common Soil-Based OWS

Watershed-scale systems

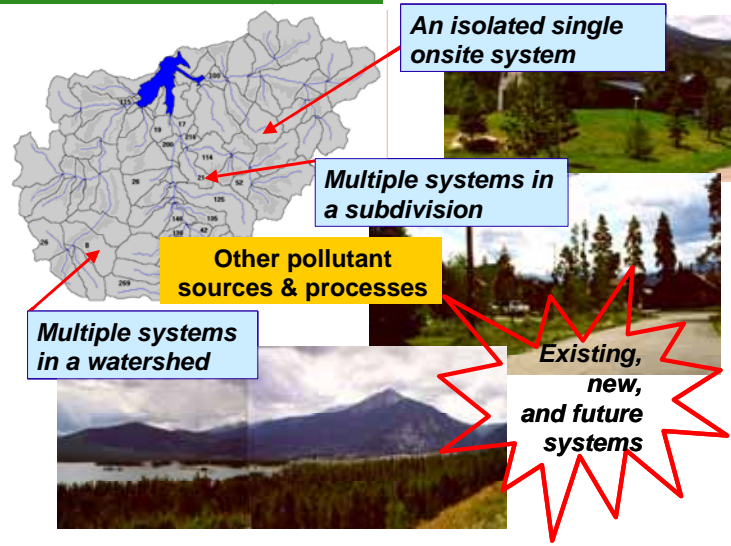


Figure 1-3
Watershed-Scale Framework Within Which Large Numbers of Individual OWS Can Occur

While considerable research has been accomplished, much of it has been empirical and has not led to quantitative understanding and predictive modeling tools. That is to say that the understanding and predictability of performance as a function of design, installation/operation, and environmental factors, as well as the risk of inadequate function and its effects, have not been fully elucidated. This knowledge gap includes spatial scales that span the single-site OWS up to a watershed scale system and temporal scales that span years to decades. The absence of fundamental OWS process understanding that enables system performance relationships to be quantified and modeled for predictive purposes makes it extremely challenging to answer questions such as those posed in Table 1-1 with any certainty.

Table 1-1
Example Questions That Quantitative Understanding and Modeling Tools Can Help Answer

Scale	Example Questions
Single site scale	How does the clogging zone develop in a soil system based on hydraulic loading rate and effluent quality?
	What is the effect on purification of increasing the dosing frequency for septic tank effluent to sandy soil from 4 to 24 times daily?
	How does the long term acceptance rate change if the effluent biochemical oxygen demand applied is reduced by 50%?
	Will 99.99% virus removal still be achieved if the unsaturated zone depth is reduced from 4 to 2 ft.?

Table 1-1
Example Questions That Quantitative Understanding and Modeling Tools Can Help
Answer (Cont.)

Scale	Example Questions
Cluster and subdivision scale	Will mounding beneath a large cluster system reduce the depth to groundwater to <3 ft.?
	What is the minimum lot size in a subdivision to keep nitrate below 10 mg-N/L in groundwater?
	Do OWS pose a current or future risk to public health in a subdivision via groundwater contamination and private wells?
Watershed scale	What portion of the total nitrogen and phosphorous load to a river comes from onsite systems?
	What is the impact (positive and/or negative) on water quality of discontinuing onsite services and extending water and/or sewer services?
	What is the impact (positive and/or negative) on water quality of requiring onsite service upgrades including advanced treatment units and/or point-of-use water treatment?
	Is there a future risk to drinking water contamination via OWS impacting groundwater if onsite systems and private wells continue to be used?

Mathematical models provide a powerful tool for understanding wastewater flow and pollutant transformations and describing the performance of OWS. Proper and careful use of single-site process models can enable optimization of system design and operation, as well as provide a quantitative understanding of how factors such as mass loading, soil type, infiltrative surface characteristics, and wastewater quality impact pollutant treatment. Site-scale models include simple spreadsheet-based equations as well as complex numerical models that can simulate unsaturated flow and reactive chemical transport.

At the other end of the spectrum of spatial scales are calibrated watershed models that can allow prediction of the impacts of decentralized wastewater systems on groundwater quality as well as assist in determination of total maximum daily loads (TMDLs) for a watershed. Such models should also be useful for planners who desire to regulate population growth in the watershed. Watershed models range from simple water-balance and chemical-mass-balance methods, to subjective or semi-quantitative geographic information system (GIS) methods, to complex numerical models that attempt to account for many different hydrologic transport processes. Modeling requires that important issues are addressed such as:

- Evaluating the appropriate level of model complexity for various purposes
- Linking the relevant single site-scale processes to watershed-scale models
- Incorporating appropriate flow and transport parameters into these models

Project Objectives

Developing an understanding and modeling tools that can help quantify site-scale system processes and watershed-scale cumulative effects of OWS is the goal of this NDWRCDP study. Specific objectives include:

- Quantification of site-scale processes and development of increased understanding and modeling tools for applications involving individual OWS
- Incorporation of project results on the dynamic quantification of site-scale processes during the refinement, application, and evaluation of watershed modeling tools
- Application of the understanding and methods developed to assess the watershed-scale effects of a broad-scale use of OWS

Project Approach

This project was designed and carried out in two phases by a collaborative team involving

- The Colorado School of Mines (CSM)
- EPRI
- Systech Engineering, Inc
- United States Geological Survey (USGS)
- The Summit County Environmental Health Department (SCEH), including participation by a stakeholder group from the study area

To accomplish the project goals and objectives, several tasks including literature review and analysis, laboratory experimentation and field monitoring, development and refinement of mathematical models, and completion of site-scale and watershed-scale model simulations were completed. Analysis of literature data along with laboratory experimentation enhanced the understanding of the transport/fate of microbes and chemicals in OWS and enabled single site-scale model development.

The site-scale source/transport/fate expressions have been incorporated into an existing watershed model, the Watershed Analysis Risk Management Framework (WARMF) model that can be used for simulating the effects of OWS relative to other pollutant sources on water quality in a watershed or sub-watershed. The WARMF model as well as the Better Assessment Science Integrating Point and Nonpoint Sources (BASINS) model were setup for the Dillon Reservoir watershed in Summit County, Colorado where there are approximately 1,500 OWS as well as other nonpoint and point sources of pollution, and more than 600 onsite drinking water wells along with community wells and surface water supplies. Dillon Reservoir is also used as a drinking water supply for the City of Denver. After setup and calibration, model simulations were completed to examine current wastewater management scenarios and the simulation results were compared to field monitoring data. Examination of future wastewater management scenarios was also completed through watershed-scale model simulations (for example, abandonment of OWS and connection to a centralized WWTP).

The project approach included the following set of interrelated tasks (Figure 1-4):

- Setup and calibrate WARMF for the Blue River study area in Summit County, Colorado
- Refine algorithms and representation of OWS
- Review literature and input parameter cumulative frequency distributions (CFDs)
- Site-scale algorithms and model formulations (HYDRUS 2-D, Biozone)
- Experiments for rate/capacity parameter estimates
- Focused water quality studies in the watershed
- Simulations for selected scenarios
- Model comparisons (WARMF, BASINS, and MANAGE)
- Verification assessment and peer review

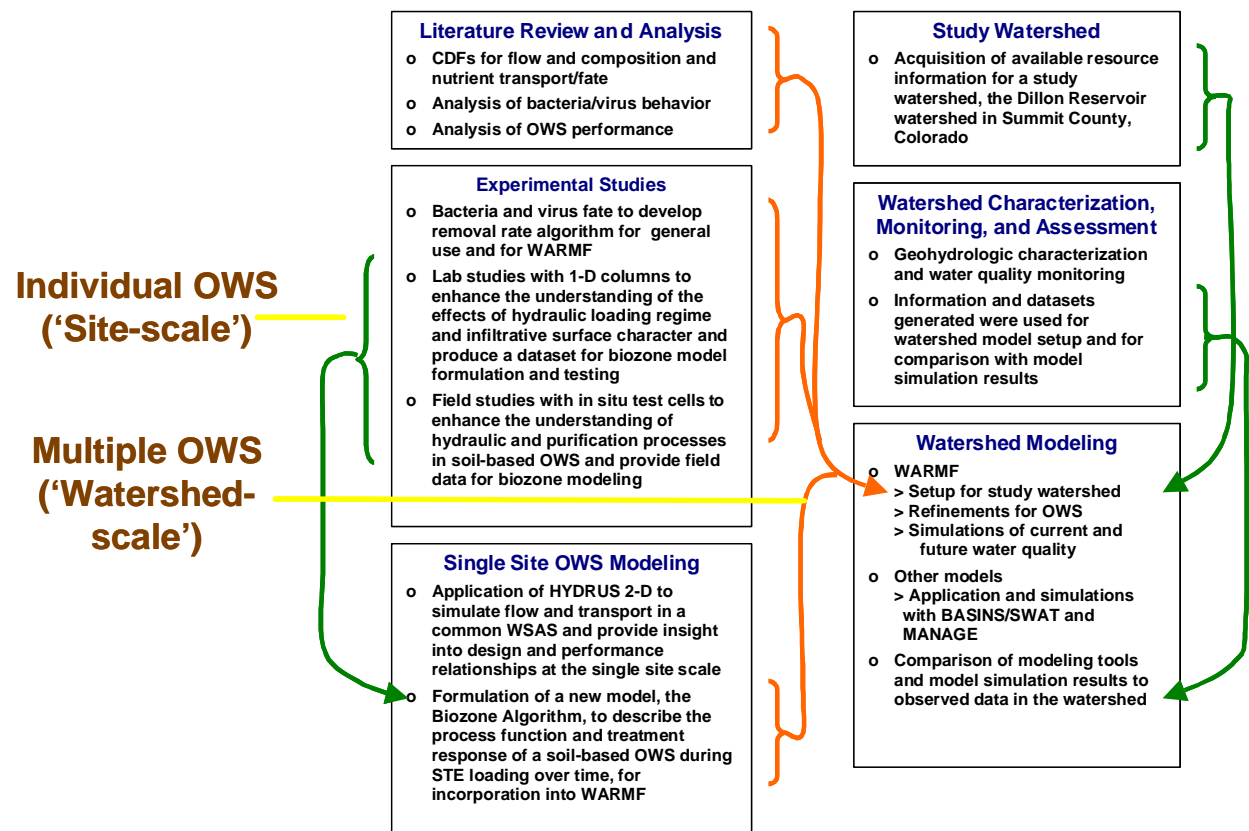


Figure 1-4
Relationships of NDWRCDP Project Tasks

The full project was completed in two integrated phases. This approach was selected to permit funding of Phase 1 initially, with funding of Phase 2 authorized one year after Phase 1 was initiated. A final element in the project was an independent peer review, which occurred during late spring and summer 2003.

The NDWRCDP project described in this report was enabled by other research recently completed or ongoing as part of the small flows research program at CSM (Figure 1-5). Existing facilities and methodologies were employed and coordination was achieved with ongoing research. This was critical to providing a knowledge base for quantitative understanding and to provide experimental datasets to aid model formulation, calibration and testing.

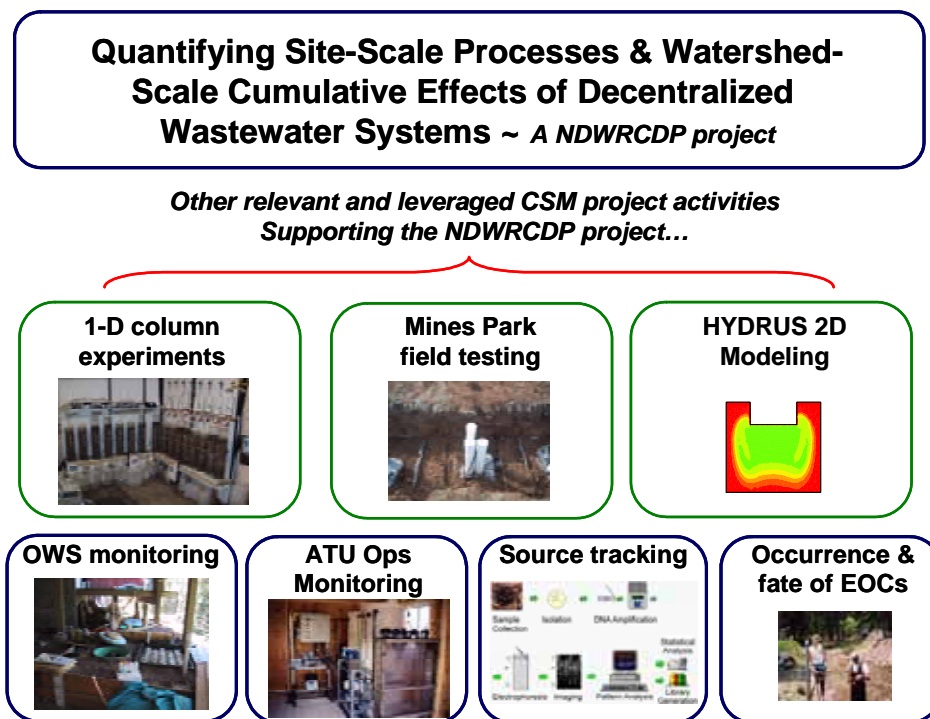


Figure 1-5
Illustration of Related CSM Research That Supported Completion of the NDWRCDP Project

Report Organization

The project included a set of interrelated tasks, which generated a substantial body of research results produced through experimental work, field monitoring, and modeling efforts (Figure 1-4). This report describes the methods and results of experimentation, environmental monitoring, and mathematical modeling completed to quantify the site-scale processes and watershed-scale cumulative effects of decentralized wastewater systems.

The report chapters provide a summary of the various facets of the project while detailed information on each component of the effort is provided in the Appendices (Table 1-2).

In addition to the information contained in this report, additional details regarding the work may be found in:

- Published CSM student theses and dissertations (Beach 2001, Kirkland 2001, Albert 2002, Guelfo 2003, Lemonds 2003, Van Cuyk 2003, Tackett 2004, Smith 2004)
- Conference proceedings papers (Chen *et al.* 2001a; Huntzinger *et al.* 2001; Siegrist *et al.* 2002; Van Cuyk and Siegrist 2001; Van Cuyk *et al.* 2002; Weintraub *et al.* 2002; Lemonds and McCray 2004; Smith *et al.* 2004; Bagdol *et al.* 2004; Tackett *et al.* 2004; Van Cuyk and Siegrist 2004; and Weintraub *et al.* 2004)
- Journal articles (Siegrist 2001; Beach and McCray 2003; Beach *et al.* 2005; McCray *et al.* 2005; and Van Cuyk *et al.* 2004)
- Forthcoming publications

Table 1-2
Reader's Guide for Supporting Information Given in Appendices to the Report

Report or Appendix	Additional Information Presented in the Appendix	Selected Related Publications
Chapter 1, <i>Introduction</i>	None	None
Chapter 2, <i>Study Watershed Environmental Setting</i>	App E, <i>Water Quality Monitoring</i>	Bagdol <i>et al.</i> 2004; Smith <i>et al.</i> 2004; Smith 2004; Guelfo 2003; Smith <i>et al.</i> 2002
Chapter 3, <i>Introduction to the Watershed Analysis Risk Management Framework (WARMF) Model</i>	App A, <i>Input Parameters for Modeling Flow and Transport in Onsite Wastewater Systems</i> App C, <i>Biozone Development and WSAS Performance: Laboratory Studies</i> App E, <i>Water Quality Monitoring</i>	Chen <i>et al.</i> 2001a; 2001b; Herr <i>et al.</i> 2000
Chapter 4, <i>Biozone Algorithm</i>	App B, <i>Pathogen Transport-Fate Studies</i> App C, <i>Biozone Development and WSAS Performance: Column Studies</i> App D, <i>Biozone Genesis and WSAS Performance: Field 3-D Test Cells</i>	Weintraub <i>et al.</i> 2002
Chapter 5, <i>Application of WARMF in the Dillon Reservoir Watershed</i>	App A, <i>Input Parameters for Modeling Flow and Transport in OWS</i>	Weintraub <i>et al.</i> 2004

Table 1-2
Reader's Guide for Supporting Information Given in Appendices to the Report (Cont.)

Report or Appendix	Additional Information Presented in the Appendix	Selected Related Publications
Chapter 6, <i>Additional Models Applied</i>	App F, <i>Site-Scale Modeling Using HYDRUS 2-D</i> App G, <i>Watershed Modeling Using BASINS/SWAT</i> App H, <i>Watershed Modeling Using MANAGE</i>	Van Cuyk <i>et al.</i> 2004; Beach and McCray 2003; Huntzinger <i>et al.</i> 2001; Van Cuyk and Siegrist 2001
Chapter 7, <i>Stakeholder and User Perspectives</i>	None	None
Chapter 8, <i>Summary, Conclusions, and Recommendations</i>	None	None
Appendix A, <i>Input Parameters for Modeling Flow and Transport in Onsite Wastewater Systems</i>	Not applicable	McCray <i>et al.</i> 2005; Kirkland 2001
Appendix B, <i>Pathogen Transport—Fate Studies</i>	Not applicable	Van Cuyk <i>et al.</i> 2004; Van Cuyk 2003; Van Cuyk <i>et al.</i> 2002; Van Cuyk and Siegrist 2001
Appendix C, <i>Biozone Development and WSAS Performance: Column Studies</i>	Not applicable	Beach 2001; Siegrist <i>et al.</i> 2002; Beach <i>et al.</i> 2005
Appendix D, <i>Biozone Genesis and WSAS Performance: Field 3-D Test Cells</i>	Not applicable	Tackett <i>et al.</i> 2004; Tackett 2004
Appendix E, <i>Water Quality Monitoring</i>	Not applicable	Guelfo 2003; Smith 2004; Bagdol <i>et al.</i> 2004; Smith <i>et al.</i> 2004
Appendix F, <i>Site-Scale Modeling Using HYDRUS 2-D</i>	Not applicable	Huntzinger <i>et al.</i> 2001; Beach and McCray 2003
Appendix G, <i>Watershed Modeling Using BASINS/SWAT</i>	Not applicable	Lemons 2003; Lemons and McCray 2004
Appendix H, <i>Watershed Modeling Using MANAGE</i>	Not applicable	None



2 STUDY WATERSHED ENVIRONMENTAL SETTING

The Dillon Reservoir watershed is located in Summit County, Colorado in the northwest quadrant of the State (Figure 2-1). The lowest elevation is 7,947 feet, and the highest elevation is 14,270 feet. Summit County has an area of 383,260 acres, or 598.8 square miles. Dillon Reservoir is located in the center of the county, and the area that drains into the reservoir is situated to the south. Dillon Reservoir was completed in 1963 and is approximately 3,140 acres in area and 246,777 acre-ft in volume (Summit County Government 1998). The reservoir serves as an aesthetic resource and also supplies approximately 25% of the drinking water for the Denver area. There are three major streams that flow into the reservoir: Tenmile Creek, Blue River, and Snake River. Since the creation of the reservoir in 1963, this area has undergone many changes. There has been a rapid increase in population, an associated increase in development, and a decrease in the mining activity in the area.



Figure 2-1
Location of the Dillon Reservoir Watershed in Summit County, Colorado (Guelfo 2003)

Introduction to the Study Area

This study included modeling and field monitoring that was focused on portions of Tenmile Creek, Blue River, and Dillon Reservoir itself (Figure 2-2).

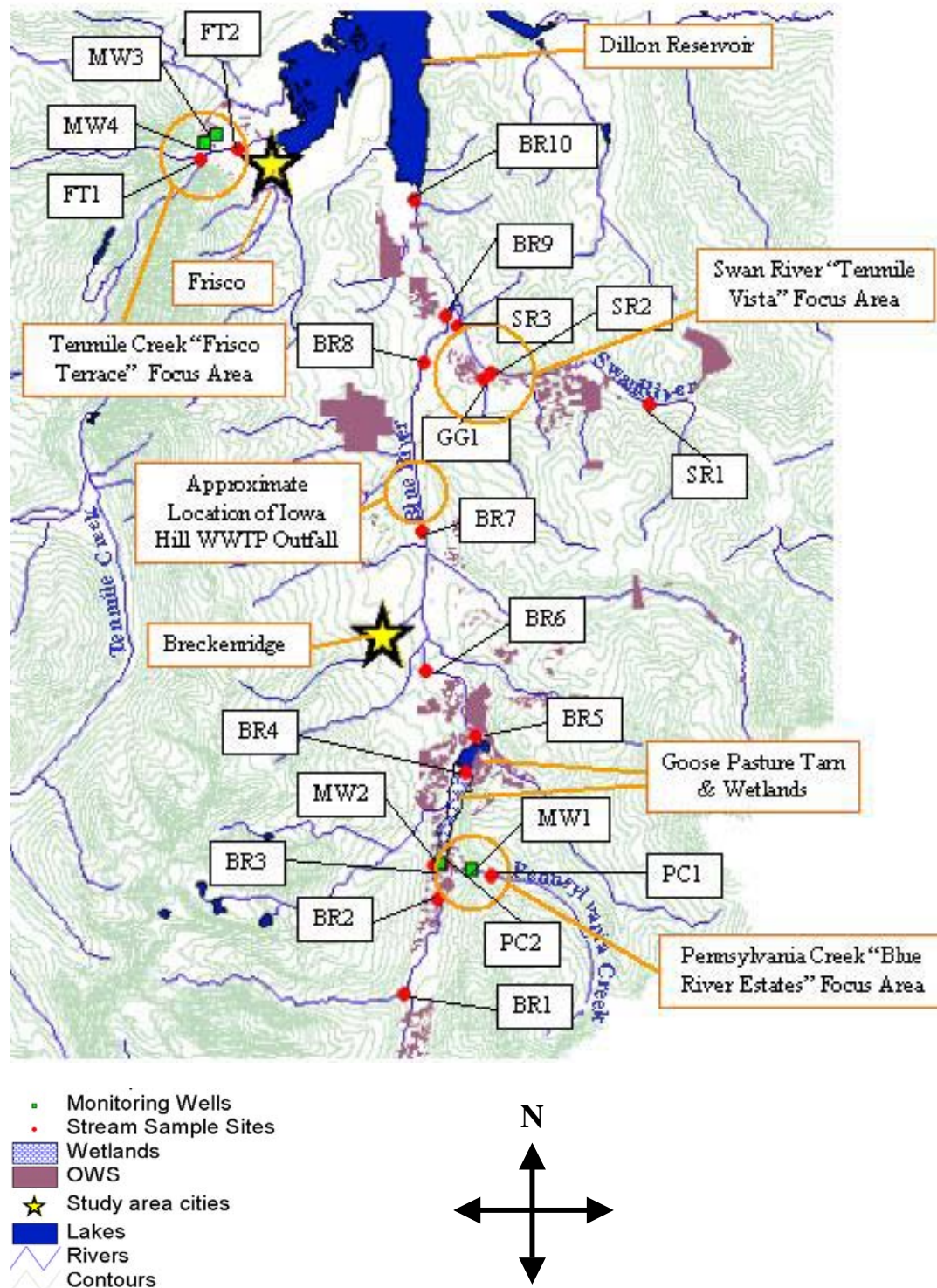


Figure 2-2
Important Geographic Features of the Study Area (Monitoring Location Identification
Includes BR for Blue River, FT for Frisco Terrace, GG for Gold Run Gulch, MW for
Monitoring Well, and SR for Swan River)

Two major areas of development upstream of Dillon Reservoir include the towns of Frisco and Breckenridge (Figure 2-2). Rapid development of these towns and others in the area caused Summit County to be the most rapidly growing county in the country from 1970 to 1980 (Summit County Government 1998). During this time period, there was a 232% increase in population. From 1980 to 1990, there was a 45.6% increase in population). From 1970 to 1998, total number of housing units increased from 2,198 to 23,019. According to the 2000 Census, the town populations of Frisco and Breckenridge are both approximately 2,500. The town of Frisco utilizes both surface water and wells as a source of drinking water. Breckenridge utilizes a small reservoir, Goose Pasture Tarn, as well as South Barton Creek for its drinking water. The towns of Frisco and Breckenridge utilize sewerage and centralized WWTPs with discharge to surface waters, while suburban and rural development relies on OWS (Figure 2-2).

Water Quality Monitoring

Water quality has been extensively monitored and studied in the primary watersheds of Summit County, Colorado for more than two decades. In the early 1980s declining water quality in the reservoir attributed to phosphorous loading, which resulted in the establishment of the Dillon Reservoir Control Regulation established by the Colorado Water Quality Control Commission. As a result, several control measures have been implemented including institution of state-of-the-art tertiary treatment systems at all publicly-operated treatment works that discharge into the watershed, several storm water retention projects, and over the last few years, an erosion control program. Additional measures have also been taken by the Summit County Environmental Health Department over the last two decades to refine the design regulations for OWS with the intent of have the most effective treatment systems installed in all parts of the county. These measures rapidly improved water quality in the reservoir in terms of nutrient loading. However, as rapid growth occurred throughout the subsequent decades, nutrient levels (in particular phosphorous) continued to creep toward regulatory limits established by the Colorado Water Quality Control Commission. The regulatory limit of 7.4 mg/L of phosphorous in the water of the reservoir as measured during the growing season (May through September) has been exceeded twice since 2001 and is attributed, in part, to the recent drought. As the major point source dischargers have continued to contribute very low levels of phosphorous to overall Dillon Reservoir nutrient loads, other contributors to phosphorous loading have been identified.

Focus Areas

Smaller focus areas were designated within the watershed study area in order to understand the effects of OWS on a smaller scale (Figure 2-2). For example, Blue River Estates, which is situated along Pennsylvania Creek, uses exclusively OWS as a means of domestic waste disposal and was chosen as a focus area for this study. Swan River (Ten Mile Vista) and portions of Tenmile Creek (Frisco Terrace) were chosen as focus areas for similar reasons. A map of the watershed showing the locations of each of the three focus areas can be found in Figure 2-2. Additionally, Table 2-1 Description of Focus Areas and Pertinent Management Questions gives a more detailed description of each focus area along with management questions applicable to each area. These management questions demonstrate the importance of more detailed study in these areas.

Table 2-1
Description of Focus Areas and Pertinent Management Questions

Focus Area	Example Management Questions
<p>Focus Area 1—Frisco Terrace: Frisco Terrace and Wiborg Park are two continuous subdivisions surrounded on three sides by incorporated sections of the Town of Frisco and on the fourth side by Interstate 70. These subdivisions were created in the mid-1960s and consist of generally one-half-acre parcels. All parcels are served by private well and sewage systems with the exception of a few properties on the fringes, which have opted to connect to the town sewer and/or water system. The western edge of both subdivisions lies at approximately 9,175 feet above sea level and drops rapidly to the east to a flat plain of approximately 9,125 feet above sea level. The total lot count in both subdivisions is about 120 with the vast majority in the alluvial plain of Tenmile Creek. Water well depths range from approximately 40 to 525 feet, with the vast majority less than 150 feet. Private water well data collected by Summit County from 1995 to date show nitrate concentrations in drinking water from approximately 2 to nearly 7 mg-N/L (milligrams nitrate per liter).</p>	<ul style="list-style-type: none"> • Is there any current risk to public health in the subdivision via private wells? • Is there a future risk to public health if OWS and private wells continue to be used? • What is the contribution of OWS to pollutant loads in Dillon Reservoir via Tenmile Creek? • What is the impact (positive and/or negative) of discontinuing onsite services and extending water and/or sewer services from the City of Frisco? • How will any infrastructure changes be financed?
<p>Focus Area 2—Ten Mile Vista: This area is located midway between Frisco and Breckenridge, just east of Colorado Highway 9. The subdivision consists of two filings. Filing 1 was platted in 1963 and consists of approximately 51 lots. The lots are generally one-half-acre in size, and the subdivision is approximately 85% built out. Filing 2, platted in 1970, lies directly to the north of Filing 1 and consists of 24 lots of generally two acres each. The subdivision slopes from west to east from an elevation of about 9,300 to 9,200 feet above sea level. Shallow soils predominate the area underlain by fractured and decomposing granite and shale formations. Shallow groundwater follows a main drainage area toward the center of the subdivision. The alluvial plain of the Swan River runs adjacent to the eastern edge of the subdivision. The Breckenridge Golf Course is located directly south of this subdivision. Drainage from the golf course generally flows east and west from a center ridgeline, which is common to the western edge of the subdivision. Water well depths in this subdivision range from 40 to 350 feet, with the majority in the 90- to 150-foot range. Due to elevation and surface topography, this subdivision is relatively isolated from surrounding land uses. Private water well data collected by Summit County from 1995 to date indicate nitrate in drinking water ranges from <1 to 7 mg-N/L.</p>	<ul style="list-style-type: none"> • Is there any current risk to public health in the subdivision via private wells? • Is there a future risk to public health if OWS and private wells continue to be used? • What is the contribution of OWS to pollutant loads in Dillon Reservoir via the Blue River? • What is the impact (positive and/or negative) of requiring onsite service upgrades including advanced treatment units and/or point-of-use water treatment? • What is the impact (positive and/or negative) of discontinuing onsite services and establishing a satellite services proximal to development area? • How will infrastructure changes be financed?

Table 2-1
Description of Focus Areas and Pertinent Management Questions (Cont.)

Focus Area	Example Management Questions
<p>Focus Area 3 —Blue River Estates: This area consists of a number of small subdivisions along a small tributary of the Blue River, Pennsylvania Creek and has widely varying soil and topography conditions in an older, more densely developed subdivision. The total lot count in the subdivisions is about 250. The subdivision lies at an elevation of about 10,000 to 10,200 feet, and because Arapaho National Forest and the Continental Divide provide a relatively pristine environment upstream from the subdivisions, there are few land uses other than the housing development in the immediate area that could affect water resources.</p>	<ul style="list-style-type: none"> • Is there any current risk to public health in the subdivision via private wells? • Is there a future risk to public health if OWS and private wells continue? • What is the contribution of OWS to pollutant loads in Dillon Reservoir via the Blue River? • What is the impact (positive and/or negative) of requiring onsite upgrades including advanced treatment units and/or water treatment? • What is the impact (positive and/or negative) of discontinuing onsite services and establishing a satellite services proximal to development area? • How will infrastructure changes be financed?

There are several features in the study area that have the potential to affect water quality. These features, shown on Figure 2-2, include the towns of Frisco and Breckenridge, the Iowa Hill wastewater treatment facility (serving Breckenridge), two riparian wetlands upstream of Goose Pasture Tarn, Goose Pasture Tarn (a small reservoir), and the presence of OWS in the study area. The Water Quality section addresses the water quality of the study area and discusses what, if any, impacts are being caused by these features.

Finally, it is important to note the locations of sampling sites (surface water and groundwater) within the study area. Approximately 20 surface water sampling sites were established within the study area (Figure 2-2). Sites were chosen in two ways:

1. To target certain features of the study area (that is, focus areas and areas of development)
2. Using a method by Sharp (1971), which ensures an even distribution of sampling points within a study area

There are also four groundwater monitoring well (MW) locations in the study area. They were emplaced in two of the focus areas: Frisco Terrace and Blue River Estates. These MW locations are shown on Figure 2-2 and include:

- A background site that is considered to be unimpacted by development at the edge of the Blue River Estates development at a higher elevation (MW1)

- A location within the development at Blue River Estates near the confluence of Blue River and Pennsylvania Creek (MW2)
- Two locations in Frisco Terrance (MW3 and MW4), which represent a highly populated area along Tenmile Creek near the exit of the stream into Dillon Reservoir

MW3 has water in both shallow and deep piezometers, so MW3 water-level measurements and groundwater samples are designated MW3U (upper) and MW3L (lower) to differentiate between the two monitoring depths at this location.

Geology and Soils

This section describes the geology and soils properties in the focus areas.

Geology

Various maps were consulted to determine the geology of the study area. These maps indicate that the bedrock in the study area consists primarily of sandstone, shale, carbonate, diorite, and gneiss of varying ages (Tweto 1973). In much of the study area the bedrock is overlain by glacial deposits, also of varying ages. In the Blue River Estates focus area, situated in the southern portion of the watershed, this bedrock is specifically comprised of the Minturn and Belden formations. The Minturn formation is Precambrian in age and includes sandstone, grit, conglomerate, and shale with scattered beds of carbonate rocks. This unit is 6,000 feet thick or more, thinning to the east. The Belden formation is also Precambrian in age and contains black shale, carbonate rock, and sandstone intruded by the Laramide intrusive rocks made up of quartz monzonite, granodiorite, and quartz diorite porphyries. This unit is approximately 900 feet thick. Well logs indicate that the overburden of glacial deposits in the Blue River Estates focus area is approximately 60 feet thick. Along the river corridor, overburden consists of young glacial drift. This glacial material is sand and gravel with unsorted bouldery deposits.

Geology of the study area remains similar to that described in the previous paragraph in much of the southern portion of the watershed. However, moving north and west in the watershed, including the Frisco Terrace focus area, bedrock geology changes into heavily faulted biotitic gneiss and migmatite containing minor layered hornblende gneiss and calcareous silicate. These rocks are also Precambrian in age. Overburden in this focus area is Pinedale and Bull Lake glacial drift deposits of bouldery till and associated sand and gravel deposits. This glacial till appears to overlay the aforementioned metamorphic deposits in an area where they come into contact with the Pierre Shale, Dakota Group, and Morrison formation. The latter are widespread in Colorado, marine in origin, and consist of conglomerate, sandstone, limestone, and shale.

Soils

Soil surveys in Summit County were completed by the Soil Conservation Service of the US Department of Agriculture in 1980 (USDA 1980). Soils in the watershed are predominantly Grenadier soils described as deep, well drained, and moderately permeable. Grenadier soils are strongly acidic (pH of 4.8–5.5), medium textured soils with a gravelly-loam surface layer (0–6 in.), a sandy-clay-loam subsoil (6–19 in.), and a cobble-loam substratum (19–60 in.). Permeability rates are reported at 0.6–2.0 in./hr at a depth of 0–19 in. and 2.0–6.0 in./hr at a depth of 19–60 in. The subsoil and substratum contain more than 35% rock fragments, by volume (USDA 1980). In the southern portion of the watershed these soils are situated on slopes ranging from 6–55%. In the northern portion of the watershed they are on a shallower slope of approximately 0–6%.

Soil core samples collected during Colorado School of Mines (CSM) MW installation activities in Summit County in fall 2001 were analyzed for physical and chemical properties. The shallow subsurface was characterized to consist of sandy-loam to loamy-sand textures (Table 2-2) in the depth interval where OWS are typically established in Summit County (that is, one to two meters of vadose zone below the infiltrative surface). Soil chemical properties within three meters below ground surface revealed median values for pH of 7.05 and organic matter at 0.2 weight percent (Table 2-3). Characteristics of the shallow subsurface at Blue River Estates and Frisco Terrace were similar, while limited data for Ten Mile Vista revealed it to have different properties (such as relatively lower pH, higher organic matter, and higher nitrogen).

Table 2-2
Physical Characteristics of the Shallow Subsurface in the Dillon Reservoir Watershed
Based on Soil Core Analyses During CSM Drilling Activities (Fall 2001)

Focus Area	Location	Depth bgs (m)	Sand (wt.%)	Silt (wt.%)	Clay (wt.%)	USDA Texture
Blue River Estates	MW1	0.75	60	27	13	Sandy loam
		1.80	63	23	14	Sandy clay loam
		3.30	81	12	7	Loamy sand
	MW2	0.60	75	19	6	Sandy loam
		1.80	73	19	8	Sandy loam
		3.00	72	19	9	Sandy loam
	SB1	0.60	78	15	7	Loamy sand
		3.00	70	20	10	Sandy loam

Table 2-2
Physical Characteristics of the Shallow Subsurface in the Dillon Reservoir Watershed
Based on Soil Core Analyses During CSM Drilling Activities (Fall 2001) (Cont.)

Focus Area	Location	Depth bgs (m)	Sand (wt.%)	Silt (wt.%)	Clay (wt.%)	USDA Texture
Frisco Terrace	MW3	0.60	78	15	7	Loamy sand
		1.80	80	14	6	Loamy sand
		3.00	76	16	8	Sandy loam
	SB2	0.60	74	18	8	Sandy loam
		3.00	81	13	6	Loamy sand
	MW4	0.60	81	13	6	Loamy sand
		1.80	88	7	5	Sand
		3.00	73	19	8	Sandy loam
Ten Mile Vista	SB3	0.60	48	13	15	Loam
		1.80	77	15	8	Sandy loam
Statistics	Minimum=		48	7	5	Sandy loam
	Maximum=		88	37	15	Loamy sand
	Median=		75.5	17.0	8.0	

Note: MW denotes monitoring well location, SB denotes soil boring location.

Table 2-3
Chemical Characteristics of the Shallow Subsurface in the Dillon Reservoir Watershed
Based on Soil Core Analyses During CSM Drilling Activities (Fall 2001)

Focus Area	Location	Depth bgs (m)	pH	Org. M. (wt.%)	Available P (mg/kg)	Total N (mg/kg)	NH ₄ -N (mg/kg)	Ca + Mg (mg/kg)
Blue River Estates	MW1	0.75	7.7	0.2	7	87	3.8	1540
		1.80	7.8	0.1	7	59	3.9	1370
		3.30	8.0	0.1	7	33	2.7	820
	MW2	0.60	6.4	1.0	16	579	4.2	1080
		1.80	7.1	0.7	14	319	3.6	1250
		3.00	8.2	0.2	8	93	0.6	1010

Table 2-3
Chemical Characteristics of the Shallow Subsurface in the Dillon Reservoir Watershed
Based on Soil Core Analyses During CSM Drilling Activities (Fall 2001) (Cont.)

Focus Area	Location	Depth bgs (m)	pH	Org. M. (wt.%)	Available P (mg/kg)	Total N (mg/kg)	NH ₄ -N (mg/kg)	Ca + Mg (mg/kg)
Blue River Estates (Cont.)	SB1	0.60	7.0	0.6	28	145	1.1	810
		3.00	7.9	0.2	8	68	11.1	850
Frisco Terrace	MW3	0.60	6.3	0.6	15	232	4.9	490
		1.80	6.8	0.2	11	91	2.6	510
		3.00	7.1	0.2	15	49	0.5	1530
	SB2	0.60	5.7	1.1	32	280	4.5	580
		3.00	6.9	0.2	5	42	0.8	1140
	MW4	0.60	6.7	0.4	22	98	0.1	450
		1.80	7.3	0.1	10	26	0.1	180
		3.00	7.2	0.2	16	44	0.1	380
Tenmile Vista	SB3	0.60	4.9	6.1	21	3931	41.5	1940
		1.80	5.9	0.6	6	232	2.0	750
Statistics	Minimum=		4.9	0.1	5	26	0.1	180
	Maximum=		8.2	6.1	32	3931	41.5	1940
	Median=		7.05	0.2	12.5	92.1	2.6	840

Note: MW denotes monitoring well location, SB denotes soil boring location.

Water Quality

This section describes the water quality in the focus areas.

Surface Water: Introduction

One of the primary goals of the surface water monitoring was to determine what, if any, are the effects of OWS on the study area, and how those effects compare to those attributed to WWTP. This question was approached by studying trends in space as well as trends in time (Guelfo 2003 and Appendix E, *Water Quality Monitoring*). This approach enables the water quality at each monitoring station to be put into context with the water quality at other times of the year and at other sites.

Studying trends in time, or seasonal trends, reveals times of the year that water quality may be more impacted than others, and studying trends in space, or upstream to downstream trends, enables the establishment of a land-use gradient. A land-use gradient can be an effective way of studying the relative effects of nonpoint and point sources of pollution. The gradient is established by sampling sites located in areas upstream of development, in areas of limited development, in areas of maximum development, and downstream of development. In this way, if constituent levels are observed from upstream to downstream, a gradient may be observed that shows where areas of impact begin, peak, and end. Temporal trends will not be presented here because little evidence was found to indicate that seasonal trends were affected by anything other than natural causes. However, spatial trends will be discussed with the focus primarily on nutrients (such as nitrogen and phosphorous species), solids, chloride, boron, and sulfur. Data is presented for the Blue River sites only, because data from other monitoring sites (Swan River, Tenmile Creek) revealed little evidence of impact.

Note that discussion of results often refers to Phases I and II. Sampling was conducted in a two-phase approach. Phase I (September 2001–March 2002) was conducted to screen the flow and water quality characteristics of all water quality stations as well as to refine field and laboratory methods. The goal of Phase II monitoring (May 2002–September 2002) was to conduct detailed monitoring of select sites by obtaining trace level nutrient data as well as producing a dataset for a broad suite of other water quality parameters.

Surface Water: Nutrient Results

Elevated nutrient levels or increasing nutrient concentration trends can potentially indicate wastewater impact. Nutrients are also elements critical for biological growth. Elevated nutrient levels can therefore cause increased biological growth and eventually eutrophication of surface waters. Nutrient species measured in this study were species of both nitrogen and phosphorous. During Phase I monitoring, analyses included nitrate, ammonia, total nitrogen, total phosphate, and total phosphorous. During Phase II, monitoring was expanded to include nitrite, organic nitrogen, dissolved phosphate, and total dissolved phosphorous.

During Phase I of this study, nearly all ammonia and total nitrogen results were below the detection limit (0.1 mg-N/L, 1 mg-N/L, respectively). Nitrate measurements in this phase ranged from 0.003 to 2.72 mg-N/L and displayed an upstream to downstream trend. (Note that it may be useful to refer back to Figure 2-2. There is a small increase in nitrate loading from BR3 to BR4 (Figure 2-3). In between these sites there is a riparian wetland that has the potential to increase nitrate through natural nutrient cycling (Hill 1996). The input of Pennsylvania Creek is also situated between these sites. Furthermore, there are many homes using OWS situated directly along the Blue River. Hence the observed increases could be natural or anthropogenic in origin. Nitrate decreases are observed from BR4 to BR5. As shown in Figure 2-2, a small reservoir, Goose Pasture Tarn, is located between those sites. The tarn is likely acting as a sink for some of the nitrate through processes such as plant uptake. The final trend to note is the large jump in nitrate mass flow beginning at site BR7. Potential causes of this trend are a WWTP outfall and the City of Breckenridge.

In Phase II, nitrate concentrations were slightly lower varying from 0.065 to 0.459 mg-N/L. Similar nitrate trends to Phase I were observed in Phase II; however, in Phase II other nitrogen species data were also available. Of the available species, nitrite and ammonia were regularly below the detection limit indicating that the majority of nitrogen in these surface waters is comprised of nitrate and organic nitrogen. Figure 2-3 reveals that at sites BR1 through BR6 both organic nitrogen and nitrate followed similar trends to those observed in Phase I nitrate data. However, comparing the two nitrogen species reveals that organic nitrogen is the dominant species of this part of the Blue River. This speciation is of note because if anthropogenic sources of nitrogen were heavily impacting the waters of this area, then nitrate would be expected to be the dominant species. In the downstream portions of the Blue River, nearer suspected anthropogenic sources, this speciation is reversed with nitrate as the dominant species.

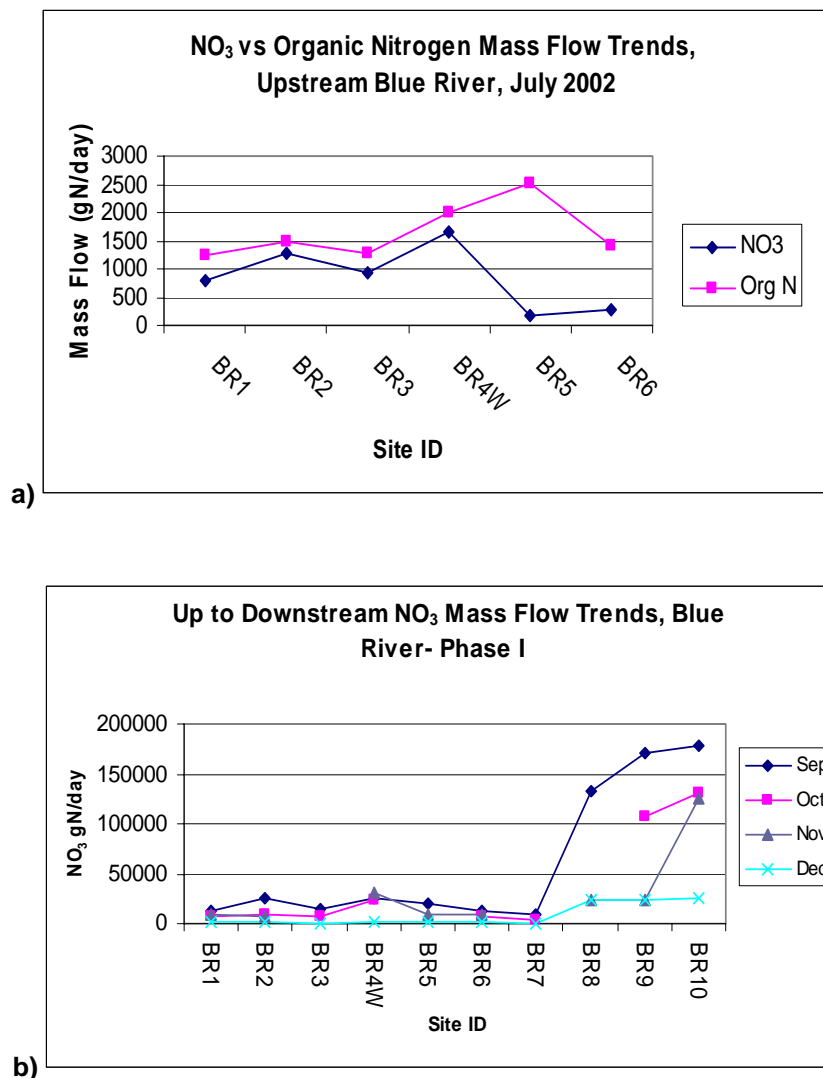


Figure 2-3
Nitrogen Mass Fluxes in the Blue River: a) Select Months of Phase I Nitrate Mass Flow Trends in the Blue River, and b) Upstream Organic Nitrate Trends in July 2002—Part of Phase II Sampling

In Phase I, all phosphorous species were below the detection limits often enough that trends in the data were hard to determine. In Phase II, lower detection limits allowed for phosphorous trends to be analyzed. Of the phosphorous species analyzed in Phase II, dissolved phosphate was below the detection limit in all cases (0.007 mg-P/L [milligrams phosphorus per liter]). Dissolved phosphorous, which would include any dissolved phosphate present, ranged from 0.002 to 0.004 mg-P/L. Total phosphorous in Phase II ranged from 0.003 to 0.013 mg-P/L. Trends in both phosphorous species are similar to those observed in nitrate (with the same potential causes as nitrate) with small increases between sites BR3 and BR4, decreases between BR4 and BR5, and increases in the downstream sites around BR7.

Surface Water: Supporting Parameter Results

Analysis of nutrient parameters revealed trends of interest with various potential causes including anthropogenic causes such as domestic wastewater discharges (Guelfo 2003). In order to better determine if some of these trends were generated by wastewater input, other parameters commonly found in wastewater were analyzed. These include chloride, boron, and sulfur.

Chlorides are naturally occurring in water due to processes such as the weathering of rocks. However, they are also found in wastewater because they are present in human excreta and in water softeners. Conventional waste treatment methods do not remove chlorides; therefore, it acts as a natural tracer. As a result, elevated chloride levels can be indicative of the presence of wastewater (Metcalf & Eddy 2003). Upstream to downstream chloride trends repeat some of those described previously (Figure 2-4). Increases were observed from BR3 to BR4, which could be due to development and OWS input, to de-icing of nearby roads, and/or the input of Pennsylvania Creek. In the downstream sites (BR6 through BR10), mass flow of chloride increases again. De-icing of roads is a potential cause, along with the WWTP input.

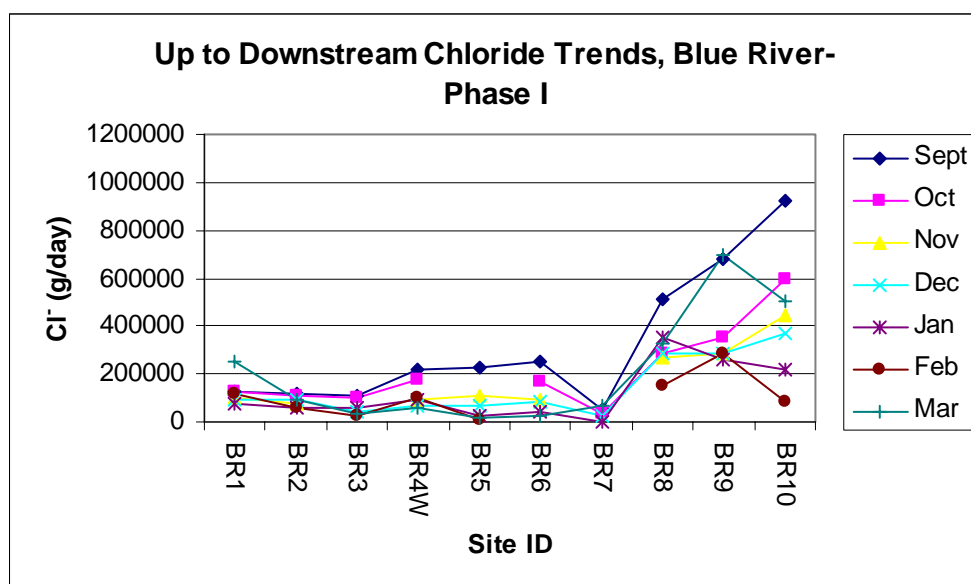


Figure 2-4
Up- to Down-Stream Mass Flow of Chloride in the Blue River

Sulfur is a naturally occurring component in surface waters, and is also a wastewater constituent. Sulfur is required in the synthesis of proteins and so is subsequently released when those proteins degrade (Metcalf & Eddy 2003). Upstream to downstream sulfur trends showed consistent increases from site BR3 to BR4 (Figure 2-5). Pennsylvania Creek or OWS input may be causing this increase. As with other parameters discussed, large increases in sulfur mass flow were observed in the Blue River downstream of site BR7.

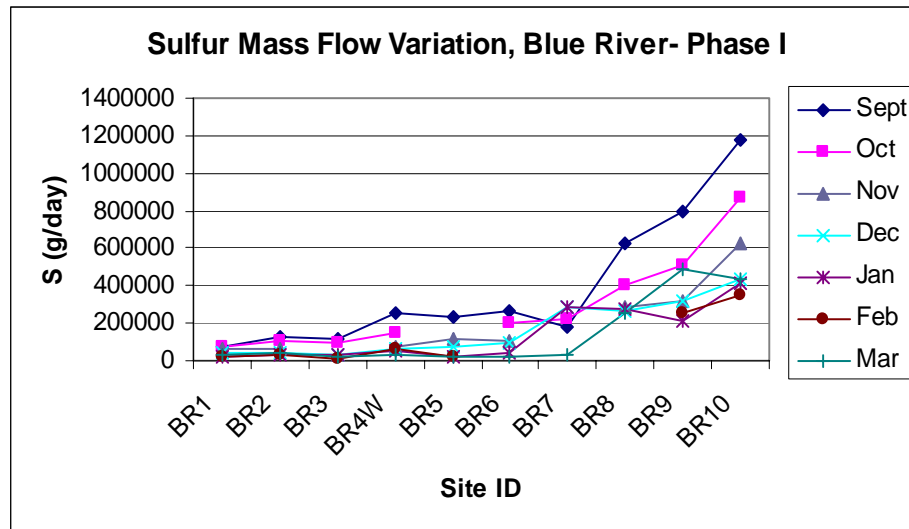


Figure 2-5
Up- to Down-Stream Mass Flow of Sulfur in the Blue River

The final supporting parameter analyzed in this assessment was boron. Similar to chloride, boron acts as a natural tracer. Boron is found in domestic wastewater as a product of the breakdown of some fruits and due to its presence in certain cleaning materials (Flynn and Barber 2000). Boron data in this study were often below the detection limit (0.0031 mg-B/L [milligrams boron per liter]); however, some upstream to downstream trends are again similar to those observed: increases from BR3 to BR4 and after BR7. In the upstream sites these trends could be due to OWS impact or the input of Pennsylvania Creek. In the downstream sites the only potential cause known for these trends is municipal wastewater effluent input from the WWTP.

Surface Water: Discussion

The results presented previously in this section show that several potential forces could be at work in the study area that may be affecting water quality trends. Two questions were asked and answered in an attempt to better determine which of the potential causes identified were actually present (Guelfo 2003). These questions are:

- Could Pennsylvania Creek stream discharge have caused the observed constituent increase from BR3 to BR4?
- Could the WWTP have caused the observed constituent increase from BR7 to BR8?

These questions are addressed in the following sections.

Pennsylvania Creek Stream Discharge Impact

In order to better determine the cause of the increases seen in several constituents between surface water sites BR3 and BR4, estimates were made to calculate whether or not Pennsylvania Creek could be causing the entirety of the observed increases. Surface water site PC2 was situated near the confluence of Pennsylvania Creek with the Blue River. For the purposes of these estimates, mass flow measured at that site was assumed to be the mass flow of Pennsylvania Creek to the Blue River. This mass flow was then compared to the increases observed between sites BR3 and BR4. Results indicate that Pennsylvania Creek could be responsible for only portions of the observed increases (Table 2-4). Anthropogenic sources (that is, OWS) coupled with some effects of riparian wetlands are likely the cause of the remaining portion of the increase.

Table 2-4
Estimates of Pennsylvania Creek Mass Flow Contributions to the Blue River

Parameter	Average Increase From BR3 to BR4 (kg/d)	Average Loading From PC2 (kg/d)	Increase in the Blue River Potentially Attributable to Pennsylvania Creek (%)
Nitrate N	1.32	0.2	16
Organic N	1.41	0.38	27
Total P	0.125	0.019	15
Dissolved P	0.059	0.007	12
Chloride	40.8	0.76	2
Sulfur	62.8	3.92	6
Boron	0.625	0.27	43

WWTP Impact

The WWTP near Breckenridge was identified as a potential cause of the observed constituent increases from BR7 to BR8. The WWTP outfall was monitored to obtain constituent concentrations and flow. Concentrations and flows were then used to calculate the mass flow levels likely to be contributed by the WWTP to the Blue River and compared to the increases observed from surface water sites upstream of the WWTP outfall to those downstream of the plant outfall (BR7 to BR8). These estimates were possible for chloride and nitrate. Comparison of the observed temperatures downstream of the WWTP with calculated temperatures downstream of the WWTP was also possible. Results for temperature and nitrate show observed increases consistent with calculated increases for both temperature and nitrate (Table 2-5).

These results indicate the WWTP discharge could be the cause of those increases. Observed chloride increases were much higher than the estimated increases that the WWTP could cause, which is likely due to the fact that chloride increases are caused by the WWTP in combination with other activities such as de-icing of the roads.

Table 2-5
Comparisons of WWTP Mass Flow Estimates to BR7–BR8 Observed Increases

	Temperature		Chloride		Nitrate	
Date	Calculated Temperature °C	Measured Temperature °C	WWTP Mass Flow (kg-Cl/day)	Measured Increase From BR7 to BR8 (kg-Cl/day)	WWTP Mass Flow (kg-N/day)	Measured Increase From BR7 to BR8 (kg-N/day)
Sept. 2001	3.7	3.9	57.3	464	21.5	123.8
Oct. 2001			53	251		
Nov. 2001			57	270	21.3	23
Dec. 2001	2.51	4.51	73.4	262	27.5	23.8
Jan. 2002	4.75	1.36	86.5	354	32.4	19.4
Feb. 2002	6.76	4.66	86.5	150	32.4	14.8
Mar. 2002			87	258	32.6	25.5

Note: A blank cell indicates data needed for calculation and comparison were not available for that month.

Surface Water: Conclusions

Analysis of upstream to downstream trends in surface water quality in the upper portion of the watershed revealed that from BR3 to BR4, the input of Pennsylvania Creek may be partially responsible for mass flow increases in the Blue River, but the presence of some wastewater parameters and increasing trends of those parameters indicates that OWS impacts are likely present to a limited extent. OWS impacts in this region are described as limited due to nitrogen speciation of the area, which shows that naturally generated organic nitrogen is the dominant species. Moreover, from BR3 to BR4, nutrient trends indicate the possibility of riparian zone effects on nutrient cycling. From BR4 to BR5, decreases in several parameters indicate that Goose Pasture Tarn acts as a sink for some constituents. Analysis of the spatial trends in the lower portion of the watershed (BR6 to BR9) revealed the effects of urbanization and WWTP discharges. In general, both WWTP and OWS are affecting water quality in the Blue River. However, rural effects (including OWS) are not a relatively more important source. Moreover, all identified impacts are limited and surface water quality of the study area is consistent with designated uses.

Groundwater: Introduction

As with surface water samples, groundwater samples were analyzed for a variety of parameters. A summary of the results for nutrients and supporting parameters can be found in the following sections. Note that due to the sparse nature of the groundwater monitoring points, trends in groundwater chemistry could not be analyzed with the same level of detail as surface water trends. Most trends can only be identified as either generally increasing or decreasing down the watershed. As a result, using groundwater trends to identify the presence of anthropogenic sources (OWS), which may cause trends at a small local scale, is difficult. However, groundwater data can be analyzed to identify elevated constituent levels in order to make some preliminary conclusions regarding anthropogenic impacts. Furthermore, geochemical fingerprint analysis was conducted on the groundwater and surface water samples together to help in determining if these waters are hydraulically connected.

Groundwater: Nutrient Results

Nitrate concentrations in the groundwater generally increased down the watershed, from the southern portion near MW1 to the northern portion near MW3 and MW4 (Figure 2-6). The highest concentrations were found in MW3 in the Frisco Terrace focus area, which also shows a seasonal trend. Potential causes are similar to those seen in the surface water trends: natural (such as forest land runoff and atmospheric deposition) or anthropogenic (such as OWS and lawn fertilization).

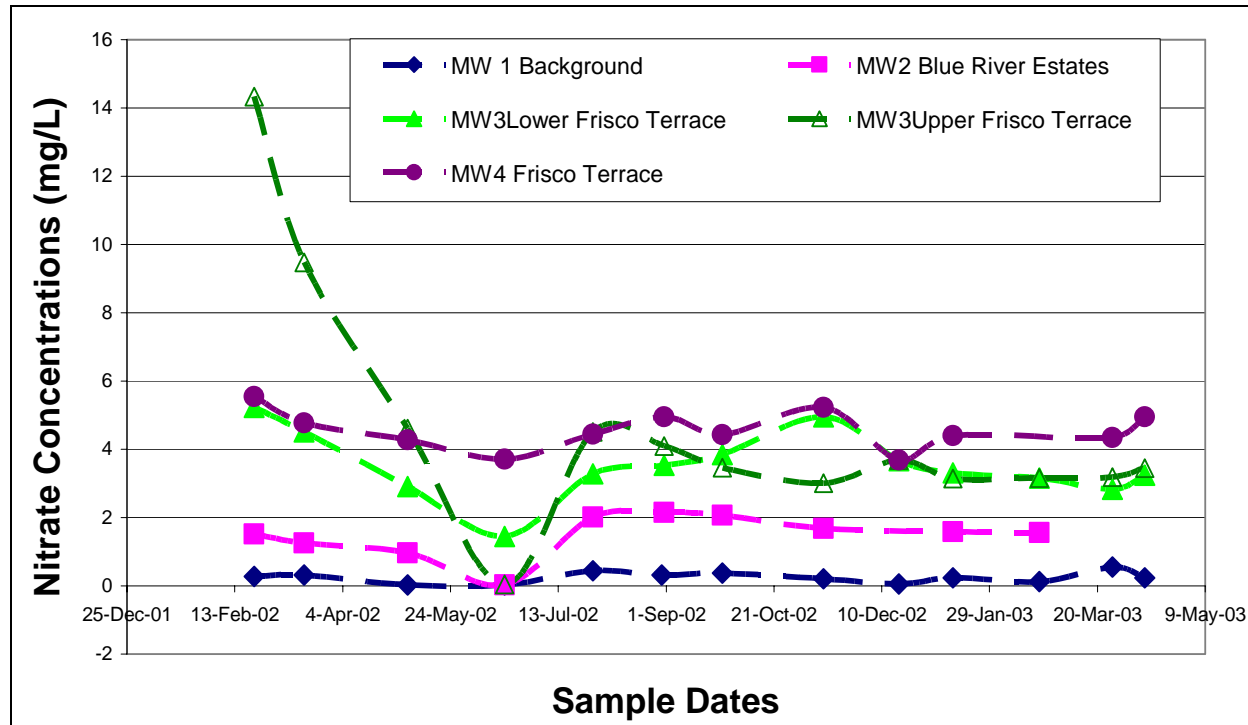


Figure 2-6
Nitrate Trends in Groundwater of the Dillon Reservoir Watershed

Groundwater: Supporting Parameter Results

Supporting parameters were measured as part of the groundwater evaluation, including solids, chloride, boron, and sulfur. All of these supporting parameters indicated an increasing trend with distance down the watershed. Note that boron (a natural tracer found in domestic wastewater as a product of the breakdown of some fruits and from certain cleaning materials) was found to be below the detection limit in the majority of cases and is not discussed further.

For groundwater sampling, solids were measured as total dissolved solids (TDS) rather than total solids as was measured in the surface water efforts. TDS showed, as with nitrate, an increasing trend with distance down the watershed. Highest concentrations were found in MW3. Factors that can contribute to the increasing trend include natural accumulation of weathered products and increased anthropogenic effects as the watershed becomes more populated moving north.

Chloride also shows an increasing trend moving down the watershed (Figure 2-7). As mentioned, chloride acts as a natural tracer. Therefore, elevated chloride levels are indicative of anthropogenic impact. The highest levels were seen in the Frisco Terrace focus area at MW4.

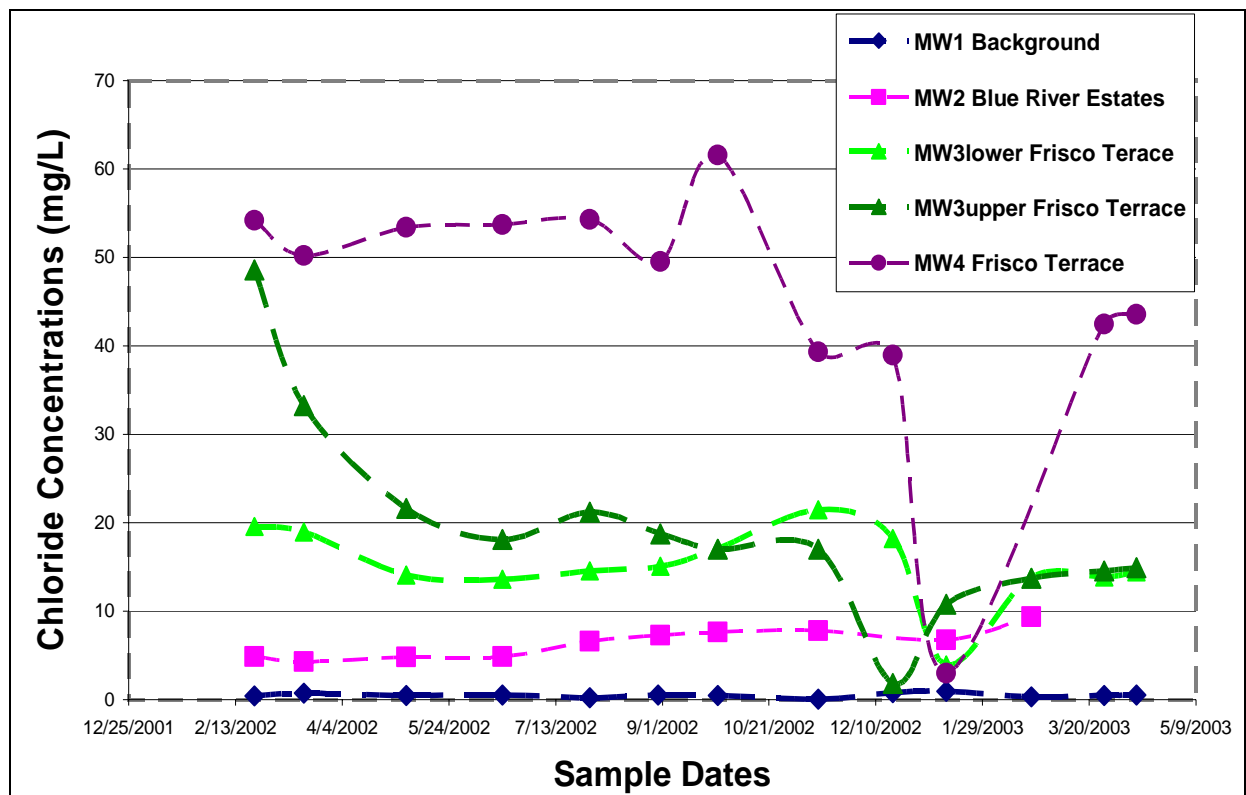


Figure 2-7
Chloride Trends in Groundwater Within the Dillon Reservoir Watershed

Groundwater: Fingerprint Analysis

A total of 76 surface and groundwater samples were taken at sites along the Blue River drainage between September 2001 and August 2002 (Figure 2-2) (Guelfo 2003). Based on geochemical evaluation, the water samples can be divided into three groups that have spatial and hydrochemical coherence. Based on sodium, potassium, calcium, magnesium, bicarbonate, sulfate, chloride, fluoride, and nitrate data, the samples can be preliminarily divided into three groups, arbitrarily numbered 1–3, each with distinct chemical signatures. The samples within a group are very similar to each other, but there is significant variation between groups. The chemical variations are primarily due to differences in sulfate, chloride, and nitrate concentrations. Figure 2-8 is a Scholler plot of the mean concentrations for each group of samples. A composite sample of septic tank effluent (STE) from a home site in Turkey Creek, a separate watershed east of Summit County, is also shown (Dano *et al.* 2003). The chemical composition of STE is distinctive with elevated chloride and nitrate. If STE is influencing the surface and groundwater chemistry, those samples will have chemical signatures with characteristics of both STE and background water.

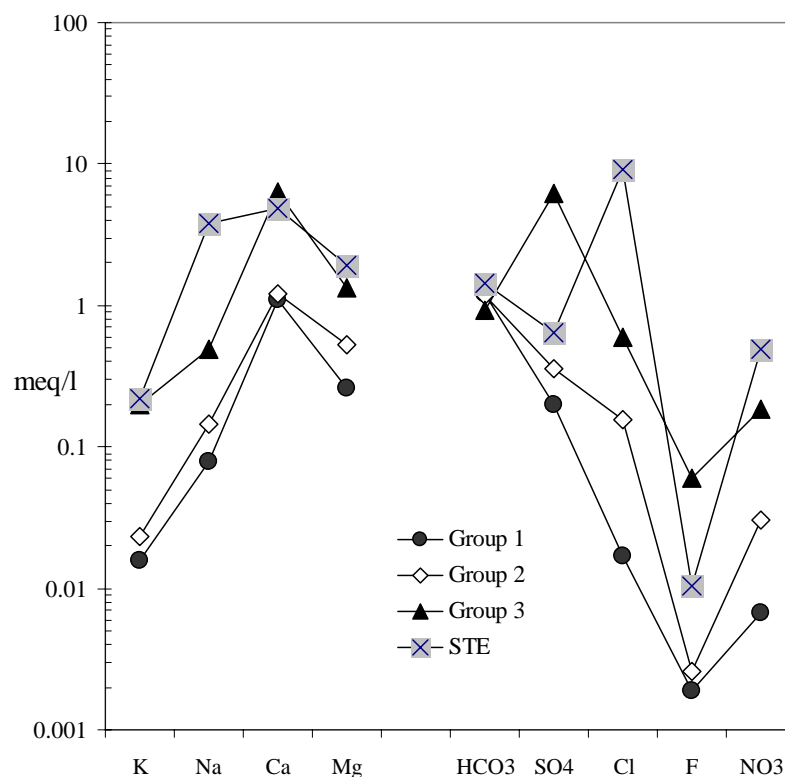


Figure 2-8
Scholler Plot of the Mean Concentrations for Water Chemistry Groups 1 Through 3 and STE

Group 1 samples ($n=14$) are from the Pennsylvania Creek, from the Swan River drainage, and MW1. The water is primarily composed of calcium and bicarbonate with low TDS, typical of mountain drainages. This chemical signature is considered natural background without any significant anthropogenic influences. All the samples come from locations with exceptionally low population density. The similarity of the Pennsylvania Creek to MW1 indicates that the MW1 is hydraulically connected to the surface water in the vicinity of the well.

Group 2 samples ($n=37$) are from the length of Blue River between Pennsylvania Creek and Dillon Reservoir and MW2. These samples have higher TDS, are primarily composed of calcium and bicarbonate, but have higher concentrations of sulfate, chloride, and nitrate than background. Chloride and nitrate are anthropogenic indicators, consistent with the fact that most development in the watershed is along the river. A portion of the elevated chloride concentrations may be a result of winter road salting; however, the elevated chlorides are found throughout the year indicating most of the impact may be from sources other than roads. Nitrate concentrations follow the trend of increasing TDS down the watershed. Potential sources of nitrate can be either natural (found in the soils), atmospheric (rain or air), or anthropogenic (OWS). Sulfate is mainly derived from mineralized rocks and mine tailings that are found in portions of Summit County including French Gulch and along Tenmile Creek. Elevated sulfate content is coupled with somewhat lower pH values and elevated trace metals such as manganese, molybdenum, strontium, tin, and zinc—a definite indicator of sulfide ore rock interaction. The similarity of the surface samples near the well and MW2 water chemistry indicates that they are hydraulically connected.

Group 3 samples ($n=25$) are from the Frisco Terrace area and include surface water samples from Tenmile Creek and groundwater samples from MW3. These samples have much higher TDS, significantly elevated sulfate, and higher chloride, fluoride, and nitrate concentrations (Figure 2-8). The chemistry is interpreted as a combination of local anthropogenic input and upstream mine tailings influence. The similarity of the water chemistry between surface water and samples from MW3 indicates that the surface water and groundwater are hydraulically connected. The four samples from MW4 have higher nitrate. This well is located near MW3, but is closer to the center of the Frisco Terrace development. The chemical difference indicates that the groundwater in MW4 may not be as well connected to the local surface water system, allowing more influence from the higher home density.

Groundwater: Conclusions

The water quality in the study area varied in a predictable and systematic fashion over the drainage area. Fingerprint analysis showed chemical signatures of the natural water in a mountain drainage, but reveal increasing impact near the bottom of the watershed. This deduction is supported by increasing trends in nutrients and supporting parameters moving down the watershed. As the surface water moved through populated areas, the chemistry acquired an anthropogenic signature that consisted of elevated chloride and nitrate. In addition, there was a chemical signature of elevated sulfate associated with mine tailings drainage.

Three of the four MWs installed in the watershed had chemical signatures identical to the local surface water showing good hydraulic connection between groundwater and surface water. In contrast, MW4 is not as well connected with the local surface water system or perhaps more influenced by the locally higher housing density.

Hydrogeology

Resources for the subsurface characterization of the study area were limited. Therefore, the evaluation was made using publicly available data as well as data collected from four MWs installed by CSM in the study area. Publicly available data consisted of well logs from the Colorado State Engineer's Office (CSEO).

More than 350 well logs were analyzed for this study. These logs revealed that the majority of wells and OWS in Summit County are installed in glacial till. Glacial till is defined as a mixture of clay, silt, sand, gravel, and boulders that range widely in size and shape. Based on the drilling logs, the glacial till in Summit County appears to be primarily coarse-grained. Logs also reveal that there is no discernable watershed-scale confining unit at depths of up to 200 ft below ground surface. This factor indicates that the groundwater and surface water in the watershed have the potential to be connected. If the groundwater and surface water in the watershed are connected, there would be a pathway for OWS effluent to eventually reach surface waters. Average depth of the wells from these logs was 80 ft below ground surface.

CSEO well logs were also used to estimate two parameters for the study area: transmissivity and hydraulic conductivity. Transmissivity (T) can be estimated using the following equation (Razack and Huntley 1991):

$$T = 1140 (SY/dd)^{0.67} \quad \text{Equation 2-1}$$

Where:

T = transmissivity in ft^2/day

SY = sustained yield in gpm

dd = drawdown in ft

This equation enabled a first estimate of T to be made for both the Blue River Estates and Frisco Terrace focus areas. The results of these estimates are provided in Table 2-6. Saturated hydraulic conductivity (K_s) can then be estimated using the following equation:

$$K_s = T/b \quad \text{Equation 2-2}$$

Where:

K_s = hydraulic conductivity

T = transmissivity

b = aquifer thickness

Table 2-6
Transmissivity Estimated From Equation 2-1 Using CSEO Well Log Information

Site Location	Average T	Std. Dev. of T	Geometric Mean of T	Data Range
Pennsylvania Creek	773 ft ² /day (8.3 cm ² /sec)	497 ft ² /day (5.3 cm ² /sec)	647 ft ² /day (6.9 cm ² /sec)	153–2106 ft ² /day (1.6–22.6 cm ² /sec)
Tenmile Creek	585 ft ² /day (6.3 cm ² /sec)	395 ft ² /day (4.2 cm ² /sec)	416 ft ² /day (4.5 cm ² /sec)	41–1403 ft ² /day (0.44–15.1 cm ² /sec)

The results of the hydraulic conductivity estimates can be found in Table 2-7.

The estimated K_s values are relatively well constrained to within a half order of magnitude. This is a significant improvement over an estimate of K_s based strictly on porous-media type, whereby K_s would vary over at least four orders of magnitude (Fetter 2001). These K_s values are consistent with K_s values expected in coarse glacial material. K_s values in the 10⁻³ range are conducive to relatively fast transport times.

Table 2-7
Hydraulic Conductivity Estimates From Equation 2-2 and CSEO Well Log Information

Site Location	Depth of Aquifer Thickness (ft)	K (cm/sec) From Average T	K (cm/sec) From Geometric Mean of T
Blue River Estates	50 (1524cm)	5.4×10^{-3}	4.6×10^{-3}
Blue River Estates	185 (5639 cm)	1.5×10^{-3}	1.2×10^{-3}
Frisco Terrace	50 (1524 cm)	4.1×10^{-3}	2.9×10^{-3}
Frisco Terrace	165 (5029 cm)	1.3×10^{-3}	8.9×10^{-4}

More detailed subsurface evaluations were focused in two of the three focus areas: Blue River Estates and Frisco Terrace. As described in the Introduction section, a total of four MWs were installed in these areas (Figure 2-2). MW1 and MW2 are in Blue River Estates; MW3 and MW4 are in Frisco Terrace. In addition to soil samples collected during well installations, hydraulic head and water quality data were obtained during routine monitoring.

Soil samples were analyzed and used to make refined estimates of the hydraulic properties of the aquifer. Soil sieve analysis on select samples from the Frisco Terrace and Blue River Estates focus areas were used to determine the effective grain size. From the effective grain size several methods can be used to estimate hydraulic conductivity. These equations include the Breyer Equation, the Modified Hazen Equation, and the Kozeny Equation (Kresic 1997). All three of these equations were used to estimate K_s . Table 2-8 presents the geometric mean K_s values calculated for each of the three methods at each focus area. These K_s values are an order of magnitude larger than the K_s values estimated using the engineer's well logs (Table 2-7). Both methods suggest the K_s at Blue River Estates is somewhat higher than at Frisco Terrace.

Table 2-8
Hydraulic Conductivity as Estimated From Grain Size Analysis Data by Three Methods

Site Location	Breyer (cm/s)	Hazen K (cm/s)	Kozeny K (cm/s)
Blue River Estates	9.4×10^{-2}	7.6×10^{-2}	4.1×10^{-2}
Frisco Terrace	5.5×10^{-2}	5.8×10^{-2}	3.1×10^{-2}

Hydraulic head data were collected in each groundwater MW for a period of one year. These data are shown for each focus area on Figure 2-9 and Figure 2-10 along with estimated head values of nearby surface water monitoring sites. An important fact to keep in mind is that stream heads are estimated from the elevation of the surface water site and that measured groundwater heads were observed during a drought year. Also note that the head of surface water sites is the elevation of the sample site taken from topographic maps. This value is only an estimate of stream head, as true stream head has the potential to fluctuate several feet or more. These fluctuations can be within the course of a day (such as during a storm event), or seasonally (such as during spring runoff or winter freeze).

Figure 2-9 shows that, in the Frisco Terrace focus area, the hydraulic heads at MW3 and MW4 are somewhat greater than the estimated head of the nearby downgradient stream water (FT2) but less than the estimated head of the upstream stream water (FT1). For this system, it is difficult to tell whether groundwater discharges to the stream or the stream discharges to groundwater, which in turn makes it difficult to determine the nature of regional groundwater flow. However, the head in MW4, which is closer to Tenmile Creek (Figure 2-2), is higher than the head in MW3 (Figure 2-9). This factor suggests that during this study the stream may be discharging to the groundwater. However, during wetter years, it is likely that groundwater discharges to the stream in this area. Thus, potential exists for OWS constituents to reach the surface water via groundwater.

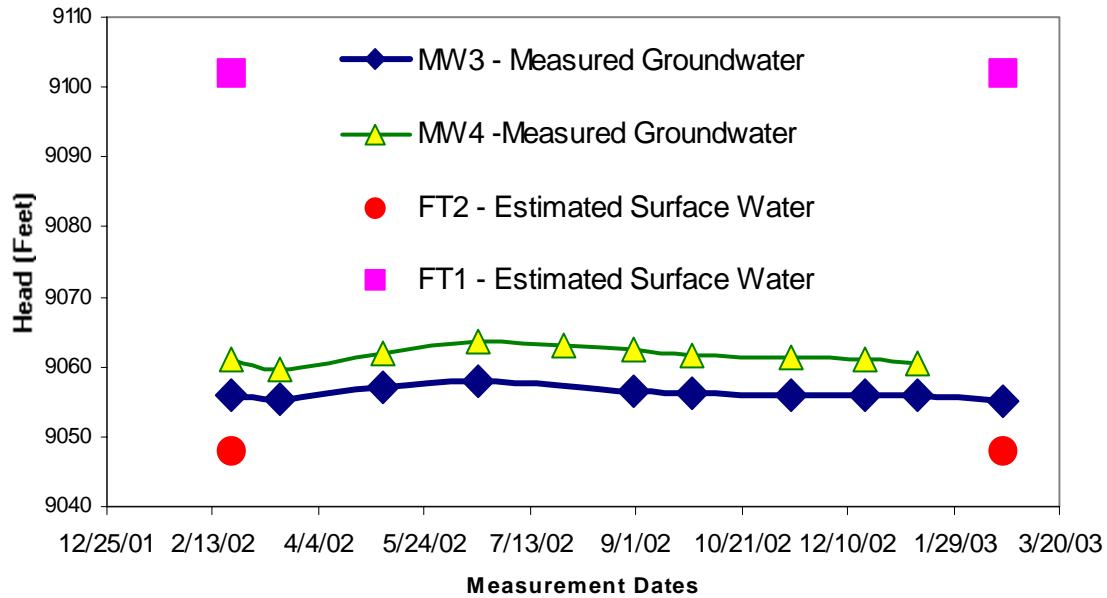


Figure 2-9
Hydraulic Head for Groundwater and Surface Water in the Frisco Terrace Focus Area

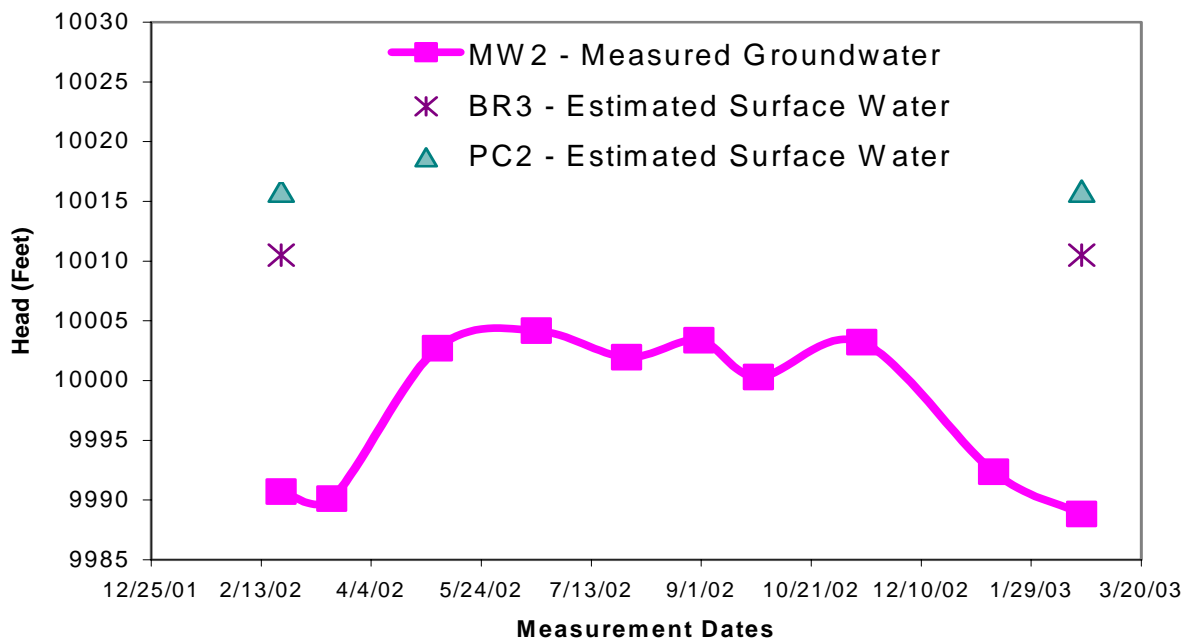


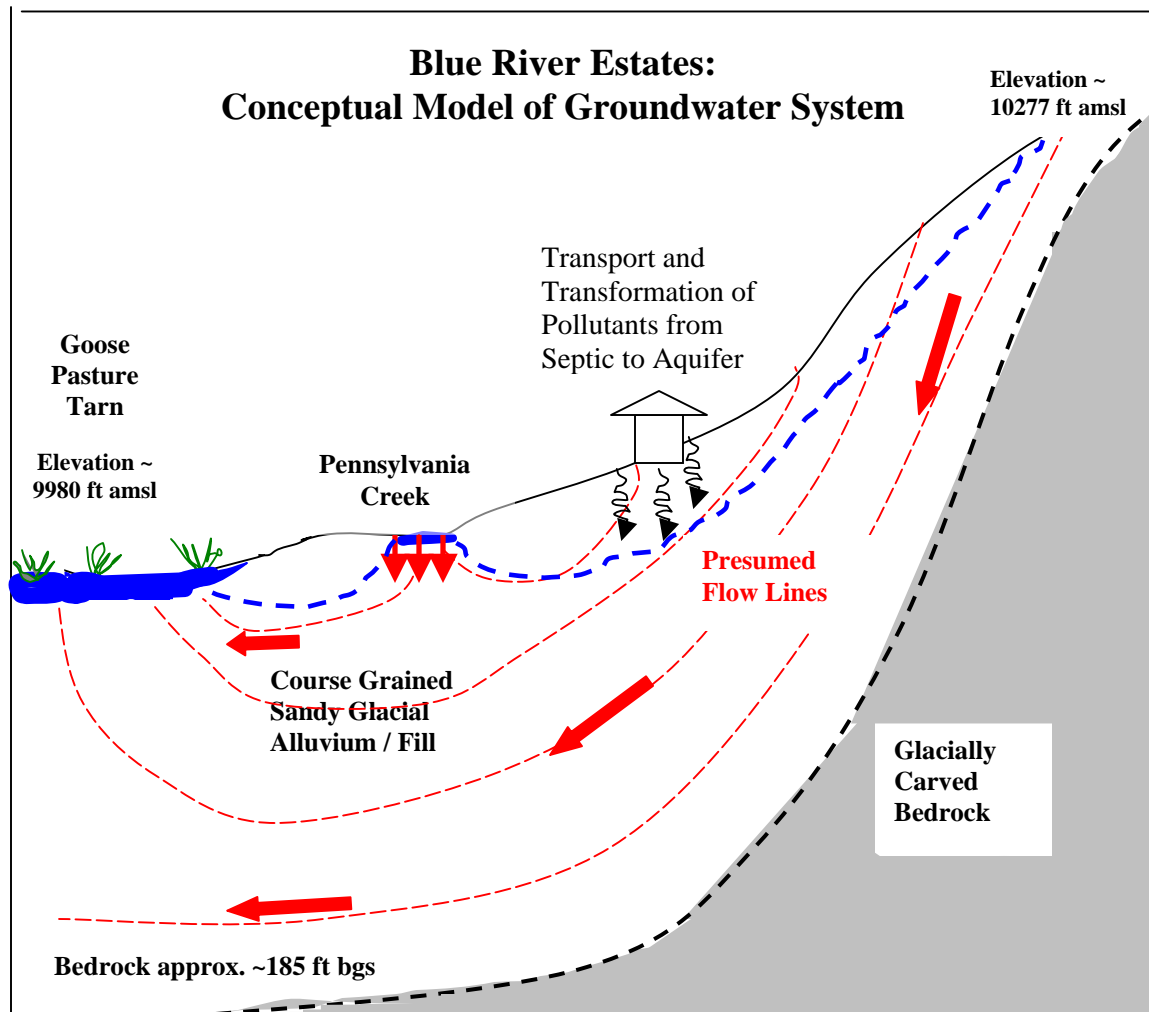
Figure 2-10
Hydraulic Head for Groundwater and Surface Water in the Blue River Estates Focus Area

Hydraulic head information, used to determine the potentiometric surface in the area, indicates that the potentiometric surface is relatively flat in Frisco Terrace. Hydraulic gradient cannot be calculated from two MW points; however it is possible to estimate the gradient by assuming that the groundwater flows toward the stream at a 45-degree angle resulting in a gradient across Frisco Terrace of approximately 0.01. This estimate can be coupled with estimates of K_s and an assumed porosity of 0.3 to hypothesize that a pollutant may travel several feet per year in this area.

The information presented in the previous section indicates that it is difficult to obtain a clear picture of the hydrogeology of the Frisco Terrace focus area from the available data. Furthermore, flow patterns are likely to be complex due to the close proximity of Dillon Reservoir, steep hills and mountains that could facilitate local recharge, and a city setting where discontinuous pavement can also cause local recharge. However, the hydraulic head information and the chemical fingerprint information (see the Groundwater: Fingerprint Analysis section) indicate that the groundwater and surface water in this area have the potential to be hydraulically connected. This area has the potential to affect nearby surface waters, though travel times are slow in comparison to other areas of the watershed (such as Blue River Estates).

MW1 is situated in the upper portion of the Blue River Estates focus area, and MW2 is situated much lower in the Blue River Estates focus area near the confluence of Pennsylvania Creek with the Blue River (Figure 2-2). Groundwater at MW1 is much higher than groundwater at MW2, showing that groundwater in Blue River Estates is moving as expected from higher to lower elevations towards the Blue River valley. There are two surface water sites near MW2: PC2 and BR3. Hydraulic head measurements over one year during this study (a drought year) indicated that groundwater at MW2 is somewhat lower than surface water in PC2 (Figure 2-10). Further investigation during the summer of 2003 using a known reference elevation and a brunton compass (accuracy to approximately 0.5-in.) also indicated the groundwater surface is lower than PC2 and somewhat lower than BR3. This suggests that Pennsylvania Creek near the confluence with the Blue River is a losing stream and that the Blue River at BR3 is also a losing stream segment. Therefore, groundwater discharge likely occurs within the next quarter of a mile of the river system in the Goose Pasture Tarn wetlands (Figure 2-11), which would concur with water quality data that indicates a small increase in various wastewater constituents between BR3 and BR4 (see the Water Quality section).

The hydraulic gradient of the groundwater beneath Blue River Estates is estimated to be 0.1. As with Frisco Terrace, this estimate was coupled with estimates of K and an assumed porosity of 0.3 to hypothesize travel times of several feet per day in the Blue River Estates area. Note that this travel time is much faster than the estimates of several feet per year in the Frisco Terrace area, indicating that groundwater pollutants would travel much faster in the Blue River Estates compared to the Frisco Terrace focus areas. This difference is primarily due to the higher gradient in the Blue River Estates. The faster travel time indicates that the Blue River Estates area may be more susceptible to OWS impacts as effluent in this area would have less contact time with soil in the saturated zone resulting in less time for treatment of OWS pollutants.



Note: Not to scale.

Figure 2-11
Cross Sectional Conceptual Model of the Groundwater System at Blue River Estates Focus Area

The potential discharge of groundwater in the Blue River Estates focus area to the Goose Pasture Tarn wetlands is thought to be indicative of the nature of the study area for the remaining downstream portions of the watershed. That is to say that portions of the Blue River are likely gaining and portions are likely losing, but the Blue River is still ultimately the source for groundwater discharge. Further evidence is found in the fact that Blue River Estates is representative of the remainder of the Blue River watershed upstream of Dillon Reservoir: a high mountain valley with steep inclines on either side of the Blue River valley. If the Blue River is the ultimate location of groundwater discharge (including any OWS effluent present), then it is important to remember that the Blue River flows into Dillon Reservoir.

Implications To This Study

The intent of this chapter is to present an overall picture of the study area as well as to emphasize the appropriateness of this watershed for a study such as the one presented in this report. The Dillon Reservoir watershed is a sensitive, alpine watershed for which there is great interest in maintaining water quality. However, there are many features in the watershed that have the potential to impact water quality including the use of OWS. Furthermore, geology and water quality analysis indicate that the surface and groundwater systems are hydraulically connected. This connection is supported by the hydrogeology of the area that indicates that, though some stretches of streams may be gaining and others losing, the ultimate destination of groundwater (and thus OWS effluent) is likely the streams that ultimately flow into Dillon Reservoir. Therefore, the environmental setting of Summit County presents a suitable location for a study investigating the watershed-scale effects of OWS on the environment. This hydrogeologic characterization confirms the importance of the other assessment activities in the Blue River portion of the watershed, including WARMF modeling activities.



3 INTRODUCTION TO THE WATERSHED ANALYSIS RISK MANAGEMENT FRAMEWORK (WARMF) MODEL

Modeling tools can provide useful information for assessing the impact of onsite wastewater systems (OWS) on a watershed-scale. The linkage between OWS discharge and water quality of the receiving waters can provide a useful means to calculate the total maximum daily loads (TMDL) of OWS that can be discharged without violating the water quality criteria of the receiving waters. Modeling tools can also be used to evaluate the effect of phasing out OWS and replacing them with a centralized sewer system.

The complexity and functionality of various models may range from simple mass balance methods, to semi-quantitative geographic information system (GIS)-mapping methods, to more complex mathematical models and decision-support systems (US EPA 1997 and McCray *et al.* 2000). Kirkland 2001 provides a thorough discussion on watershed-scale assessment methods and provides an extensive table of available models.

Mass Balance Methods

Mass balance assessment methods can include simple back-of-the envelope calculations or spreadsheet tools developed using hydrology or water-quality transport equations. Although useful for quick answers and available at a relatively low cost to implement, these tools require numerous simplifying assumptions and parameter estimations. Examples of simple mass balance assessment tools include TOXROUTE and STREAMDO.

GIS-Mapping-Based Methods

The next category of tools includes GIS-mapping-based assessment methods. These tools often provide a link between simple mass-balance models and large databases. Many GIS-mapping methods produce maps highlighting the sensitive and vulnerable regions of a watershed with respect to water quantity and quality. Stakeholders and decision makers often find the mapping information interesting, but lacking in quantitative information about the impacts of OWS on the receiving waters. As part of this project, the GIS-mapping tool MANAGE was applied to the Blue River watershed (see Chapter 6, *Additional Models Applied* and Appendix H, *Watershed Modeling Using MANAGE*).

The need for a watershed-scale model that considers OWS loading was demonstrated in a US EPA Chesapeake Bay Study. A goal of a 40% nitrogen and phosphorus load reduction required an accurate assessment of specific sources of nutrient loading to groundwater, surface water, and Chesapeake Bay. For the study, US EPA used the Hydrologic Simulation Program Fortran (HSPF) as the watershed scale model (Linker *et al.* 1999). Because HSPF does not explicitly model OWS, it required an externally calculated “edge-of-drainfield loading” of OWS.

US EPA developed a GIS-based method to estimate the “edge-of-drainfield load” of nitrogen (Maizel *et al.* 1997). In HSPF, this load was deposited directly to river segments. Census Block Group data was used to determine the number of occupied housing units in the watershed, and the distribution between urban (70.9%), rural (26.4%), and farm (0.6%). The nitrogen load from OWS was estimated assuming 25% of housing units used OWS, 2.6 persons per household, and an average nitrogen OWS loading of 9.35 lbs/capita/year. No allowance was made for loss to denitrification, and phosphorus was assumed to be adsorbed completely by the soil. This GIS-based method is strictly a method of estimation. Because the calculations are based on assumptions, there is no way to calibrate or verify the calculations. Recommendations of this study included an integration of source loadings with water resources to determine direct and off-site impacts of septic effluent. Therefore, estimation of the “edge-of-drainfield load” is problematic and a watershed-scale model that incorporates OWS directly is more desirable.

Mathematical Models

Mathematical models are more complex tools based on a set of differential equations that describe physical processes. In general, these models are more rigorous, physically based, and provide a dynamic simulation of the system. Most research in OWS has been empirical in nature. Much knowledge has been accumulated. The time has come to advance empirical observations into theory of processes involved and incorporate them into a watershed model. Such a model can track the fate of all OWS discharges through soil to the receiving waters of a river basin. The model can calculate the nonpoint source loads of OWS that reach the surface waters. The model can also predict the water quality of the receiving waters due to the combined effect of all point and nonpoint source loads, including those contributed by OWS.

One goal of this project was to develop a watershed scale model based on the findings of OWS research. Model calculations should be based on scientific principles. The model should accept the basic data of households served by OWS, number of people per household, characteristics of septic tank effluent (STE), meteorology, and other data sources, all of which are readily available. The model should calculate the “edge-of-drainfield pollution loads,” rather than requiring them as input. In addition, the model should predict flow and water quality concentrations that can be verified by observed data. Such a model can be incorporated into a decision-support system that provides information in the form of decision road maps, GIS displays, risk assessment evaluations, and cost benefit analyses all driven by an underlying mathematical model.

Ideally, an existing watershed model could be enhanced to incorporate OWS discharges. WARMF was selected for that purpose. WARMF is a physically-based model that simulates flow and water quality of groundwater in soil layers.

This physically-based formulation was extremely beneficial because OWS loading could be explicitly modeled based on available physical data. Many other models use a mass export coefficient method to account for subsurface loading. This purely empirical method is less flexible when there is a need to model a new loading process. Because it is physically based rather than empirically based, WARMF is more transferable to other watersheds that may have different climate, soils, or population density conditions. Also, WARMF is a decision-support system, not just a model. Scenarios are easily set up in WARMF and the graphical user interface makes it easy to compare multiple scenarios. WARMF is designed to accommodate stakeholders' needs for long-term planning and assessment of watershed cumulative impacts.

WARMF Model Overview

WARMF is a decision-support system designed to support the watershed approach involving stakeholders (Chen *et al.* 2001b; Herr *et al.* 2000). WARMF guides stakeholders to develop and evaluate water quality management alternatives for a watershed. The system takes them through a series of steps and presents them with information in a logical manner so that they can understand their watershed and make informed decisions. WARMF also provides a procedure to calculate the TMDL of a pollutant that can be discharged to a water body without violating the water quality criteria for its designated uses.

WARMF has five modules (Data, Engineering, Knowledge, TMDL and Consensus) integrated by a Windows-based graphical user interface (GUI) (Figure 3-1). The modules work together and support each other.

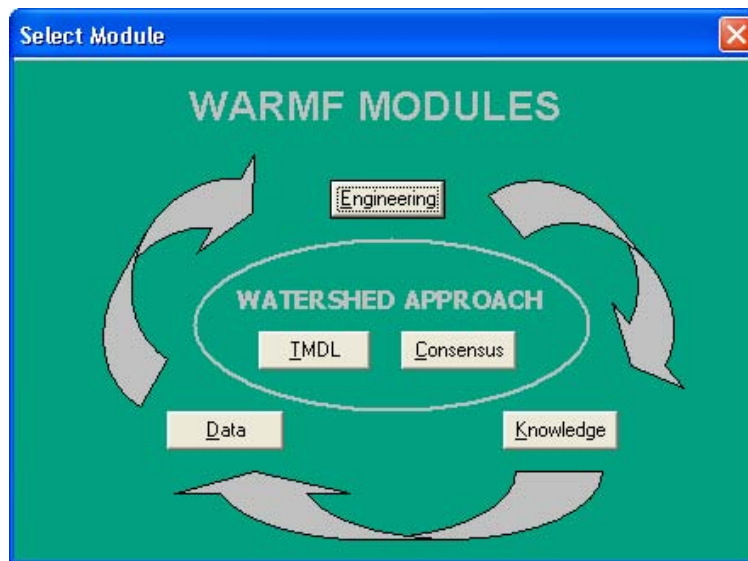


Figure 3-1
The Five Modules of WARMF

The Engineering module is a dynamic watershed simulation model that calculates daily runoff, groundwater flow and quality, hydrology and water quality of river segments, and stratified reservoirs. The Data module contains meteorology, air quality, point source, reservoir release, and flow diversion data. The Knowledge module contains reference information about legal constraints. The TMDL module is a decision module that provides a step-by-step procedure to calculate TMDLs. The Consensus module is a decision module that guides stakeholders in selecting an acceptable TMDL considering economic, social, and political factors.

Figure 3-2 shows the seven-step road map of the Consensus module. Several publications have documented the decision-support capabilities of WARMF (Chen *et al.* 1997; Chen *et al.* 1999; Chen *et al.* 2000; Weintraub *et al.* 2001; and Herr *et al.* 2002).

The five modules of WARMF are integrated by a GUI. The GUI not only provides menus for the user to issue commands, but also automatically furnishes data to the models and stores output for display in color-coded GIS maps, bar charts, and spreadsheets.

Consensus Road Map			
Module	Scenario		
1. Stakeholders	List		Organization
2. Work Plan	Mission		Tasks & Schedule
3. Water Quality Issues	Designated Use		Criteria
4. Learning Process	Simulate	Loading	Water Quality
5. Management Alternatives	<div> Scenario: Base052903 Describe </div> <div> Edit... Point Sources </div>		
6. Analysis	Cost / Benefit		Cost Sharing
7. Resolution	Pros & Cons		Consensus?

Figure 3-2
Consensus Module Road Map in WARMF

Model Description

The Engineering module of WARMF contains a dynamic watershed simulation model that calculates daily surface runoff, groundwater flow and quality, non-point source loads, hydrology, and water quality of river segments and stratified reservoirs.

The Data module furnishes input data including meteorology, air quality, point source load, reservoir releases, and flow diversions. The Data module also contains observed flow and water quality data.

Hydrologic Network

To facilitate the simulation, the watershed is divided into a network of land catchments, river segments, and reservoir layers. Land catchments are further divided into land-surface and soil layers. These watershed compartments (that is, soil layer, river segment, or lake layer) are seamlessly connected to form a network for hydrologic and water quality simulations.

WARMF assumes uniform characteristics for each watershed compartment. The characteristics can vary from one compartment to the next. Each compartment is treated as a continuously stirred tank reactor (CSTR) in which various physical, chemical, and biological processes can occur.

Figure 3-3 shows a schematic representation of a catchment in WARMF containing land surface and soil layer compartments. The land surface is characterized its by land uses and cover, which may include forested areas, agriculture lands, urbanized cities, and other land uses and cover. The soil layers consist of solid, liquid, and gaseous fractions. Up to four soil layers can be modeled in a watershed application of WARMF.

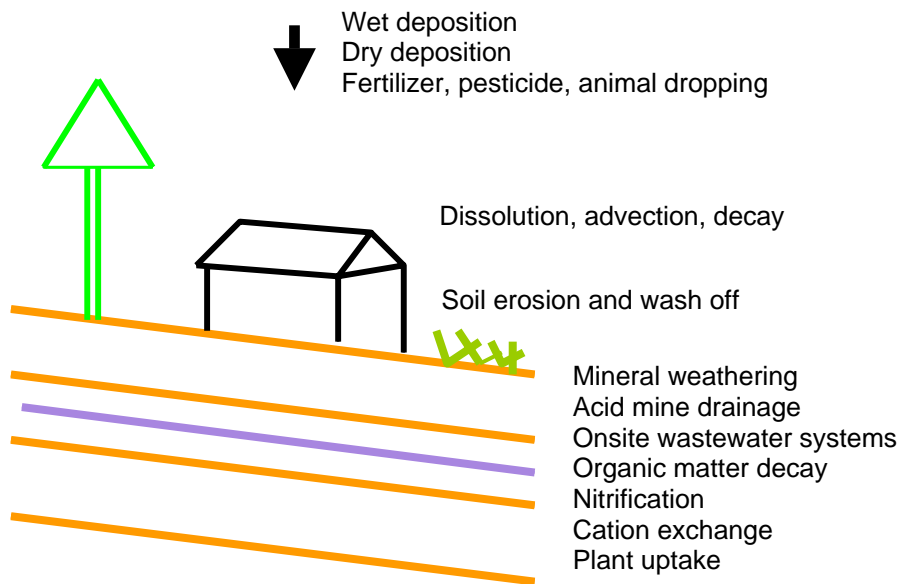


Figure 3-3
Definition Sketch of Land Catchment for WARMF

Rainfall and snowmelt water infiltrates through the land surface as a function of the percent pervious area of land surface and the infiltration capacity of the soil layer below. For impervious areas, precipitation on the land surface does not infiltrate and instead becomes overland flow. For pervious areas, the infiltration capacity of the soil is calculated as a function of soil moisture content and vertical conductivity. As water percolates from one layer down to the next, a water balance is performed to track the change of soil moisture in each layer. Lateral flow occurs when a soil layer becomes saturated. When the infiltration rate of water is higher than the lateral flow, the saturated zone may rise to the surface and initiate surface runoff.

Hydrology Simulation

Daily precipitation, which includes rainfall or snow, is deposited on the land catchments. WARMF performs daily simulations of snow and soil hydrology to calculate surface runoff and groundwater accretion to river segments. The water is then routed from one river segment to the next downstream river segment until it reaches the terminus of the watershed. The flow and associated loads of point source discharges are added to the appropriate receiving waters (river or lake segment).

Nonpoint Sources Load

Nonpoint sources of pollution can contribute significant pollutant loads to a waterbody. Sources of nonpoint loads other than OWS include trash, pet droppings, and lawn fertilizer carried with storm water in urban areas, fertilizer running off agricultural lands, livestock droppings on pasture land, and air deposition on land. Fertilizer and pesticide application, trash, and animal droppings are deposited onto the land surface. Air pollutants are deposited onto the foliage canopy. During precipitation events, the pollutants accumulated on the canopy are washed down to the land surface as throughfall. As water reaches the land surface, the pollutants accumulated on the land surface are dissolved. The resulting pollutant concentrations are assigned to the infiltrating groundwater and to the surface runoff. As surface runoff flows to a nearby river segment it may also erode soil particles and carry adsorbed nutrients and minerals to the river. Thus, WARMF accounts for nonpoint source load associated with surface runoff. Storm water is accounted for in WARMF as part of the surface runoff and associated dissolved pollutants from impervious urban areas.

In addition to overland flow, processes below the land surface contribute to the pollutant loadings. Solid phase minerals are weathered to release cations and anions. Litter is decomposed into humus to release its constituent cations and anions. Ammonia is nitrified to nitrate. Cations and anions are removed by tree and crop uptake. The percolating water dissolves the cations and anions into soil solution and subjects the cations to competitive exchange with the cation exchange sites of the soil particles. When the percolating water reaches the saturated zone, the flow becomes lateral. The lateral flow discharges groundwater and its chemical constituents to the river segment, which accounts for nonpoint source loads of groundwater accretion.

Point Source Load

WARMF accepts point source load as input data (WWTP discharge). The input file, one for each point source discharge, contains the time series of daily flow and pollutant loads for various constituents. Point source data can vary on a daily basis and do not need to be specified at equal time intervals.

The model uses a step function approach, in which the discharge values at one time remain the same until the values for the next time become available. If a yearly value is provided in the input file, the model will discharge the same amount every day for that year. If monthly values are provided, the model will change the daily discharge month by month. Likewise, if daily values are provided in the input file, the model will change the daily discharge day by day.

Water Quality Simulation

Heat budget and mass balance calculations are performed to calculate the temperature and concentrations of various constituents in each river segment and lake layer. The mass balance and heat budget equations account for advection, sinks, and sources, and are similar to equations used in the well-known QUAL2E model. The main difference is that QUAL2E is a steady-state model and WARMF is a dynamic model. With a steady-state model, the flow is assumed to be constant for a given time period and the water volume of the river segment does not change with time. A dynamic model accounts for the changes in flow and water volume each day, similar to daily changes in an actual system.

Sources of Algorithms

The algorithms of WARMF were derived from many well-established codes. The main computational engine of WARMF was adapted from the Integrated Lake-Watershed Acidification Study (ILWAS) model (Chen *et al.* 1983; Gherini *et al.* 1985). Algorithms for snow hydrology, groundwater hydrology, river hydrology, lake hydrodynamics, and mass balance for acid base chemistry were based on the ILWAS model. Algorithms for erosion, deposition, re-suspension, and transport of sediment were adapted from ANSWERS (Beasley *et al.* 1980; Beasley and Huggins 1991). Pollutant accumulation on the land surface was adapted from the Storm Water Management Model (SWMM) (Chen and Shubinski 1971; Huber and Dickinson 1988; US EPA 1992). In WARMF, instead of using export coefficients as in SWMM, an algorithm for mixing and washoff is used to simulate the processes that generate nonpoint source loading. The first order decay of coliform bacteria and biochemical oxygen demand (BOD) and its impact on dissolved oxygen follow traditional water quality models. The sediment sorption-desorption of pesticides and phosphorus and the kinetics of nutrients and algal dynamics were adapted from WASP5 (Ambrose *et al.* 1991). Periphyton algorithms were adapted from the Dynamic Stream Simulation and Assessment Model with temperature (DSSAMt) (Caupp *et al.* 1998). A complete description of the WARMF formulations can be found in the WARMF technical documentation report (Chen *et al.* 2001b).

WARMF Applications

WARMF has been applied to several watersheds in the US (Figure 3-4). In the Catawba River watershed (NC and SC), WARMF has been used for nutrient, fecal coliform bacteria, sediment, and copper TMDLs. WARMF has also been used for reservoir tailwater evaluation and cumulative impact analysis. The Truckee River (CA and NV) application of WARMF is providing nonpoint source loading estimates under current and future conditions to help drive TMDL and environmental impact statement analysis using several river water-quality models. WARMF was used to calculate an acid mine drainage TMDL for the Cheat River (WV) and nutrient, sediment, and metals TMDLs for Chartiers Creek (PA). A sediment TMDL was calculated using WARMF for Oostanaula Creek (TN), and a comparison between WARMF and HSPF flow simulation was completed for the Mica Creek (ID). An application of WARMF to the Santa Clara watershed (CA) was used to calculate nutrient TMDLs. The focus of an application to the St. Louis River (MN) is to investigate a fate and transport of mercury.

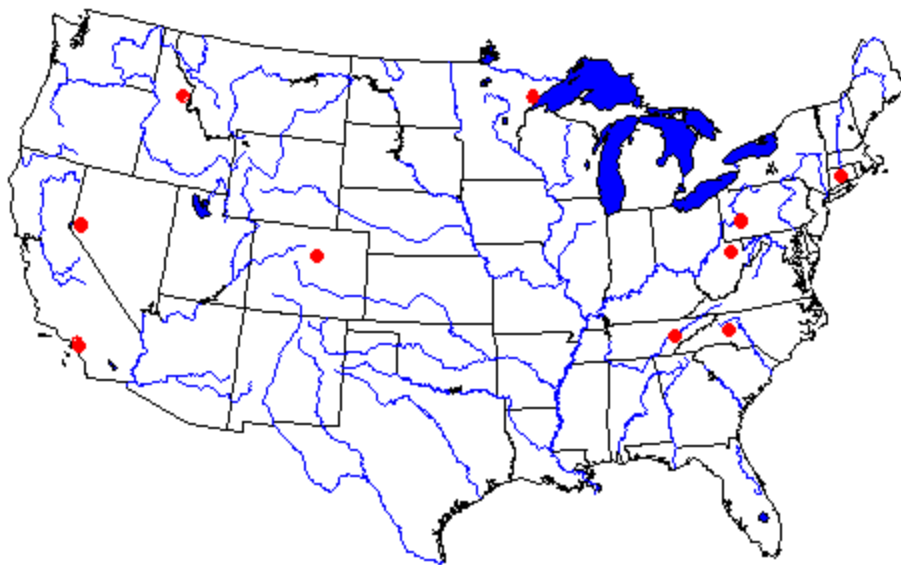


Figure 3-4
Map Showing Locations of WARMF Watershed Applications

Modifications for OWS: Biozone Algorithm

For this project, WARMF was enhanced to model the loading of OWS to the soil. An initial model test was performed by modifying the original code of WARMF to accept and apply the OWS effluents to the top layer of soil (Figure 3-3). The original algorithm was used to simulate groundwater quality. Thus, ammonia was retained by the soil through competitive cation exchange and was nitrified according to a kinetic rate coefficient. Phosphorus was adsorbed to soil according to a linear adsorption isotherm.

The results showed that the model was able to track the transport and fate of nutrients through the subsurface to the surface waters. However, the nitrification rate had to be increased substantially over the typical value normally used in the simulation of forested watersheds, where nitrogen was typically limiting (Chen *et al.* 2001a). The research conducted in this study clearly showed that OWS effluents created a biozone to adsorb pollutants for accelerated nitrification and pathogen deactivation. Model enhancements were made to add the biozone algorithm to process the OWS effluents before releasing them to the soil (Weintraub *et al.* 2002).

The biozone algorithm simulates the growth of bacteria biomass in the top 2 cm of soil that receives STE. The bacteria biomass acts like a sponge to adsorb water that contains ammonia, pathogens and other pollutants. The process accelerates the ammonia nitrification and pathogen deactivation. It also leads to the gradual build up of plaque (dead bacteria and solid residue), which reduces infiltration. Over time, infiltration capacity can decline and under some conditions, a hydraulic failure can occur. Under such conditions, WARMF will simulate surface seepage of STE co-mingled with precipitation and spread it across the surface of a land catchment. The stored effluent can then infiltrate into soil in the areas without the biozone. It can also be water for surface runoff. Details of the biozone algorithm are discussed in Chapter 4, *Biozone Algorithm*.

Necessary Input Parameters

The application of WARMF to a specific watershed requires digital elevation model (DEM) data to set up the network of catchments, river segments, and stratified reservoirs. It also requires land use shapefile to describe the characteristics of the land surface and soil data to describe the surface as well as subsurface soil properties. It needs meteorological data to drive the model and observed stream flow and water quality data to verify the results.

With enhancements to simulate the water quality impacts of OWS, the model requires input data to characterize OWS. Table 3-1 summarizes data for OWS, including the source of data for the Dillon Reservoir watershed application and chapter number where a full discussion on that data can be found.

Table 3-1
OWS-Related Data Required by WARMF

Data Type	Source	Location in Report
OWS spatial distribution in watershed	GIS Data, Summit County	Chapter 5, OWS Characterization section
Typical STE flows	Literature review	Appendix A
Typical STE water quality	Literature review	Appendix A
Soil reaction rates	Literature review	Appendix A
Phosphorus adsorption rates	Literature review	Appendix A

Table 3-1
OWS-Related Data Required by WARMF (Cont.)

Data Type	Source	Location in Report
Calibration data for biozone algorithm	Laboratory experiments	Appendix C
In-stream water quality	Field data collection	Appendix E
Groundwater characterization	Field data collection	Appendix E



4 BIOZONE ALGORITHM

WARMF was enhanced to model the processes occurring in the biogeochemically-active biozone of an OWS before releasing its effluent to the subsurface. The work included:

1. Developing algorithms to represent the hydrologic and biogeochemical processes of a biozone
2. Testing and calibrating the biozone module with data collected in column experiments
3. Incorporating the biozone module into a watershed-scale model (WARMF)
4. Testing it under field conditions.

This chapter describes the first two tasks: development and testing of the biozone algorithm.

Description of the Biozone

A biozone layer is usually formed within the soil at and below the infiltrative surface. This zone is created by the buildup of bacteria biomass, which enhances sorption, nitrification, biological decay, and bacterial die-off. The biozone is a dynamic region that includes a clogging zone where permeability loss occurs (often within the initial 0 to 2 cm of soil) and hydraulic effects can be pronounced. The biozone also includes a biochemically-active treatment zone (often in the top 10 to 15 cm) where physical and biological processes can contribute to substantial pollutant transformation and removal. A well-developed biozone is often saturated and anoxic/anaerobic near the infiltrative surface with a transition to an unsaturated and aerobic condition within 10 to 15 cm below the infiltrative surface in most soils. The biozone is represented as a small control volume that accepts septic tank effluent (STE). The flow and quality of STE are modified as it passes through the biozone and then into the unsaturated soil layers below.

Motivation

Early in the project, WARMF was initially set up to simulate OWS on a watershed scale without taking into account a separate control volume for the biozone (Chen *et al.* 2001a). In these exercises, use of a very high nitrification rate in the soil layers was necessary to achieve a good result. For WARMF to be more robust, including the biozone as an independent control volume was deemed necessary. The biogeochemically-active biozone provides a high nitrification rate so that the nitrification rate coefficient of the underlying soil layers can be returned to normal values.

With a biozone algorithm, WARMF can simulate the build up of plaque (dead bacteria and solid residue), which in time can cause loss in infiltration capacity and under some conditions, a hydraulic failure of OWS. The capability to predict the hydraulic failure of OWS was thought to be an important added feature of WARMF.

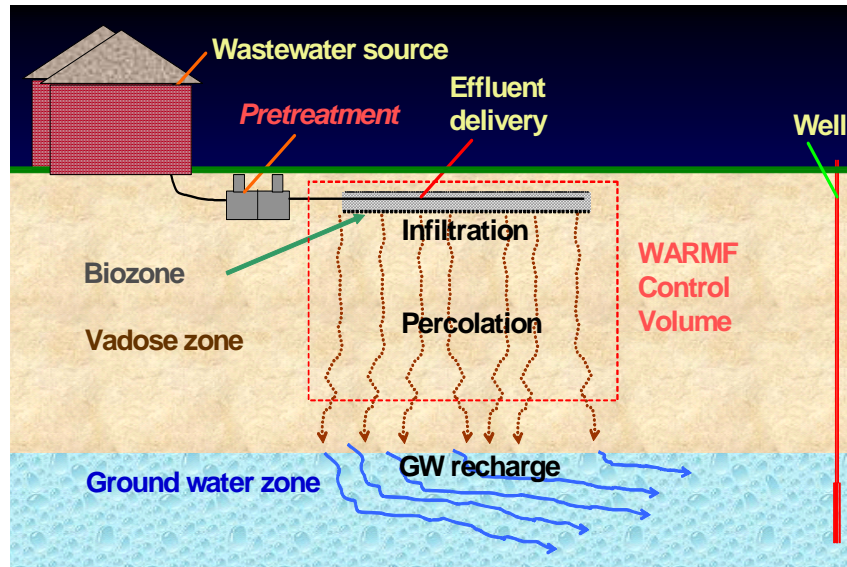


Figure 4-1
Schematic Showing the Biozone Location in an OWS

Another motivation for the development of the biozone algorithm also came from earlier work, in which the steady-state model, HYDRUS 2-D, was used to simulate the hydraulic behavior of a WSAS for site-scale modeling (Appendix F, *Site-Scale Modeling Using HYDRUS 2-D*). HYDRUS 2-D assumed a constant hydraulic conductivity. This assumption was found to be limiting, which pointed out the need for a dynamic model to account for the changing hydraulic conductivity of the biozone.

From a research standpoint, the behaviors of OWS have empirically been observed and documented. To advance our knowledge of OWS operation and performance, translating the empirical observations into quantitative theories is desirable. These theories, expressed in terms of equations for various physical, chemical, and biological processes within a biozone, can be incorporated into a mathematical model to test their validity with observed data.

Theory and Formulation of Biozone Algorithm

The biozone algorithm was first developed in a stand-alone module. After calibration and testing, the module was incorporated into WARMF. The development of the biozone algorithm was based on a conceptual model of how a biozone develops and functions as determined through laboratory and field research.

Research has shown that a biozone develops in a WSAS. A theory is that the biozone is formed by the growth of microorganisms feeding on the organic matter (BOD) of STE. The biomass increases the field capacity of the biozone, due to the filamentous material of the live biomass, creating a higher surface area. This higher surface area retains additional water, much like a sponge. As biomass dies off, plaque remains in the pore space. The plaque is composed of only solids material, which takes up space. The plaque does not contain filamentous material like the live biomass. As the plaque builds up, the porosity of the biozone decreases. Over time, the gap between field capacity and porosity becomes narrower, and the infiltration rate through the biozone decreases. If loading of STE is continued, ponding may occur and eventually lead to a hydraulic failure of the OWS.

Further theorized is that the biozone consists of an intense region of biomass accumulation and pore filling near the infiltrative surface (top 2 cm) that affects infiltration rate properties and provides treatment through physical and biological processes, as well as a more extensive zone of biofilm accumulation (initial 10 to 15 cm of soil) that enables pollutant transformation and removal to occur. The live biomass within the entire biozone is the primary force for reactions such as BOD decay, nitrification, and coliform die-off. The rates of such reactions depend on the amount of biomass present in the biozone and as the biozone matures over time, the reaction rates increase.

The equations to represent the above mentioned processes are presented in the following sections.

Buildup of Biomass

The BOD contained in STE promotes the growth and build up of live bacteria biomass at the infiltrative surface. The mass balance equation of live bacteria is:

$$\frac{d(Bio)}{dt} = \alpha \left[\sum Q C_{BOD,in} - \left(\frac{I_p}{\Delta t} \right) C_{BOD} \right] - R_{resp} - R_{mort} - R_{slough} \quad \text{Equation 4-1}$$

where Bio = biomass of live bacteria in biozone, mg
 $C_{BOD,in}$ = BOD concentration in STE, mg/L
 C_{BOD} = BOD concentration in biozone, mg/L
 α = gram biomass / gram BOD in STE, unitless
 Q = the flow rate of STE, cm³/s
 I_p = percolation out of the biozone, cm³
 R_{resp} = respiration of bacteria, mg/s
 R_{mort} = mortality of bacteria, mg/s
 R_{slough} = sloughed off bacteria, mg/s

For each timestep, a portion of the live biomass is removed during respiration and death. The reactions for biomass respiration and mortality are calculated as follows:

$$R_{resp} = \left[\frac{\gamma}{\theta_s Z A} \right] (Bio) \quad \text{Equation 4-2}$$

$$R_{mort} = \left[\frac{\phi}{\theta_s Z A} \right] (Bio) \quad \text{Equation 4-3}$$

where θ_s = saturated moisture content of biozone, unitless

Z = thickness of biozone, usually ~2 cm

A = biozone area, cm²

γ, ϕ = rate coefficients, cm³/s

These empirical equations are scaled by $1 / (\theta_s Z A)$, which is equal to $1 / \text{pore volume}$. This scaling is done so that the reaction rate can be translated from small-scale (laboratory column) to large-scale field conditions without unintended amplification due to a higher mass of biomass.

Biomass can also be sloughed off and removed from the biozone by a high pore velocity of infiltrating water. The mass of sloughed bacteria is calculated as:

$$R_{slough} = \eta v_p^\delta \quad \text{Equation 4-4}$$

where v_p = pore velocity = $\Sigma Q / (A \theta_s)$, cm/s

η = calibration parameter, mg/cm

δ = calibration parameter, unitless

Buildup of Plaque

As the biomass dies, a portion of it is transformed into plaque. Plaque is also built up from total solids contained in the STE. Plaque can also be sloughed off and removed from the biozone by a high pore velocity of infiltrating water. The sloughing formulation is the same as was presented in equation 4.4 for live biomass. The mass balance equation of plaque is:

$$\frac{d(Plaque)}{dt} = R_{mort} + \sigma \sum Q * TS - R_{slough} \quad \text{Equation 4-5}$$

where σ = calibration parameter to convert total solids in STE to plaque, unitless

Q = flow rate of STE, cm³/s

TS = total solids contained in STE, approximately 500 to 600 mg/L

Impacts of Field Capacity, Saturated Moisture, and Hydraulic Conductivity

The field capacity of natural soil is a constant. However, the field capacity of a biozone is dynamic because it is dependent on the amount of live bacteria biomass. As the biomass increases, the filamentous material of the biomass allows the layer to retain additional water, much like a sponge. The field capacity is adjusted for each time step as follows:

$$\theta_{f,t} = \theta_{f,t-1} + \Phi(\theta_{s,t-1} - \theta_{f,t-1})^{\xi} \left[\frac{d(Bio)}{dt} \Delta t \right] (\rho_b ZA)$$
Equation 4-6

where $\theta_{f,t}$ = field capacity at time t , unitless
 $\theta_{f,t-1}$ = field capacity at time $t-1$, unitless
 $\theta_{s,t-1}$ = saturated moisture at time $t-1$, unitless
 Φ, ξ = calibration parameters, unitless
 $d(Bio)/dt$ = live biomass growth rate, mg/s
 Δt = time step of calculation, seconds
 ρ_b = density of biomass, mg/cm³

The saturated moisture content (porosity) of natural soil is usually constant. However, in a biozone, the porosity may change with time due to the build up of plaque from dead bacteria biomass and solid residue. This build up of solids reduces the available pore space:

$$\theta_s = \theta_{sm} - \frac{Plaque}{\rho_p ZA}$$
Equation 4-7

where θ_s = actual saturated moisture content of biozone, unitless
 θ_{sm} = porosity of parent soil with zero plaque, unitless
 $Plaque$ = biomass of dead bacteria and residue, mg
 ρ_p = density of biomass, mg/cm³

The potential percolation through a biozone (I_{P1} , cm³) is controlled by the field capacity, saturated moisture (porosity) and hydraulic conductivity. Assuming homogenous soil conditions within the biozone, potential percolation is calculated as follows:

$$I_{P1} = P_v A \Delta t$$
Equation 4-8

where A = surface area of biozone, cm²
 Δt = time step of model calculation, s
 P_v = hydraulic conductivity, cm/s

The hydraulic conductivity is a function of moisture content in the biozone:

$$P_v = K_v \frac{\theta - \theta_f}{\theta_s - \theta_f} \quad \text{Equation 4-9}$$

where K_v = the intrinsic hydraulic conductivity, cm/s
 θ = moisture content of biozone, unitless
 θ_f = field capacity of biozone, unitless
 θ_s = saturated moisture content of biozone, unitless

The minimum percolation is the free water in the biozone:

$$I_{p2} = (AZ)(\theta - \theta_f) \quad \text{Equation 4-10}$$

The actual percolation through the biozone is the smaller of I_{p1} and I_{p2} , that is:

$$I_p = \min(I_{p1}, I_{p2}) \quad \text{Equation 4-11}$$

For each time step, a water balance is performed to update the moisture content of biozone:

$$\theta_t = \theta_{t-1} + \frac{(Q\Delta t - I_p - E)}{ZA} \quad \text{Equation 4-12}$$

where θ_t = moisture content of biozone at time t , unitless
 θ_{t-1} = moisture content of biozone at time $t-1$, unitless
 Q = STE flow into biozone, cm³/s
 E = evapotranspiration from biozone, cm³

Transformation and Decay Reactions

Transformation and decay of pollutants in a biozone is simulated using a first order reaction:

$$C = C_o e^{-K_i \Delta t} \quad \text{Equation 4-13}$$

where C = concentration in biozone at time t , mg/L
 C_o = concentration in biozone at time $t-1$, mg/L
 K_i = first order reaction rate, 1/day
 t = time, day

Reaction rates for each constituent are calculated as follows:

$$K_i = \left[\frac{K_{l,i}}{\theta_s Z A} \right] (Bio) \quad \text{Equation 4-14}$$

where $K_{l,i}$ = the reaction rate calibration parameter for each constituent i . As with the biomass respiration and mortality, the empirical reaction rates are scaled by $1 / (\theta_s Z A)$, which is equal to $1 / \text{pore volume}$. This scaling is done so that the reaction rate can be translated from small-scale (laboratory column) to large-scale field conditions without unintended amplification due to a much higher mass of biomass. The primary reactions that occur in the biozone are nitrification, denitrification, BOD decay, and fecal coliform bacteria decay.

Phosphorus Adsorption

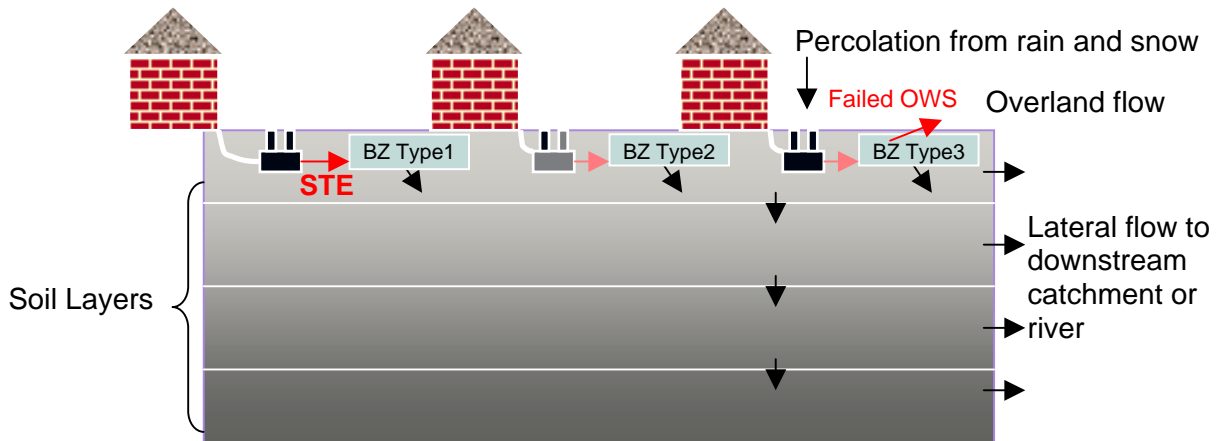
Phosphorus adsorption takes place in the soil media below the biozone. WARMF uses a linear isotherm represented by the equation:

$$S = K_D C \quad \text{Equation 4-15}$$

where S is the mass solute sorbed per unit dry weight of solid (mg/kg), C is the concentration of the solute in solution equilibrium with the mass of solute sorbed onto the solid (mg/L), and K_D is the linear distribution coefficient (L/kg). One limitation of a linear isotherm is that it does not limit the amount of solute that can be sorbed onto the soil. With no upper limit, the soil would have an infinite capacity for phosphorus loading from OWS. To remedy this, a parameter setting the upper limit on phosphorus adsorption sites was introduced into WARMF.

Discharge to Soil Layers

After STE passes through the biozone, it is discharged into the soil layers below. Here, the constituents are subject to additional transport/fate processes as would be expected to occur in natural soils. Figure 4-2 shows the pathways of flow after STE exits the biozone.



Note: WARMF assumes vertical flow between layers. When a layer reaches field capacity or greater, lateral flow will occur. When a layer reaches saturation, excess water will "back up" into the layer above. When all layers are above field capacity, all layers will experience lateral flow.

Figure 4-2
Schematic Showing of Pathways of Subsurface Flow in WARMF

To account for three types of OWS, WARMF was programmed to model up to three different biozones in each land catchment. When the field capacity has reached the level of the saturated moisture content to cause hydraulic failure, the excess STE will be added to detention storage on the catchment surface. After being added to the detention storage, the STE water can percolate through the soil layers if the moisture level is not saturated. If the soil is saturated, the STE water and pollutants, held in detention storage, will become available for surface runoff in the next time step.

Other Assumptions

As with any model development, establishing several model assumptions in order to represent the physical system of a biozone in a modeling framework was necessary. The following assumptions were based on laboratory observation and available knowledge:

- Typical biozone thickness is 2 cm.
- The composition of bacteria biomass is 8% nitrogen and 2% phosphorus by weight.
- The biozone receives a continuous daily loading of STE. Intermittent dosing over the course of one day is not considered.
- When the biozone is clogged and the STE backs up, it is added to the detention storage of the catchment.
- Total solids and TDS concentrations of STE are the same.

Calibration and Testing

The biozone formulations described above include coefficients such as field capacity, saturated moisture content (porosity), and a BOD to live bacteria biomass conversion factor, among others. The field capacity and porosity of typical soils can be estimated from literature values. Other coefficients can be measured scientifically. Several parameters are empirical and their values are estimated and adjusted through a model calibration procedure.

Data from a one-dimensional column experiment were used for verification and calibration (Appendix C, *Biozone Development and WSAS Performance: Column Studies*). This column experiment compressed the time scale of observation by accelerated loading of STE (Siegrist *et al.* 2002). This section describes set up of the model to simulate the laboratory conditions under the controlled experiment allowing the rate coefficients for various biozone processes to be established. Subsequent calibration will be made for field data being collected at Mines Park (Appendix D, *Biozone Genesis and WSAS Performance: Field 3-D Test Cells*).

Column Study Data

Sixteen experimental data sets were obtained from Colorado School of Mines (CSM). The experiments were conducted by applying STE to sand columns under accelerated loading conditions (5 to 30 times the typical design application rate). Results were provided for replicate columns dosed under four loading regimes for 138 days (Siegrist *et al.* 2002).

Table 4-1 summarizes the daily hydraulic loading rates for each data set. Although columns 3 and 4 were set up for intermittent dosing conditions (four doses per day), their average dosing rates were used for model testing. For each loading rate, columns A and B were set up with a gravel-free infiltrative surface whereas columns C and D included a washed gravel layer at the infiltrative surface. Columns A and B were used for model comparison.

Table 4-1
Experimental Dosing Rates

Column	Design Loading Rate
1 (A,B)	35.36 L/d
2 (A,B)	17.68 L/d
3 (A,B)	8.84 L/d
4 (A,B)	4.42 L/d

To alleviate severe anoxic conditions observed in the columns after two weeks of operation, aeration holes were drilled in the column sidewalls. The anoxic condition likely contributed to the severe outlier data points measured for several columns on day 13. Therefore, data points for day 13 were omitted from the data set for model comparison. Appendix C, *Biozone Development and WSAS Performance: Column Studies* provides more details on the one-dimensional column laboratory studies.

In the experiments, columns were loaded with STE from a nearby multi-family housing unit. The STE quality used in the calibration runs was representative of the effluent applied during the laboratory experiments. Table 4-2 summarizes the water quality of STE used for calibration.

Table 4-2
Water Quality of STE Used for Simulation Runs

Parameter	Concentration, mg/L
BOD ₅	181
Total suspended solids*	126.5
Ammonia (as NH ₄ -N)	65
Nitrate (as NO ₃ -N)	1
Phosphate (as PO ₄ -P)	26
Fecal coliform bacteria (MPN/100 mL)	1500

*Note: Total suspended solids were not simulated. Data provided for informational purposes only.

Model Coefficients

Several model coefficients were adjusted during the calibration process. Adjusted first were field capacity and sloughing coefficients that affect the hydraulic capacity of the biozone. Then decay rates were adjusted to match observed water quality concentrations.

Table 4-3 shows the calibrated coefficients. In addition, the field capacity and saturated moisture content were set to 0.235 and 0.5 respectively. These values are consistent with clean sand.

A sensitivity analysis was performed to characterize the sensitivity of the empirical calibration parameters that were set during calibration. Column 3 data was randomly selected for the sensitivity analysis exercise. Multiple simulations were performed to determine which calibration parameters from Table 4-3 were most sensitive. While holding all other coefficients constant, each parameter was increase by 50% and then decreased by 50%. Simulated flow was then compared to the calibrated case. The following three calibration parameters stood out as being the most sensitive:

- α , gm biomass/gm BOD in STE
- Φ , Field capacity coefficient 1
- ξ , Field capacity coefficient 2

For the remaining parameters, perturbation of $\pm 50\%$ did not produce significant change in flow predictions.

Table 4-3
Calibrated Coefficients of the Biozone Module

Symbol	Value	Description
α	0.42	Gram biomass/gram BOD in STE
γ	0.18	Respiration rate coefficient, cm^3/s
ϕ	0.29	Mortality rate coefficient, cm^3/s
η	4.0×10^{-4}	Sloughing coefficient 1, mg/cm
δ	1.5	Sloughing coefficient 2, unitless
σ	0.1	Plaque coefficient for TDS, unitless
Φ	30	Field capacity coefficient 1, unitless
ξ	0.7	Field capacity coefficient 2, unitless
ρ_b	1000	Density of biomass, mg/cm^3
$K_{1,\text{nitr}}$	1.0	Nitrification rate coefficient, cm^3/s
$K_{1,\text{denitr}}$	0.05	Denitrification rate coefficient, cm^3/s
$K_{1,\text{BOD}}$	108	BOD decay rate coefficient, cm^3/s
$K_{1,\text{fecal}}$	15	Fecal coliform bacteria decay rate coefficient, cm^3/s

Simulations Results

The model was configured to represent the laboratory conditions as closely as possible. The area of the infiltrative surface was set to equal that of the experimental columns (diameter = 15 cm, area = 176.7 cm^2). In addition to modeling a 2-cm-thick biozone on the infiltrative surface, the model included infiltration through a 60-cm soil layer below the biozone. Simulations of the entire column length (biozone and underlying sand) were performed for each flow regime for a period of five months (153 days). For each flow, simulated results of flow and quality at the bottom of the sand layer were compared to four sets of experimental data.

Simulation of Biomass Build Up and Hydraulic Conductivity

Figure 4-3 shows the simulated build up of live and dead bacteria in the biozone. There is no observed data for comparison. The biomass growth appears to taper off after approximately 80 days due to the increase of pore velocity, which sloughs off bacteria. A delay in significant biomass buildup was simulated for all columns with the longest delay (approximately 18 days) observed in column 1.

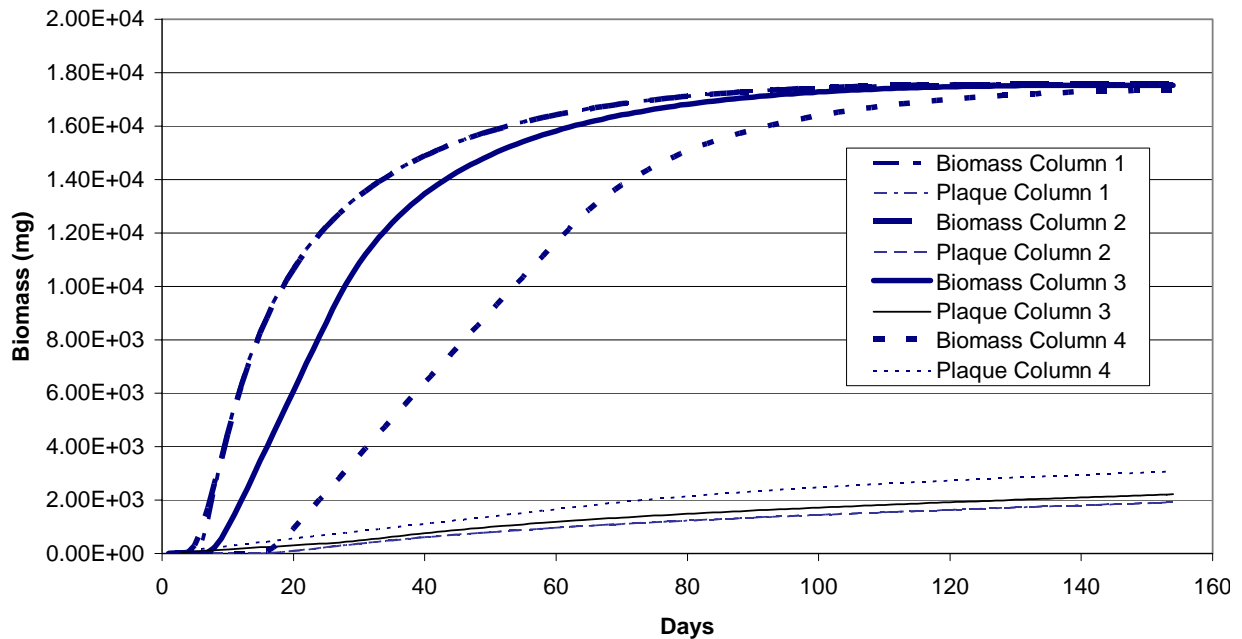


Figure 4-3
Simulated Bacteria Biomass in the Biozone for Columns 1, 2, 3, and 4

The higher flow rates for columns 1 and 2 appear to have caused the bacteria to slough off in these early days resulting in a delay for biomass buildup. The dead bacteria biomass (plaque) increases with the live bacteria biomass. The highest build up of plaque is observed with the lowest loaded column 4, which is likely due to lower sloughing of plaque at lower loading rates. All of these trends are reasonable.

The hypothesis is that the hydraulic failure of OWS can be caused by excessive pore clogging in the biozone. Figure 4-4 shows the simulated field capacity and saturated moisture for each column. Under the experimental condition of a high loading rate, the rapid build-up of bacteria caused the field capacity to approach the saturated moisture content (porosity) in 20 to 40 days. At that point, the model predicts a hydraulic failure, which caused the experimental columns to overflow, as observed in the laboratory.

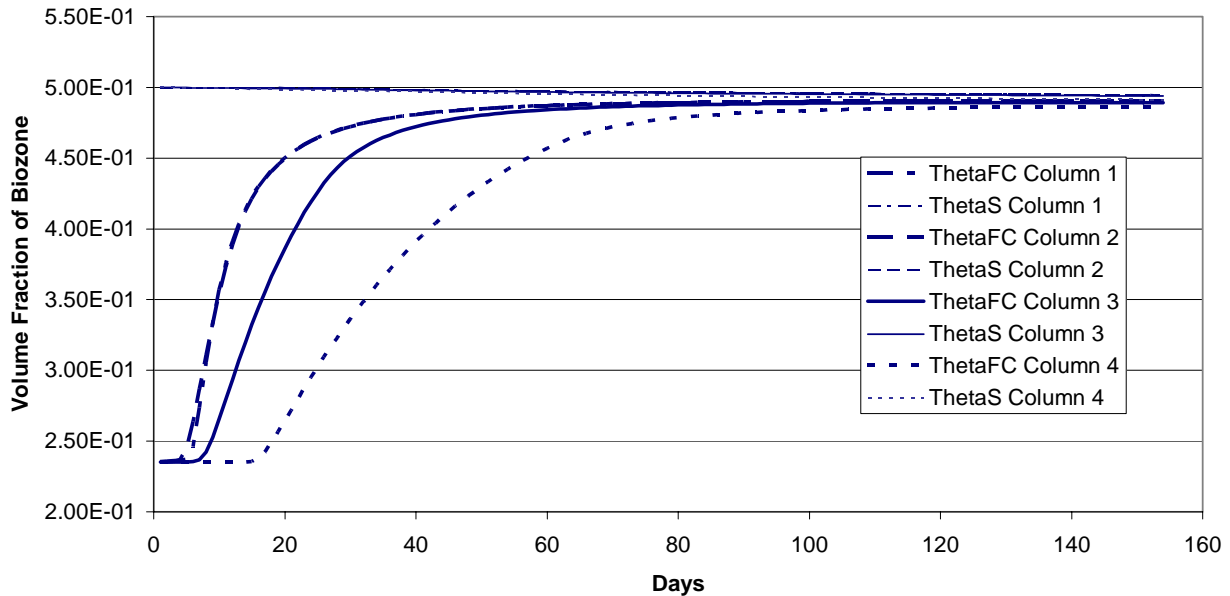


Figure 4-4
Simulated Field Capacity (ThetaFC) and Saturate Moisture Content (ThetaS) of Column Experiments

Hydrology Calibration

Figure 4-5 through Figure 4-8 compare the simulated and observed throughput of the column experiments. All simulations are of the entire length of the column including both the biozone and underlying sand. For all columns, the model showed an initial increase in flow up to a maximum value equal to the input flow rate. The maximum flow was reached in approximately four days for all cases. After a period of time, the flow out of the bottom of the column was reduced due to decreased infiltration into the biozone and ponding at the surface.

Ponding occurred earlier for the higher loading rates (approximately 10 days for column 1) and later for the lower loading rate (approximately 60 days for column 4). After approximately 100 days, the simulated flow out of the column approached a steady state flow of approximately $1 \times 10^{-8} \text{ m}^3/\text{s}$ or 4–5 cm/day for all cases (similar to rates measured in the lab at the end of the study [111 days]).

With the same model coefficients, the model reasonably simulated a wide range of loading conditions. R-squared values were greater than 0.7 for several columns. Though observed data is presented for replicate columns at each loading rate, the high amount of scatter when comparing columns A and B for each loading rate suggests inherent variability in the system. The poorest match of simulated versus observed was for column 4, which showed the highest degree of scatter in observed data.

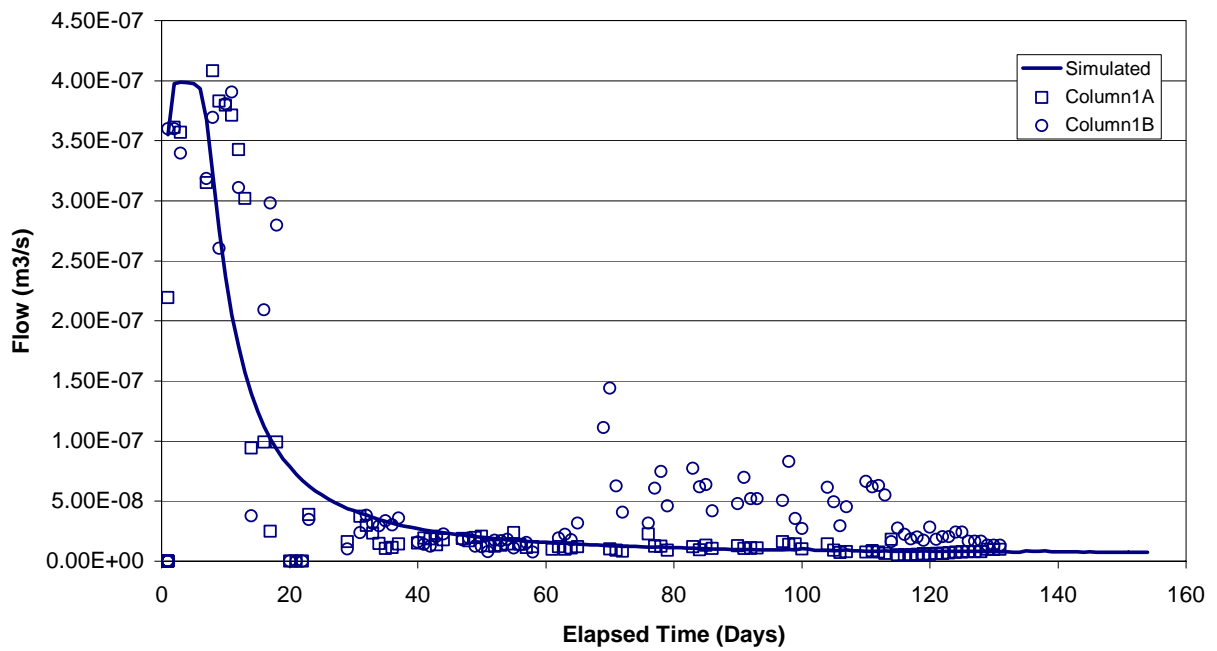


Figure 4-5
Simulated and Observed Flow for Column 1. $R^2 = 0.72$ (1A), $R^2 = 0.59$ (1B)

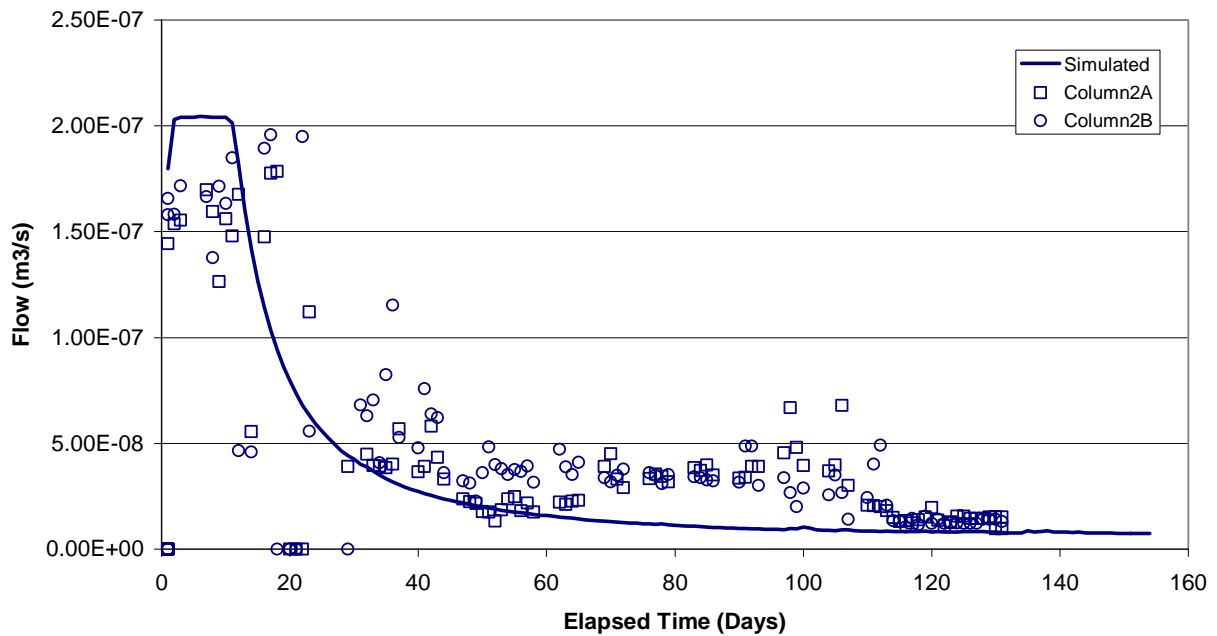


Figure 4-6
Simulated and Observed Flow for Column 2. $R^2 = 0.62$ (2A), $R^2 = 0.54$ (2B)

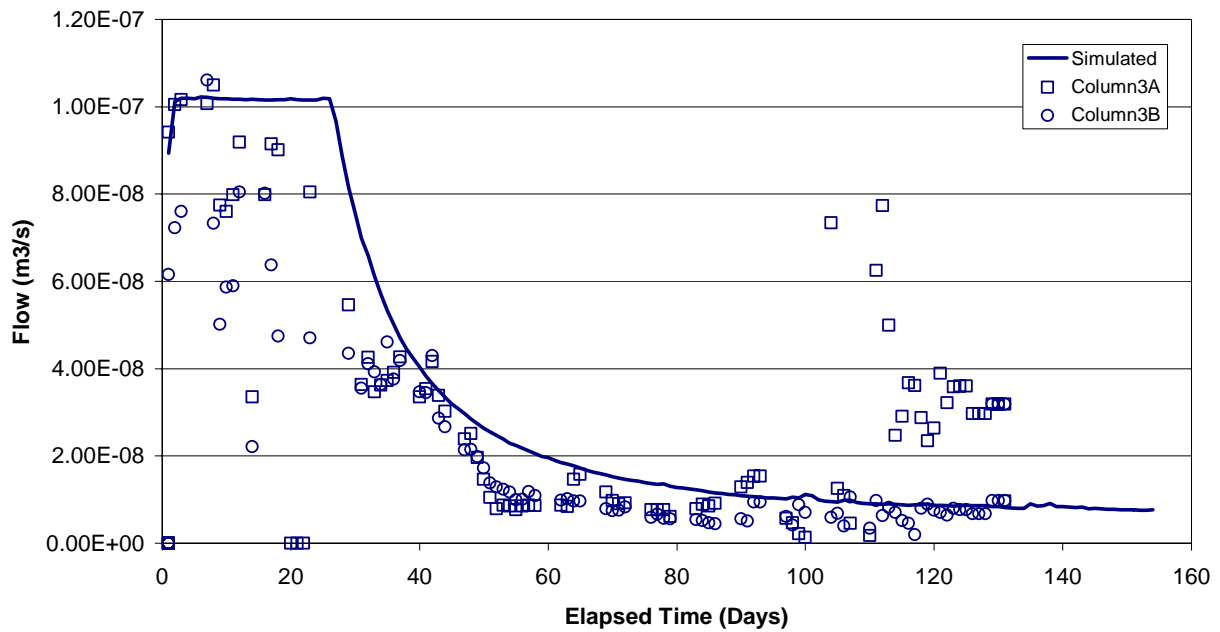


Figure 4-7
Simulated and Observed Flow for Column 3. $R^2 = 0.36$ (3A), $R^2 = 0.78$ (3B)

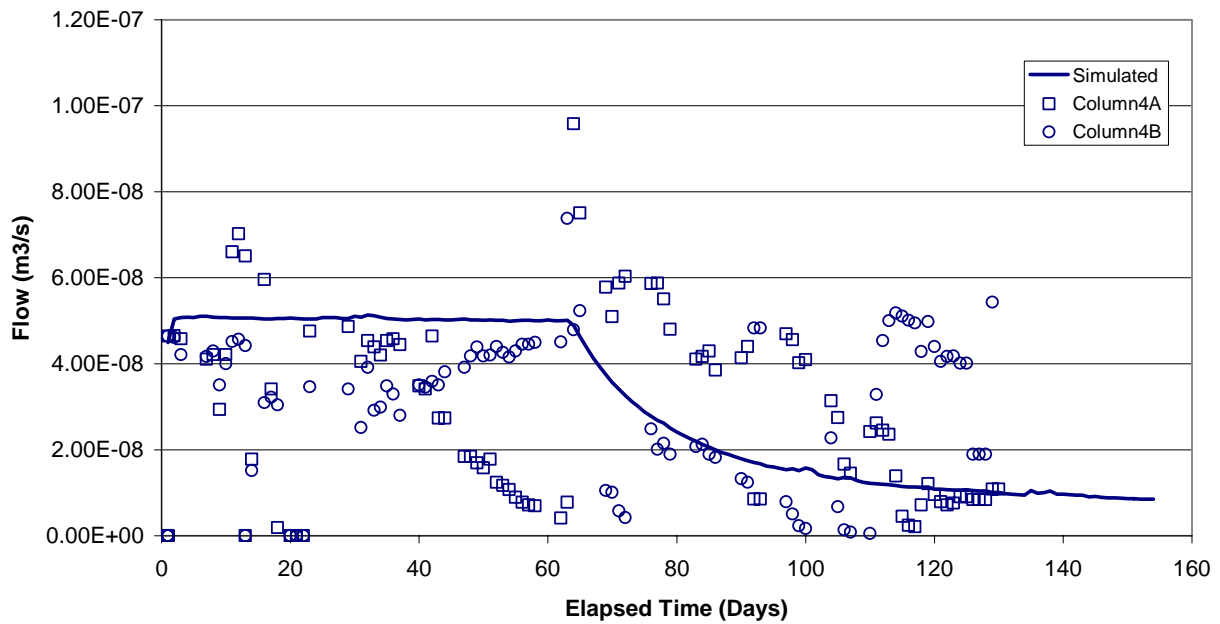


Figure 4-8
Simulated and Observed Flow for Column 4. $R^2 = 0.06$ (4A), $R^2 = 0.02$ (4B)

Water Quality Calibration

This section compares the simulated and observed water quality of column experiments. All simulations are of the entire length of the column including both the biozone and underlying sand. All measured water qualities are of the water leaving the bottom of the sand column.

Figure 4-9 through Figure 4-12 compare the simulated and observed ammonia nitrogen. For all columns the simulated ammonia concentration rises quickly to a peak concentration of 60–70 mg/L. After the biomass begins to mature and nitrification increases, the ammonia concentration sharply decreases and steadily decreases to a constant value after approximately 60 days. Laboratory column data shows a similar pattern for all loading rates. One exception, however, was observed for column 1B. Laboratory data suggest little nitrification occurred in this column because high ammonia concentration, low nitrate concentrations, depressed alkalinity, and high levels of BOD measured as late as 80 to 100 days into the experiment.

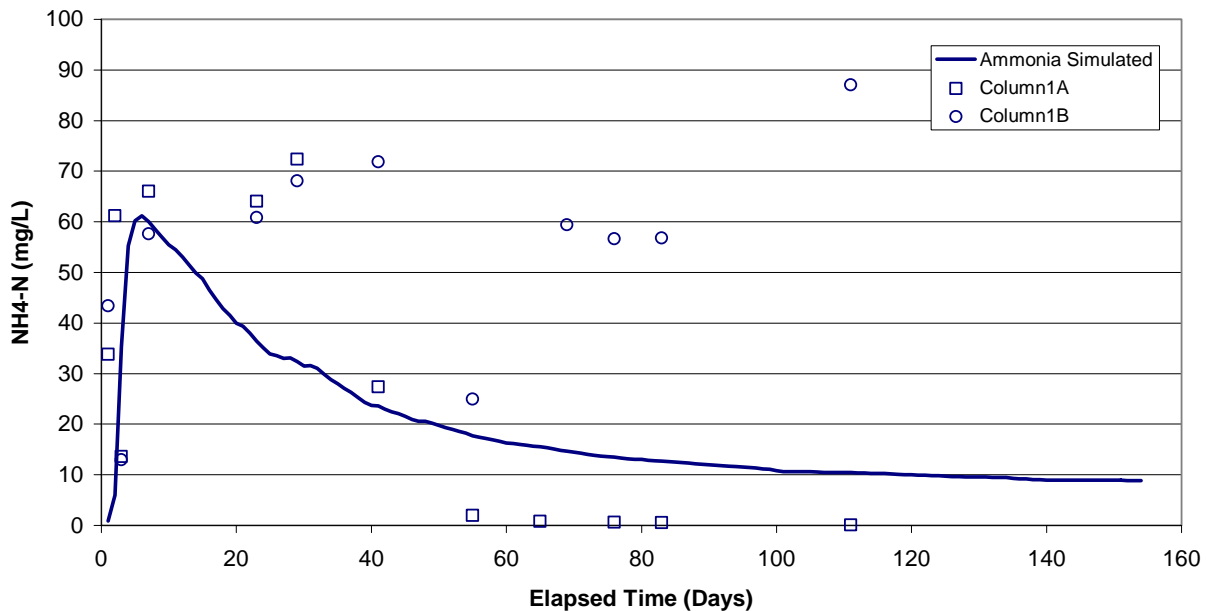


Figure 4-9
Simulated and Observed Ammonia for Column 1

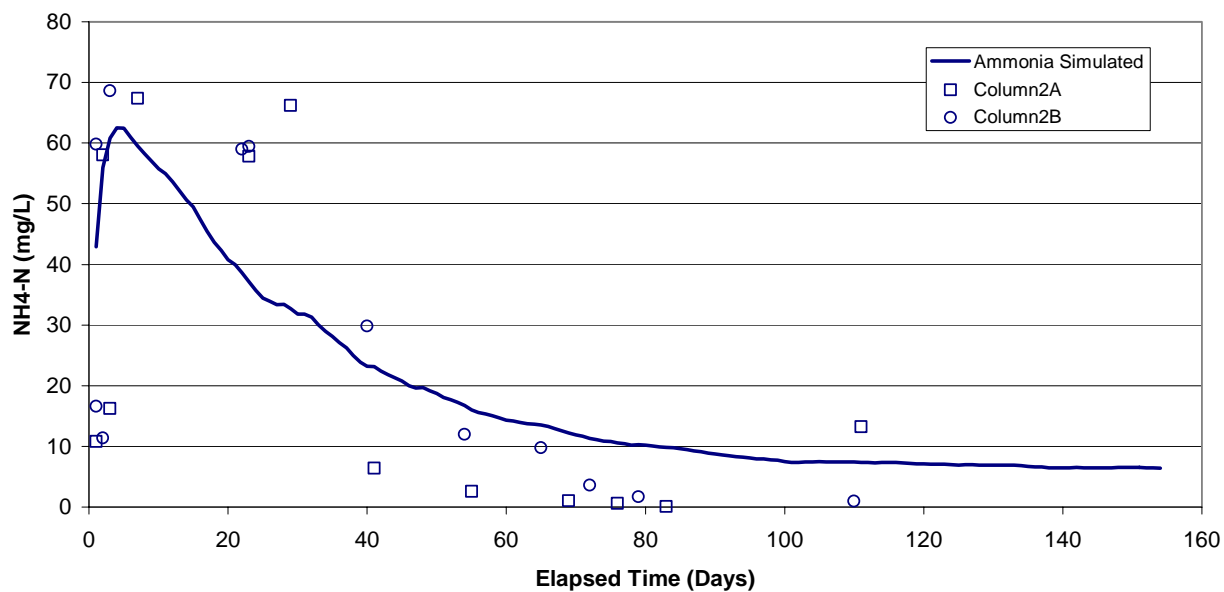


Figure 4-10
Simulated and Observed Ammonia for Column 2

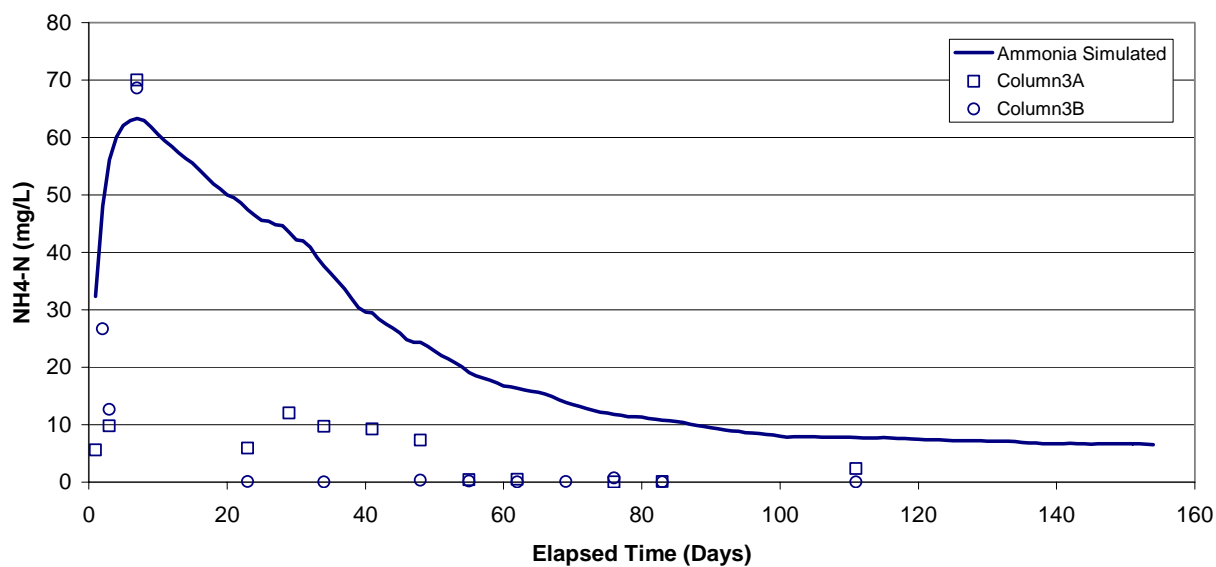


Figure 4-11
Simulated and Observed Ammonia for Column 3

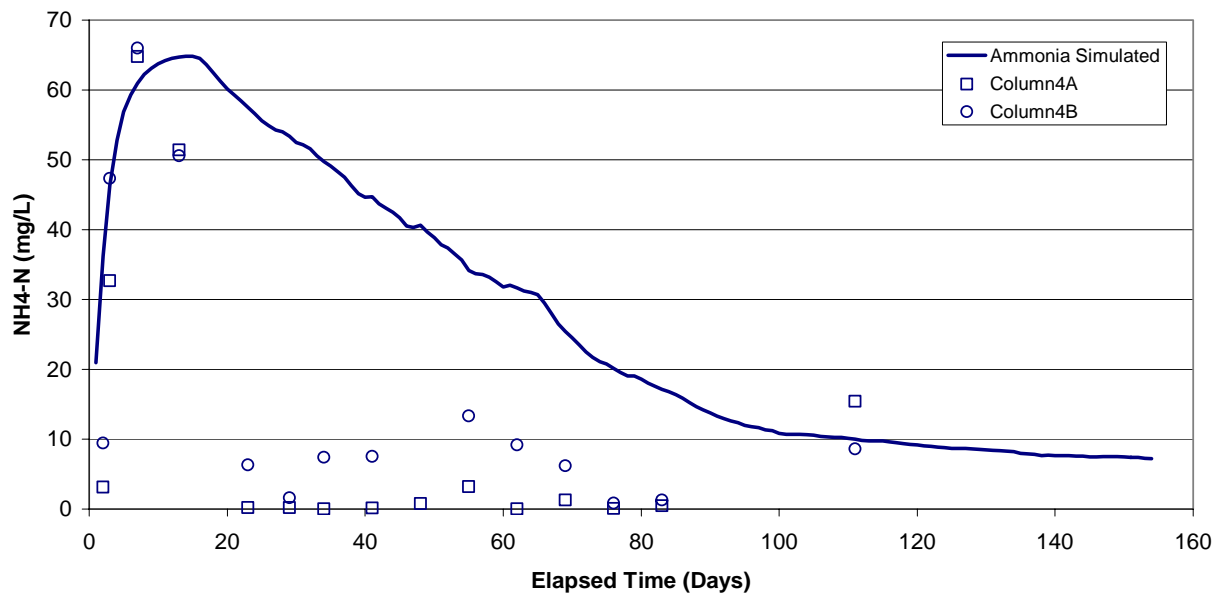


Figure 4-12
Simulated and Observed Ammonia for Column 4

Figure 4-13 through Figure 4-16 compare the simulated and observed nitrate nitrogen. For all cases, the simulation shows a steady increase in nitrate concentration as the biozone matures and nitrification increases. As the flow rate decreases, a decreasing trend in nitrate is observed. The model predicts trends consistent with the observed data for all columns. The best match between simulated and observed nitrate is seen in columns 3 and 4. For columns 1 and 2, the model appears to be predicting the increase in nitrate too early. This lag in observed data may be due to a slower growth rate of nitrifying bacteria as compared to other types of bacteria. This phenomenon would not be captured by the model due to the linear relationship between biomass and nitrification rate used in the algorithm. As previously mentioned, observed data for column 1B indicated little nitrification occurred in this column.

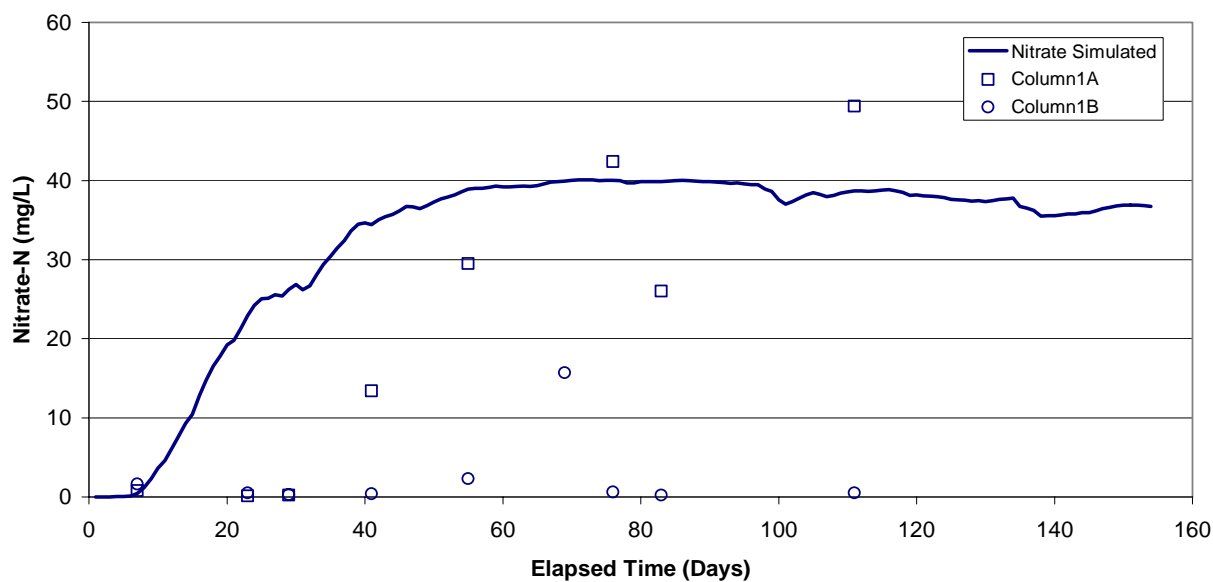


Figure 4-13
Simulated and Observed Nitrate for Column 1

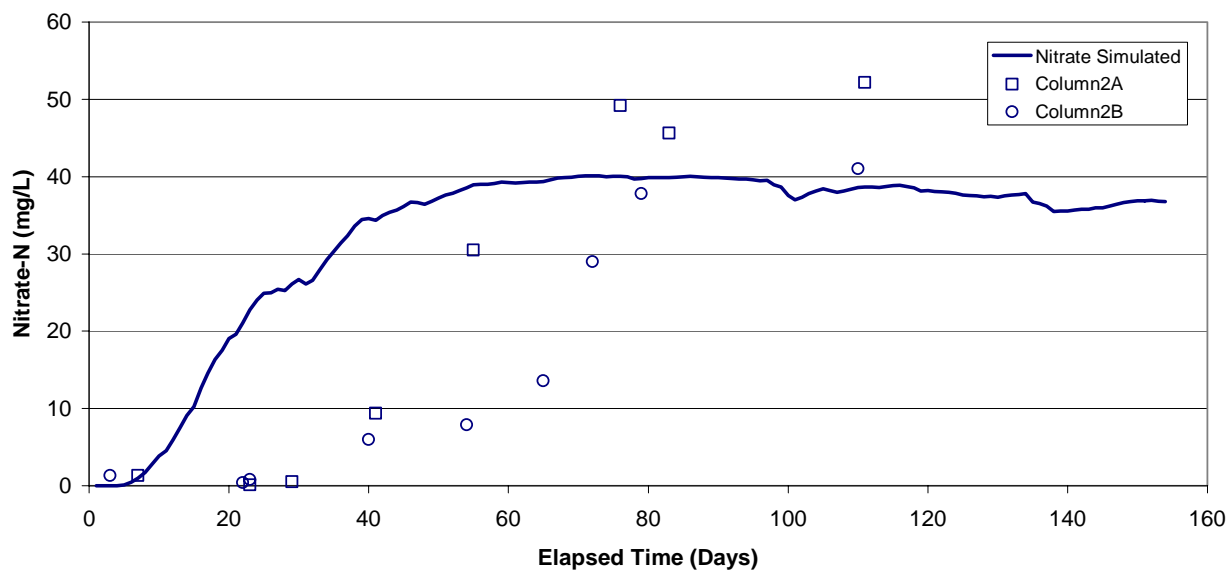


Figure 4-14
Simulated and Observed Nitrate for Column 2

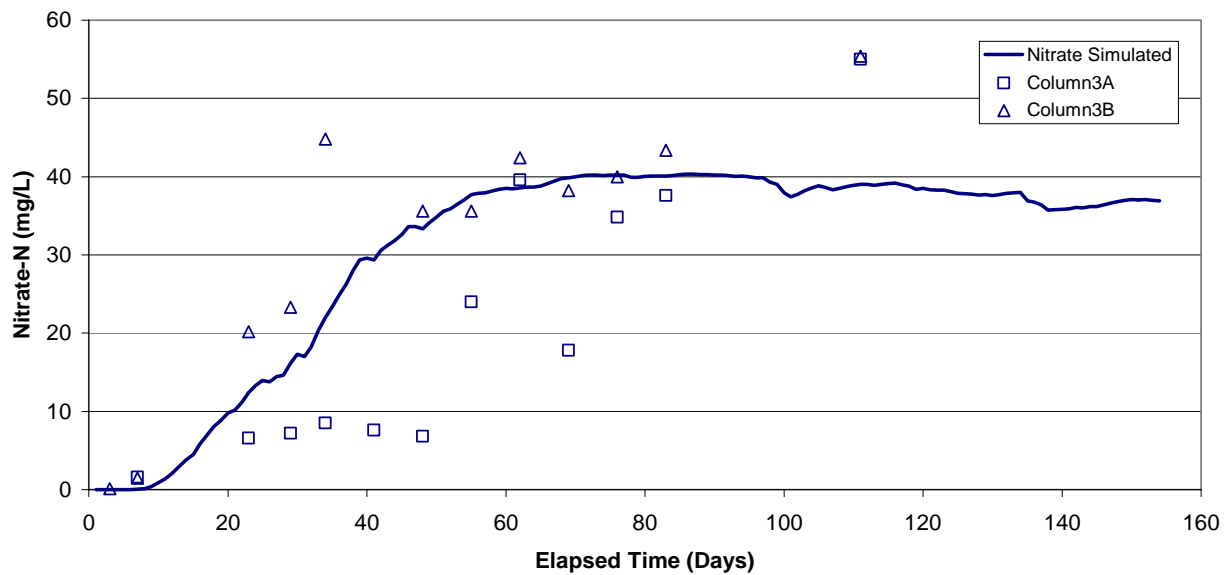


Figure 4-15
Simulated and Observed Nitrate for Column 3

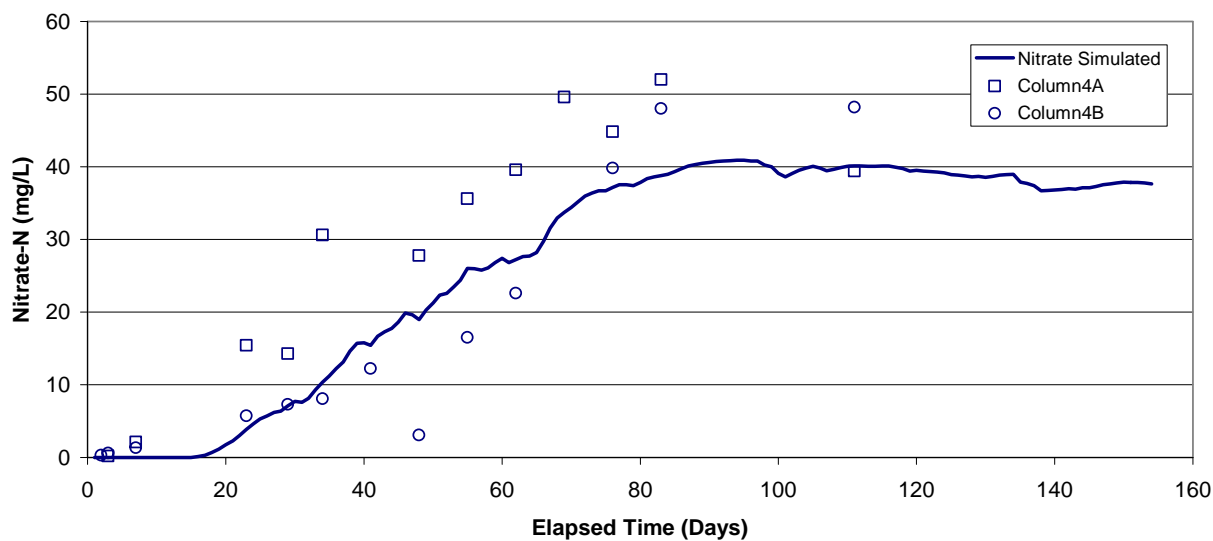


Figure 4-16
Simulated and Observed Nitrate for Column 4

Simulated and observed results for fecal coliform bacteria are presented in Figure 4-17 through Figure 4-20. The simulated results indicate a decreasing trend of fecal coliform bacteria followed the maturation of the biozone, which caused an increase of decay rate. For all cases, simulated values fall within the range of observed values.

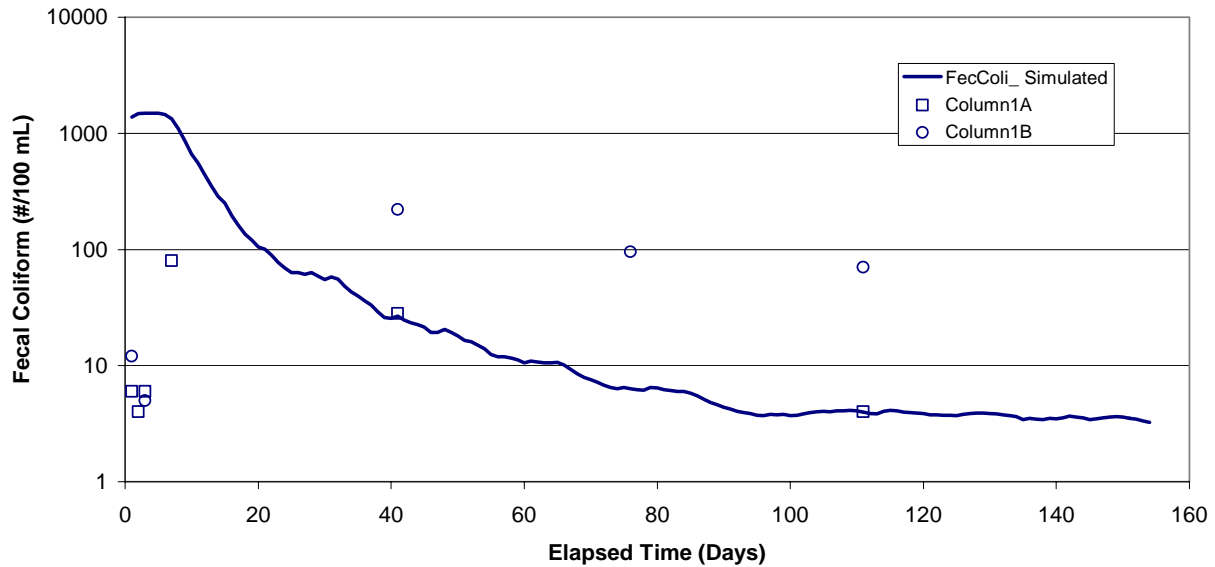


Figure 4-17
Simulated and Observed Fecal Coliform Bacteria for Column 1

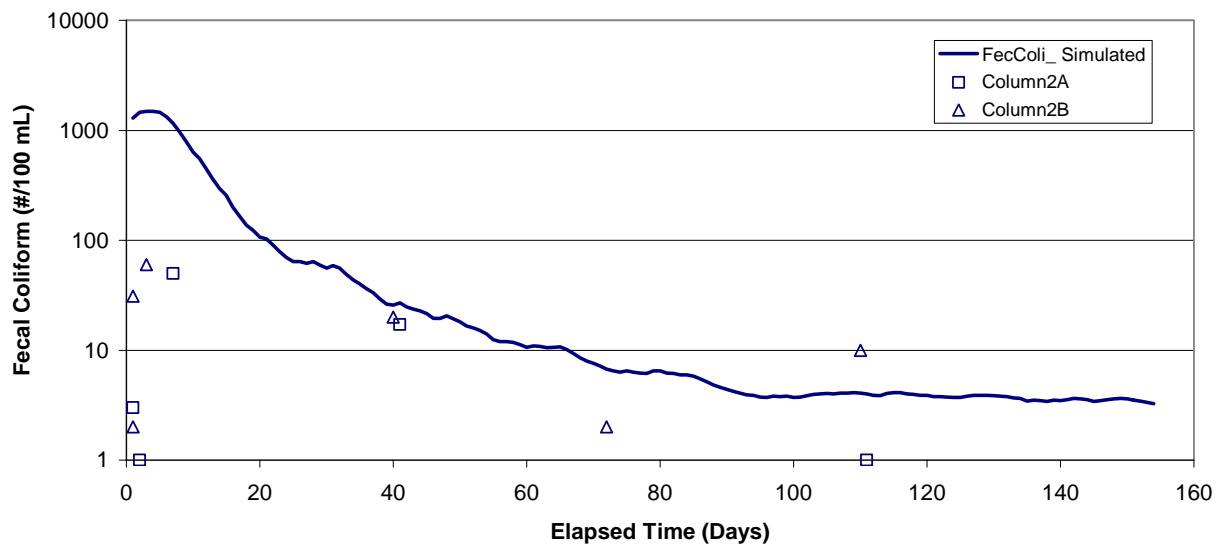


Figure 4-18
Simulated and Observed Fecal Coliform Bacteria for Column 2

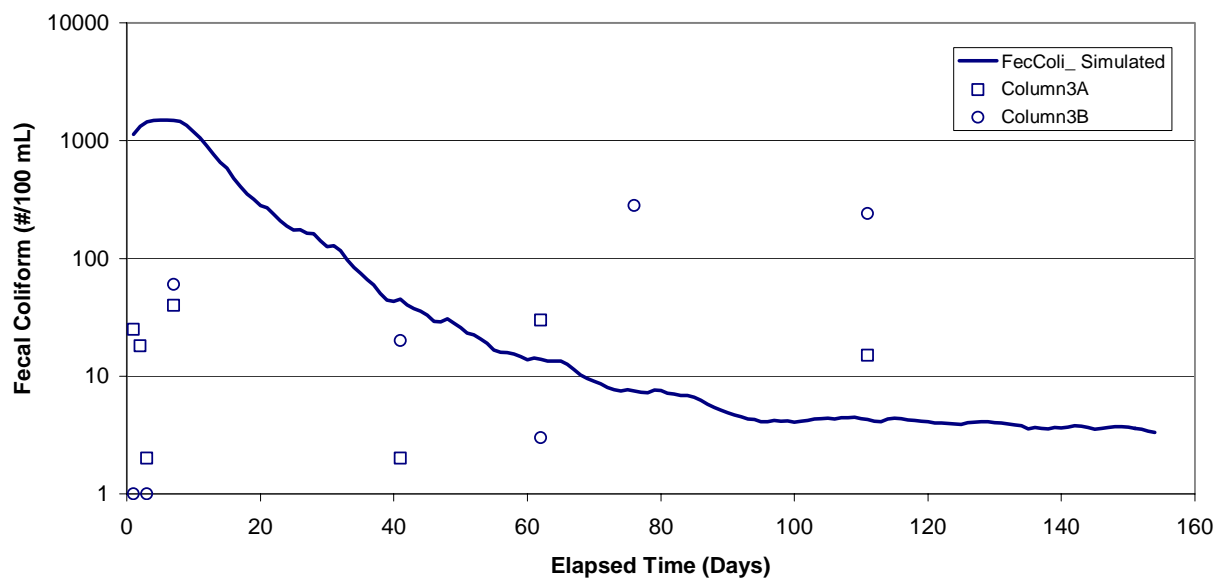


Figure 4-19
Simulated and Observed Fecal Coliform Bacteria for Column 3

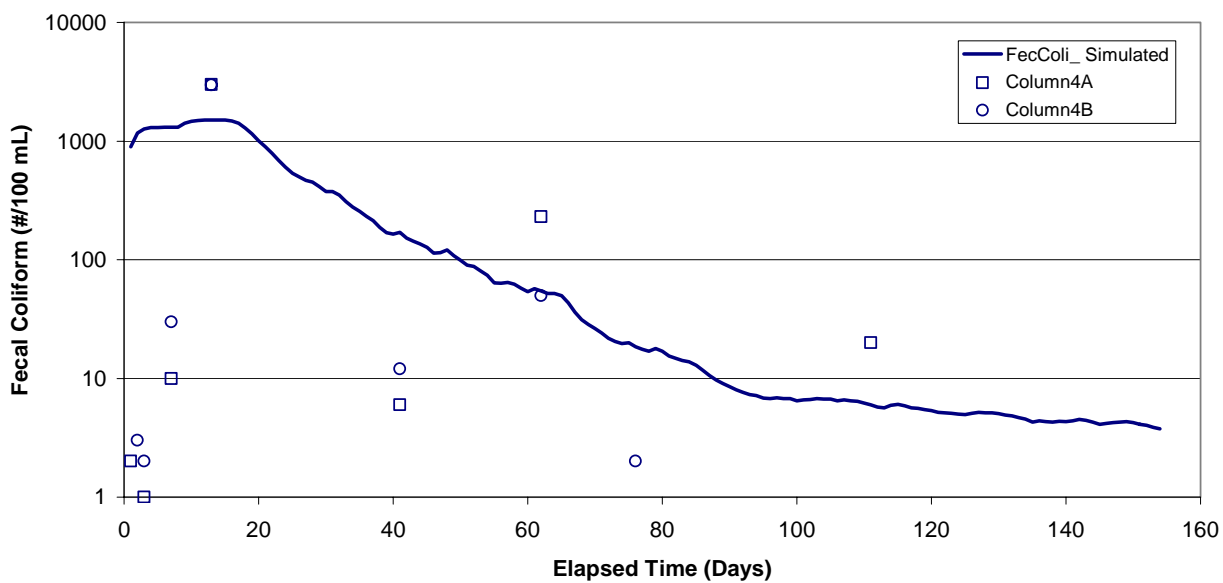


Figure 4-20
Simulated and Observed Fecal Coliform Bacteria for Column 4

Figure 4-21 through Figure 4-24 compare simulated and observed BOD. Simulated results indicate a sudden drop of BOD concentration after approximately 10 to 20 days is noted for all cases. This drop is due to the biozone consuming BOD to build up biomass. Though not a perfect fit, the simulation follows the trends of experimental data for most cases.

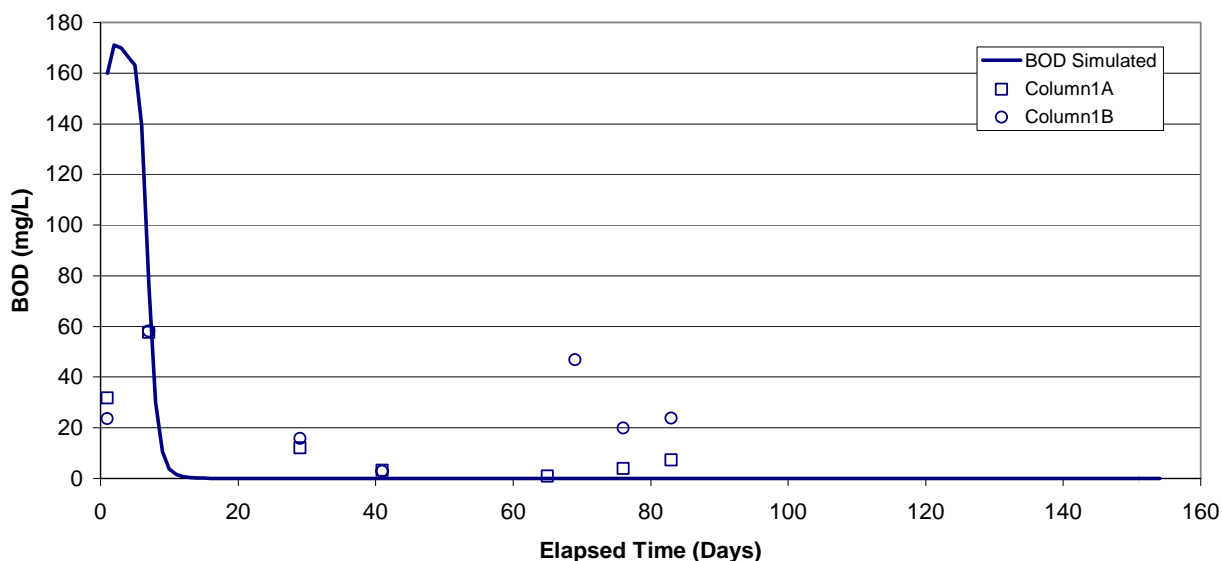


Figure 4-21
Simulated and Observed BOD for Column 1

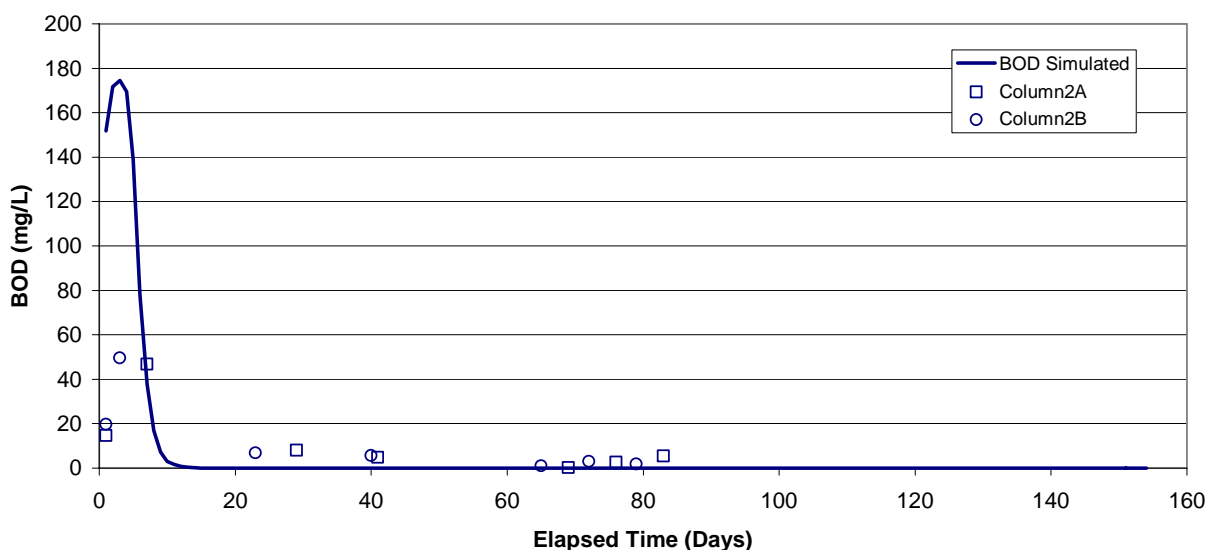


Figure 4-22
Simulated and Observed BOD for Column 2

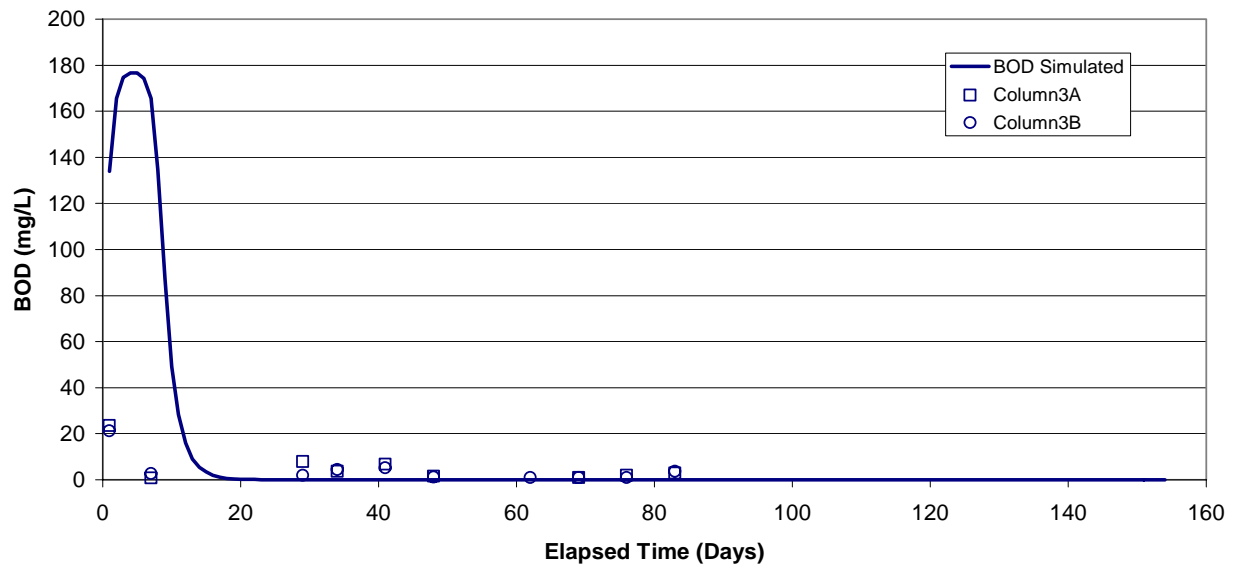


Figure 4-23
Simulated and Observed BOD for Column 3

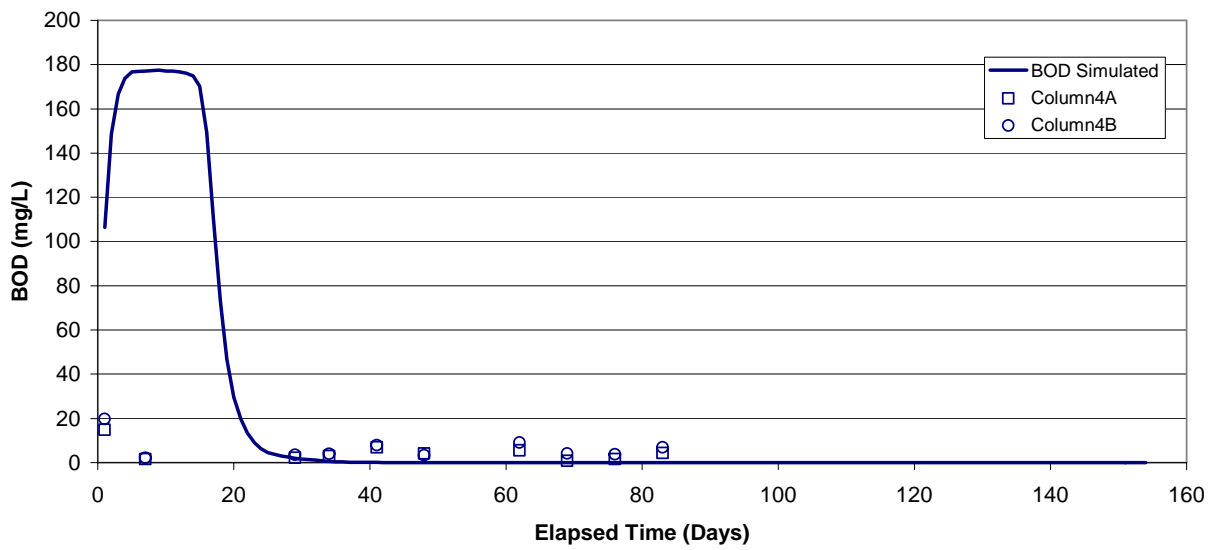


Figure 4-24
Simulated and Observed BOD for Column 4

Figure 4-25 through Figure 4-28 show the simulated and observed total phosphorus. Simulated results show a low initial concentration for 10 to 60 days, up to a point of breakthrough where the concentration rises quickly and then tapers off. This point of breakthrough corresponds to the point of maximum adsorption at which all phosphorus adsorption sites have been occupied. The simulated pattern is logical in that the higher dosed columns reach a breakthrough point sooner than the lower dosed columns. However, the measured column data shows an unexpected opposite trend when comparing columns 1 through 4, likely attributed to several factors including sampling and analyses methods, column operation, and changing conditions within the column (for example, microbial activity).

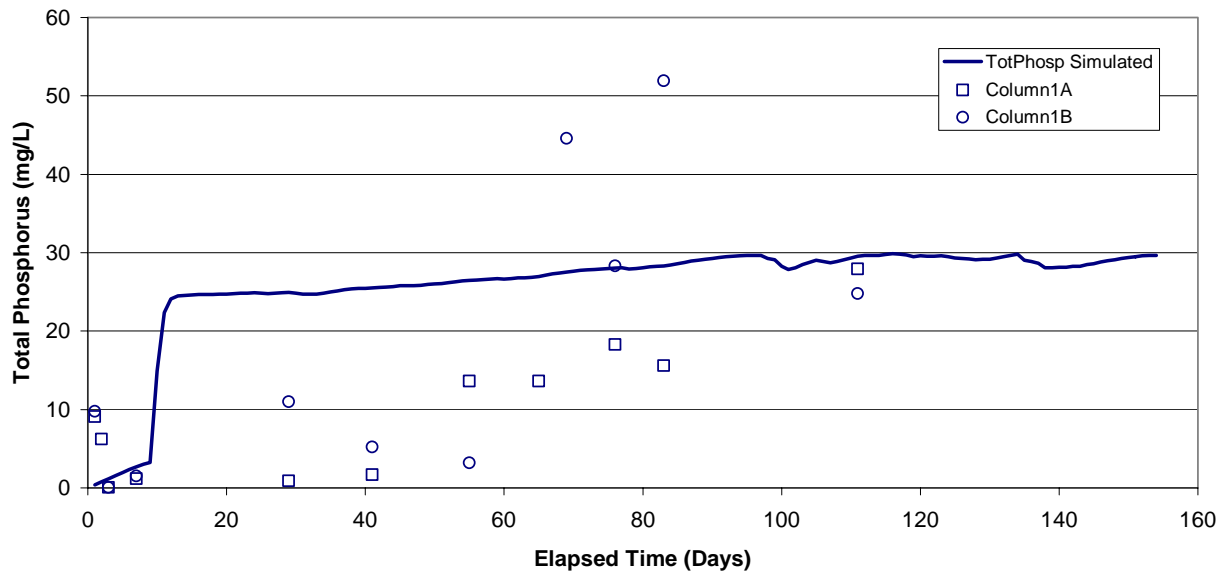


Figure 4-25
Simulated and Observed Total Phosphorus for Column 1

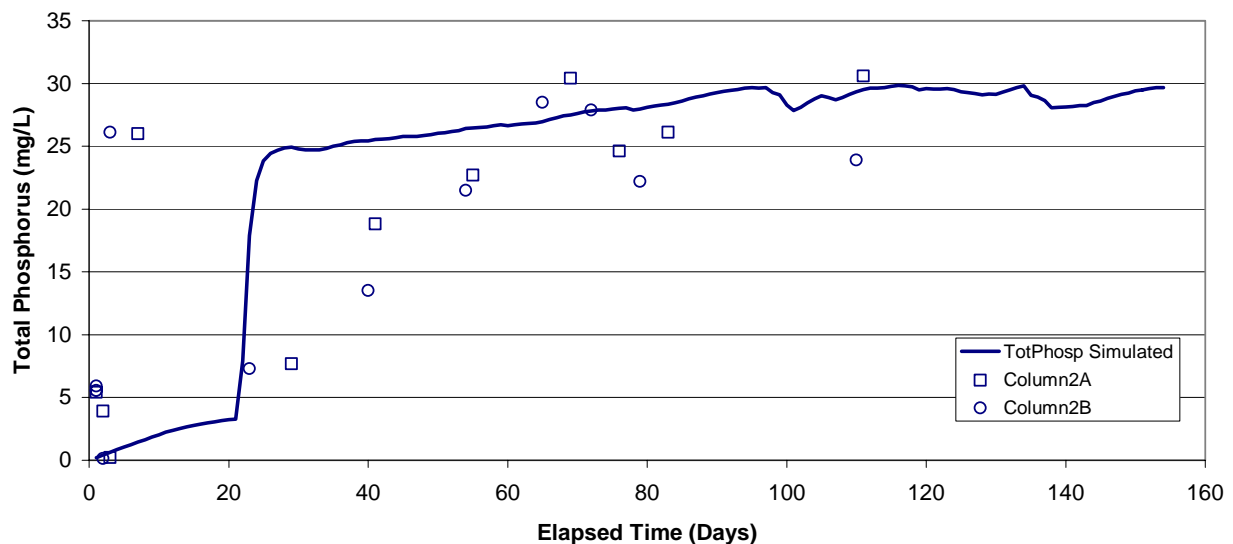


Figure 4-26
Simulated and Observed Total Phosphorus for Column 2

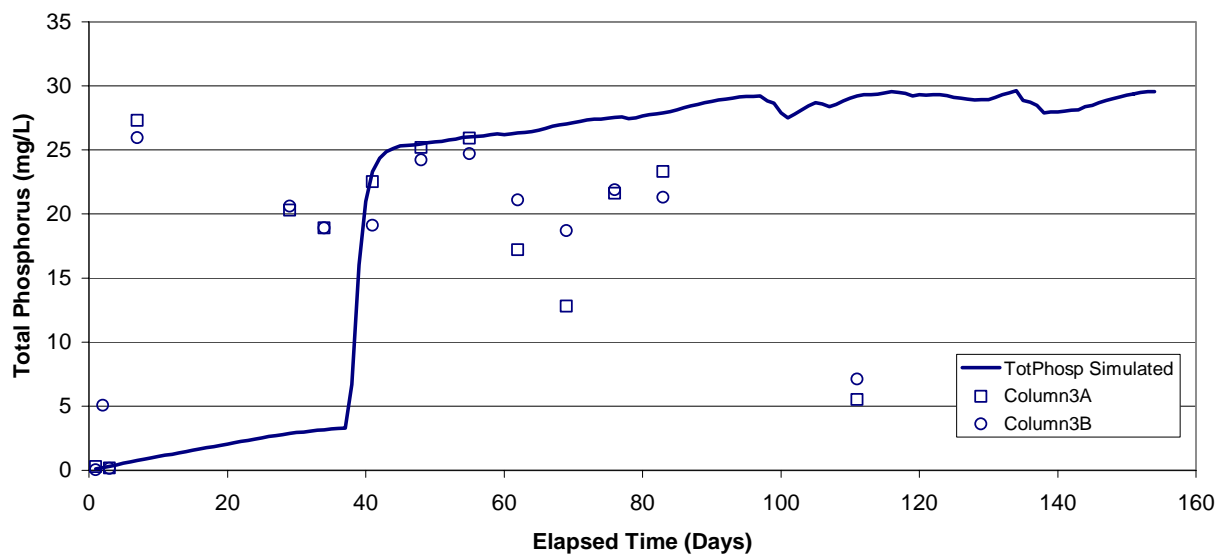


Figure 4-27
Simulated and Observed Total Phosphorus for Column 3

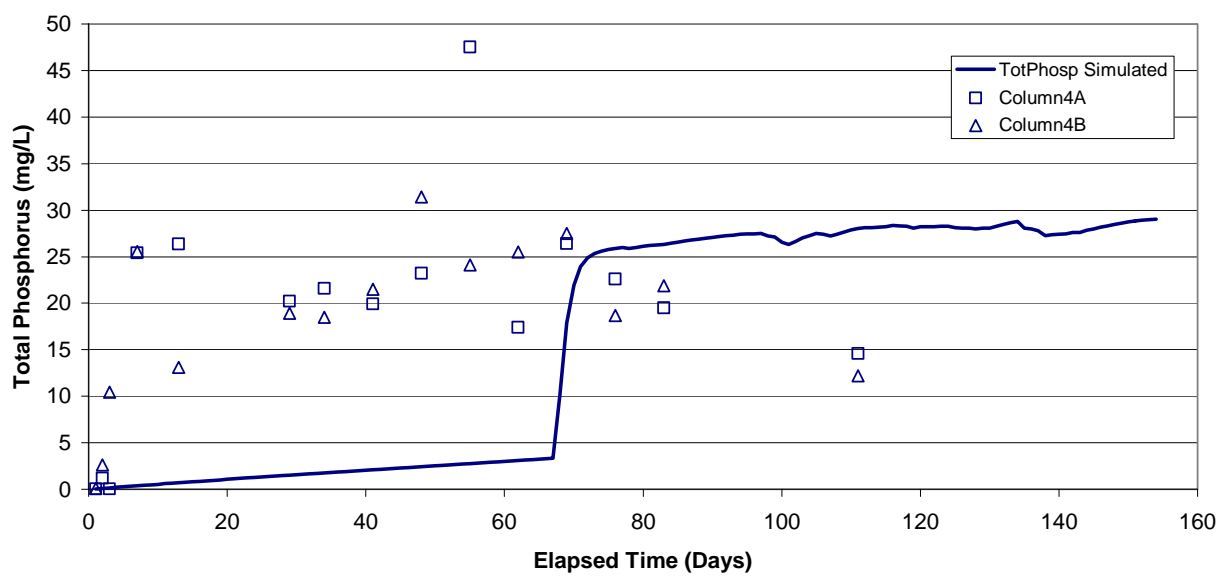


Figure 4-28
Simulated and Observed Total Phosphorus for Column 4

Simulated and observed total nitrogen are presented in Figure 4-29 through Figure 4-32. Simulated total nitrogen increases to a maximum value in a matter of one to two days for all columns. After that, a slow decrease in total nitrogen is observed. For most cases, the experimental data shows a slower climb to a peak nitrogen concentration. In general, the simulation falls within the wide range of observed values for most cases.

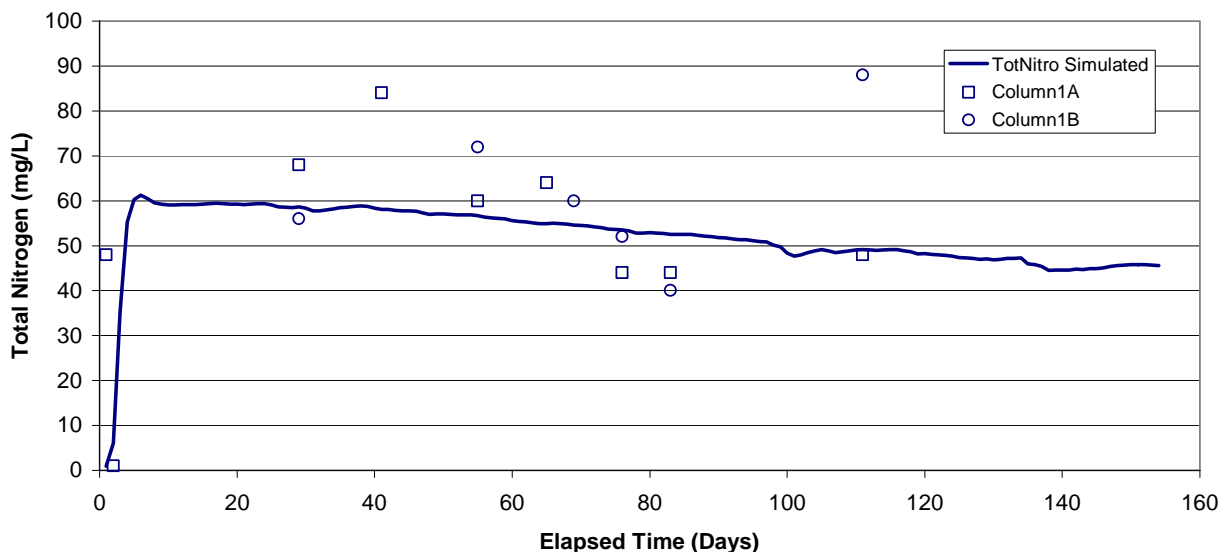


Figure 4-29
Simulated and Observed Total Nitrogen for Column 1

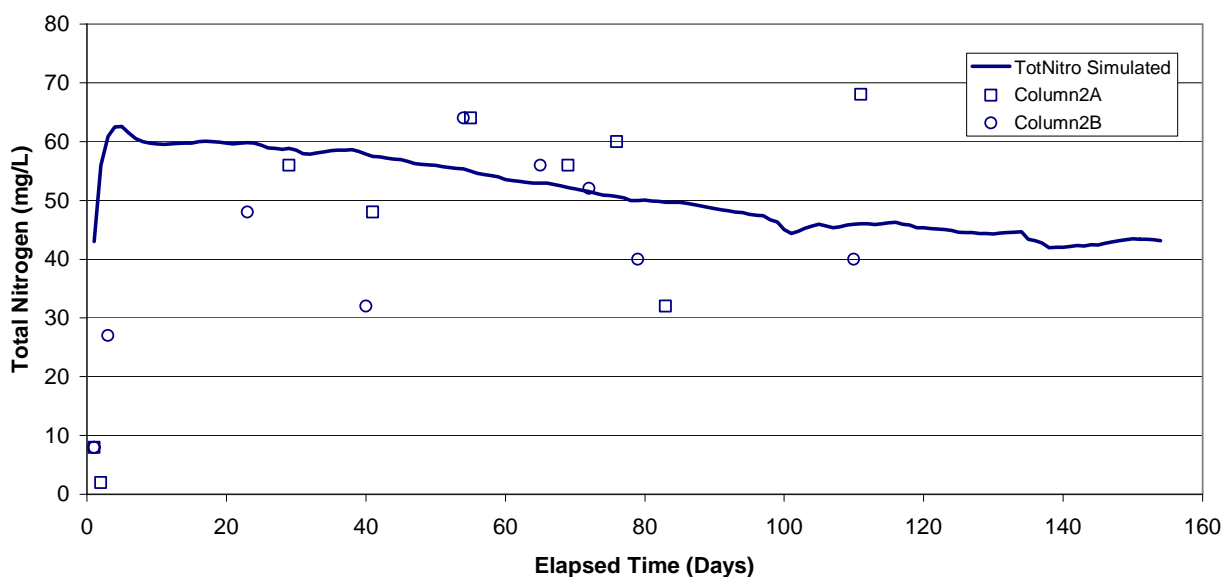


Figure 4-30
Simulated and Observed Total Nitrogen for Column 2

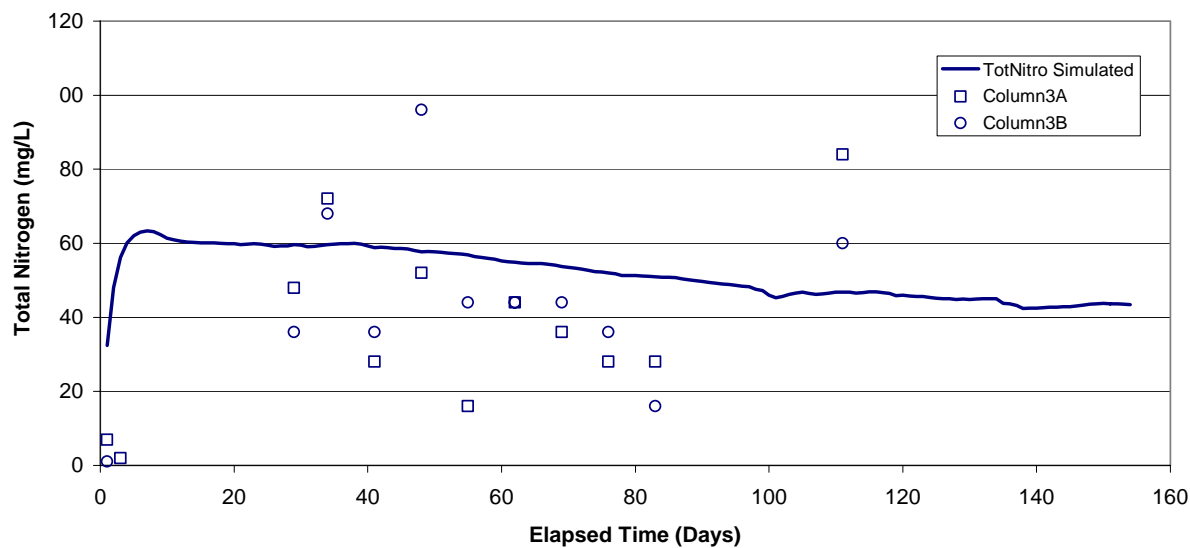


Figure 4-31
Simulated and Observed Total Nitrogen for Column 3

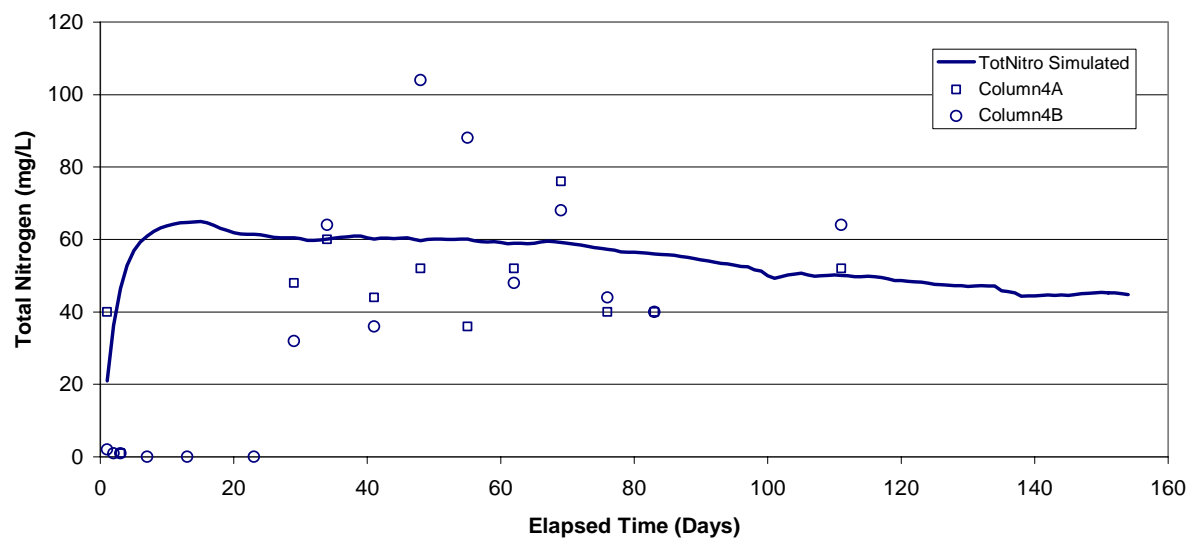


Figure 4-32
Simulated and Observed Total Nitrogen for Column 4

When bacteria in the biozone nitrifies ammonia (a cation) to nitrate (an anion), the model will predict a decrease of alkalinity and pH. Figure 4-33 through Figure 4-36 compare simulated and observed alkalinity for each column. For all columns, simulated alkalinity starts high (approximately 400 mg/L calcium carbonate [CaCO_3]) and eventually drops to a steady level of approximately 50 mg/L CaCO_3 after 60 to 80 days. This pattern is observed in the laboratory and predicted by the model. For column 1B, the alkalinity stays at a constant high value throughout the experiment, which is consistent with the observation that no nitrification occurred in this column.

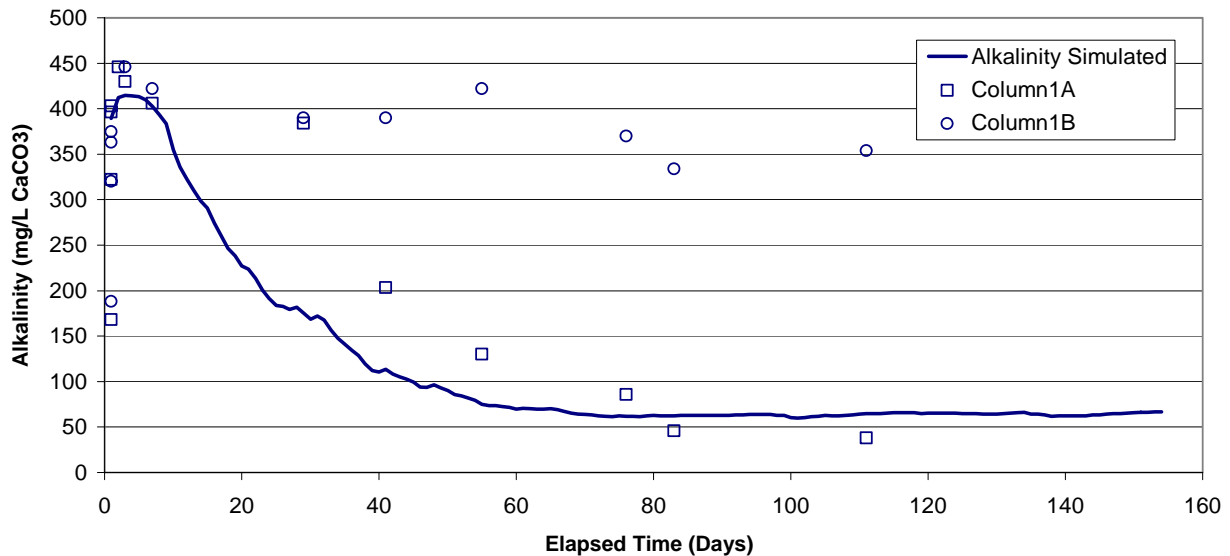


Figure 4-33
Simulated and Observed Alkalinity for Column 1

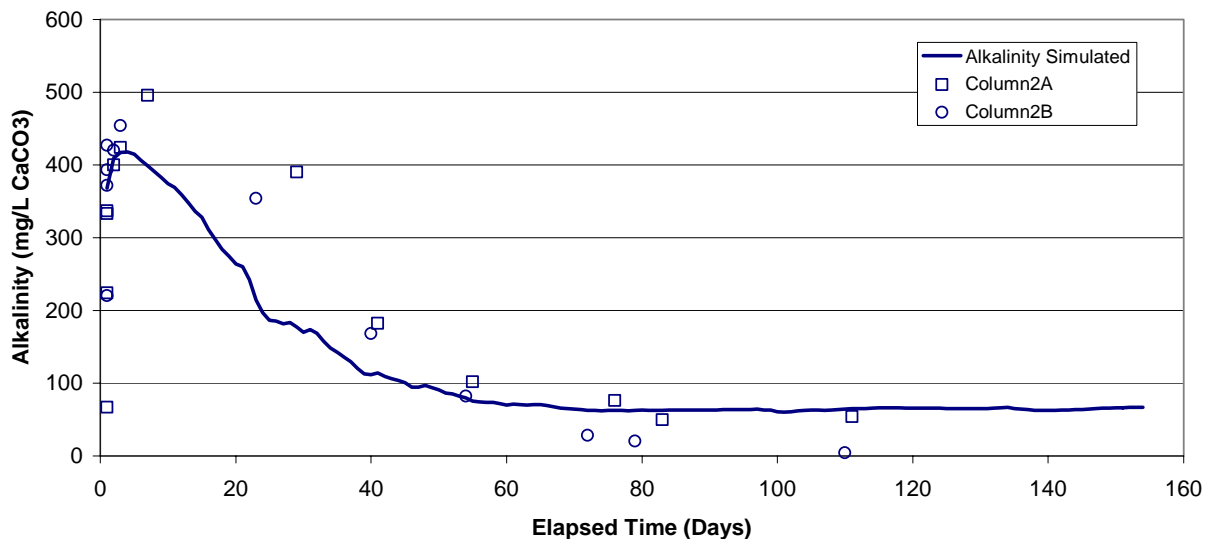


Figure 4-34
Simulated and Observed Alkalinity for Column 2

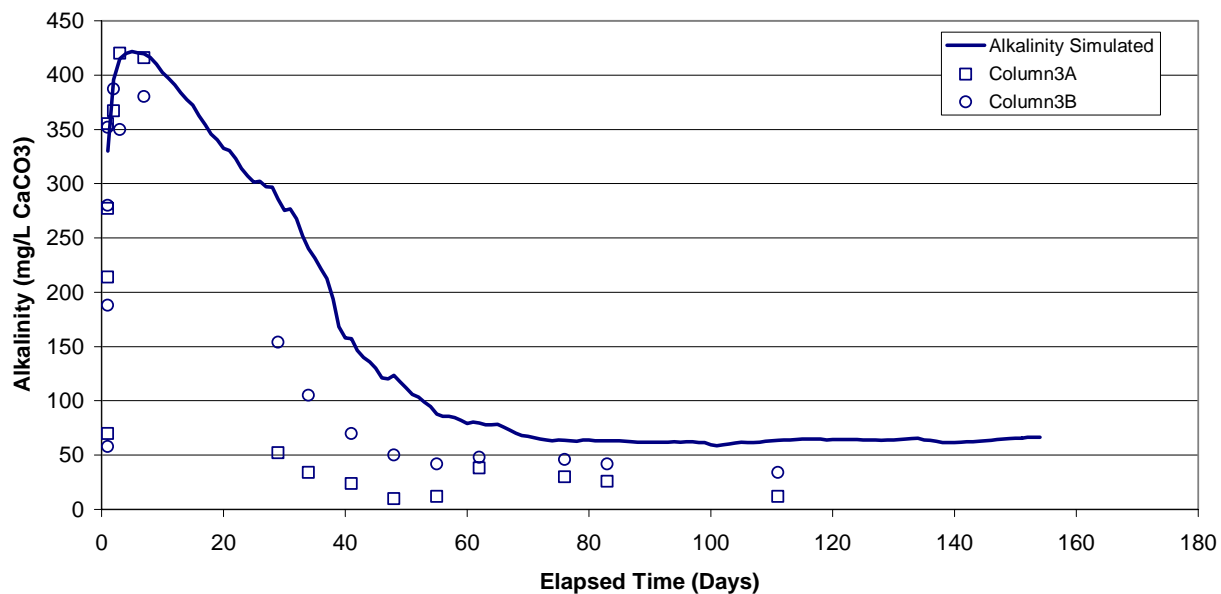


Figure 4-35
Simulated and Observed Alkalinity for Column 3

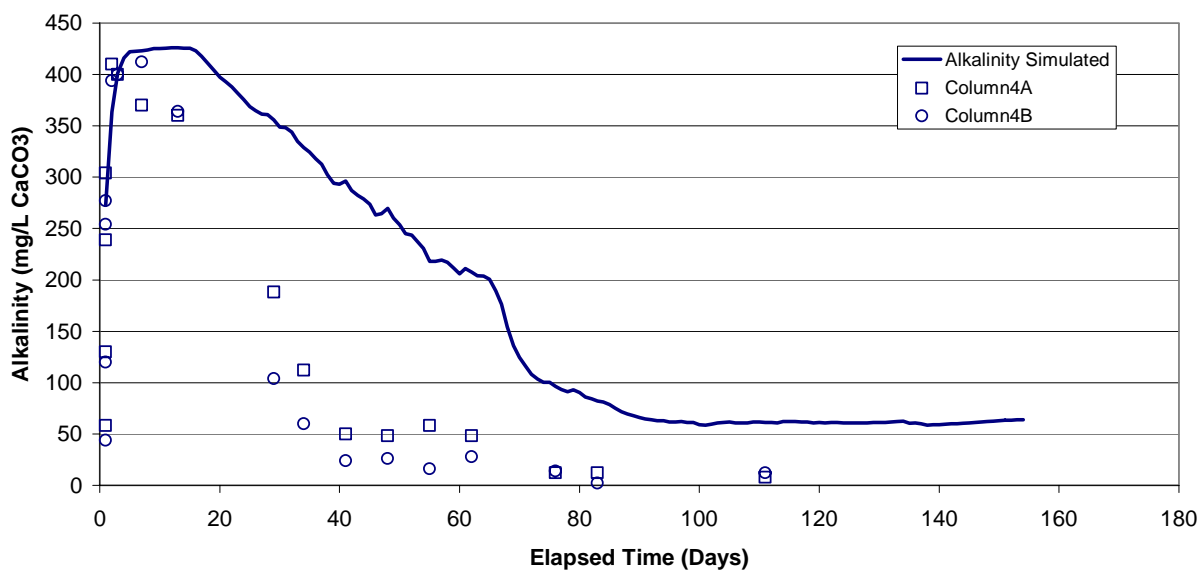


Figure 4-36
Simulated and Observed Alkalinity for Column 4

Figure 4-37 through Figure 4-40 compare simulated and observed pH for each column. For all columns, the simulated pH fell from 8 to 7 over the period of simulation. Observed pH showed similar trends though values dipped to as low as 5 for several columns.

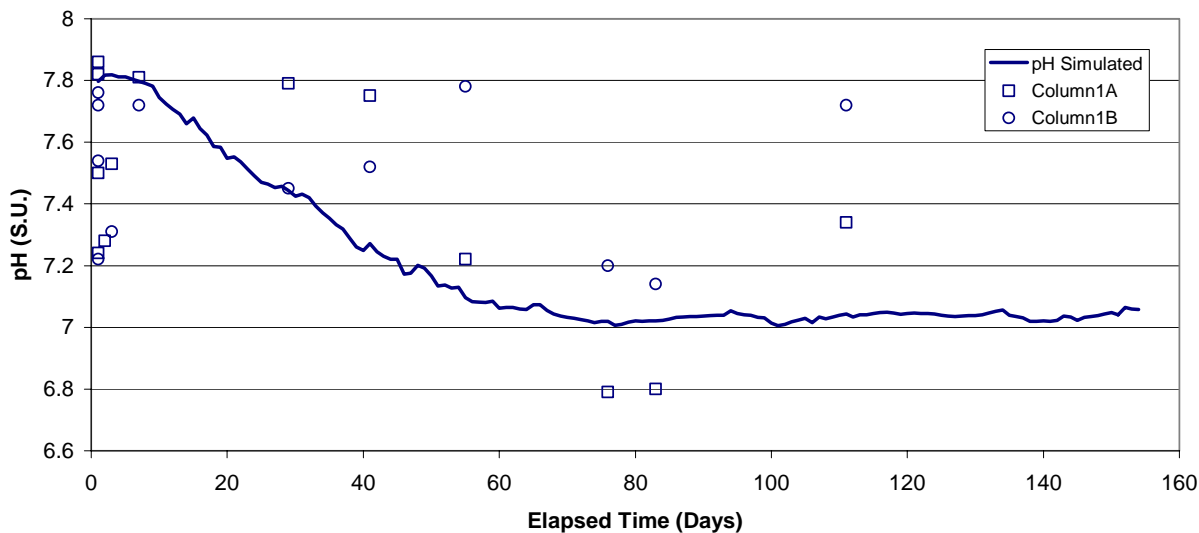


Figure 4-37
Simulated and Observed pH for Column 1

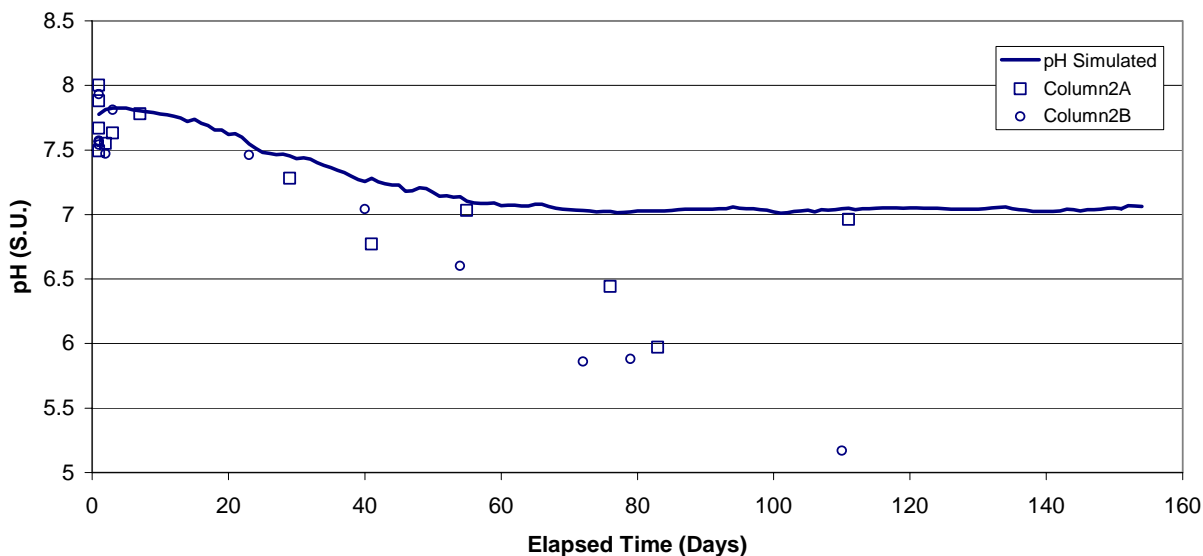


Figure 4-38
Simulated and Observed pH for Column 2

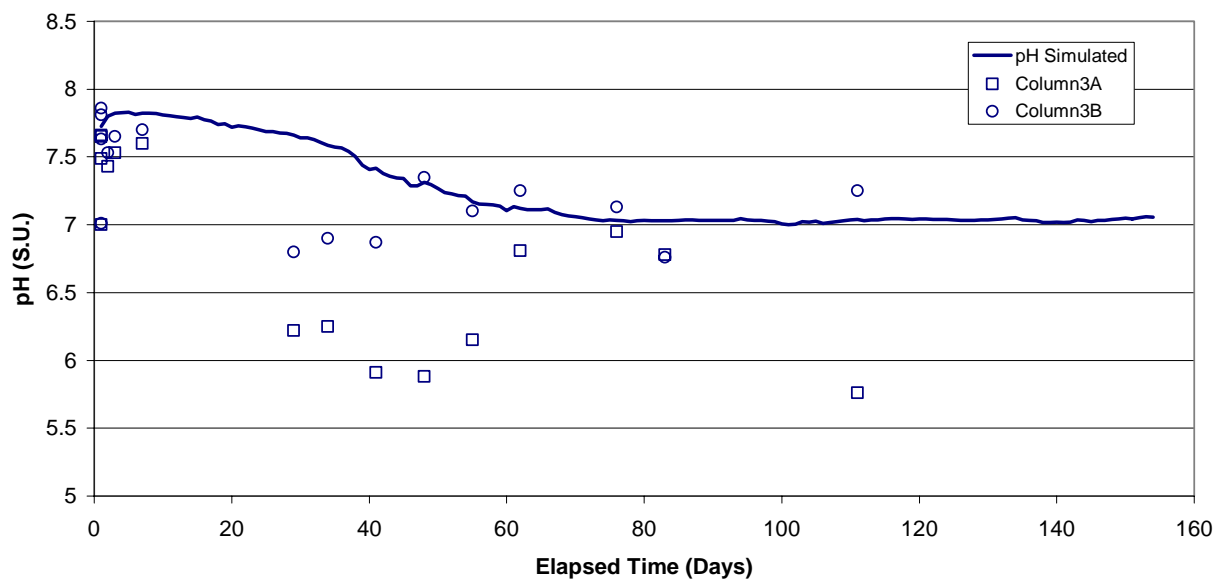


Figure 4-39
Simulated and Observed pH for Column 3

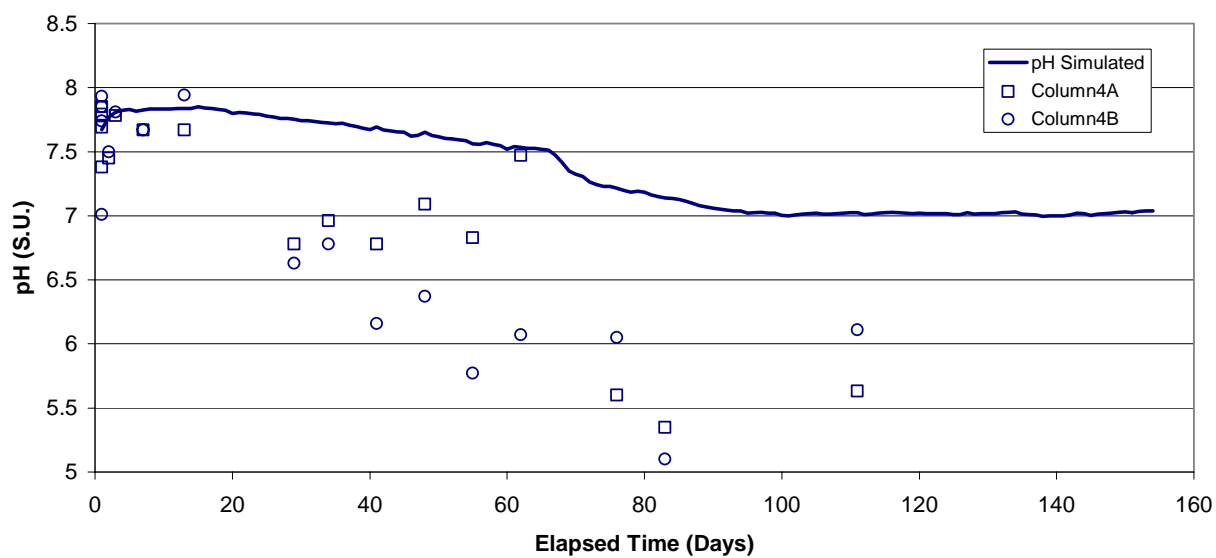


Figure 4-40
Simulated and Observed pH for Column 4

Statistical Analysis

To provide a statistical summary of the goodness of fit, the R^2 values and mean flows and concentrations for each column were compared. Figure 4-41 shows the maximum R^2 values for each calibration run. Most R^2 values fell between 0.4 and 0.8. High R^2 values were calculated for flow, nitrate, pH, and alkalinity. Lower R^2 values were calculated for fecal coliform bacteria, BOD, total nitrogen, and total phosphorous. The low R^2 values calculated for column 4 illustrated the difficulty of matching model simulations with the highly scattered data for this column.

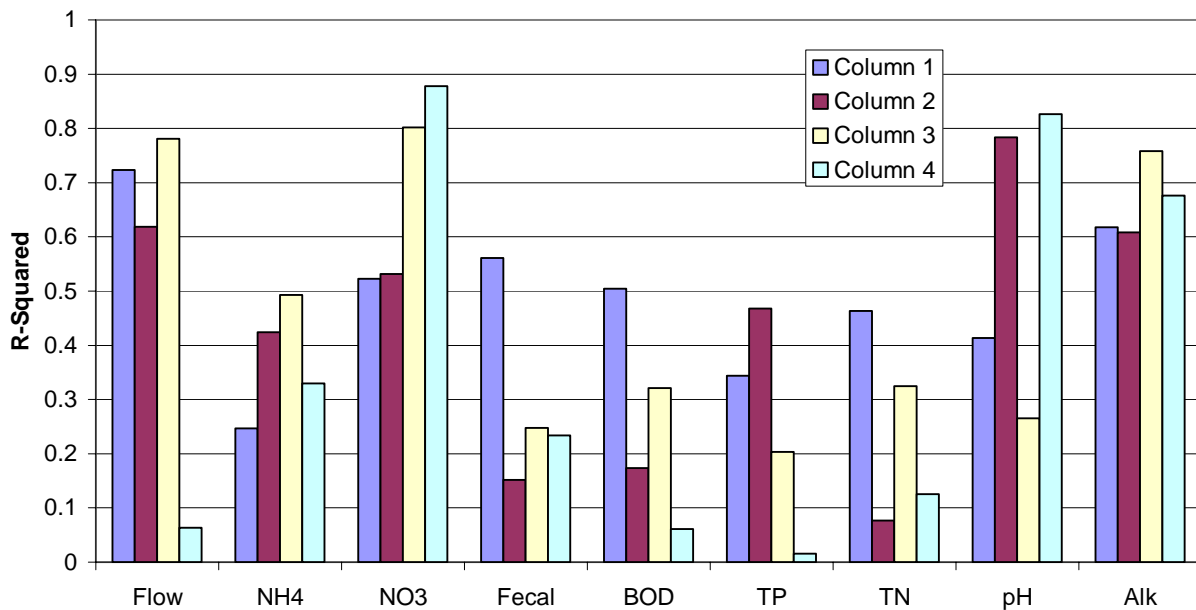


Figure 4-41
 R^2 Values for Each Parameter and Column

The comparison of mean flow and concentrations for each simulation and data set provides another mechanism for evaluating model performance with respect to observed data. Figure 4-42 through Figure 4-50 show the mean values for flow, ammonia, nitrate, fecal coliform bacteria, BOD, total phosphorus, total nitrogen, alkalinity, and pH respectively. For most parameters, the simulated means lie within the range of the observed means. The best comparison is observed for flow, total phosphorus and total nitrogen. The poorest comparison of means is observed for ammonia and BOD. The results for column 1B show little nitrification as compared to the model.

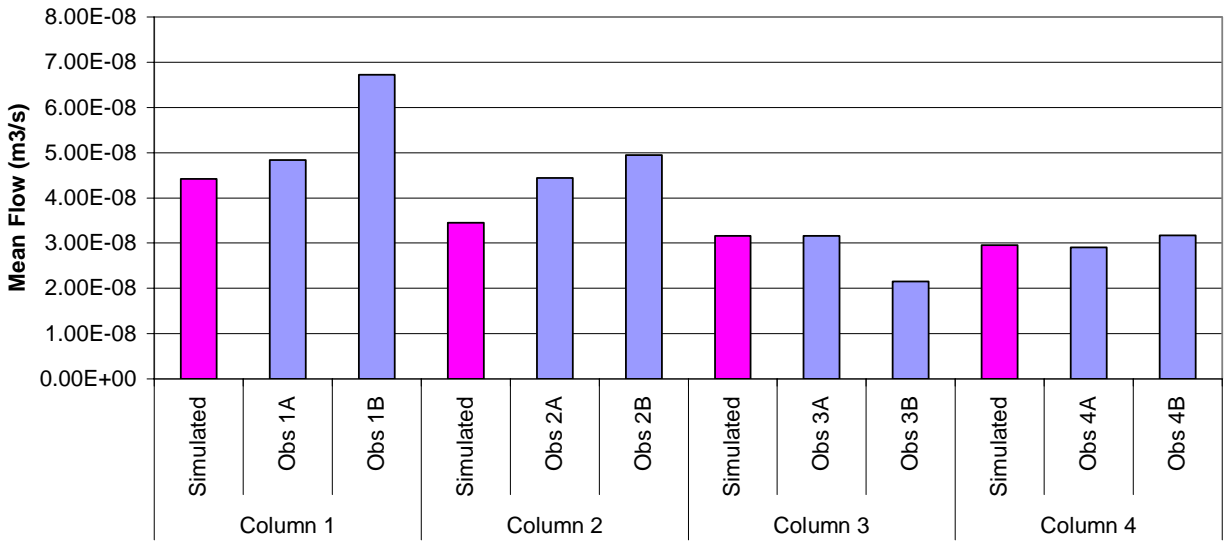


Figure 4-42
Simulated Mean Biozone Flow Compared to Mean Measured Flow for Each Column

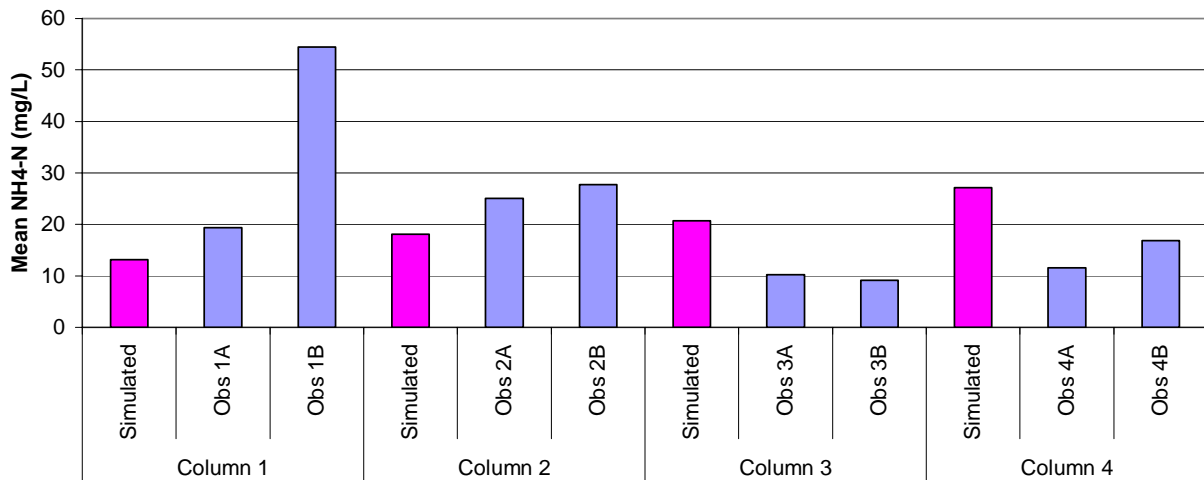


Figure 4-43
Simulated Mean Biozone Ammonia Compared to Mean Measured Ammonia for Each Column

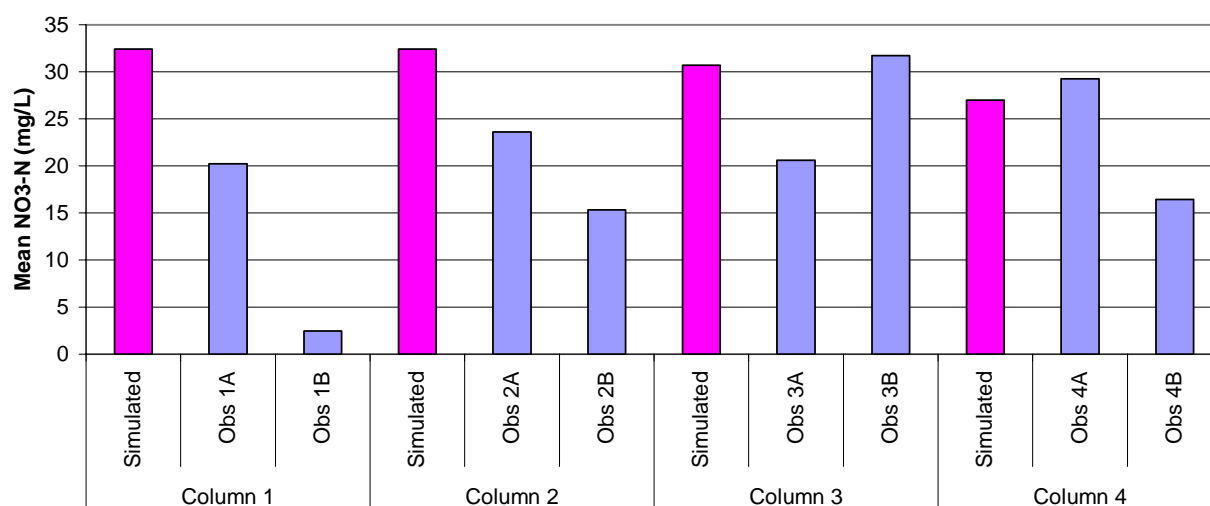


Figure 4-44
Simulated Mean Biozone Nitrate Compared to Mean Measured Nitrate for Each Column

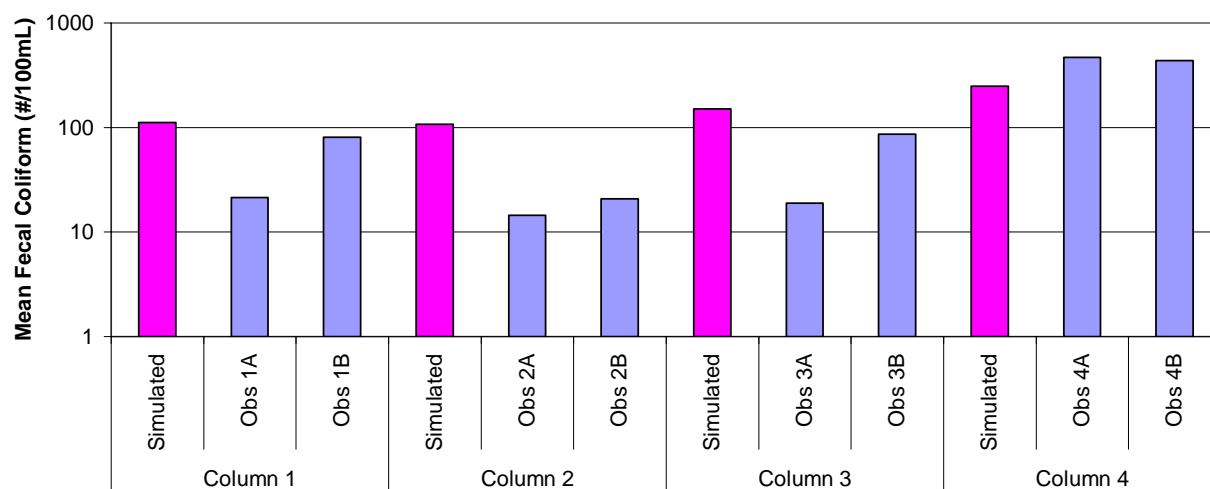


Figure 4-45
Simulated Mean Biozone Fecal Coliform Bacteria Compared to Mean Measured Fecal Coliform Bacteria for Each Column

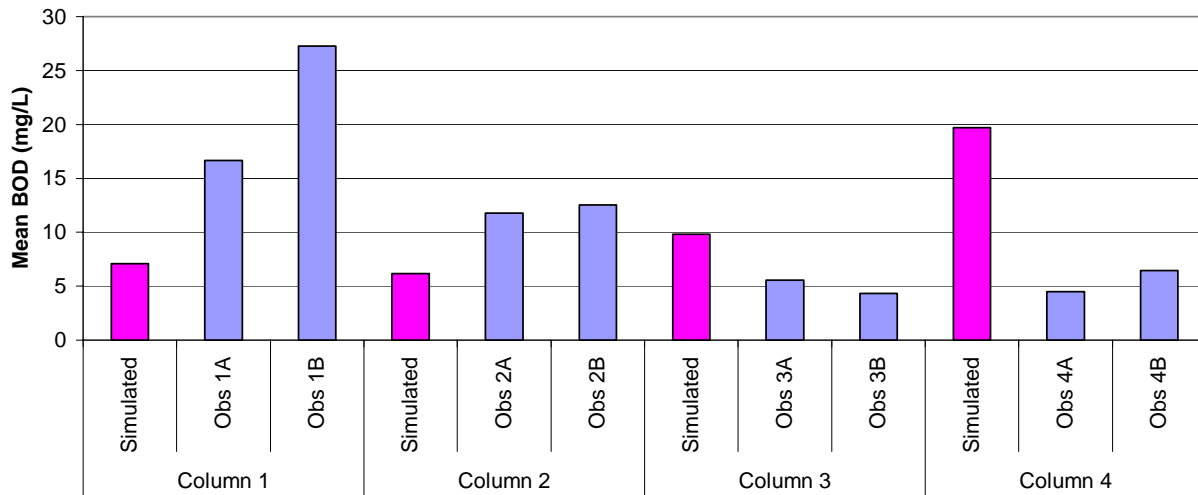


Figure 4-46
Simulated Mean Biozone BOD Compared to Mean Measured BOD for Each Column

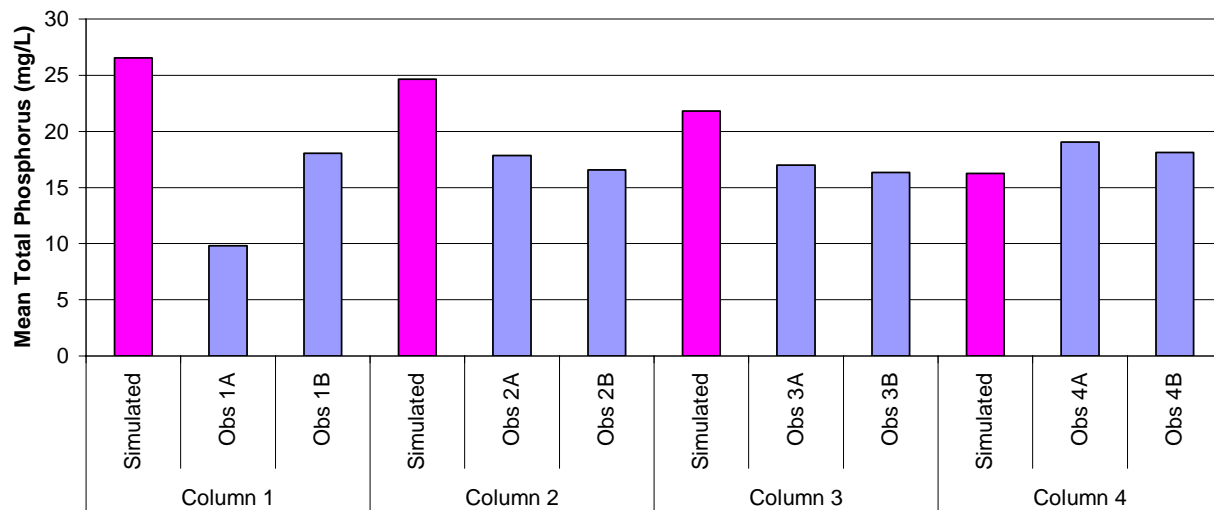


Figure 4-47
Simulated Mean Biozone Total Phosphorus Compared to Mean Measured Total Phosphorus for Each Column

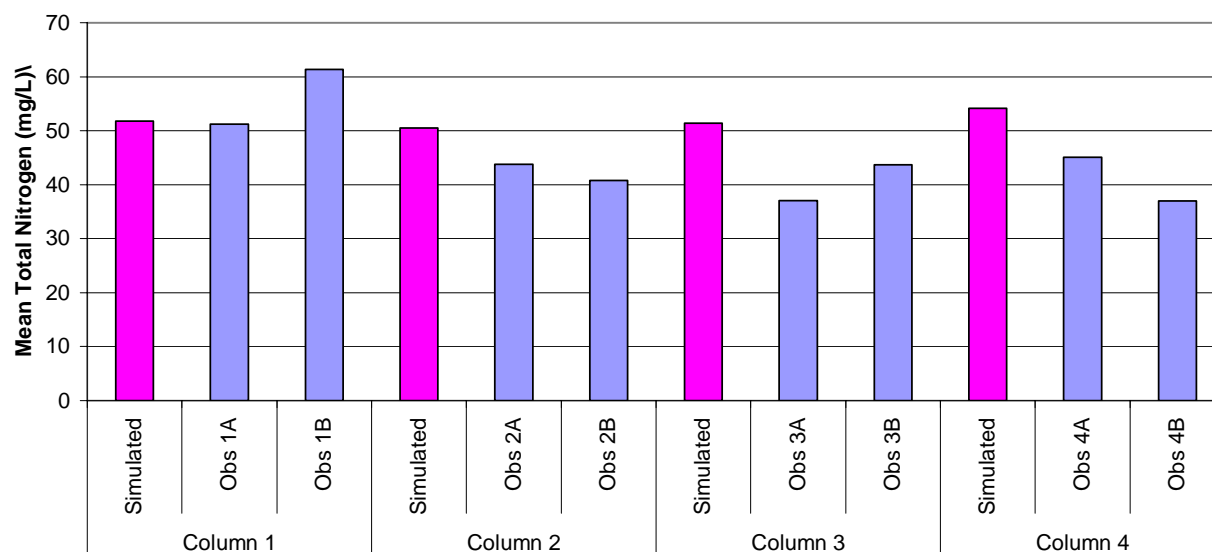


Figure 4-48
Simulated Mean Biozone Total Nitrogen Compared to Mean Measured Total Nitrogen for Each Column

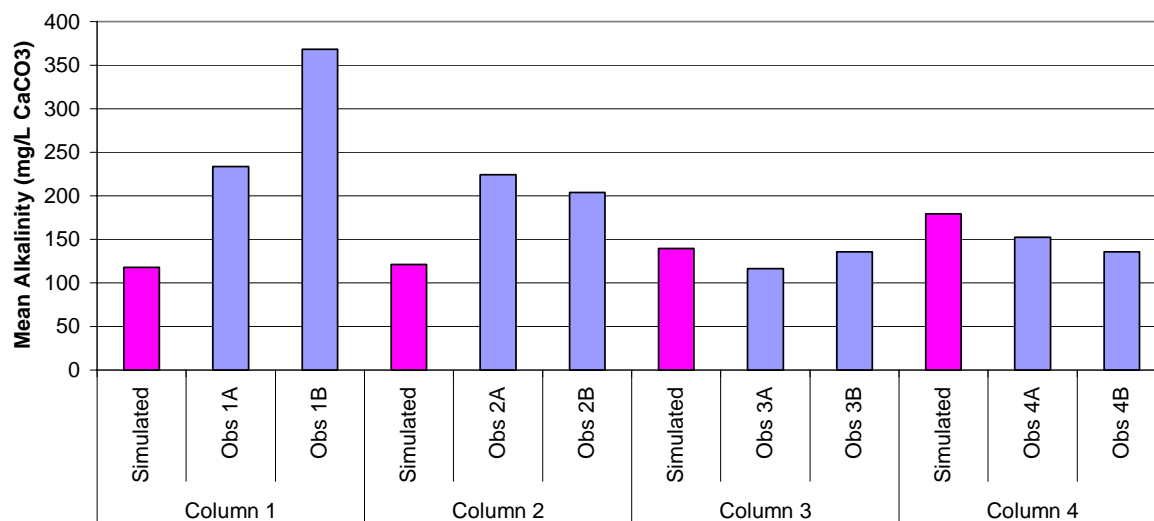


Figure 4-49
Simulated Mean Biozone Alkalinity Compared to Mean Measured Alkalinity for Each Column

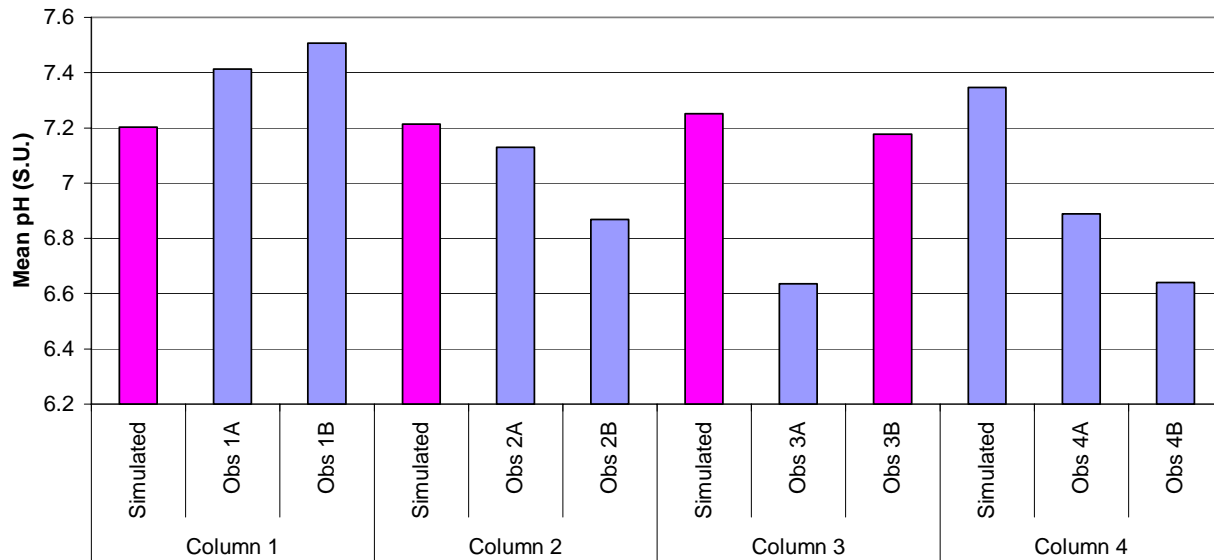


Figure 4-50
Simulated Mean Biozone Ph Compared to Mean Measured Ph for Each Column

Discussion

The goal of calibration of the biozone algorithm to the one-dimensional column data was to establish reasonable values for the empirical coefficients contained in the model formulations. The model was tested against all four dosing rates applied during the experiment and all model coefficients were kept the same among simulation runs. All simulations were of the entire length of the column including both the biozone and underlying sand. The model produced reasonable trends that were comparable to most column data sets. Model results were compared to observed data using visual match and comparisons of correlation coefficients and means. In several cases, the scatter of observed data due to the inherent variability of a physical system was not reproduced by the model. However, results indicated that the model did capture the effect of the biozone development on infiltration, purification processes, and constituent transformation.

This calibration is only the initial effort of model calibration. Further calibration and algorithm refinement can be made in the future with field data being collected at Mines Park (Appendix D, *Biozone Genesis and WSAS Performance: Field 3-D Test Cells*).

Simulation of Field Scale OWS

A normal OWS has a WSAS substantially larger than the cross-sectional area of the columns used in the laboratory experiment. On a per unit area basis, the daily hydraulic loading rates of a full-scale OWS are substantially lower than the rates used in the laboratory (such as 2 to 4 cm/d versus 16 to 160 cm/d). The next step is to apply the biozone module to simulate a full-scale OWS, using the model coefficients obtained in the calibrations using the laboratory data.

Unfortunately for this test, there were no observed flow or water quality data to compare against the model results. The reasonableness of the model can be judged by whether it predicts the time of hydraulic failure of OWS comparable to previous field experience.

Being a deterministic model, the biozone module will predict the same failure time for all OWS under the same operating conditions. However, field experience indicates that not all OWS fail at the same time. A theory is that all systems of a given type of OWS (such as STE to a WSAS) may not be operated under uniform conditions. For example, each OWS in the field may receive different loading rates of STE with different effluent concentrations, the WSAS may be installed differently, and/or the WSAS may be installed in different soil or climatic conditions. Thus, the time for the hydraulic failures of field OWS will have a range of values.

A Jackknife simulation has previously been adapted from Efron (1982) and Efron and Gong (1983) for sensitivity analysis with WARMF (Chen *et al.* 2001b). This technique was used to determine the range of times for hydraulic failure of field OWS. For the Jackknife simulations, STE flow rates were taken from the 10th percentile (90 L/c/day), 50th percentile (165 L/c/day) and the 90th percentile (300 L/c/day) as discussed in Appendix A, *Input Parameters for Modeling Flow and Transport in Onsite Wastewater Systems*. With an average WSAS area of 125 m², this translates to daily loading rates ranging from 0.2 to 0.6 cm/day/person. BOD concentrations of STE typically range from 140 to 200 mg/L (Siegrist *et al.* 2001). Low, medium, and high values of BOD in STE were 140, 170, and 200 mg/L respectively.

A Jackknife table was prepared for all possible combinations of low, medium, and high values of STE flow rates and BOD concentrations of STE shown in Table 4-4. The model was set up to perform a simulation for each combination, one at a time. The outputs were analyzed for the statistical spread of time for hydraulic failure of a conventional OWS.

Table 4-4
Low, Medium, and High Values of Dosing Rates and BOD Concentrations

Parameters	STE Flow Rate (L/c/day)	STE BOD Concentration (mg/L)
Low Value	90	140
Medium Value	165	170
High Value	300	200

The project team soon found that there was no official definition for the hydraulic failure of a field OWS. From a modeling standpoint, one end point for the hydraulic failure can be defined as the time when the infiltration through the biozone is compromised and the ponding first starts. The other end point can be the complete failure when the infiltration rate through the biozone becomes virtually zero, or minimum.

Figure 4-51 presents the statistical distribution of predicted times to first ponding and minimum infiltration for the nine Jackknife simulations. The time to failure ranges from approximately six years to greater than 35 years. The model predicts a 70% chance that failure of a conventional OWS would occur before 25 years, and that the time between first ponding and minimum infiltration through the biozone would be approximately one year. These results are reasonable with respect to typical OWS life spans of 10 to 25 years (Siegrist *et al.* 2001).

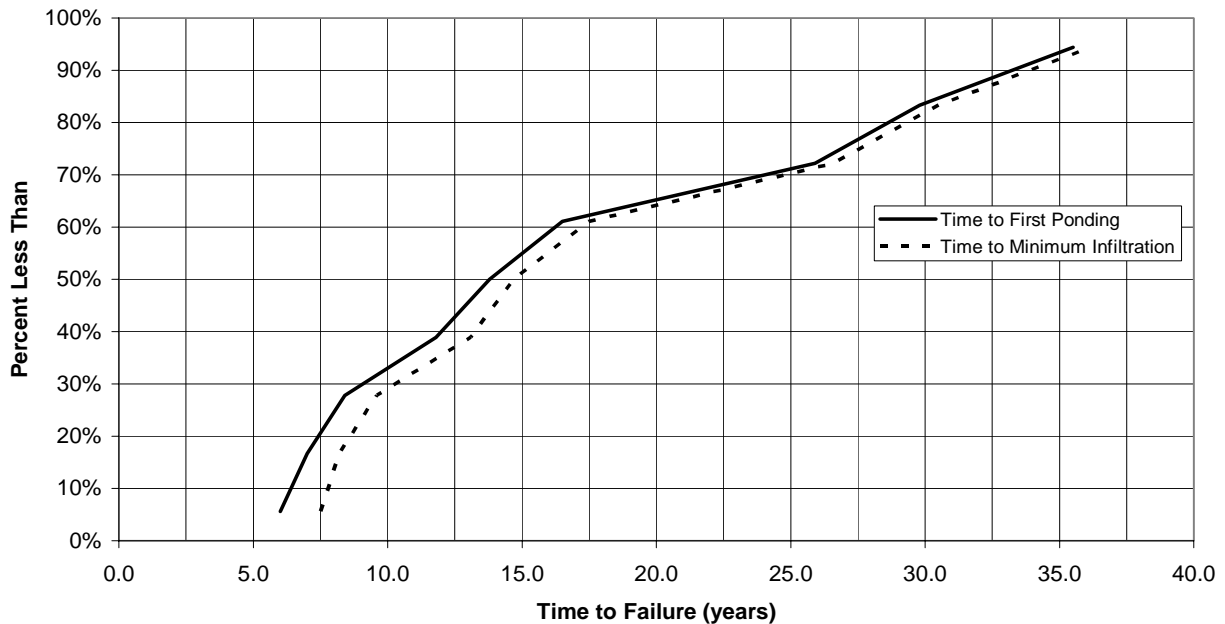


Figure 4-51
Frequency Distribution of Time to Failure for OWS Simulated with the Biozone Algorithm

Implementation in WARMF

After the calibration with laboratory data and the testing for simulating a full-scale OWS, the biozone module was incorporated into WARMF. The work included the development of input dialogs for users to enter biozone reaction rates (Figure 4-52) and biozone coefficients (Figure 4-53). The model coefficients, calibrated with experimental data, were imported into WARMF for default values.

An option was provided for users to bypass the biozone algorithm. For that, the biozone area of the catchments is set to zero. Then the users must, instead of inputting typical STE quality, specify the water quality concentrations of ammonia, nitrate, BOD and fecal coliform bacteria leaving the biozone and entering the soil. With WARMF, the OWS can be varied yielding a maximum of three types within a watershed. Each OWS of the same type will have the same daily loading rate, pollutant concentrations, biomass buildup, infiltration, and hydraulic failure (for example, all conventional OWS may have a daily loading rate of 5 cm/d while all OWS with sand filters may have a daily loading rate of 25 cm/d).

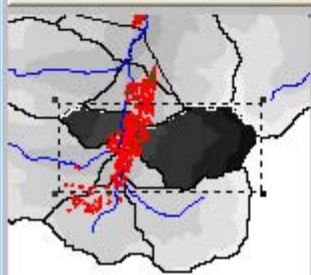
WARMF will start the simulation with the initial biomass concentration of the biozone set to zero. For that reason, the first few months of simulation will not be accurate for a watershed where the biozone is already mature. There are three options to handle this inaccuracy. One is to simply ignore the simulation results of the first few months. Another is to specify initial biomass of the mature biozone. Lastly, one can run the model for one year using a warm start procedure of WARMF. WARMF will save the intermediate results including the initial biomass of the biozone for a continued simulation. More details on the application of WARMF to the Dillon Reservoir watershed are given in Chapter 5, *Application of WARMF in the Dillon Reservoir Watershed*.

Subcatchment 187

Physical Data | Meteorology | Land Uses | Land Application | Irrigation | Sediment | BMP's
 Point Sources | Pumping | Septic Sys. | Reactions | Soil Layers | Mining | CE-QUAL-W2

Reaction Rates

	Soil	Surface	Canopy	Biozone
BOD Decay, 1/d	0.000055	0	0	108
Organic Carbon Decay, 1/d	0.000055	0	0	0
Nitrification, 1/d	0.1	0.1	0.01	3
Denitrification, 1/d	0.025	0	0	0.05
Sulfate Reduction, 1/d	0	0	0	0
Pesticide 1 Decay, 1/d	1	0	1	0
Pesticide 2 Decay, 1/d	1	0	1	0
Pesticide 3 Decay, 1/d	1	0	1	0
Sediment 1 Settling, m/d	0	0	0	0
Sediment 2 Settling, m/d	0	0	0	0
Sediment 3 Settling, m/d	0	0	0	0
Algae 1 Growth, 1/d	1.1	0	0	0



☐ Apply Changes To Selected
☐ Apply Changes To All
☒ Write Output To File

Figure 4-52
 WARMF Input Dialog for Biozone Reaction Rates

Subcatchment 1633

Physical Data | Meteorology | Land Uses | Land Application | Irrigation | Sediment | BMP's
 Point Sources | Pumping | Septic Sys. | Reactions | Soil Layers | Mining | CE-QUAL-W2

Discharge Layer

Population Served by Septics

Distribution of Septic Systems (total should = 100)

Treatment Type 1 (%)

Treatment Type 2 (%)

Treatment Type 3 (%)

Initial Biomass (g/cm2)

Biomass Thickness (cm)

Biozone Area (m2)

Biomass Respiration (1/d)

Biomass Mortality (1/d)

☐ Apply Changes To Selected
☐ Apply Changes To All
☒ Write Output To File

Figure 4-53
WARMF Input Dialog for OWS and Biozone Coefficients

Summary

The biozone algorithm was developed and tested with the data from laboratory column experiments. The model predicted the build up of biomass bacteria, an increase in field capacity, a decrease in porosity and a decrease in throughput over time. The model also predicted the nitrification of ammonia, denitrification of nitrate, and the decay of BOD and fecal coliform bacteria. After calibration, the biozone module was incorporated into the watershed scale model WARMF. The operation time before potential hydraulic failure of a conventional OWS was also tested using Jackknife simulations of a full-scale OWS.



5 APPLICATION OF WARMF IN THE DILLON RESERVOIR WATERSHED

This chapter provides information pertaining to the application of WARMF to the Dillon Reservoir watershed. The reservoir is west of Denver, Colorado and provides the city of Denver with drinking water.

Introduction

WARMF was applied to the Dillon Reservoir watershed using data from several sources. The model was calibrated against stream water quality data collected during this study (Appendix E, *Water Quality Monitoring*). Verification was performed using an existing data set from the early 1990s. WARMF was then used to simulate several management scenarios including the replacement of OWS with sewerage and a centralized WWTP.

General Input Data

The site-specific data of the Dillon Reservoir watershed were imported into WARMF during the model set-up. Some data were readily available from national databases over the Internet and other data were either collected as part of this project or tracked down from local sources.

Digital Elevation Model (DEM)

WARMF imports DEM data, which were used to delineate the watershed into subcatchments, rivers, and lake. These data are readily available from the United States Geological Survey (USGS) at a 30-meter resolution (<http://edc.usgs.gov/geodata/>). During the delineation, decisions are made regarding the resolution of catchment, river, and reservoir segmentation. Generally, regions with a higher variance of land use and a higher density of urban activity, point sources, and water quality sampling stations are set up with a higher resolution than undeveloped regions that contribute little loading.

Figure 5-1 presents the base map of the Dillon Reservoir watershed created by WARMF. The total drainage area of Dillon Reservoir watershed is 842 km² (325 mile²). Based on the DEM data, the watershed was divided into 122 land catchments, 98 stream segments, and one reservoir containing roughly 30 layers. WARMF calculates the area, aspect, and slope of land catchments and the upstream and downstream elevations of stream segments. The watershed has four major tributaries: Snake River, Swan River, Blue River, and Tenmile Creek.

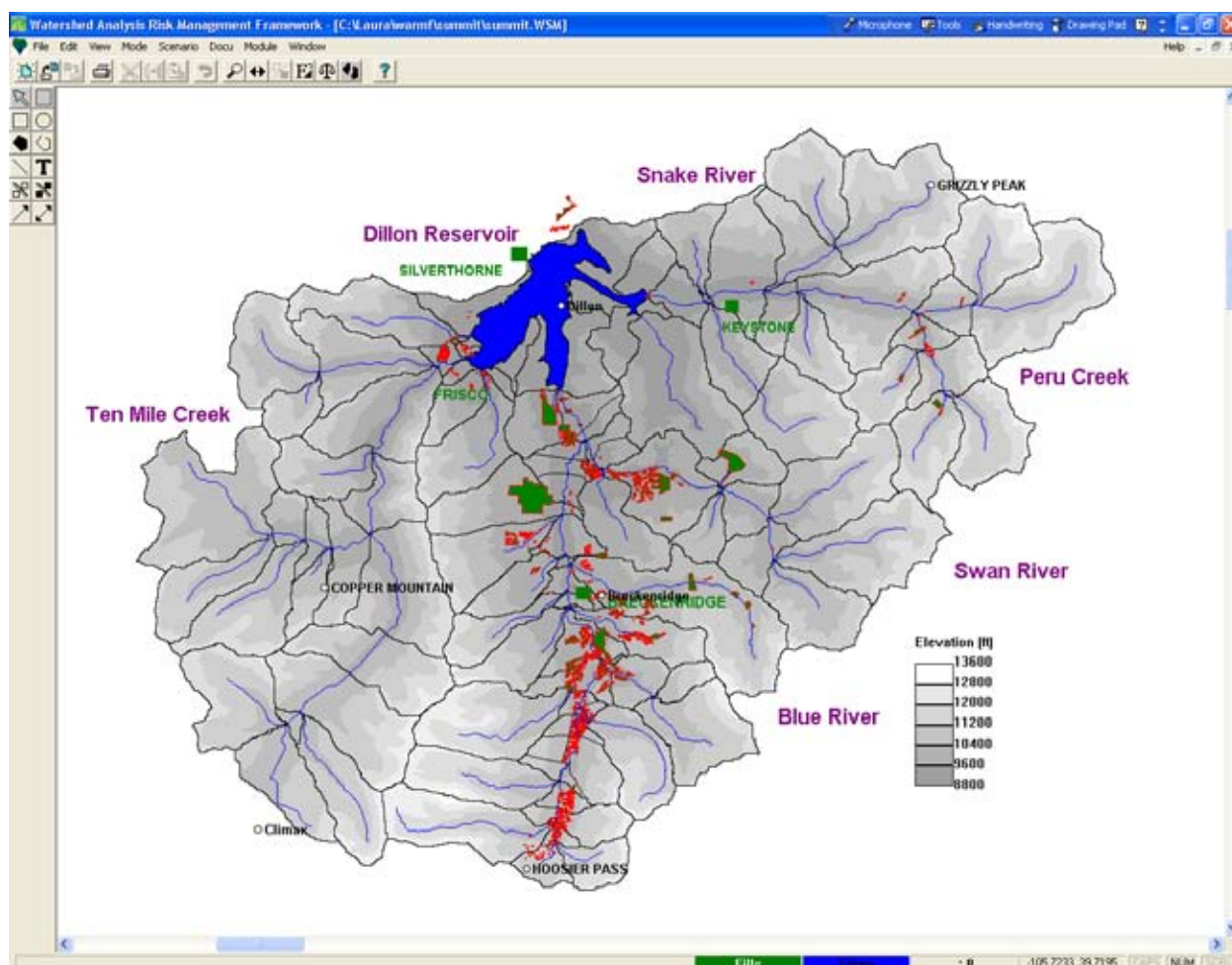


Figure 5-1
WARMF Map of the Dillon Reservoir Watershed

Meteorology

WARMF hydrology calculations are driven by meteorology. The meteorology data includes daily values of precipitation, minimum temperature, maximum temperature, cloud cover, dewpoint temperature, air pressure, and wind speed. Precipitation and temperature data were compiled for six stations in or near the Dillon Reservoir watershed for 1989 through 2002 (Table 5-1). Dewpoint temperature and wind speed data were obtained from Eagle County Airport. Due to lack of data for a nearby station, air pressure information from Denver was used after an adjustment was made to account for the elevation difference. Cloud cover for each station was estimated from temperature, precipitation, and dewpoint temperature.

Each catchment is assigned a nearby meteorological station. Precipitation weighting and temperature lapse factors are used to account for orographic effects between the catchment and its meteorology station. The estimate of adjustment factors was based on a review of precipitation isohyetal maps, ground elevation, and prevailing wind.

Table 5-1
Meteorology Stations for WARMF Application of Blue River Watershed

Station Name	ID Number	Source	Latitude	Longitude
Breckenridge	050909	NCDC	39.480	-106.030
Climax	051660	NCDC	39.383	-106.200
Copper Mountain	05019	NRCS-SNOTEL	39.483	-106.167
Dillon	052281	NCDC	39.600	-106.050
Grizzly Peak	05028	NRCS-SNOTEL	39.650	-105.867
Hoosier Pass	05030	NRCS-SNOTEL	39.367	-106.067

NCDC = National Climatic Data Center

NRCS-SNOTEL = National Resources Conservation Service SNOpack TELemetry system

Air Quality

Wet and dry deposition of various water quality constituents are important input to the watershed. Air quality data were obtained from the EPA Clean Air Status and Trends Network (CASTNET). The closest station to the watershed was GOTHIC (GTH161), located approximately 64 miles southwest of the watershed (Latitude: 38.9573, Longitude: -106.985). Air deposition data are usually broken down into wet and dry fractions. Dry deposition will fall on any given day and accumulate on the ground surface. Wet deposition is based on the average concentration of constituents in precipitation. This concentration is multiplied by the daily precipitation to determine a wet deposition load.

Point Sources

Available point source data for all discharges in the Dillon Reservoir watershed were also compiled and imported into WARMF (Table 5-2). This data included five major discharges and eight minor discharges. Major stations have flows greater than 0.25 million gallons per day (MGD). Nine point sources are discharged to surface waters. Three minor point sources are discharged to groundwater.

Table 5-2
Point Source Dischargers in Dillon Reservoir Watershed

Name	NPDES #	Average Discharge (MGD)	Type	Receiving Water	Ave. NH ₄ Load (kg/d) ¹	Ave. NO ₃ Load (kg/d) ¹	Ave. P Load (kg/d) ¹
Frisco WWTP	CO 0020451	0.499	Major—Municipal	Reservoir	4.67	20.16	0.12
Breckenridge WWTP	CO 0021539	1.178	Major—Municipal	Reservoir	55.54	23.98	0.17
Copper Mountain WWTP	CO 0021598	0.261	Major—Municipal	River	4.39	9.89	0.070
Iowa Hills Water Reclamation WWTP	CO 0045420	0.607	Major—Municipal	River	1.45	26.65	0.79
Snake River WWTP	CO 0029955	0.500	Major—Municipal	Reservoir	1.08	25.58	0.035
Ralston Resorts, Keystone	CO 0027995	0.006	Minor—Ski Resort	River	—	0.078	0.00067
Arapahoe Basin Ski Area	CO 0023876	0.007	Minor—Ski Resort	River	0.13	—	0.00046
Alpine Rock Company McCain Pit	COG 500141	0.180	Minor—Industrial	River	—	—	0.0026
Frisco, Wayne Bristol Water Supply	COG 640067	0.046	Minor—Municipal	Reservoir	—	—	0.035
CDOH—Vail Pass Rest Area	CO 0042731	0.003	Minor—Rest Area	Ground-water	—	0.026	0.0012
BSD McDill Placer Aspen	CO 0029211	0.004	Minor—Municipal	Ground-water	—	0.040	0.00041
BSD Valley of the Blue	CO 0027197	0.001	Minor—Municipal	Ground-water	—	0.0089	0.00026
BSD South Blue River WWTP	CO 0041581	0.017	Minor—Municipal	Ground-water	—	0.16	0.015

¹ Flow and loading data is model input based on available discharge monitoring data for each discharge from 1984 to 2002.

Land Use

A geographic information system (GIS) shape file for land use, developed by USGS Land Use Land Cover (LULC), was obtained from the BASINS database and imported into WARMF (Figure 5-2). The polygons of land uses were overlaid with those of catchments to calculate the percents of land uses for each catchment. The land use of the Dillon Reservoir watershed is primarily coniferous forest, herbaceous, shrub/brush, and alpine rock. Most commercial and residential land is concentrated along the Blue River Valley or near Dillon Reservoir. Several ski resorts populate the region as well.

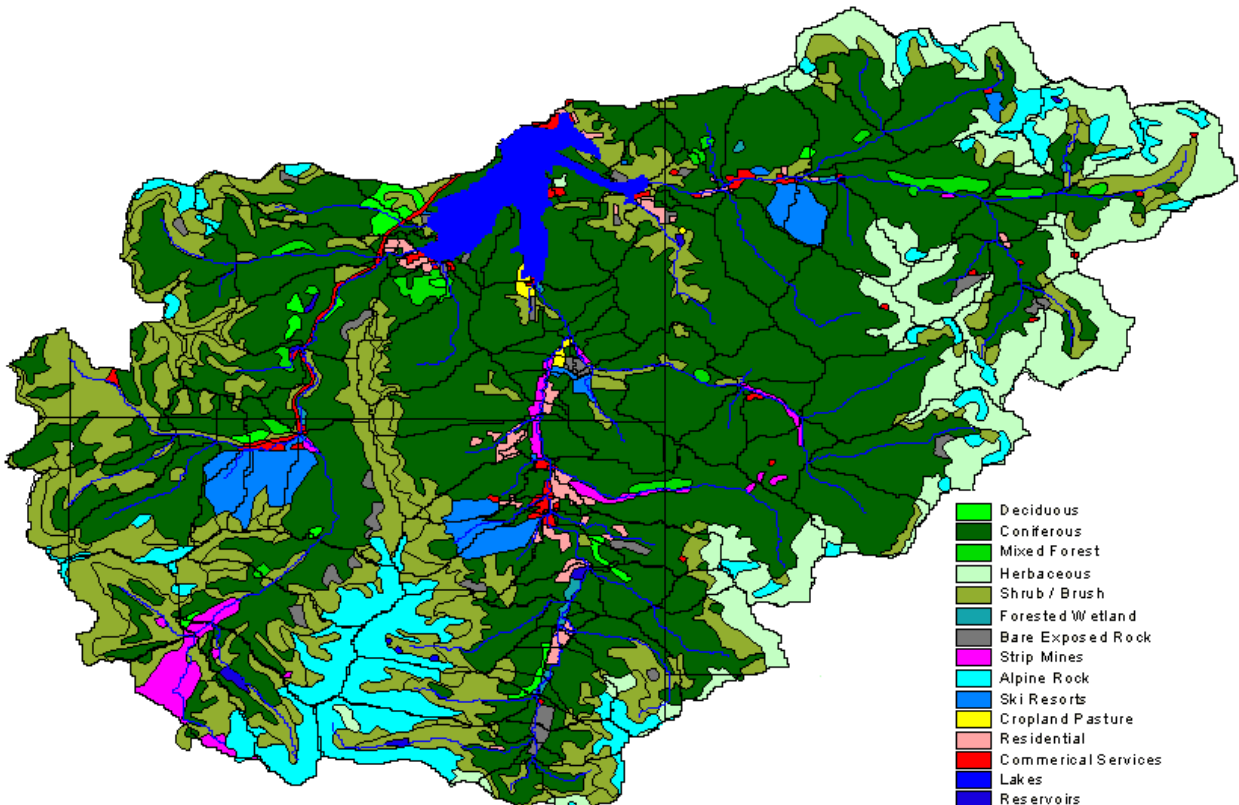


Figure 5-2
Land Use Map of the Dillon Reservoir Watershed

Managed Flow

Managed flow includes diversions from rivers and reservoirs, and reservoir releases and spills. Table 5-3 lists the managed flow for the Dillon Reservoir watershed. Three small diversions remove water from the tributaries and upper reaches of the Blue River near Hoosier Pass. The water diverted is transported over the Continental Divide and out of the watershed. Dillon Reservoir releases flow to the Lower Blue River and Roberts Tunnel transports water to the City of Denver.

Table 5-3
Managed Flow in the Dillon Reservoir Watershed

Managed Flow	Location	Data Source
McCullough-Sp-Diversion	Hoosier Pass	USGS 09044800
Bemrose-Hoosier Diversion	Hoosier Pass	USGS 09044300
Monte Cristo Diversion	Hoosier Pass	USGS 09041900
Dillon Reservoir Release	Dillon Reservoir	USGS 09050700
Roberts Tunnel Diversion	Dillon Reservoir	Denver Water

Observed Stream Flow

Observed stream flow data were used for comparison to model predictions during hydrology calibration. Data from nine stations within the watershed were obtained and imported into WARMF (Table 5-4).

Table 5-4
Observed Stream Flow Stations in Dillon Reservoir Watershed

File Name	Station	Source	Latitude	Longitude	Period of Record
Blueriv1	Blue River at Blue River, Co.	USGS 09046490	39.4558	-106.031	Continuous, 1989–2002
Blueriv2	Blue River near Dillon, Co.	USGS 09046600	39.5667	-106.049	Continuous, 1989–2002
French	French Gulch at Breckenridge	USGS 09046530	39.4931	-106.044	Continuous, 1989–2002
Keygulch	Keystone Gulch near Dillon, Co.	USGS 09047700	39.5944	-105.972	Continuous, 1989–2002
Miners	Miners Cr. above L. Dillon	Summit Co. –MIN	39.57	-106.088	Bi-monthly, 1984–1995
Snake	Snake River near Montezuma, Co.	USGS 09047500	39.6056	-105.933	Continuous, 1989–2002
Snake2	Snake River above Dillon Reservoir	Summit Co.—SRL	39.6017	-105.996	Bi-monthly, 1984–1995
Soda	Soda Cr. above L. Dillon	Summit Co.—SOD	39.595	-106.008	Bi-monthly, 1984–1995
Tenmile	Tenmile Creek Bl North Tenmile Cr., at Frisco, Co.	USGS 09050100	39.5769	-106.109	Continuous, 1989–2002

Observed Water Quality

Observed water quality data for six major stations and 14 minor stations were also compiled and entered into WARMF (Table 5-5). In addition, the field data collected by the Colorado School of Mines (CSM) were also entered into WARMF. The sampling from these stations is discussed in Appendix E, *Water Quality Monitoring*. In WARMF, the observed water quality data were used only for comparison to model predictions.

Table 5-5
Observed Water Quality Stations in Dillon Reservoir Watershed

File Name	Station	Source	Latitude	Longitude
blue2	Blue R. above Blue R., CO	STORET	39.410	-106.047
blue4	Blue R. near Dillon, CO	STORET	39.549	-106.039
blueadam	Blue R. at Adams Street	STORET	39.479	-106.046
BR-1	Blue R. above McCollough Gulch	CSM	39.403	-106.050
BR-10	Blue R. above Dillon Reservoir	CSM/STORET/ Summit Co.	39.567	-106.050
BR-2	Blue R. above Penn. Gulch	CSM	39.423	-106.042
BR-3	Blue R. above Penn. Gulch	CSM	39.430	-106.043
BR-5	Blue R. at Blue River, CO	CSM/STORET	39.456	-106.031
BR-6	Blue R. below Blue River, CO	CSM	39.469	-106.045
BR-7	Blue R. below French Gulch	CSM/STORET	39.498	-106.047
BR-8	Blue R. west of Ten Mile Vista	CSM	39.533	-106.047
BR-9	Blue River above Swan River	CSM	39.543	-106.040
BR-4W	Blue River below Penn. Gulch	CSM	39.448	-106.034
deer	Deer Creek	STORET	39.564	-105.861
french1	French Gulch above Rich Gulch	STORET	39.486	-105.977
FT-1	Tenmile Cr. blw N. Tenmile Cr.	CSM/STORET	39.575	-106.110
FT-2	Tenmile Creek at Frisco	CSM/STORET/ Summit Co.	39.579	-106.097
GG-1	Gold Run Gulch	CSM	39.530	-106.029
keystone	Keystone Gulch near Dillon, CO	STORET	39.594	-105.972

Table 5-5
Observed Water Quality Stations in Dillon Reservoir Watershed (Cont.)

File Name	Station	Source	Latitude	Longitude
miners	Miners Creek above Dillon Reservoir	Sum. Co.	39.570	-106.088
PC-1	Upper Pennsylvania Gulch	CSM	39.428	-106.027
PC-2	Pennsylvania Gulch (S. Fork)	CSM	39.430	-106.041
PC-3	Pennsylvania Gulch (N. Fork)	CSM	39.434	-106.040
peru	Peru Creek at mouth	STORET	39.597	-105.872
SC-1	Spruce Creek	CSM	39.441	-106.047
snake1	Snake River above Keystone	STORET	39.606	-105.942
snake2	Snake River below Keystone	STORET/ Summit Co.	39.602	-105.996
Soda	Soda Creek above Dillon Reservoir	Summit Co.	39.595	-106.008
SR-1	Upper Swan River	CSM	39.525	-105.982
SR-2	Swan River above Gold Run Gulch	CSM	39.531	-106.027
SR-3	Swan River at mouth near Frisco	CSM / STORET	39.541	-106.037
Stjohn	St. Johns at Montezuma	STORET	39.579	-105.878
tenmile2	Tenmile Creek at Kokomo	STORET	39.450	-106.200
w10mile1	W. Tenmile Creek below Copper	STORET	39.503	-106.167
w10mile2	W. Tenmile Creek at Shrine Pass	STORET	39.500	-106.167

STORET = US EPA's STOrage and RETrieval database (www.epa.gov/storet)

Monitoring Well Data

Monitoring well (MW) data were collected in the Dillon Reservoir watershed as part of this project. Details regarding these data are presented in Appendix E, *Water Quality Monitoring*. Soil profile and water table data taken during well drilling were used to define the soil layer thickness. Soil sieve analysis data provided estimates for the composition of clay, silt, and sand. The cation exchange capacity measured in the soil samples were input into WARMF. Hydraulic conductivity of the soil was estimated to range from 300 to 8,000 cm/day. Hydraulic conductivity of soil in WARMF was set to range from 800 to 2,000 cm/day.

Water qualities of well samples were used to compare against groundwater concentrations predicted by WARMF. Table 5-6 shows the average concentrations of two wells sampled in the Blue River Estates region (MW1 and MW2) compared with the average concentrations calculated by WARMF in nearby catchments. Most concentrations are within the same order of magnitude for both simulated and observed.

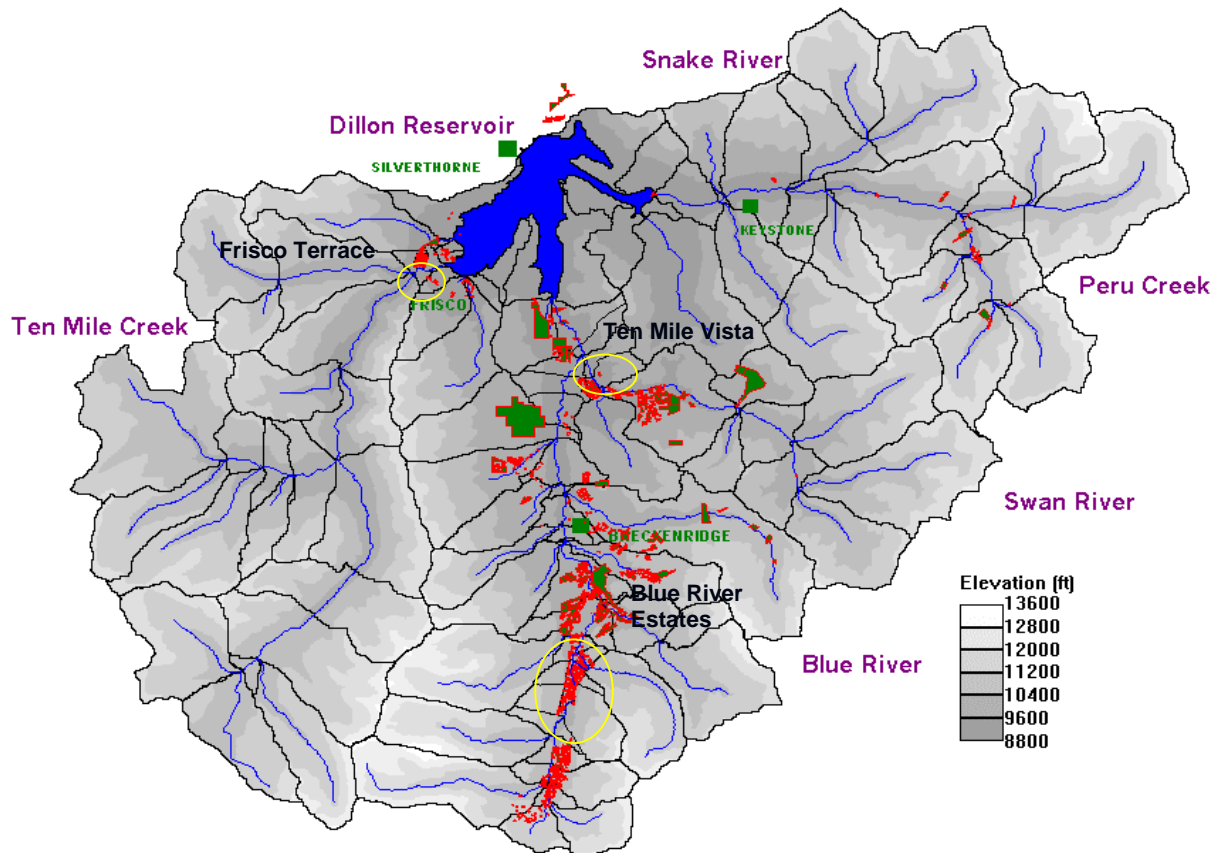
Table 5-6
Comparison of Well Sampling Data and WARMF Predicted Soil Solution Concentrations for Blue River Estates

Parameter	Ave. Well Sampling Data: MW1, MW2 (mg/L)	Ave. WARMF Layer 4 Concentration (mg/L)
Ammonia	0.09	0.01
Calcium	53.33	44.31
Magnesium	10.10	8.29
Potassium	0.78	0.67
Sodium	2.61	3.99
Sulfate	6.08	3.50
Nitrate	0.85	0.14
Chloride	3.03	2.41
Phosphate	0.05	0.004
Dissolved oxygen	13.17	5.94

Study Focus Areas

An effort was made to identify three focus areas within the Dillon Reservoir watershed that would be the locations of more intense sampling and modeling efforts. Figure 5-3 shows the locations of the three focus areas on the watershed map. These regions were selected according to the following criteria:

- Subdivisions of 50 or more homes with OWS
- Good County records on land use, onsite system type, design, and operational age
- Availability of existing environmental monitoring data
- Access to land for additional surface water and groundwater monitoring



Note: Green areas with a red outline indicate parcels with OWS. Small parcels appear as red.

Figure 5-3
Focus Areas of Dillon Reservoir Watershed Study

Frisko Terrace

Frisko Terrace and Wiborg Park are two contiguous subdivisions surrounded on three sides by incorporated sections of the Town of Frisko and on the fourth side by Interstate 70. These subdivisions were created in the mid-1960s and consist of generally one-half-acre parcels. All parcels are served by private well and sewage systems with the exception of a few properties on the fringes, which have opted to connect to the town sewer and/or water system. The western edge of both subdivisions lies 9,175 feet above sea level and drops rapidly to the east to a flat plain of 9,125 feet. The total lot count in both subdivisions is about 120 with the vast majority in the alluvial plain of Tenmile Creek. Soils and geology are characterized by shallow soils and rock outcrops at the western edge to alluvial soils to the east.

Ten Mile Vista

This area is located midway between Frisco and Breckenridge, just east of Colorado Highway 9. The subdivision consists of two filings. Filing 1 was platted in 1963 and consists of approximately 51 lots. The lots are generally one-half-acre in size and the subdivision is approximately 85% built out. The Filing 2, platted in 1970, lies directly to the north of Filing 1 and consists of 24 lots of generally two acres each. The subdivision slopes from west to east from elevation 9,300 to 9,200 feet above sea level.

Shallow soils predominate the area underlain by fractured and decomposing granite and shale formations. Shallow groundwater follows a main drainage area toward the center of the subdivision. The alluvial plain of the Swan River runs adjacent to the eastern edge of the subdivision. The Breckenridge Golf Course is located directly south of this subdivision. Drainage from the golf course generally flows east and west from a center ridgeline, which is common to the western edge of the subdivision. Due to elevation and surface topography, this subdivision is relatively isolated from surrounding land areas.

Blue River Estates

This focus area includes a number of small subdivisions along Pennsylvania Creek, a small tributary of the Blue River. This is an older, more densely developed subdivision as compared to the other focus areas, that has a total of 360 OWS. Because of the surrounding Arapaho National Forest and the Continental Divide, there are few land development uses other than the housing development in the immediate area.

Map Modifications

To accommodate the high density of OWS in the three focus areas, the delineation of land catchments in WARMF was modified from its original configuration. Originally, catchment boundaries were set based on natural topography, which controlled the flow path. Catchments were split at subdivision borders and at locations where surface water sampling would take place. Figure 5-4 shows the revised catchment delineation for the Blue River Estates area. Land parcels with OWS are shown as green squares with a red outline on the map. Water quality sampling stations are also labeled on the map (that is, BR-1, BR-2).

The new catchment configuration required catchments to be linked to downstream catchments instead of streams. Available well data and geology data were referenced when setting up the catchment linkages. Figure 5-5 shows the catchment linkages for the Blue River Estates region with black arrows. The current configuration of WARMF assumes that all land catchments are hydraulically connected to downstream rivers. Therefore in WARMF, all streams were considered to be gaining due to overland flow and subsurface flow draining from upland catchments. However, groundwater characterization performed in this study (Chapter 2, *Study Watershed Environmental Setting*) suggests that the surface water in the Pennsylvania Creek is recharging the shallow groundwater and therefore Pennsylvania Creek is a losing stream.

Whether or not the Blue River is also a losing stream in this area is unclear. Based on interpretation of the available groundwater MW data, the groundwater in this region appears to be moving in a northwesterly direction, and Goose Pasture Tarn is the likely discharge point for groundwater into the surface water system.

Given the uncertainty of the groundwater connectivity in this localized region, it is necessary to evaluate the impacts of OWS from the Blue River Estates at a point downstream of Goose Pasture Tarn where subsurface flow from the area has recharged to the surface water. When additional sampling provides more information regarding the characteristics of gaining and losing streams in this area, WARMF can be adapted to reflect this flowpath. Required data would include daily estimates of flow seeping from a local stream and the percentage of this flow that will later enter a downstream water body (stream or lake).

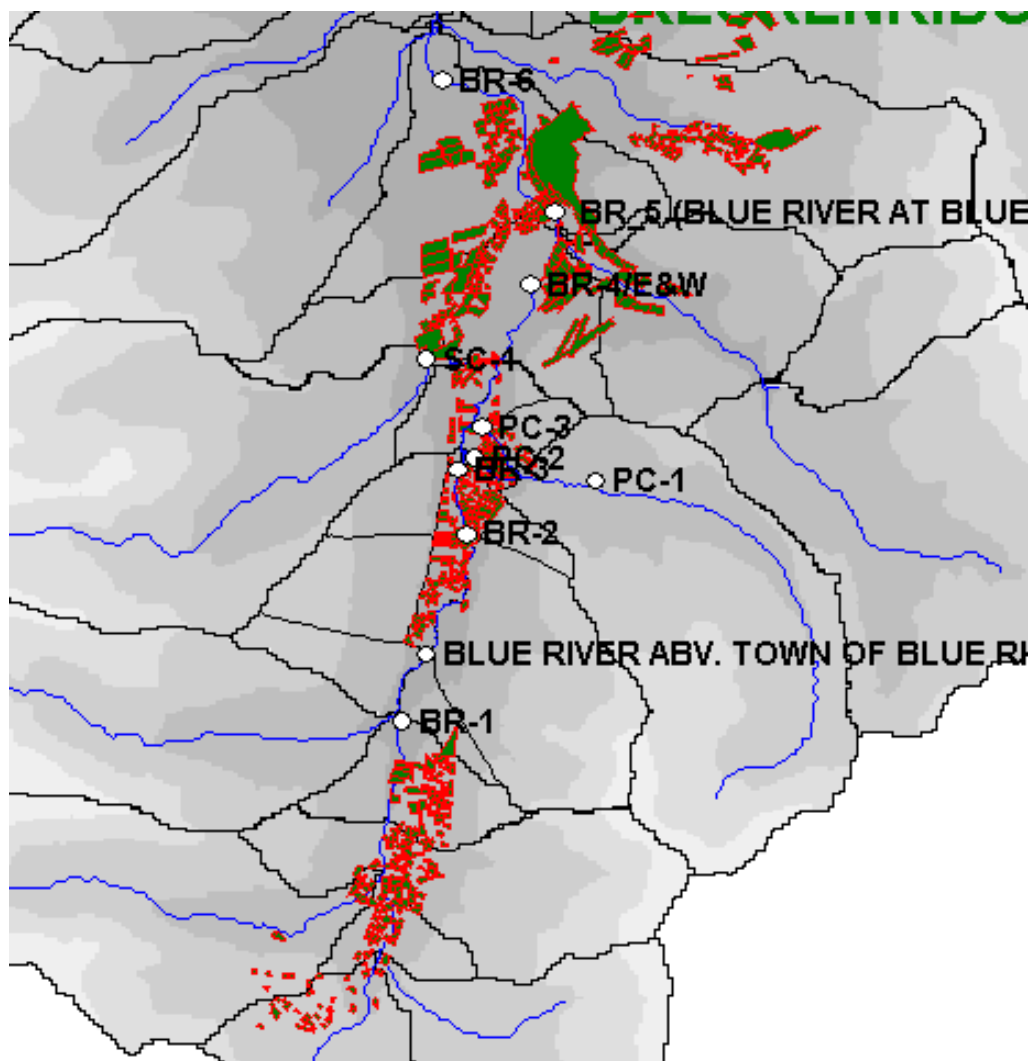


Figure 5-4
Catchment Delineation in the Blue River Estates Focus Area

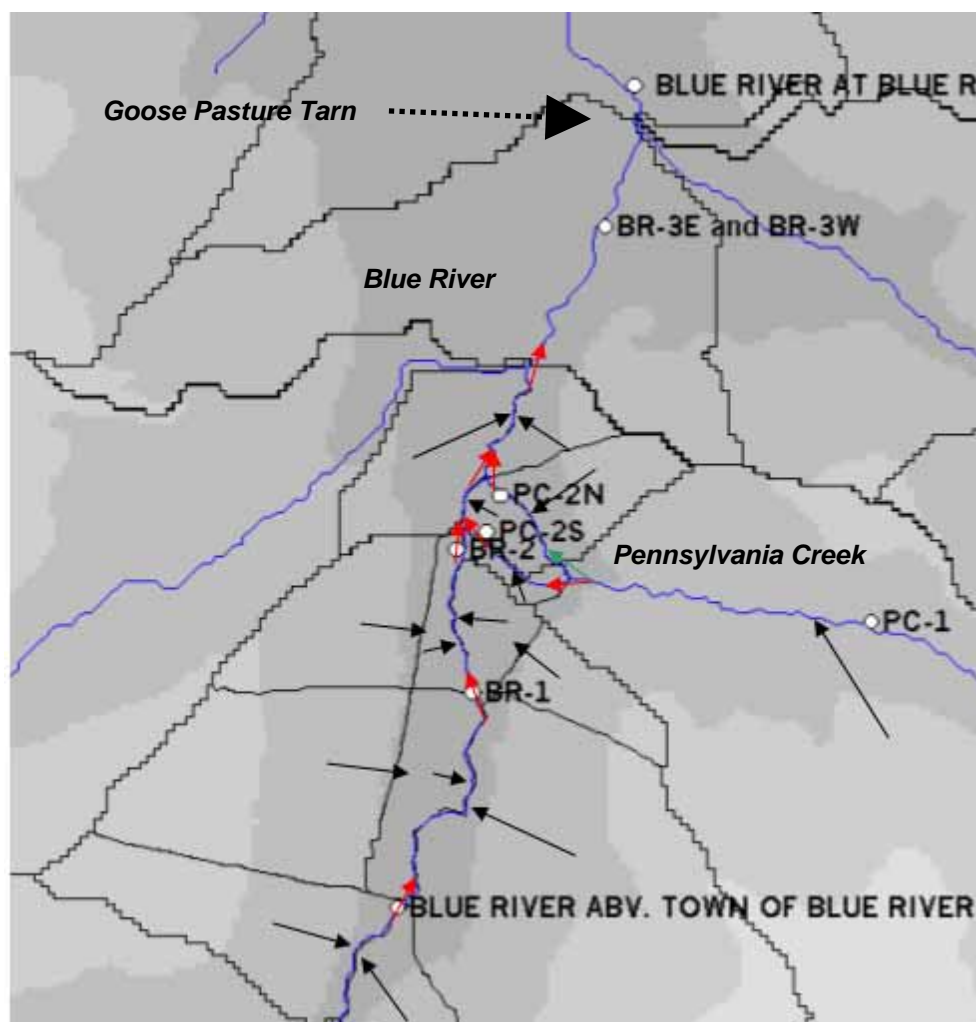


Figure 5-5
Catchment Flow Paths for the Blue River Estates Focus Area

OWS Characterization

There are approximately 1,500 OWS in the Dillon Reservoir watershed. The locations of these OWS were obtained from Summit County Environmental Health Department (SCEH). The GIS layer of OWS was imported into WARMF and is shown as green parcels with a red outline on the map (Figure 5-3). The number of OWS within each catchment was counted and entered into WARMF. It was assumed that each household contained 2.5 people. WARMF can simulate three types of OWS within a given catchment (for example, conventional STE WSASs, sand filter effluent to higher rate WSASs). Another catchment input in WARMF is the distribution of systems between the three types. Figure 5-6 shows OWS inputs for a catchment located in the Ten Mile Vista focus area.

Subcatchment 166

Physical Data | Meteorology | Land Uses | Land Application | Irrigation | Sediment | BMP's
 Point Sources | Pumping | **Septic Sys.** | Reactions | Soil Layers | Mining | CE-QUAL-W2

Discharge Layer: 1
 Population Served by Septics: 40
 Distribution of Septic Systems (total should = 100)
 Treatment Type 1 (%): 100
 Treatment Type 2 (%): 0
 Treatment Type 3 (%): 0
 Initial Biomass (g/cm²): 0
 Biomass Thickness (cm): 2
 Biozone Area (m²): 50
 Biomass Respiration (1/d): 0.18
 Biomass Mortality (1/d): 0.29

☐ Apply Changes To Selected
☐ Apply Changes To All
☒ Write Output To File

OK Cancel Help

Figure 5-6
Septic System Input for a Catchment in WARMF

STE Flow and Quality

The flow and quality characteristics of each OWS type were estimated. Cumulative frequency distribution plots of typical STE flow and quality were obtained from Kirkland (2001). Details of the data are presented in Appendix A, *Input Parameters for Modeling Flow and Transport in Onsite Wastewater Systems*. The 50th-percentile values were extracted from the distribution plots and input to the model (Table 5-7). For other parameters, such as calcium and magnesium, STE quality was set to be similar to background concentrations in the soil in order to avoid any dilution effects. Figure 5-7 shows the STE quantity and quality input dialog in WARMF.

Table 5-7
50th-Percentile Values for STE (Kirkland 2001)

Parameter	Value	Units
Flow	165	L/capita/day
Biochemical oxygen demand (BOD)	170	mg/L
Ammonia (as NH ₄ -N)	58	mg/L
Nitrate (as NO ₃ -N)	0	mg/L
Phosphate (as PO ₄ -P)	9.8	mg/L
Fecal coliform bacteria	1.0 E7	MPN/100 mL

System Coefficients

Physical Data | Land Uses | Snow/Ice | Heat/Light | Canopy | Litter | Reactions
 Septic Sys. | Minerals | Sediment | Phytoplankton | Periphyton | Parameters

Flow (L/cap/day)

Septic System Discharge Quality (mg/L)

	Type 1	Type 2	Type 3
Ammonia	58	0	0
Aluminum	0	0	0
Calcium	20	0	0
Magnesium	5	0	0
Potassium	0.25	0	0
Sodium	5	0	0
Sulfate	3	0	0
Nitrate	0	0	0
Chloride	5	0	0
Phosphate	9.8	0	0
Org. Carbon	0	0	0

OK Cancel Help

Figure 5-7
STE Input Data

OWS Types

WARMF can simulate up to three types of OWS. Each type will have its own quality characteristics. For example, an OWS with a sand filter will have a lower BOD and fecal coliform bacteria concentration than a standard OWS. Literature values of STE quality for various OWS types were compiled and entered into WARMF's help system (Table 5-8). The help system can be accessed by clicking on the Help button, which is located as shown in Figure 5-7.

Table 5-8
STE Quality for Various OWS Types

Type	Description	Reference	BOD (mg/L)	TSS (mg/L)	TN (mg-N/L)	NH4 (mg-N/L)	NO3 (mg-N/L)	TP (mg-P/L)
1 Septic								
a	Septic w/ SAS		170	75	70	60	0	10
b	Septic w/ SAS	Siegrist et al., 2001	140-200	50-100	40-100			5-15
2 Septic w/ N removal								
a	Septic w/ in-tank N removal and SAS		170	80	20	0	20	10
b	Septic tank w/ effluent N removal and recycle	Siegrist et al., 2001	80-120	50-80	10-30			5-15
c	Septic w/ corrugated plastic trickling filter	Ball, 1995	20	10	7.7	2.4	7.1	
d	Septic w/ open-cell foam trickling filter	Ball, 1995	18	17	11	5.6	4.1	
3 Septic w/ single pass sand filter								
a	Single pass sand filter	Loomis et al., 2001	3-4	1-3	37-39			
b	Single pass sand filter	Ronayne et al., 1984	3.2	9	30			
c	Single pass sand filter	Effert et al., 1984	4	17	37.5			14.1
d	Single pass sand filter	Darby, J., G. Tchobanoglous, et al., 1996	75.1	29.1	15.5	10.6	0.3	
4 Septic w/ recirculating sand filter								
a	At grade recirculating sand filter	Loomis et al., 2001	3-4	3-4	11-16			
b	Maryland style RSF	Loomis et al., 2001	3-7	4-9	21-40			
c	Recirculating sand filter	Christopherson et al., 2001	9-14	12-15	24-29	5-6	15-23	6
5 Constructed wetlands								
a	Septic tank w/ constructed wetland and surface water discharge	Henneck et al., 2001	9-44	8-16	16-60			0.4-11
b	Municipal wastewater w/ constructed wetland and surface water discharge	USEPA, 1993	27	15				
c	Municipal wastewater w/ constructed wetland and surface water discharge	USEPA, 1993		4.2		0.86		0.24
d	Municipal wastewater w/ constructed wetland	USEPA, 1993	3-12	3-25		0.15-6.43		
e	Municipal wastewater w/ lagoon and constructed wetland	USEPA, 1993	2.5-9	4-15		0.05-3.9		
6 Biofilters								
a	Waterloo biofilter (plastic media)	Loomis et al., 2001	3-54	0-37	10-106			
b	Waterloo biofilter (plastic media)	Jowett and McMaster, 1995	16.8 ^a	5		10.2	5.7	
c	Peat Biofilter	Lindbo and MacConnell, 2001	3-6	6-7	1-4.1	0.4-1.5	18-22.1	1.9-4
d	Peat Biofilter	Brookes et al., 1984	14-24	9-16	8.1-20.2	2.4-17.7	0.3-4.4	0.5-14.9
7 Textile Filter								
a	Recirculating Textile Filter	Loomis et al., 2001	6-49	7-25	7-46			
b	Foam or textile filter effluent	Siegrist et al., 2001	5-15	5-10	30-60			
8 Systems w/ disinfection								
a	Septic, recirculating gravel filter, UV disinfection	Crites et al., 1997	0 to <5	4.9	0.4	0	12.2	

a. BOD value for this entry is 7 day BOD
b. Value is for total coliforms

Private Drinking Water Well Withdrawals

To perform the water balance calculation, it is necessary to estimate the well pumping that occurs in parcels not serviced by a central water-supply system. Typical domestic water use ranges from 75 to 380 L/c/day (McGhee 1991). For the Dillon Reservoir watershed, a pumping rate of 200 L/c/day was assumed. This rate of pumping results in roughly a 20% consumption of pumped water with the remaining 80% being discharged back to the groundwater via the OWS. Pumping rates were assigned to each catchment with OWS present.

Subsurface Characterization

The subsurface characteristics of soil were estimated from well log data (Smith 2004). Three unsaturated soil layers of 0.5, 1.5, and 2 m in thickness were used to represent the subsurface. The hydraulic conductivity of the soil layers was estimated to range from 800 to 2,000 cm/day, consistent with the values obtained during well installation. The depth to the groundwater table is typically 4 m. Layer 4 was saturated bedrock 15-m thick with a hydraulic conductivity of 5 cm/day. This bottom layer is hydraulically connected to the stream and provides a steady base-flow through the simulation. Layers 1, 2, and 3 can become saturated and can contribute flow during the spring melt and runoff periods.

Hydrology Calibration

WARMF accepts daily meteorology to simulate runoff from catchments. The runoff from catchments drains to stream segments. The flows in stream segments are routed through small creeks to the main tributaries of the Dillon Reservoir watershed. The simulation is performed for every catchment and river segment every day. The output is a daily time series of flow for all river segments. The predicted flows can be compared to observed data at various locations and times.

Calibration Parameters

During calibration, model coefficients are adjusted to improve the matches between predicted and observed values. Important hydrology calibration parameters include precipitation weighting factors, evaporation coefficients, soil field capacity and saturated moisture content, snow melt coefficients, and hydraulic conductivity. Precipitation weighting factors translate the amount of precipitation that occurs at the weather station to the amount falling on a specified land catchment. This factor accounts for orographic effects due to elevation differences. The factor is modified in conjunction with the evaporation coefficient so that the correct amount of precipitation is applied to the catchments to produce the right amount of runoff by WARMF. Snowmelt coefficients control the rising limb of the hydrograph in the spring. Field capacity, horizontal and vertical hydraulic conductivity, and saturated moisture of the soil control the recession limb of the hydrograph and the dynamic fluctuations between storms.

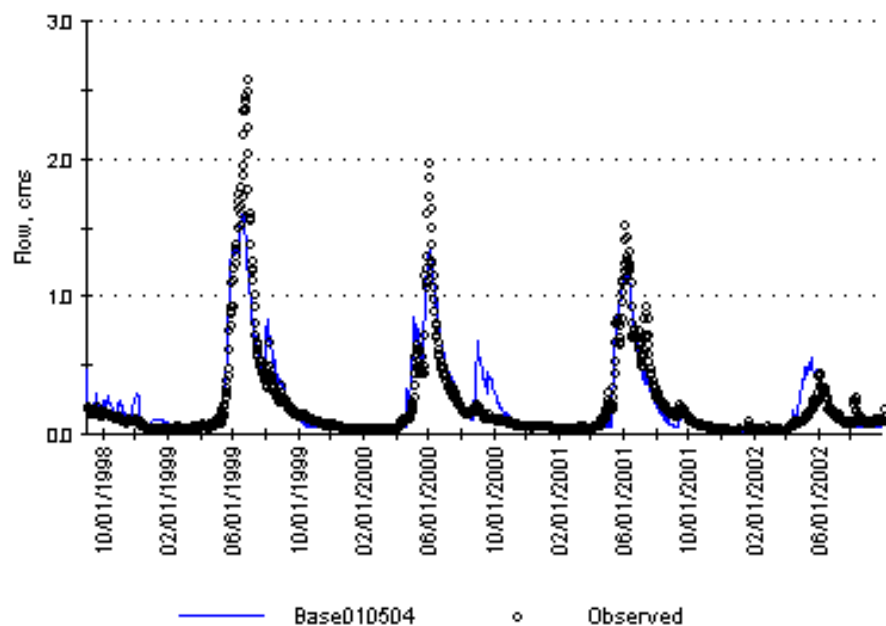
Model Results

WARMF produces four graphical outputs:

- Instantaneous hydrograph
- Cumulative hydrograph
- Frequency distribution
- Scatter plot with a statistical summary of comparison between simulated and observed data

To match the monitoring efforts of this project, a simulation period of October 1, 1998 to September 30, 2002 was chosen for calibration. The following plots present results for several locations in the Dillon Reservoir watershed: French Gulch, Blue River at Blue River, CO, Blue River above Dillon Reservoir, Tenmile, and the Snake River.

Figure 5-8 presents the comparison of simulated and observed stream flow for French Gulch, a tributary of the upper Blue River. For the period of 1998 to 2002, the model under predicted peak flows for 1999 and 2000. The predictions were much closer for 2001 and 2002. The model appeared to have simulated the low flow for the dry year of 2002 and for all years, the recession curve of the base flow was simulated well. Figure 5-9 shows a statistical output and scatter plot for the calibration. The overall correlation coefficient was 0.849 for the simulated and observed values. Figure 5-10 and Figure 5-11 show plots for frequency distribution and cumulative flow. Both plots indicate a good match for low, high, and cumulative flows.



Note: 1cms = 35.3 cfs

Figure 5-8
Simulated and Observed Stream Flow for French Gulch

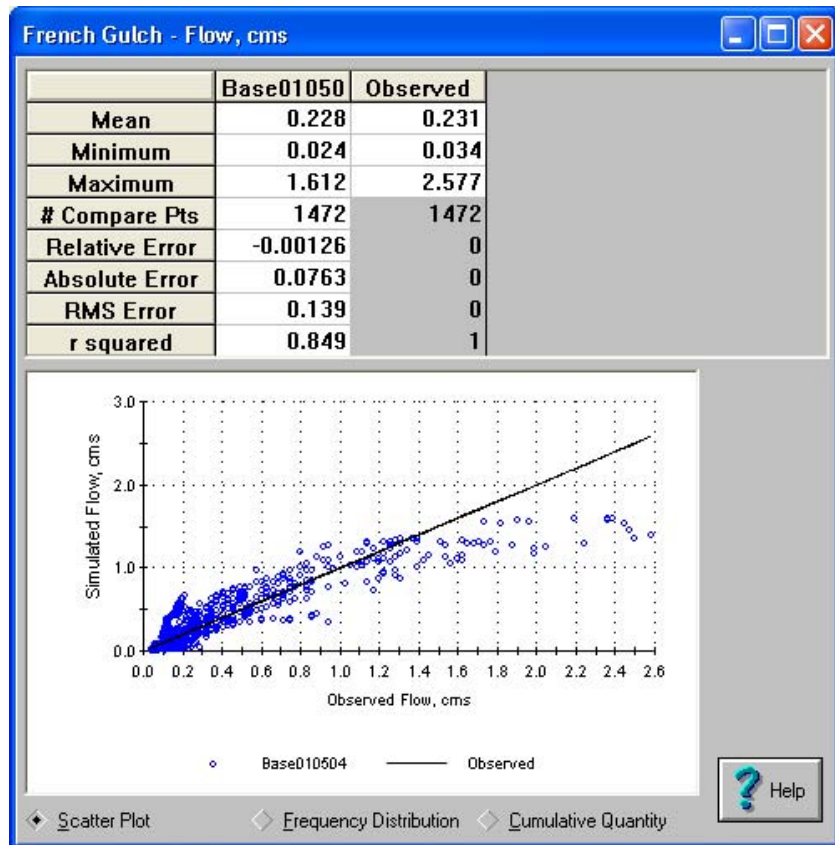
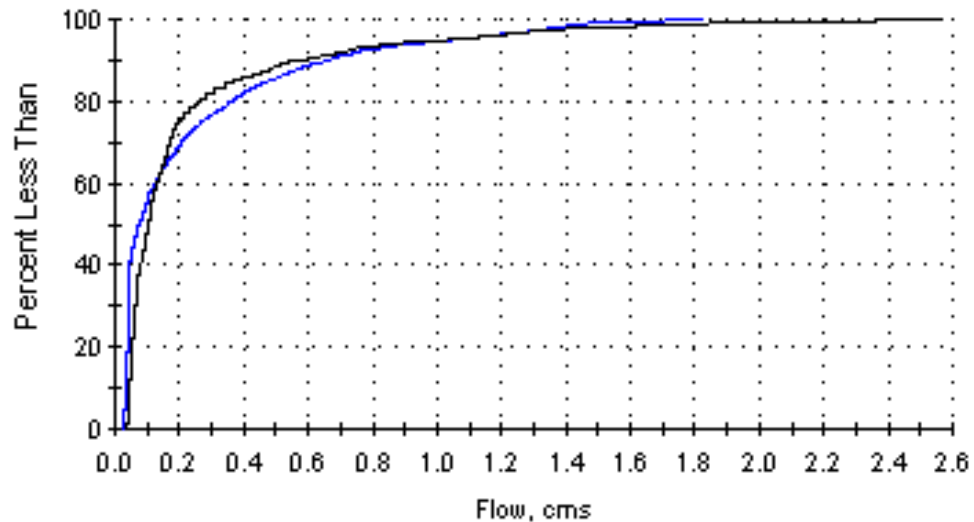
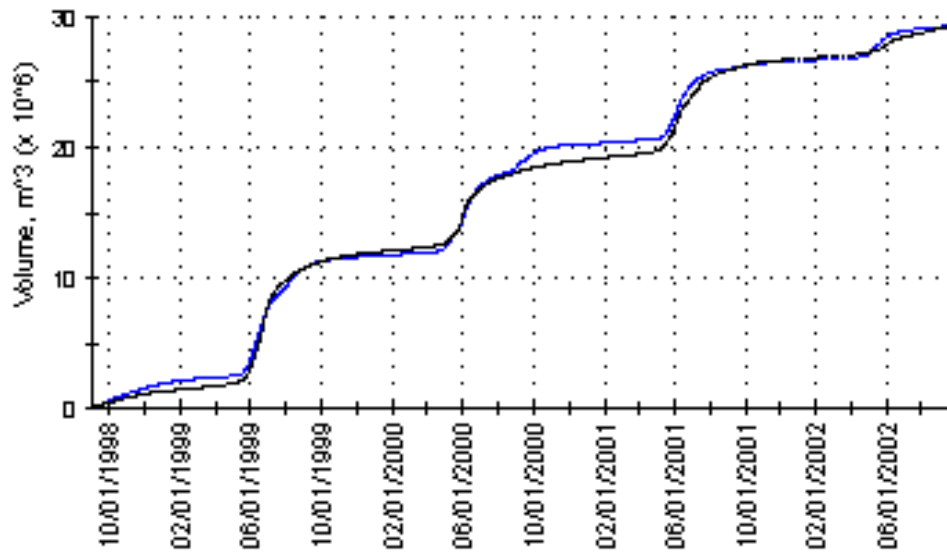


Figure 5-9
Statistical Output and Scatter Plot for French Gulch



Note: Black line is observed; blue line is simulated.

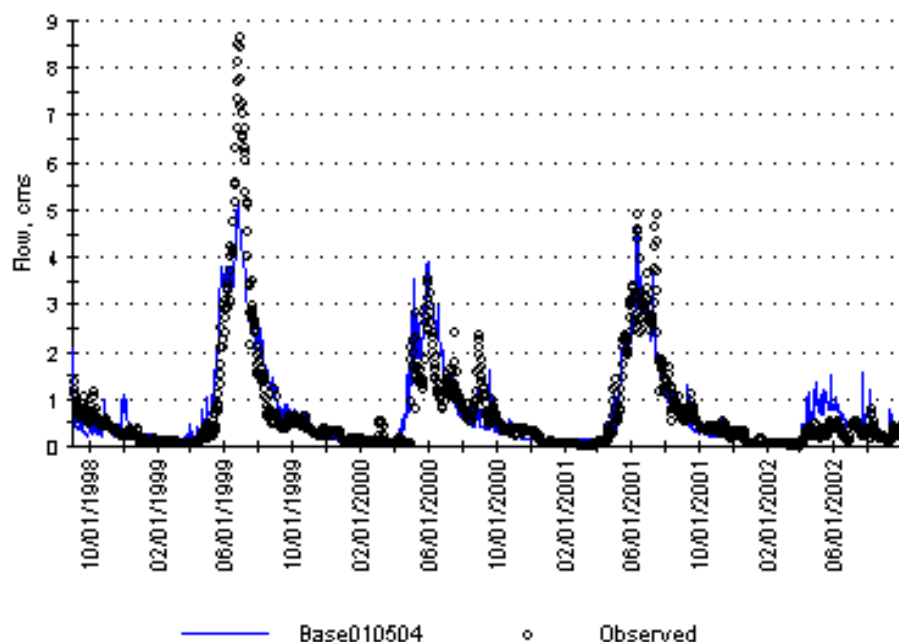
Figure 5-10
Frequency Distribution Plot for French Gulch



Note: Black line is observed; blue line is simulated.

Figure 5-11
Cumulative Quantity Plot for French Gulch

Figure 5-12 shows simulated and observed streamflow for the Blue River at Blue River, CO. For this location, peak flows were under predicted for 1999, over predicted for 2002, but matched well for 2000 and 2001. The general pattern of seasonal runoff and recession was simulated well. Figure 5-13 through Figure 5-15 show statistical results, a scatter plot, a frequency distribution plot, and a cumulative hydrograph. The correlation coefficient for this location is 0.813.



Note: 1 cms = 35.3 cfs

Figure 5-12
Simulated and Observed Flow for the Blue River at Blue River, CO

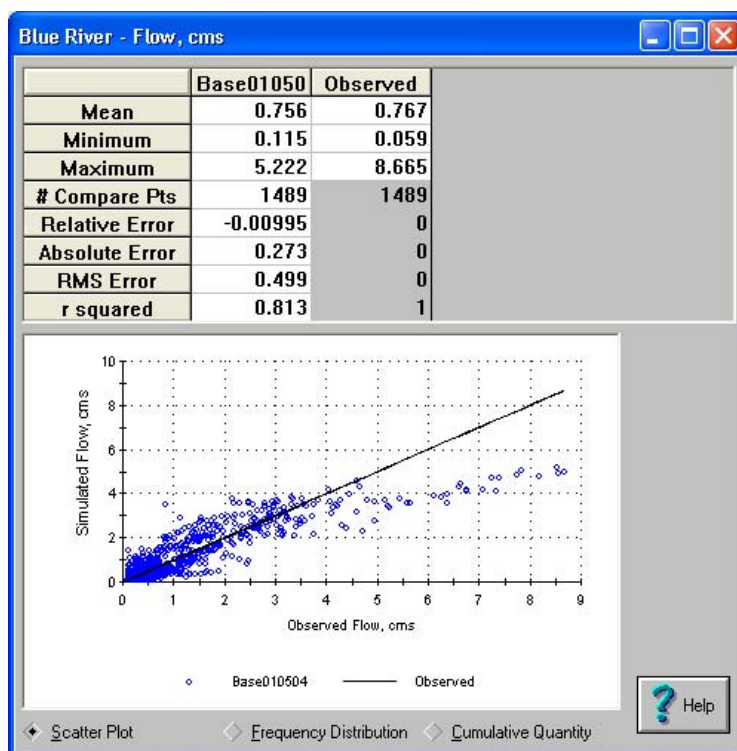
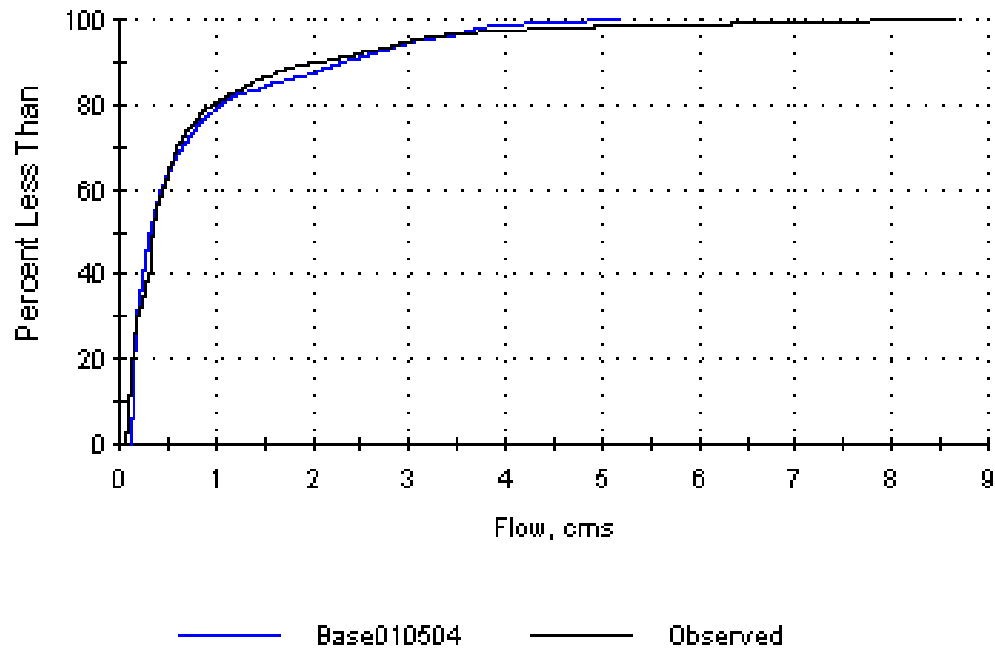
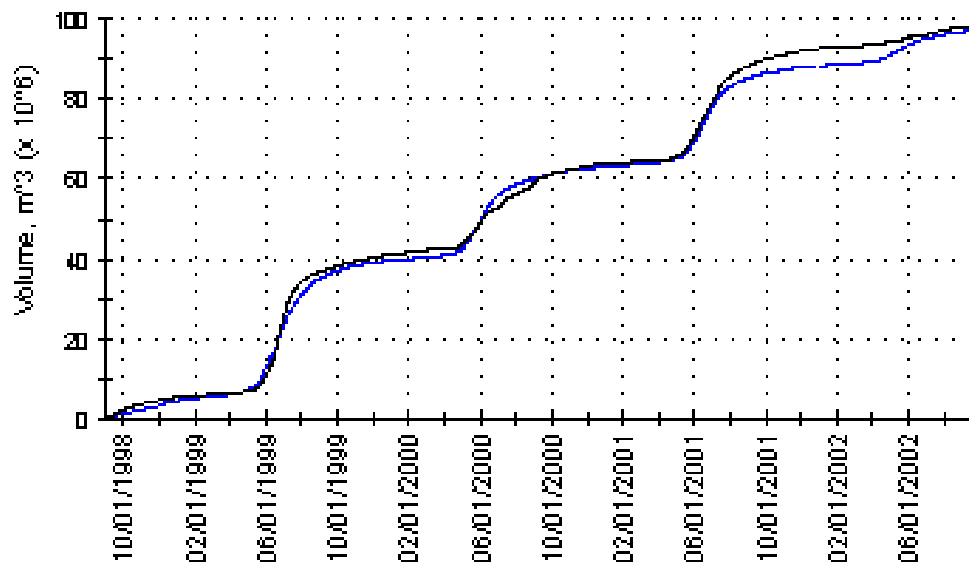


Figure 5-13
Statistical Output and Scatter Plot for the Blue River at Blue River, CO



Note: Black line is observed; blue line is simulated.

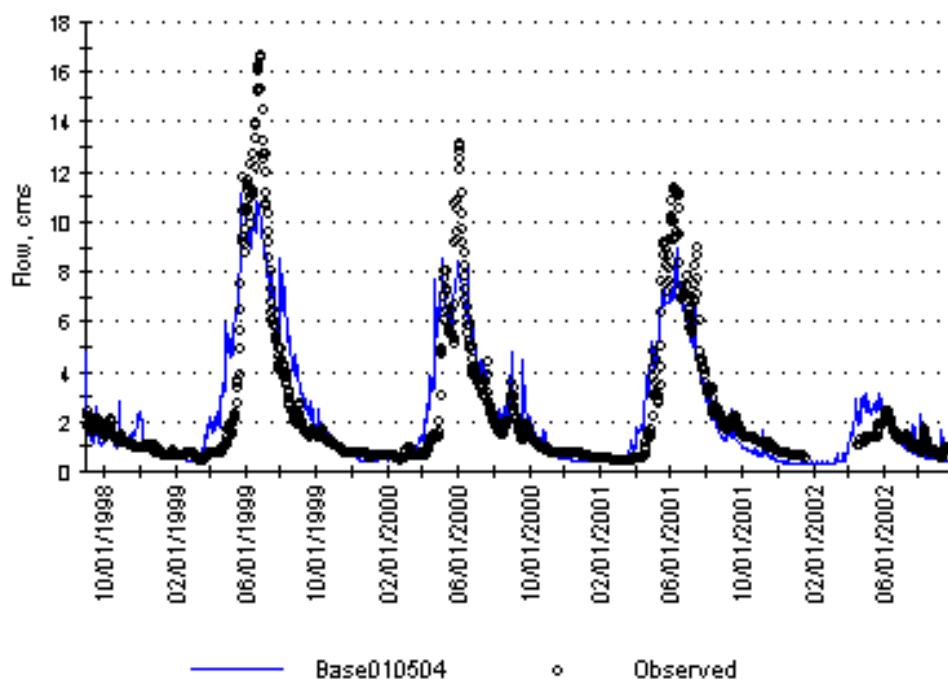
Figure 5-14
Frequency Distribution Plot for the Blue River at Blue River, CO



Note: Black line is observed; blue line is simulated.

Figure 5-15
Cumulative Quantity Plot for the Blue River at Blue River, CO

Figure 5-16 shows simulated and observed stream flow for the Blue River above Dillon Reservoir. For this location, the general pattern of seasonal snow melt is simulated well; however, the rising limb of the hydrograph is a little early. The peak flows for 1999 and 2000 were under predicted, but the simulations for 2001 and 2002 showed a better match. Figure 5-17 through Figure 5-19 show statistical results, a scatter plot, a frequency distribution plot, and a cumulative hydrograph. The correlation coefficient for this location 0.826. The cumulative hydrograph indicates a slight over prediction of cumulative flow through the simulation period.



Note: 1 cms = 35.3 cfs

Figure 5-16
Simulated and Observed Flow for the Blue River Above Dillon Reservoir

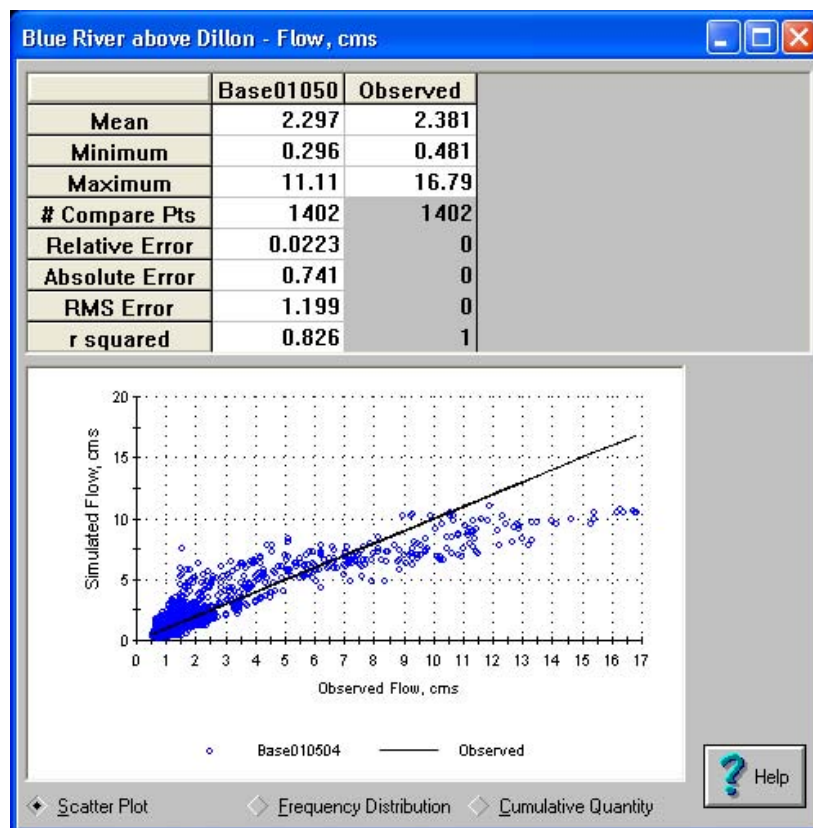
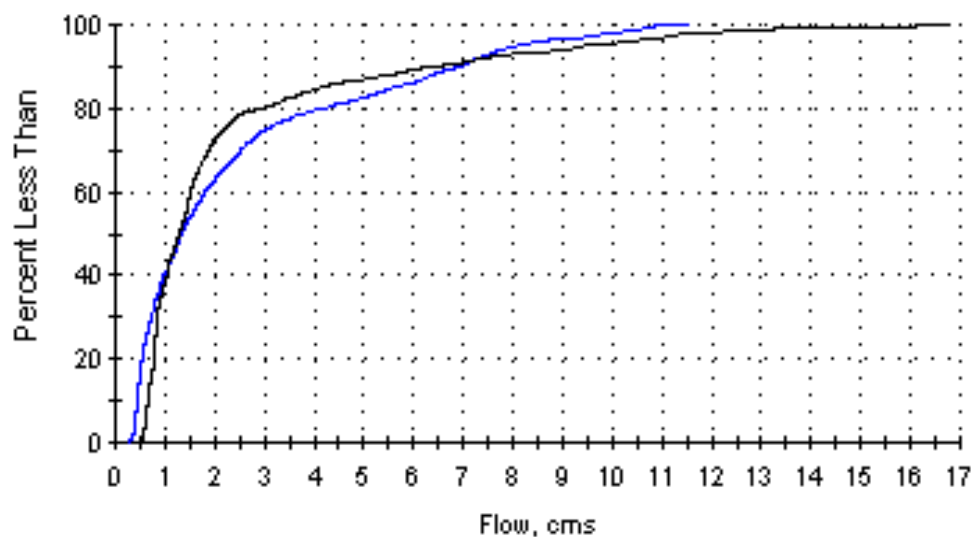
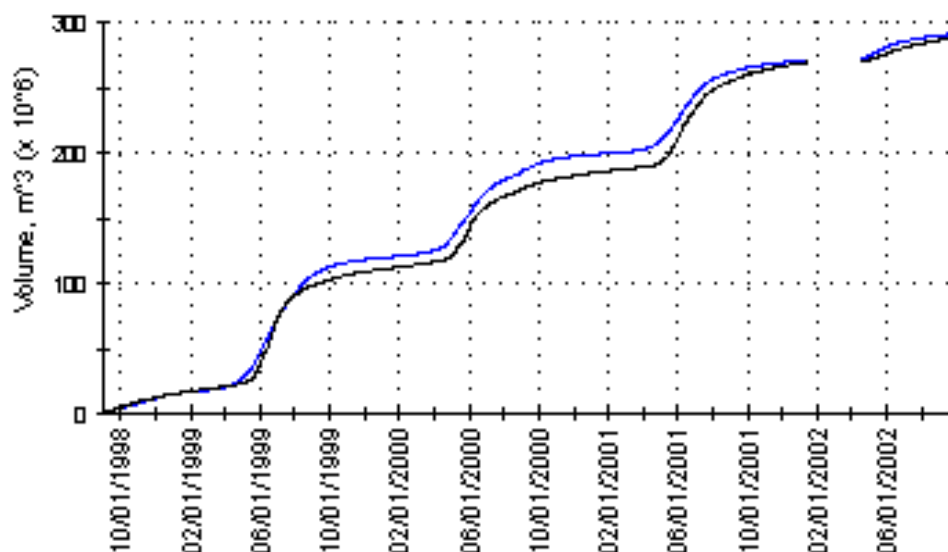


Figure 5-17
Statistical Output and Scatter Plot for the Blue River Above Dillon Reservoir



Note: Black line is observed; blue line is simulated.

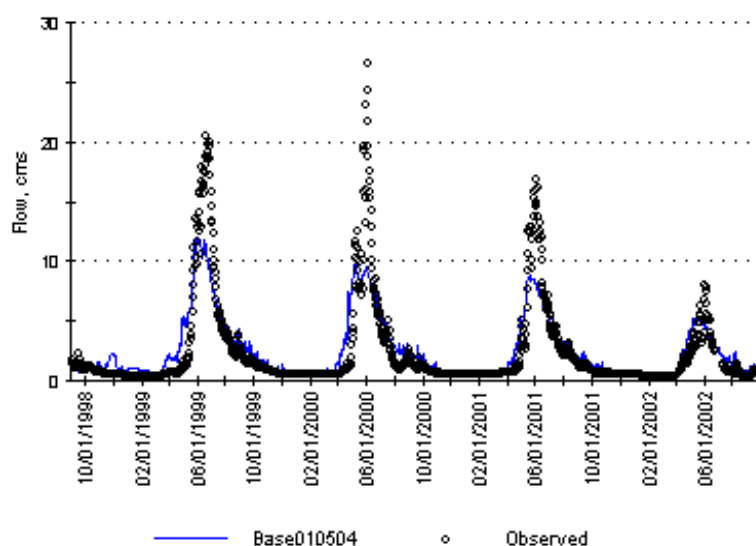
Figure 5-18
Frequency Distribution Plot for the Blue River Above Dillon Reservoir



Note: Black line is observed; blue line is simulated.

Figure 5-19
Cumulative Quantity Plot for the Blue River Above Dillon Reservoir

Figure 5-20 shows simulated and observed stream flow for Tenmile Creek above Dillon Reservoir. As with the other stations, the hydrograph pattern was simulated well; however, several peak flows were under predicted. Figure 5-21 through Figure 5-23 show statistical results, a scatter plot, a frequency distribution plot, and a cumulative hydrograph. The correlation coefficient for this location 0.815.



Note: 1 cms = 35.3 cfs

Figure 5-20
Simulated and Observed Flow for Tenmile Creek

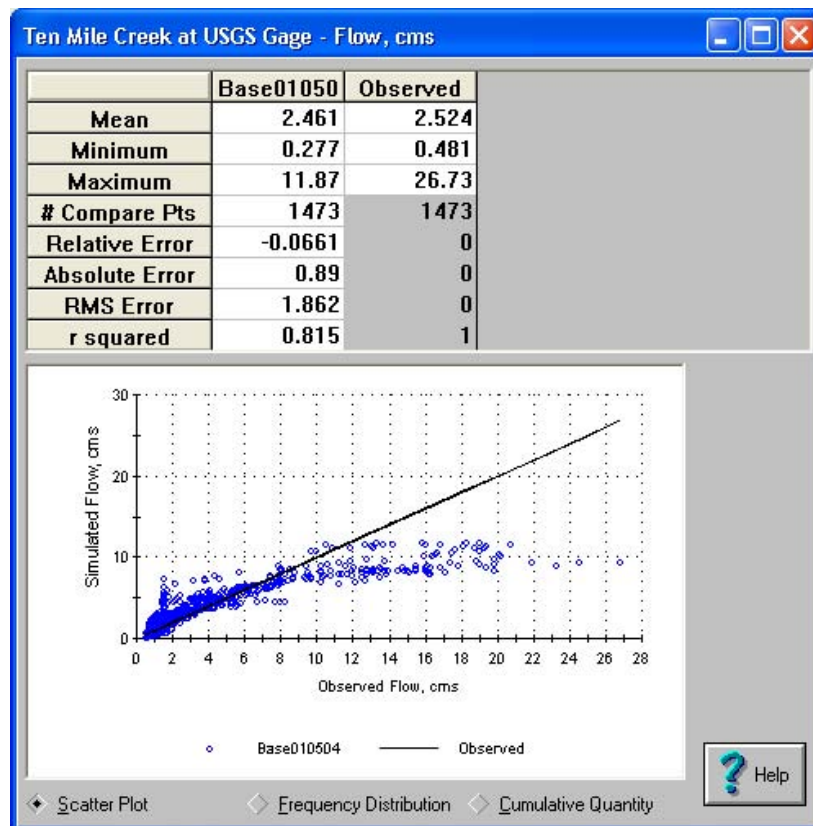
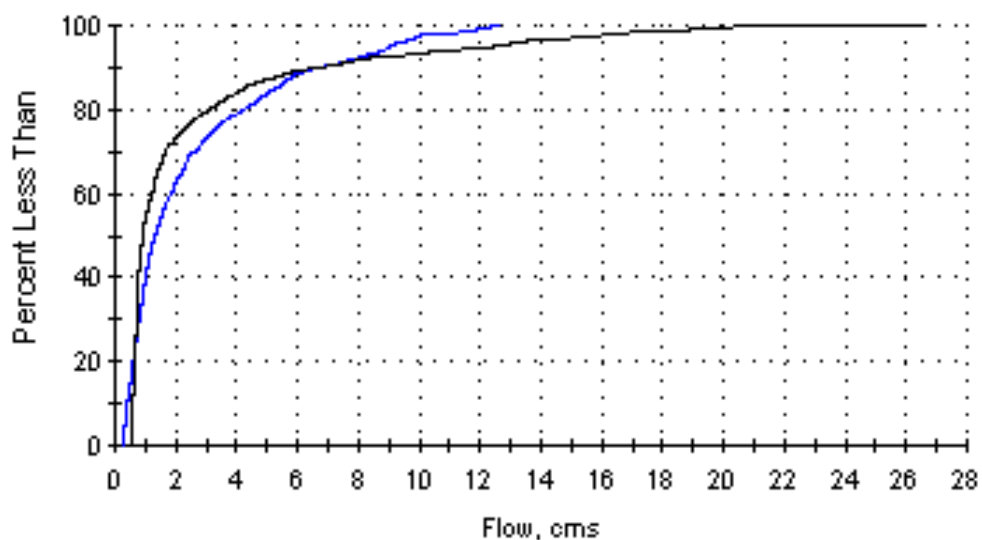
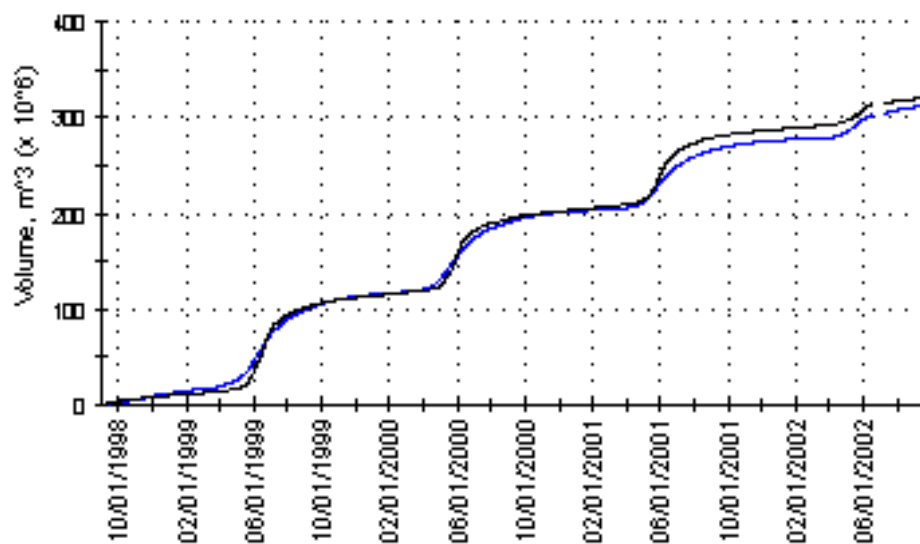


Figure 5-21
Statistical Output and Scatter Plot for Tenmile Creek



Note: Black line is observed; blue line is simulated.

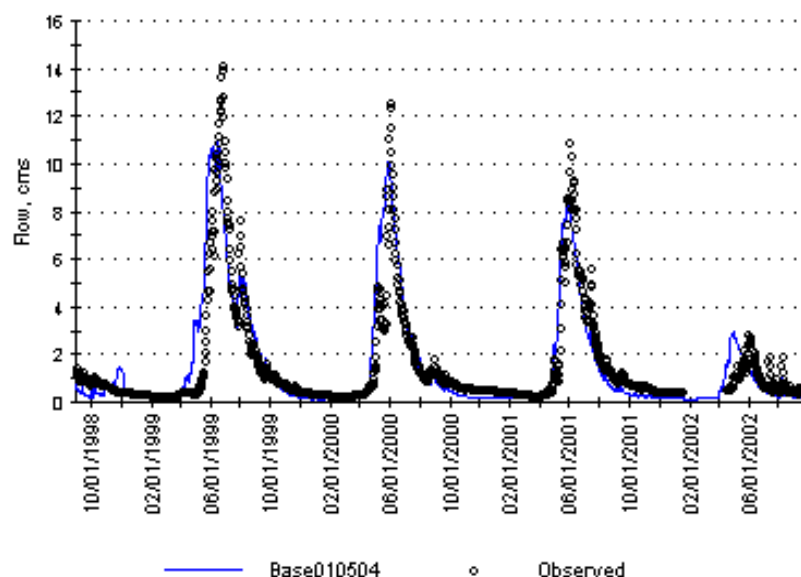
Figure 5-22
Frequency Distribution Plot for Tenmile Creek



Note: Black line is observed; blue line is simulated.

Figure 5-23
Cumulative Quantity Plot for Tenmile Creek

Figure 5-24 shows simulated and observed stream flow for the Snake River above the N. Fork Snake River. The peak flows for this location matched quite well. Figure 5-25 through Figure 5-27 show statistical results, a scatter plot, a frequency distribution plot, and a cumulative hydrograph. The cumulative hydrograph shows a slight over prediction of flow volume, and the correlation coefficient for this location, 0.839.



Note: 1 cms = 35.3 cfs

Figure 5-24
Simulated and Observed Flow for the Snake River Above N. Fork

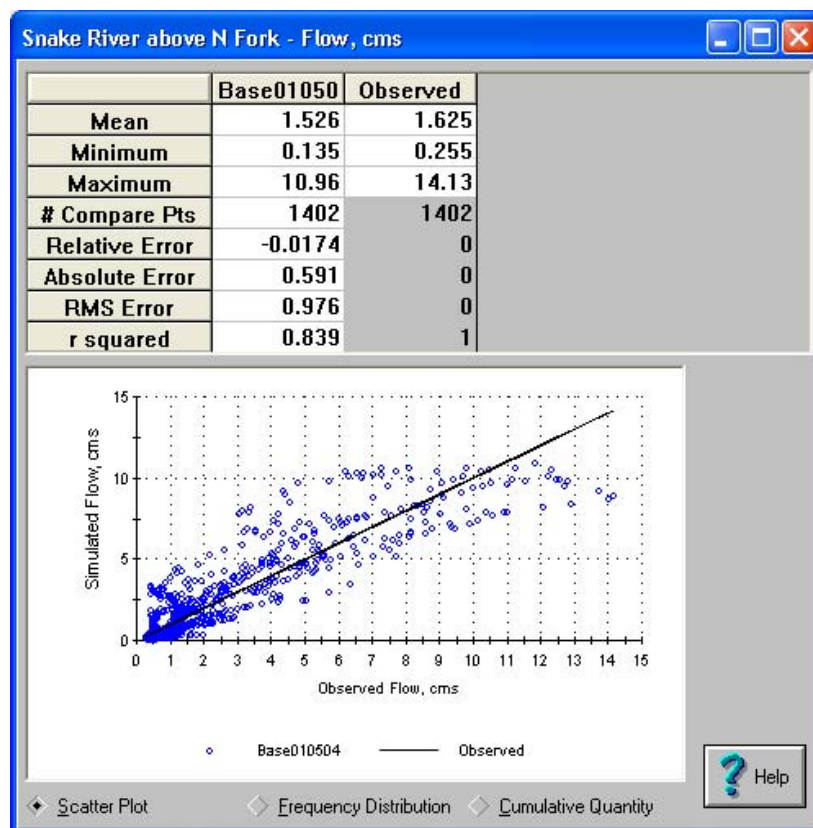
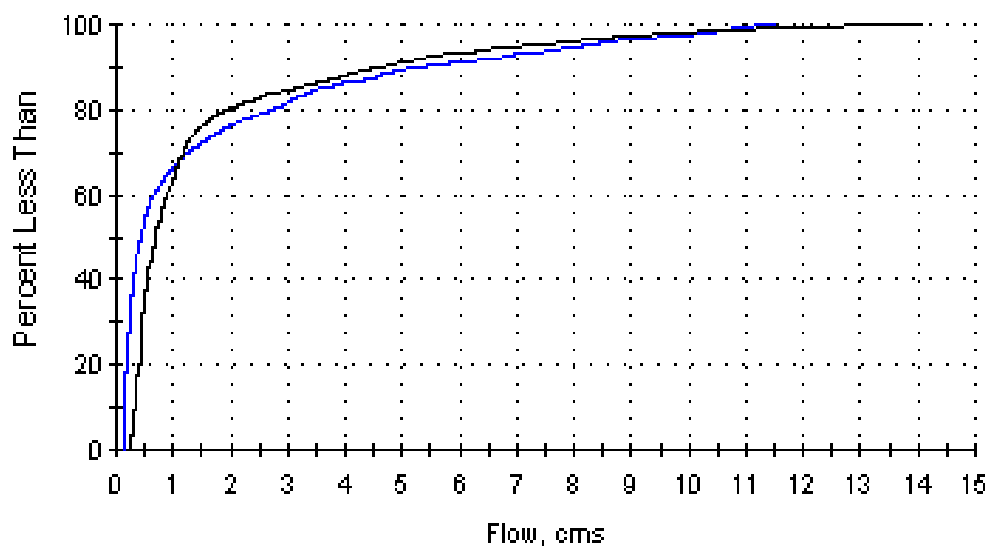


Figure 5-25
Statistical Output and Scatter Plot for the Snake River Above N. Fork



Note: Black line is observed; blue line is simulated.

Figure 5-26
Frequency Distribution Plot for the Snake River Above N. Fork

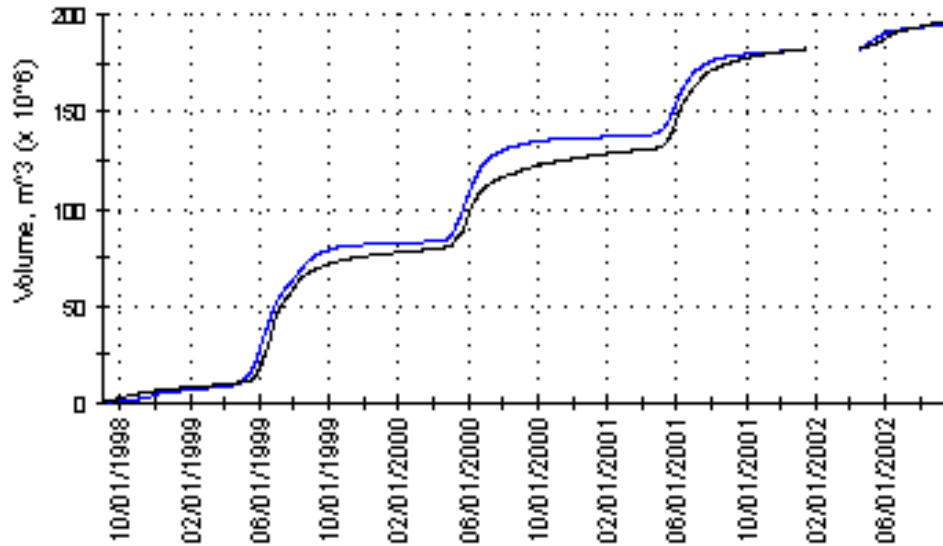


Figure 5-27
Cumulative Quantity Plot for the Snake River Above N. Fork

Water Balance

As part of the hydrology calibration, the overall water balance was calculated for each water year (Figure 5-28). For the total simulation period from 1992 to 2002, total precipitation was $6.77 \times 10^9 \text{ m}^3$. Total water diverted from the watershed including Denver water supply from Dillon Reservoir and three additional diversions near Hoosier Pass amounted to $1.13 \times 10^9 \text{ m}^3$. The total reservoir releases during this time period were $2.3 \times 10^9 \text{ m}^3$ and total evaporative losses were $3.42 \times 10^9 \text{ m}^3$. The net change in reservoir storage in the reservoir from the beginning of simulation in 1992 to the end of simulation in 2002 was $-7.2 \times 10^6 \text{ m}^3$. Nearly 99% of the precipitation input to the watershed is accounted for in the outputs and change in storage.

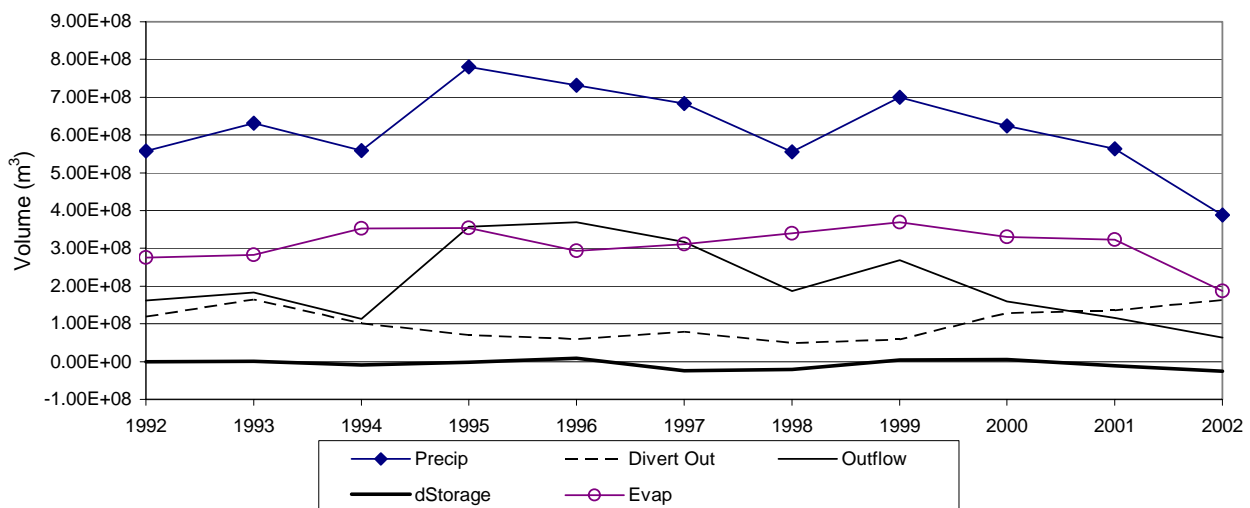


Figure 5-28
Calculated Water Balance Volumes for Each Water Year

Water Quality Calibration

WARMF routes all pollutants through the subsurface to the surface waters. The output is the time-dependent concentrations of pollutants for various stream segments. The water-quality constituents simulated include temperature, dissolved oxygen, phosphorus, ammonia, nitrate, and fecal coliform bacteria, among others. For stream segments with monitoring data, the predicted concentrations can be plotted for comparison to the observed values.

Calibration Parameters

The calibration of water quality is performed one constituent at a time. The calibration sequence of water quality constituents must follow a logical hierarchy. For example, BOD, ammonia, and temperature can affect the dissolved oxygen concentration and are calibrated before dissolved oxygen. Calibration parameters for water quality vary by constituent. The initial soil concentrations, phosphate adsorption coefficient, and decay rates are first set with default values in WARMF. Then adjustments are made to improve the match between simulated and observed values.

Model Results

Samples of water quality results are presented for the following water quality stations

- Blue River above Pennsylvania Creek (BR3)
- S. Fork of Pennsylvania Gulch (PC2)
- Blue River below Pennsylvania Creek (BR4)
- Swan River near mouth at Frisco (SR3)
- Blue River above Dillon Reservoir (BR10)

Note that the WARMF model provides additional output that is not presented here but could be viewed through the WARMF model CD.

The graphical comparison indicates that the model predictions are in the range of the observed data. WARMF provides plots for time series, correlation statistics, frequency distribution, and cumulative curve of water quality constituents similar to those for stream flow. However, far fewer data points are collected for water quality than for stream flow, which makes it more difficult to make statistical comparisons.

Temperature

Figure 5-29 through Figure 5-33 present the temperature simulations for each location. For all locations, WARMF predicts the seasonal temperature cycle correctly. Most simulations compare well to observed data, though the peak temperature in 2002 was under predicted at BR3 and BR4 and over predicted at PC2.

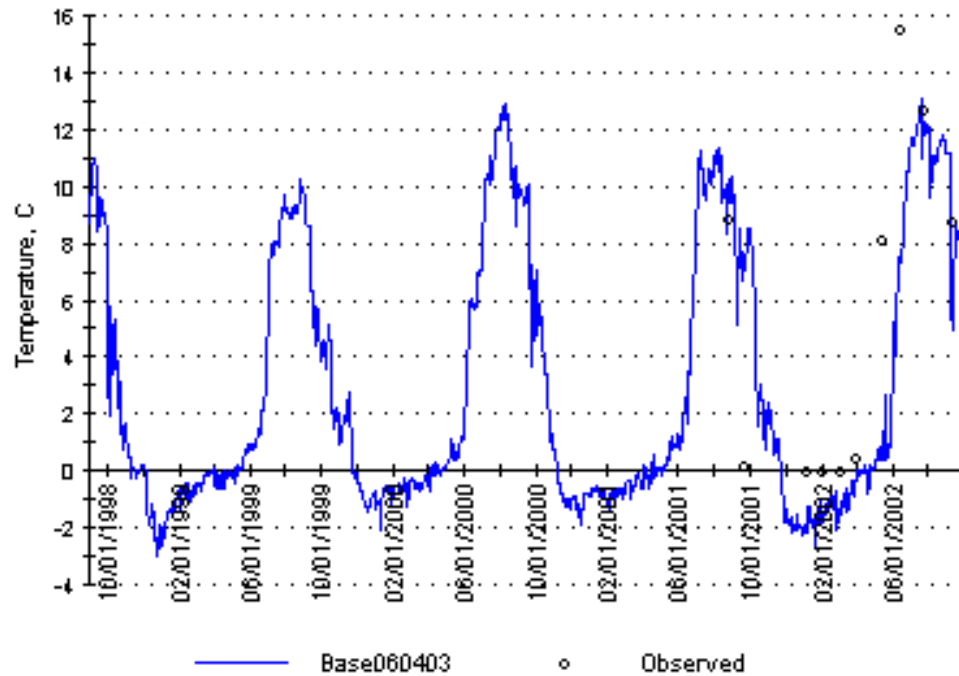


Figure 5-29
Simulated and Observed Temperature at BR3

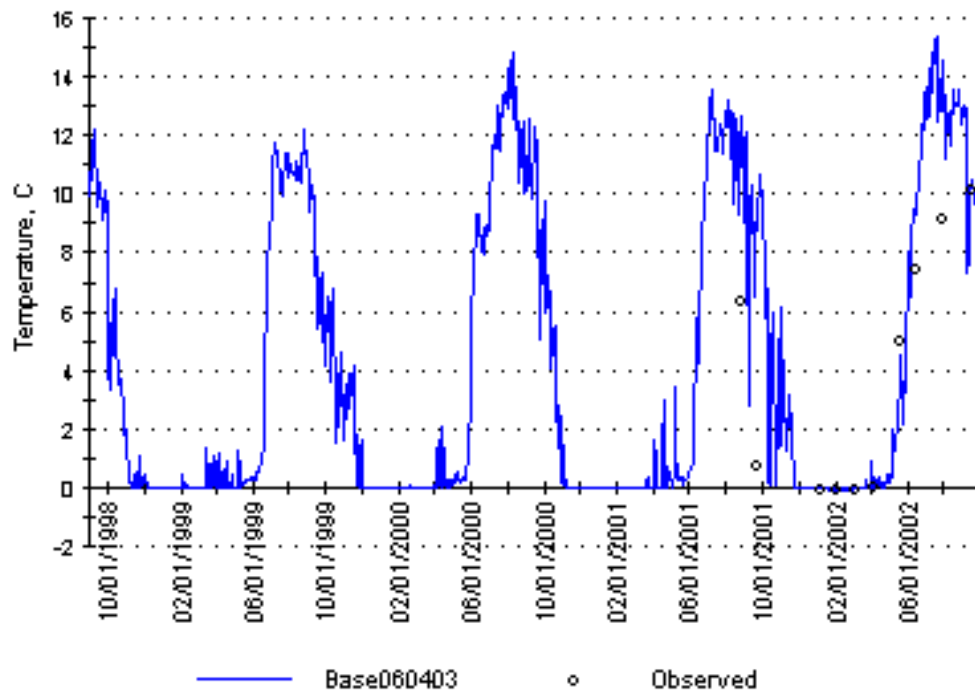


Figure 5-30
Simulated and Observed Temperature at PC2

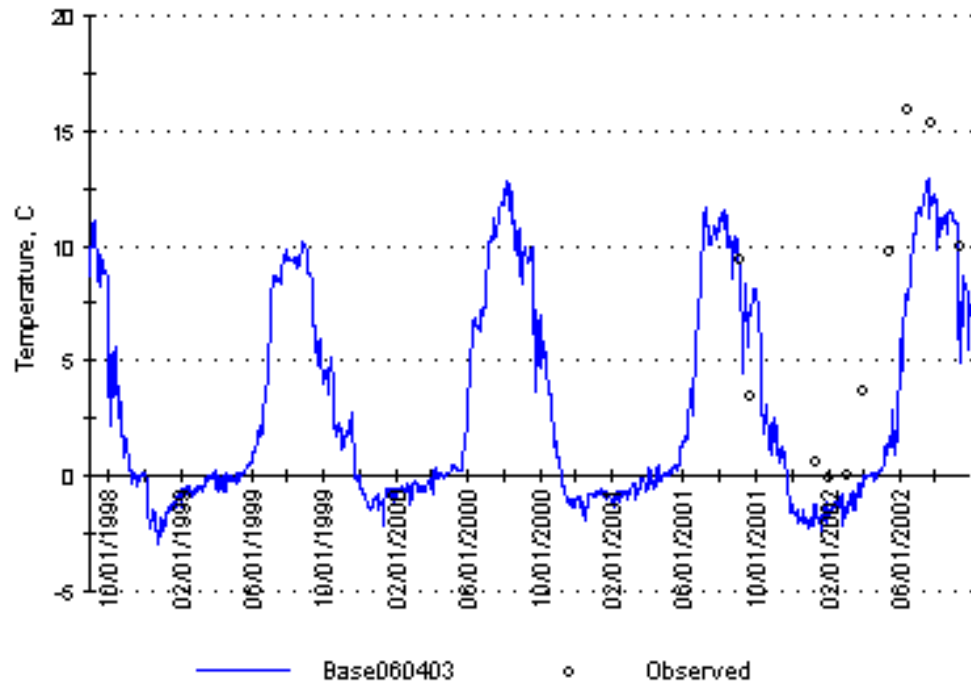


Figure 5-31
Simulated and Observed Temperature at BR4

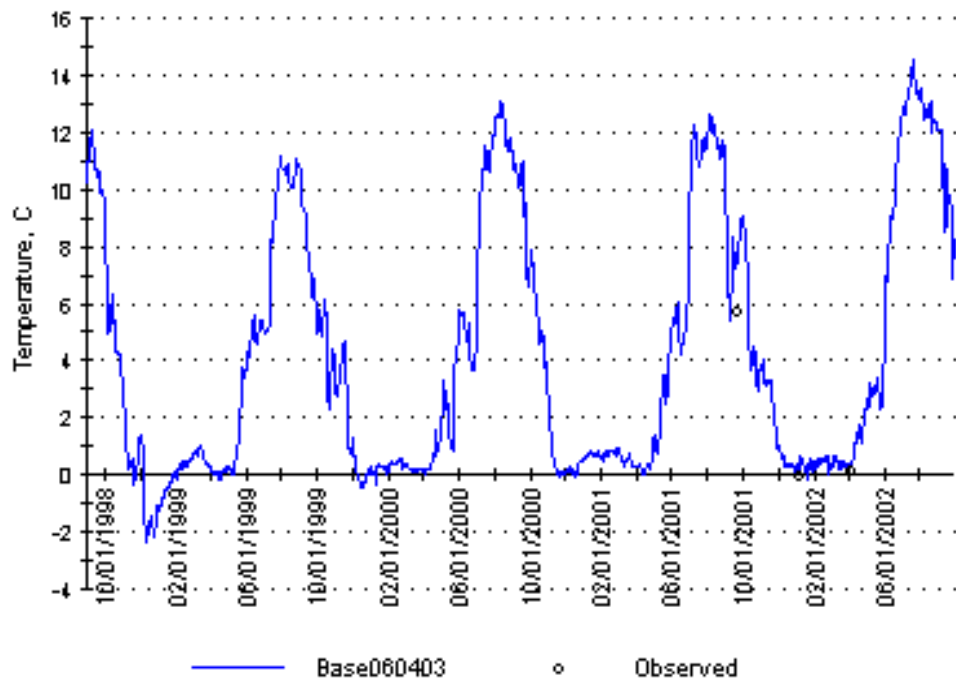


Figure 5-32
Simulated and Observed Temperature at SR3

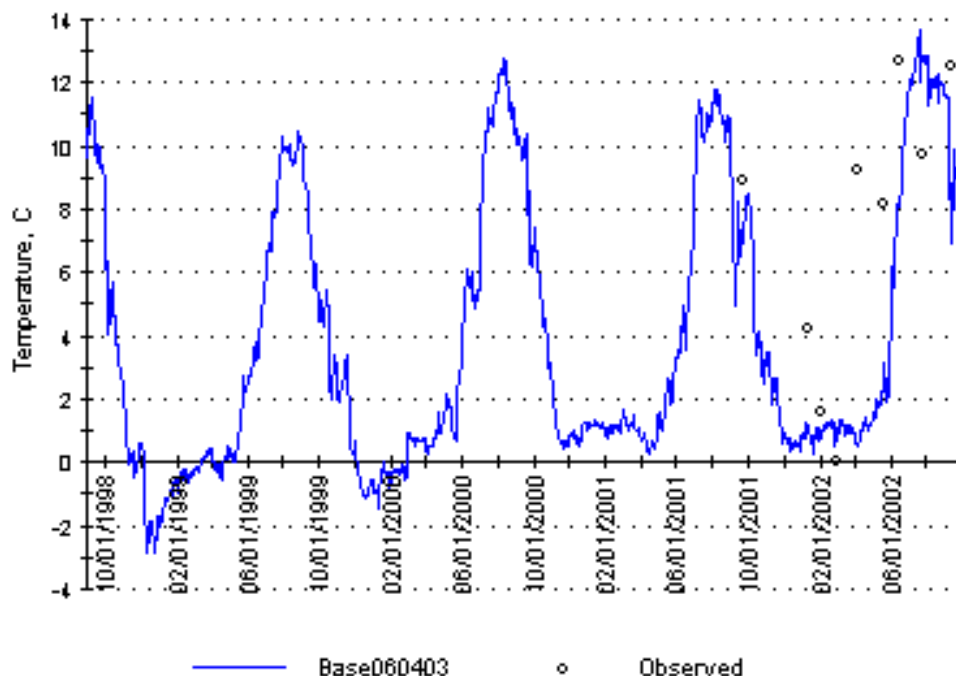


Figure 5-33
Simulated and Observed Temperature at BR10

Ammonia

Figure 5-34 through Figure 5-38 show the simulated and observed ammonia results for the five selected locations. For most locations, the baseline concentration of ammonia was simulated well, and the simulated peak concentrations were also in the range of observed concentrations. For BR10, the baseline ammonia concentration is over predicted. This over prediction is believed to be due to the large point source upstream at Iowa Hill WWTP. The loading data available for this point source was limited. More accurate point source data may help improve the simulation at this location.

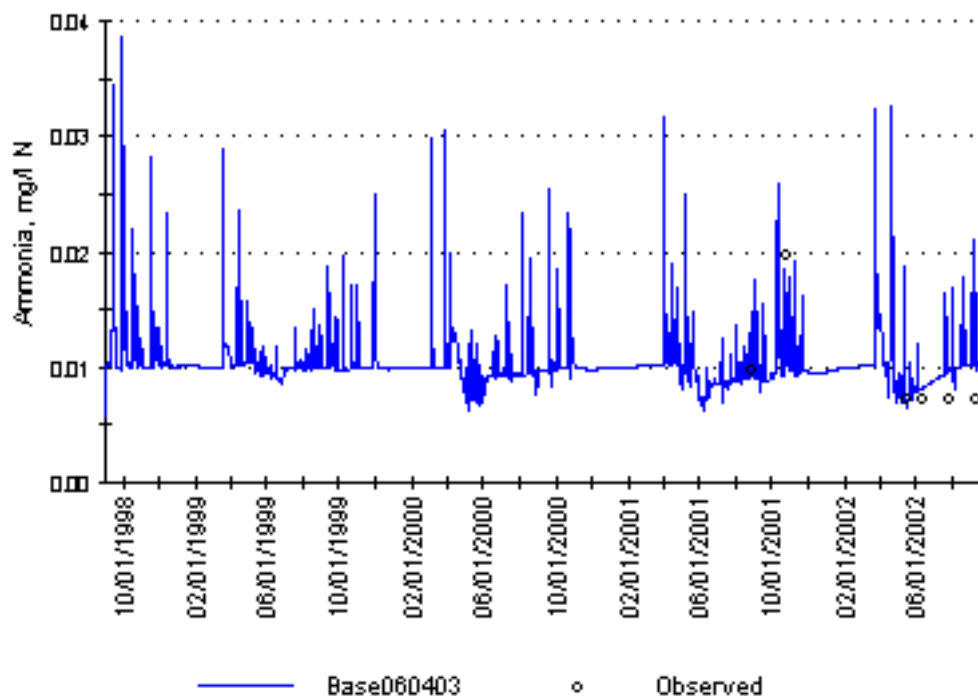


Figure 5-34
Simulated and Observed Ammonia (as $\text{NH}_4\text{-N}$) at BR3

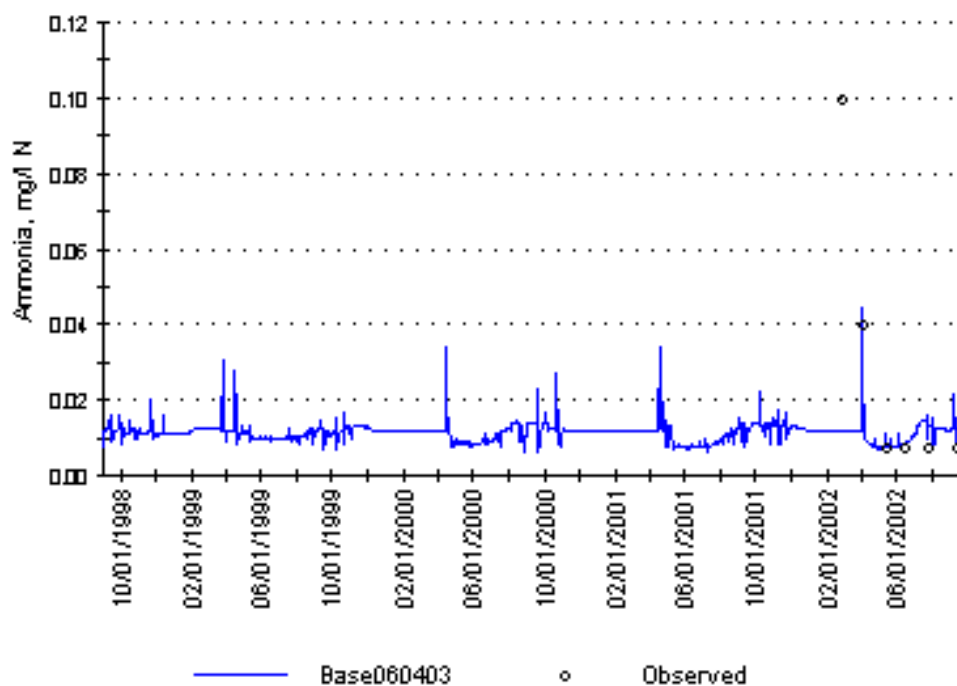


Figure 5-35
Simulated and Observed Ammonia (as $\text{NH}_4\text{-N}$) at PC2

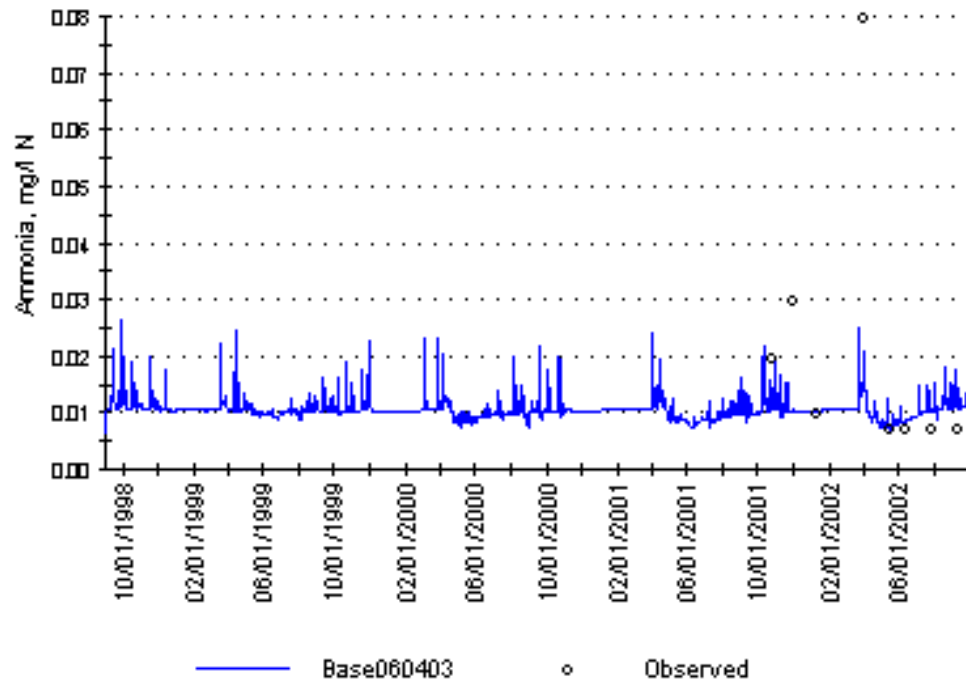


Figure 5-36
Simulated and Observed Ammonia (as $\text{NH}_4\text{-N}$) at BR4

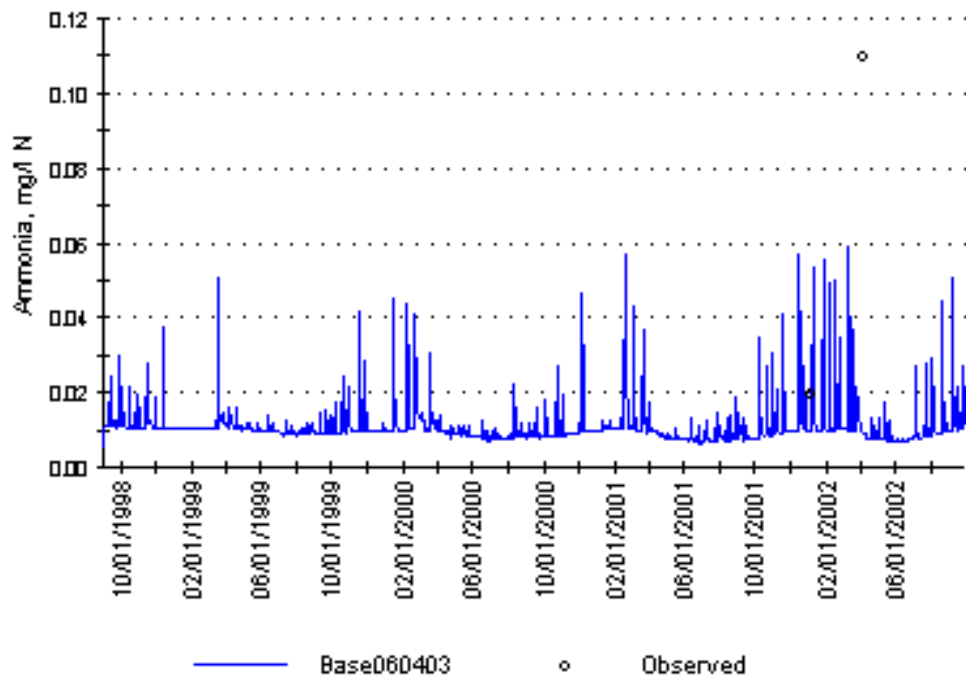


Figure 5-37
Simulated and Observed Ammonia (as $\text{NH}_4\text{-N}$) at SR3

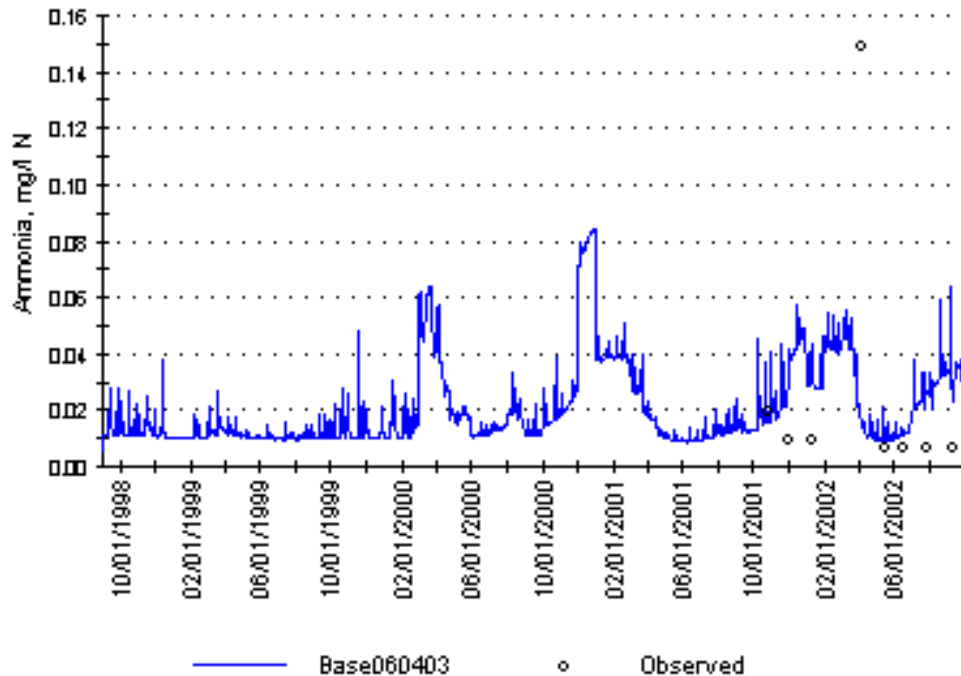


Figure 5-38
Simulated and Observed Ammonia (as $\text{NH}_4\text{-N}$) at BR10

Nitrate

Simulated nitrate concentrations at the five sample locations are compared to observed data in Figure 5-39 through Figure 5-43. For all locations, the general trends and ranges of simulated concentrations match the observed data quite well. At BR10, the over prediction of nitrate below the Iowa Hill WWTP is contributed to the limited point source data available for the plant, as discussed earlier.

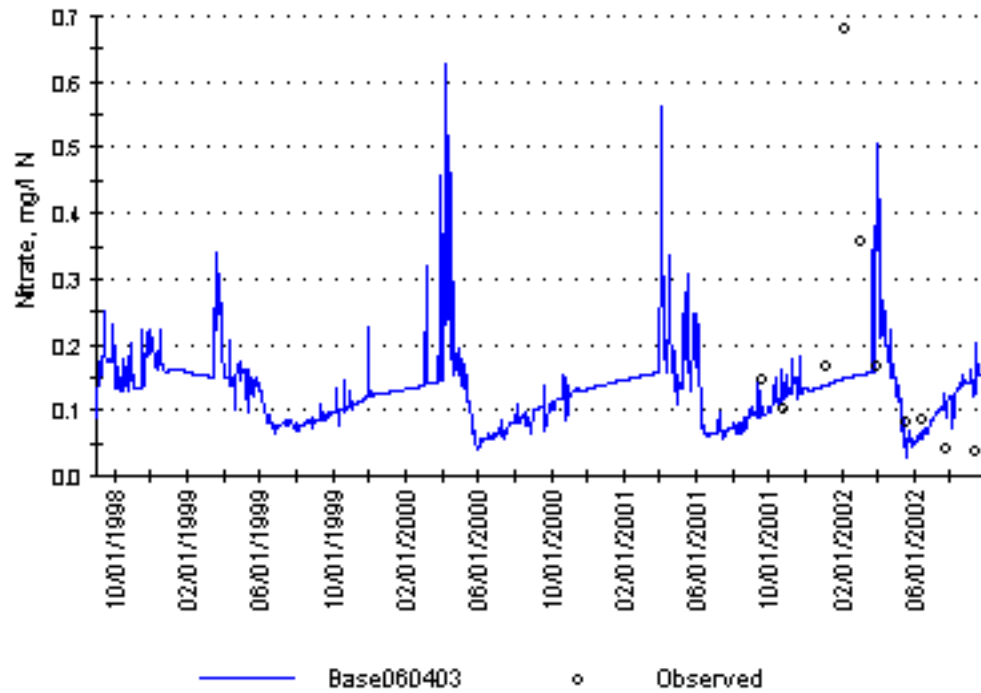


Figure 5-39
Simulated and Observed Nitrate (as $\text{NO}_3\text{-N}$) at BR3

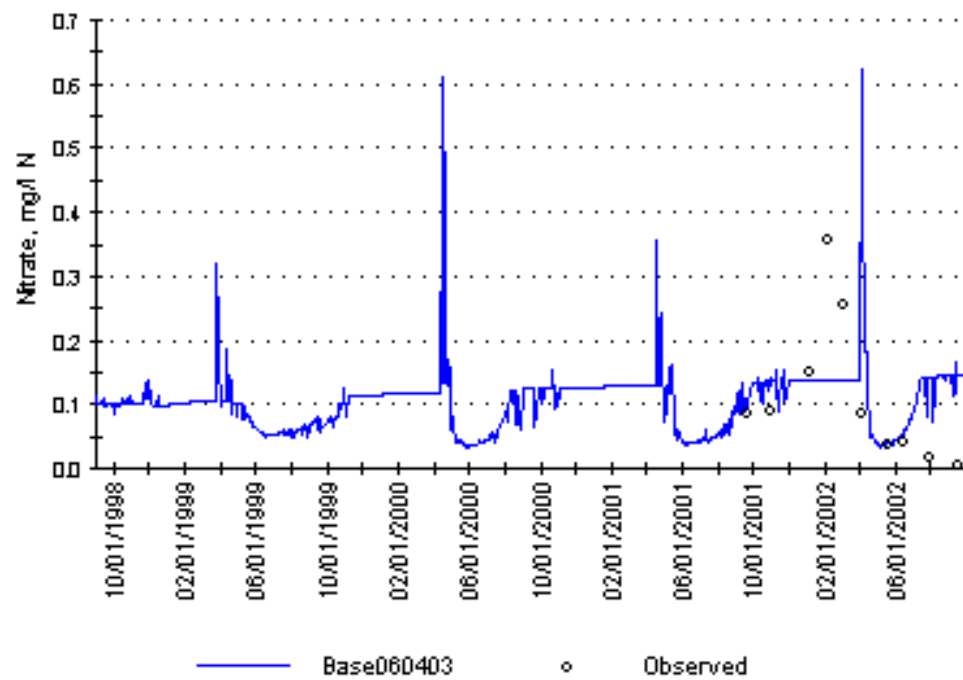


Figure 5-40
Simulated and Observed Nitrate (as $\text{NO}_3\text{-N}$) at PC2

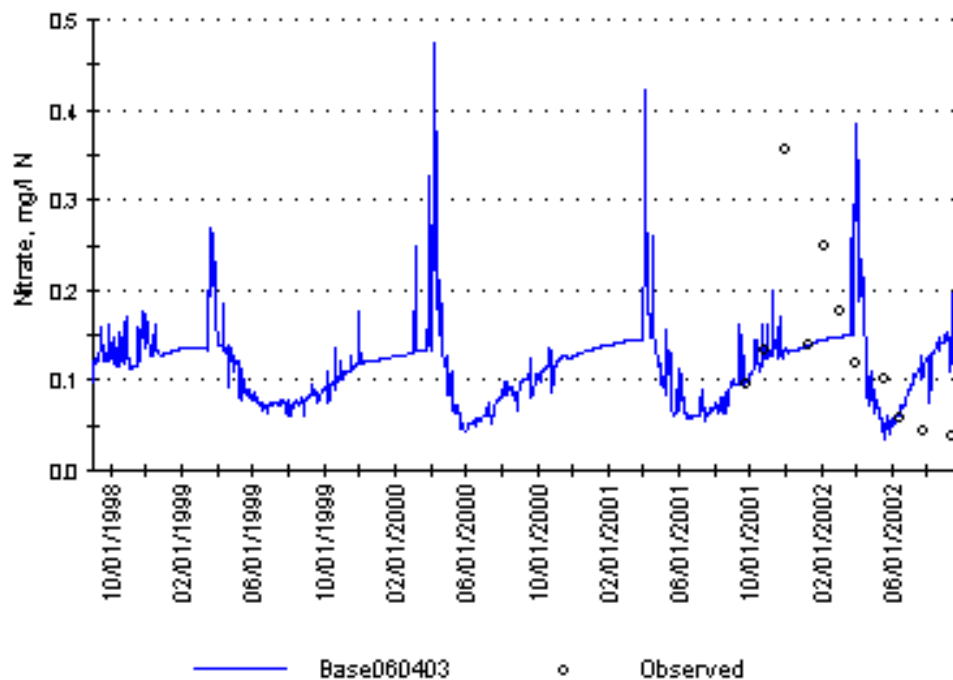


Figure 5-41
Simulated and Observed Nitrate (as NO₃-N) at BR4

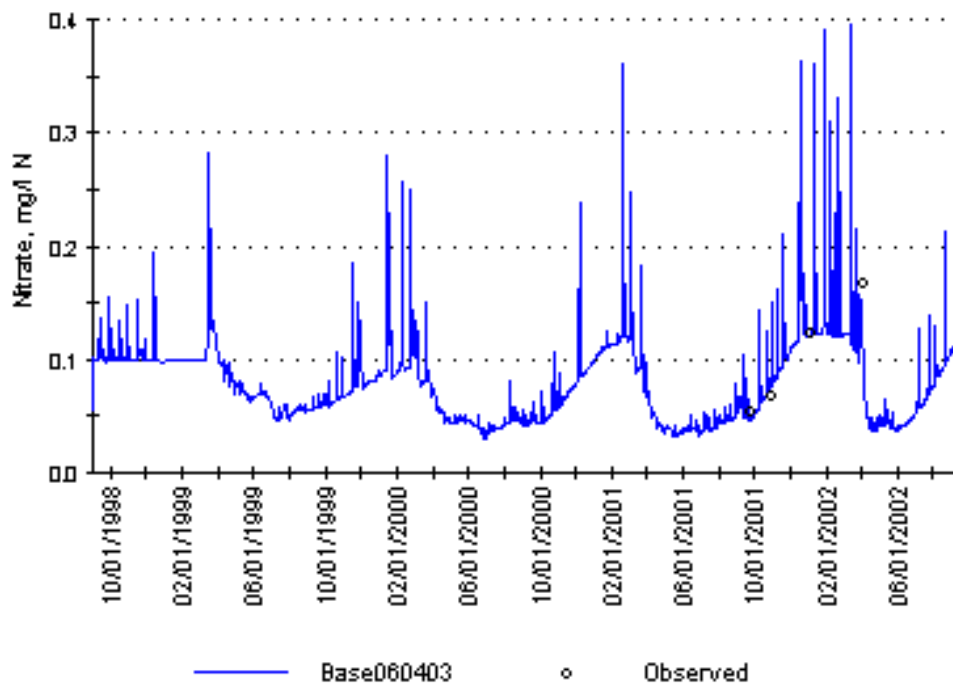


Figure 5-42
Simulated and Observed Nitrate (as NO₃-N) at SR3

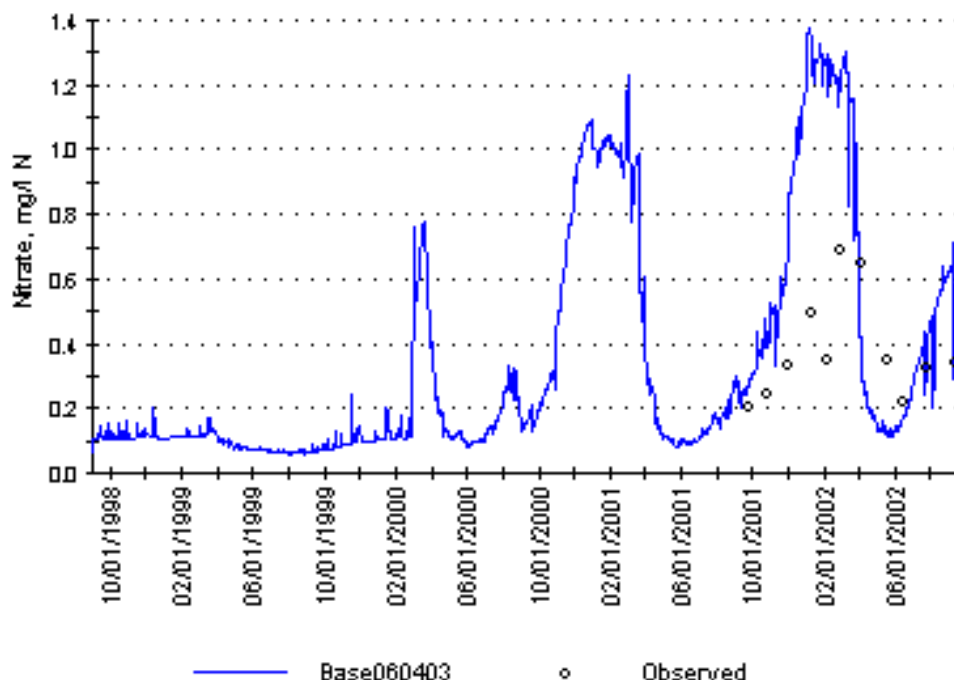


Figure 5-43
Simulated and Observed Nitrate (as NO₃-N) at BR10

Total Nitrogen

Figure 5-44 through Figure 5-48 show simulated total nitrogen compared to observed data. The general trends and ranges of observed data are tracked by the model. One point to note is that the total nitrogen data from 2001 was collected using a method with a relatively high detection limit (Phase I sampling), whereas data collected in 2002 used a more accurate method with a lower detection limit (Phase II sampling). This change in the detection limit may explain why WARMF under predicted total nitrogen concentrations at several locations in 2001.

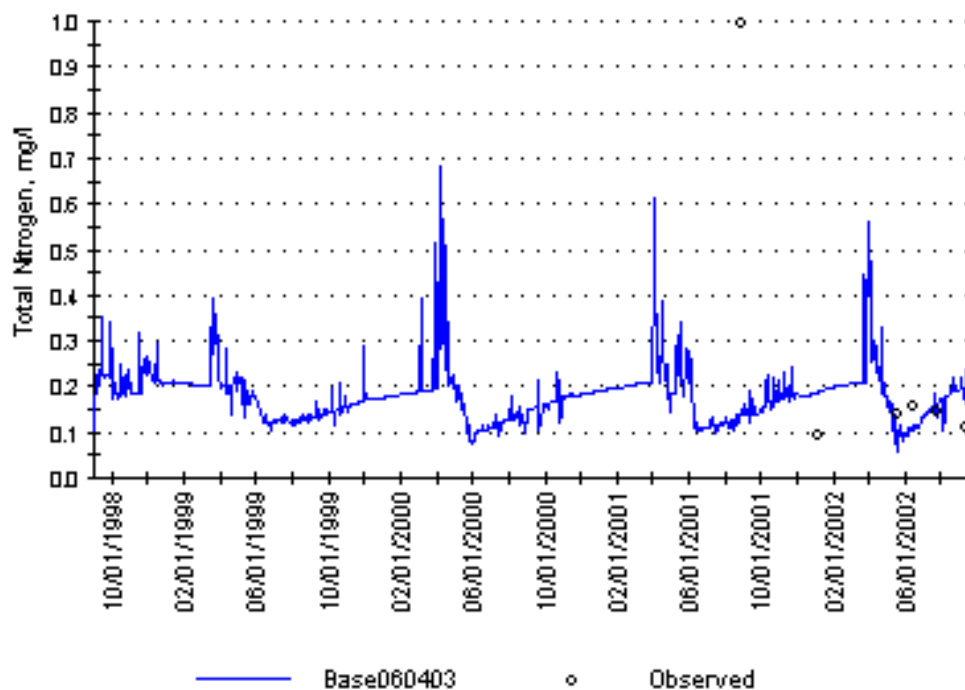


Figure 5-44
Simulated and Observed Total Nitrogen at BR3

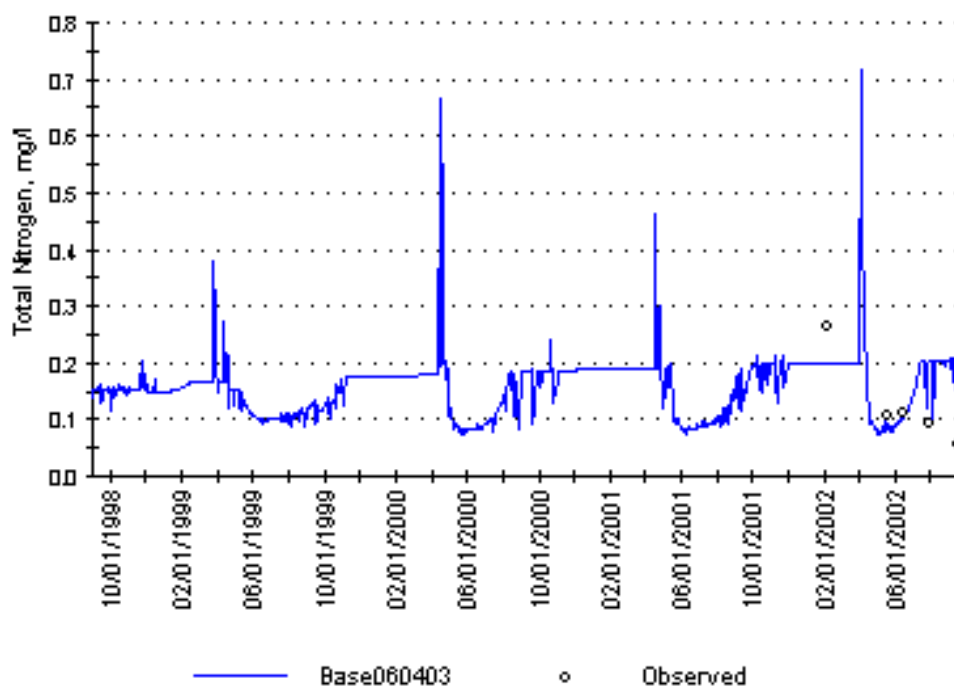


Figure 5-45
Simulated and Observed Total Nitrogen at PC2

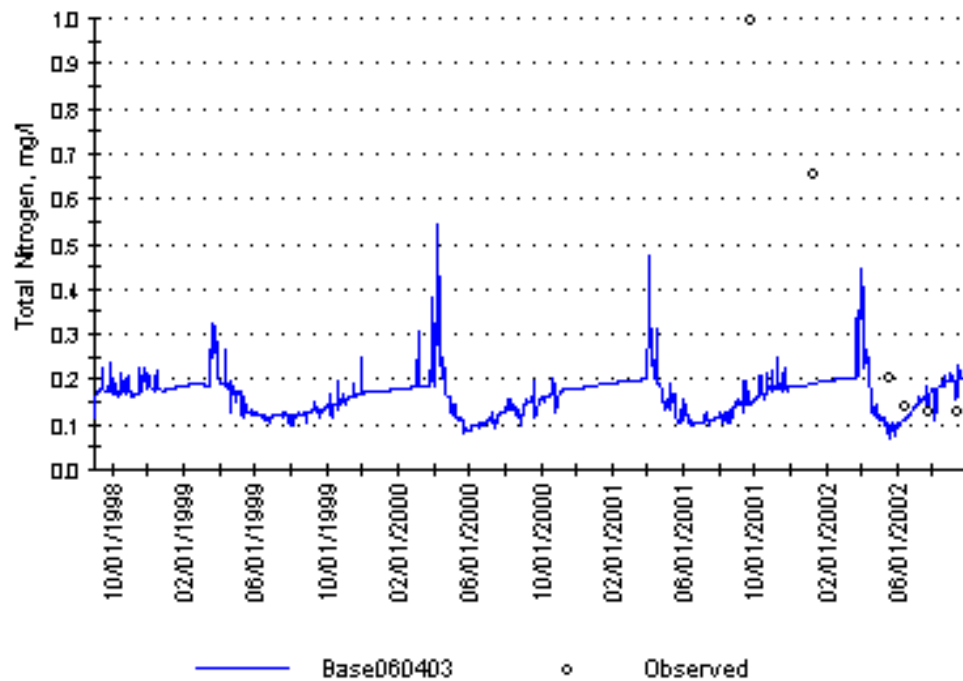


Figure 5-46
Simulated and Observed Total Nitrogen at BR4

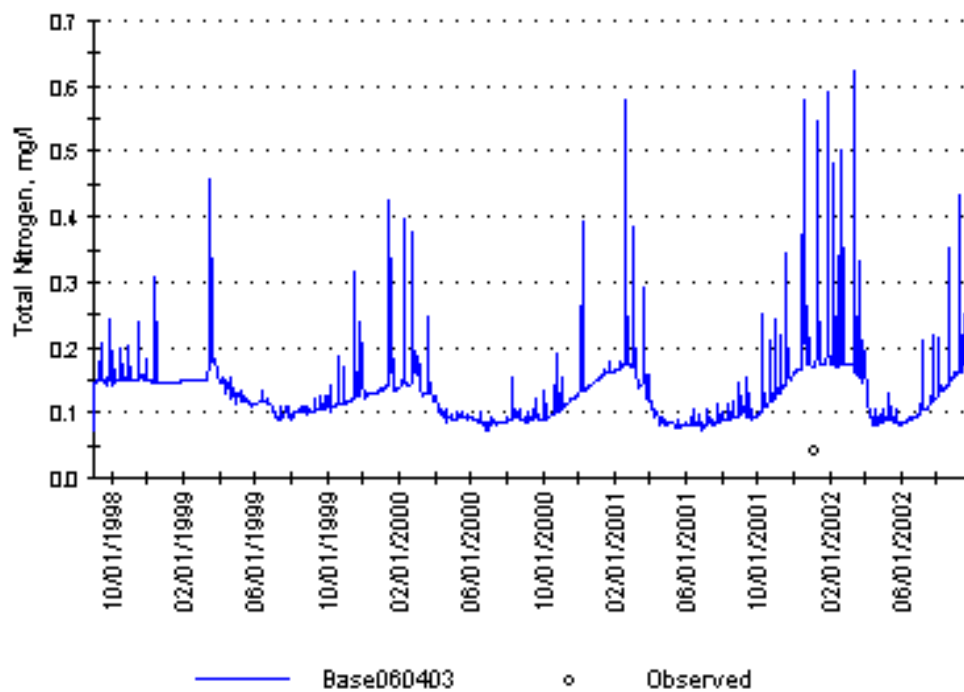


Figure 5-47
Simulated and Observed Total Nitrogen at SR3

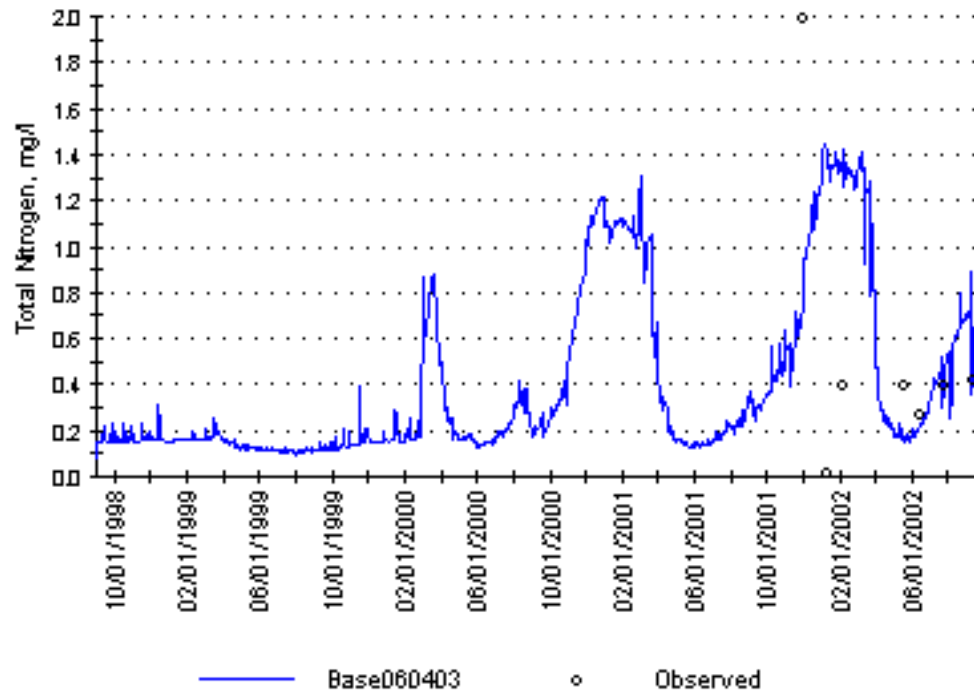


Figure 5-48
Simulated and Observed Total Nitrogen at BR10

Phosphate

Simulated and observed concentrations of phosphate are presented in Figure 5-49 through Figure 5-53. For most locations, the concentration of phosphate during the base-flow period was predicted well; however, it was over predicted at PC2, BR4 and BR10 during the early winter of 2002. Peak concentrations were simulated to be in within the range of observed for all locations.

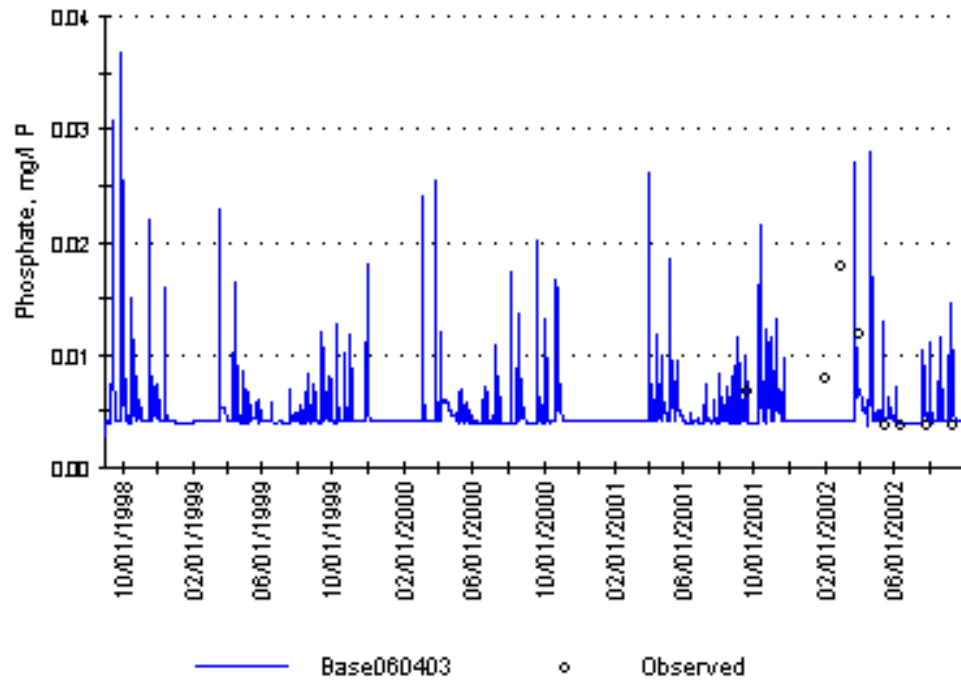


Figure 5-49
Simulated and Observed Phosphate (as $\text{PO}_4\text{-P}$) at BR3

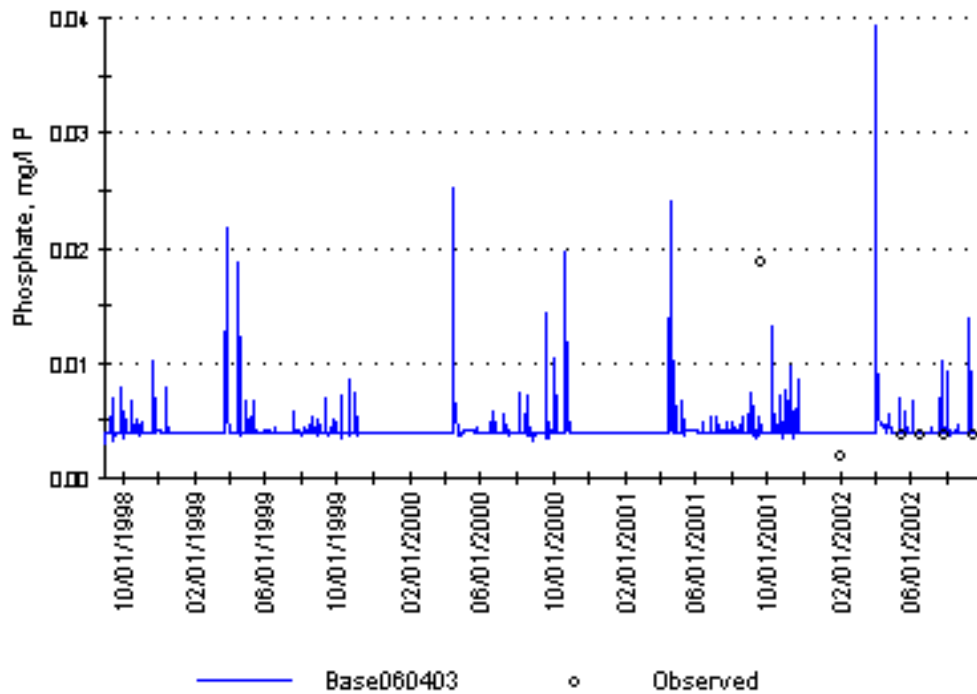


Figure 5-50
Simulated and Observed Phosphate (as $\text{PO}_4\text{-P}$) at PC2

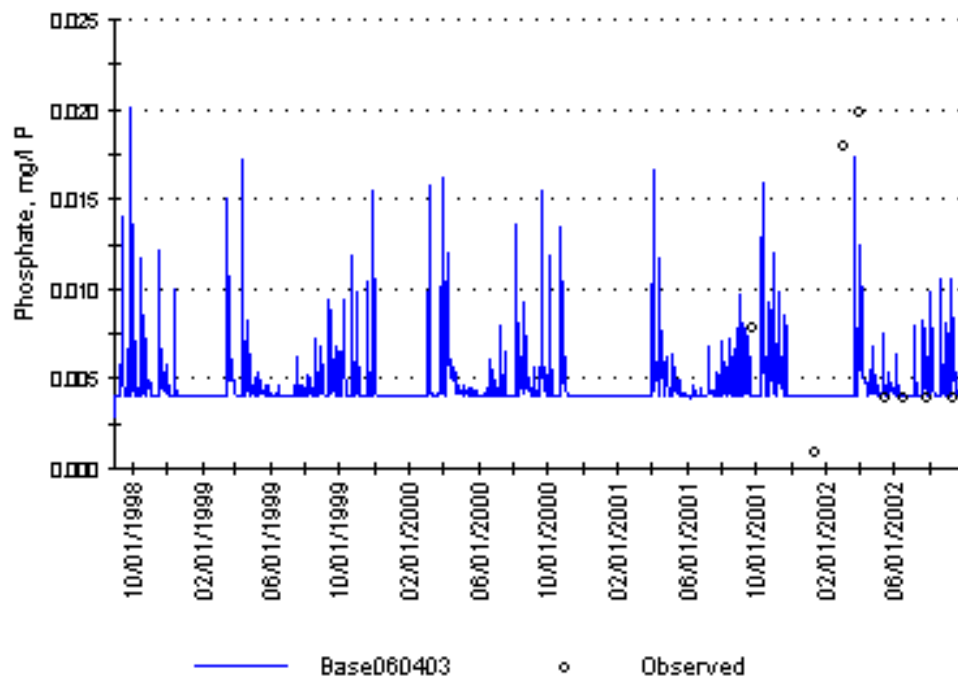


Figure 5-51
Simulated and Observed Phosphate (as PO₄-P) at BR4

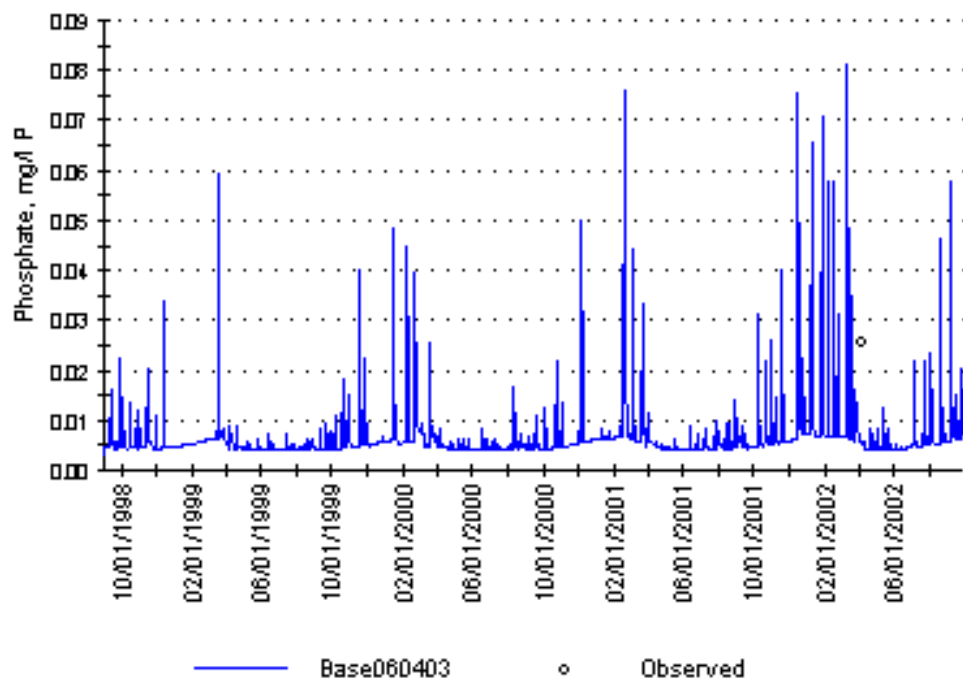


Figure 5-52
Simulated and Observed Phosphate (as PO₄-P) at SR3

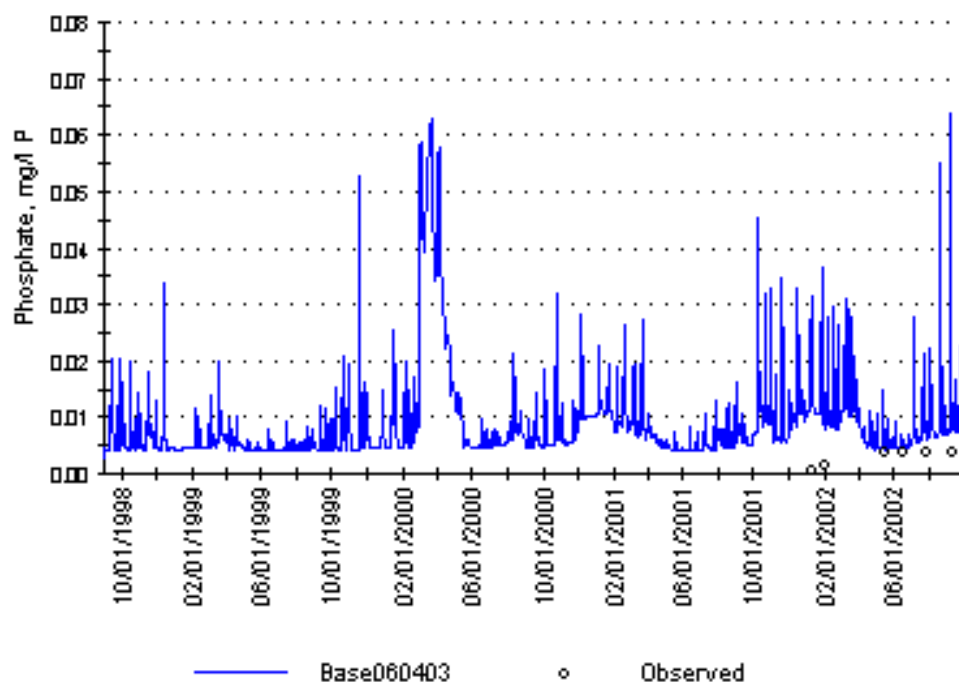


Figure 5-53
Simulated and Observed Phosphate (as $\text{PO}_4\text{-P}$) at BR10

Total Phosphorus

Figure 5-54 through Figure 5-58 show simulated and observed total phosphorus at the five locations. The trends and ranges of observed data were simulated by WARMF at all locations. Total phosphorus data was not collected at station SR2; however, simulated total phosphorus is presented in Figure 5-58.

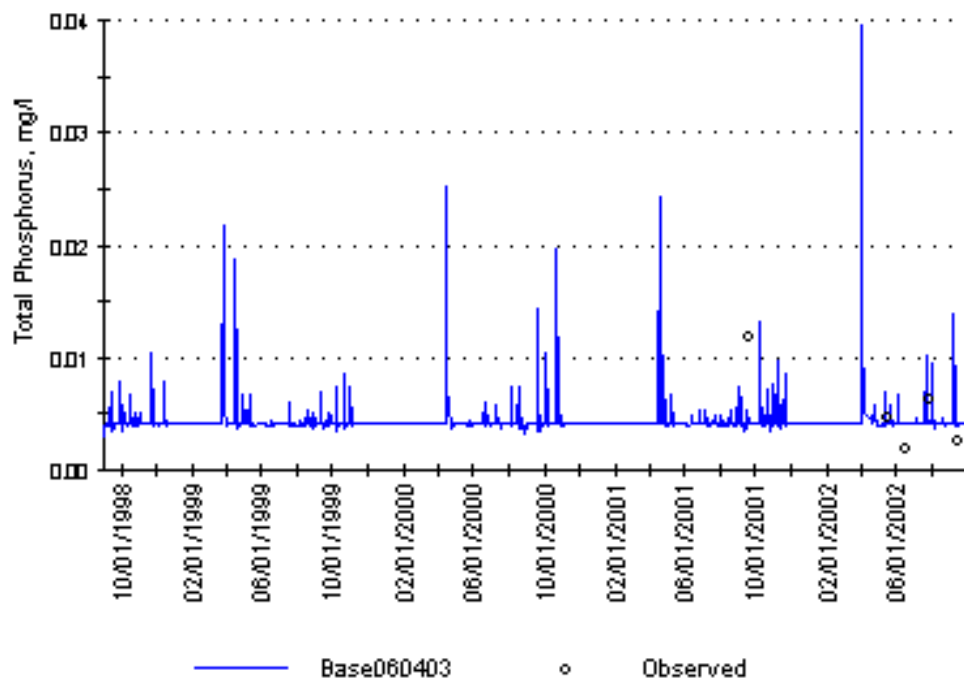


Figure 5-54
Simulated and Observed Total Phosphorus at PC2

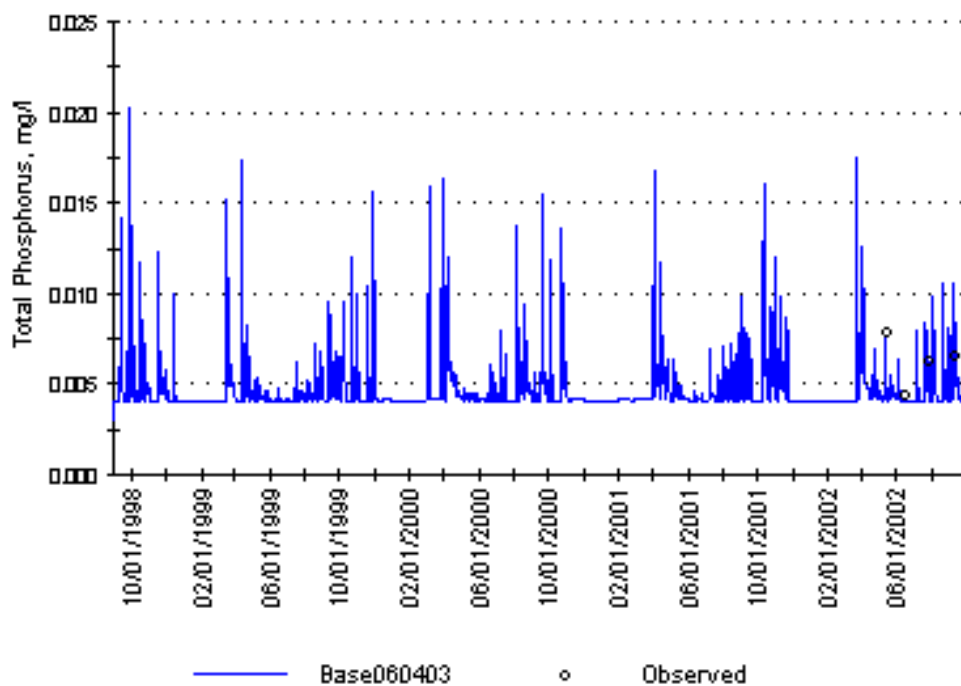


Figure 5-55
Simulated and Observed Total Phosphorus at BR4

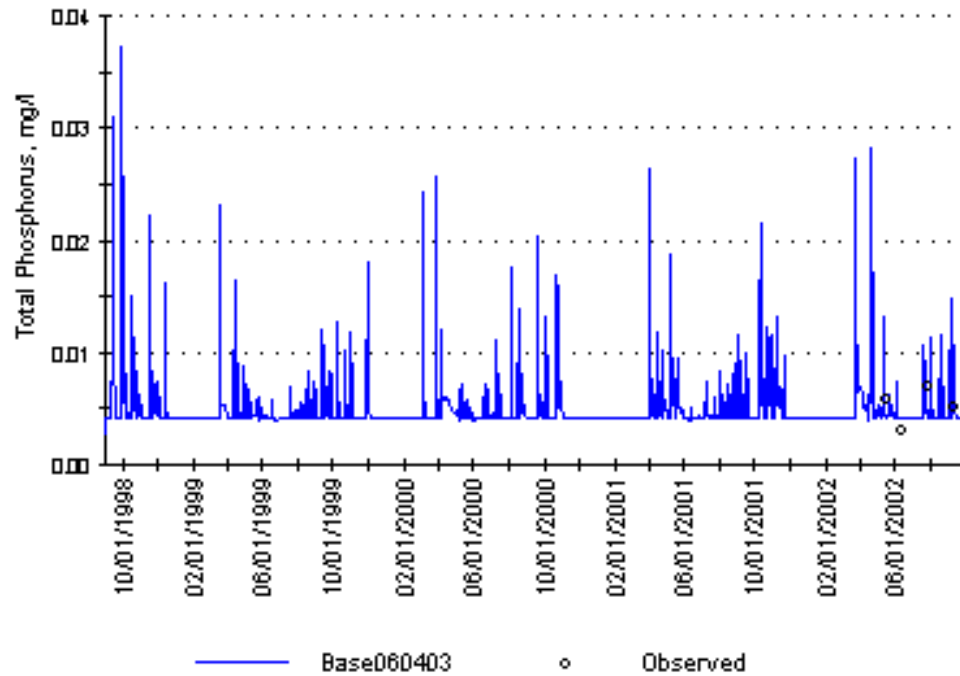


Figure 5-56
Simulated and Observed Total Phosphorus at BR3

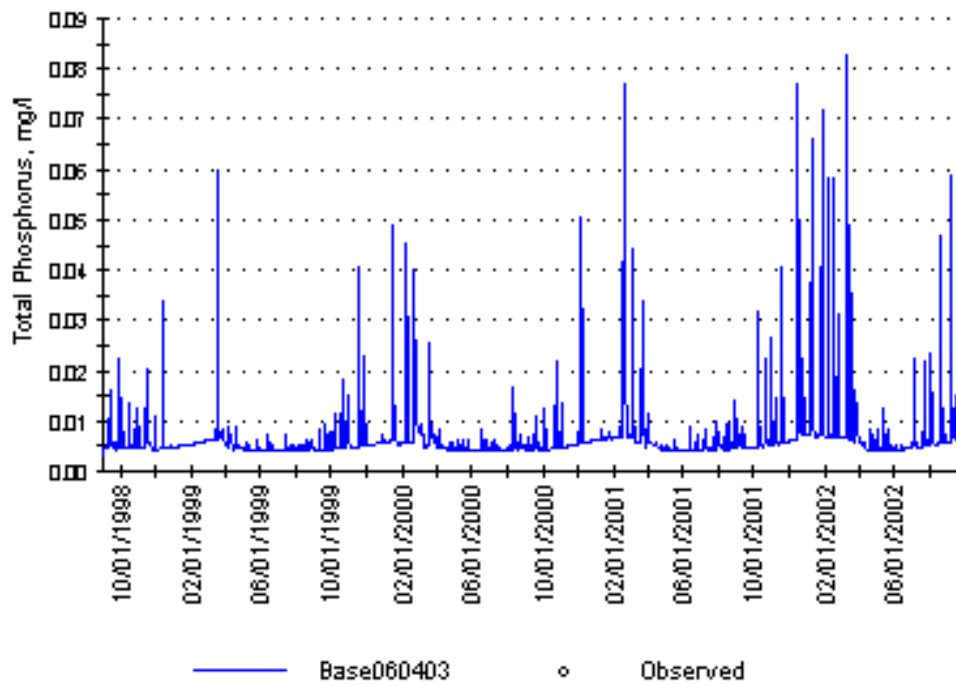


Figure 5-57
Simulated and Observed Total Phosphorus at SR3

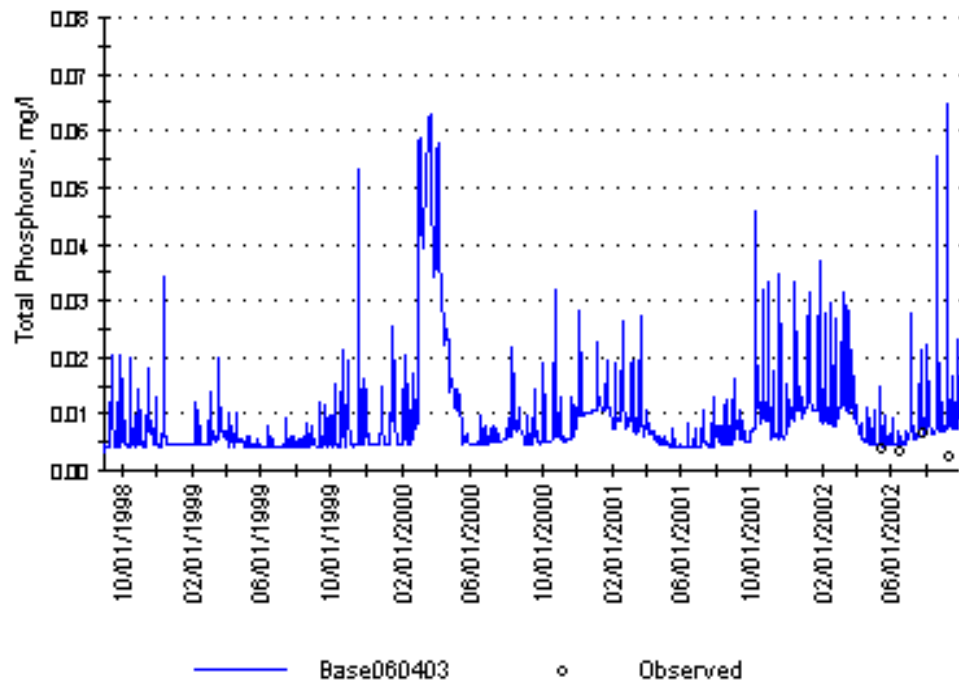


Figure 5-58
Simulated and Observed Total Phosphorus at BR10

Fecal Coliform Bacteria

Simulated and observed fecal coliform bacteria results are presented in Figure 5-59 through Figure 5-63. The results are plotted on a log scale. The predicted surface water concentrations ranged from 1.0E-3 to 1,000 MPN/100 mL for various locations. The observed data were in the same range.

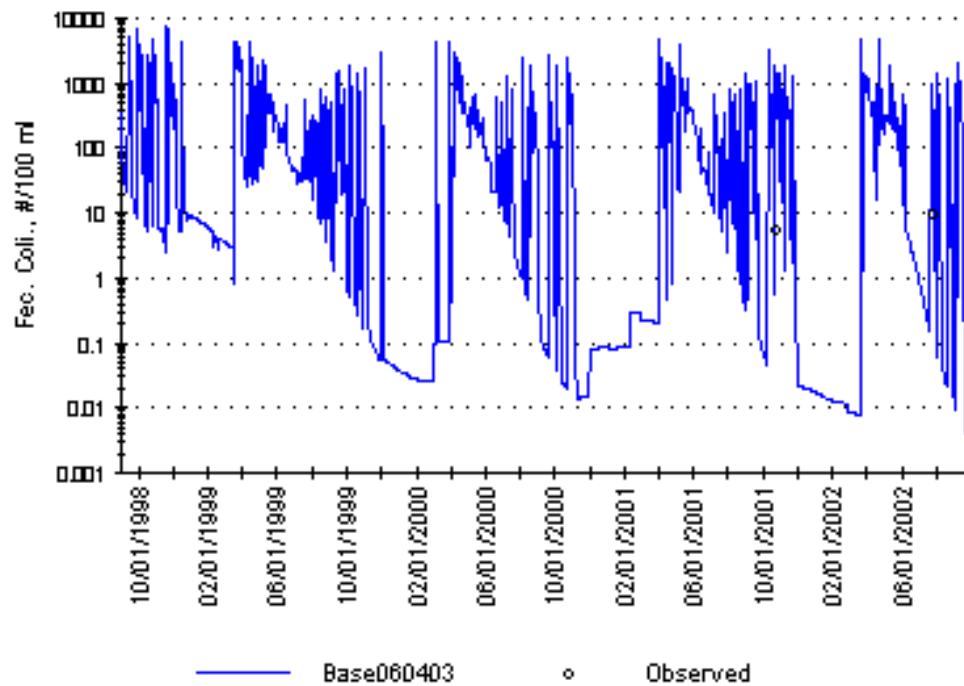


Figure 5-59
Simulated and Observed Fecal Coliform Bacteria at BR3

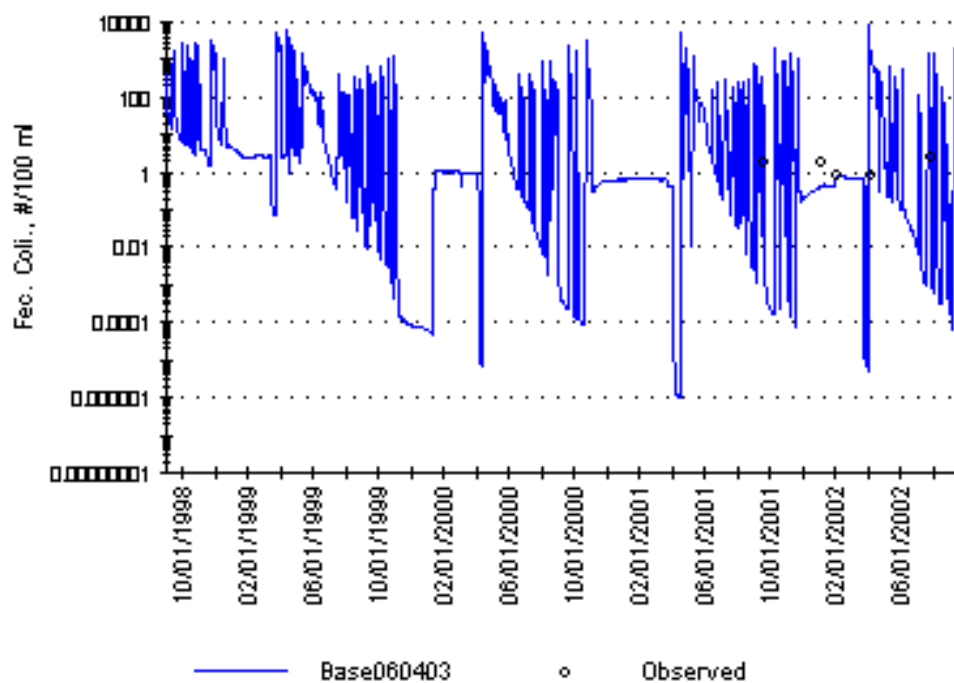


Figure 5-60
Simulated and Observed Fecal Coliform Bacteria at PC2

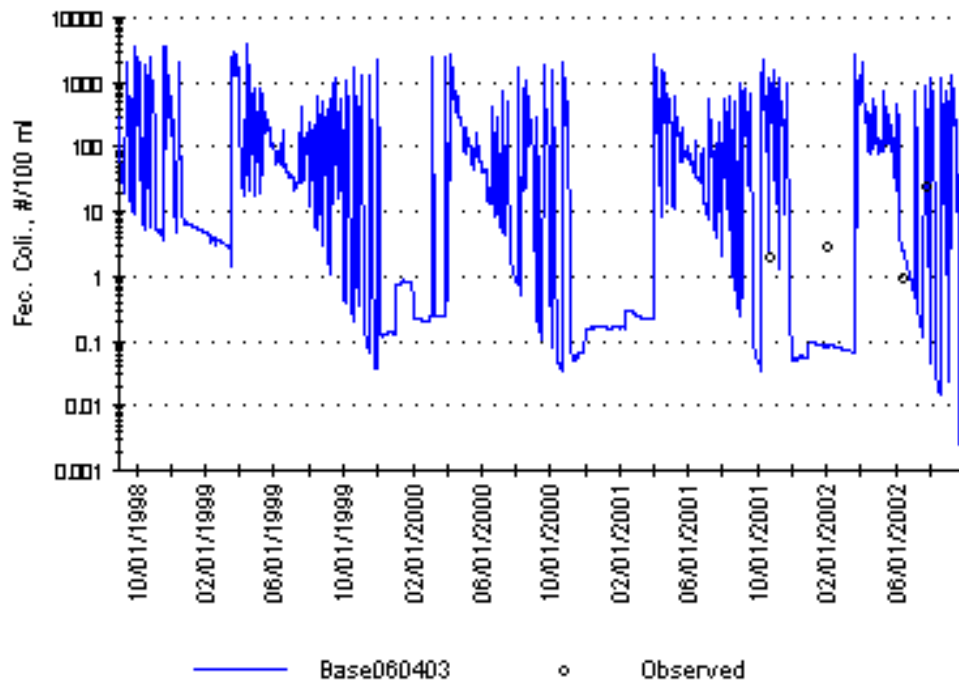


Figure 5-61
Simulated and Observed Fecal Coliform Bacteria at BR4

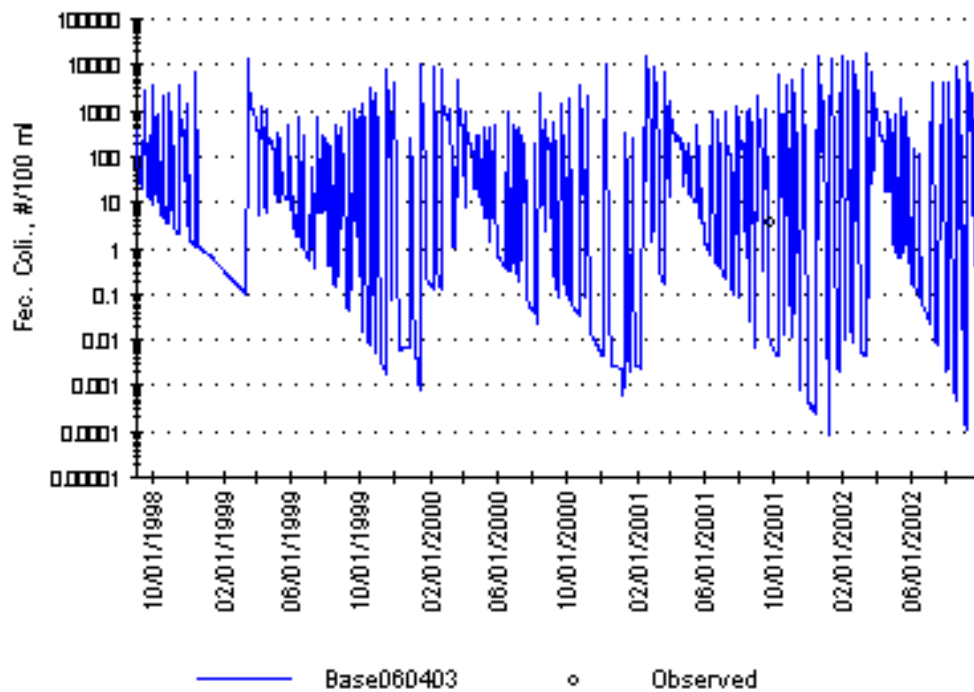


Figure 5-62
Simulated and Observed Fecal Coliform Bacteria at SR3

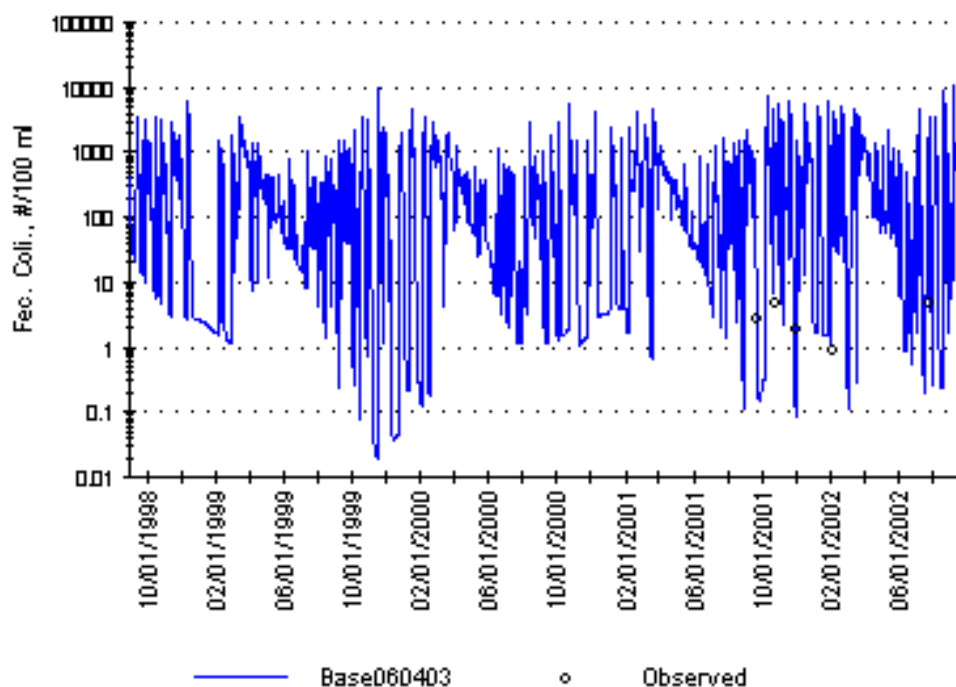


Figure 5-63
Simulated and Observed Fecal Coliform Bacteria at BR10

Dissolved Oxygen

Figure 5-64 through Figure 5-68 compare simulated and observed dissolved oxygen concentrations for five locations. For all locations, the range of observed dissolved oxygen data was predicted well by WARMF; however, the pattern does not show a temporal match. Typically, dissolved oxygen concentrations are low in the summer and high in the winter because lower water temperatures allow for a higher saturation limit. WARMF consistently predicts this seasonal pattern, whereas the observed data shows a reverse pattern with the lowest concentrations occurring in the winter. The reason for the abnormal behavior of the observed dissolved oxygen concentrations needs to be investigated.

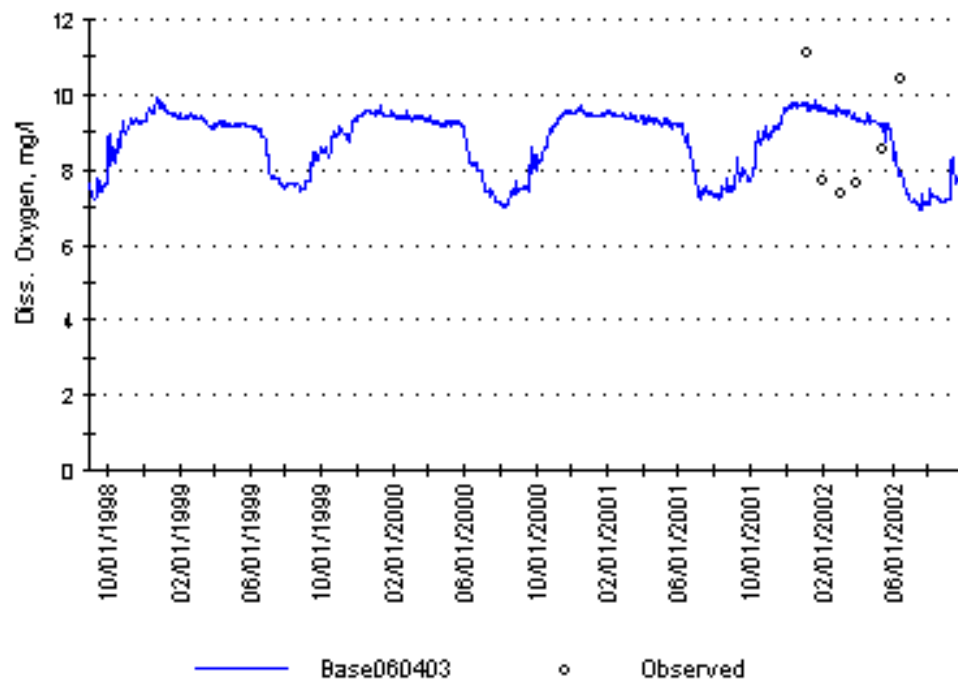


Figure 5-64
Simulated and Observed Dissolved Oxygen at BR3

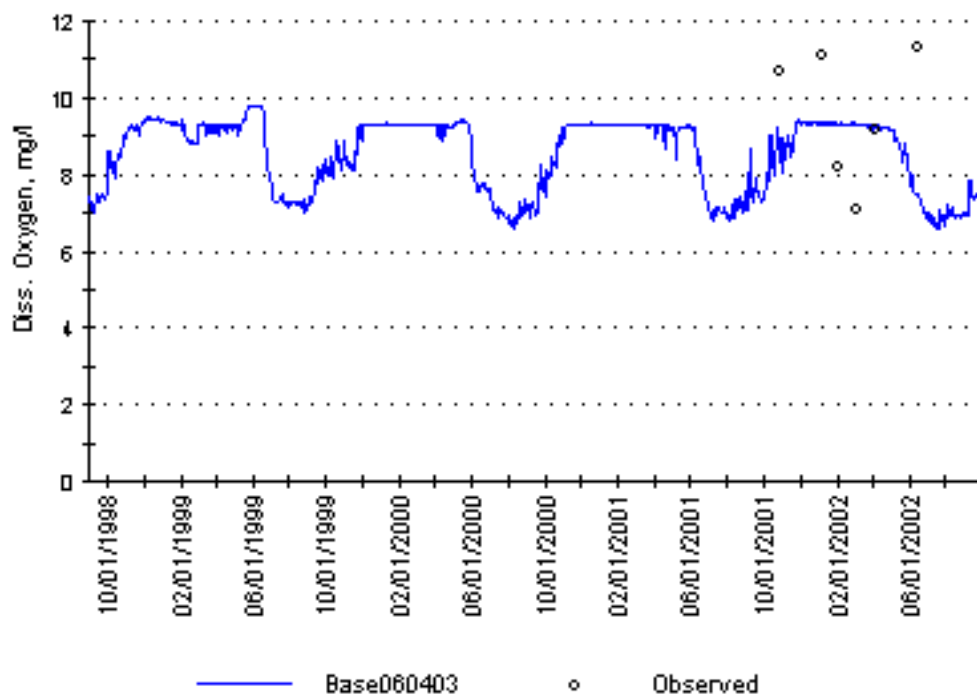


Figure 5-65
Simulated and Observed Dissolved Oxygen at PC2

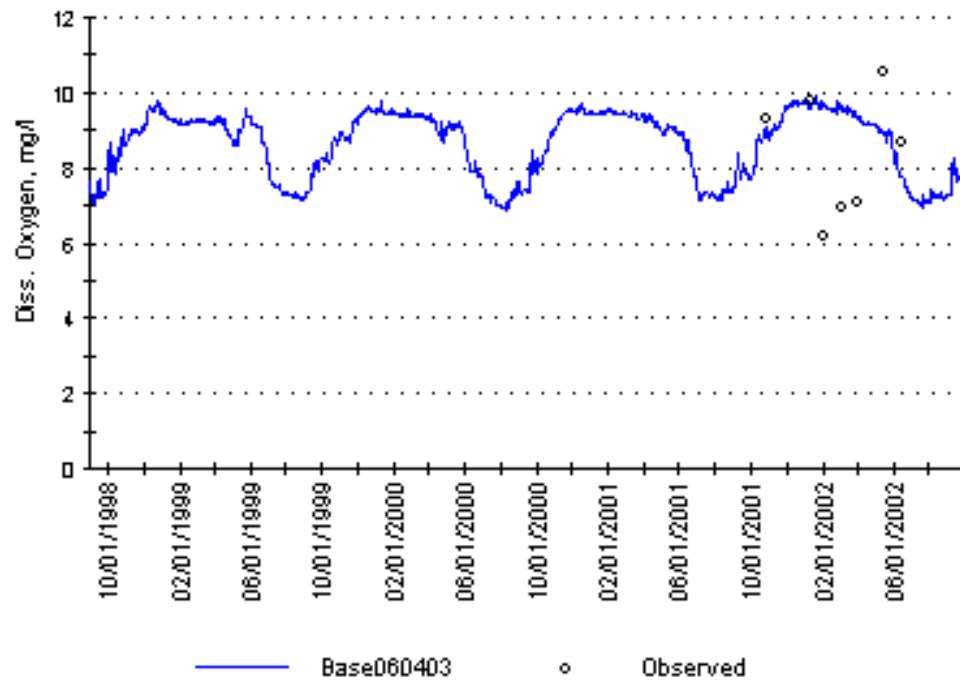


Figure 5-66
Simulated and Observed Dissolved Oxygen at BR4

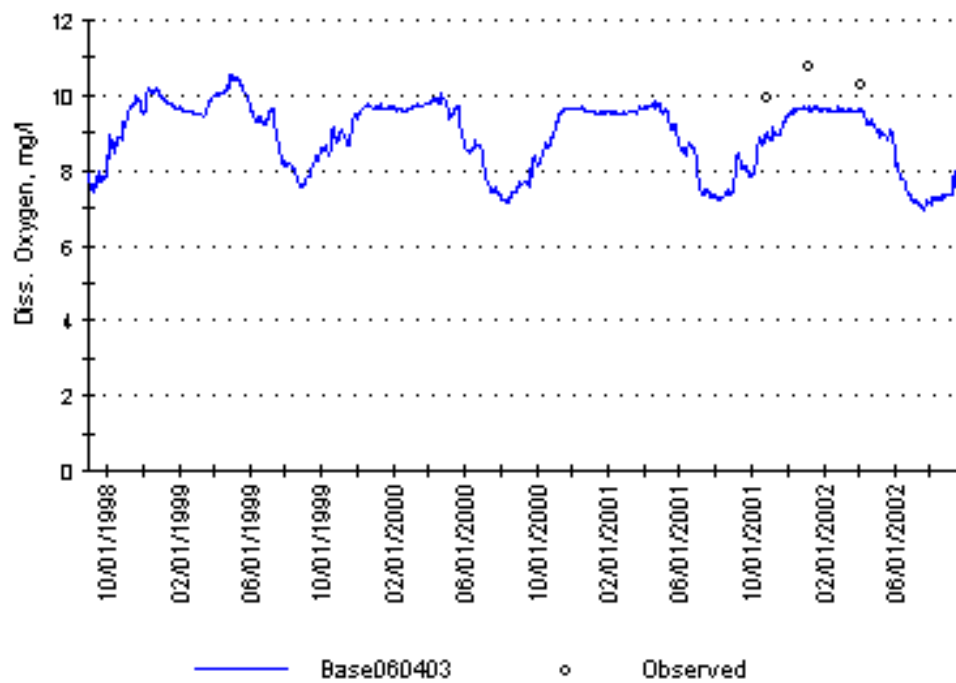


Figure 5-67
Simulated and Observed Dissolved Oxygen at SR3

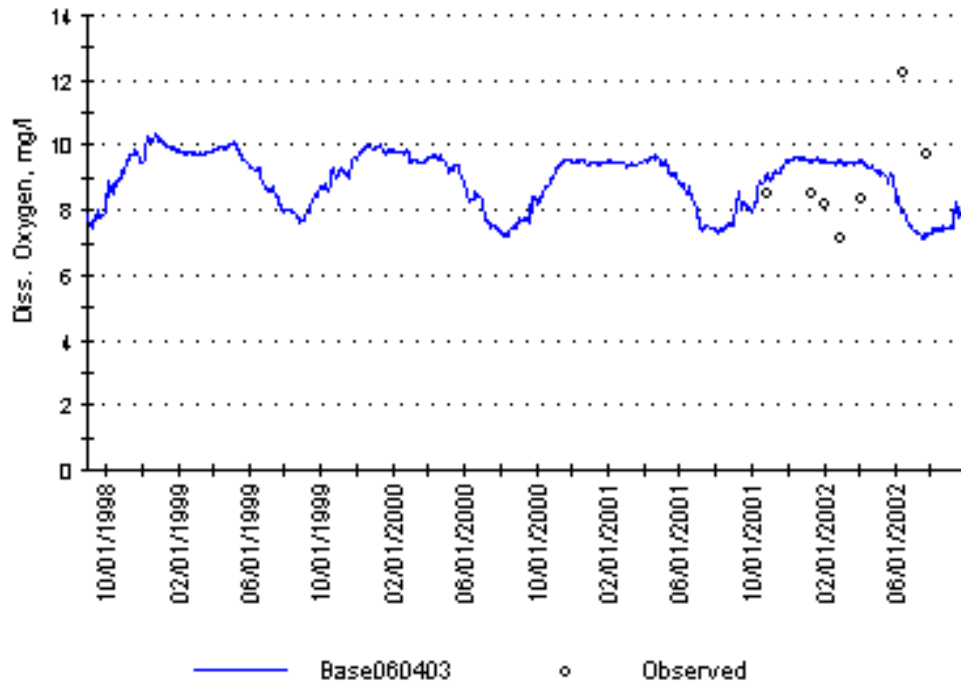


Figure 5-68
Simulated and Observed Dissolved Oxygen at BR10

Verification

Model verification involves testing the model performance for a different time period while using the calibrated coefficients without modification. A time period of 1990 to 1995 was selected for verification. Results are presented in the following sections.

Hydrology Verification

Figure 5-69 compares simulated and measured stream flow at Blue River at Blue River, CO. Figure 5-70 through Figure 5-72 show statistical results, a scatter plot, a frequency distribution plot, and a cumulative hydrograph for this location. The timing and magnitude of seasonal peak flows matched well for most years. However, for the exceptionally wet year of 1995, the peak flow was under predicted. The cumulative plot shows a slight under prediction of flow volume and the correlation coefficient for this location of 0.756.

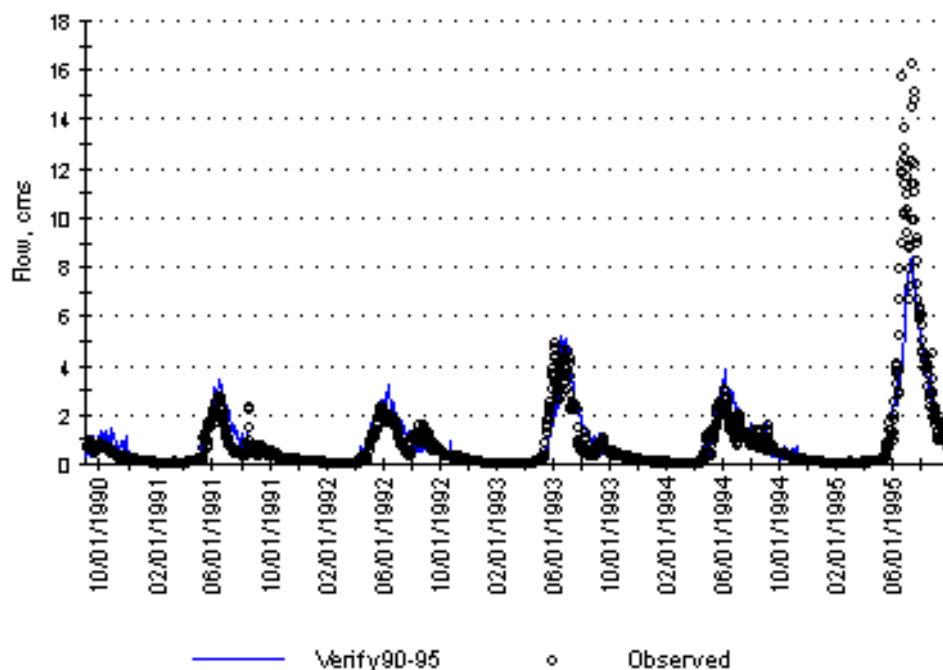


Figure 5-69
Simulated and Observed Flow for Blue River at Blue River, CO

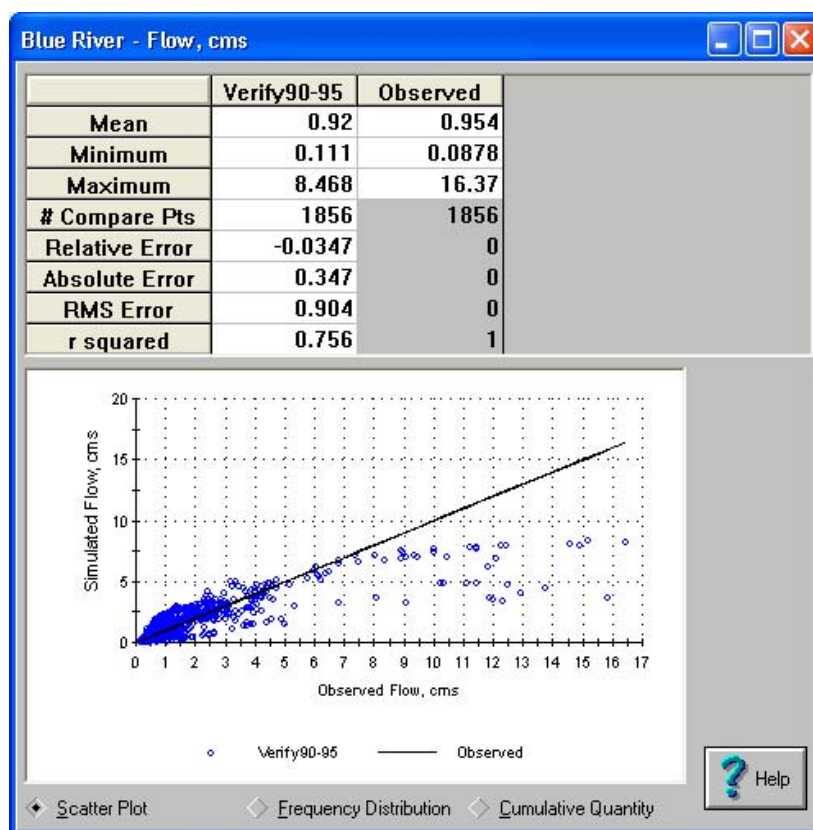
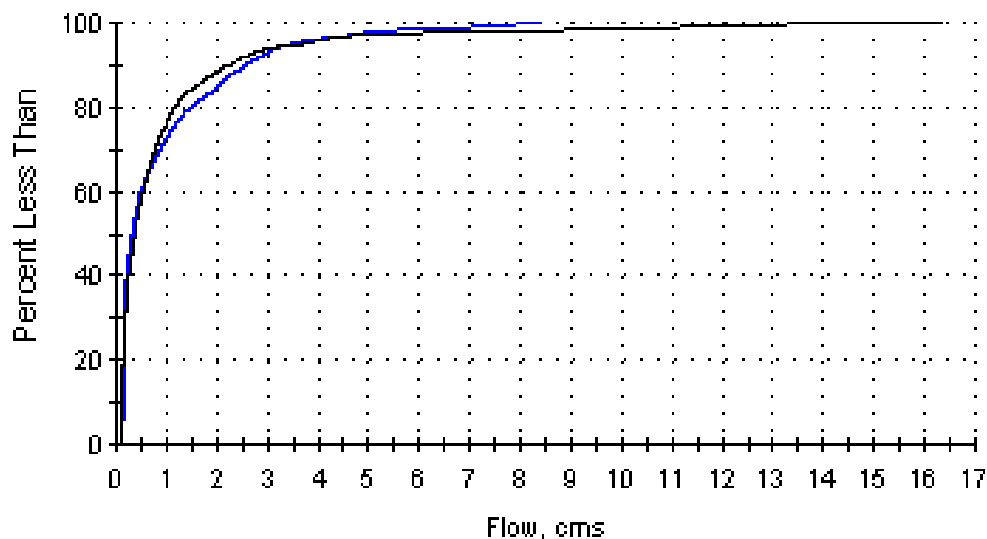
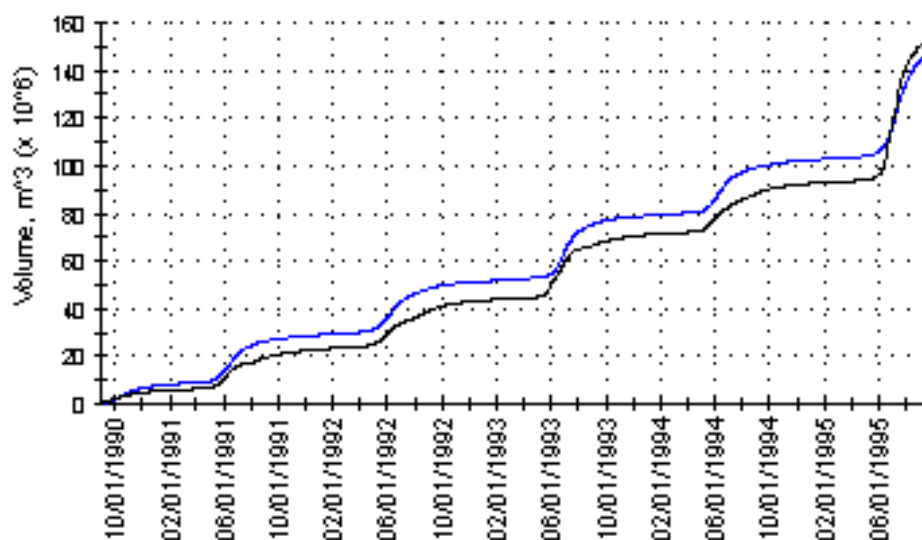


Figure 5-70
Statistical Output and Scatter Plot for Blue River at Blue River, CO



Note: Black line is observed; blue line is simulated.

Figure 5-71
Frequency Distribution Plot for Blue River at Blue River, CO



Note: Black line is observed; blue line is simulated.

Figure 5-72
Cumulative Quantity Plot for Blue River at Blue River, CO

Figure 5-73 presents simulated and observed flow for the Blue River above Dillon Reservoir. Figure 5-74 through Figure 5-76 show statistical results, a scatter plot, a frequency distribution plot, and a cumulative hydrograph for this location. The timing and magnitude of seasonal peak flows matched well for most years. Also, the peak flow was under predicted for 1995. The cumulative plot shows a good prediction of flow volume and the correlation coefficient for this location of 0.826.

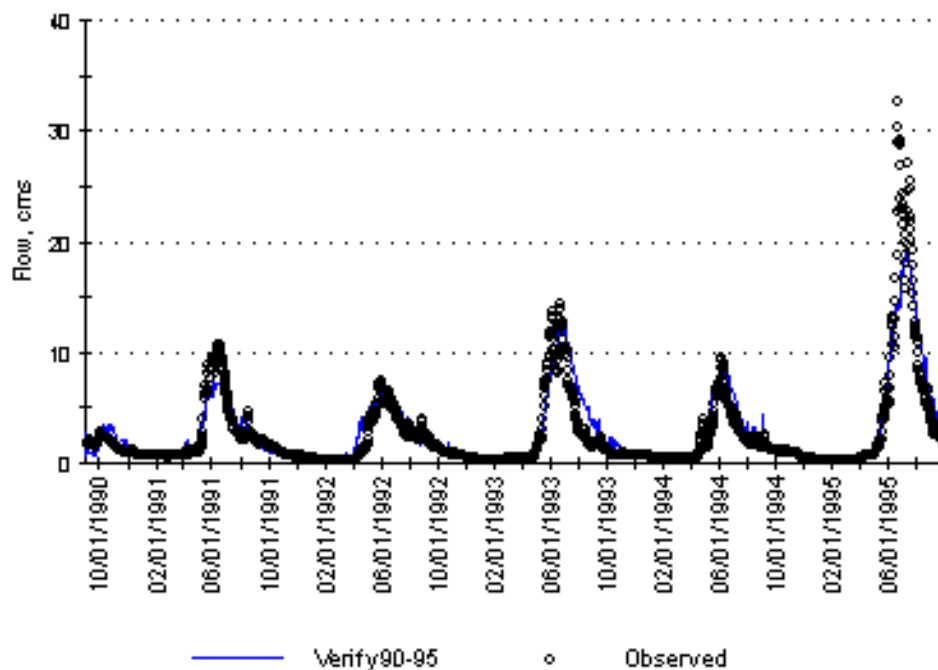


Figure 5-73
Simulated and Observed Flow for Blue River Above Dillon Reservoir

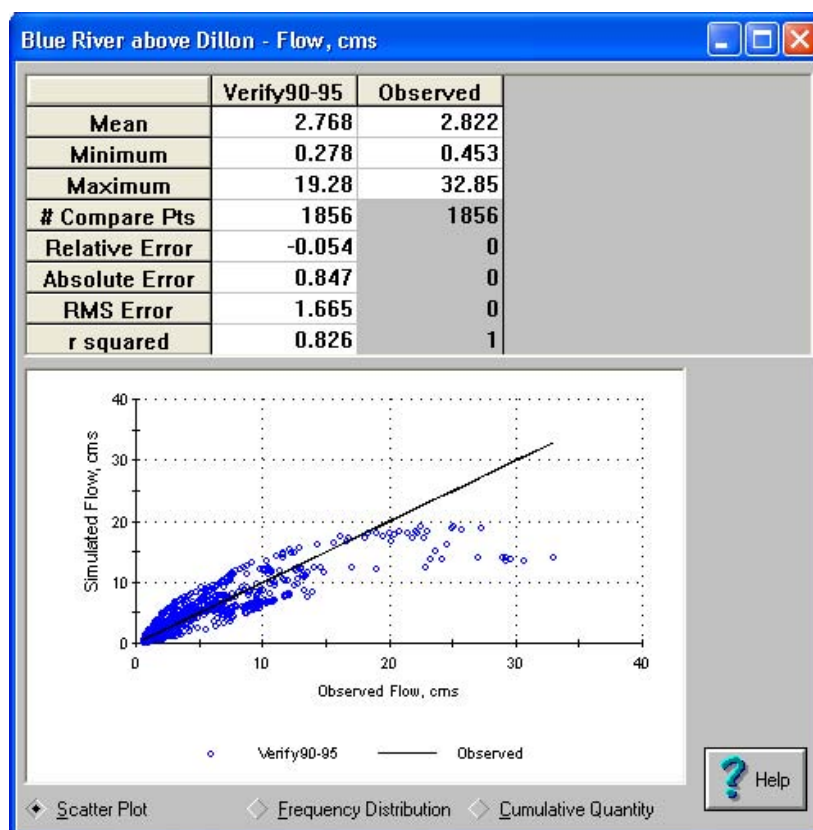
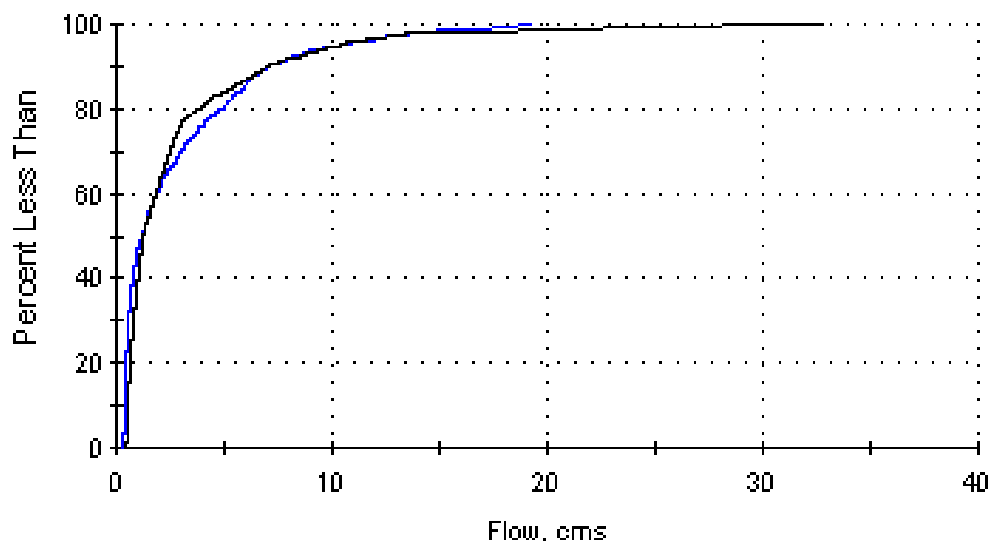
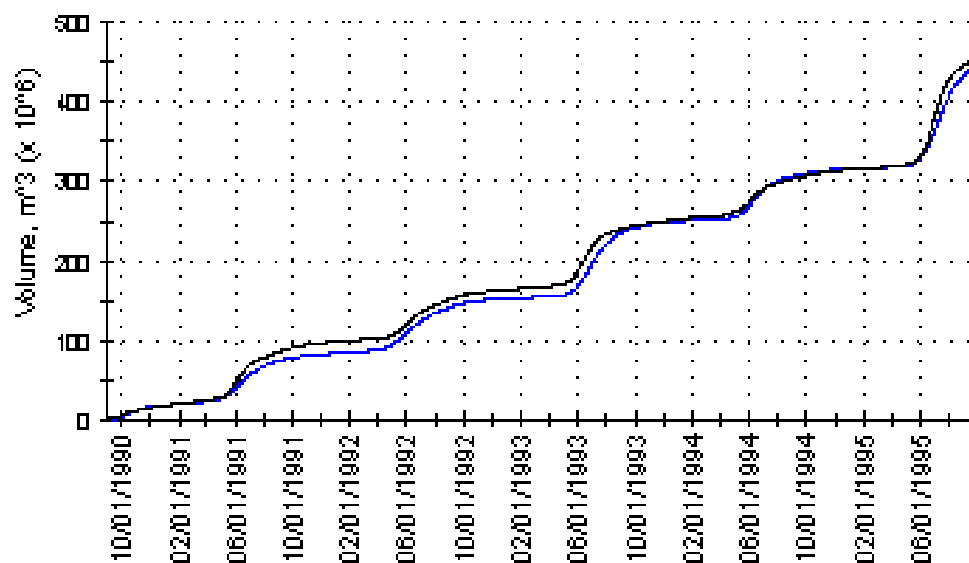


Figure 5-74
Statistical Output and Scatter Plot for Blue River Above Dillon Reservoir



Note: Black line is observed; blue line is simulated.

Figure 5-75
Frequency Distribution Plot for Blue River Above Dillon Reservoir



Note: Black line is observed; blue line is simulated.

Figure 5-76
Cumulative Quantity Plot for Blue River Above Dillon Reservoir

Figure 5-77 compares simulated and measured stream flow at Tenmile Creek. Figure 5-78 through Figure 5-80 show statistical results, a scatter plot, a frequency distribution plot, and a cumulative hydrograph for this location. The hydrograph pattern was simulated well; however, several peak flows were under predicted. The cumulative plot shows a slight under prediction of flow volume and the correlation coefficient for this location of 0.738.

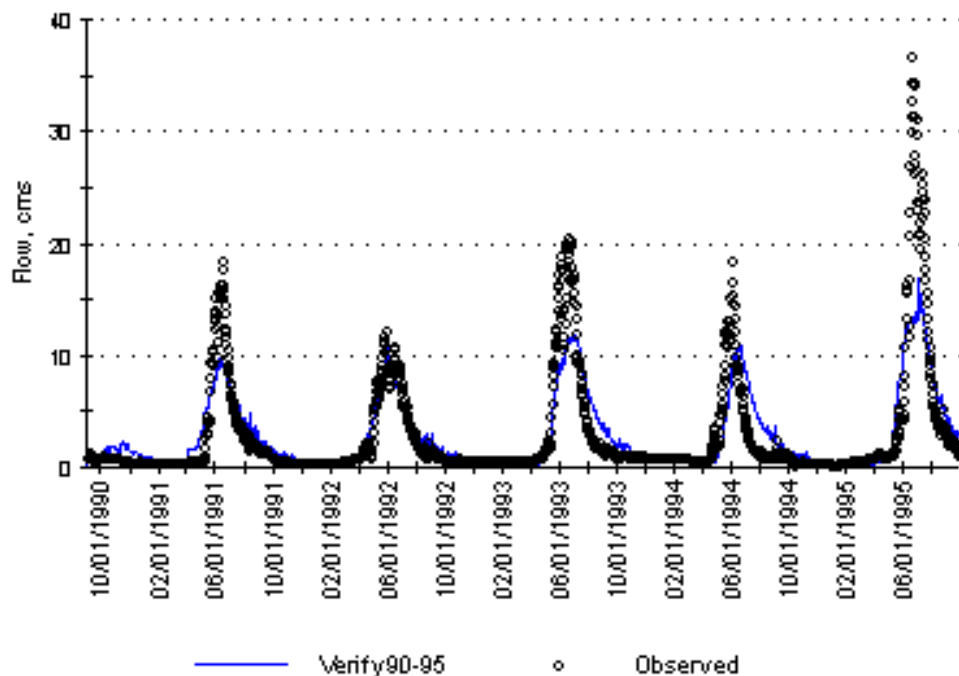


Figure 5-77
Simulated and Observed Flow for Tenmile Creek at USGS Gage

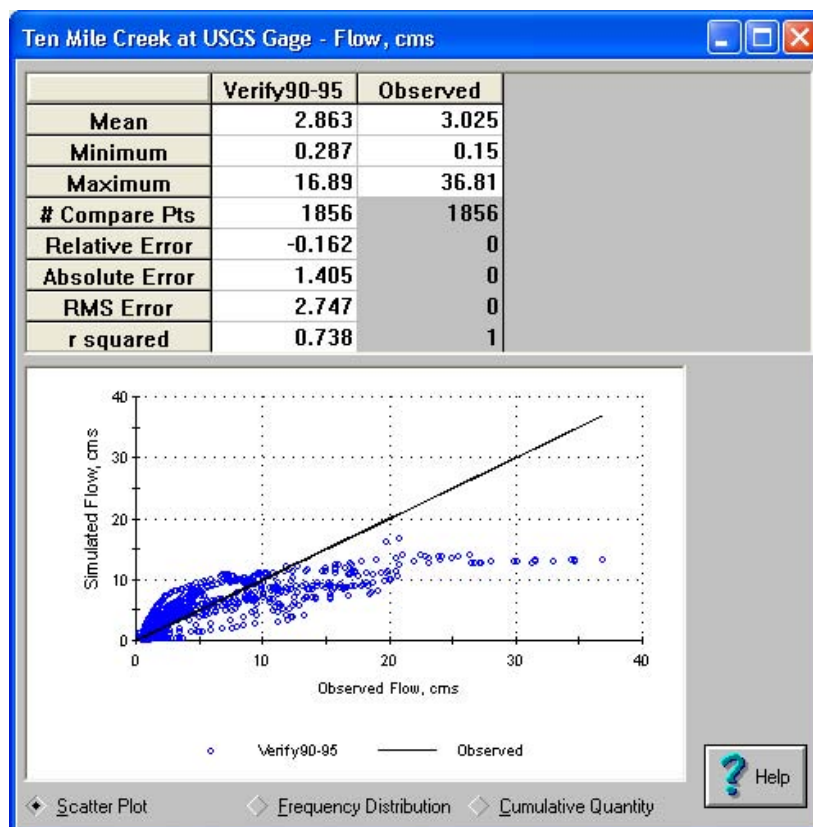
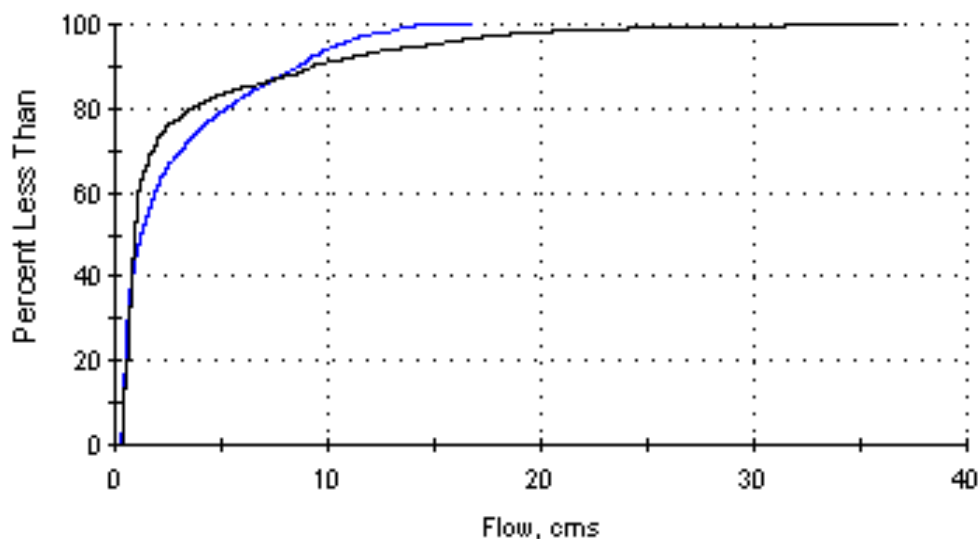
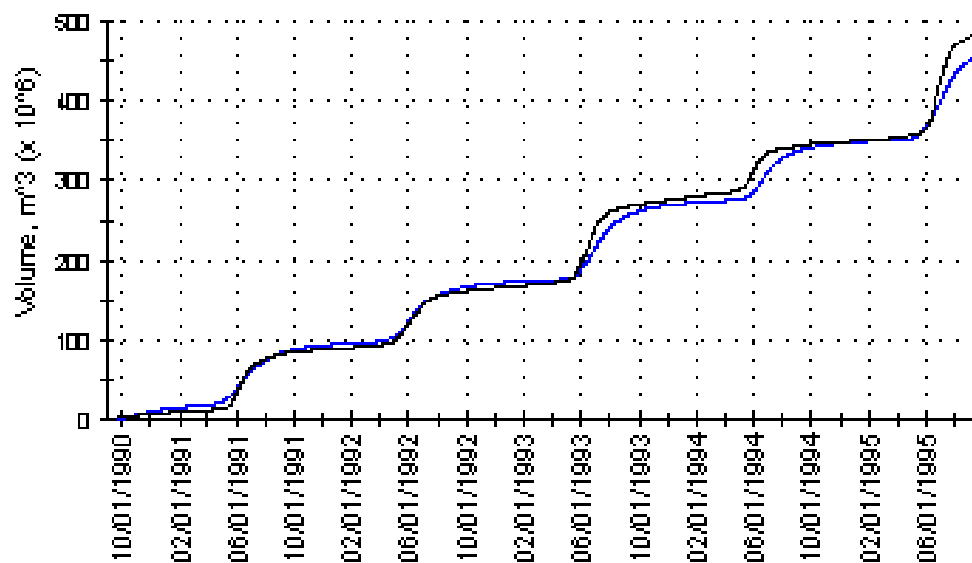


Figure 5-78
Statistical Output and Scatter Plot for Tenmile Creek at USGS Gage



Note: Black line is observed; blue line is simulated.

Figure 5-79
Frequency Distribution Plot for Tenmile Creek at USGS Gage



Note: Black line is observed; blue line is simulated.

Figure 5-80
Cumulative Quantity Plot for Tenmile Creek at USGS Gage

Figure 5-81 shows simulated and observed stream flow for Snake River above North Fork. The hydrograph pattern was simulated well; however, peak flows for 1994 and 1995 were under predicted and peak flow for 1992 was slightly over predicted. Figure 5-82 through Figure 5-84 show statistical results, a scatter plot, a frequency distribution plot, and a cumulative hydrograph. The correlation coefficient for this location is 0.814.

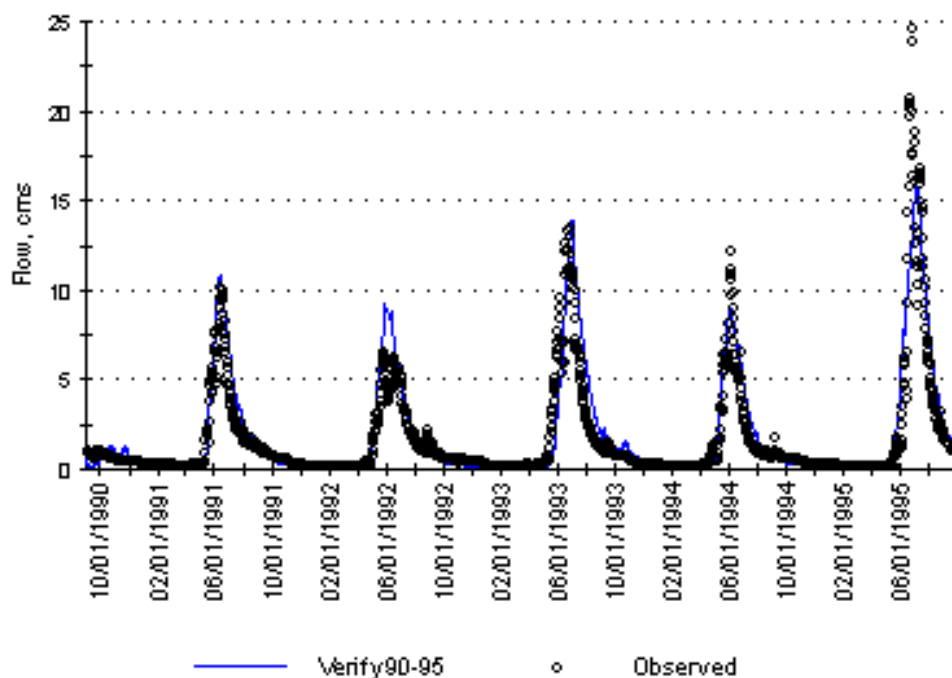


Figure 5-81
Simulated and Observed Flow for Snake River Above North Fork

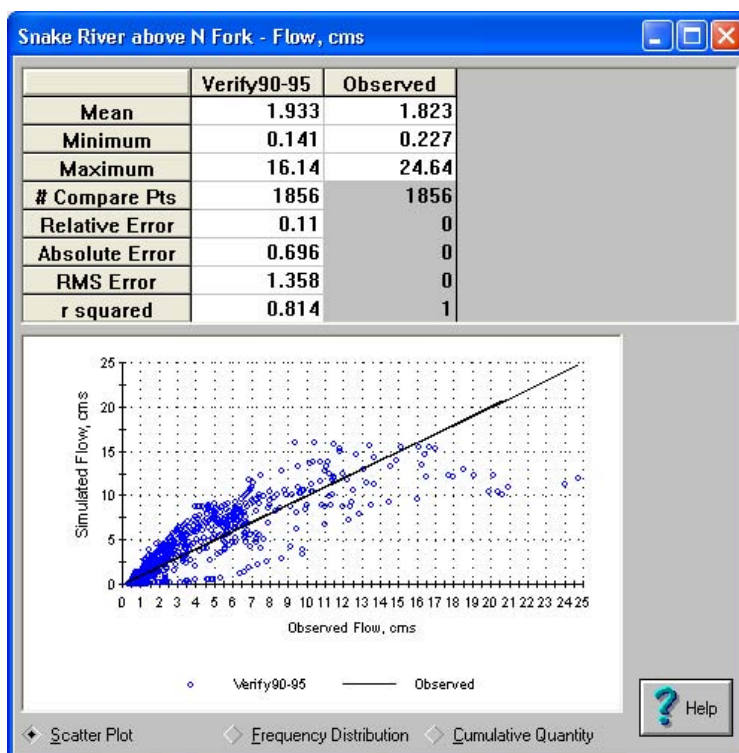
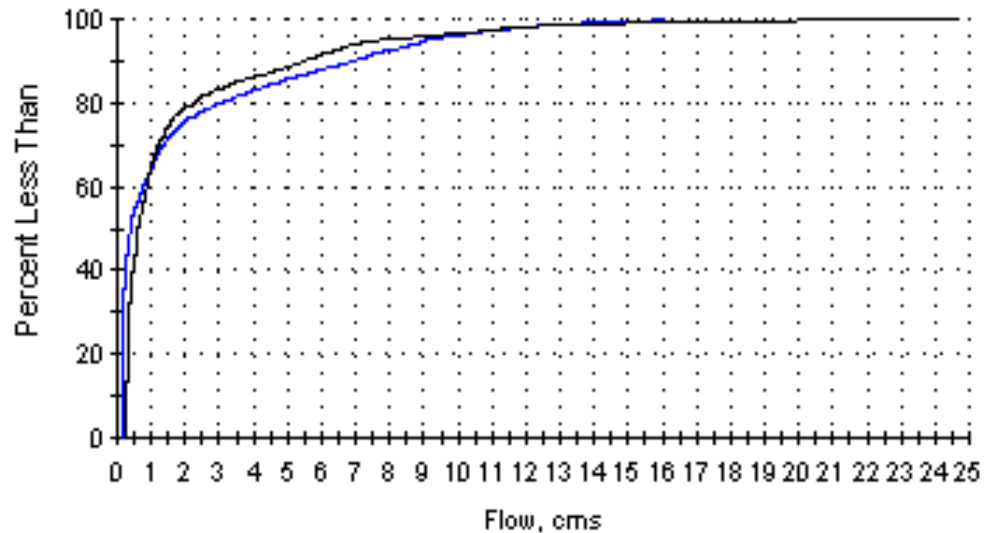
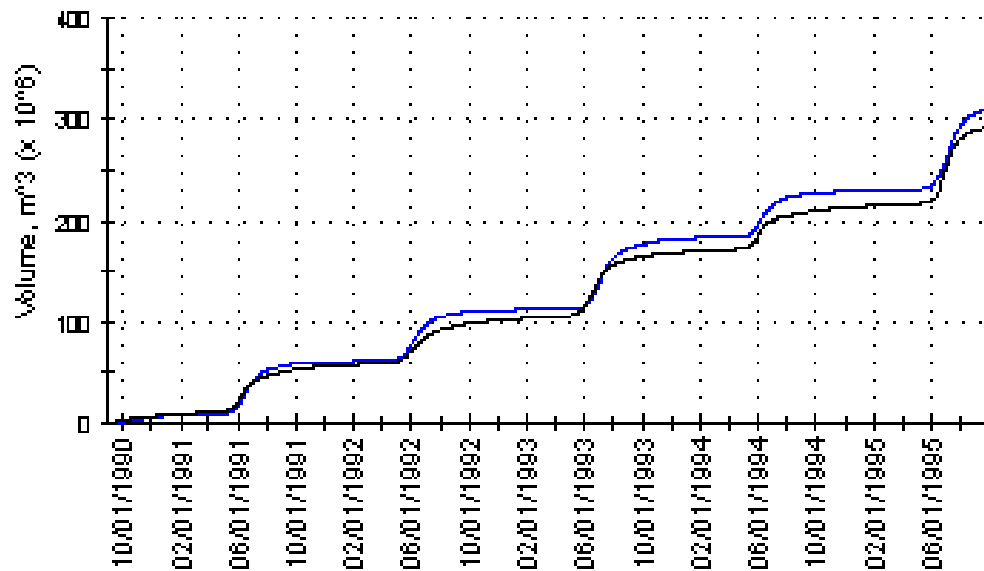


Figure 5-82
Statistical Output and Scatter Plot for Snake River Above North Fork



Note: Black line is observed; blue line is simulated.

Figure 5-83
Frequency Distribution Plot for Snake River Above North Fork



Note: Black line is observed; blue line is simulated.

Figure 5-84
Cumulative Quantity Plot for Snake River Above North Fork

Water Quality Verification

The stream water quality data collected during this project and used for model calibration covered a large spatial area along the Blue River and included several water quality parameters. The data collection effort did not focus on the other main Dillon Reservoir tributaries (Tenmile Creek and Snake River). In contrast, water quality data available for verification from 1990 to 1995 were only collected for a few parameters at three main sites located at the mouth of the major tributaries just upstream from Dillon Reservoir.

Figure 5-85 through Figure 5-87 compare simulated and measured nitrate for the Blue River above Dillon Reservoir, Tenmile Creek above Dillon and Snake River above North Fork. For all stations, the measured seasonal pattern of low nitrate in the late summer climbing to higher nitrate in the early spring was captured by the model. The simulated concentration of nitrate generally fell within the range of observed concentration for all stations. Tenmile Creek shows a much higher concentration than the other tributaries as it is greatly influenced by the upstream point sources. The nitrate concentration for the Blue River above Dillon during the verification period is roughly three times lower than the calibration period (simulated mean verification = 0.1 mg/L, simulated mean calibration = 0.3 mg/L). Both the model and the observed data captured the water quality impacts of the Iowa Hill WWTP, which did not begin operation until 2000.

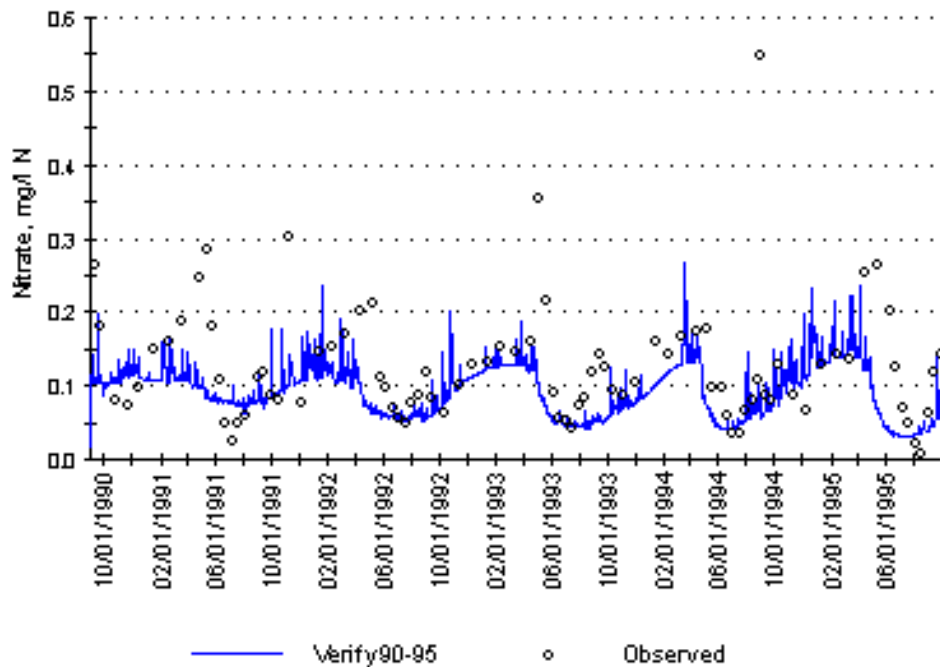


Figure 5-85
Simulated and Observed Nitrate for Blue River Above Dillon Reservoir

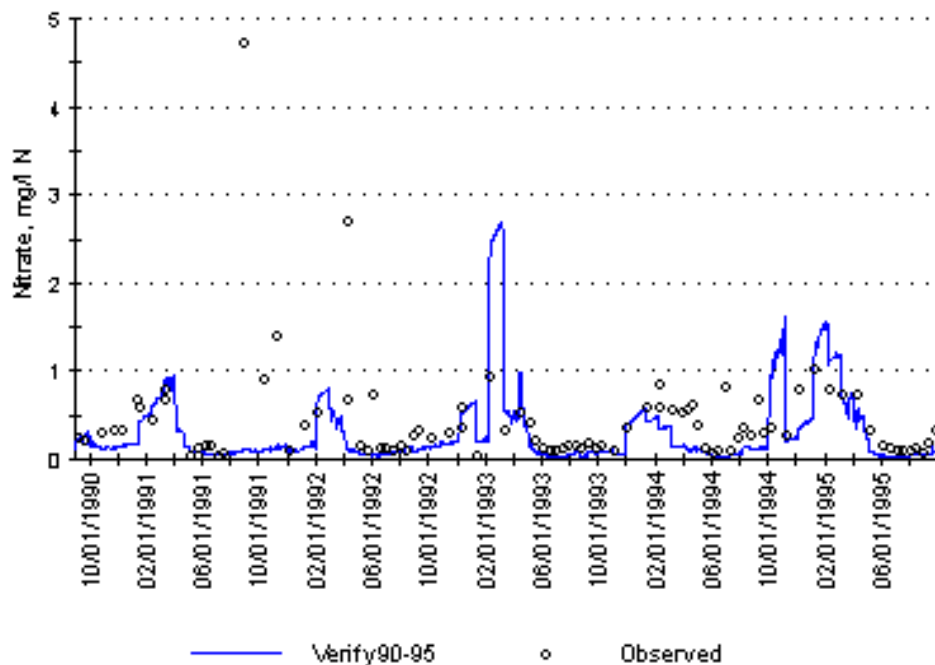


Figure 5-86
Simulated and Observed Nitrate For Tenmile Creek Above Dillon Reservoir

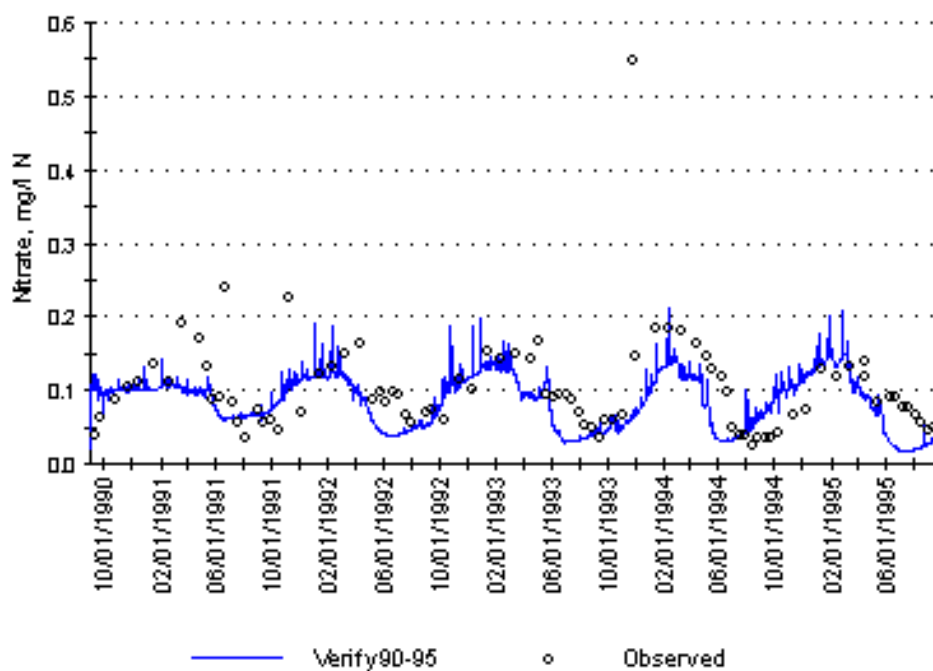


Figure 5-87
Simulated and Observed Nitrate for Snake River Above Dillon Reservoir

Figure 5-88 through Figure 5-90 compare simulated and observed total phosphorus for the three sites. For all three locations, the base-flow total phosphorus concentration was simulated well. Spikes of total phosphorus are believed to be attributed to phosphorus transported with sediment during high runoff periods. Though not all peaks were matched, the simulated concentrations fell within the range of observed concentrations.

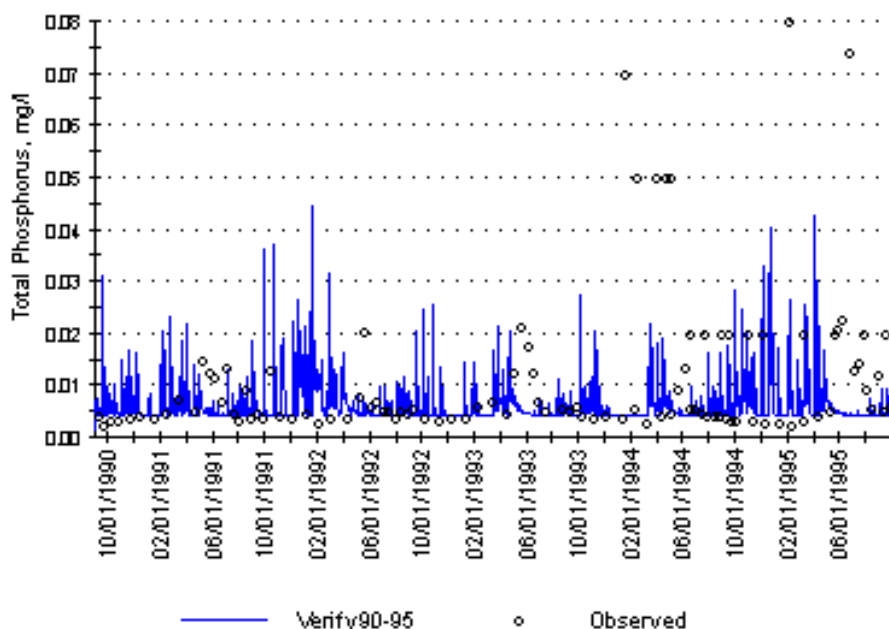


Figure 5-88
Simulated and Observed Total Phosphorus for Blue River Above Dillon Reservoir

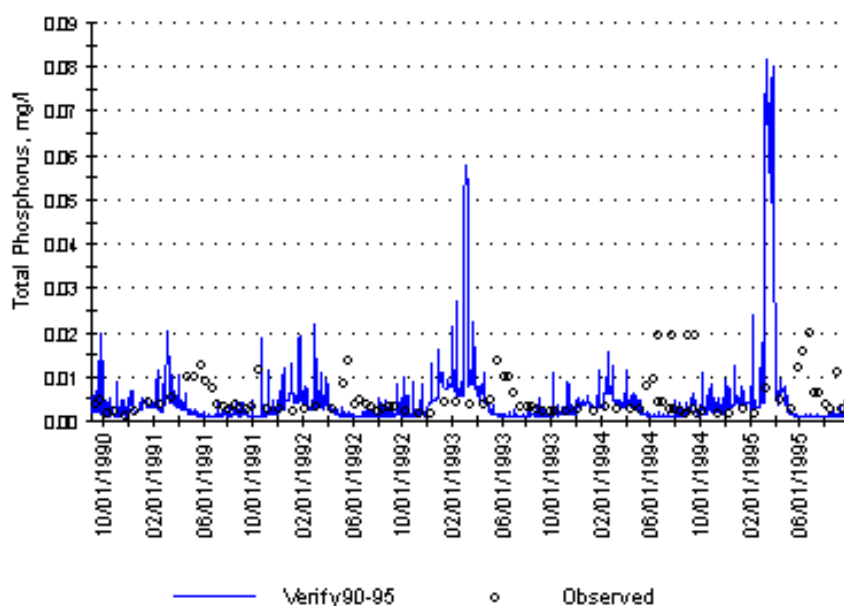


Figure 5-89
Simulated and Observed Total Phosphorus for Tenmile Creek Above Dillon Reservoir

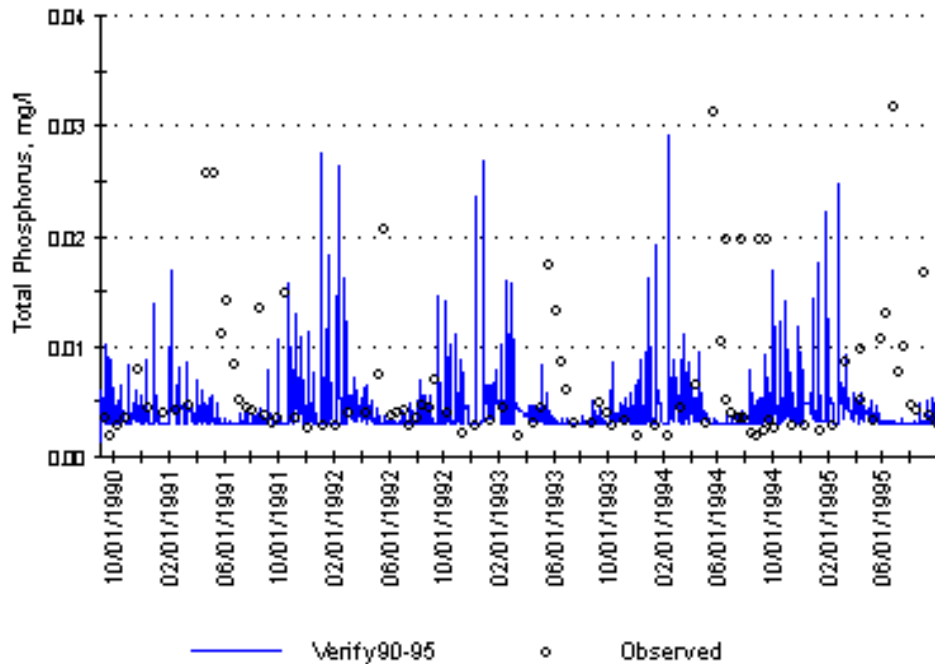


Figure 5-90
Simulated and Observed Total Phosphorus for Snake River Above Dillon Reservoir

Discussion

Calibration and verification for hydrology produced a reasonable prediction of stream hydrology with correlation coefficients ranging from 0.74 to 0.85. For all locations, the timing of the snow melt was well predicted though the peak flows were sometimes over or under predicted for several locations. Water quality data sets for different spatial regions were used for comparison with model simulations for calibration and verification. For both comparisons, WARMF simulated major water quality parameters within the range of those observed and followed most seasonal trends. Though model calibration and refinement could continue with the collection of additional water quality data, the model is sufficiently calibrated at this point to examine the relative impacts of OWS in the Dillon Reservoir watershed.

Management Scenarios

A valuable use of WARMF is the evaluation of management alternatives. WARMF can be used to analyze the effect of the replacement of OWS with sewerage and a centralized WWTP together with the projected growth and development in a watershed due to further urbanization. The effect can be evaluated in terms of the changes in pollution loads and receiving water quality.

After calibration and verification, WARMF was used to evaluate several hypothetical management scenarios. Due to the research emphasis of this project, the scenarios were purely hypothetical. Two scenarios presented in this report are

- Scenario 1: The impact of no OWS in the watershed as compared to the existing conditions
- Scenario 2: The conversion of OWS in the Blue River Estates area to centralized WWTP

Scenario 1: No OWS in the Watershed

The first scenario tested was a comparison of the base condition with OWS to a condition without OWS in the watershed (no corresponding load to a centralized WWTP was added). This scenario will help provide an understanding of the relative impact of OWS in the region.

The “population served by septics” input was set to zero for all catchments in the watershed. Examination of time-series plots (not shown) showed no noticeable difference in nutrient or fecal coliform bacteria concentrations in the main downstream location of the Blue River (BR10). Noticeable differences were seen in smaller tributaries or the upper reaches of the Blue River. Figure 5-91 shows the simulated nitrate concentration in the Blue River above Pennsylvania Creek (BR2). Without OWS, spikes of nitrate during high flow periods in the spring were greatly reduced.

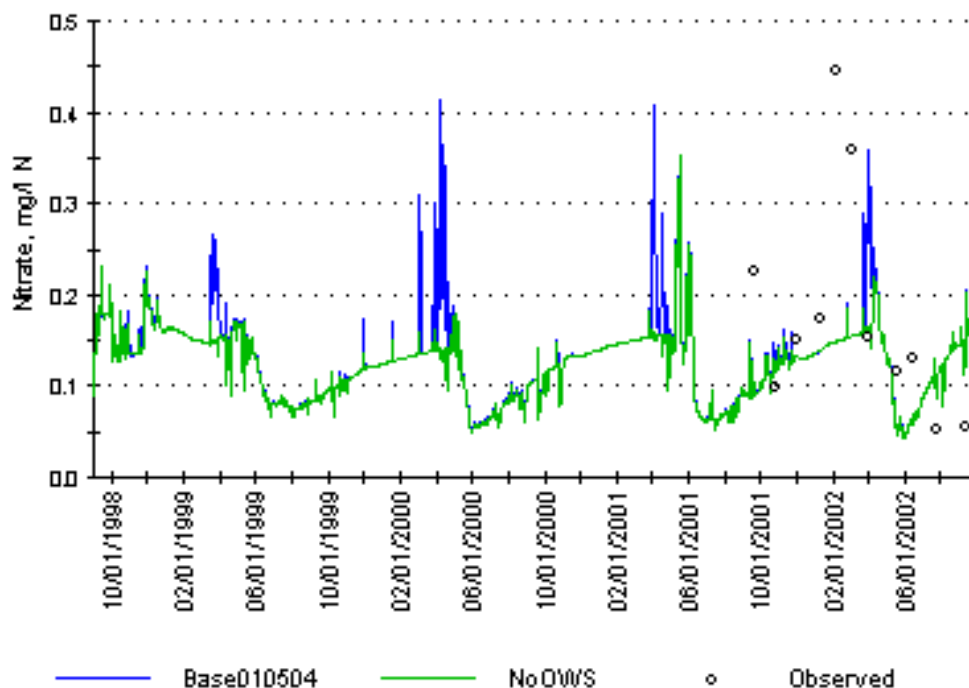


Figure 5-91
Simulated Nitrate at BR-2 With and Without OWS

Because Dillon Reservoir provides drinking water to the City of Denver, nutrient loading to the reservoir is of concern. Figure 5-92 compares the total phosphorus loading to the reservoir for the two conditions of this scenario. The figure shows two bar charts: one for the base condition with OWS (Base01050) and one for the no-OWS case (NoOWS). For each case, there is nonpoint source load of phosphorus at the bottom (green) and point source load of phosphorus at the top (magenta). The no-OWS case has a lower nonpoint source load of phosphorus. However, this decrease is rather slight in terms of total loading to the reservoir, which includes point and nonpoint loads. OWS only contribute 3.63% of the total loading to the reservoir. In terms of nonpoint loading to the reservoir, OWS contribute roughly 4.87%. Figure 5-93 shows a close-up view of the loading table displayed in WARMF.

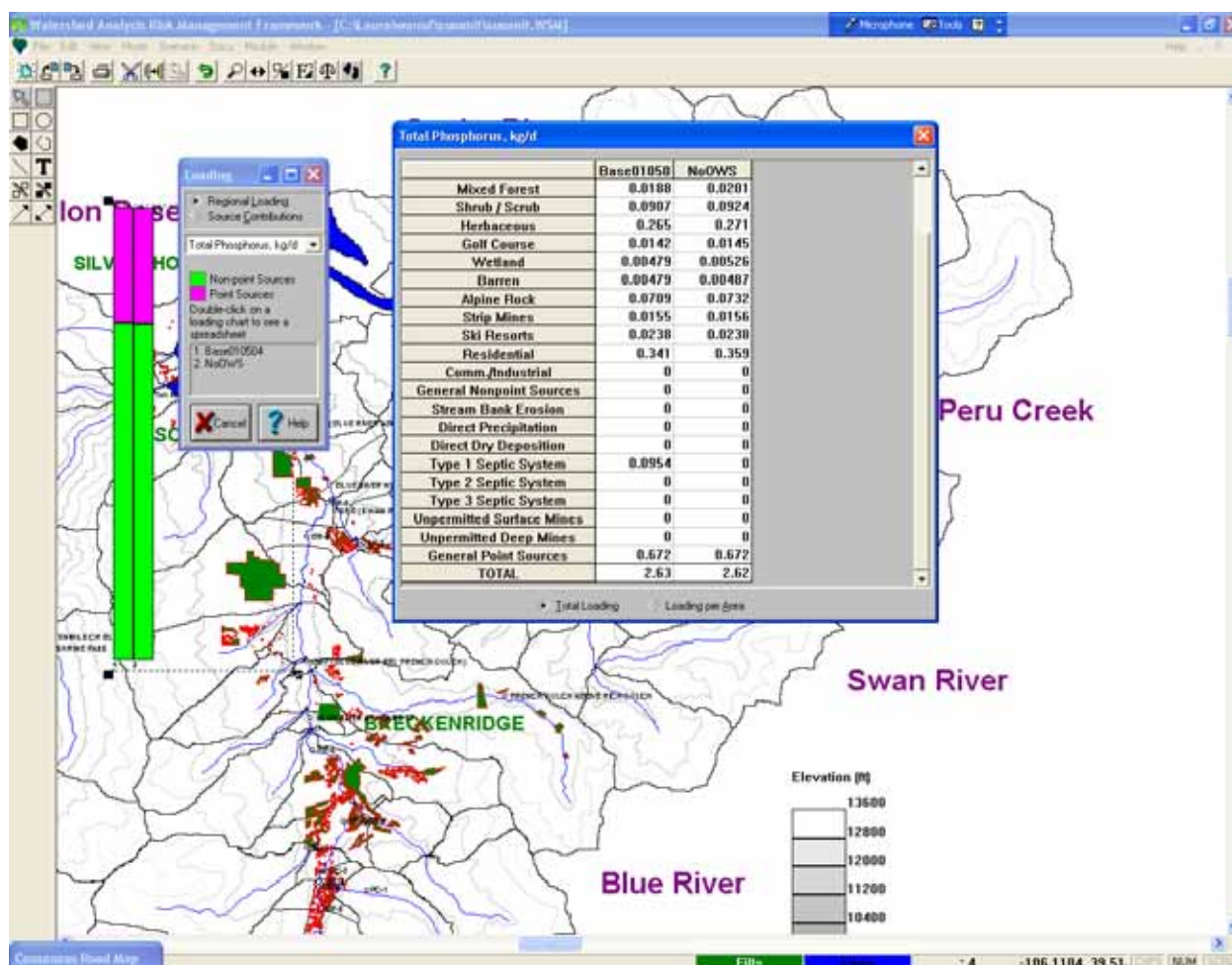


Figure 5-92
Total Phosphorus Loading to Dillon Reservoir With and Without OWS

	Base01050	NoOWS
Mixed Forest	0.0188	0.0201
Shrub / Scrub	0.0907	0.0924
Herbaceous	0.265	0.271
Golf Course	0.0142	0.0145
Wetland	0.00479	0.00526
Barren	0.00479	0.00487
Alpine Rock	0.0709	0.0732
Strip Mines	0.0155	0.0156
Ski Resorts	0.0238	0.0238
Residential	0.341	0.359
Comm./Industrial	0	0
General Nonpoint Sources	0	0
Stream Bank Erosion	0	0
Direct Precipitation	0	0
Direct Dry Deposition	0	0
Type 1 Septic System	0.0954	0
Type 2 Septic System	0	0
Type 3 Septic System	0	0
Unpermitted Surface Mines	0	0
Unpermitted Deep Mines	0	0
General Point Sources	0.672	0.672
TOTAL	2.63	2.62

☒ Total Loading
 ☐ Loading per Area

Figure 5-93
Closeup of Total Phosphorus Loading to Dillon Reservoir With and Without OWS

Figure 5-94 shows the comparison for total nitrogen loading to Dillon Reservoir. Only a slight decrease in loading is observed when all OWS are removed. OWS contribute roughly 0.16% of the total nitrogen loading to the reservoir and 0.47% of the total nonpoint nitrogen loading. Figure 5-95 shows a close-up view of the loading table displayed in WARMF. This type of information can help stakeholders understand the relative impact of OWS on the watershed.

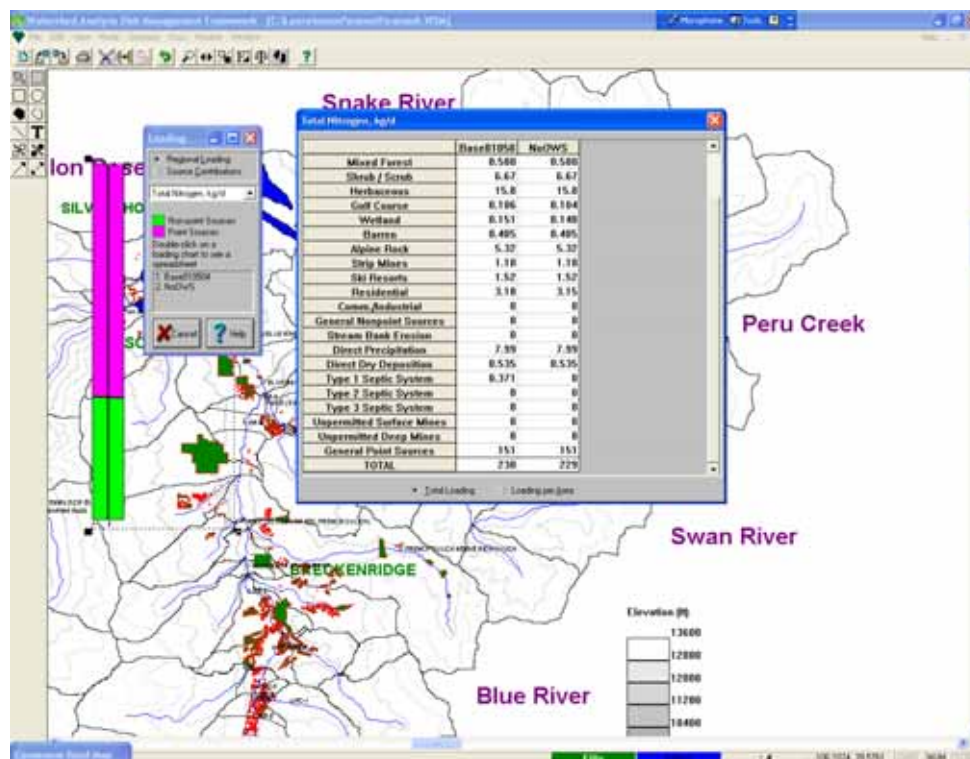


Figure 5-94
Total Nitrogen Loading to Dillon Reservoir With and Without OWS

Total Nitrogen, kg/d		
	Base01050	NoOWS
Mixed Forest	0.580	0.580
Shrub / Scrub	6.67	6.67
Herbaceous	15.8	15.8
Golf Course	0.106	0.104
Wetland	0.151	0.148
Barren	0.405	0.405
Alpine Rock	5.32	5.32
Strip Mines	1.10	1.10
Ski Resorts	1.52	1.52
Residential	3.18	3.15
Comm./Industrial	0	0
General Nonpoint Sources	0	0
Stream Bank Erosion	0	0
Direct Precipitation	7.99	7.99
Direct Dry Deposition	0.535	0.535
Type 1 Septic System	0.371	0
Type 2 Septic System	0	0
Type 3 Septic System	0	0
Unpermitted Surface Mines	0	0
Unpermitted Deep Mines	0	0
General Point Sources	151	151
TOTAL	230	229

Figure 5-95
Closeup of Total Nitrogen Loading to Dillon Reservoir With and Without OWS

Scenario 2: Convert Blue River Estates to Centralized Sewers

Figure 5-96 presents a schematic of a second management scenario. In this scenario, the 362 OWS in the Blue River Estates subdivision were converted to the centralized sewer system and WWTP. The sewage would be pumped to the South Blue River Wastewater Treatment Plant (SBRWWTP), which currently discharges its effluent to the subsurface. Sewering will foster more development and increase the plant capacity, requiring a surface water discharge to the Blue River just upstream of Blue River Estates.

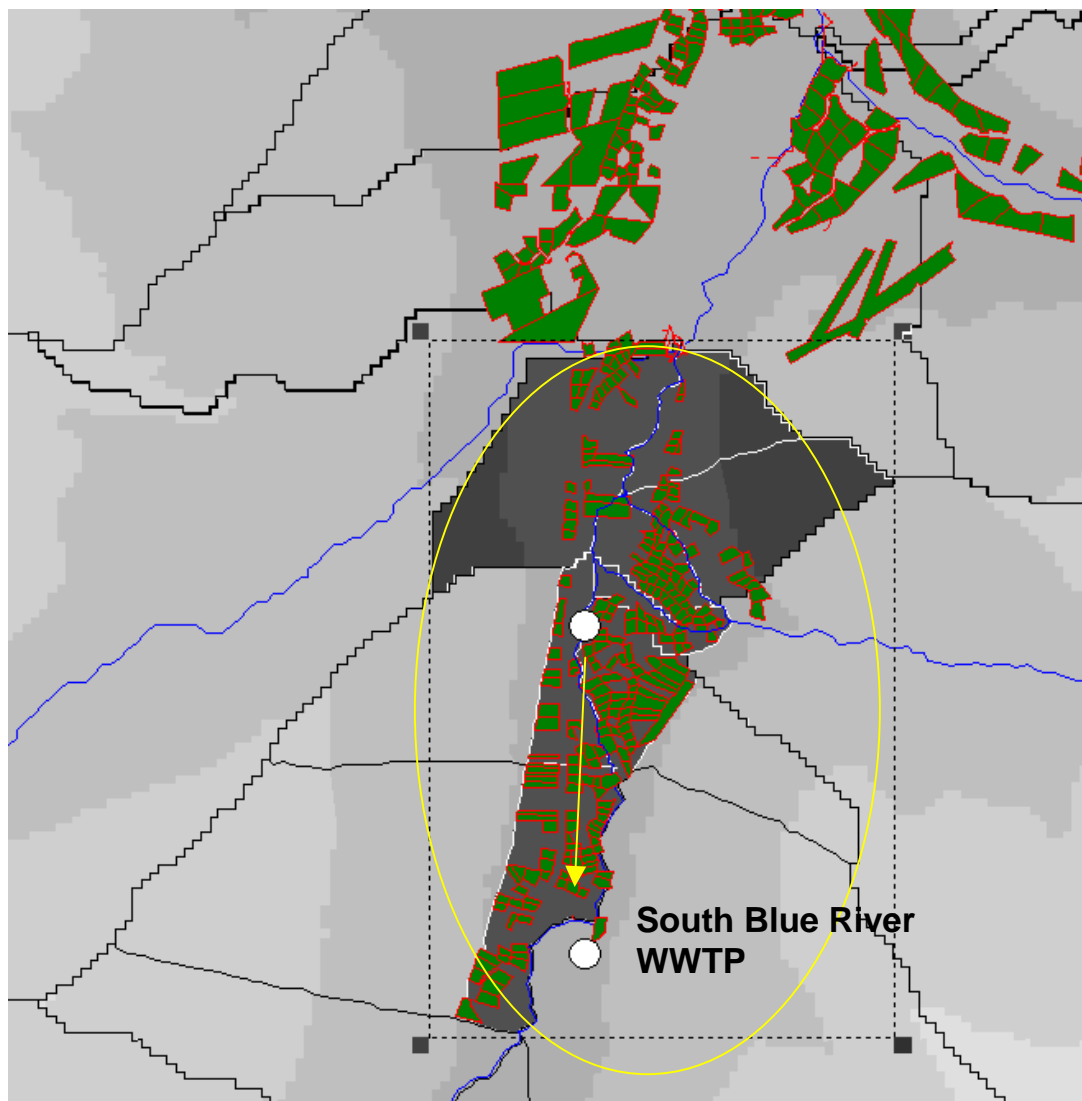


Figure 5-96
A Schematic of the Proposed Management Scenario to Convert Blue River Estates OWS to a Centralized Sewer System

For the scenario, the catchment input for “population served by septics” was set to zero for the affected catchments. A new point source file was created to account for the wastewater loading from these homes. The flow of the point source file was equivalent to the per capita flow rate times the number of people whose service would now be provided by a centralized WWTP. Loading for the point source file was calculated based on the flow and typical concentrations from the existing SBRWWTP. The treatment level currently achieved by the plant was assumed to be the same with the added capacity.

Figure 5-97 shows the simulated nitrate concentrations in a catchment of Blue River Estates. The base scenario (Base060403) is in blue and the management scenario (ConvPennCr) is in green. This figure shows a significant decrease in nitrate from the catchment when the OWS have been removed. Figure 5-98 shows the simulated total phosphorus concentrations for both scenarios from a local catchment. In this plot, the two simulated lines are virtually on top of each other. This suggests that the total phosphorus loading from the catchment was not greatly reduced once the OWS were removed, and that OWS phosphorus loading is adsorbed well by the subsurface soil in this region.

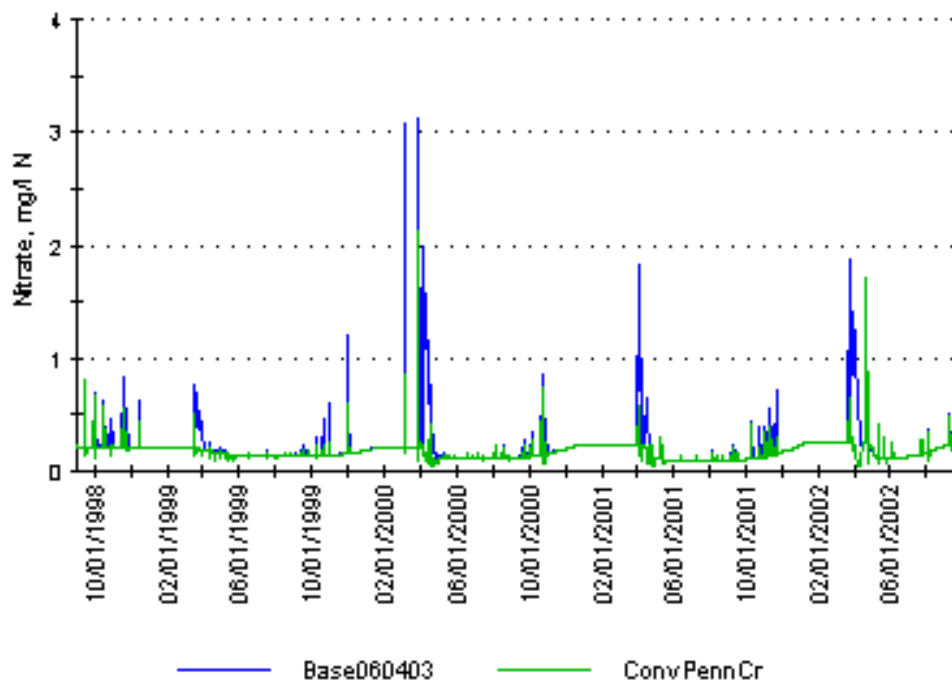


Figure 5-97
Simulated Nitrate Concentration in a Local Catchment for Blue River Estates Without OWS (ConvPennCr) Compared With OWS (Base060403)

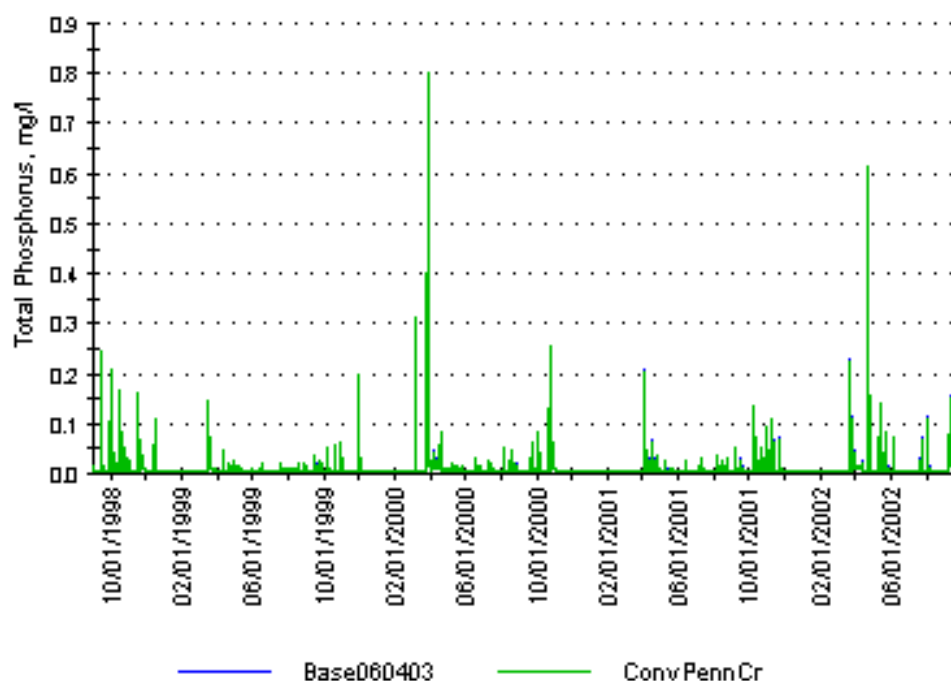


Figure 5-98
Simulated Total Phosphorus Concentration in a Local Catchment for Blue River Estates
Without OWS (ConvPennCr) Compared With OWS (Base060403)

Figure 5-99 and Figure 5-100 show the simulated nitrate and total phosphorus concentrations in the Blue River below the SBRWWTP for the management scenario compared to base conditions. When the OWS are removed and waste load is now a point source from the WWTP, the peak concentration of nitrate during wet, runoff periods are lower, but the base flow concentration of nitrate is considerably higher. For total phosphorus, a higher concentration in the river is observed when the loading is treated by the WWTP instead of individual OWS.

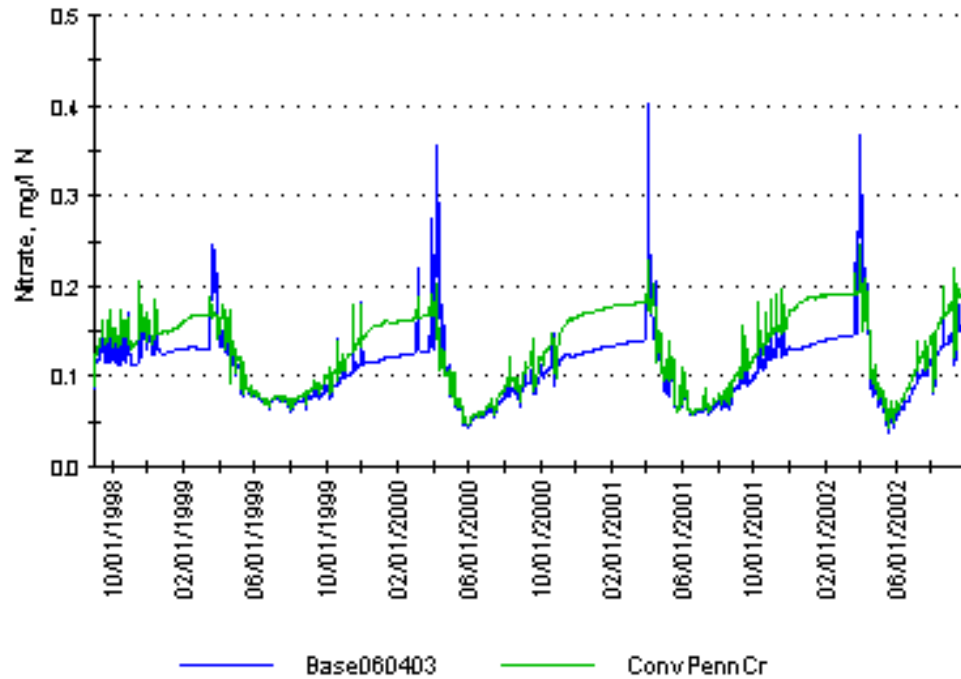


Figure 5-99
Simulated Nitrate in the Blue River Below SBRWWTP and Goose Pasture Tarn (BR-6) Comparing With OWS (Base060403) and Without OWS (ConvPennCr)

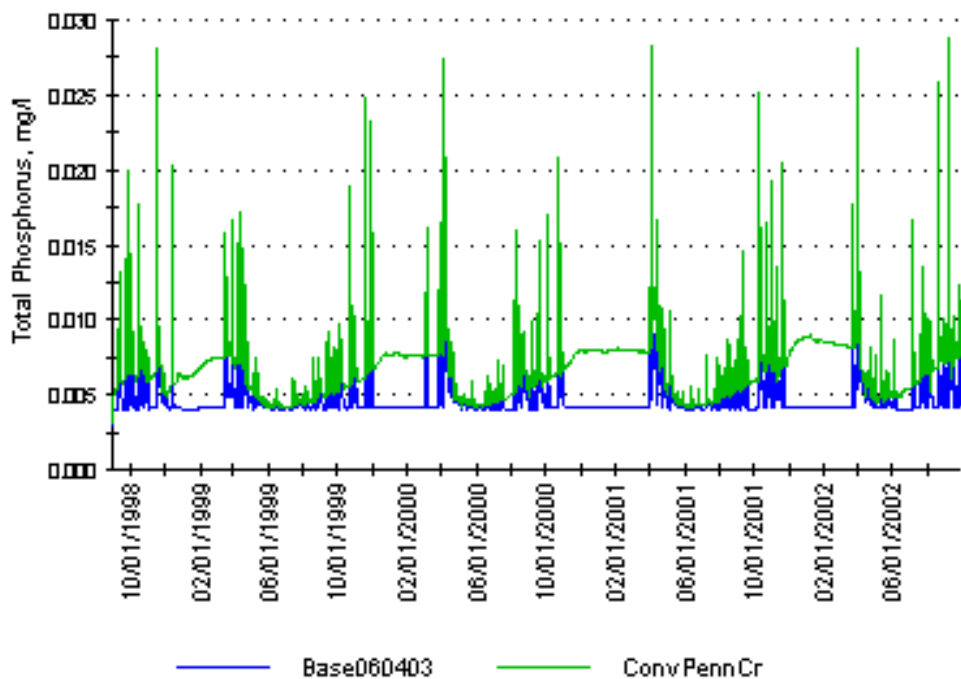


Figure 5-100
Simulated Total Phosphorus in the Blue River Below SBRWWTP and Goose Pasture Tarn (BR-6) Comparing With OWS (Base060403) and Without OWS (ConvPennCr)

Figure 5-101 presents the phosphorus loading to the Blue River. The loading was compared near Goose Pasture Tarn, the point along the Blue River at which it is believed that all local catchment flow has been returned to the surface water. When the OWS have been removed, the nonpoint source load of phosphorus decreases because of the reduced contribution from OWS. However, after conversion to centralized sewers, the point source load of phosphorus increases due to the increase of treated wastewater from the treatment plant. The net result is an overall increase of phosphorus loading after converting OWS to the centralized WWTP. The model shows that the STE that is removed by soil adsorption under the base condition is greater than the treatment level that can be achieved by the WWTP. Figure 5-102 shows a close-up view of the loading values for the comparison.

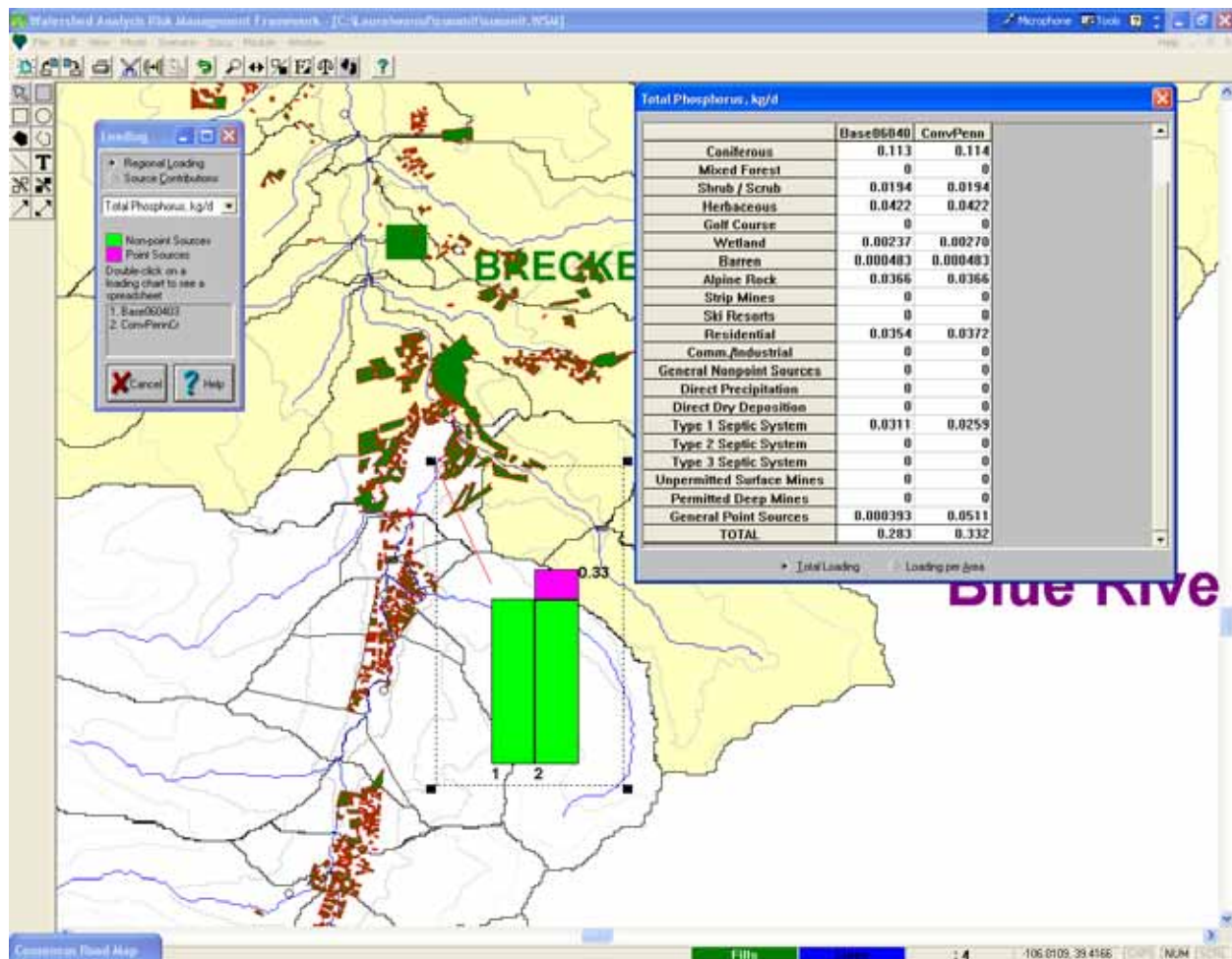


Figure 5-101
Total Phosphorus Loading Output for With OWS (Base060403) Compared to Without OWS (ConvPennCr)

Total Phosphorus, kg/d		
	Base06040	ConvPenn
Coniferous	0.113	0.114
Mixed Forest	0	0
Shrub / Scrub	0.0194	0.0194
Herbaceous	0.0422	0.0422
Golf Course	0	0
Wetland	0.00237	0.00270
Barren	0.000483	0.000483
Alpine Rock	0.0366	0.0366
Strip Mines	0	0
Ski Resorts	0	0
Residential	0.0354	0.0372
Comm./Industrial	0	0
General Nonpoint Sources	0	0
Direct Precipitation	0	0
Direct Dry Deposition	0	0
Type 1 Septic System	0.0311	0.0259
Type 2 Septic System	0	0
Type 3 Septic System	0	0
Unpermitted Surface Mines	0	0
Permitted Deep Mines	0	0
General Point Sources	0.000393	0.0511
TOTAL	0.283	0.332

☒ Total Loading
 ☐ Loading per Area

Figure 5-102
Closeup of Total Phosphorus Loading Output With OWS (Base060403) Compared to Without OWS (ConvPennCr)

Figure 5-103 presents the loading output of total nitrogen to the Blue River. Figure 5-104 shows a close-up view of the loading values for comparison. Although the nonpoint loading of total nitrogen is reduced when the OWS are converted to centralized sewers, the overall loading to the river has increased due to the nitrogen now being released as a point source from the WWTP. These results indicate that in order for the conversion of OWS in this region to be beneficial, an exceptionally high level of treatment would be required of the WWTP.

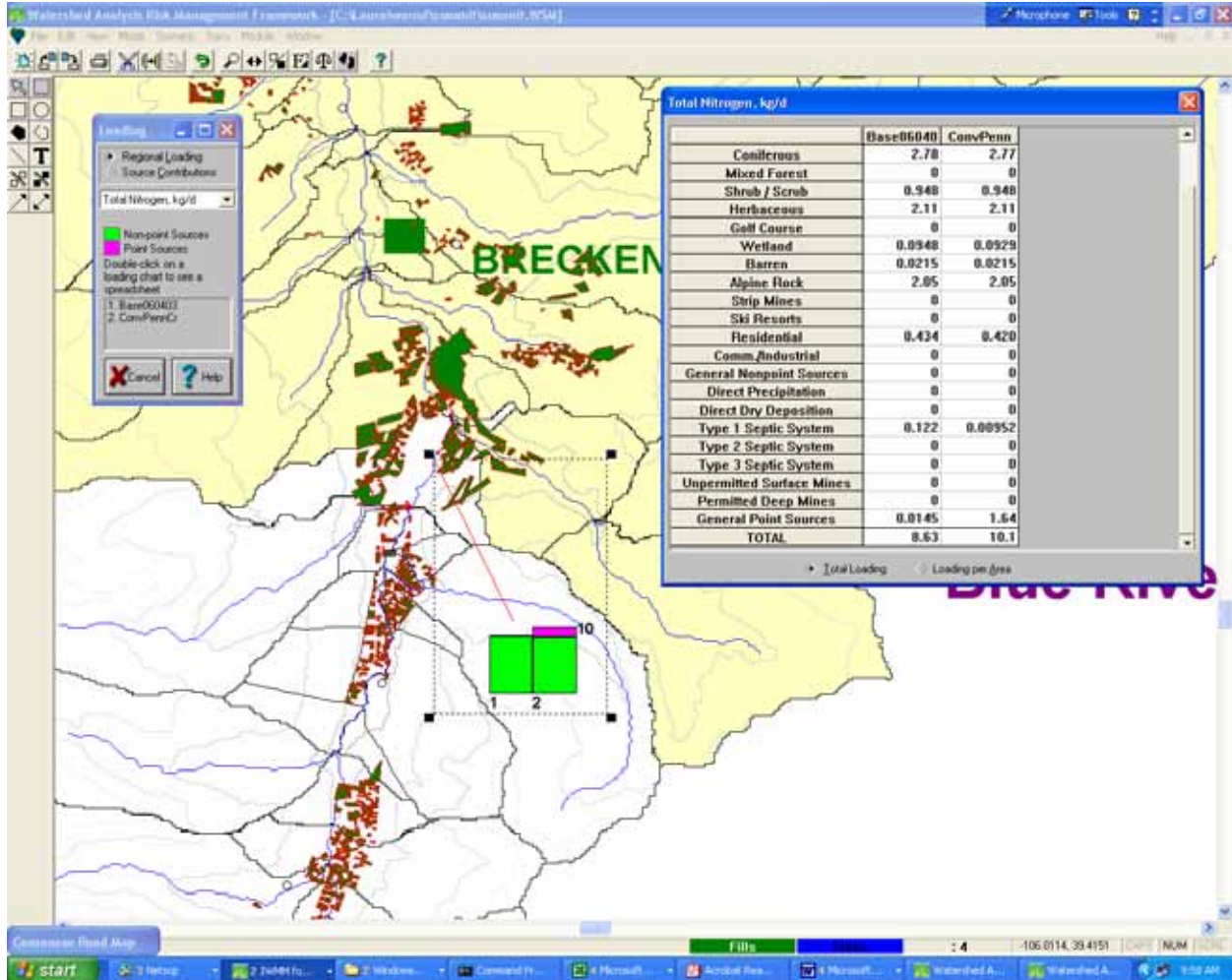
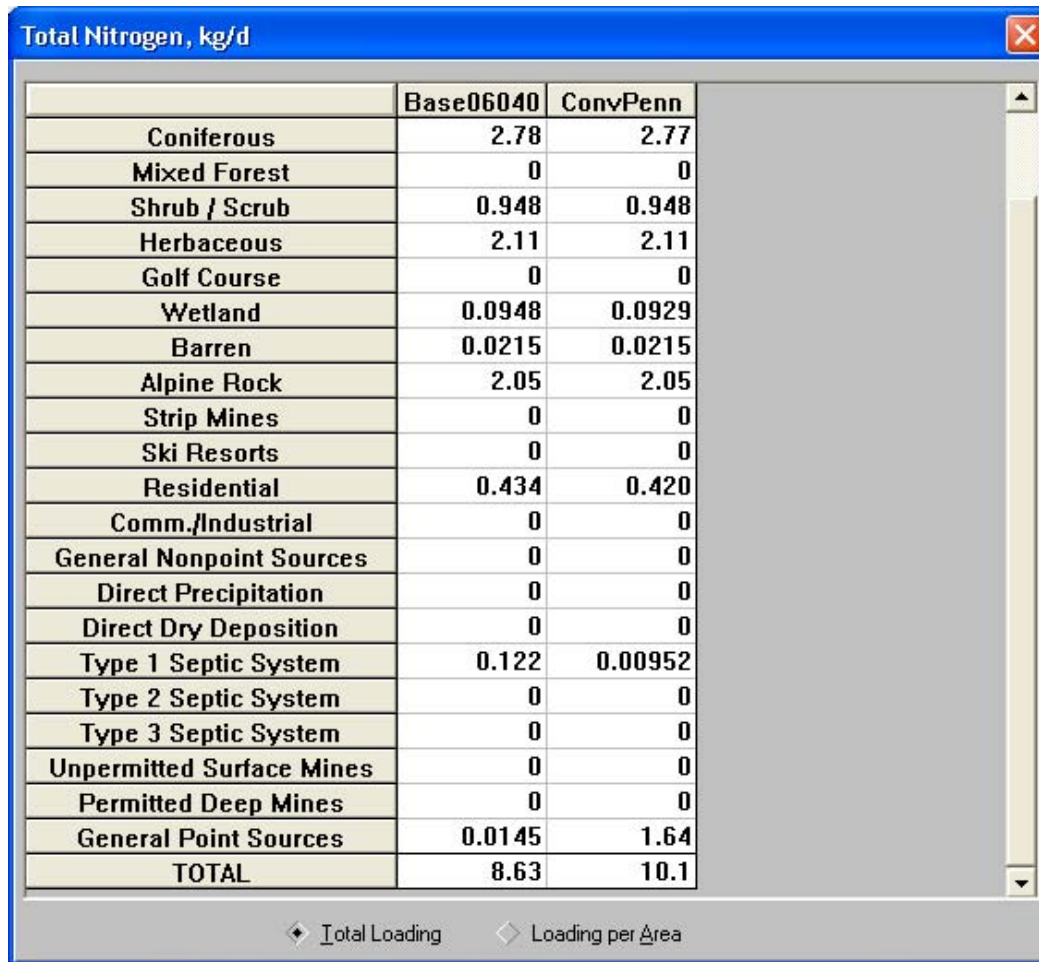


Figure 5-103
Total Nitrogen Loading Output With OWS (Base060403) Compared to Without OWS (ConvPennCr)



	Base06040	ConvPenn
Coniferous	2.78	2.77
Mixed Forest	0	0
Shrub / Scrub	0.948	0.948
Herbaceous	2.11	2.11
Golf Course	0	0
Wetland	0.0948	0.0929
Barren	0.0215	0.0215
Alpine Rock	2.05	2.05
Strip Mines	0	0
Ski Resorts	0	0
Residential	0.434	0.420
Comm./Industrial	0	0
General Nonpoint Sources	0	0
Direct Precipitation	0	0
Direct Dry Deposition	0	0
Type 1 Septic System	0.122	0.00952
Type 2 Septic System	0	0
Type 3 Septic System	0	0
Unpermitted Surface Mines	0	0
Permitted Deep Mines	0	0
General Point Sources	0.0145	1.64
TOTAL	8.63	10.1

☒ Total Loading
 ☐ Loading per Area

Figure 5-104
 Closeup of Total Nitrogen Loading Output With OWS (Base060403) Compared to Without OWS (ConvPennCr)

This section has shown how WARMF can be used as a planning tool for stakeholders to decide whether it would be cost-effective or beneficial to convert existing OWS to centralized sewers. This scenario is just one simple example that was chosen for demonstrative purposes. Many other types of scenarios related to growth, land use change, and system conversion can be easily set up and analyzed by WARMF.

Summary

WARMF, was adapted to simulate the impact of OWS within a watershed. WARMF is a GIS-based watershed management tool that combines a dynamic simulation model with a data module and decision support modules for consensus building and TMDL development.

WARMF was applied to the 840-km² (325-mile²) Dillon Reservoir Watershed in Colorado where about 1,500 OWS can be found along the Blue River. WARMF was set up with available DEM, meteorology, point source, and land use data. Additional data collected in the watershed for this project included surface water quality, soil properties, well data, and the spatial distribution of OWS in the watershed. Site-specific rates for nitrification, phosphorus adsorption, and coliform decay were also determined and included in the model. WARMF algorithms were modified to include the loading from OWS. In addition, a biozone module was developed to represent the biologically-active infiltration zone that develops in a soil system receiving STE. Hydrology and water quality simulations were run and the model was calibrated to available observed data.

After establishing a base case, management scenarios related to OWS in three specific study areas (Frisco Terrace, Ten Mile Vista, and Pennsylvania Creek) were tested with WARMF. These scenarios included a comparison of nutrient loading to Dillon Reservoir with and without OWS and the conversion of existing OWS to centralized sewers in the Blue River Estates area. The results of these scenario runs provide useful information for decision makers of Summit County related to the trade-offs between OWS and centralized sewer systems as well as the general impact of OWS on water quality.



6 ADDITIONAL MODELS APPLIED

Quantitative understanding of flow and transport processes controlling the performance of an individual OWS is needed to support effective design and operation of individual systems as well as to represent individual system inputs into watershed-scale modeling efforts.

Site-Scale Models

As part of this project, mathematical modeling was used to investigate the impact of the clogging zone (CZ) on the hydraulic performance and nutrient treatment and transport in a WSAS. This CZ creates an increased resistance to infiltration, which can lead to unsaturated flow conditions and a concomitant increase in hydraulic retention times in the subsurface. The CZ is increasingly referred to as a biozone since it can also be biogeochemically more reactive than clean soil and provide more rapid and extensive pollutant removal than clean soil. A certain degree of clogging may improve the treatment of wastewater by causing an unsaturated flow regime and improved reaction rates and extents. However, excessive clogging can lead to eventual system failure if the CZ becomes essentially impermeable and wastewater can no longer infiltrate (Siegrist 1987 and Siegrist and Boyle 1987). The service life of an OWS is often gauged by its hydraulic performance, which is closely related to CZ development and the long-term infiltration or acceptance rate of the system (Siegrist *et al.* 2001).

HYDRUS-2D

The influence of the biozone, on the two-dimensional unsaturated flow regime within an OWS was evaluated using the HYDRUS-2D model (Beach and McCray 2003). This modeling study focused on two cases: one where the biozone has not formed, and one where the biozone is mature (quasi-steady-state condition). Two soil types were used for each case. The effort did not attempt to address the temporal formation of the biozone or the influence of the biozone on treatment. HYDRUS-2D (Simunek *et al.* 1999) solves the mixed form of Richards' equation (Celia *et al.* 1990) for variably saturated water flow using the standard Galerkin linear finite-element method (Appendix F, *Site-Scale Modeling Using HYDRUS 2-D*). The capillary pressure head versus water content relationships in HYDRUS-2D are based on the van Genuchten (1980) relationships.

Initially, an unsaturated soil can accept exceptionally high infiltration rates in a capillary-dominated flow regime. For a homogeneous soil under capillary-dominant conditions, the long-term infiltration rate will approach the K_s value of the soil. Consequently, when the application rate of water is greater than the K_s of the surface layer (in this case the CZ) in a steady-state system, the surface layer becomes saturated and ponding will occur.

For a surface-clogged soil with a more permeable subsoil, unsaturated conditions and therefore negative-pressure heads develop below the CZ due to a capillary-barrier effect. For ponded infiltration into permeable soil with a saturated CZ, the hydraulic-head gradient across the zone of clogging can be quite large (positive pressure heads above the CZ, negative pressure heads below the CZ, and a short infiltration distance across the CZ).

This modeling investigation demonstrated that the hydraulic properties of both the CZ and the subsoil play an important role in controlling the hydraulic residence times and water-content distributions within OWS (Beach and McCray 2003). Figure 6-1 shows the simulated water content distribution throughout the WSAS. The results illustrate that the clogging layer acts as a hydraulic impedance, causing flow through the clogged soil system to be dependent upon the hydraulic head above the infiltrative surface (ponding depth), K_s of the CZ, and the hydraulic characteristics of the subsoil. These latter findings substantiate those of Hargett *et al.* (1982), who reached similar conclusions using less quantitative methods. For both sand and silt subsoil cases, increasing the hydraulic resistance of the CZ (decreasing K_s) caused increased sidewall flow and resulted in greater hydraulic residence times.

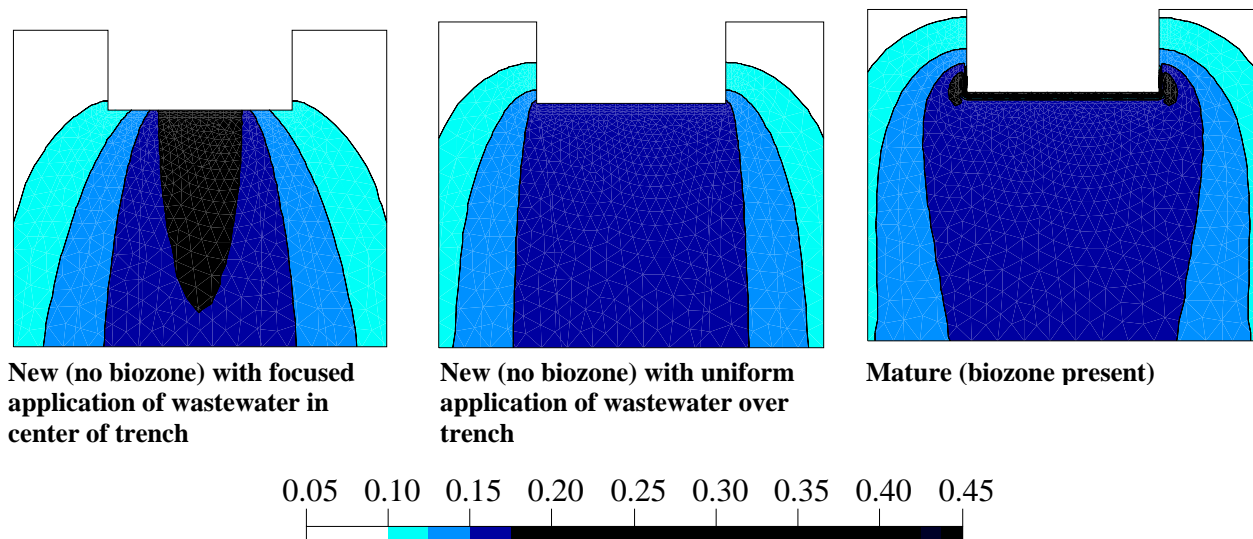


Figure 6-1
Steady-State Water Contents for a WSAS System

The model simulations also demonstrated that increasing the hydraulic resistance of the base and sidewall CZ by factors of three and four, respectively, increased the ponding height required to sustain a constant volumetric flow rate, caused lower water contents in the subsoil, and resulted in larger hydraulic residence times (lower velocities). The most significant difference occurred in the sand case, where an increase in the CZ hydraulic resistance required a five-fold increase in ponding height to sustain the same daily processing rate.

The impact of infiltrative-surface CZs were not as great for the silt subsoil (ponding level increased by a factor of about two), likely due to the relative similarity between the hydraulic properties of the simulated CZ and the silt subsoil. The increases in hydraulic residence times due to changes in CZ properties were not as great. Generally, less than a 50% difference in velocities was observed between the cases for low- and high-degrees of clogging. Wastewater in the more mature (lower K_s) systems appears to be more widely distributed, effecting greater soil contact, and thus enabling enhanced treatment compared to the less mature systems.

HYDRUS-2D simulations illustrated that an accurate knowledge of the hydraulic properties of the CZ and subsoil for various types of parent soil in an OWS is important for understanding and predicting the hydraulic efficiency of OWS, and therefore treatment efficiency of wastewater pollutants. Interestingly, the STE acceptance rates for silt are not largely different than for sand systems when a CZ has developed.

A third modeling study was also performed to investigate flow and transport of nitrogen species and phosphorus in a WSAS, but did not explicitly account for biozone processes on treatment. Figure 6-2 illustrates the steady-state phosphate concentrations in a mature system. In this study, the effects of the biozone on flow and transport are indirectly included by using long-term infiltration rates or ponding levels measured in operating WSASs. This study is not presented in this chapter. Rather, it is detailed in Appendix F, *Site-Scale Modeling Using HYDRUS 2-D*.

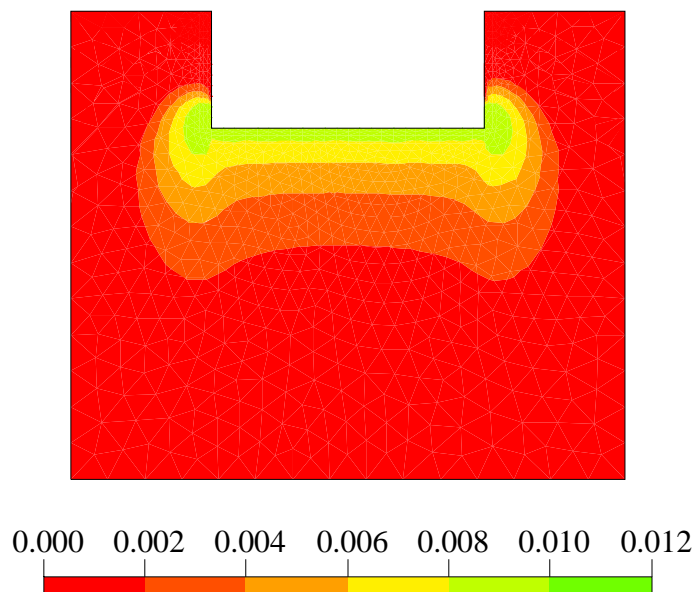


Figure 6-2
Steady-State Phosphate Concentrations in the WSAS (mg/mL) for a Mature (Biozone Present) System

Virus Fate and Transport

In concert with this project, a series of experiments were conducted to elucidate the transport-fate of bacteria and virus during wastewater renovation in WSASs. Information on the attachment and inactivation/die-off behavior gathered in the laboratory using material and temperatures representative of field conditions (Harvey 1997; Van Cuyk *et al.* 2001; Navigato 1999; and Loveland *et al.* 1996) is summarized in Table 6-1. Information related to the effects of daily hydraulic loading rates and methods, effluent quality, temperature, pH, and organic carbon on virus removal, inactivation rates, and transport are presented in Appendix B, *Pathogen Transport-Fate Studies* (see also Van Cuyk 2003; Van Cuyk *et al.* 2004; and Van Cuyk and Siegrist 2004).

Table 6-1
Calculated Inactivation Rates ($-k_i$) for Viruses Observed Here and Reported by Other Investigators Under Various Conditions

Researcher	Porous Media?	Temp (C)	Rates ($-k_i$) (day ⁻¹)	Virus	Comments
Reddy <i>et al.</i> (1981)	Yes and No		0.04–3.69	many	Compilation of data
Bertucci <i>et al.</i> (1974)	No	12	2.21	echovirus 11	Anaerobic digestion
Bertucci <i>et al.</i> (1974)	No	12	2.53	MS-1	Anaerobic digestion
Larkin <i>et al.</i> (1976)	Yes	12(?)	0.1	poliovirus	Soil flooded with inoculated, non-chlorinated secondary effluent
Navigato (1999)	No	5	0.022	PRD-1	Contaminated groundwater
Navigato (1999)	No	5	0.056	PRD-1	Radiolabeled phage
Navigato (1999)	No	5	0.083	MS-2	Contaminated groundwater
Navigato (1999)	No	5	0.093	MS-2	Radiolabeled phage
Yates (1995)	No	4	0.018–0.15	MS-2	Groundwater
Powelson <i>et al.</i> (1990)	No	4	0.041	MS-2	Groundwater
Powelson <i>et al.</i> (1993)	No	7	0–0.092	MS-2, PRD-1	Groundwater
Schijven <i>et al.</i> (1999)	No		0.12	PRD-1	Groundwater
Schijven <i>et al.</i> (1999)	No		0.030	MS-2	Groundwater
Van Cuyk <i>et al.</i> (2001)	medium sand	18	0.26–1	PRD-1	Wastewater, too little MS-2 breakthrough to measure

Table 6-1
Calculated Inactivation Rates (-k_i) for Viruses Observed Here and Reported by Other Investigators Under Various Conditions (Cont.)

Researcher	Porous Media?	Temp (C)	Rates (-k _i) (day ⁻¹)	Virus	Comments
Van Cuyk (2003)	No	23	0.0336	PRD-1, pH 5	AGW ^b
Van Cuyk (2003)	No	23	0.0552	PRD-1 pH 7	AGW
Van Cuyk (2003)	No	23	~0 ^a	PRD-1, pH 9	AGW
Van Cuyk (2003)	No	23	0.02688	MS-2, pH 5	AGW
Van Cuyk (2003)	No	23	~0 ^a	MS-2, pH 7	AGW
Van Cuyk (2003)	No	23	~0 ^a	MS-2, pH 9	AGW

^aNot enough virus breakthrough to quantify removal rate

^bArtificial groundwater at pH 7.

Static columns and two bacteriophages, MS-2 and PRD-1, were used as surrogates for human pathogenic enteric viruses. The removal of viruses in non-disinfected wastewater effluent released into the subsurface may depend almost completely upon the permanent attachment of viruses to subsurface solids and/or their inactivation due to strong intersurface forces occurring during reversible or intermittent attachment. Models that are utilized to predict the transport of viruses must include the loss of virus from soil solution or groundwater due to the attachment based on the physical and chemical properties of the soil and the groundwater. Laboratory experiments were conducted to examine the effect of temperature, pH, and the presence of organic carbon on virus attachment behavior using small, static mini-columns that are filled with medium sand that has been used previously in laboratory studies (Van Cuyk *et al.* 2001; Van Cuyk 2003). In addition, the effects of different porous media, and various carrier solutions (artificial groundwater [AGW], and STE) on the removal of viruses at the infiltrative surface were investigated. This work involved a novel unsaturated column assembly used to simulate the infiltrative surface by applying a vacuum to simulate underlying unsaturated soil, which allowed for the collection of percolate samples immediately below the infiltrative surface. Detailed discussion related to experimental design and results is presented in Appendix B, *Pathogen Transport-Fate Studies*.

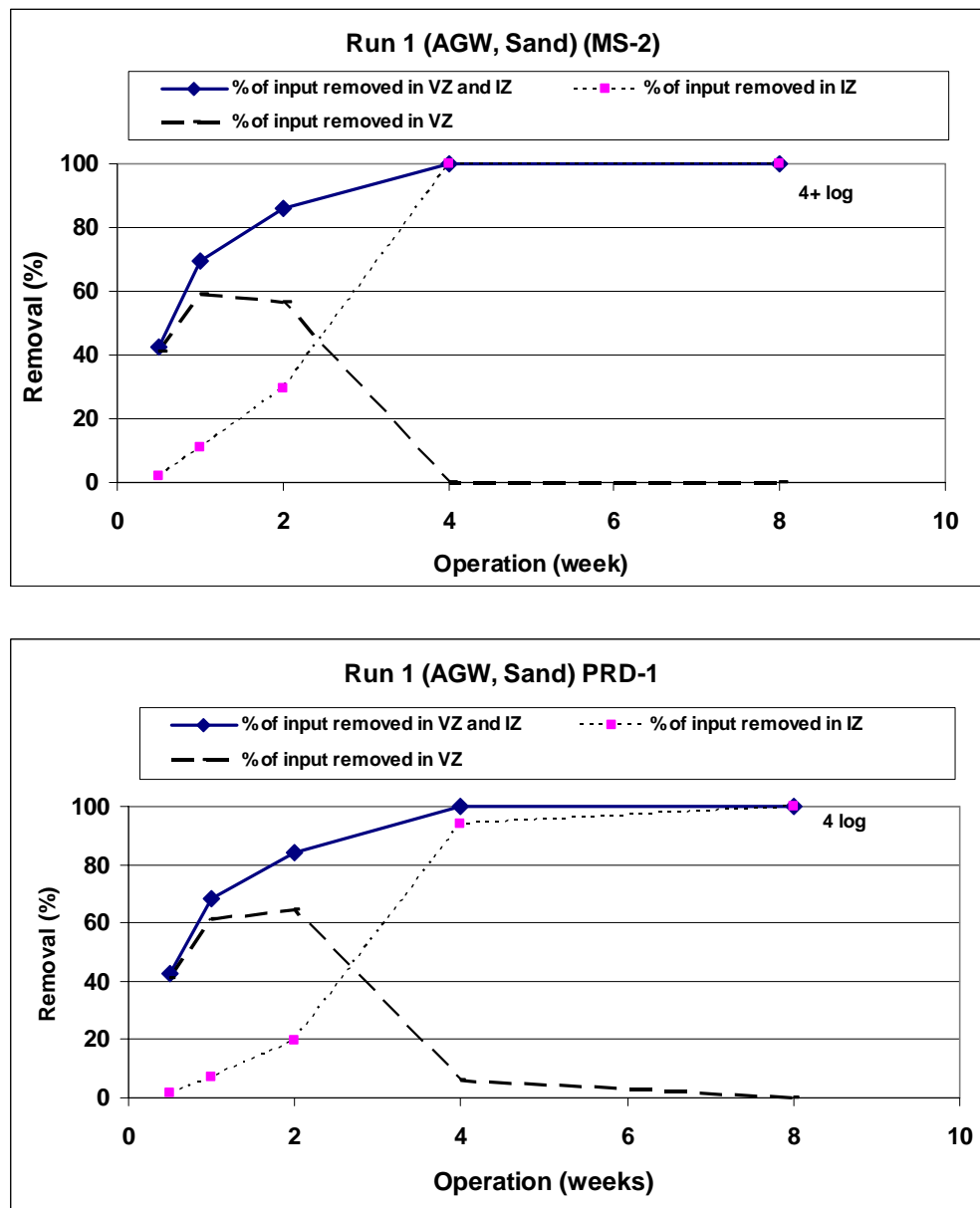
Using the data from the static mini-column experiments, a simple model was used to gain an understanding of the importance of the infiltrative surface in the overall removal of viral surrogates in porous media biofilters. This spreadsheet model assumes first-order removal and divides the porous media filter into two sections. The first is the infiltrative zone (IZ), estimated at a 4-cm depth and the second is the vadose zone (VZ) at 56 cm (for a total soil depth from infiltrative surface to groundwater of 60 cm). Sand was used in these simulations to enable comparison to data collected in previous Colorado School of Mines (CSM) laboratory studies.

Simulations were run using STE or AGW as the applied effluent with effluent dosing at 5 cm/day and initial virus concentrations of 1×10^7 plaque forming units (PFU)/100 mL. Average retention time (t), in hours, in each soil zone was calculated using the following equation:

$$t = (L * N_e) * (ISU) / (q) \quad \text{Equation 6-1}$$

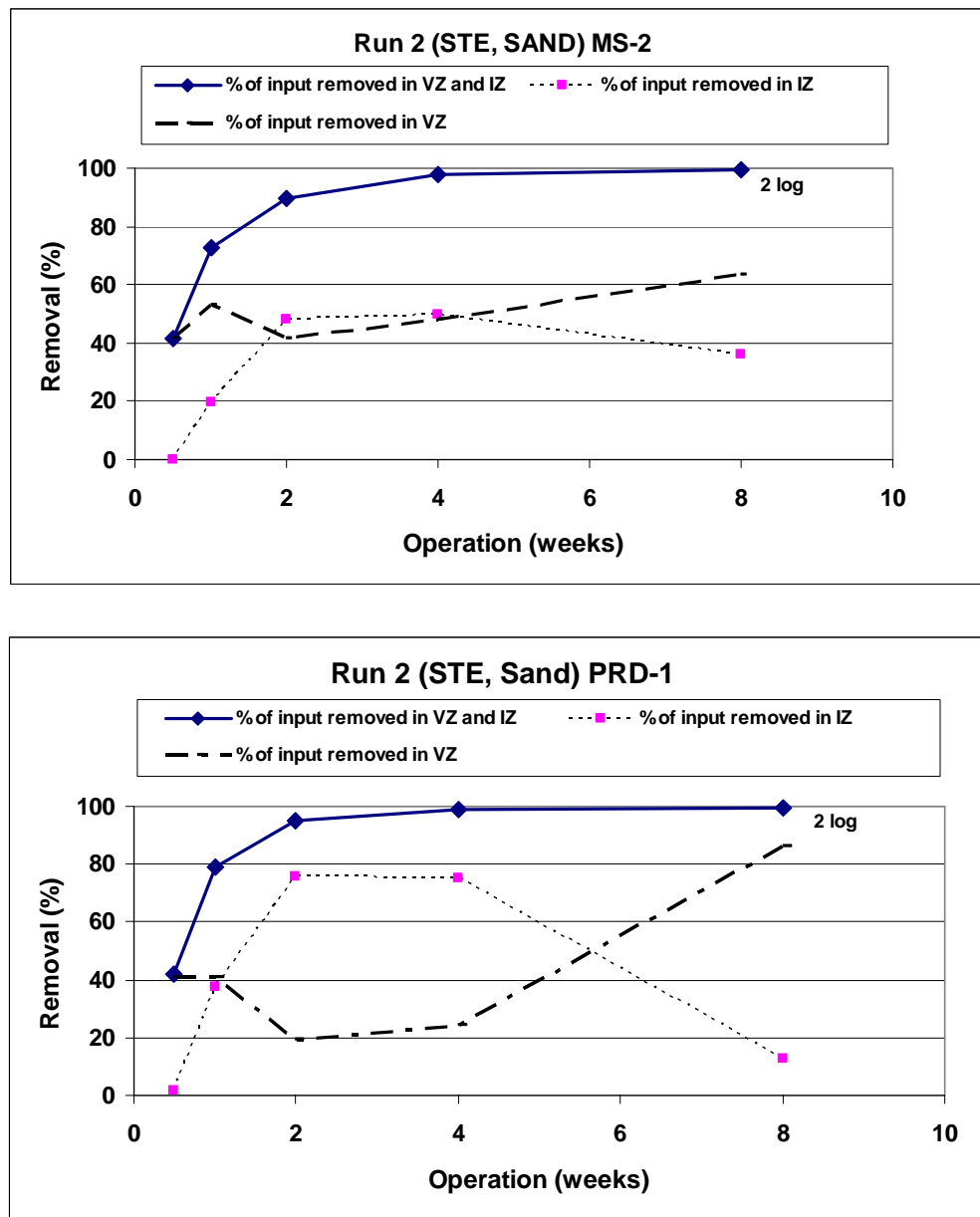
where L is length of soil including infiltrative surface and vadose zone, N_e is effective porosity (v/v), ISU is infiltrative surface utilization (fraction utilized), and q is application rate (cm/hr).

The importance of the vadose zone in the early period of operations is illustrated from the Run 1 (AGW) results (Figure 6-3). An increased importance of the IZ on the removal of MS-2 and PRD-1 with time of operation is also illustrated. High total removal (4 log and higher) is achieved in these systems by week eight of operation, with most of this removal occurring in the IZ. Results from Run 2 (STE) show that by week eight a 2-log removal of both MS-2 and PRD-1 is achieved, but the importance of the IZ at this time in the overall removal is less than that of the vadose zone (Figure 6-4). These results parallel what was observed in the CSM 3-D lysimeter work (Van Cuyk 2003), where initial breakthrough was observed, followed by 4-log removal of added bacteriophage following a longer period of operation.



Note: 1×10^7 PFU/mL of Virus Added in AGW Dosed at 5 cm/d. IZ = Infiltrative Surface Zone, First 4 cm of Depth; VZ = Vadose Zone From 4 to 60 cm Depth

Figure 6-3
Virus Removal Simulation Assuming First Order Removal With Respect to Concentration
With Increasing Time of Operation



Note: 1×10^7 PFU/mL of Virus Added in STE Dosed at 5 cm/d. IZ = Infiltrative Surface Zone, First 4 cm of Depth; VZ = Vadose Zone From 4 to 60 cm Depth

Figure 6-4
Virus Removal Simulation Assuming First Order Removal With Respect to Concentration
With Increasing Time of Operation

Watershed-Scale Models and Comparisons

As part of this project, a comparative analysis of alternative methods for site-scale and watershed scale assessment was completed. To date, two models, BASINS/Soil and Water Assessment Tool (SWAT) and MANAGE, have been compared with WARMF. Attributes for comparison include model capabilities, setup, calibration, and results.

Purpose

A model comparison between the three models is useful to demonstrate how models of varying complexity are used for assessing watershed-scale impacts of wastewater pollutants, and also to validate the results of the two watershed-scale numerical models. Details on the theory, formulation, model set up, and calibration of the SWAT and MANAGE models are presented in Appendix G, *Watershed Modeling Using BASINS/SWAT* and Appendix H, *Watershed Modeling Using MANAGE*.

Soil Water Assessment Tool (SWAT)

BASINS is the watershed modeling system promoted by the US EPA, and the software may be acquired at no cost. However, BASINS is not a watershed model. Rather, it is a graphical user interface and data manipulation software for several hydrology-water quality models (HSPF, SWAT, QUAL2E, PFLOW). The BASINS model chosen for this study was SWAT (Neitsch *et al.* 2000). This model was chosen because, like WARMF, it seems well-suited for conducting watershed-scale simulations of hydrology and pollutant transport, including pollutant sources in the upland portions of a watershed. The other models in BASINS are perhaps more rigorous for in-stream processes, but do not simulate upland processes (such as land use, land-climate interactions, and other upland processes). For this study, the BASINS graphical user interface was not used because it was rather cumbersome compared to the free user-interface provided by the SWAT model. Thus, the SWAT user interface was utilized for this study.

Method for Assessment, Nutrient-loading, and Geographic Evaluation (MANAGE)

MANAGE is a model that was created by the University of Rhode Island Cooperative Extension to be applied in the communities of Rhode Island to aid in assessment and management of nonpoint pollution sources and management of water resources (Joubert and Lucht 2000). MANAGE has been referred to as a “screening-level pollution risk assessment method” (Joubert and Lucht 2000), and it involves three main components:

- Use of geographic information systems (GIS) to create maps for use in analysis and identification of pollutant hotspots
- Use of watershed characteristics as indicators that can be used to assess the risk that pollutant inputs and other factors will lead to an adverse water quality impact
- Nutrient loading estimates via mass balance calculations

Comparison of Model Theoretical Basis

SWAT is similar to WARMF with respect to the theory and the numerical formulation of the hydrology and transport. Specifically, hydrologic and transport processes incorporated in WARMF are also generally included in SWAT, but the exact equations for each process may differ. For example, there are more than a dozen equations that are considered appropriate for estimating evapotranspiration based on temperature, relative humidity, aspect, elevation, plant cover, and other factors. SWAT and WARMF use different equations for evapotranspiration. However, fundamentally, either equation should work equally well if applied properly. Perhaps the most significant difference is that SWAT has a complex formulation for phosphorus transport because of SWAT's origin in agricultural hydrology. Organic and inorganic phosphorus is simulated, as well as active and inactive reservoirs of phosphorus, and rate-limited mass transfer between the different reservoirs and the water phase. WARMF, on the other hand, uses a relatively simple formulation that assumes first-order, equilibrium sorption of inorganic phosphorus to soils. This assumption appears to be appropriate for OWS applications (Kirkland 2001). In addition, this is possibly an advantage for WARMF because it is difficult to manipulate the equations in SWAT to simulate the primarily inorganic phosphorus in OWS effluent.

The theory behind the numerical component of MANAGE differs significantly in nature from that of either WARMF or SWAT. Nutrient loading is estimated using a mass balance approach (Joubert and Lucht 2000). The mass balance uses a water and nutrient budget to determine the nutrient inputs and outputs of a system. Outputs occur as either nutrients entering surface water run off or recharge to groundwater. This mass balance is set up in an Excel spreadsheet format. Necessary input data can be obtained from available GIS coverages such as soil and land use data, population estimates, and number of OWS. The mass balance equation itself was set up using values from available data and literature including average annual precipitation, nitrogen and phosphorous inputs to surface water, and nitrogen inputs to groundwater. Note that this is a simplified mass balance that does not take into account such factors as situations where the per acre nutrient loading may be higher than the average, the effects of storm events, other pollutants, and nutrient uptake through natural processes (Joubert and Lucht 2000).

For more information about the theory behind each model, refer to the documentation for each model.

Model Capabilities

Because the hydrologic and pollutant transport formulations for the SWAT and WARMF are similar, the ultimate capabilities of the two models are inherently similar. Both models use a GIS format to include publicly-available input and calibration data for the model. However, there are some important differences.

The primary technical difference between SWAT and WARMF is that WARMF specifically incorporates a method to apply STE from an OWS into the shallow subsurface. SWAT does not have this option, so the amounts of wastewater pollutants (for example, nitrogen and phosphorous) were calculated based on the number of people in each subbasin. This calculated mass of pollutant was then applied in the form of fertilizer in the second soil layer (to avoid transport of pollutants by runoff, which would not normally influence OWS pollutants). This application is problematic because it assumed that natural rainfall percolation infiltrated all the wastewater pollutants (Appendix G, *Watershed Modeling Using BASINS/SWAT*).

Another important difference between SWAT and WARMF is that WARMF has more sophisticated output displays. For example, distribution of loads from different sources can be displayed on a watershed map at various locations, and predicted exceedences of some water-quality limit or TMDL is displayed in a separate color. Model output from SWAT can be manipulated to produce the same data, but external software must be used.

WARMF can also more easily allow simulation of various hypothetical scenarios. Such scenarios might include simulating more OWS due to growth, or reducing OWS-effluent pollutant concentrations to simulate use of advanced treatment systems. This varied simulation is done in WARMF simply by changing entries on a single screen and re-running the model. In SWAT; however, the user must rebuild the model (with respect to hydrologic input, OWS input, and other factors) each time a different scenario is simulated.

Finally, WARMF includes two separate modules that are extremely useful for watershed managers. One module performs TMDL calculations and assessments, allows the user to test various scenarios of load reduction, and helps the user choose the best approach to meet assigned TMDLs. WARMF also includes a module for stakeholder involvement. In this module, contact information for all stakeholders can be entered, as well as a means for various stakeholders to choose or recommend various options. Both modules are easy to use via a Windows-based environment. Because of these modules, WARMF is a more complete watershed management tool.

The three components of MANAGE provide screening-level risk assessment capabilities. Hotspot mapping enables locating areas that are at a high risk for pollutant impacts and identifying locations of certain risk factors. In addition, qualitative pollutant risks can be compared as watershed indicators. While indicators do not quantify pollution effects, the risk from a pollutant input or physical stress that could adversely affect water quality can be compared. Finally, nutrient loading is estimated using a simplified mass balance.

Calibration Comparison

Two measures are used for this comparison: the plot of observed versus simulated streamflow, and observed versus simulated phosphorous concentrations. Both comparisons are for the location on the Blue River just before it enters Dillon Reservoir.

Systech Engineering completed calibrations for WARMF, while CSM completed SWAT calibrations. Because the numerical component of MANAGE differs significantly in nature from that of either WARMF or SWAT, a comparison using MANAGE was not completed.

Figure 6-5 shows the WARMF streamflow calibration. Figure 6-6 shows the SWAT calibration. Both model calibrations are exceptionally good for watershed-scale streamflow predictions, particularly for the stream location that is farthest downstream. The WARMF calibration does a better job of matching the receding flows, while the SWAT calibration is somewhat better at matching peak flows. However, this outcome was primarily a choice for the modeler because both peak flows and receding flows could not be simulated with precision. Based on this comparison, there is essentially no difference between the results of the two different models.

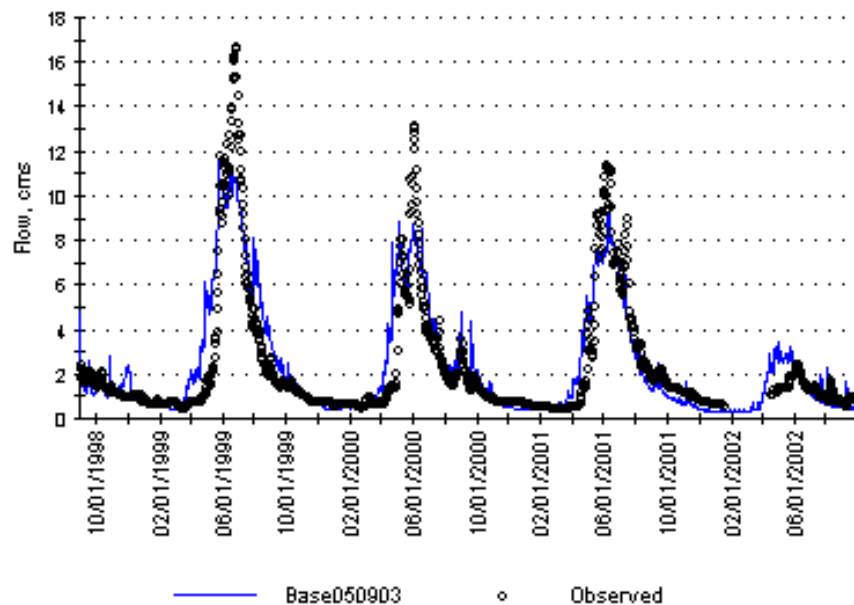


Figure 6-5
WARMF Simulated and Observed Stream Flow for Blue River Above Dillon Reservoir

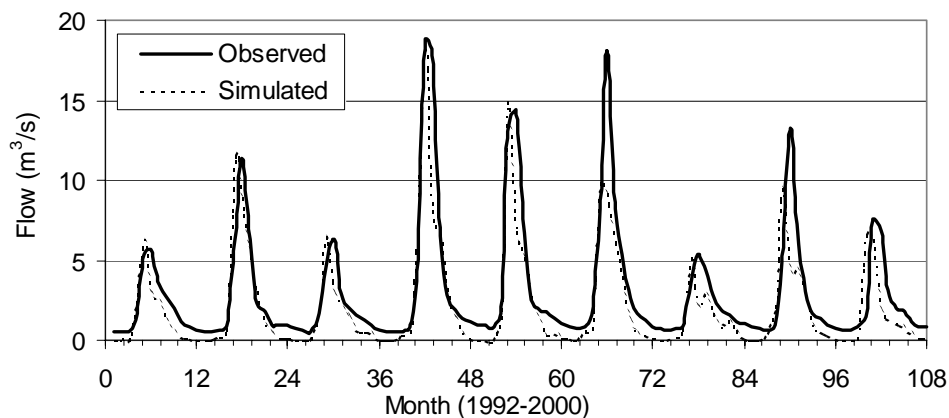


Figure 6-6
SWAT Simulated and Observed Stream Flow for Blue River Above Dillon Reservoir

Figure 6-7 shows the phosphorous calibration for SWAT, and Figure 6-8 illustrates the comparison between SWAT and WARMF. Figure 6-7 is shown separately to enable a better inspection of SWAT results for a phosphorous calibration. The calibration is not excellent for either simulation. However, the results are similarly good for the two models. In addition, while the results for both models are probably not good enough to predict future concentrations of phosphorous, the models could certainly be used to evaluate different management scenarios.

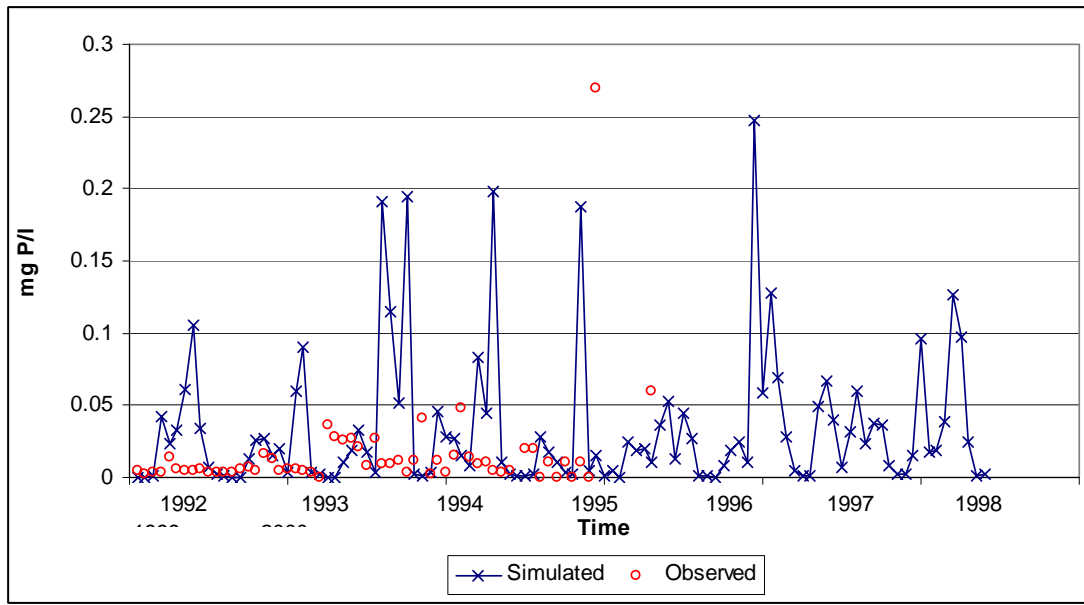


Figure 6-7
SWAT Simulated and Observed Phosphate at Blue River Above Dillon Reservoir

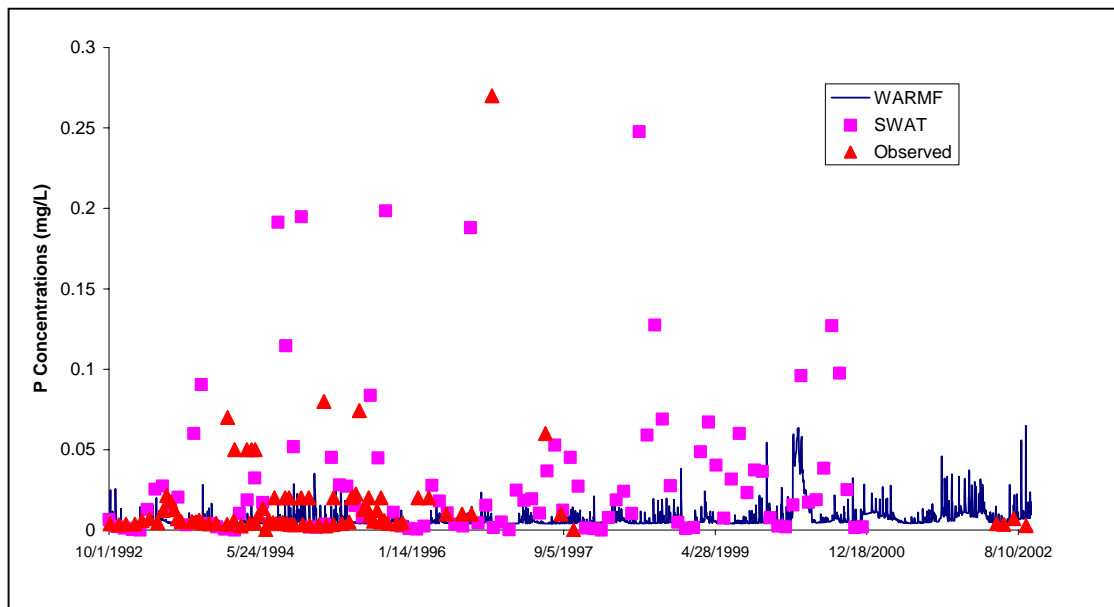


Figure 6-8
Comparison of WARMF and SWAT Phosphate Concentrations for the Blue River Above Dillon Reservoir

Model Availability

BASINS/SWAT is available free of charge from the US EPA (Office of Water, Office of Science and Technology). Free documentation on theory and use of the model is included. MANAGE is available free of charge from University of Rhode Island. WARMF may be obtained from the model developers, Systech Engineering (San Ramon, California). Presently, Systech Engineering performs model setup and calibration for most applications of WARMF. Consulting fee costs for Systech Engineering to deliver a calibrated watershed model typically range between \$75,000 and \$350,000 depending on the size of the watershed. Once the WARMF application has been calibrated, Systech Engineering provides training on how stakeholders can use the model to simulate various management scenarios. There are no licensing fees or restrictions on its usage and distribution.

Resource Requirements

Application of the WARMF and BASINS/SWAT models to the Dillon Reservoir watershed required approximately one year of effort for a hydrologic modeler working at about 30% effort. WARMF must be obtained from the developer under a consulting contract. However, personnel with limited technical background can then use it to test various management scenarios.

SWAT software can be obtained free of charge. However, a trained hydrologic modeler is required to apply and run the model for a given situation. If a consulting firm were hired to construct the SWAT model, it is anticipated that the end costs for both models would be similar. In fact, because SWAT would require a professional modeler for management-scenario simulations, the cost of SWAT could be significantly greater if many scenarios are desired. If the watershed stakeholders already employ a trained hydrogeologist with modeling experience, then SWAT might be more cost effective, but the modeler would be taken away from his typical duties (which are presumably considerable if he or she is in full-time employment with the watershed entity).

MANAGE is also available at no cost, but a GIS expert with some knowledge of soils and water-quality is required to implement it. Fortunately, most counties in the US and all large cities typically employ a GIS specialist.

High-end computational computers are required to run BASINS/SWAT and WARMF. A practical requirement is 1 GB of RAM, 1 GHz speed, and a relative large memory capacity (30 GB minimum required). For MANAGE 500 MB of RAM, 400 MHz, and 30 GB hard-drive memory are recommended minimum requirements

Comparative Model Summary

Summaries of model features, attributes, and selection features of the models (WARMF, BASINS/SWAT, and MANAGE) that were used in this project are presented in Table 6-2 through Table 6-4.

Table 6-2
Summary of Model Attributes

Model Attributes	WARMF	BASINS-SWAT	MANAGE
Model Configuration	Self-contained decision support system with dynamic watershed model, data module, and decision-support tools.	Graphical user interface and data manipulation software for several hydrology-water quality models including SWAT.	Planning-level, watershed-scale tool that couples GIS mapping with a simple, Excel-based nutrient load calculation.
Important Model Inputs	Land use, meteorology, DEM data.	Land use, meteorology, DEM data, soils data.	GIS data for soils and land use, population estimates, and number of OWS.
Hydrology	Dynamic water balance; simulates physical processes of snow, soil, and surface hydrology; uses Manning's equation for kinematic wave routing of flow in rivers; diversions can be specified to remove water from or add water to a river segment.	Soil Conservation Service runoff method for surface hydrology; directly simulates saturated flow; unsaturated flow between layers indirectly modeled with depth distribution of plant water uptake and soil water evaporation; storage routing or the Muskingum river routing method.	Uses precipitation data coupled with amount data on impervious surface, land use, and soil to calculate vertical infiltration and runoff. However, does not account for subsurface storage or movement of groundwater and associated constituents.
Water Quality	Dynamic mass balance in soil solution and in rivers; simulates build up and wash off of pollutants on soil surface; calculates nutrient cycling, sediment transport, chlorophyll-a, pesticides and fecal coliform bacteria.	Mass balance of nutrients, pesticides, plant uptake, fertilizer application; nonpoint loadings of sediment and nutrients are determined using USGS linear regression equations or buildup and washoff methods.	Pollutant hotspots identified with GIS maps; water quality impact assessed based on watershed characteristics; nutrient loading estimates via simplified mass balance calculations based on literature data for precipitation and nutrient input to surface water and groundwater.
OWS Loading	Simulates up to three types of OWS; loading is input to soil layer after processing by biozone module.	No explicit mechanism for simulating OWS loading.	No discrete OWS calculation, estimates impact based on GIS data.
Time Scale	Continuous simulation; daily time step; output in daily time series and average loading rates (kg/d).	Continuous simulation; daily time step; daily, monthly or yearly output available.	Average annual mass balance.

Table 6-3
Summary of Model Features

Model Features	WARMF	BASINS-SWAT	MANAGE
Graphical User Interface (GUI)	GIS-based map, spreadsheet data module, graphical model output with statistical analysis, self-contained modeling tool.	GUI-based map; input dialogs; text output requiring external post processing.	ArcView GUI linked with Excel spreadsheets.
Decision Support System Capabilities	Modules for TMDL calculation and stakeholder consensus building; easy to run alternative scenarios.	Limited; difficult to generate alternative management scenarios; no guidance for consensus or TMDLs.	GIS maps provide screening leveling information.
Documentation/ Help	Technical documentation; user's manual; and context sensitive help system.	User's manual; input definitions in GUI; tech support from USDA-ARS; user's forums on email.	Documentation available from the initial use of MANAGE at http://www.edc.uri.edu/cewq/manage.html .
GIS Capability	Can import ArcView shapefiles (DEM, land use).	Uses an ArcView GUI; can import ArcView shapefiles (DEM, land use).	Can interface with ArcInfo to obtain information from relevant ArcInfo files. An interface with ArcView is in progress.

Table 6-4
Summary of Model Selection Criteria

Model Selection Criteria	WARMF	SWAT	MANAGE
Scale	Small subwatershed up to large watershed system; resolution determined by available DEM data.	Small subwatershed up to large watershed system; resolution determined by available DEM data.	Cannot delineate subwatersheds, but if subwatershed delineations are available (from another model), MANAGE can be run for each subwatershed.
OWS Management Questions Model Can Answer	Benefit of converting existing OWS to centralized sewers; potential impact of growth in region; benefit of advanced versus standard OWS.	Relative impact of OWS on water quality; difficult to develop alternative management scenarios.	Screening level pollution risk of OWS.

Table 6-4
Summary of Model Selection Criteria (Cont.)

Model Selection Criteria	WARMF	SWAT	MANAGE
Resources Required to Apply Model	Approximately 4–6 man-months of time to set up and calibrate 500 sq mile watershed.	Approximately 4–6 man-months of time to set up and calibrate 500 sq mile watershed.	Approximately 1–2 man-months of time depending on the availability of GIS data.
System Requirements	1 GB of RAM, 1 GHz speed, 30 GB hard drive	1 GB of RAM, 1 GHz speed, 30 GB hard drive; ArcView application also required; Spatial Analyst is helpful but not required.	500 MB of RAM, 400 MHz speed, and 30 GB hard drive. ArcView of Arc Info application also required.
Previous Applications	Small and large watersheds throughout US	Small and large watersheds throughout US	Site-specific application to Wickford Harbor, RI.
Model Limitations and Simplifying Assumptions	Complex model; multiple OWS lumped within single catchment.	Complex model; does not explicitly model OWS.	Simple model; does not handle dynamic nature of watershed.
Data Requirements	High	High	Moderate
Model Availability	Front-end effort by model developers required; model turned over to user with no licensing restrictions; calibration performed by hydrologic modeler; scenarios created and run by end user with minimal modeling experience.	Public domain from US EPA or USDA-ARS; a trained hydrologic modeler is required to apply model, calibrate, and run alternative scenarios.	Public domain from URI; requires GIS expert with soils and water-quality knowledge to implement.



7 STAKEHOLDER AND USER PERSPECTIVES

Water quality has been extensively monitored and studied in the primary watersheds of Summit County, Colorado for over two decades. As a result of declining water quality in Dillon Reservoir during the early 1980s, extensive improvements were made to several WWTP that discharge into Dillon Reservoir. These treatment upgrades rapidly improved water quality in the reservoir in terms of nutrient loading. However, as rapid growth has occurred throughout the subsequent decades, nutrient levels, in particular phosphorous, have continued to creep toward regulatory limits established by the Colorado Water Quality Control Commission. As the major point source dischargers have continued to contribute very low levels of phosphorous to overall Dillon Reservoir nutrient loads, other contributors to phosphorous loading have been identified. Several local studies have attributed the largest percentage of anthropogenic non-point source phosphorous loading in the reservoir to OWS systems scattered throughout the watershed.

OWS are used by approximately 12% of the residences in the Dillon Reservoir watershed. Rapid development throughout the 1990s has increased local interest in understanding the contribution of OWS to nutrient loading and other water-quality impacts within the watershed as well as at the sub-watershed level.

WARMF Has Stakeholder Appeal

Development of the WARMF application for OWS appealed to potential Summit County water-quality stakeholders for many reasons. Many areas currently served by OWS are under pressure by contiguous sanitation districts to extend sanitary sewers. The expense of such infrastructure development projects concerns many residents and public officials in terms of the cost benefit of sewerage versus upgrading existing OWS. Others question the benefits of sewerage in light of little understood public-health or water-quality risks associated with continued use of OWS.

Most areas that are facing pressure to construct sewer systems are served by private water wells. Little is understood about the water quantity impacts of sewerage areas and moving wastewater miles away from its source. Public water systems are often not available to these areas and would be cost prohibitive to property owners to develop or extend from existing facilities.

Officials Desire a Better Understanding of Water-Quality Impacts

Summit County officials also desire to better understand more about water-quality impacts of OWS related to high-density development areas. Many of these areas are served by OWS and drinking water wells. Many of the more established, densely developed OWS are in valley bottoms either close to or in floodplains with shallow wells that draw from alluvial aquifers.

Information is needed as to anticipated human-health and water-quality risks that may be created by development of OWS in these areas. Interest exists in utilization of the engineering and consensus-building modules for addressing community decisions around use of OWS versus central sewer service.

Although a few individual studies have been conducted in the watershed, the cumulative non-point source phosphorous loading contributed by OWS is not clearly understood nor agreed upon by local water-quality stakeholders. Also, little is clearly understood about the actual contribution of failed OWS to phosphorous and other contaminant loading in the watershed. Furthermore, little is understood about the relative differences between water-quality impacts of different types of OWS. Useful tools are currently unavailable to compare costs of various wastewater alternative solutions at the subdivision level. In addition, since the same research group has conducted most water quality studies surrounding OWS impacts, concerns have been raised about potential biases. Community interest exists in comparing the findings of the WARMF model to the Lake Dillon Model regarding the relative contribution of phosphorous to Dillon Reservoir.

Summit County officials look forward to the opportunity to investigate many of the community issues surrounding the continued use of OWS in various watersheds. WARMF provides useful tools for water quality professionals to concerned citizens to make informed decisions about these issues. Local officials hope that use of the model will be intuitive and the findings of various scenario applications will contribute significantly to ongoing, productive public process concerning the continued use and management of OWS in the future.



8 SUMMARY, CONCLUSIONS, AND RECOMMENDATIONS

This project encompassed an extensive array of experimental work, field monitoring, and modeling efforts in order to quantify the site-scale processes and watershed-scale cumulative effects of decentralized wastewater systems. Numerous conclusions have been reached based on the findings of the research. Specific conclusions of individual research efforts are presented in the preceding chapters and subsequent appendix sections.

Summary and Conclusions

In summary, for common OWS, quantitative understanding of site-scale processes has been improved and site-scale models and decision-support tools have been developed and tested in this project, including the:

- Development of cumulative frequency distributions (CFDs) for OWS source concentrations and loads and values for nutrient transport/fate parameters based on literature data
- Development of fundamental understanding of bacteria and virus transport/fate in soil-based OWS through a series of experimental studies
- Initial development and testing of a new experimental design methodology based on life-cycle acceleration of soil-based OWS
- Application of HYDRUS 2-D to soil-based OWS to enable site-scale scenario analyses regarding hydraulic and purification performance
- Initial development and testing of a Biozone Algorithm to describe the biozone development in a soil-based OWS and the hydraulic and purification performance of that OWS

Site-scale quantitative understanding and mathematical modeling can provide insight into the process function and performance of an OWS and enable design and interpretation of experimental studies and the extrapolation of data collected in those studies to other conditions. Modeling can also help answer questions such as those posed in Table 1-1 regarding how changes in siting, design, and operation can affect OWS performance with respect to hydraulic and purification efficiencies.

For larger-scale applications of individual OWS, which can occur within a watershed, watershed-scale assessment and mathematical modeling can enable an evaluation of the effects of OWS compared to other pollutant sources in a watershed.

Assessment and modeling approaches can facilitate minor and major decision-making regarding infrastructure alterations and land-use planning based on their environmental effects (positive or negative) and the relative benefits/costs of different actions being contemplated.

A major focus of this project was on refinement, application, and testing of an existing watershed-scale model, Watershed Analysis Risk Management Framework (WARMF), which has been modified to include explicit representation of OWS of different performance features, an integrated Biozone Algorithm, and CFDs for source concentrations and transport/fate parameters.

As demonstrated in this project for the Blue River basin of the Dillon Reservoir watershed, the water-quality effects of OWS were simulated using WARMF and compared to a water-quality dataset generated during the project. Simulations were also completed to assess realistic decision-making scenarios concerning wastewater infrastructure in the watershed and to determine the comparative effects on water quality.

In addition to the work with WARMF, the BASINS/SWAT model was setup, calibrated and applied to the Dillon Reservoir watershed. Compared to WARMF, the BASINS/SWAT model does not explicitly account for OWS, is less efficient in running scenario analyses, and does not include modules for TMDL analysis and stakeholder consensus building. In terms of setup and application to a given watershed, both models will require considerable resources either in the form of the upfront purchase price for a setup and calibrated model (WARMF) or for the consultant or in-house labor costs to setup, calibrate, and run a public domain model (BASINS/SWAT).

In this project, the MANAGE model was also reviewed and applied to the study watershed. MANAGE is a comparatively simple geographic information system (GIS)-based vulnerability mapping tool to identify potential hotspots and is similar in many respects to mass balance calculation approaches that could be formulated and applied to a particular potential problem area.

The environmental monitoring and subsurface characterization efforts of this project were focused on developing sufficient understanding of the Dillon Reservoir watershed to enable model setup and initial calibration. The water-quality monitoring was focused on surface water flow and quality at up to 20 monitoring locations in the watershed. Quality data include routine water-quality parameters, wastewater-related pollutants, and some chemical and biological tracers. In performing the characterization work we attempted to use limited and potentially uncertain data and to assess the reliability of that approach.

At the watershed-scale in the Dillon Reservoir watershed, compared to urbanized development and WWTP discharges, OWS are not a principal source of water pollutants as evidenced by:

- Source load mass balance calculations
- WARMF and BASINS/SWAT model simulation results
- Water-quality monitoring and analysis of spatial and temporal trends

Application of a watershed-scale decision-support tool such as WARMF can enable analysis of wastewater management scenarios and provide critical insight into the water-quality benefits of one management option compared to another. Based on WARMF simulations of different wastewater management scenarios in the Blue River basin, extending central sewers and conversion of OWS to a central WWTP appears to offer little or no benefit in terms of water-quality protection, and in some cases may lead to water-quality degradation.

Recommendations

While the research completed during this project has advanced the science and engineering of OWS, there are gaps in understanding that further research should attempt to fill. In general, there continues to be a need for quantitative understanding to enable proper OWS design to yield a desired performance level. Such understanding also enables the design and implementation of monitoring devices and methodologies for process control and performance assurance.

The biozone algorithm developed for WARMF is recommended to be further tested and refined based on additional data collected in the laboratory and the field (for example, Mines Park Test Site). Laboratory experiments and long-term field testing to measure and assess biomass build up and quantification of pollutant removal efficiencies in the biozone and subsurface soil could be used to further calibrate the biozone module. Incorporation of a virus constituent into WARMF based on the knowledge gained during this study with respect to reaction rates and transport mechanisms would be valuable. In addition, it may be beneficial to develop the biozone module as a stand-alone piece of software to enable evaluation of individual OWS under specific site conditions by homeowners applying for OWS permits and county officials evaluating permit applications.

The methodology and tools developed in this project are recommended to be applied to support decision making in Summit County, Colorado and the benefits gained from this decision support should be documented and used to assess the benefit/cost of quantitative decision-support such as reported herein. In addition, the methods and tools developed in this project should be applied and tested for other situations and environmental conditions to determine the extent of extrapolation possible.

Given the scope of the research completed in this project, those components of the work that would be most valuable to enabling application to another geographic region of the US for watershed-scale management would include: WARMF (and a comparative model) model refinement, setup, calibration and simulations, and environmental characterization and watershed monitoring.

Depending on the goals of the research during a similar project in another region of the US, additional site-scale testing and experimentation (to generate site-specific input data and algorithms for modeling) might also be warranted.



9 REFERENCES

- Albert, J. 2002. *Assessment of Bacterial Source Tracking Using Rep-PCR and Classification Methods for Identification of Fecal Contamination*. M.S. Thesis. Environmental Science & Engineering Division, Colorado School of Mines, Golden, CO.
- Ambrose, R. B. Jr., T. A. Wool, J. L. Martin, J. P. Connolly, and R. W. Schanz. 1991. *WASP5x, A Hydrodynamic and Water Quality Model—Model Theory, User's Manual, and Programmer's Guide*. Environmental Research Laboratory, Environmental Protection Agency, Athens, GA.
- Bagdol, J. L., R. L. Siegrist, and K. S. Lowe. 2004. "Mass Balance Modeling and Water Quality Monitoring for Impact Assessment of Development with Onsite Wastewater Systems Compared to That with Centralized Treatment Plants." *Proceedings of the Tenth National Symposium on Individual and Small Community Sewage Systems*. American Society of Agricultural Engineers, Sacramento, CA. 146–155.
- Beach, D. N. 2001. *The Use of One-Dimensional Columns and Unsaturated Flow Modeling to Assess the Hydraulic Processes in Soil-Based Wastewater Treatment Systems*. M. S. Thesis. Department of Geology and Geological Engineering, Colorado School of Mines, Golden, CO.
- Beach, D. N. and J. E. McCray. 2003. "Numerical Modeling of Unsaturated Flow in Mature Wastewater Soil Absorption Systems." *Ground Water Monitoring and Remediation*. 23(2), 64–72.
- Beach, D. N., J. E. McCray, K. S. Lowe, and R. L. Siegrist. 2005. "Temporal Changes in Hydraulic Conductivity of Sand Porous Media Biofilters During Wastewater Infiltration: Experimental Evaluation." *Journal of Hydrology*. In press.
- Beasley, D. B., L. F. Huggins, and E. J. Monke. 1980. *ANSWERS—A Model for Watershed Planning*. American Society of Agricultural Engineers. 23(4), 938–944.
- Beasley, D. B. and L. F. Huggins. 1991. *ANSWERS User's Manual*. Publication 5, Agricultural Engineering Department, University of Georgia, Coastal Plain Experiment Station, Tifton, GA.
- Bertucci, J. C. Lue-Hing, D. Zene, and S. J. Sedita. 1974. *Studies on the Inactivation of Four Enteric Viruses in Anaerobically Digesting Sludge*. Metropolitan Sanitary District of Greater Chicago, Res. and Dev. Department Report No. 74–19. Cicero, IL.

- Caupp, C. L., J. T. Brock, and H. M. Runke. 1998. *Application of the Dynamic Stream Simulation and Assessment Model (DSSAMt) to the Truckee River Below Reno, Nevada: Model Formulation and Overview*. Technical Report No. RCR98-1. Rapid Creek Research, Inc., Boise, ID.
- Celia, M. A., E. T. Bouloutas, and R. L. Zarba. 1990. "A General Mass-Conservative Numerical Solution for the Unsaturated Flow Equation." *Water Resources Research*. 26, 1483–1496.
- Chen, C. W. and R. P. Shubinski. 1971. "Computer Simulation of Urban Storm Water Runoff." *Journal of Hydrology*. 97(2), 289–301.
- Chen, C. W., S. A. Gherini, R. J. M. Hudson, and J. D. Dean. 1983. *Integrated Lake-Watershed Acidification Study—Volume 1: Model Principles and Application Procedures*. Final Report EA-3221. Electric Power Research Institute, Palo Alto, CA.
- Chen, C. W., J. Herr, L. Ziemelis, M. C. Griggs, L. Olmsted, and R. A. Goldstein. 1997. "Consensus Module to Guide Watershed Management Decisions for Catawba River Basin." *Environmental Professional*. 19, 75–79.
- Chen, C. W., J. Herr, L. Ziemelis, R. A. Goldstein, and L. Olmsted. 1999. "Decision Support System for Total Maximum Daily Load." *Journal of Environmental Engineering*. 125(7), 653–659.
- Chen, C. W., J. Herr, and L. Weintraub. 2000. *Watershed Analysis Risk Management Framework (WARMF) User's Guide: Documentation of Graphical User Interface*. Report TR-1000729. Electric Power Research Institute, Palo Alto, CA.
- Chen, C. W., L. Weintraub, R. A. Goldstein, R. L. Siegrist, and S. Kirkland. 2001a. "Framework to Account for Onsite Wastewater Systems in Calculating Total Maximum Daily Loads." *Onsite Wastewater Treatment*. Publication No. 701P0101. American Society of Agricultural Engineers, St. Joseph, MI. 524–532.
- Chen, C. W., J. Herr, and L. Weintraub. 2001b. *Watershed Analysis Risk Management Framework (WARMF): Update One—A Decision Support System for Watershed Analysis and Total Maximum Daily Load Calculation, Allocation and Implementation*. Publication No. 1005181. Electric Power Research Institute, Palo Alto, CA.
- Crites, R. and G. Tchobanoglous. 1998. *Small and Decentralized Wastewater Management Systems*. McGraw-Hill, Boston, MA.
- Dano, K. E; E. Poeter, and G. Thyne. 2003. "Geochemical and Geophysical Determination of the Fate of Septic Tank Effluent in Turkey Creek Basin, Colorado." *Geol. Soc. Amer.*, Abstracts with Programs, 3.
- Efron, B. 1982. *The Jackknife, the Bootstrap, and Other Resampling Plans*. Society of Industrial and Applied Mathematics, Philadelphia, PA.

- Efron, B. and G. Gong. 1983. "A Leisure Look at the Bootstrap, the Jackknife, and Cross Validation." *American Statistics*. 37(1), 36–48.
- Electric Power Research Institute (EPRI). 2001. *National Research Needs Conference Proceedings: Risk-Based Decision Making for On-site Wastewater Treatment*. Project No. 1001446. EPRI, Palo Alto, CA, US EPA and National Decentralized Water Resources Capacity Development Project. March 15, 2001.
- Fetter, C. W. 2001. *Applied Hydrogeology, Fourth Edition*. Prentice Hall, Inc., Upper Saddle River, NJ.
- Flynn, J. L. and L. B. Barber. 2000. *Quality of Ground Water and Surface Water in an Area of Individual Sewage Disposal System Use Near Barker Reservoir, Nederland, Colorado August through September 1998*. US Geological Survey Open File Report 00-214.
- Gherini, S. A., L. Mok, R. J. Hudson, G. Davis, C. W. Chen, and R. A. Goldstein. 1985. "The ILWAS Model: Formulation and Application." *Water, Air, and Soil Pollution*. 26, 425–459.
- Guelfo, J. L. 2003. *Water Quality Monitoring in the Lake Dillon Watershed, Colorado to Enable Assessment of Development Impacts*. M. S. Thesis. Environmental Science & Engineering Division, Colorado School of Mines, Golden, CO.
- Hargett, D. L., E. J. Tyler, and R. L. Siegrist. 1982. "Soil Infiltration Capacity as Affected by Septic Tank Effluent Application Strategies." *Onsite Sewage Treatment*. Publication 1-82. American Society of Civil Engineers. 72–84.
- Harvey, R. W. 1997. "Microorganisms as Tracers in Groundwater Injection and Recovery Experiments: A Review." *FEMS Microbiology Reviews*. 20, 461–472.
- Herr, J. W., L. H. Z. Weintraub, and C. W. Chen. 2000. *User's Guide to WARMF (Documentation to the Graphical User Interface)*. Report 100729. Electric Power Research Institute, Palo Alto, CA.
- Herr J., C. W. Chen, R. A. Goldstein, and J. Brogdon. 2002. "A Tool for Sediment TMDL Development on Oostanaula Creek." *Watershed Management to Meet Emerging TMDL Environmental Regulations, Conference and Exhibits*, March 11–13, 2002, Radisson Plaza, Fort Worth, TX.
- Hill, A. R. 1996. Nitrate Removal in Stream Riparian Zones. *Journal of Environmental Quality*. 25, 743–755.
- Huber, W. C. and R. E. Dickinson. 1988. *Storm Water Management Model User's Manual, Version 4*. EPA/600/3-88/001a (NTIS PB88-236641/AS). Environmental Protection Agency, Athens, GA.

- Huntzinger, D., J. McCray, R. L. Siegrist, and S. Van Cuyk. 2001. "Mathematical Modeling of Unsaturated Flow in Wastewater Soil Absorption Systems with Clogging Zones." *Onsite Wastewater Treatment*. Publication No. 701P0101. American Society of Agricultural Engineers, St. Joseph, MI. 106–115.
- Jenssen, P. D. and R. L. Siegrist. 1990. "Technology Assessment of Wastewater Treatment by Soil Infiltration Systems." *Wat. Sci. Tech.* 22(3/4), 83–92.
- Joubert, L. and J. Lucht. 2000. *Wickford Harbor Watershed Assessment*. Report #00-03, Contribution #3847. University of Rhode Island, College of Environment and Life Sciences, Kingston, RI.
- Kirkland, S. L. 2001. *Coupling Site-Scale Fate and Transport with Watershed-Scale Modeling to Assess the Cumulative Effects of Nutrients from Decentralized Wastewater Systems*. M.S. Thesis. Department of Geology and Geological Engineering, Colorado School of Mines, Golden, CO.
- Kresic, N. 1997. *Quantitative Solutions in Hydrogeology and Ground Water Modeling*. Lewis Publishers, Boca Raton, FL.
- Larkin, E. P., J. T. Tiernay, and R. Sullivan. 1976. "Persistence of Poliovirus 1 in Soil and on Vegetables Irrigated with Sewage Wastes: Potential Problems." *Virus Aspects of Applying Municipal Waste to Land*. L. B. Baldwin *et al.* (ed.), University of Florida. US Environmental Protection Agency. 119–130.
- Lemons, P. J. 2003. *Modeling Pollution Transport and Fate to Assess the Effects of Onsite Wastewater Systems on the Lake Dillon Watershed, Colorado*. M. S. Thesis. Department of Geology and Geological Engineering, Colorado School of Mines, Golden, CO.
- Lemons, P. J. and J. E. McCray. 2004. "Watershed-Scale Transport Modeling of Onsite Wastewater Pollutants in the Blue River Drainage Basin." *Proceedings of the Tenth National Symposium on Individual and Small Community Sewage Systems*. American Society of Agricultural Engineers, Sacramento, CA. 19–26.
- Linker, L. C., G. W. Shenk, R. L. Dennis, and J. L. Sweeny. 1999. *Cross-Media Models for the Chesapeake Bay Watershed and Airshed*. Chesapeake Bay Program Office, Annapolis, MD. November 1999.
- Loveland, J. P., J. N. Ryan, G. L. Amy, and R. W. Harvey. 1996. "The Reversibility of Virus Attachment to Mineral Surfaces." *Colloids and Surfaces*. 107, 205–221.
- Lowe, K. S. and R. L. Siegrist. 2002. *Site Evaluation Report for the Wastewater Reclamation Test Site*. Prepared for the Jefferson County Department of Health and Environment by the Colorado School of Mines, Golden, CO. June 2002.

- Maizel, M. S. and P. Muehlbach, *et al.* 1997. *The Potential for Nutrient Loadings from Septic Systems to Ground and Surface Water Resources and the Chesapeake Bay*. EPA #903-R-97-006, Report #CBP/TRS 166/97.
- McCray, J. E., D. N. Huntzinger, S. Van Cuyk, and R. Siegrist. 2000. "Mathematical Modeling of Unsaturated Flow and Transport in Soil-Based Wastewater Treatment Systems." *WEFTEC 2000 Conference Proceedings*. Anaheim, CA. Water Environment Federation, Alexandria, VA.
- McCray, J. E., S. L. Kirkland, R. L. Siegrist, and G. D. Thyne. 2005. "Hydrologic Modeling of Nutrients from Onsite Wastewater Systems: Review of Input Parameters." *J. Ground Water*. Accepted and in press.
- McGee, T. J. 1991. *Water Supply and Sewerage*. Sixth Edition. McGraw-Hill, Boston, MA..
- Metcalf & Eddy, Inc. 2003. *Wastewater Engineering: Treatment, Disposal, and Reuse*. McGraw-Hill, Boston, MA.
- Neitsch, S. L., J. G. Arnold, J. R. Kiniry, and J. R. Williams. 2000. *Soil and Water Assessment Tool Theoretical Documentation, Version 2000*.
- Navigato, T. 1999. *Virus Attachment Versus Inactivation in Aquifer Sediments*. M. S. Thesis. University of Colorado, Boulder, CO.
- Powelson, D. C., Simpson, J. R., and Gerba C. P. 1990. "Virus Removal from Sewage Effluents During Saturated and Unsaturated Flow Through Soil Columns." *J. Environ. Quality*. 19, 396–401.
- Powelson, D. K., C. P. Gerba, and M. T. Yahya. 1993. "Virus Transport and Removal in Wastewater During Aquifer Recharge." *Wat. Res.* 27(4), 583–590.
- Powelson, D. K. and C. P. Gerba. 1994. "Virus Removal from Sewage Effluents During Saturated and Unsaturated Flow Through Soil Columns." *Wat. Res.* 28(10), 2175–2181.
- Razack, M. and D. Huntley. 1991. "Assessing the Transmissivity from Specific Capacity Data in a Large and Heterogeneous Alluvial Aquifer." *Ground Water*. 29(6), 856–861.
- Reddy, K. R., R. Khaleel, and M. R. Overcash. 1981. "Behavior and Transport of Microbial Pathogens and Indicator Organisms in Soils Treated with Organic Wastes." *J. Environ. Quality*. 10(3), 255–266.
- Schijven, J. F., W. Hoogenboezem, S. M. Hassanizadeh, and J. H. Peters. 1999. "Modeling Removal of Bacteriophages MS2 and PRD1 by Dune Recharge at Castricum, Netherlands." *Water Resources Research*. 35, 1101–1111.
- Sharp, W. E. 1971. "A Topologically Optimum Water-Sampling Plan for Rivers and Streams." *Water Resources Research*. 7(6), 1641–1646.

Siegrist, R. L. 1987. "Soil Clogging During Subsurface Wastewater Infiltration as Affected by Effluent Composition and Loading Rate." *J. Environmental Quality*. 16, 181–187.

Siegrist, R. L. and W. C. Boyle. 1987. "Wastewater Induced Soil Clogging Development." *J. Environmental Engineering*. 113(3), 550–566.

Siegrist, R. L. 2001. "Perspectives on the Science and Engineering of Onsite Wastewater Systems." *Small Flows Journal*. 2(4), 8–13.

Siegrist, R. L., E. J. Tyler, and P. D. Jenssen. 2001. "Design and Performance of Onsite Wastewater Soil Absorption Systems." *National Research Needs Conference Proceedings: Risk-Based Decision Making for On-site Wastewater Treatment*. Project No. 1001446. EPRI, Palo Alto, CA, US EPA and National Decentralized Water Resources Capacity Development Project. March 15, 2001.

Siegrist, R. L., K. S. Lowe, J. McCray, B. Beach, and S. Van Cuyk. 2002. "Accelerated Loading for Evaluation of Long-Term Performance of Soil PMBs Used for Wastewater Renovation." *Proceedings of the Eleventh Northwest On-Site Wastewater Treatment Short Course and Equipment Exhibition*. April 3–4, 2002, Seattle, WA.

Simunek, J., M. Sejna, and M. T. van Genuchten. 1999. *The HYDRUS-2D Software Package for Simulating Water Flow and Solute Transport in Two-Dimensional Variably Saturated Media, Version 2.0*. IGWMC-TPS-53C. International Groundwater Modeling Center, Colorado School of Mines, Golden, CO.

Smith, H. E. 2004. *Watershed Scale Impacts of Pollutants in an Alpine Groundwater System*. M.S. Thesis. Department of Geology and Geological Engineering, Colorado School of Mines, Golden, CO.

Smith, H. E., G. D. Thyne, J. E. McCray, K. S. Lowe, J. Guelfo, and R. L. Siegrist. 2004. "Preliminary Evaluation of Anthropogenic Effects on Water Quality Within the Blue River Watershed, Summit County, Colorado." *Proceedings of the Tenth National Symposium on Individual and Small Community Sewage Systems*. American Society of Agricultural Engineers, Sacramento, CA. 668–678.

Summit County Government. 1998. Population and Housing Data 1970–1998. <http://www.co.summit.co.us/>.

Tackett, K. N. 2004. *Vadose Zone Treatment During Effluent Reclamation as Affected by Infiltrative Surface Architecture and Hydraulic Loading Rate*. M. S. Thesis. Environmental Science & Engineering Division, Colorado School of Mines, Golden, CO.

Tackett, K. N., K. S. Lowe, R. L. Siegrist, and S. M. VanCuyk. 2004. "Vadose Zone Treatment During Effluent Reclamation as Affected by Infiltrative Surface Architecture and Hydraulic Loading Rate." *Proceedings of the Tenth National Symposium on Individual and Small*

Community Sewage Systems. American Society of Agricultural Engineers, Sacramento, CA. 655–667.

Tweto, O. 1973. *Reconnaissance Geologic Map of the Dillon 15-Minute Quadrangle, Summit, Eagle, and Grand Counties, Colorado*. USGS Open File Report 73-285.

United States Department of Agriculture (USDA). 1980. *Soil Survey of Summit County Area, Colorado*. USDA, Soil Conservation Service, Washington, DC.

United States Environmental Protection Agency (US EPA). 1978. *Management of Small Waste Flows*. EPA-600/2-78-173. Report of Small Scale Waste Management Project, University of Wisconsin, Madison, WI. US EPA, Municipal Environmental Res. Lab., Cincinnati, OH.

US EPA. 1992. *SWMM: Storm Water Management Model, Version 4.2*. Center of Exposure Assessment Modeling. Environmental Protection Agency, Athens, GA.

US EPA. 1997. *Response to Congress on Use of Decentralized Wastewater Treatment Systems*. US EPA, Office of Water, Washington, DC.

US EPA. 2002. *Onsite Wastewater Treatment Systems Manual*. EPA 625/R-00/008. US EPA, Office of Water, Washington, DC.

Van Cuyk, S. and R. L. Siegrist. 2001. “Pathogen Fate in Wastewater Soil Absorption Systems as Affected by Effluent Quality and Soil Clogging Genesis.” *Ninth National Symposium on Individual and Small Community Sewage Systems*. Fort Worth, TX.

Van Cuyk, S., R. L. Siegrist, A. Logan, S. Masson, E. Fischer, and L. Figueroa. 2001. “Hydraulic and Purification Behaviors and Their Interactions During Wastewater Treatment in Soil Infiltration Systems.” *Water Research*. 35(4), 953–964.

Van Cuyk, S., R. L. Siegrist, and R. W. Harvey. 2002. “Fate of Viruses During Wastewater Reclamation in Small-Scale Systems that Rely on Soil Treatment Before Groundwater Recharge.” *WEFTEC Conference Proceedings*. October 2002, Chicago, IL. Water Environment Federation, Alexandria, VA.

Van Cuyk, S. M. 2003. *Fate of Virus during Wastewater Renovation in Porous Media Biofilters*. Ph.D. Dissertation. Environmental Science & Engineering Division, Colorado School of Mines, Golden, CO.

Van Cuyk, S., R. L. Siegrist, K. Lowe, and R. W. Harvey. 2004. “Evaluating Microbial Purification During Soil Treatment on Wastewater with Multicomponent Tracer and Surrogate Tests.” *J. Environ. Qual.* 33, 316–329.

Van Cuyk, S. M. and R. L. Siegrist. 2004. "Fate of Viruses in the Infiltrative Surface Zone of Systems that Rely on Soil Treatment for Wastewater Renovation." *Proceedings of the Tenth National Symposium on Individual and Small Community Sewage Systems*. American Society of Agricultural Engineers, Sacramento, CA. 387–399.

van Genuchten, M. T. 1980. "A Closed-Form Equation for Predicting the Hydraulic Conductivity of Unsaturated Soil." *Journal of the Soil Science Society of America*. 44, 892–892.

Weintraub, L. H. Z., C. W. Chen, and J. Herr. 2001. "Demonstration of WARMF: A Decision Support Tool for TMDL Development." *Proceedings from the WEF TMDL Science Issues Conference*. March 4–7, 2001, St. Louis, MO.

Weintraub, L., C. W. Chen, W. Tsai, J. Herr, R. A. Goldstein, and R. L. Siegrist. 2002. "Modifications of WARMF to Assess the Efficacy of Onsite Wastewater Systems on Public Health." *WEFTEC Conference Proceedings*. October 2002, Chicago, IL. Water Environment Federation, Alexandria, VA.

Weintraub, L. H. Z., C. W. Chen, R. A. Goldstein, and R. L. Siegrist. 2004. "WARMF: A Watershed Modeling Tool for Onsite Wastewater Systems." *Proceedings of the Tenth National Symposium on Individual and Small Community Sewage Systems*. American Society of Agricultural Engineers, Sacramento, CA. 636–646.

Yates, M. V. 1995. "Field Evaluation of the GWDR's Natural Disinfection Criteria." *J. American Water Works Assoc.* 87, 76–85.



10 ACRONYMS, ABBREVIATIONS, AND SYMBOLS

Acronyms and Abbreviations

AGW	Artificial groundwater
AMD	Acid mine drainage
ANOVA	Analysis of variance
ATU	Advanced treatment unit
BASINS	Better Assessment Science Integrating Point and Nonpoint Sources
BDL	Below detection limit
BOD	Biochemical oxygen demand
BOD ₅	5-day BOD
BR	Blue River
BST	Bacterial source tracking
Ca	Calcium
CASNET	Clean Air Status and trends Network
cBOD	Carbonaceous BOD
CFD	Cumulative frequency distribution
CFU	Colony forming unit
Cl	Chloride
COD	Chemical oxygen demand
CSEO	Colorado State Engineer's Office
CSM	Colorado School of Mines
CSTR	Continuously stirred tank reactor
CZ	Clogging zone
DEM	Digital elevation model

DO	Dissolved oxygen
DOC	Dissolved organic carbon
DSS	Decision support system
DSSAMt	Dynamic Stream Simulation and Assessment Model with temperature
EPRI	Electric Power Research Institute
F	Fluoride
FC	Fecal coliform bacteria
GIS	Geographic information system
GUI	Graphical user interface
GWR	Ground Water Rule
HCO ₃	Bicarbonate
HLR	Hydraulic loading rate
HSPF	Hydrologic Simulation Program Fortran
IC	Ion chromatograph
ICP	Inductively coupled plasma
ILWAS	Integrated Lake-Watershed Acidification Study
IR	Infiltration rate
ISU	Infiltrative surface utilization
IZ	Infiltrative zone
K	Potassium
K_s	Saturated hydraulic conductivity
LR	Loading regime
LULC	Land use land coverage
MANAGE	Method for Assessment, Nutrient-loading, and Geographic Evaluation
mg/L	Milligrams per liter
Mg	Magnesium
MGD	Million gallons per day
Mn	Manganese
Mo	Molybdenum
MW	Monitoring well

N	Nitrogen
Na	Sodium
NCDC	National Climatic Data Center
NDWRCDP	National Decentralized Water Resources Capacity Development Project
NO ₃	Nitrate
NRCS	National Resources Conservation Service
NWQL	National Water Quality Laboratory
OWS	Onsite wastewater system
P	Phosphorous
PFU	Plaque forming unit
RSF	Recirculating sand filter
SB	Soil boring
SBRWWTP	South Blue River wastewater treatment plant
SC	Specific conductance
SCEH	Summit County Environmental Health Department
SCS	Soil Conservation Service
Sn	Tin
SNOTEL	SNOpack TELelemetry system
SO ₄	Sulfate
SPE	Soil percolate effluent
Sr	Strontium
STATSGO	State Soil Geographic Database
STE	Septic tank effluent
STORET	STOage and RETrieval database (www.epa.gov/storet)
SWAT	Soil and Water Assessment Tool
SWMM	Stormwater Management Model
SWTR	Surface Water Treatment Rule
TDS	Total dissolved solids
TMDL	Total maximum daily load
TOC	Total organic carbon

TKN	Total Kjeldahl nitrogen
TN	Total nitrogen
TP	Total phosphorous
TS	Total solids
TSS	Total suspended solids
TW	Tapwater
USDA	United States Department of Agriculture
US EPA	United States Environmental Protection Agency
USGS	United States Geological Survey
VZ	Vadose zone
WARMF	Watershed Analysis Risk Management Framework
WC	Water content
WSAS	Wastewater soil absorption system
WWTP	Wastewater treatment plant
Zn	Zinc

Symbols

A	Biozone surface area, cm^2
Bio	Biomass of live bacteria in biozone, mg
b	Aquifer thickness, feet or cm
C	Concentration in biozone at time t , mg/L (Equation 4-13)
C	Concentration of the solute in solution equilibrium with the mass of solute sorbed onto the solid, mg/L (Equation 4-15)
C_o	Concentration in biozone at time $t-1$, mg/L
$C_{BOD,in}$	BOD concentration in STE, mg/L
C_{BOD}	BOD concentration in biozone, mg/L
$d(Bio)/dt$	Live biomass growth rate, mg/s
dd	Aquifer drawdown, feet
E	Evapotranspiration from biozone, cm^3
I_p	Percolation out of the biozone, cm^3

ISU	Fraction of infiltrative surface utilization, unitless
K_D	Linear distribution coefficient, L/kg
K_i	First order reaction rate, 1/day
$K_{l,i}$	Reaction rate coefficient for each constituent i , cm^3/s
K_s	Saturated hydraulic conductivity, ft/d or cm/s
K_v	Intrinsic hydraulic conductivity, cm/s
$K_{l,nitr}$	Nitrification rate coefficient, cm^3/s
$K_{l,denitr}$	Denitrification rate coefficient, cm^3/s
$K_{l,BOD}$	BOD decay rate coefficient, cm^3/s
$K_{l,feecal}$	Fecal coliform bacteria decay rate coefficient, cm^3/s
L	Length of soil including infiltrative surface and vadose zone, cm
N_e	Effective porosity, unitless (vol/vol)
Plaque	Biomass of dead bacteria and residue, mg
P_v	Hydraulic conductivity, cm/s
Q	Flow rate of STE into biozone, cm^3/s
q	Application rate, cm/hr
R_{resp}	Respiration of bacteria, mg/s
R_{mort}	Mortality of bacteria, mg/s
R_{slough}	Sloughed off bacteria, mg/s
S	Mass solute sorbed per unit dry weight of solid, mg/kg
SY	Sustained yield, gallons per minute
T	Transmissivity, ft^2/day or cm^2/s
t	Time, s or hr or day
Δt	Time step of (model) calculation, s
TS	Total solids contained in STE, approximately 500 to 600 mg/L
Z	Thickness of biozone, usually approximately 2 cm

α	Gram biomass/gram BOD in STE, unitless
δ	Sloughing coefficient 2, unitless

ξ	Field capacity coefficient 2, unitless
Φ	Field capacity coefficient 1, unitless
ϕ	Mortality rate coefficient, cm^3/s
γ	Respiration rate coefficient, cm^3/s
η	Sloughing coefficient 1, mg/cm
θ	Moisture content of biozone, unitless
θ_f	Field capacity of biozone, unitless
$\theta_{f,t}$	Field capacity at time t , unitless
$\theta_{f,t-1}$	field capacity at time $t-1$, unitless
θ_t	Moisture content of biozone at time t , unitless
θ_{t-1}	Moisture content of biozone at time $t-1$, unitless
θ_s	Saturated moisture content of biozone, unitless
$\theta_{s,t-1}$	Saturated moisture at time $t-1$, unitless
θ_{sm}	Porosity of parent soil with zero plaque, unitless
ρ_b	Density of biomass, mg/cm^3
σ	Plaque coefficient for TDS, unitless
v_p	Pore velocity = $\Sigma Q/(A\theta_s)$, cm/s



A INPUT PARAMETERS FOR MODELING FLOW AND TRANSPORT IN ONSITE WASTEWATER SYSTEMS

Mathematical modeling is a powerful tool for assessing the impacts of onsite wastewater systems (OWS) on water quantity and quality from the single site to watershed scales. However, models require input parameters to describe the hydrologic system, wastewater chemical and biological concentrations, and pollutant transport parameters. Estimation of hydrologic input parameters has long been a topic of the literature. Hydrologic-parameter estimation at large scales is uncertain, but national databases exist to help the user define these properties. The recent use of geographical information systems (GIS) and remote sensing has greatly facilitated these efforts. However, methods to estimate wastewater constituents and pollutant transport parameters are not readily available in the literature. Of course, direct measurement is the preferred method; but given the spatial and temporal variability in fate and transport parameters at typical modeling scales, direct measurement is not always possible. In these cases, it is useful to have a database of relevant, statistically supported input parameters to choose from.

Overview

The purpose of this section is to present the range, frequency, and median values for selected wastewater pollutant concentration and transport parameters. The source of the reported data is a thorough literature review. When feasible, cumulative frequency distributions (CFDs) are presented. Summary tables with the median values, and often a range of values, are also reported. Use of the CFDs for modeling at various scales and for various purposes is discussed.

First, a summary of OWS effluent concentration values for a variety of system types is presented. Second, a discussion is presented regarding the importance of virus on water quality. CFDs and tables for nutrient concentrations in septic tank effluent (STE) and transport parameters, such as nitrogen reaction rates and phosphorus sorption coefficients, are presented. Finally, information on daily flow for residential dwellings is given.

Effluent Concentrations From OWS

Table A-1 follows and presents typical OWS effluent concentrations for various types of OWS systems. The remainder of this report presents parameters for conventional OWS systems. Few parameter values for non-conventional systems are available in the literature. The information in Table A-1 might be useful, for example, when conducting hypothetical watershed-scale model simulations to assess the effect of installing different types of OWS systems on watershed water quality.

Table A-1
Expected OWS Performance for Various System Types

Type	Description	Reference	BOD (mg/L)	TSS (mg/L)	TN (mg-N/L)	NH4 (mg-N/L)	NO3 (mg-N/L)	TP (mg-P/L)	F. Coli (cfu/100mL)
1 Septic									
a	Septic w/ SAS		170	75	70	60	0	10	1.00E+07
b	Septic w/ SAS	Siegrist et al., 2001	140-200	50-100	40-100			5-15	1E6-1E8
2 Septic w/ N removal									
a	Septic w/ in-tank N removal and SAS		170	80	20	0	20	10	1.00E+06
b	Septic tank w/ effluent N removal and recycle	Siegrist et al., 2001	80-120	50-80	10-30			5-15	1E6-1E8
c	Septic w/ corrugated plastic trickling filter	Ball, 1995	20	10	7.7	2.4	7.1		
d	Septic w/ open-cell foam trickling filter	Ball, 1995	18	17	11	5.6	4.1		
3 Septic w/ single pass sand filter									
a	Single pass sand filter	Loomis et al., 2001	3-4	1-3	37-39				200-520
b	Single pass sand filter	Ronayne et al., 1982b	3.2	9	30				407
c	Single pass sand filter	Effert et al., 1984	4	17	37.5			14.1	123-1600
d	Single pass sand filter	Darby, J., G. Tchobanoglous, et al., 1996	75.1	29.1	15.5	10.6	0.3		
4 Septic w/ recirculating sand filter									
a	At grade recirculating sand filter	Loomis et al., 2001	3-4	3-4	11-16				240-5100
b	Maryland style RSF	Loomis et al., 2001	3-7	4-9	21-40				660-5400
c	Recirculating sand filter	Christopherson et al., 2001	9-14	12-15	24-29	5-6	15-23	6	5.1E4-6.1E4
5 Constructed wetlands									
a	Septic tank w/ constructed wetland and surface water discharge	Henneck et al., 2001	9-44	8-16	16-60			0.4-11	35-1900
b	Municipal wastewater w/ constructed wetland and surface water disch	USEPA, 1993	27	15					
c	Municipal wastewater w/ constructed wetland and surface water disch	USEPA, 1993		4.2		0.86		0.24	77
d	Municipal wastewater w/ constructed wetland	USEPA, 1993	3-12	3-25		0.15-6.43			
e	Municipal wastewater w/lagoon and constructed wetland	USEPA, 1993	2.5-9	4-15		0.05-3.9			
6 Biofilters									
a	Waterloo biofilter (plastic media)	Loomis et al., 2001	3-54	0-37	10-106				
b	Waterloo biofilter (plastic media)	Jowett and McMaster, 1995	16.8 ^a	5		10.2	5.7		1.9E5
c	Peat Biofilter	Lindbo and MacConnell, 2001	3-6	6-7	1-4.1	0.4-1.5	18-22.1	1.9-4	2.9E2-1.6E3
7 Textile Filter									
a	Recirculating Textile Filter	Loomis et al., 2001	6-49	7-25	7-46				580-101000
b	Foam or textile filter effluent	Siegrist et al., 2001	5-15	5-10	30-60				10-1E3
8 Systems w/ disinfection									
a	Septic, recirculating gravel filter, UV disinfection	Crites et al., 1997	0 to <5	4.9	0.4	0	12.2		<2-12.5 ^b

a. BOD value for this entry is 7 day BOD

b. Value is for total coliforms

Bacteria and Virus Concentrations

Viruses of concern are the human enteric viruses, which replicate in the gastrointestinal tract and are present in the feces of infected individuals. Most persons have at least one virus infection per year, so it is likely that a septic tank system will receive virus-laden wastewater at some time over the course of a year (Gerba 2002). Hain and O'Brien (1979) isolated enteric viruses from all of the four septic tanks they sampled in New Mexico. One of these septic tanks was positive for enteric viruses on five different sampling times occurring over the course of a year. Typical concentrations of enteric viruses in septic tank effluent and raw wastewater have been quantified at 10^3 to 10^4 plaque-forming units (PFU) per 100 mL (Crook 1998; Crites and Tchobanoglous 1999). The US EPA (2002) states that the number of specific virus (hepatitis, polio, echo, coxsackie, coliphage) is in the range of 0 – 10^5 PFU/mL, with episodic presence at high levels. Coliphage are typically found in STE at approximately the same level (Crook 1998, Crites and Tchobanoglous 1999).

Table A-2 presents a list of human viruses that are potentially present in untreated domestic wastewater (Crites and Tchobanoglous 1999, Crook 1998, Feachem *et al* 1983). Two studies have found that infected individuals can excrete from 10^6 – 10^8 enteric viruses per gram of feces (Tyrrell and Kapikian 1982, Sabin 1955).

Work by Anderson *et al.* (1991) showed that approximately 33% of stool samples in one subdivision in Florida yielded detectable viral agents. Infected residents in this subdivision were found to shed virus for periods in excess of 30 days. A recent study in household wells in Wisconsin (Borchardt *et al.* 2003) found 8% of wells tested to be positive for virus by reverse transcriptase polymerase chain reaction (RT-PCR). These wells were positive for Hepatitis A, rotavirus, and Norwalk-like virus. These researchers stressed the idea that virus contamination can be intermittent and that the vulnerability of a well to viral contamination cannot be characterized from a single sample.

Ward *et al.* (1986) demonstrated that enteric viruses have an exceptionally low infectious dose (unlike many pathogenic enteric bacteria). Their studies conducted with human volunteers suggest that ingestion of 1–10 viruses may be all that is needed to induce enteric virus infection.

Because the cells (hosts) needed for replication of human pathogenic virus are present in low concentrations in groundwater systems, long-term transport of virus is often assumed unlikely. Keswick *et al.* (1982) showed that poliovirus, coxsackie virus, and rotavirus survive much longer (on the order of weeks to months) in the subsurface environment than had generally been assumed. Transport of virus in the vadose and unsaturated zone has been found to be substantial (Rose *et al.* 1999; Keswick and Gerba 1980). However, studies of soil-based wastewater systems have demonstrated the high removal efficiency of these systems for virus. Additional information related to the effects of daily hydraulic loading rates and methods, effluent quality, temperature, pH, and organic carbon on virus removal, inactivation rates and transport are presented in Appendix B, *Pathogen Transport-Fate Studies* (see also Van Cuyk 2003).

Table A-2
Human Viruses Potentially Present in Untreated Domestic Wastewater

Virus	Disease(s)
Adenovirus (31 types)	Respiratory disease
Enteroviruses (72 types, polio, echo, and coxsackie viruses)	Gastroenteritis, heart anomalies, meningitis
Hepatitis A virus	Infectious hepatitis
Norwalk agent	Gastroenteritis
Parvovirus (3 types)	Gastroenteritis
Rotavirus	Gastroenteritis

(Crites and Tchobanoglous 1999; Crook 1997; and Feachem *et al.* 1983)

Nutrient Concentrations and Transport Parameters

Humans generate approximately 13.3 g nitrogen (N) per capita per day (Crites and Tchobanoglous 1998). Assuming an average density of 2.4 people per household and one house per acre-lot, the annual nitrogen-loading rate from a subdivision is potentially $7,460 \text{ kg sq mi}^{-1} \text{ yr}^{-1}$. In some areas, the housing density is much greater. This value compares to nitrogen loading rates of approximately $1,500\text{--}3,000 \text{ kg sq mi}^{-1} \text{ yr}^{-1}$ from atmospheric deposition (Howarth *et al.* 1996) and approximately $25,000\text{--}50,000 \text{ kg sq mi}^{-1} \text{ yr}^{-1}$ from fertilizer applied to row crop agriculture (Keeney 1986). Because of the large amount of fertilizer used in agriculture and the large amounts of nutrients deposited by animals in large livestock farms, agriculture's impact is potentially much greater than the impact of onsite systems overall in areas where agricultural production is dominant. However, in nonagricultural areas, OWS can be a significant contributor to groundwater and potentially to surface water nitrogen loadings.

Humans generate approximately 3.28 g phosphorus (P) per capita per day in domestic wastewater (Crites and Tchobanoglous 1998). Annual phosphorus loading rates from OWS depend on several factors, but primarily on OWS density (Gold and Sims 2001). Assuming the same population density as in the previous example with nitrogen, the annual phosphorus-loading rate from a subdivision is potentially $1,840 \text{ kg sq mi}^{-1} \text{ yr}^{-1}$. This compares to phosphorus loadings of less than $256 \text{ kg sq mi}^{-1} \text{ yr}^{-1}$ from atmospheric deposition, approximately $1,280 \text{ kg sq mi}^{-1} \text{ yr}^{-1}$ from maintenance fertilization of lawns, and 2,560 to $38,400 \text{ kg sq mi}^{-1} \text{ yr}^{-1}$ as fertilizer or manure in agricultural production systems (Gold and Sims 2001).

Methodology

Data related to OWS nutrient concentrations in STE and nutrient transport and transformation parameters were collected from studies published in the literature. This data is presented in detail in Kirkland (2001). Summary tables of compiled data, including the median, range, and number of data gathered for each OWS parameter, are presented in this report. These data were used to create CFD diagrams. CFD diagrams may be used to estimate the proportion of the members of a population whose measured values exceed or fall short of some stated level. CFD diagrams were created for STE concentrations of nitrogen and phosphorus, nitrification rates, denitrification rates, and linear sorption isotherm constants for phosphorus (P). While P is known to precipitate as well as sorb, particularly under suitable electrochemical conditions, too few data were found in literature sources to include phosphorus precipitation parameters using the CFD methodology. The cumulative frequency as a percentage is presented on the vertical axis of the CFD diagrams and the upper limits of the STE concentration or the nutrient transformation rate constant is presented on the horizontal axis. Data points represent values obtained or calculated from data gathered from literature sources. Trend lines are presented as solid lines. For this report, median values and other percentile values that were obtained from the CFD plots are derived from the trend lines or interpolated between particular data points.

The data used to construct these CFD diagrams were obtained from numerous literature sources. These sources used various experimental methodologies and data-reporting styles. For example, some studies report an average value of many samples collected in one study. In other papers, only one value is collected and reported. In other studies, only a range of measured values was given. For this type of report, the median value was used for inclusion into the CFD. If multiple data were given for a single site (for example, different sampling times), the value reported or calculated as the median of the data was used.

In the literature, nitrogen (N) species in STE were not consistently reported as N concentrations (that is, ammonium-nitrogen [$\text{NH}_4\text{-N}$], nitrate-nitrogen [$\text{NO}_3\text{-N}$]). However, for this study, all nitrate (NO_3^{-2}) concentrations are reported as N-equivalent concentrations based on molecular-weight ratios. In some cases, total Kjeldahl nitrogen (TKN) was reported in lieu of total N. Because nitrates and nitrites generally comprise a legible fraction of total N, TKN was assumed to be a satisfactory estimate for total N. Nitrogen and denitrification rates were reported in varying units. Sometimes a zero-order rate was reported (such as mg N per kg soil per day), which was converted to first-order rate constant units (1/day) using the reported soil properties. When necessary, a soil particle density of 2.65 g/cm^3 and porosity of 40% were assumed for this conversion.

Reported STE phosphorus concentrations were sometimes ambiguous. While phosphate concentrations were generally reported as total phosphorus (TP) or phosphate-phosphorus ($\text{PO}_4\text{-P}$), concentrations were also reported as PO_4^{-3} , and P. $\text{PO}_4\text{-P}$ is the phosphorus concentration due only to phosphate. Whether values reported as P represented $\text{PO}_4\text{-P}$ or TP was often unclear. Because 85% to 90% of TP in STE is usually considered to consist of the phosphate form (Wilhelm *et al.* 1994; Correll 1998; Willman *et al.* 1981), all concentrations reported simply as P, with no explanation, were assumed to represent $\text{PO}_4\text{-P}$ concentrations for this study.

To obtain consistent phosphorus concentration parameters, PO_4^{3-} and TP concentrations are converted to $\text{PO}_4\text{-P}$ concentrations. When TP is reported, the $\text{PO}_4\text{-P}$ concentration is assumed equal to 0.85 TP. Reported phosphate (as PO_4^{3-}) concentrations are converted to $\text{PO}_4\text{-P}$ concentrations (as P) based on molecular-weight ratios. $\text{PO}_4\text{-P}$ concentrations (or the concentration of PO_4^{3-} as P) in STE are less than the concentrations of PO_4^{3-} by a factor of approximately three.

Nitrogen Concentrations and Transport Parameters

Common forms of inorganic nitrogen associated with wastewater include ammonium (NH_4^+), NO_3^{-2} , nitrite (NO_2^-), and nitrogen gas (N_2). Nitrogen present in fresh wastewater is contained primarily in protein-rich matter and urea. Decomposition by bacteria readily changes organic N to ammonium in the septic tank (Crites and Tchobanoglous 1998). Approximately 75 to 85% of the TKN (organic N plus ammonium) consists of NH_4^+ in STE (Kirkland 2001). Table A-3 summarizes the data collected in this study, as well as average values reported by the *Onsite Wastewater Treatment Systems Manual* (US EPA 2002). Data from Anderson *et al.* (1994) was the source of the nitrates and phosphates data reported by US EPA (2002).

Nitrogen Concentrations

Nitrogen concentrations in STE vary depending on the wastewater generation and water use at the source, especially over time due to changing water-use practices. Keeney (1986) reported the total nitrogen concentration of typical effluent from a septic tank ranges from 50 to 70 mg N L^{-1} , about 75% as ammonium and 25% as organic nitrogen. Crites and Tchobanoglous (1998) reported similar values with organic nitrogen in STE ranging 20 to 40 mg N L^{-1} and $\text{NH}_4\text{-N}$ ranging 30 to 50 mg N L^{-1} . US EPA (2002) cites ranges of 40 to 100 mg L^{-1} for total nitrogen and 0.01 to 0.16 mg L^{-1} for $\text{NO}_3\text{-N}$ for typical residential wastewater. These specific data from the EPA study could not be obtained. Therefore, the STE nutrient pollutant concentrations provided herein present an independent evaluation using more data. However, the average value of each constituent from this EPA study (Table A-3) is included as one data point for this study's analysis. In addition, the EPA (2002) evaluation does not present the data in a CFD as is done for this study. These CFD diagrams are useful for planning, designing, and modeling, as will be discussed in more detail later.

As shown in Table A-3, this study's recent compilation of data relates to STE concentrations from operating OWS range from 17 to 178 mg N L^{-1} for NH_4 and 9.5 to 15 mg N L^{-1} organic N. $\text{NO}_3\text{-N}$ concentrations are much lower, as is expected since nitrification would not transform NH_4 to NO_3 in the anaerobic conditions of the septic tank. Surprisingly, the range and median of NH_3 concentrations reported in the literature is larger than the total N concentrations. However, STE concentration data for these two species were generally derived from different sources.

Table A-3
Summary of N and P Concentrations in STE^{a,b,c}.

Pollutant	Concentration (mg/L)			
	Median	Range	Number of Data	Average Value from US EPA (2002)
Total N (mg N L ⁻¹)	44	12–453	18	44.2 ^d
Organic N (mg N L ⁻¹)	14	9.4–15	6	^e
Ammonium (mg N L ⁻¹)	60	17–178	37	^e
Nitrate (mg N L ⁻¹)	0.2	0–1.94	33	0.04
Phosphate (mg P L ⁻¹)	9.0	1.2–21.8	35	8.6 ^f

a N and P data sources: Kirkland (2001), Robertson *et al.* (1998), Robertson and Blowes (1995), Wilhelm *et al.* (1996), Wilhelm *et al.* (1994), Robertson and Cherry (1992), Sherman and Anderson (1991), SSWMP (1978), Harkin *et al.* (1979), Brown *et al.* (1977), Robertson *et al.* (1991), Reneau *et al.* (1989), Cogger *et al.* (1988), Whelan (1988), Crites (1985), Willman *et al.* (1981), Kristiansen (1981), US EPA (2002), Viraraghavan and Warnock (1976), Magdoff *et al.* (1974), Otis *et al.* (1973), Walker *et al.* (1973), Ronayne *et al.* (1982a), Ayres Assoc. (1993, 1996), Otis (1978)

b N data sources: Converse (1999), DeSimone and Howes (1998), Harman *et al.* (1996), Bowne (1982), Pell and Nyberg (1989)

c P data sources: Fischer (1999), Ptacek (1998), Zanini *et al.* (1998), Harman *et al.* (1996), Robertson (1995), Nagpal (1986), Reneau (1979), Lance (1977), Reneau and Pettry (1976)

d NH₄ plus organic N (n = 11)

e not reported

f total P (n = 11)

Figure A-1 illustrates a CFD diagram for NH₄-N concentrations in residential STE based on data compilation from this study. CFD diagrams were not created for NO₃-N or NO₂-N because STE concentrations are generally negligible and are thus not generally reported in detail. Data for organic N was not sufficient to construct a CFD.

Due to nitrification in the vadose zone, OWS can generate NO₃-N concentrations at the water table from 25–80 mg N L⁻¹ in most situations, even though NO₃-N concentrations in STE are usually less than 2 mg N L⁻¹ (Gold *et al.* 1999). Conversely, NH₄-N concentrations at the water table are most often low, if any NH₄-N reaches the water table at all (Robertson *et al.* 1998). The US EPA drinking water standard for NO₃-N is 10 mg N L⁻¹ (US EPA 2000). The European Union groundwater standard for NO₃ is 50 mg-NO₃/L (11.3 mg-N/L). Considering many residences serviced by OWS also draw their water from onsite drinking water wells, N contributions from OWS may have local groundwater impacts in some areas, as well as potential impacts to groundwater and surface-water loadings in the watershed.

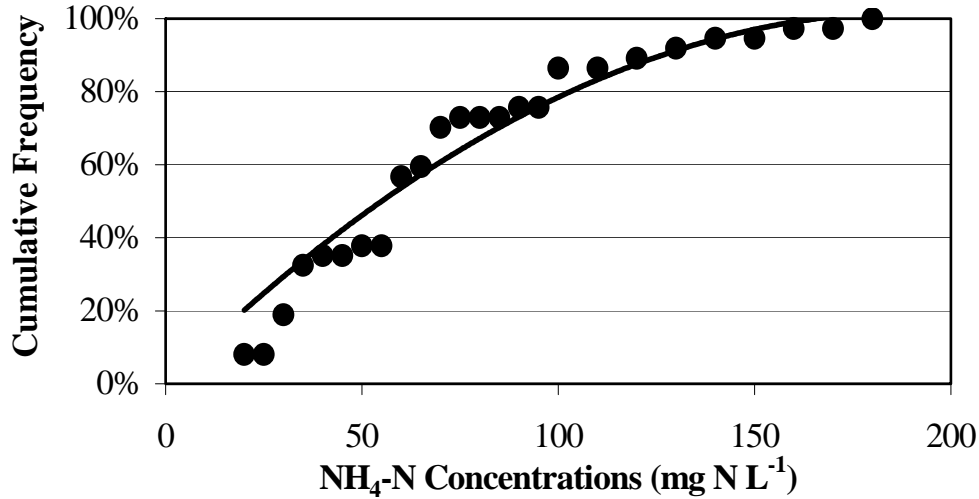


Figure A-1
Cumulative Frequency Distribution for NH₄-N Concentrations in Domestic STE

Dilution may play a part in reducing nitrogen concentrations in the short term. Groundwater will normally provide some dilution, but mixing is not always efficient and plumes of higher concentrations will exist (Converse 1999). In a study of two groundwater NO₃ plumes in sand aquifers (Cambridge and Muskoka sites in central Canada) that originated from wastewater sources, Robertson *et al.* (1991) found exceptionally low transverse and longitudinal dispersivity leading to well-defined NO₃ plumes in groundwater. Furthermore, even though nitrogen concentrations may be reduced through dilution, mass loadings are not. As the density and aerial extent of unsewered development grows, the dilution capacity of undeveloped lands is diminished (Gold *et al.* 1999). Therefore, dilution as the primary means of reducing nitrogen concentrations is not always a practical long-term solution. To assess these problems in a more rigorous fashion, mathematical models may be used. Other transport parameters for nitrogen, such as degradation rates, are also necessary, and are discussed in detail in the following section.

Nitrogen Transport and Transformation

Processes affecting the fate and transport of N from OWS include nitrification and denitrification. Nitrification is the process whereby ammonium (NH₄⁺), the primary constituent in STE is converted to NO₂⁻, and then to NO₃⁻². However, the conversion to NO₂⁻ is so rapid that nitrification can be assumed to occur in a single step (NH₄⁺ to NO₃⁻). Nitrification has been described using zero-order (Equation A-1a or Equation A-1b) and first-order (Equation A-2) reactions. During denitrification, NO₃⁻² is converted to N₂. Denitrification rates are typically described using first-order reactions (Equation A-3). Reaction rate constants reported in literature sources are summarized in Table A-4.

$$\frac{\partial(NO_3)}{\partial t} = -\frac{\partial(NH_4)}{\partial t} = \mu \quad \text{Equation A-1a}$$

$$-\frac{\partial(NH_4)}{\partial t} = \mu' = \mu M_{NH_4} \quad \text{Equation A-1b}$$

$$\frac{\partial(NO_3)}{\partial t} = -\frac{\partial(NH_4)}{\partial t} = k_1(NH_4) \quad \text{Equation A-2}$$

$$\frac{\partial(NO_3)}{\partial t} = -k_2(NO_3) \quad \text{Equation A-3}$$

where the parentheses indicate molar concentrations of the enclosed chemical species (mol/L), k_1 and k_2 are first-order rate constants (days^{-1}), μ is the zero-order rate constant reported on a molar basis ($\text{mol L}^{-1}\text{day}^{-1}$), μ' is the zero-order rate constant reported on a ammonium mass basis ($\text{mg L}^{-1}\text{day}^{-1}$), and M_{NH_4} is the molecular weight of ammonium (18,000 mg/L).

Table A-4 presents a wide range of reaction rates for nitrification. This wide range is due to the fact that reported nitrification or denitrification rates for OWS were sparse, and because rates were also tabulated from studies of nitrification in natural soil, and not specifically OWS. With the wide range of values reported, selecting a single value for a nitrification rate is difficult. Field observations of onsite systems have shown little, if any, ammonium reaches the groundwater below an OWS infiltration trench. This observation should be taken into account when evaluating the adequacy of a nitrification rate to be used in modeling efforts. Figure A-2 is a CFD of first-order nitrification rates summarized from literature sources. Due to the large variability of the limited literature data, nitrification rates cannot currently be distinguished by soil type.

Table A-4
Summary of Nitrification and Denitrification Rates Reported in Literature Sources^a.

Process/Reaction Order	Median	Range	Number of Data
Nitrification—Zero-order, μ' ($\text{mg L}^{-1}\text{day}^{-1}$)	264	156–1464	7
Nitrification—First-order, k_1 (day^{-1})	2.9	0.0768–211.2	19
Denitrification—First-order, k_2 (day^{-1})	0.025	0.004–2.27	53

^a Geng *et al.* (1996), Cho (1971), Ling and El-Kadi (1998), Yamaguchi *et al.* (1996), Starr *et al.* (1974), Starr and Gillham (1993), Misra *et al.* (1974), Ardakani *et al.* (1974a, 1974b), Lind (1983), Slater and Capone (1987), Anderson (1998), Trudell *et al.* (1986), Smith and Duff (1988), Bengtsson and Annadotter (1989), Francis *et al.* (1989), Obenhuber and Lowrance (1991), Smith *et al.* (1991), Ekpote and Cornfield (1965), Christensen *et al.* (1989), Bradley *et al.* (1992), Tesoriero *et al.* (2000), Smith *et al.* (1996), Lawrence and Foster (1986), Korom (1992), Hiscock *et al.* (1991).

Denitrification is possible both at anaerobic microsites in the vadose zone and in anaerobic groundwater when an available source of carbon is present. However, while many studies have been performed on NO_3^{-2} removal in the subsurface via denitrification, it is still neither well understood nor well quantified. First-order denitrification rates vary widely in literature sources. No zero-order rates were found in the literature to describe denitrification. The first-order reaction rates for denitrification summarized in Table A-4 are presented in a CFD in Figure A-3. Due to the large variability in literature data, denitrification rates could not be segregated by soil type.

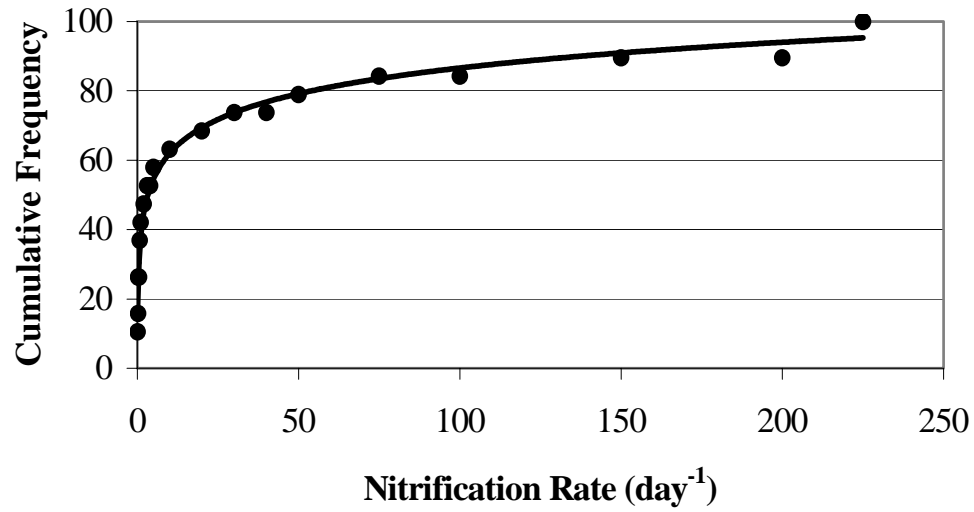


Figure A-2
Cumulative Frequency Distribution for First-Order Nitrification Rate

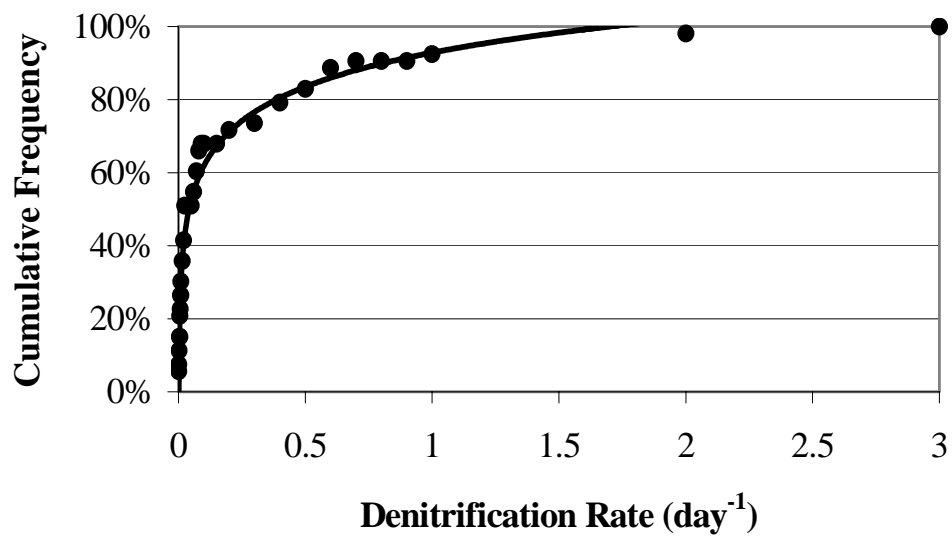


Figure A-3
Cumulative Frequency Distribution for First-Order Denitrification Rate

Phosphorus Concentrations and Transport Parameters

Phosphorus in domestic wastewater is derived generally from human waste and synthetic detergents, although modern detergents contain minimal P.

Phosphorus Concentrations

Concentrations of P in STE will vary according to the type of source, volume of wastewater generated, and the extent of synthetic detergent use. Concentrations of P normally found in OWS effluent (1 to 22 mg P L⁻¹) much exceed the lower P concentrations (0.01 to 0.10 mg P L⁻¹) that have been observed to stimulate algae growth in aquatic environments (Gold and Sims 2001). The majority of P in wastewater is in the form of soluble orthophosphate (PO₄³⁻). The orthophosphate form is considered the most hazardous in the environment due to its abundance and the availability for biological metabolism without further breakdown. P in organic molecules and polyphosphates is hydrolyzed to PO₄³⁻ in the septic tank (Wilhelm *et al.* 1994), contributing to the high percentage of total phosphorus (TP) as orthophosphate (PO₄) in STE. Orthophosphate equaling 85% of TP in STE is often reported to be a typical value, although values ranging from 76% to over 95% have been measured (Magdoff *et al.* 1974; Wilhelm *et al.* 1994; Correll 1998; Willman *et al.* 1981).

Table A-3 summarizes P concentrations in STE reported in various literature sources (Kirkland 2001). The PO₄-P concentrations reported in Table A-3 are consistent with values reported by the US EPA (2002) of 5–17 mg TP L⁻¹. However, the design manual does not present the frequency distribution of reported P concentrations in STE. Figure A-4 presents a CFD diagram for P concentrations in domestic STE created from data summarized in Table A-3.

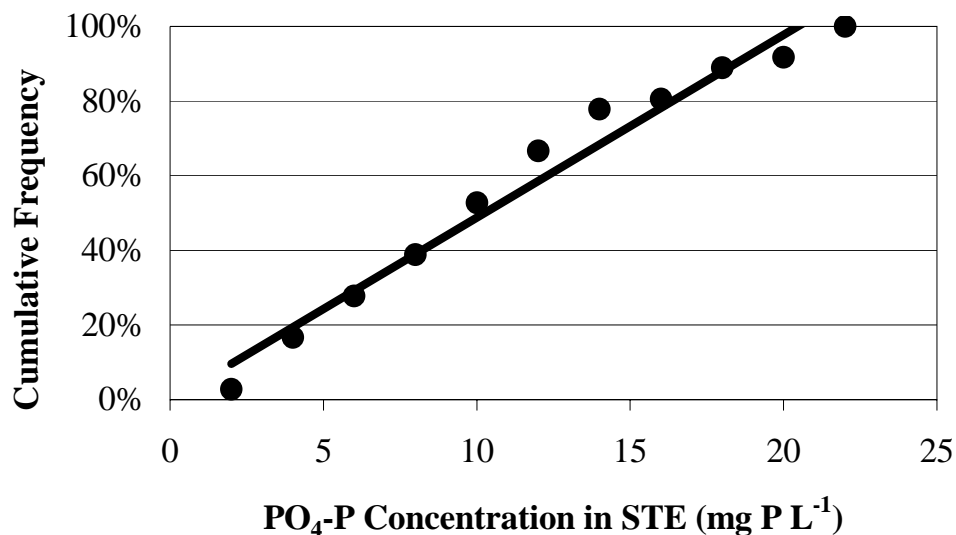


Figure A-4
Cumulative Frequency Distribution for PO₄-P Concentrations in STE

Increasing public awareness in the 1960s of the adverse effects of P over-enrichment of surface waters led to various actions by political units, detergent manufacturers, and consumers to limit the use of phosphate in detergents (Hem 1992). Phosphate detergent bans went into effect in the mid- to late-1980s in many states. An overall decreasing temporal trend in STE phosphate concentrations in available STE data from the 1970s to the present was observed in the data collected for this study. Based on data collected in papers published in the decade of 1970 to 1980, the range of reported $\text{PO}_4\text{-P}$ concentrations for this decade was 5.5 to 21.8 mg/L with an average of 13.1 mg/L. In the 1980s, the reported range was 2.1–20.6 mg/L with an average of 11.1 mg/L. Finally, in the 1990s, the reported range was 1.2–14.2 mg/L with an average of 8.4 mg/L.

Phosphorus Transport and Transformation

Most OWS rely on chemical processes such as sorption and precipitation during vadose zone percolation to prevent P from entering the groundwater and eventually discharging to surface waters. The effectiveness of soils and underlying aquifer materials in attenuating P movement to subsurface and surface waters depends upon a number of factors including the soil chemical and physical properties, the chemical properties and loading rate of the wastewater, site hydrology, proximity of the site to surface waters, and the design and management of the OWS (Robertson *et al.* 1998; Gold and Sims 2001). Mechanisms for P transformation related to OWS systems have not been fully elucidated, although Robertson (1995) provides a good review of what is known about P transformation mechanisms. Sorption of P in soils is well documented and is often thought to be associated with metal-oxide minerals that can possess a positive surface charge at typical pH ranges, allowing sorption of the anionic phosphate. Some researchers have suggested a two-stage attenuation process with an initial reversible reaction representing sorption, and an irreversible reaction that causes loss of P from the aqueous phase, which is sometimes considered to represent precipitation of sparingly soluble phosphate minerals (Robertson 1995). Several phosphate minerals have been suggested as controls on phosphate in natural waters. Most of these mineral phases involve iron, although calcium and aluminum may also be important (Robertson and Blowes 1995).

Sorption has been described in many ways. Kirkland (2001) summarizes linear, and nonlinear (Freundlich and Langmuir) P sorption isotherms reported in numerous literature sources. P sorption isotherms could not be separated specifically by soil type, with the exception of maximum sorption capacity, which was often reported in studies where no isotherm was measured. The first isotherm to be discussed is the linear isotherm. The low concentrations of P found below an OWS infiltrative surface are often in the linear range of reported nonlinear isotherms. In addition, the amount of data available is often insufficient to justify a more sophisticated approach, thus the linear sorption isotherm is the most widely used in hydrologic models (Drever 1997). A linear isotherm is represented by the equation:

$$S = K_D C \quad \text{Equation A-4}$$

where S is the mass of solute sorbed per unit dry weight of solid (mg kg^{-1}), C is the concentration of the solute in solution in equilibrium with the mass of solute sorbed onto the solid (mg L^{-1}), and K_D is linear distribution coefficient (L kg^{-1}).

K_D values were obtained directly from those reported in literature sources or calculated from reported or assumed aquifer porosity and bulk density properties of the soil material and the reported retardation factor using the following equation:

$$R_f = 1 + \frac{\rho_b}{\phi} K_D \quad \text{Equation A-5}$$

where ρ_b is the dry bulk density of the aquifer solids (g cm^{-3}) and ϕ is the aquifer porosity (dimensionless).

Studies that reported retardation factors were generally obtained from wastewater-derived plumes in saturated zones. Sorption parameters for unsaturated soil were not generally specified in the literature. However, the K_D values are theoretically independent of the water content, provided the soils in the unsaturated and saturated zones are similar. A major limitation of the linear sorption isotherm is that it does not limit the amount of solute that can be sorbed onto the solid (Fetter 1999). This assumption is clearly not physically realistic, as there must be an upper limit of the amount of solute that can be sorbed to a given solid particle. However, this assumption is often appropriate because low aqueous concentrations in groundwater may not supply enough chemicals to saturate sorption sites, particularly for non-continuous plumes.

The Freundlich sorption isotherm is a more general description of sorption and may be described by the general equation:

$$S = KC^N \quad \text{Equation A-6}$$

where K and N are empirical constants. Freundlich isotherms are nonlinear and usually obtained through empirical fits to experimental data. As with the linear isotherm, a major limitation of the Freundlich isotherm is that there is no upper limit to the amount of solute that could be sorbed for $N > 1$. However, for $N < 1$, an asymptotic limit may be approached. For $N = 1$, the Freundlich isotherm reduces to the linear sorption isotherm where $K = K_D$.

The Langmuir sorption isotherm is a more complex sorption isotherm. The Langmuir sorption isotherm incorporates the assumption that a finite number of sorption sites exist on a solid and may be described by the equation:

$$\frac{C}{S} = \frac{1}{\alpha\beta} + \frac{C}{\beta} \quad \text{Equation A-7}$$

where α is an adsorption constant related to the binding energy (L mg^{-1}) and β is the maximum amount of a solute that can be absorbed by the solid (mg kg^{-1}) (Fetter 1998). Because the Langmuir isotherm can simulate maximum adsorption capacity, it is probably the most rigorous and potentially accurate isotherm for P sorption. Maximum sorption capacities for soils reported in literature sources are summarized in Table A-5. Maximum sorption capacities of soils were not reported in many studies. Note that the maximum soil capacities could be used for the beta parameter in the Langmuir expression (Equation A-7).

Table A-5
Summary of Maximum P Sorption Capacities by Soil Type From Literature^a

Soil Type	Soil Concentration (mg/kg)		
	Median	Range	Number of Data
Sandy Loam	405	116–1640	13
Sand	40	15–1368	12
Not Specified	220	0–17,600	13
All Soil Types	237	0–17,600	38

a Hill and Sawhney (1981), Harman *et al.* (1996), Nagpal (1986), Childs *et al.* (1974), Tofflemire and Chen (1977), Fischer (1999).

A Langmuir-type or Freundlich-type nonlinear isotherm is generally best overall for modeling phosphate sorption, as they both can account for limited sorption capacities in soils. However, if the range of P concentrations present in onsite wastewater systems are within the initial linear portion of a nonlinear isotherm, a linear isotherm may adequately describe phosphate sorption, especially over a watershed-scale application. An advantage to using the linear sorption isotherm is that it may be described by only one parameter, whereas Freundlich and Langmuir isotherms require two parameters each. Use of the linear sorption isotherm is the simplest method of representing P sorption, and is thus advantageous when implementing sorption into an already complex hydrologic model.

The linear range of the nonlinear isotherms in the literature varies from less than 1 mg P L⁻¹ to 10 mg P L⁻¹. This variability is likely due largely to varying soil types and P solution concentrations used in the isotherm experiments. Another limitation of the Langmuir data located in the literature is the limited overall range of the isotherm. Some of these isotherms only represent concentrations of P that are less than 1 mg P L⁻¹. These data may be misinterpreted as linear when a nonlinear isotherm would be more appropriate over a larger range of concentrations.

There was insufficient data to allow a rigorous evaluation of the nonlinear-isotherm fitting coefficients (except for maximum sorption capacity). For this reason, and because linear isotherms are the most widely used in hydrologic models (the range of P concentrations below OWS are often in the linear range of nonlinear isotherms), nonlinear isotherms were transformed to linear isotherms to obtain equivalent K_D values. An equivalent “linearized” sorption coefficient may be obtained from a nonlinear isotherm by an integral transform approach presented by van Genuchten (1974) and also used by Neville *et al.* (2000). This method was employed over the concentrations of P typically seen in onsite systems. For concentrations of P from 0 to 10 mg P L⁻¹, the linearized sorption coefficient, K_D^l , is defined by:

$$\int_0^{10} K_D^l C dc = \int_0^{10} K_f C^N dC \quad \text{Equation A-8}$$

Values of the linear distribution coefficient, K_D , reported in literature sources or calculated from data presented in the literature, including reported linear values as well as transformed values, vary from 1.4 to 478 L kg⁻¹ (see Table A-6).

Table A-6
Summary of Linear Sorption Isotherm Constants (K_D) for P From the Literature^a

P Linear Sorption Isotherm Constant (L kg⁻¹)	Median	Range	Number of Data
Reported directly in the literature	2.7	1.4–7.3	3
Calculated from retardation factor	7.9	3.9–20.4	6
Calculated from a nonlinear isotherm	35.8	6.2–478	9
All methods	15.1	1.4–478	18

a Robertson and Harman (1999), Lee *et al.* (1998), Robertson *et al.* (1998); DeCamargo *et al.* (1979), Sawhney and Hill (1975).

Some linear sorption isotherm coefficients summarized in Table A-6 were reported directly in literature sources. Other coefficients were back-calculated from a reported retardation factor obtained from field measurements using Equation A-5, or were “linearized” from a nonlinear isotherm (van Genuchten 1974) using Equation A-8. Note that precipitation, and not just sorption, may have contributed to the “solid-phase” P concentrations attributed solely to sorption in the research results summarized in Table A-6. However, it was not possible to separate the contributions of these two mechanisms.

The median STE concentration of P is approximately 10 mg P L⁻¹. A linear sorption isotherm for P may not appear to be appropriate at the OWS site scale, such as in the vadose zone below the effluent delivery system, based on isotherm data presented in this study. However, dilution of P in the soil below the OWS will occur quickly (McCray *et al.* 2000), and thus P concentrations in the soil solution and groundwater are likely to be considerably less than 10 mg/L. In addition, in the literature sources reviewed, P concentrations in the groundwater are reported to be less than 1 mg P L⁻¹. This factor is probably due to sorption, dilution, and dispersion in the unsaturated soil water and groundwater. Consequently, the use of a linear sorption isotherm for OWS applications is recommended.

All P sorption data were collected from studies related to wastewater sources as well as studies concerned with P sorption to soils in non-wastewater-related systems. Only studies of P sorption in the subsurface soils were reviewed. No studies of P sorption in river or lake sediments were examined. Figure A-5 presents the P sorption isotherm data in a cumulative frequency distribution diagram.

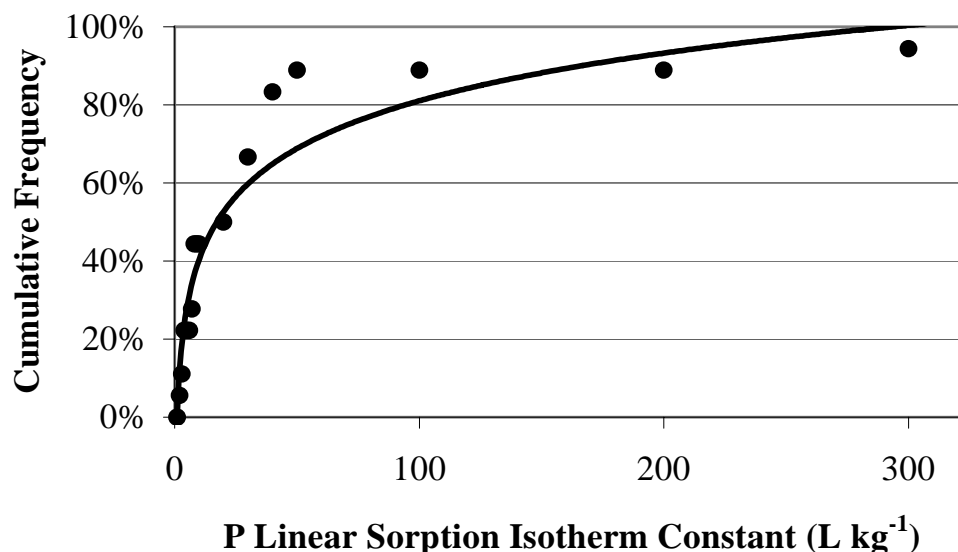


Figure A-5
Cumulative Frequency Distribution for Linear Sorption Isotherm Constants in Soil and Groundwater Sediments

As described previously, precipitation is another process known to affect P fate and transport in the subsurface. Precipitation is often lumped into the sorption isotherm or ignored in modeling efforts. However, several attempts to model precipitation as a first-order decay reaction have also been attempted. Mansell *et al.* (1977a,b) examined two types of first-order irreversible precipitation or chemical immobilization terms and concluded a finite sink term would have been more appropriate in their study than the infinite sink term they used. Enfield *et al.* (1981) used a first-order mass-loss term. Several studies (Shutter *et al.* 1994, Lee *et al.* 1998, and McCray *et al.* 2000) have used a first-order decay-type term to account for precipitation, while also considering reversible sorption. Although several studies regarding P precipitation exist in the literature, reported rate constants or mass-law constants are not reported for most cases. Precipitation depends greatly on groundwater chemistry as well as soil type. Thus, an attempt to generalize precipitation parameters was not attempted for this project.

P deposition in soil below an infiltrative surface can be modeled as a zero-order mass loss from the aqueous phase to the soil phase. In this model, P is deposited in the soil, independent of the soil water concentration, until some maximum soil concentration is reached. This type of mass transfer would be consistent with irreversible sorption or precipitation. However, the analysis provided in the following section indicates that a traditional sorption isotherm approach is probably more appropriate.

Zanini *et al.* (1998) reported zones of P enrichment below the wastewater infiltrative surface at four OWS sites in central Canada. These authors reported typical PO₄-P concentrations of approximately 800 mg kg⁻¹ soil in zones of enrichment 0.75 to 2.25 m in depth. However, these enrichment zones were not continuous due to preferential flow processes occurring in the subsurface.

In a long-term laboratory study, Hill and Sawhney (1981) observed enriched P zones of approximately 400 mg kg^{-1} within 30 cm of the infiltrative surface. Concentrations of $\text{PO}_4\text{-P}$ observed in uniform zones, generally within 20–50 cm of the infiltrative surface, were approximately 1.36 kg P m^{-3} of soil (or approximately 850 mg P per kg soil assuming a dry soil bulk density of 1.6 g cm^{-3}). Therefore, for this analysis, a median enrichment depth of 1.5 m for the preferential flow dominated zones described above, and a uniform high-P concentration depth of 0.5 m were assumed.

Next, a comparison was made of this soil loading with the typical P emitted by an OWS system. Assuming a median $\text{PO}_4\text{-P}$ concentration in STE of approximately 10 mg P L^{-1} , and the flow and population densities described earlier (260 liters/capacity/day [Lpcd] and 2.4 people per household), an OWS will generate approximately 22.8 kg $\text{PO}_4\text{-P}$ over a 10-year period. Considering an OWS infiltrative surface area of 1.4 m^2 , this mass of $\text{PO}_4\text{-P}$ would result in a uniform high-P soil concentration zone of depth equal to 11.9 m. This depth would be 35.8 m if preferential flow is dominating at the same density assumed previously. Accordingly, if only irreversible sorption or precipitation processes are occurring, the high-P concentration zones in soil are expected to be much deeper than 2 meters, which is reported in the literature. Furthermore, a modeling study conducted by McCray *et al.* (2000) demonstrated that high P concentrations in soil would develop within 1 m below the infiltrative surface if only reversible, linear, equilibrium sorption were considered (assuming soil P concentrations similar to those as reported in the literature—see Appendix F, *Site-Scale Modeling Using HYDRUS 2-D*). This aspect suggests that reversible sorption processes are appropriate for simulating P retention in soil below the OWS infiltrative surface.

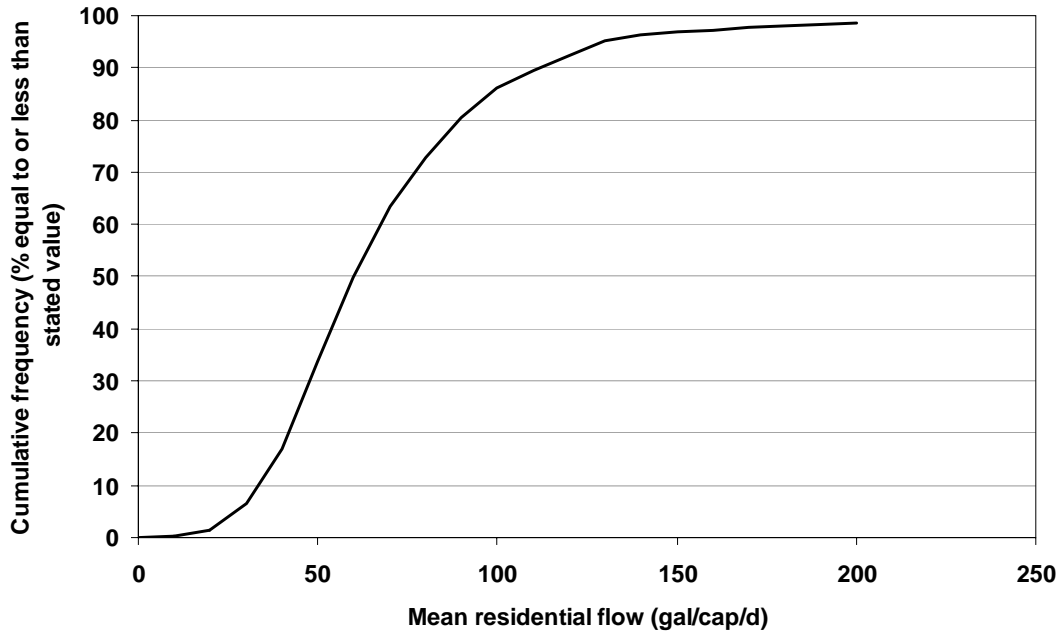
Wastewater Flow

In a study conducted by Mayer *et al.* (1999) water use from 1,188 homes at 12 study sites (95 to 100 homes at each of the 12 locations) across the USA were logged. Based on this study, the indoor water use by site ranged from 57.1 to 83.5 gallons/capacity/day (gpcd) with a mean of 69.3 gpcd (standard deviation for indoor water use was 39.6 gpcd) and the outdoor water use by site ranged from 54.0 to 63.8 gpcd with a mean of 60.5 gpcd. A summary of the flow rate information from this study is presented in Table A-7 and a CFD is presented in Figure A-6. Table A-8 summarizes domestic STE flow rate information gained from four studies.

Table A-7
Residential Wastewater Flows

Avg. Home Indoor Q (gpcd)	Value From Figure A-6 (%)	Adj. Value to Yield 100% (%)	Avg. Home Indoor Q (gpcd)	Cumm. Value (%)
0	0	0	0	0.0
10	0.15	0.1	10	0.1
20	1.2	1.2	20	1.3
30	5.1	5.1	30	6.4
40	10.5	10.5	40	16.9
50	16.8	16.7	50	33.6
60	16.3	16.2	60	49.9
70	13.6	13.6	70	63.4
80	9.4	9.4	80	72.8
90	7.7	7.7	90	80.5
100	5.6	5.6	100	86.0
110	3.6	3.6	110	89.6
120	2.8	2.8	120	92.4
130	2.8	2.8	130	95.2
140	1	1.0	140	96.2
150	0.8	0.8	150	97.0
160	0.2	0.2	160	97.2
170	0.5	0.5	170	97.7
180	0.3	0.3	180	98.0
190	0.2	0.2	190	98.2
200	0.3	0.3	200	98.5
>200	1.5	1.5		100.0
	100.35	100.0		

(US EPA 2002 as modified from Mayer *et al.* 1999)



(US EPA 2002 modified from Mayer *et al.* 1999)

Figure A-6
Cumulative Frequency Distribution of Mean Residential Indoor Water Use

Table A-8
Average Daily Wastewater Flows Based on Indoor Water Use Monitoring^a

Study	Number of OWS Systems	Study Duration (Months)	Average Flow (L/ person/ day)	Range of Flows (L/person/day)
Anderson and Siegrist (1989)	90	3	268.0	249.4–289.9
Anderson <i>et al.</i> (1993)	25	3	191.9	98.9–322.5
Brown and Caldwell (1984)	210	20	250.6	216.9–276.3
Mayer <i>et al.</i> (1999)	1188	1	262.3	216.1–316.1

a Not based on wastewater flow monitoring. Assumes all water used indoors becomes wastewater.

Often, attempts to quantify the cumulative effects of OWS on water quality require calculations of mass loadings, which are accomplished by multiplying a concentration by a flow rate. For example, a goal might be to model the potential for P pollution of a sensitive small wetland near an OWS that serves a family of four. For this extreme case, one may wish to be highly conservative and assume a high flow rate of 300 L/day per person and the 90th percentile concentration of 19 mg/L in a modeling effort, which would represent a mass loading of 22.8 grams per day. For this scenario, a conservative 10th percentile K_D value of 5 L/kg might also be used in this model.

If a Langmuir isotherm is used, then a low maximum sorption capacity might also be used. However, for a watershed-scale simulation, a reasonable assumption is that the average input for each home can be estimated using 50th percentile values for all of the parameters (250 L/person/day, P concentration of 9 mg/L, mass loading of 9 g/day, K_D of 15 L/Kg, maximum sorption capacity of 237 mg/kg).

Combining factors such as flow rate and concentration, however, at a conservative level for each (for example, 90th-percentile frequency) results in a mass loading that is more conservative than the 90th percentile suggests. In such a situation, perhaps combining a median flow rate value and a 90th percentile concentration value, or other similar combinations, would provide a more appropriate, yet still conservative result. A user should choose values based on his or her particular goal.

Summary

In this study, OWS source, fate, and transport data were gathered from literature sources including data on nutrient concentrations in STE, nitrification rates, denitrification rates, and phosphorus sorption and precipitation data. CFD diagrams were constructed from literature-reported data for nitrogen and phosphorus STE concentrations, first-order nitrification rates, first-order denitrification rates, and linear sorption isotherm constants for phosphorus. The purpose of these CFD diagrams is to serve as a tool in selecting appropriate water quality input parameters for analysis and modeling of OWS nutrients because limited data exists in the literature for estimating model-input parameters.

The CFD plots may be useful for applying mathematical models to assess the influence of OWS systems on water quality. A 90th percentile value may be used, for example, as a very conservative (high-concentration) estimate for a single home or a small group of homes. This estimate might be useful when trying to determine OWS-separation distance from a local drinking water well or other surface-water body, or if contamination in a well is due to the OWS system. However, as the number of individual homes being considered increases (to more than five or ten), the average parameter value approaches the 50th percentile value, thus providing a better estimate for larger subdivisions or small communities. If an enhanced-treatment system is used, such as an intermittent sand filter for example, then values smaller than the 50th percentile values could be assumed for an OWS source concentration.

Data is generally not available for quantifying nitrification and denitrification of nitrogen or sorption and precipitation of phosphorus in the subsurface based on soil type or soil-related parameters. Relatively few studies were found that quantified nitrification rates specifically for OWS, although nitrification is known to be a dominant process in OWS. Although many studies have been reported on denitrification in the subsurface, the factors affecting denitrification and the variability of reported denitrification rates vary extensively.

A high level of inconsistency was found to exist in the reporting methods for phosphorus concentrations and P sorption-isotherm data. Based on analysis of linear and nonlinear sorption isotherm data for P and comparison to typical P concentrations in soil below OWS, a linear, reversible, equilibrium isotherm is recommended to represent sorption of P from OWS at the watershed scale. This method is recommended because of its simplicity, and because of lack of more detailed data on other P reaction mechanisms for OWS. Some attempts to describe phosphorus (P) precipitation in the subsurface with a first-order decay-type loss term have been made. However, the rate coefficient and its dependence on soil geochemical conditions have not been adequately quantified. The issue of phosphorus precipitation needs to be examined further through a continued literature search and laboratory work to support quantification of P precipitation. Also, geochemical modeling could be performed with data collected from a field site to provide a better understanding of P sorption and precipitation processes. The data used in this study were gathered from varying literature sources that spanned over approximately 30 years of research and used differing methodologies and reporting styles. Therefore, careful consideration when using these results for engineering applications is recommended.

References

- Anderson D. L. and R. L. Siegrist. 1989. "The Performance of Ultra-Low-Volume Flush Toilets in Phoenix." *J. Amer. Water Works Assoc.* 81(3), 52–57.
- Anderson, D. L., A. L. Lewis, and K. M. Sherman. 1991. "Human Enterovirus Monitoring at Onsite Sewage Disposal Systems in Florida." *Proceedings of the Sixth National Symposium on Small Sewage Systems*. American Society of Agricultural Engineers, St. Joseph, MI. 94–104.
- Anderson, D. L., D. M. Mulville-Friel, and W. L. Nero. 1993. "The Impact of Water Conserving Plumbing Fixtures on Residential Water Use Characteristics in Tampa FL." *Proceedings of the Conserv93 Conference*, Dec. 12–16, 1993, Las Vegas, NV.
- Anderson, D. L., R. J. Otis, J. I. McNeillie, and R. A. Apfel. 1994. "In-Situ Lysimeter Investigation Pollutant Attenuation in the Vadose Zone of a Fine Sand, On-Site Wastewater Treatment." *Proceedings of the Seventh International Symposium on Individual and Small Community Sewage Systems*. American Society of Agricultural Engineers, St. Joseph, MI.
- Anderson, D. L. 1998. "Natural Denitrification in Groundwater Impacted by Onsite Wastewater Systems, On-Site Wastewater Treatment." *Proceedings of the Eighth International Symposium on Individual and Small Community Sewage Systems*. American Society of Agricultural Engineers, St. Joseph, MI. 336–345.
- Ardakani, M. S., J. T. Rehbock, and A. D. McLaren. 1974a. "Oxidation of Ammonium to Nitrate in a Soil Column." *Soil Science Society of America Proceedings*. 38, 96–99.
- Ardakani, M. S., R. K. Schulz, and A. D. McLaren. 1974b. "A Kinetic Study of Ammonium and Nitrate Oxidation in a Soil Field Plot." *Soil Science Society of America Proceedings*. 38, 273–277.

Ayres Associates. 1993. *Onsite Sewage Disposal System Research in Florida: An Evaluation of Current OSDS Practices in Florida*. Florida Department of Health and Rehabilitative Services, Environmental Health Program, Tallahassee, FL.

Ayres Associates. 1996. *Contaminant Transport Investigation from an OWS in Fine Sand, Phase 3 Report*. Soap and Detergent Association, New York, NY.

Ball, H. L. 1995. "Nitrogen Reduction in an Onsite Trickling Filter/Upflow Filter System." *Proceedings of the Eighth Northwest On-Site Wastewater Treatment Short Course*, Seattle, WA. 259–268.

Bengtsson, G. and H. Annadotter. 1989. "Nitrate Reduction in a Groundwater Microcosm Determined by ^{15}N Gas Chromatography-Mass Spectrometry." *Appl. Environ. Micro.* 55(11), 2861–2870.

Borchardt, M. A., P. D. Bertz, S. K. Spencer, and D. A. Battigelli. 2003. "Incidence of Enteric Viruses in Groundwater from Household Wells in Wisconsin." *Applied Environ. Micro.* 69(2), 1172–1180.

Bowne, W. C. 1982. *Characteristics and Treatment of STEP Pressure Sewer Collection Wastewater*. Report submitted to US EPA, MERL, Cincinnati, OH.

Bradley, P. M., M. Fernandez, and F. H. Chapelle. 1992. "Carbon Limitation of Denitrification Rates in an Anaerobic Groundwater System." *Environ. Sci. Technol.* 26(12), 2377–2381.

Brown, K. W., J. F. Slowey, and H. W. Wolf. 1977. *Accumulation and Passage of Pollutants in Domestic Septic Tank Disposal Fields*. Report for Project R801955. Texas A & M Research Foundation, College Station, TX.

Brown and Caldwell. 1984. *Residential Water Conservation Projects*. Research Report 903. US Department of Housing and Urban Development, Office of Policy Development, Washington, DC.

Childs, K. E., S. B. Upchurch, and B. Ellis. 1974. "Sampling of Variable, Waste-Migration Patterns in Groundwater." *Ground Water*. 12(6), 369–376.

Cho, C. M. 1971. "Convective Transport of Ammonium with Nitrification in Soil." *Can. J. Soil Sci.* 51, 339–350.

Christensen, P. B., L. P. Nielsen, N. P. Revsbech, and J. Sorensen. 1989. "Microzonation of Denitrification Activity in Stream Sediments as Studied with a Combined Oxygen and Nitrous Oxide Microsensor." *Appl. Environ. Micro.* 55(5), 1234–1241.

Christopherson, S. H., J. L. Anderson, and D. M. Gustafson. 2001. "Evaluation of Recirculating Sand Filters in Minnesota." *Proceedings of the Ninth National Symposium on Individual and Small Community Sewage Systems*. American Society of Agricultural Engineers, Fort Worth, TX. 207–214.

Cogger, C. G., L. M. Hajjar, C. L. Moe, and M. D. Sobsey. 1988. "Septic System Performance on a Coastal Barrier Island." *J. Environ. Qual.* 17(3), 401–408.

Converse, J. C. 1999. "Nitrogen as it Relates to On-Site Wastewater Treatment with Emphasis on Pretreatment Removal and Profiles Beneath Dispersal Units." *Proceedings of the Tenth Northwest On-Site Wastewater Treatment Short Course*, April 3–4, 2002, Seattle, WA. 171–184.

Correll, D. L. 1998. "The Role of Phosphorus Eutrophication of Receiving Waters: A Review." *J. Environ. Qual.* 27, 261–266.

Crites, R. W. 1985. "Nitrogen Removal in Rapid Infiltration Systems." *J. Environ. Engr.* 111(6), 865–873.

Crites, R., C. Lekven, S. Wert, and G. Tchobanoglous. 1997. "A Decentralized Wastewater System For Small Residential Development in California." *Small Flows Journal.* 3(1):3–11.

Crites, R. and G. Tchobanoglous. 1998. *Small and Decentralized Wastewater Management Systems*. McGraw-Hill Publishing Company, Boston, MA.

Crook, J. 1998. "Water Reclamation and Reuse Criteria." T. Asano (ed.), *Wastewater Reclamation and Reuse*. Technomic Publishing, Lancaster, PA.

Darby, J., G. Tchobanoglous, M. Astrinor, and D. Maciolek. 1996. "Shallow Intermittent Sand Filtration: Performance Evaluation." *Small Flows Journal.* 2(1), 3–15.

De Camargo, O. A., J. W. Biggar, and D. R. Nielsen. 1979. "Transport of Inorganic Phosphorus in an Alfisol." *Soil Sci. Soc. Amer. J.* 43, 884–890.

DeSimone, L. A. and B. L. Howes. 1998. "Nitrogen Transport and Transformations in a Shallow Aquifer Receiving Wastewater Discharge: A Mass Balance Approach." *Water Resour. Res.* 34(2), 271–285.

Drever, J. I. 1997. *The Geochemistry of Natural Waters, Third Edition*. Prentice Hall, Inc., Upper Saddle River, NJ.

Effert, D., J. Morand, and M. Cashell. 1984. "Field Performance of Three Onsite Effluent Polishing Units." *Proceedings of the Fourth National Symposium on Individual and Small Community Sewage Systems*, American Society of Agricultural Engineers, New Orleans, LA. 351–361.

Ektepe, D. M. and A. H. Cornfield. 1965. "Effect of pH and Addition of Organic Materials on Denitrification Losses from Soil." *Nature.* 208, 1200.

Enfield, C. G., T. Phan, and D. M. Walters. 1981. "Kinetic Model for Phosphate Transport and Transformation in Calcareous Soils II: Laboratory and Field Transport." *Soil Sci. Soc. Amer. J.* 45, 1064–1070.

Feachem, R. G., D. J. Bradley, H. Garelick, and D. D. Mara. 1983. *Sanitation and Disease: Health Aspects of Excreta and Wastewater Management*. John Wiley & Sons, New York, NY.

Fetter, C. W. 1999. *Contaminant Hydrology, Second Edition*. Prentice Hall Publishers, Upper Saddle River, NJ.

Fischer, E. 1999. *Nutrient Transformation and Fate During Intermittent Sand Filtration of Wastewater*. M.S. Thesis. Environmental Science and Engineering Division, Colorado School of Mines, Golden, CO.

Francis, A. J., J. M. Slater, and C. J. Dodge. 1989. "Denitrification in Deep Subsurface Sediments." *Geomicrobio. J.* 7(1), 103–116.

Geng, Q. Z., G. Girard, and E. Ledoux. 1996. "Modeling of Nitrogen Cycle and Nitrate Transfer in Regional Hydrogeologic Systems." *Ground Water*. 34(2), 293–304.

Gerba, C. P. 2002. "Virus Transport and Fate in Ground Water." *Proceedings of the Eleventh Northwest On-Site Wastewater Treatment Short Course*, April 3–4, 2002, Seattle, WA.

Gold, A. J. and J. T. Sims. 2001. "Research Needs In Decentralized Wastewater Treatment And Management: A Risk-Based Approach To Nutrient Contamination." *National Research Needs Conference Proceedings: Risk-Based Decision Making for On-site Wastewater Treatment*. Project No. 1001446. EPRI, Palo Alto, CA, US EPA and National Decentralized Water Resources Capacity Development Project. March 15, 2001.

Hain, K. E. and R. T. O'Brien. 1979. *The Survival of Enteric Viruses in Septic Tank Drain Fields*. New Mexico Water Resources Research Institute, Report 108. Las Cruces, NM.

Harkin, J. M., C. J. Fitzgerald, C. P. Duffy, and D. G. Kroll. 1979. *Evaluation of Mound Systems for Purification of Septic Tank Effluent*. Technical Report—Wisconsin WRC 79-05. Water Resources Center, University of Wisconsin, Madison, WI.

Harman, J., W. D. Robertson, J. A. Cherry, and L. Zanini. 1996. "Impacts on a Sand Aquifer from an Old Septic System: Nitrate and Phosphate." *Ground Water*. 34(6), 1105–1114.

Hem, J. D. 1992. *Study and Interpretation of the Chemical Characteristics of Natural Water, Third Edition*. US Geological Survey (USGS) Water Supply Paper 2254. USGS, Washington, DC.

Henneck, J., R. Axler, B. McCarthy, S. Monson Geerts, S. Heger Christopherson, J. Anderson, and J. Crosby. 2001. "Onsite Treatment of Septic Tank Effluent in Minnesota Using SSF Constructed Wetlands: Performance, Cost and Maintenance." *Proceedings of the Ninth National Symposium on Individual and Small Community Sewage Systems*. American Society of Agricultural Engineers, Fort Worth, TX. 650–662.

Hill, D. E. and B. L. Sawhney. 1981. "Removal of Phosphorus from Wastewater by Soil Under Aerobic and Anaerobic Conditions." *J. Environ. Qual.* 10(3), 401–405.

- Hiscock, K. M., J. W. Lloyd, and D. N. Lerner. 1991. "Review of Natural and Artificial Denitrification of Groundwater." *Water Research*. 25(9), 1099–1111.
- Howarth, R. W., G. Billen, D. Swaney, A. Townsend, N. Jaworski, K. Lajtha, J. A. Downing, R. Elmgren, N. Caraco, T. Jorday, F. Berendse, J. Freney, V. Kudeyarov, P. Murdoch, and Zhu Zhao-Liang. 1996. "Regional N Budgets and Riverine N and P Fluxes for the Drainages to the North Atlantic Ocean: Natural and Human Influences." *Biogeochem*. 35, 75–139.
- Jowett, E. C. and M. L. McMaster. 1994. "Absorbent Aerobic Biofiltration for On-Site Wastewater Treatment – Laboratory and Winter Field Results." *Proceedings of the Seventh National Symposium on Individual and Small Community Sewage Systems*. American Society of Agricultural Engineers, Atlanta, GA. 424–431.
- Keeney, D. R. 1986. "Sources of Nitrate to Ground Water." *Crit. Rev. Environ. Cont.* 16, 257–304.
- Keswick, B. H. and C. P. Gerba. 1980. "Viruses in Groundwater." *Environ. Sci. Technol.* 14(11), 1290–1297.
- Keswick, B. H., D. Wang, and C. P. Gerba. 1982. "The Use of Microorganisms as Groundwater Tracers: A Review." *Ground Water*. 20(2), 142–149
- Kirkland, S. L. 2001. *Coupling Site-Scale Fate and Transport with Watershed-Scale Modeling to Assess the Cumulative Effects of Nutrients from Decentralized Wastewater Systems*. M.S. Thesis. Department of Geology and Geological Engineering, Colorado School of Mines, Golden, CO.
- Korom, S. 1992. "Natural Denitrification In The Saturated Zone: A Review." *Water Resour. Res.* 28(6), 1657–1668
- Kristiansen, R. 1981. "Sand-filter Trenches for Purification of Septic Tank Effluent: I. The Clogging Mechanism and Soil Physical Environment." *J. Environ. Qual.* 10(3), 353–357.
- Lance, J. C. 1977. "Phosphate Removal From Sewage Water by Soil Columns." *J. Environ. Qual.* 6(3), 279–284.
- Lawrence, A. R. and S. S. D. Foster. 1986. "Denitrification in a Limestone Aquifer In Relation To The Security Of Low-Nitrate Groundwater Supplies." *J. Indust. Water Engr. Sci.* 40, 159–172.
- Lee, S., D. C. McAvoy, J. Szydluk, and J. L. Schnoor. 1998. "Modeling the Fate and Transport of Household Chemicals in Septic Systems." *Ground Water*. 36(1), 123–132.
- Lind, A. M. 1983. "Nitrate Reduction in the Subsoil." *Denitrification in the Nitrogen Cycle*, H. L. Golterman (ed.). Plenum, NY. 145–156.

Lindbo, D. L. and V. L. MacConnell. 2001. "Evaluation of a Peat Biofilter Treatment System." *Proceedings of the Ninth National Symposium on Individual and Small Community Sewage Systems*. American Society of Agricultural Engineers, Fort Worth, TX. 225–234.

Ling, G. and A. I. El-Kadi. 1998. "A Lumped Parameter Model For Nitrogen Transformation In the Unsaturated Zone." *Water Resour. Res.* 34(2), 203–212.

Loomis, G. W., D. B. Dow, M. H. Stolt, A. D. Sykes, and A. J. Gold. 2001. "Performance Evaluation of Innovative Treatment Technologies Used to Remediate Failed Septic Systems." *Proceedings of the Ninth National Symposium on Individual and Small Community Sewage Systems*, American Society of Agricultural Engineers, Fort Worth, TX. 52–61.

Magdoff, F. R., D. R. Keeney, J. Bouma, and W. A. Ziebell. 1974. "Columns Representing Mound-Type Disposal Systems for Septic Tank Effluent: II. Nutrient Transformations and Bacterial Populations." *J. Environ. Qual.* 3(3), 228–234.

Mansell, R. S., H. M. Selim, and J. G. A. Fiskell. 1977a. "Simulated Transformations and Transport of Phosphorus in Soil." *Soil Science*. 124(2), 102–109.

Mansell, R. S., H. M. Selim, P. Kanchanasut, J. M. Davidson, and J. G. A. Fiskell. 1977b. "Experimental and Simulated Transport of Phosphorus through Sandy Soil." *Water Resources Research*. 13(1), 189–194.

Mayer, P. W., W. B. DeOreo, E. M. Opitz, J. C. Kiefer, W. Davis, B. Dziegielewski, and J. Nelson. 1999. *Residential End Uses of Water*. AWWARF and American Water Works Association, Denver, CO.

McCray, J. E., D. N. Huntzinger, S. Van Cuyk, and R. Siegrist. 2000. "Mathematical Modeling of Unsaturated Flow and Transport in Soil-Based Wastewater Treatment Systems." *WEFTEC 2000 Conference Proceedings*. Anaheim, CA. Water Environment Federation, Alexandria, VA.

Misra, C., D. R. Nielsen, and J. W. Biggar. 1974. "Nitrogen Transformations In Soil During Leaching: II. Steady State Nitrification And Nitrate Reduction." *Soil Sci. Soc. Amer. Proc.* 38, 294–299.

Nagpal, N. K. 1986. "Effect of Soil and Effluent Characteristics on Phosphorus Sorption in Dosed Columns." *J. Environ. Qual.* 15(1), 73–78.

Neville, C. J., M. Ibaraki, and E. A. Sudicky. 2000. "Solute Transport with Multiprocess Nonequilibrium: a Semi-Analytical Solution Approach." *J. Contam. Hydrol.* 44, 141–159.

Obenhuber, D. C. and R. Lowrance. 1991. "Reduction of Nitrate in Aquifer Microcosms by Carbon Additions." *J. Environ. Qual.* 20, 255–258.

Otis, R. J., W. C. Boyle, and D. K. Sauer. 1973. *Annual Report, Small-Scale Waste Management Program*. University of Wisconsin, Madison, WI.

Otis, R. J. 1978. *An Alternative Public Wastewater Facility for a Small Rural Community, Small Scale Wastewater Management Program*. University of Wisconsin, Madison, WI.

Pell, M. and F. Nyberg. 1989. "Infiltration of Wastewater in a Newly Started Pilot Sand-Filter System: III. Transformation of Nitrogen." *J. Environ. Qual.* 18, 463–467.

Ptacek, C. J. 1998. "Geochemistry of a Septic-System Plume in a Coastal Barrier Bar, Point Pelee, Ontario, Canada." *J. Contam. Hydrol.* 33, 293–312.

Reneau, R. B. and D. E. Pettry. 1976. "Phosphorus Distribution from Septic Tank Effluent in Coastal Plain Soils." *J. Environ. Qual.* 5(1), 34–39.

Reneau, R. B. 1979. "Changes in Concentrations of Selected Chemical Pollutants in Wet, Tile-Drained Soil Systems as Influenced by Disposal of Septic Tank Effluents." *J. Environ. Qual.* 8(2), 189–196.

Reneau, R. B. Jr., C. Hagedorn, and M. J. Degen. 1989. "Fate and Transport of Biological and Inorganic Contaminants from On-Site Disposal of Domestic Wastewater." *J. Environ. Qual.* 18(2), 135–144.

Robertson, W. D., J. A. Cherry, and E. A. Sudicky. 1991. "Ground-Water Contamination From Two Small Septic Systems on Sand Aquifers." *Ground Water.* 29(1), 82–92.

Robertson, W. D. and J. A. Cherry. 1992. "Hydrogeology of an Unconfined Sand Aquifer and Its Effect on the Behavior of Nitrogen from a Large-Flux Septic System." *Applied Hydrogeol.* 1, 32–44.

Robertson, W. D. 1995. "Development of Steady-State Phosphate Concentrations in Septic System Plumes." *J. Contam. Hydrol.* 19, 289–305.

Robertson, W. D. and D. W. Blowes. 1995. "Major Ion and Trace Metal Geochemistry of an Acid Septic-System Plume in Silt." *Ground Water.* 33(2), 275–283.

Robertson, W. D., S. L. Schiff, and C. J. Ptacek. 1998. "Review of Phosphate Mobility and Persistence in 10 Septic System Plumes." *Ground Water.* 36(6), 1000–1010.

Robertson, W. D. and J. Harman. 1999. "Phosphate Plume Persistence at Two Decommissioned System Sites." *Ground Water.* 37(2), 228–236.

Ronayne, M. P., R. C. Paeth, and S. A. Wilson. 1982a. *Oregon On-Site Experimental Systems, Final Report*. US EPA Project No. 5806349. Oregon Department of Environmental Quality, Salem, OR.

Ronayne, M. P., R. C. Paeth, and T. J. Osborne. 1982b. "Intermittent Sand Filter Design and Performance – An Update." *Proceedings of the Fourth Northwest On-Site Wastewater Disposal Short Course*. Sept 21–22, 1982, Seattle, WA. 127–142.

- Rose, J. B., D. W. Griffin, and L. W. Nicosia. 1999. "Virus Transport from Septic Tanks to Coastal Waters." *Proceedings of the Tenth Northwest On-Site Wastewater Treatment Short Course*, September 20–21, 1999, Seattle, WA. 71–80.
- Sabin, A. B. 1955. "Behavior of Chimpanzee-Avirulent Poliomyelitis Viruses in Experimentally Infected Human Volunteers." *Am. J. Med. Sci.* 230, 1–8.
- Sawhney, B. L. and D. E. Hill. 1975. "Phosphate Sorption Characteristics of Soils Treated with Waste Water." *J. Environ. Qual.* 4(3), 342–346.
- Sherman, K. M. and D. L. Anderson. 1991. *An Evaluation of Volatile Organic Compounds and Conventional Parameters from On-Site Sewage Disposal Systems in Florida On-Site Wastewater Treatment*. American Society of Agricultural Engineers, St. Joseph, MI. 62–75.
- Shutter, S. B., E. A. Sudicky, and W. D. Robertson. 1994. "Chemical Fate and Transport in a Domestic Septic System: Application of a Variably Saturated Model for Chemical Movement." *Environ. Toxicol. Chem.* 13(2), 223–231.
- Siegrist, R. L., E. J. Tyler, and P. D. Jenssen. 2001. "Design and Performance of Onsite Wastewater Soil Absorption Systems." *National Research Needs Conference Proceedings: Risk-Based Decision Making for On-site Wastewater Treatment*. Project No. 1001446. EPRI, Palo Alto, CA, US EPA and National Decentralized Water Resources Capacity Development Project. March 15, 2001.
- Slater, J. M. and D. G. Capone. 1987. "Denitrification in Aquifer Soil and Nearshore Marine Sediments Influenced By Groundwater Nitrate." *Appl. Environ. Micro.* 53(6), 1292–1297.
- Small Scale Waste Management Project (SSWMP). 1978. *Management of Small Waste Flows*. EPA 600/2/78-173. MERL, US EPA, Cincinnati, OH.
- Smith, R. L., and J. H. Duff. 1988. "Denitrification in a Sand and Gravel Aquifer." *Appl. Environ. Micro.* 54(4), 1071–1078.
- Smith, R. L., B. L. Howes, and J. H. Duff. 1991. "Denitrification in Nitrate-Contaminated Groundwater: Occurrence in Steep Vertical Geochemical Gradients." *Geochim. Cosmochim. Acta*, 55(7), 1815–1825.
- Smith, R. L., S. P. Garabedian, and M. H. Brooks. 1996. "Comparison of Denitrification Activity Measurement in Groundwater Using Cores and Natural-Gradient Tracer Tests." *Environ. Sci. Technol.* 30(12), 3448–3456.
- Starr, J. L., F. E. Broadbent, and D. R. Nielsen. 1974. "Nitrogen Transformations During Continuous Leaching." *Soil Sci. Soc. Amer. Proc.* 38, 283–289.
- Starr, R. C. and R. W. Gillham. 1993. "Denitrification and Organic Carbon Availability In Two Aquifers." *Ground Water*. 31, 934–947.

- Tesoriero, A. J., H. Liebscher, and S. E. Cox. 2000. "Mechanism and Rate of Denitrification in an Agricultural Watershed: Electron and Mass Balance along Groundwater Flow Paths." *Water Resour. Res.* 36(6), 1545–1559.
- Tofflemire, T. J. and M. Chen. 1977. "Phosphate Removal by Sands and Soils." *Ground Water*. 15(5), 377–387.
- Trudell, M. R., R. W. Gillham, and J. A. Cherry. 1986. "An In-Situ Study of the Occurrence and Rate of Denitrification in a Shallow Unconfined Sand Aquifer." *J. Hydrol.* 83, 251–268.
- Tyrrell, D. A. and A. Z. Kapikian. 1982. *Virus Infections of the Gastrointestinal Tract*. Marcel Dekker, Inc. New York, NY.
- US Environmental Protection Agency (US EPA). 1993. *Subsurface Flow Constructed Wetlands for Wastewater Treatment: A Technology Assessment*. EPA832-R-93-001. US EPA Office of Water, Washington, DC.
- US EPA. 2000. *Drinking Water Standards and Health Advisories*. EPA 822-B-00-001. US EPA Office of Water, Washington, DC.
- US EPA. 2002. *Onsite Wastewater Treatment Systems Manual*. EPA 625/R-00/008. US EPA Office of Water, Washington, DC.
- van Genuchten, M. 1974. *Mass Transfer Studies in Sorbing Porous Media*. PhD Dissertation. New Mexico State University, Las Cruces, NM.
- Viraraghavan, T. and R. G. Warnock. 1976. "Treatment Through Soil of Septic Tank Effluent." *Water, Air Soil Pollutio.* 5, 214–233.
- Ward, R. L., D. I. Bernstein, and E. C. Young. 1986. "Human Rotavirus Studies in Volunteers of Dose and Serological Response to Infection." *J. Infect. Dis.* 154, 871–877.
- Walker, W. G., J. Bouma, D. R. Keeney, and F. R. Magdoff. 1973. "Nitrogen Transformations During Subsurface Disposal of Septic Tank Effluent in Sands: I. Soil Transformations." *J. Environ. Qual.* 2(4), 475–480.
- Whelan, B. R. 1988. "Disposal of Septic Tank Effluent in Calcareous Sands." *J. Environ. Qual.* 17(2), 272–277.
- Wilhelm, S. R., S. L. Schiff, and W. D. Robertson. 1994. "Chemical Fate and Transport in a Domestic Septic System: Unsaturated and Saturated Zone Geochemistry." *Environ. Toxicol. Chem.* 13(2), 193–203.
- Wilhelm, S. R., S. L. Schiff, and W. D. Robertson. 1996. "Biogeochemical Evolution of Domestic Wastewater in Septic Systems: 2. Application of Conceptual Model in Sandy Aquifers." *Ground Water*. 34(5), 853–864.

Willman, B. P., G. W. Petersen, and D. D. Fritton. 1981. "Renovation of Septic Tank Effluent in Sand-Clay Mixtures." *J. Environ. Qual.* 10(4).

Yamaguchi, T., P. Moldrup, E. E. Rolston, S. Ito, and S. Teranishi. 1996. "Nitrification in Porous Media During Rapid Unsaturated Water Flow." *Water Res.* 30(3), 531–540.

Zanini, L., W. D. Robertson, C. J. Ptacek, S. L. Schiff, and T. Mayer. 1998. "Phosphorus Characterization in Sediments Impacted by Septic Effluent at Four Sites in Central Canada." *J. Contam. Hydrol.* 33, 405–429



B PATHOGEN TRANSPORT-FATE STUDIES

Infiltration and percolation of wastewater through soil is relied on to renovate and polish partially treated wastewater and produce a percolate quality that does not contaminate groundwater and cause adverse public health or environmental impacts. The removal of pathogenic bacteria and virus is often of critical concern due to the public health implications should these organisms reach groundwater at high concentrations and contaminate drinking water supplies. Depending on the source concentration of virus, up to a 12-log removal of viruses must be achieved from the “toilet to tap” in order ensure an annual risk of infection of less than 1:10,000.

In concert with this project, a series of experiments were conducted to elucidate the transport-fate of bacteria and virus during wastewater renovation in wastewater soil absorption systems (WSASs). This appendix describes a series of experiments including a description of the methods employed and the results observed. Further details regarding the work described herein may be found in Van Cuyk (2003), Van Cuyk and Siegrist (2004), and Van Cuyk *et al.* (2004).

Purification of Bacteria and Virus in WSASs: One-Dimensional Column Study

More than 25% of the US population and 35% of all new development is served by onsite and small-scale wastewater systems, the majority of which rely on percolation of primary treated effluent through soil to achieve purification prior to recharge to the groundwater (US EPA 1978, 1980, 1997, Jenssen and Siegrist 1990, Crites and Tchobanoglous 1998). This practice is increasingly being scrutinized since there are over 25 million systems in operation, with the number increasing, and over 100 million people are served by drinking water systems using groundwater as the source water.

Human pathogens are known to exist in sewage effluents and the removal of pathogens is essential in preventing contamination of groundwater and drinking water sources. Attempts to exploit the benefits of decentralized system approaches have resulted in innovations in design approaches and technologies that are emerging at a growing rate. Alternative designs are being promoted that employ advanced pretreatment to reduce the suspended solids and biochemical oxygen demand and thereby enable increased hydraulic loading rates (HLRs) to soil (10-fold increase HLR). While such practices may be sound based on hydraulics, purification of pathogens (bacteria and virus) has not been proven.

Much work has been conducted on the transport of viruses and other pathogens in the groundwater environment, both at the laboratory and field scales. However, limited investigations have been conducted to elucidate the transport of virus through WSASs, that is, through the infiltrative surface and the vadose zone into the underlying groundwater.

Nicosia *et al.* (2001) conducted a field investigation on the removal of PRD-1 in infiltration cells dosed with wastewater located at a research station in Florida. These researchers found PRD-1 attachment to be reversible, with slow desorption of the phage over time.

Many factors have been shown to be important in the removal of viruses in the subsurface. These include the virus type and characteristics of the grain surface and solution chemistry such as: pH, organic matter content, and presence of surface active agents (Bales *et al.* 1991, Loveland *et al.* 1996, Navigato 1999). Understanding the impact of organic matter on the fate of pollutants is important since the source of viral contamination is frequently sewage-derived organic matter. The importance of organic matter on the fate of viruses is not completely understood and contradictory results have been presented in the literature. Some research suggests that organic matter may increase the attachment of virus on soil due to the adsorption to mineral surfaces on the soil grains and perhaps adding hydrophobic sites (Bales *et al.* 1991, 1993; Zerda *et al.* 1985; and Navigato 1999). Other research suggests a decrease in the attachment of virus to surfaces with increased organic matter (Burge and Enkiri 1978; Gerba *et al.* 1981; Pieper *et al.* 1997; Ryan *et al.* 1999; and Sobsey *et al.* 1980). These studies present the theory that the organic matter is absorbed to mineral surfaces on the soil grains and both blocks attachment sites and adds electrostatic repulsion by reversing the surface charge, which results in increased viral transport.

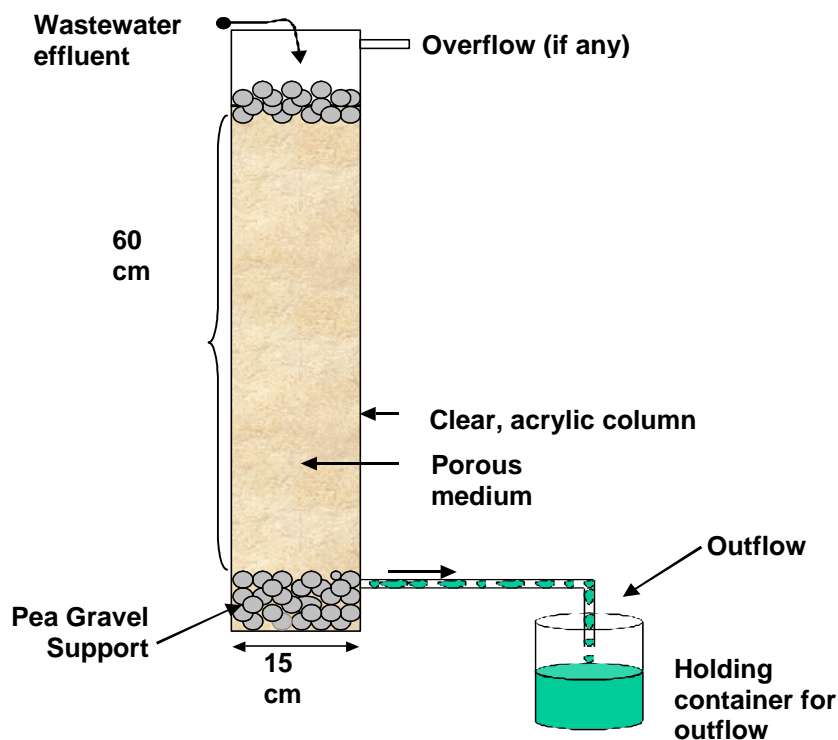
The work described herein focuses on the role of the infiltrative surface and the vadose zone of WSASs on the removal of virus. Effluent composition and loading rate impacts on the development of the clogging zone and virus fate were also studied using one-dimensional (1-D) sand-filled columns. Previous and forthcoming papers describe the operation, water quality characteristics, and numerical modeling of the flow regime (see Appendix C, *Biozone Development and WSAS Performance: Column Studies*, and Beach 2001; Lowe *et al.* 2005; and Beach *et al.* 2005). The research presented in these papers was used to refine the relationship between infiltration rate response and cumulative mass loading of total biochemical oxygen demand (tBOD) and total suspended solids (TSS). A comparison of infiltration rate responses in aggregate-laden versus aggregate-free systems and an assessment of the role of aggregate on the loss of infiltration rate and the magnitude of an equilibrium rate was also conducted (Beach *et al.* 2005).

Materials and Methods

This section provides detailed information regarding the materials and methods used in the 1-D column study on the role of the infiltrative surface and the vadose zone of WSASs on the removal of virus.

Column Preparation and Operation

Sixteen 1-D columns were constructed from clear acrylic pipe, 15 cm in diameter and 75 cm in length with 30 cm extensions to allow for additional space above the infiltrative surface (see Figure B-1). Each column was packed with moist sand (approximately 5.5% water by weight, $d_{10} = 0.22$ mm, $d_{60} = 0.60$ mm, total organic carbon (TOC) = 0.017 dry wt %) in 5 cm lifts. This sand was the same medium sand as used in previous lysimeter studies (Van Cuyk *et al.* 2001). For eight of the columns, after the final lift was added, a layer of washed gravel (nominal 2 cm diameter) was placed on the scarified surface and dry sand was used to fill the void in spaces with additional gravel added to a height of 10 cm above the soil surface. This arrangement was done to simulate gravel embedment, which is known to occur in WSASs.



Note: Columns were cloaked with black plastic to prevent algae growth

Figure B-1
Schematic of 1-D Column Apparatus

Columns were operated under various loading regimes (Table B-1) to simulate different field conditions. All columns received septic tank effluent (STE) for 138 days and were monitored for hydraulic properties and purification performance. Monitoring of water quality included sampling and analysis of the STE applied to the columns as well as the percolate outflow from each column. Sampling and analysis of the applied STE was conducted during three separate days each week. The STE used in this study was typical of residential STE and was collected from a multifamily student housing unit located in Golden, CO. Sampling and analysis of the percolates from the columns was conducted at least once every two weeks, with more frequent sample collection and analysis during initial operation and during tracer tests.

Table B-1
Experimental Conditions for the Column Operation

Loading Regime	Column	Infiltrative Surface Character	Design HLR ¹	Loading Rate Representative of...	Loading Method Features	Effluent Applied
LR1	1A, 1B	Gravel-Free	200 cm/d	Random gravity in a serial distribution trench network	Continuous delivery at 24.56 mL/min	STE
	1C, 1D	Gravel-Laden	35.36 L/d per column			
LR2	2A, 2B	Gravel-Free	100 cm/d	Random gravity in a trench network with distribution	Continuous delivery at 12.28 mL/min	STE
	2C, 2D	Gravel-Laden	17.68 L/d per column			
LR3	3A, 3B	Gravel-Free	50 cm/d	Dosed, non uniformly distributed between orifices	Dosed 4x/d at 8, 12, 4, 8 hr. 12.5 cm/dose or 2.20 L/dose 1.10 L/min for 2 min	STE
	3C, 3D	Gravel-Laden	8.84 L/d per column			
LR4	4A, 4B	Gravel-Free	25 cm/d	Uniform distribution between orifices	Dosed 4x/d at 8, 12, 4, 8 hr. 6.25 cm/dose or 1.10 L/dose 1.10 L/min for 1 min	STE
	4C, 4D	Gravel-Laden	4.42 L/d per column			
LR5	5A, 5B	Gravel-Free	50 cm/d 8.84 L/d per column	Sand filter effluent, non-uniformly dosed between orifices	Dosed 4x/d at 8, 12, 4, 8 hr. 12.5 cm/dose or 2.20 L/dose 1.10 L/min for 2 min	SPE ²

¹ Actual daily loading rates were 65 to 82% of the design rate (see Appendix C).

² SPE = soil percolate effluent, consisting of the combined percolate from LR3 and LR4 columns.

Percolate samples were collected from the outflow containers by pouring percolate from the container into precleaned 250 mL plastic bottles. All samples were labeled and stored at 4 °C until analysis. All laboratory analysis of the percolate samples was performed within 24 hours of sample collection.

To evaluate laboratory analysis methods, 10% duplicate sample analyses were performed. The following characteristics were determined following standard methods: (APHA 1998)

- pH was measured electrometrically
- Alkalinity was measured (total alkalinity) via titration with sulfuric acid according to APHA method 2320B
- Carbonaceous biochemical oxygen demand (cBOD₅) was measured according to APHA method 5210B
- Chemical oxygen demand (COD) analysis was performed using a Hach reactor digestion, colorimetric method (Hach 1998, US EPA-approved)
- Total solids (TS) and TSS were measured according to APHA methods 2540B and 2540D
- Total nitrogen (TN) was measured by persulfate digestion, nitrate nitrogen by chromotropic acid method, and ammonia nitrogen by salicylate method (Hach 1998, US EPA-approved)
- Total phosphorus (TP) was measured according to EPA acid persulfate method (US EPA 365.2)
- Fecal coliform analysis was performed by membrane filtration according to APHA method 9222D

In addition to the 16 columns described previously, two gravel-free columns were constructed following the same procedure. These columns, 5A and 5B, received the combined percolate from the LR3 and LR4 columns (designated soil percolate effluent [SPE]) at a design loading rate of 50 cm/day in four doses (same dosing interval and rate as LR3).

Prior to system startup and gravel placement (in aggregate/gravel-laden columns), the saturated hydraulic conductivity of each column was measured using a falling head test (Beach 2001). Statistical tests performed on all possible pairs of loading regimes indicated no significant difference (at a 95% confidence level) in measured saturated hydraulic conductivity between any combination of loading regimes (Beach 2001). This factor indicates that the packing procedure was reproducible and that differences in baseline hydraulic properties between columns were insignificant.

Hydraulic monitoring of the columns included soil moisture tension, soil moisture content, column throughput rates as measured by percolate volume, ponding heights, and bromide tracer tests (see Appendix C, *Biozone Development and WSAS Performance: Column Studies* and Beach 2001).

The percolate from each column was directed into an outflow container, which was calibrated by recording its empty weight prior to system operation. All volume measurements were made by weight using an electric balance. At the beginning of the column study, outflow volume was measured just prior to each dosing event. As conditions moved towards steady-state throughput (continuously ponded), the frequency of monitoring decreased to twice per day and eventually to once every 24 hours four times per week. Percolate volumes were collected through day 131 of column operation. The percolate samples were also used to assess system performance by measuring water quality parameter concentrations. These percolate samples were collected at a higher frequency during tracer tests and were used to measure the level of added surrogates and tracers in the column outflow.

In all columns, during some point in operation, the application rate exceeded the infiltration rate and ponding ensued. The level of ponding was periodically monitored throughout the operation of the columns from a reference point made at the top of the infiltrative surface. In LR1, LR2, and periodically in LR3 and LR4, ponding levels increased to the point of overflow (approximately 20 cm).

Multicomponent Surrogate and Tracer Test

To evaluate mean travel times (hydraulic performance) and the purification performance of these columns with respect to viruses under each loading regime during the life of the columns, tracer tests were conducted prior to wastewater addition (dosed with tap water, tracer test 1) and during weeks 1 (tracer test 2), 6 (tracer test 3), and 15 (tracer test 4). During these tracer tests a multicomponent mixture of viral surrogates (two bacteriophages) and a conservative tracer (bromide) were added to the STE in a 300 gallon holding tank before application to the columns. This multicomponent tracer mixture was applied to the columns for three days and percolate samples were collected and monitored. All of the percolate coming from the columns was collected initially four times per day (collected over a six-hour time interval) and later 24 to 48 hour collection intervals.

During the tap water tracer test, bromide was added at a concentration of approximately 1,000 mg-Br/L. Bromide was added to STE to a final concentration of 500 mg-Br/L in the week 1 and week 6 tests. Bromide was added to the applied effluent and dosed to each column at the prescribed design rate (Table B-1).

The MS-2 and PRD-1 were added to the applied effluent at a target concentration of 1×10^7 PFU/mL. MS-2 is an icosahedral single-stranded RNA coliphage with an average diameter of approximately 25 nm and an isoelectric point (pH_{iep}) of 3.9 (VanDuin 1988, Powelson *et al.* 1990, Bales *et al.* 1991). PRD-1 is an icosahedral lipid phage with a diameter of 62 nm, a pH_{iep} of < 4.5 and a *Salmonella typhimurium* host (Ryan *et al.* 1999; Bales *et al.* 1991; and Olsen *et al.* 1974). MS-2 and PRD-1 have been extensively used as viral surrogates (Harvey 1997a, b). Levels of the two bacteriophages and bromide were measured in percolate samples to determine virus retardation and removal efficiencies. The shape of the breakthrough curves was used to provide insight into dispersion within the columns as well as heterogeneities that may develop due to continued wastewater application.

Percent removal was calculated using the following equation:

$$100 \times \frac{[(V_t)(C_o)] - \left[\sum_{j=1}^n (V_j)(C_j) \right]}{[(V_t)(C_o)]} = \% \text{ Removal} \quad \text{Equation B-1}$$

where V_t is the total volume of the dose containing bacteriophages (mL), C_o is the concentration of bacteriophage added to the dose volume (PFU/mL), V_j is the volume of column outflow collected over a sampling time (mL), C_j is the concentration of viruses measured in the outflow (PFU/mL) and n is the number of outflow samples collected.

Column Dismantling and Media Characterization

After 138 days (19 weeks) of operation, the columns were shut down and final infiltration rates were measured by monitoring the ponding level or head drop in the columns over time. Approximately one to three hours following cessation of ponding, sand sample collection from the columns commenced. Infiltrative surface samples were scraped off the top of the columns using a sterile spatula and placed in a sterile container. Samples were also collected at depth intervals of 5 to 8 cm, 10 to 13 cm, and 25 to 28 cm below the infiltrative surface using precleaned sterile beakers. Samples of the infiltrative surface (0 to 3 cm) were also collected at two locations in each cored column. LR1 columns were not dismantled due to additional experiments. Sand core samples were not taken from columns 2D and 3B.

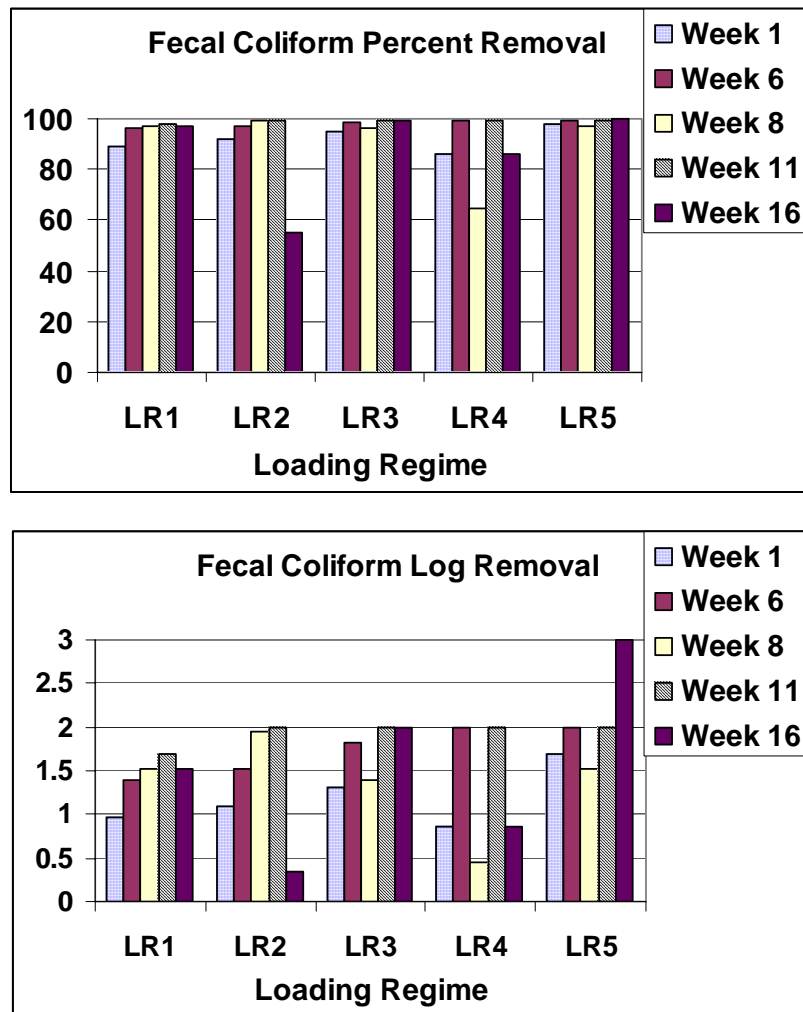
The sand samples were analyzed for water content, fecal coliform (FC) bacteria, MS-2, and PRD-1 bacteriophages. Water content analysis was performed by drying the samples in a 105 °C oven (APHA 1998). Total carbon analysis was conducted on selected samples. Total carbon analysis was performed using a CM 5014 CO₂ Coulometer (Coulometrics, Joliet, IL). Fecal coliform and bacteriophage samples were extracted by taking approximately four grams of soil and placing it into a 50 mL conical, adding 40 mL of 1.5% beef extract (a 1:10 extraction) and rotating on an orbital mixer for two minutes. Samples were settled for one minute at which time an aliquot was withdrawn from mid-depth for fecal coliform and bacteriophage analysis. Fecal coliform analysis was conducted using the membrane filtration method with serial dilutions (APHA 1998). MS-2 and PRD-1 bacteriophage assays were made following the plaque forming unit technique on lawns of bacteria hosts (*Escherichia coli* and *Salmonella typhimurium* host, respectively) described in Adams (1959).

Results and Discussion

Throughout the operation of these columns, water quality data from percolate samples were collected. This report focuses on the microbial parameters while the physical and chemical data are presented elsewhere (see Appendix C, *Biozine Development and WSAS Performance: Column Studies* and Lowe *et al.* 2005).

Water Quality Observations

Briefly, all columns proved to have high removal efficiencies for added STE constituents. Ninety percent of added cBOD₅ was removed in these columns. Nitrification was observed in all columns and it commenced in LR1 and LR2 between 30 and 40 days of operation, and following approximately 15 days of operation in LR3 and LR4. The difference in time to nitrification at the various loading rates might be due to the presence of more unsaturated flow in the intermittently dosed LR3 and LR4, allowing nitrifying communities to establish early on, while the presence of a biozone at the infiltrative surface of LR1 and LR2 was needed for unsaturated flow to occur and nitrifying communities to establish. High removal of phosphorous (P) was observed in most columns, though P breakthrough was observed in LR1 and LR2, most likely due to the relatively higher effluent loading. Figure B-2 presents the average percent removal of FC for each loading rate at different times of operation.



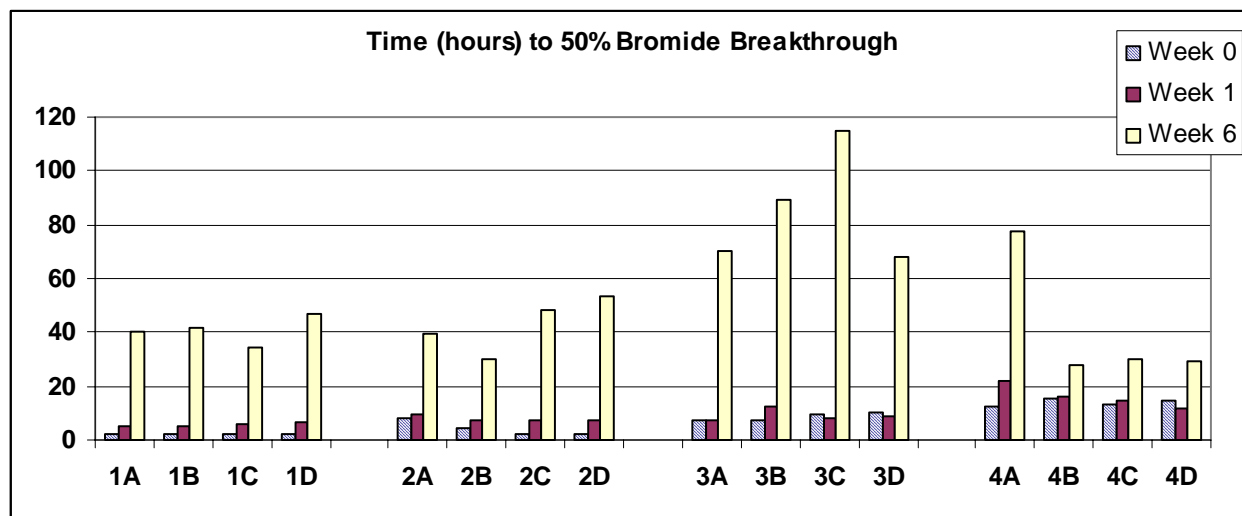
Note: Percent Removal of FC averaged for each loading rate (LR1–LR5) for weeks 1, 6, 8, 11, and 16 of column Operation. Log removal for the same data is also shown. Average Influent concentration for STE was 2.25×10^5 cfu/mL

Figure B-2
Percent Removal of Fecal Coliform

This graph demonstrates that high removals were observed early on during column operation (86 to 98% removal at the week 1 test). Percent removal was calculated by measuring the average influent concentration and volume dosed at a given time period and comparing that to percolate samples collected over 24 hours (entire percolate volume collected).

Virus Surrogate and Tracer Tests

Results from bromide-tracer tests indicate that bromide breakthrough occurs at roughly the same time in the first two tracer tests (clean-water baseline and week 1) in all columns from LR1, LR2, and LR4 (Figure B-3).



Note: Week 0 represents clean tap-water dosing.

Figure B-3
Comparison of 50% Bromide Breakthrough During Tracer Tests 1, 2, and 3 In All Loading Regimes

Bromide breakthrough of tracer test 2 (week 1) was significantly delayed in all columns in LR3 compared to the clean-water test. Since the second tracer test was initiated after only a week of wastewater application, little or no noticeable change is expected to occur between these two tests. However, during the third tracer test, bromide breakthrough occurs later in all columns and significant tailing effects can be observed. Assuming (1) that modification to infiltrative surface properties and subsequent changes in hydraulic acceptance is the main control on changes in the shape and position of the bromide breakthrough curves, and (2) that the changes in soil properties beneath the clogging zone are negligible, the changes observed during the third tracer test compared to the clean-water tracer test are attributed to the development of soil clogging at the infiltrative surface.

Higher water contents and lower permeability in the biozone caused lower water transport rates and an increased time to observed bromide breakthrough. In addition, variations in travel paths (on the pore scale) at the clogging zone/subsoil interface can cause tailing effects (Beach 2001, Beach *et al.* 2005).

Results of bromide tracer tests indicate that for each successive tracer test, the mean travel time through the columns increased (Figure B-3). The most significant increase occurred between the second and third tracer test (that is, between weeks 1 and 6). During this time, continuously ponded conditions, presumed to be due to the development of a restrictive biozone at the infiltrative surface, were observed in all but two columns (4B and 4C). The presence of the biozone decreases the infiltrative surface permeability and results in an increased hydraulic residence time as observed during the third tracer test.

Figure B-4 shows results for the clean-water tracer tests (week 0) in duplicate columns dosed at 50 cm/day (LR3) with MS-2 and PRD-1. This clean-water tracer test provides baseline breakthrough curves and allows for the calculation of retardation factors for the virus added to these columns.

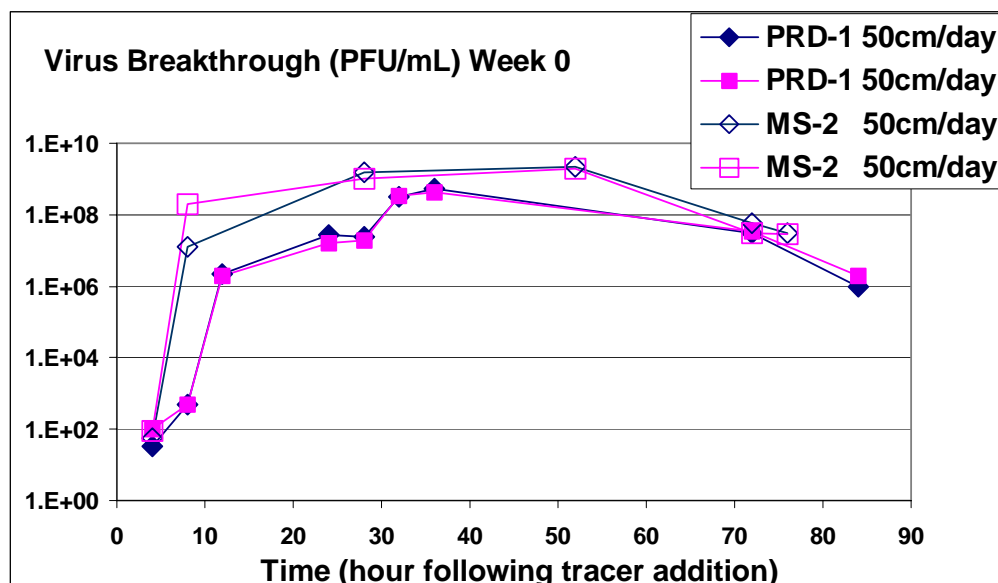
Table B-2 summarizes the time to 10% and 50% breakthrough for bromide (BT₁₀ and BT₅₀), PRD-1 and MS-2 at the week 0 tracer test. Retardation of viruses is calculated using the following expression (Powelson *et al.* 1993):

$$\Theta_w = \Theta_{Br} / R_{Br} \quad \text{Equation B-2}$$

where Θ_w and Θ_{Br} are the travel time for infiltration of water and bromide to reach the depth of interest (60 cm). Assuming that R_{Br} equals 1 then:

$$\Theta_{vir} = \Theta_{Br} / R_{vir} \quad \text{Equation B-3}$$

By comparing the retention time (BT₁₀ or BT₅₀) of bromide and virus, R_{vir} can be calculated. Based on BT₁₀, retardation factors in these columns were calculated at 6.4 and 6.0 for PRD-1 and MS-2, respectively. Powelson *et al.* (1993) found virus transport to be retarded ($R = 1.9$) initially but increased transport was observed ($R = 0.47$) after 4 days of flooding (saturated conditions). Powelson *et al.* (1990) found R_{vir} of 0.75 in unsaturated sand-filled columns dosed at rates of 0.13 m/day, which suggests charge exclusion from part of the water volume in this system. These investigators also observed greater R_{vir} with secondary effluent versus tertiary, and suggested this may possibly be due to a greater amount of organic colloids deposited by secondary effluent, which may result in greater adsorption of virus.



Note: Duplicate columns loaded at 50 cm/day (LR5) intermittently (4 equal doses). MS-2 and PRD-1 in the influent were 1×10^{10} and 1×10^9 PFU/mL, respectively

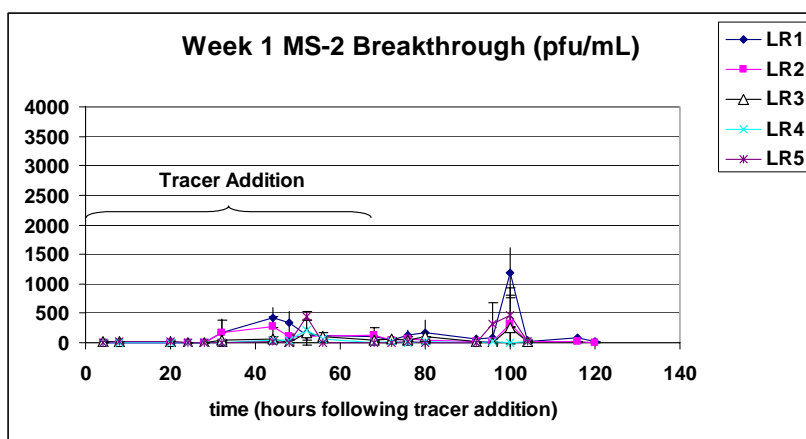
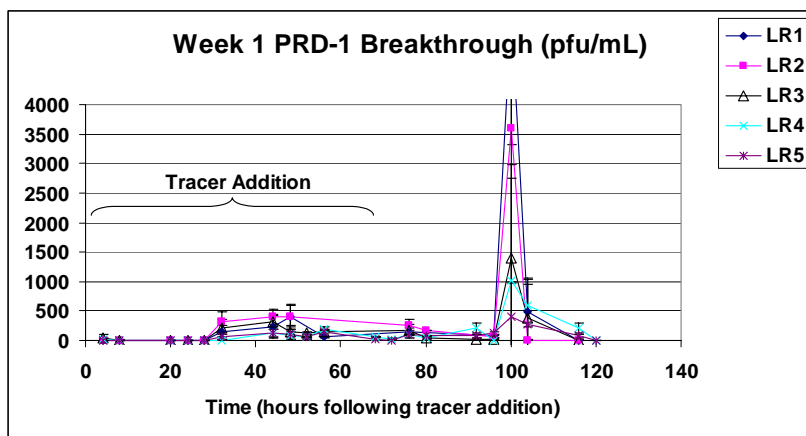
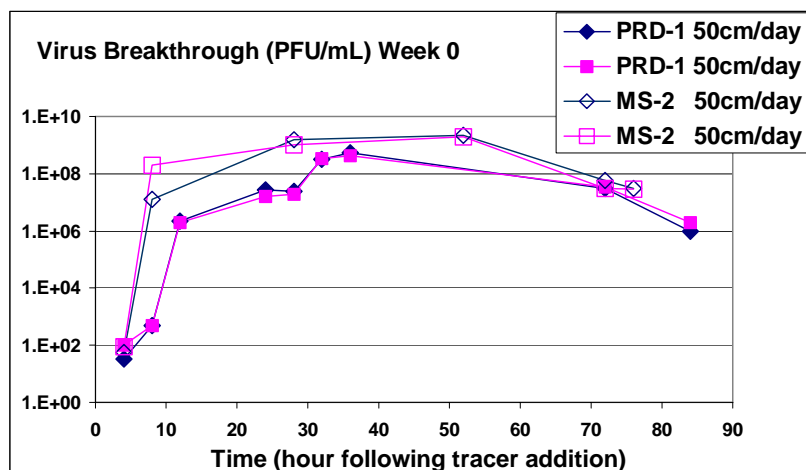
Figure B-4
PRD-1 and MS-2 Breakthrough During Clean-Water Tracer Test (Week 0)

Table B-2
Approximate Time (Hours) to 10% and 50% Breakthrough During Clean-Water Tracer Test (Week 0)

	Bromide (hr)	PRD-1 (hr)	MS-2 (hr)	Calculated R_{vir}	
				PRD-1	MS-2
10% BT	5	32	30	6.4	6.0
50% BT	10	36	40	3.6	4.0

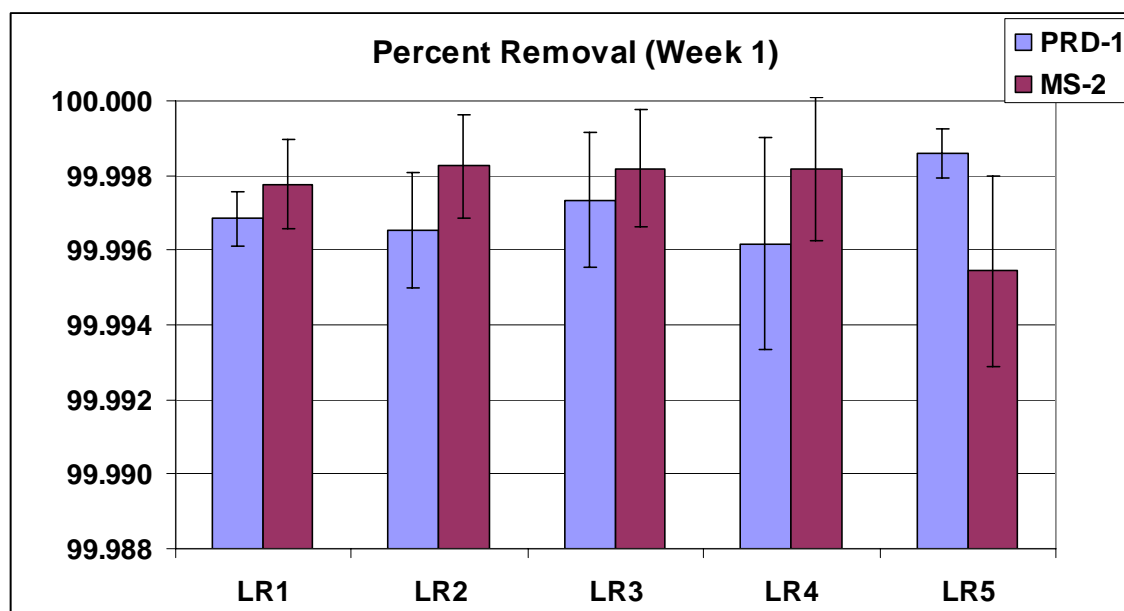
Note: Duplicate columns dosed intermittently at 50 cm/day. Virus retardation (R_{vir}) calculated based on expressions from Powelson 1993 (see Equation B-3).

Figure B-5 presents the breakthrough curves for MS-2 and PRD-1 for the week 1 tracer test. R_{vir} could not be calculated for PRD-1 or MS-2 in subsequent tracer tests due to the limited breakthrough (high removal) of the bacteriophages in the columns. Average values for each of the four sets of duplicate columns in LR1–LR4 are shown. Total removal of added bacteriophage was approximately four-logs or higher during this tracer test, as shown in Figure B-6 (the cause of the spike at 100 hours is unknown). These total removals are based on collection of the total volume of percolate (100% of column effluent). Percolate samples were collected until three consecutive days of non-detectable levels of virus in the samples were observed (virus detection level = 1 PFU/1mL).



Note: All data points \pm 1 standard deviation. Average values for each loading regime shown for tracer test beginning one week after initiation of STE loading.

Figure B-5
Breakthrough Curves for MS-2 and PRD-1 for LR1–LR4



Note: +/- 1 Standard Deviation. Average of the four columns in each loading regime.

Figure B-6
Average Percent Removal of MS-2 and PRD-1 During the Week 1 Tracer Test

Tracer tests conducted at week 6 and week 15 showed exceedingly high removal of viruses added. Exceptionally few percolate samples had detectable levels of virus during both of these tracer tests. From percolate samples collected for 300 hours following the addition of the tracer and virus surrogates to the STE, less than 20 samples had detectable levels of virus in them and all were below 16 PFU/mL. The detection limit for analysis is 1 PFU/mL. Percent removals were higher at week 6 and 15 than at week 1; all showed a 5-log (99.999%) or higher removal.

The impact of loading sand media with a higher quality effluent (SPE consisting of the percolate collected from LR3 and LR4 columns) on the hydraulic and purification performance was also investigated. This study involved a duplicate set of columns, similar to the main experiment, but to which a higher quality effluent was applied. The time-dependent changes in virus removal were compared between the STE loaded columns and the higher quality effluent (SPE) loaded columns.

These two additional columns (5A and 5B) were filled with the same sand to obtain a vadose zone depth of 60 cm. Their infiltrative surfaces were open (or aggregate-free). These columns were dosed with the combined percolates collected from the LR3 and LR4 columns (discussed above). This effluent was initially expected to be similar to sand filter effluent (SFE), but during the start up phase of the column operation it had much higher levels of TSS, chemical oxygen demand (COD), and ammonia (NH₄) (see Table B-3). The effluent was applied to the columns at 50 cm/day in four equal doses at 8, 12, 16, 20 hours (the same as LR3).

Table B-3
Composition of Effluent Applied to LR5 Columns (5A and 5B)

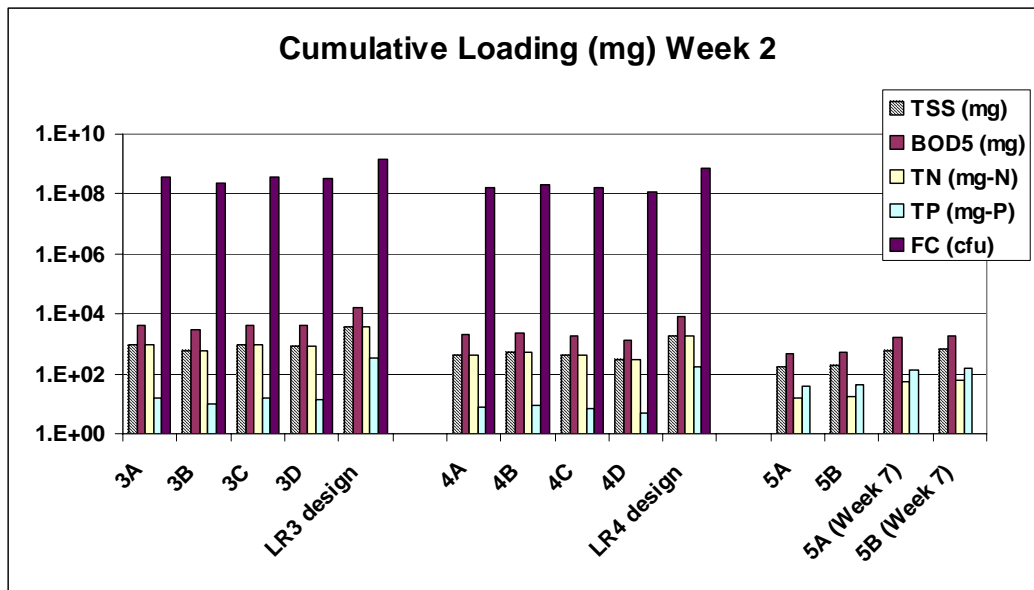
	TSS (mg/L)	COD (mg/L)	TN (mg/L)	NH ₄ (mg/L)	TP (mg-P/L)	FC (cfu/100mL)
SPE Average ¹	15.7	91.5	27.3	22.2	15.4	–
SPE High	27.5	173	36	54	20.6	9.4×10^4
SPE Low	nd	61	2.4	0.1	6.5	nd
SFE ²	10–15	30–40	20–30	20–25	0–5	0–1000
STE Average (this study)	126.5	457.5	55.5	60	26.5	2.2×10^4 – 5.5×10^5

¹Soil percolate effluent (combined effluent from LR3 and LR4 columns), n = 9.

²Sand filter effluent from literature values.

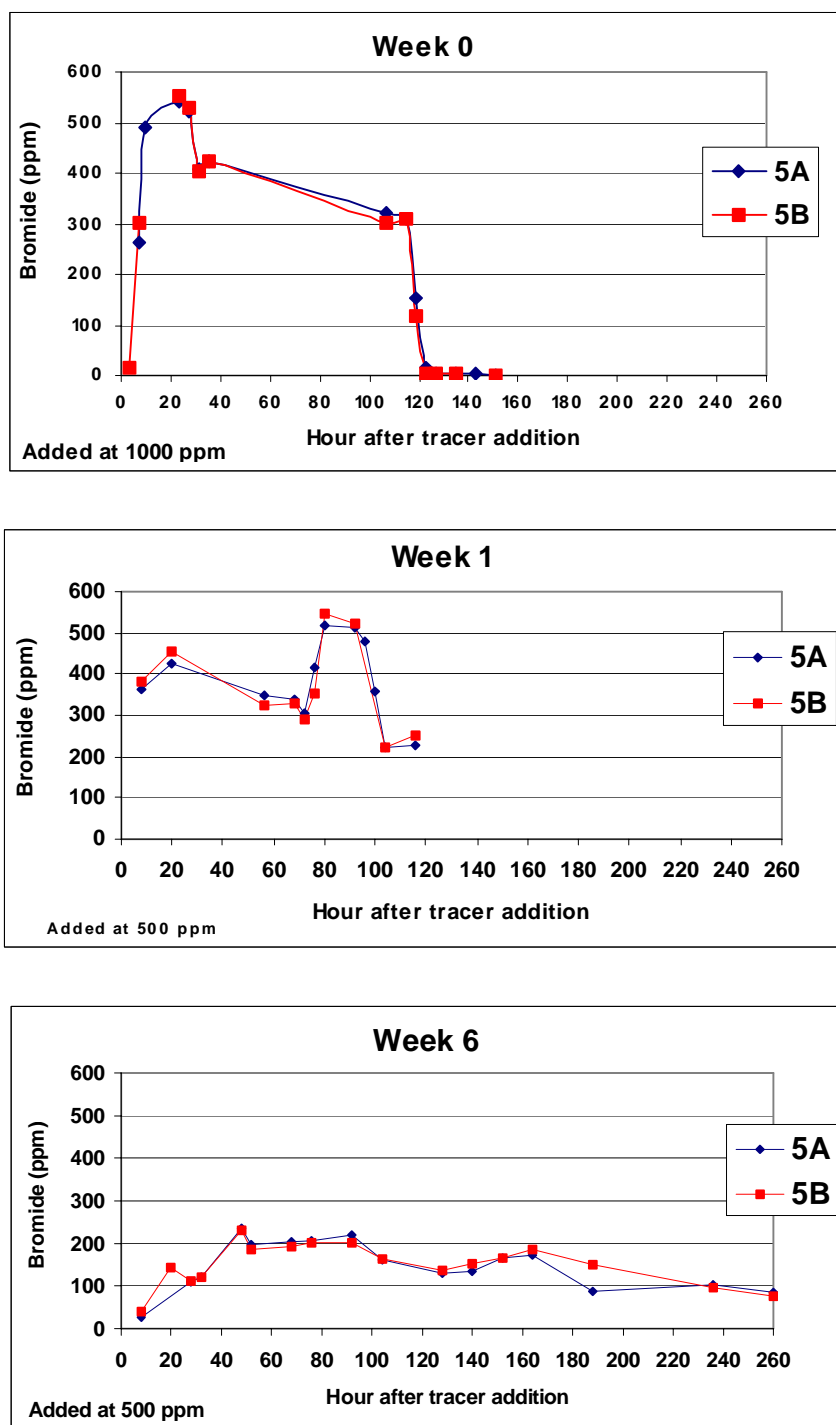
nd = non-detectable.

Comparison of columns 5A and 5B to the columns of LR3 and LR4 was made for the cumulative loading of effluent constituents (Figure B-7). Similar levels of BOD₅ and TSS were applied but relatively lower levels of fecal coliform bacteria were added to 5A and 5B due to the high removal within the LR3 and LR4 columns. Bromide tracer curves for these columns (5A and 5B) for week 0, 1, and 6 are presented in Figure B-8. Figure B-9 presents PRD-1 and MS-2 breakthrough over the time following addition of these bacteriophages.



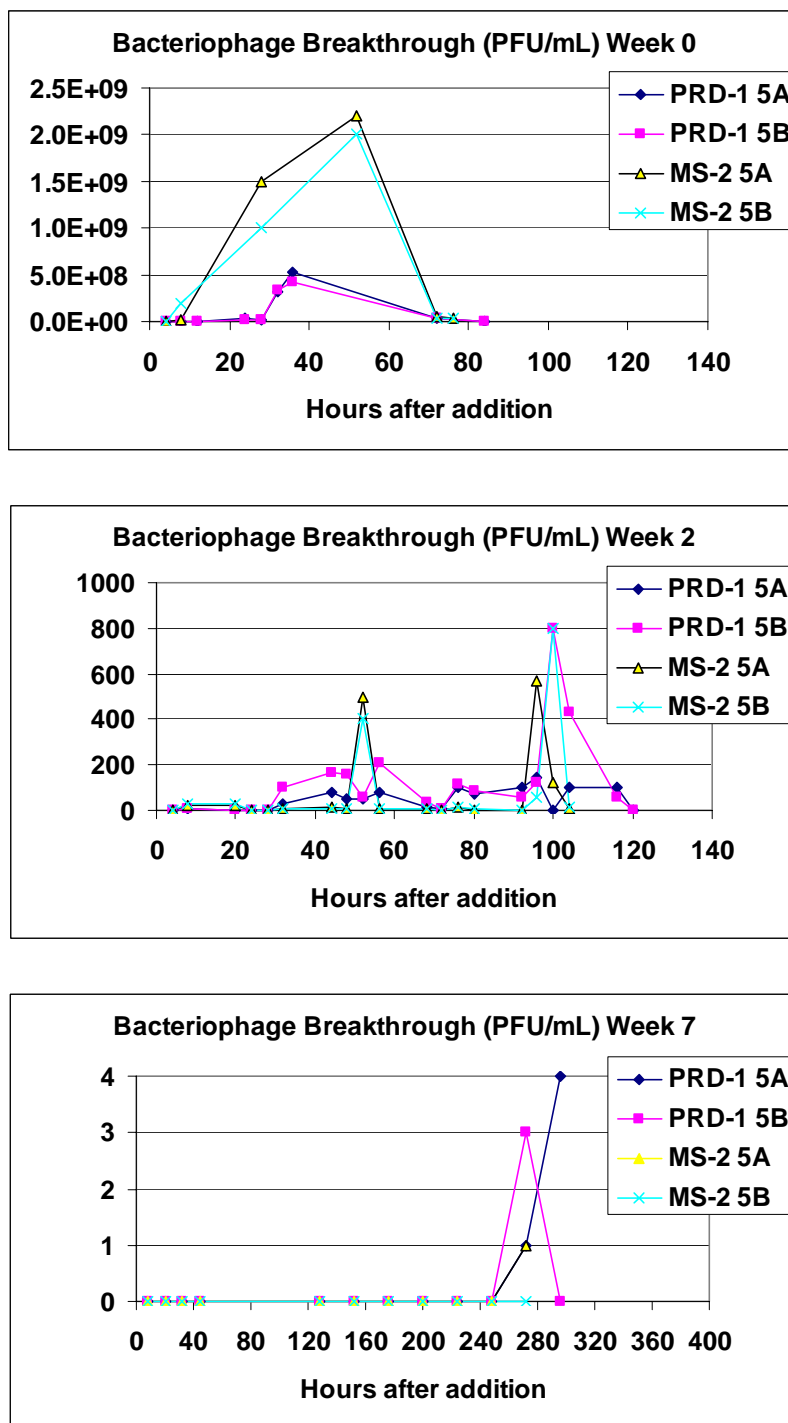
Note: Columns 5A and 5B (LR 5) mass loadings prior to the second tracer test are also shown.

Figure B-7
Estimated Cumulative Loading of Constituents in Applied Effluent to LR3, LR4, and LR5 Columns Just Prior to the Start of the Week 1 Tracer Test



Note: Tracer was added over the first 72 hours.

Figure B-8
Bromide Breakthrough Curves for Columns 5A and 5B at Week 0, 1, and 6 Tracer Tests



Note: Tracer was added over the first 72 hours—x and y scales are different.

Figure B-9
PRD-1 and MS-2 Breakthrough in Columns 5A and 5B at the Week 0, 1, and 6 Tracer Tests

Table B-4 presents the time to BT_{10} and BT_{50} for each of the tracer tests. The values given are representative of both columns (5A and 5B). The data show that the most dramatic differences in hydraulics occurred between the week 1 and the week 6 tests, similar to observations of LR1, LR2, and LR4.

Table B-4
Time (Hours) to BT_{10} and BT_{50} During Tracer Tests Conducted in Columns 5A and 5B at Week 0, 1, and 6 of Column Operation

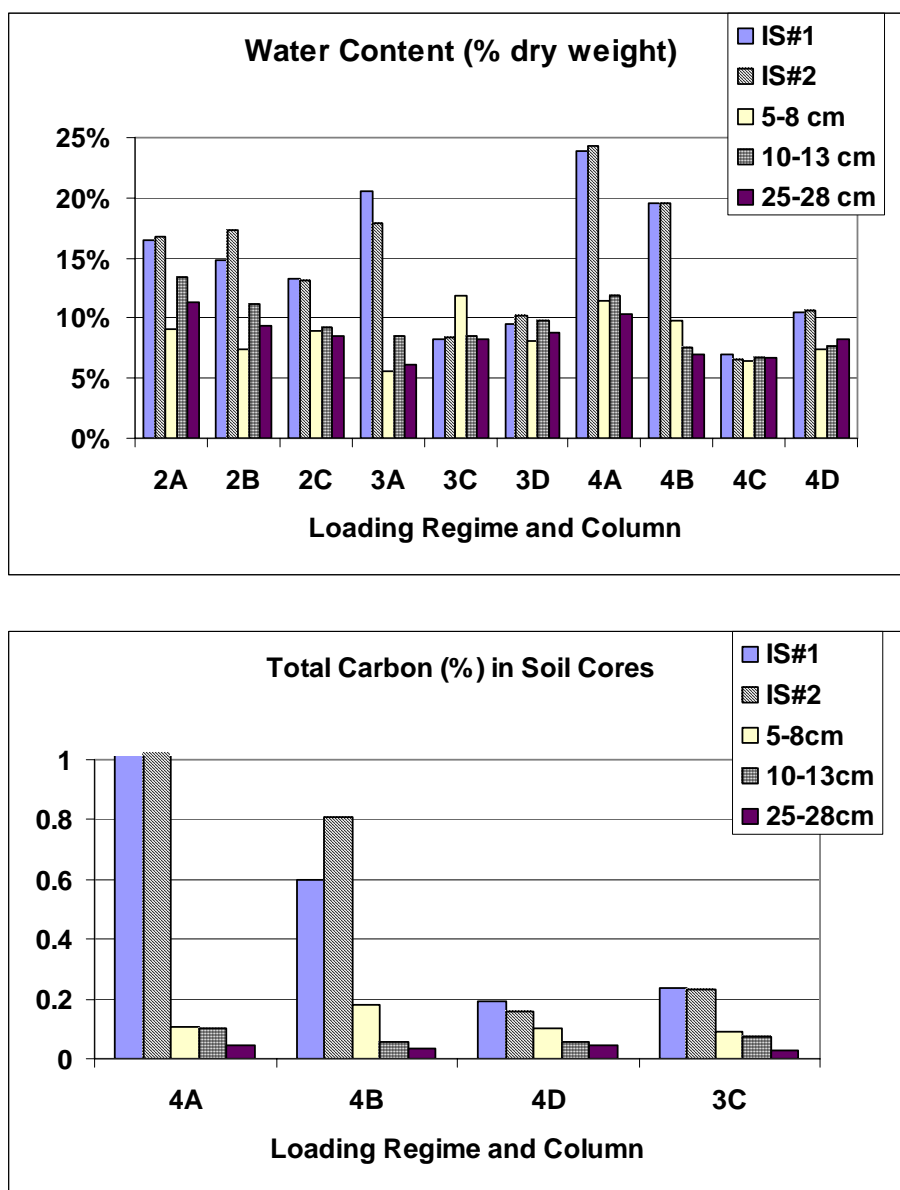
Bromide	Week 0 (hr)	Week 1 (hr)	Week 6 (hr)
BT_{10}	7	5	8
BT_{50}	10	10	8

The bromide tracer tests showed an increase in the hydraulic retention time (HRT) with time of operation and significant changes in LR3 and LR4 in the first two weeks of operation, while the higher quality effluent columns (5A and 5B) showed more significant changes in HRT by the week 6 tracer test. At the week 0 tracer test, significant breakthrough of virus was observed in columns 5A and 5B, while at the week 1 tracer test the removal of virus was high (4- to 5-log for both PRD-1 and MS-2) in these columns even with little change in the HRT. Therefore, at the week 1 tracer test, an increase in the removal of virus was observed in these columns that cannot be attributed simply to hydraulic changes in this system. The “conditioning” of the porous media due to application of SPE (even relatively higher quality effluent versus STE) appears to play an important role in the removal of these viruses, and the appearance of a visibly developed biomat at the infiltrative surface and a concomitant change in the hydraulic loading may not be required.

Terminal Coring and Infiltrative Surface Characterization

Water and carbon content values for soil samples were taken from three representative columns. The results indicate increases in water content and carbon content at the infiltrative surface zone (IS#1 and IS#2) compared to the remainder of the column (Figure B-10). These increases are expected due to the accumulation of pore-filling agents as a result of continued wastewater application (Siegrist 1987).

The differences in the water content values with individual columns seem to be greater in the columns with an open infiltrative surface (A and B columns) versus those with gravel at the infiltrative surface (C and D). This variation may be due to the more disruptive method of obtaining infiltrative surface samples in the gravel laden columns, where gravel was picked off the top of the columns until it was completely removed, at which time two infiltrative surface samples were collected.



Notes:

IS = infiltrative surface (two samples were taken from this layer).

A and B have open infiltrative surface, C and D have gravel infiltrative surface.

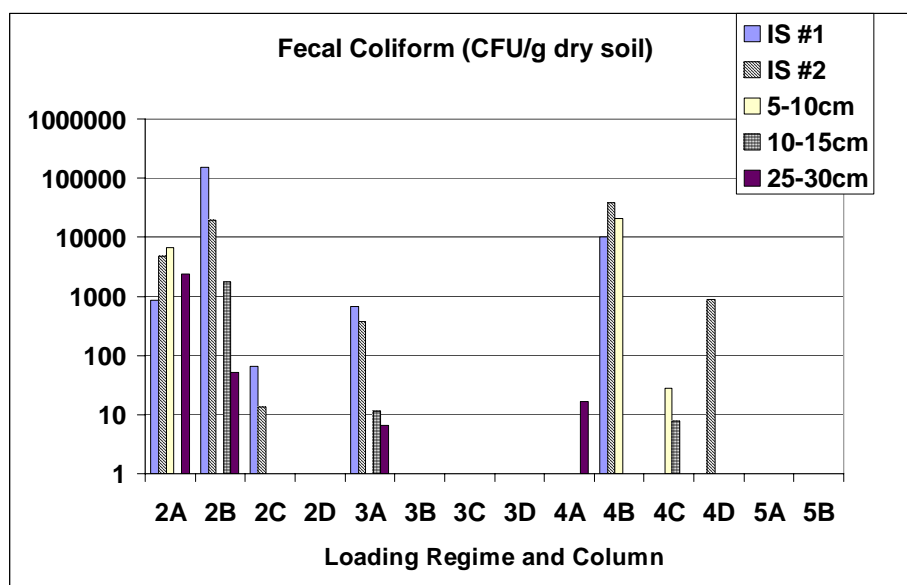
Design loading rates are LR1 = 200 cm/day, LR2 = 100 cm/day, LR3 = 50 cm/day, and LR4 = 25 cm/day.

Actual daily loading rates were 65 to 82% of design rates.

Figure B-10

Water Content and Total Carbon Values for Soil Samples Collected From Cored Columns

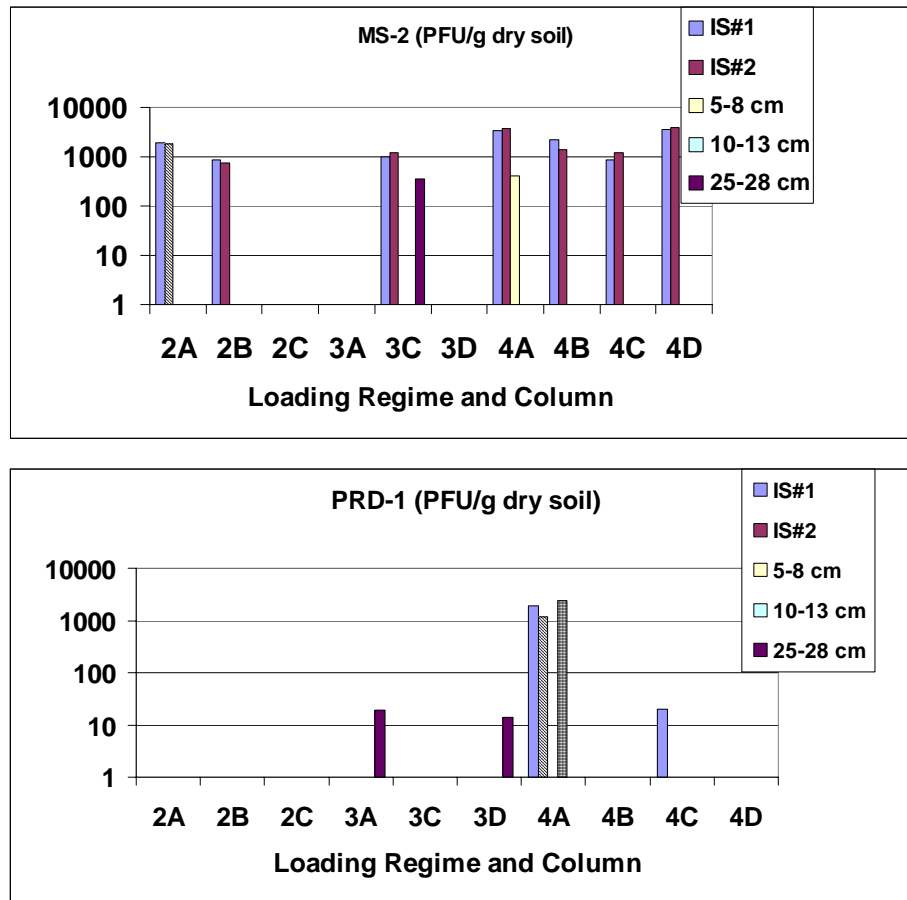
Few fecal coliforms were found in sand below 15 cm, though columns 2A, 2B, 3A, and 4A all had detectable levels at the 25–30 cm depth (Figure B-11). In columns where fecal coliform bacteria were measured in soil core extracts, there is a general trend of decreasing levels with increasing depth below the infiltrative surface.



Note: No bar represents non-detectable levels. Columns 2D and 3B not cored.

Figure B-11
Fecal Coliform Levels From Extracted Soil Samples at the Infiltrative Surface and at Three Intervals Below

Figure B-12 shows MS-2 and PRD-1 extracted from these same soil samples. PRD-1 was detected in notably few soil samples. Column 4A had the highest level of extracted PRD-1, while columns 3A and 3D had PRD-1 present in soil cores from 25–28 cm depth. MS-2 was frequently found in infiltrative surface cores (found in 7 of the 10 columns analyzed). This finding suggests the importance of the infiltrative surface and the “conditioning” of the columns in the removal of certain viruses.



Note: No bar represents non-detectable levels. Columns 2D and 3B not cored.

Figure B-12

MS-2 and PRD-1 Found in Soil Samples Taken From Extracted Soil Samples at the Infiltrative Surface and at Three Intervals Below

Summary and Conclusions

A 1-D column study was conducted to evaluate the infiltrative surface biozone genesis effects on virus removal. These columns were filled with the same medium sand and were dosed with STE at four loading rates:

- LR1 columns dosed with STE at an experimental design rate of 200 cm/day continuously dosed
- LR2 continuously dosed at 100 cm/day
- LR3 intermittently dosed (four times daily) at 50 cm/day
- LR4 intermittently dosed (four times daily) at 25 cm/day

Actual loading rates were measured and observed to range from 65 to 82% of the design rates. Within each loading rate, duplicate columns were run with either an aggregate-free or an aggregate-laden infiltrative surface and a 60 cm soil vadose zone depth. Two additional gravel-free columns were set up and dosed with the combined percolate collected from LR3 and LR4 (SPE) at 50 cm/day to simulate pretreated effluent applied at a higher hydraulic loading rate (HLR). Multicomponent surrogate and tracer tests were conducted by adding the conservative tracer bromide and the viral surrogates MS-2 and PRD-1 to the applied effluent.

At the completion of the study, soil cores were collected and analyzed for chemical and microbial constituents. This appendix focuses on the removal of viruses and bacteria in STE applied to these columns with time of operation as well as relatively higher quality effluent dosed onto other columns.

Results demonstrate a maturation of the columns dosed with wastewater effluent with incipient ponding observed in LR1 by week 1, LR2 by week 2, LR3 by week 4 and LR4 by week 6, except for one column where ponding did not occur until week 19. Bromide tracer tests showed an increase in the hydraulic retention time with time of operation for all columns, with the most significant changes observed during the first two weeks of operation for the columns loaded with STE (LR1–LR4). Fecal coliform removal was high (greater than 99% removal) in these STE-loaded columns early on and continued to be so throughout the study.

Results from the pretreated effluent columns showed that, with a limited amount of effluent conditioning of the sand, no visible biozone formation, and no appreciable change in the hydraulic retention times, enhanced removal of virus was observed. The columns loaded with SPE (columns 5A and 5B) showed the most dramatic changes in the hydraulic regime after the first six weeks of operation. Lower fecal coliform removal was observed in these two columns and the added bacteriophages, MS-2 and PRD-1, showed substantial breakthrough in the clean-water tracer test conducted just prior to the addition of percolate. High removal of added virus was observed in both columns by the week 1 tracer test. This result suggests that an increased removal of virus may not be attributed to hydraulic changes, but to the conditioning of the porous media that results from dosing the columns with percolate from columns dosed with STE (lower pollutant concentrations than STE). While lacking a visible biozone at the infiltrative surface or a flow regime change indicative of biozone development, conditioning of the sand is important to the removal of viruses in such systems. The importance of a developed infiltrative zone and its impact on removal rates and the hydraulic character of these systems were examined on a smaller scale as presented in the following section (Van Cuyk 2003).

Fate of Viruses in WSASs: Mini-Column Studies

Wastewater systems for onsite and small-scale applications are commonly designed for intermittent dosing of primary treated wastewater into natural soil where it infiltrates and percolates through the vadose zone before it recharges into the underlying groundwater. These systems are widely used due to their high purification performance with respect to organics, solids, and nutrients, with relatively low cost and limited operation and maintenance requirements. However, with such systems increasingly being used as permanent solutions for wastewater treatment and at increasing numbers and densities, there is a growing awareness and concern over system performance with respect to bacteria and virus.

Since human pathogens are known to exist in sewage effluents, their removal during soil treatment of wastewater is essential in preventing contamination of groundwater, which can be used for drinking water purposes. There have been incidences of disease outbreaks by contaminated drinking water due to the source waters being contaminated (Craun 1985, US EPA 2000). In fact, some investigators have claimed that septic systems are the most frequently reported cause of groundwater contamination associated with disease in the US (Powelson and Gerba 1994).

Virus transport distance and transport times estimated by models are extremely sensitive to the choice of attachment and inactivation rate coefficients (Yates 1995, Navigato 1999). These parameters and the processes that control attachment and inactivation are not readily available or well understood, particularly for soil systems used to treat domestic wastewater effluent onsite. This appendix describes laboratory experiments that attempt to understand what controls the natural disinfection of virus in the subsurface, primarily in soils receiving STE.

Figure B-13 presents a generalized schematic of a soil-based treatment system. These systems include a broad spectrum of types and designs. Soil may be used to treat high-quality effluent (such as sand filter effluent) that may have low levels of carbon, nutrients, and pathogens, or it may be used to treat primary effluent (such as STE) that contains high levels of carbon, nutrients, and bacteria. The underlying soil and groundwater may or may not be changed by the applied effluent.

Important areas for treatment in these systems include the

- Biozone, which may be formed at the infiltrative surface
- Vadose zone, the depth of which may vary from one foot or less to many hundreds of feet
- Saturated groundwater zone

The groundwater transport distance to receptors from such a system can vary anywhere from hundreds of feet to miles.

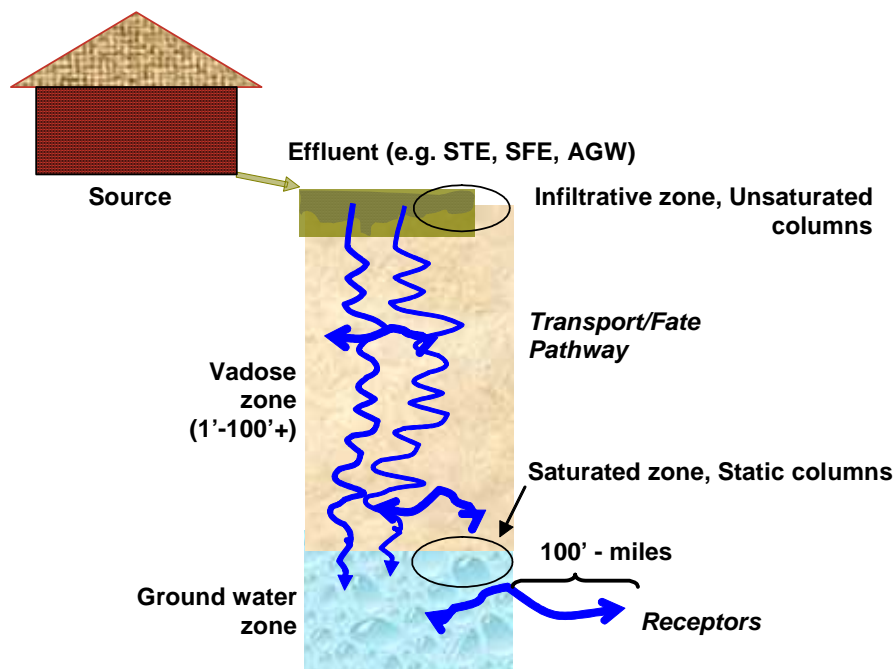


Figure B-13
General Schematic Showing Components of a Soil-Based Treatment System

In order to address the issue of virus fate and transport, information on attachment and inactivation/die-off behavior has been gathered in the laboratory using material and temperatures representative of field conditions following established methods (Harvey 1997a, b; Van Cuyk *et al.* 2001; Navigato 1999; Loveland 1996). Similar to the 1-D column experiment, two bacteriophages, MS-2 and PRD-1, were used as surrogates for human pathogenic enteric viruses (see the Virus Surrogate and Tracer Tests section). The removal of viruses in non-disinfected wastewater effluent released into the subsurface may depend almost completely upon the permanent attachment of viruses to subsurface solids and/or their inactivation due to strong intersurface forces occurring during reversible or intermittent attachment. Models that are utilized to predict the transport of virus must include the loss of virus from soil solution or groundwater due to the attachment based on the physical and chemical properties of the soil and the groundwater.

The column work presented here examines the pH-dependency of virus attachment behavior using small, static mini-columns that are filled with medium sand that has been used previously in laboratory studies (Van Cuyk *et al.* 2001). The effect of temperature, pH, and the presence of organic carbon on attachment was studied. In addition, the effects of different porous media and various carrier solutions (groundwater and STE) on the removal of viruses at the infiltrative surface were investigated. This work involved a novel unsaturated column assembly used to simulate the infiltrative surface alone. This assembly used a vacuum manifold to simulate underlying unsaturated soil, which allowed for the collection of percolate samples immediately below the infiltrative surface.

Materials and Methods

Two bacteriophages, MS-2 and PRD-1, were used in this study as models for human pathogenic enteric viruses (see the Multicomponent Surrogate and Tracer Test section). Liquid samples and extracted soil core samples were analyzed for these bacteriophages following the PFU technique as described by Adams (1959). For this assay, all samples were serially diluted in phosphate buffered saline (PBS), plated with the bacterial host on a layer of agar and incubated overnight at 37 °C. Plates were enumerated by counting plaques formed in the host lawn. MS-2 and PRD-1 bacteriophages and host bacteria were obtained from the United States Geological Survey (USGS) in Boulder, CO. Viruses were added to applied effluent (STE, dilute STE, or artificial groundwater) at target concentrations of approximately 10^4 – 10^7 PFU/mL.

Static Saturated Mini-Columns

Static columns have been used by researchers in the past and are advantageous because they allow for equilibrium attachment studies to be conducted at solid-solution ratios that are similar to the soil groundwater environment (Loveland 1996, Harvey 1997a, Navigato 1999). Since energy is not added to the system, Brownian diffusion is the only mechanism transporting the viruses in groundwater to the soil surface. That the flow is only in the downward direction may alter the dispersion of viruses and their attachment on grain surfaces. Loveland noted that the lack of tangential flow in these columns may alter the distribution of viruses as compared to natural groundwater settings (Loveland 1996), but for this research, which is focused on the vertical entry into the groundwater zone (see Figure B-13), the columns are ideal.

Static columns used in this investigation were prepared as described by Loveland (1996) (Figure B-14). Briefly, the column materials (50 mL glass syringe, Popper and Sons) were rinsed with deionized water and then soaked for three hours in 0.1M hydrochloric acid (HCl) to remove trace metals. Residual organic matter was oxidized by baking the columns overnight at 450 °C. The same procedure was used for the polypropylene mesh placed at the base of the columns.

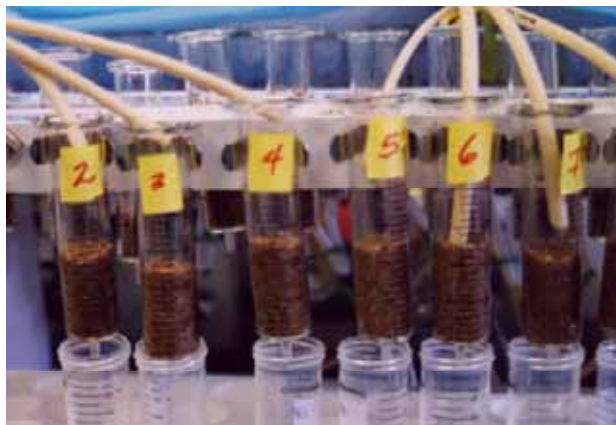
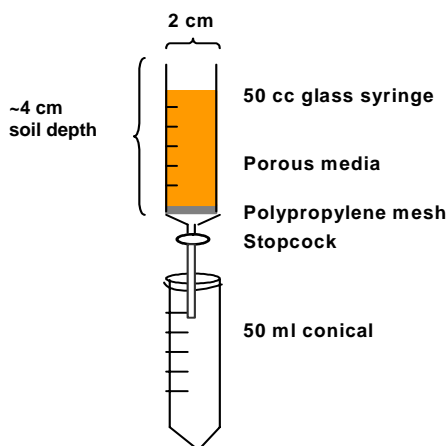


Figure B-14
Static Mini-Column Assembly Used for Saturated Conditions Experiments

These columns were then packed with approximately 10g of moist sand (10% water content, dry wt %). This sand has the following characteristics (Sheldon 1999, Van Cuyk *et al.* 2001) (Table B-5):

- $d_{10} = 0.22$ mm, $d_{60} = 0.60$ mm
- pH = 6.8
- total organic carbon (TOC) = 0.017 dry wt %
- $K_{sat} = 0.032$ cm sec⁻¹

Elemental analyses were made using a JEOL JXA-840 scanning microanalyzer at the Colorado School of Mines (CSM). Columns were equilibrated to the desired pH by flushing with groundwater or other dilute STE matrix at the pH of interest until flow through pH values were within 0.5 pH units of the desired value. When necessary, the pH of the aqueous matrix was adjusted by adding sodium hydroxide (NaOH) or HCl. pH values were measured using an electrode.

Table B-5
Soil Physical and Chemical Properties

Soil Properties	Units	Sand	Silty Sand
Dry bulk density ^a	g/cm ³	1.70	1.68
Organic carbon content ^b	Dry weight %	0.00130 (0.0169) ^c	0.226 (+/- 0.009)
pH		6.8	6.5
Metal elemental composition	Dry weight % ^d	Al 8.182 (0.779)	Al 7.574 (0.602)
		Ca 0.360 (0.268)	Ca 2.476 (0.309)
		Fe 4.138 (0.642)	Fe 3.432 (0.625)
		Mg nd	Mg 0.952 (0.344)
		Si 33.076 (1.012)	Si 28.21 (0.806)

^a Dry bulk density = dry soil mass/ volume of soil

^b Mean percent organic carbon content (+/- one standard error)

^c +/- 0.0015 (from Sheldon 1999)

^d Mean percent (5 replicates) measured by scanning microanalysis (+/- one standard error); nd = non-detect

Artificial groundwater (AGW) was prepared in the laboratory following the method of Struse (1999). The final composition of the AGW was (see Table B-6):

- 0.83 mg/L KCl
- 1.0 mg/L NaNO₃
- 1.28 mg/L FeCl₃

- 68.8 mg/L MgCl₂
- 104 mg/L CaSO₄

STE was collected from a multifamily housing unit and characterized for chemical and biological properties, revealing the following average concentrations:

- TSS = 69 mg/L
- cBOD₅ = 227 mg/L
- TN = 57 mg-N/L
- TP = 4.6 mg-P/L
- fecal coliforms = 5.4×10^5 cfu/100mL

Table B-6
Properties of Septic Tank Effluent and Artificial Groundwater Used in Mini-Column Studies

Parameter	STE ^a	AGW
Alkalinity (mg-CaCO ₃ /L)	209	40
cBOD ₅ (mg/L)	276	–
COD (mg/L)	504	21.7
DOC (mg/L)	4	–
TS (mg/L)	585	237.5
TSS (mg/L)	60	5
FC (colony forming unit/mL)	2.2×10^5	nd
pH ^b	Approximately 6.8	6.0

^a Average values presented

^b Static saturated mini-columns had pH values adjusted

nd = non detect

– = not measured

In the static mini-columns, run under saturated conditions, STE was diluted 1:100 in AGW and dissolved organic carbon (DOC) was added as citric acid to a final concentration of 4 mg/L. This value for DOC represents the level measured in STE collected by the CSM research group and values measured by Pieper *et al.* (1999) in the groundwater collected from a sewage contaminated zone of an aquifer at a field site on Cape Cod, MA. Diluting the STE allowed for low concentrations of solids, BOD₅, nitrogen, and phosphorous in the aqueous matrix while keeping fecal coliform levels high (approximately 5×10^3 cfu/100mL). Addition of DOC to 4 mg/L, in the saturated mini-column, allowed for simulation of a STE-impacted soil for use in comparing the impact of organic carbon on the removal of virus in this portion of the system.

After columns were equilibrated and saturated, the liquid meniscus was brought to a level just above the soil grains at the upper end of the column and one pore volume of virus solution (in either diluted (1:100) STE with 4 mg/L DOC or AGW, at desired concentration and pH) was added. The pore volume was calculated gravimetrically. The virus suspension was drawn into the column by opening the clamp at the bottom of the column and draining slowly one pore volume of liquid (over approximately one minute). Static columns were run at either 6 °C or 23 °C. These columns were not cloaked.

Once the solution containing the added viruses was delivered onto the columns, the columns were allowed to equilibrate overnight. Samples were then taken by draining off the interstitial groundwater after adding one pore-volume (approximately 2 mL) of the sample matrix (AGW or diluted STE with 4 mg/L DOC) to the top of the column. Columns were run in replicates of six and, unless otherwise noted, values shown are the average of these six columns.

Percent attachment was calculated using the following equation (Loveland 1996):

$$\% \text{ Attachment} = 100 \times \frac{C_o - C_{fl}}{C_o} \quad \text{Equation B-4}$$

where C_o is the initial concentration of virus (or bacteria) (PFU/mL) added and C_{fl} is the concentration of virus (or bacteria) measured in the sampled solution (first pore volume collected, PFU/mL).

Inactivation rates for each virus under various conditions can be calculated from these controls by graphing infective virus in each sample over time. Inactivation is assumed to be a first-order kinetic process described by the following equation (Gerba *et al.* 1991, Powelson and Gerba 1994):

$$C = C_o e^{-k_i t} \quad \text{Equation B-5}$$

where C is the concentration at time t (PFU/mL), C_o is the initial concentration (PFU/mL) and k_i is the inactivation rate (time⁻¹).

Unsaturated Mini-Columns

Unsaturated mini-columns were prepared in the same manner as the saturated static mini-columns as described in the Column Preparation and Operation section. Columns were packed with approximately 10 g of sand or silty sand. Physical properties of the sand and silty sand have been characterized previously by Sheldon (1999) (Table B-5).

After packing, columns were upflow saturated with deionized water and approximately five pore volumes were flushed before allowing downflow of water. Column experiments were designed in a full 2⁴ factorial design (Table B-7), with effluent (STE [straight] or AGW [at pH 7]) dosed onto the sand or silty-sand columns at a rate of either 5 or 25 cm/day. Columns were dosed in equal doses, for a total of 4 or 24 such doses per day.

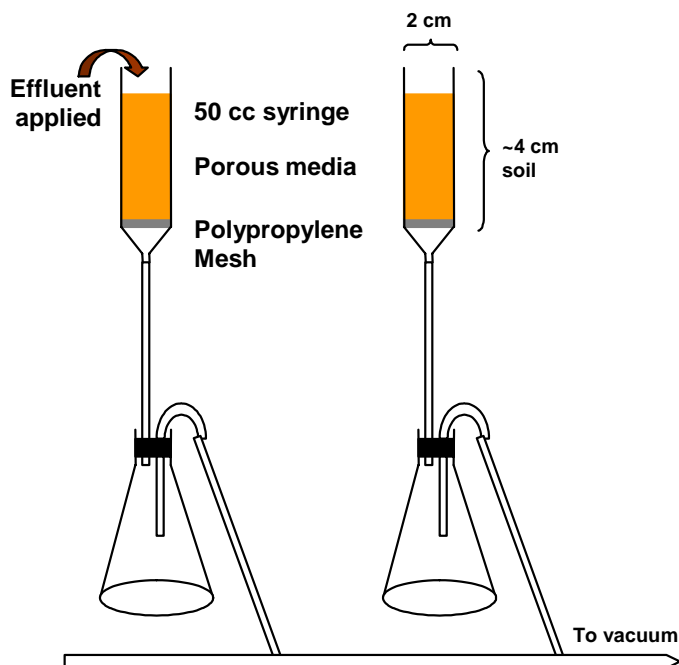
A vacuum was pulled under each column during each dosing period and for five minutes following dosing. This applied vacuum pulled a consistent suction equivalent to that of approximately 60 cm of unsaturated soil (see Figure B-15 for the unsaturated mini-column apparatus). All dosing and delivery of effluent was automated using a programmable Chronotrol device. AGW pH 7 was made daily from stock solutions. STE was collected weekly and stored quiescent and cloaked at 18 °C.

Table B-7
Replicated 2⁴ Full Factorial Design of Flow-Through Unsaturated Mini-Column Experiments

	Column #	Effluent	Porous Media	HLR (cm/day)	Dose (#/day)
Run 1	1–3	AGW	Sand	5	4
	4–6			25	4
	7–9			25	24
	10–12			5	24
Run 2	1–3	STE	Sand	5	4
	4–6			25	4
	7–9			25	24
	10–12			5	24
Run 3	1–3	STE	Silty sand	5	4
	4–6			25	4
	7–9			25	24
	10–12			5	24
Run 4	1–3	AGW	Silty sand	5	4
	4–6			25	4
	7–9			25	24
	10–12			5	24

Note: All columns run in triplicate.

Soil depth in mini-columns was approximately 4 cm, representing the infiltrative surface zone of a WSAS.



Note: Vacuum manifold designed to simulate approximately 60 cm of unsaturated soil

Figure B-15
Unsaturated Mini-Column Apparatus

During tracer tests, MS-2 and PRD-1 were added directly to the column dose pot. Effluent, with MS-2 and PRD-1 added, was dosed for a full 24-hour period. Dose pot samples were collected and analyzed at the start ($t = 0$) and at the end ($t = 24$ hr) of delivery of the virus. Little soil free inactivation was observed in this 24 hour period, but in cases where measured concentrations of added virus differed in the liquid samples collected at the start and at the end of the 24-hour period, average values were used for the initial concentration of virus in removal calculations. At the end of addition of the virus, all effluent delivery lines were flushed with virus-free AGW or STE.

Percolate samples were collected from each column at six-hour intervals during tracer tests, until low levels of viruses (less than 1 PFU/mL) were measured in samples, at which point collection of samples occurred at 12 or 24 hour intervals. Samples were stored at 4 °C and plated for MS-2 and PRD-1 infective units (PFUs) within 48 hours of collection. The first tracer test commenced at a time point that represents one week of operation at 5 cm/day or 25 cm/day of effluent loading. The second tracer test commenced at week six of column operation. Surrogate tracer tests occurred at these time points in order to gain an understanding of the early development of the infiltrative surface.

Percent removal was calculated in the same manner as during the 1-D column experiment as described in the Multicomponent Surrogate and Tracer Test section using Equation B-1.

Column dismantling occurred at week 10 of column operation for all columns except for columns in run 2. Run 2 columns were dismantled following 11 weeks of operation. Prior to coring, the column dosing was ceased and the columns “rested” for approximately 2.5 hours before dismantling.

All of the soil was aseptically removed from columns, mixed using sterile utensils, and divided into three subsamples. The first portion was used for water-content analysis. This soil was added to preweighed aluminum weigh boats, dried at 105 °C overnight and percent water content calculated on a dry weight basis (APHA 1998).

The second portion was added to a sterile conical and extracted using 1.5 wt % beef extract solution (1:10 w/w soil: beef extract), shaken on an orbital shaker for two minutes at 250 rpm, followed by one minute of settling after which a supernatant subsample was taken and analyzed for fecal coliform bacteria (via membrane filtration, APHA 1998), heterotrophic plate count (HPC) (APHA 1998), and MS-2 and PRD-1 bacteriophage. Numbers of bacteria and virus found in the extracted soil supernatant were converted to number per gram dry soil via the water-content values. The third portion of soil was stored at 4 °C for possible future analysis.

Analysis of many of the results was conducted using analysis of variance. In all cases the confidence limit was 95%. This work was performed using Microsoft Excel.

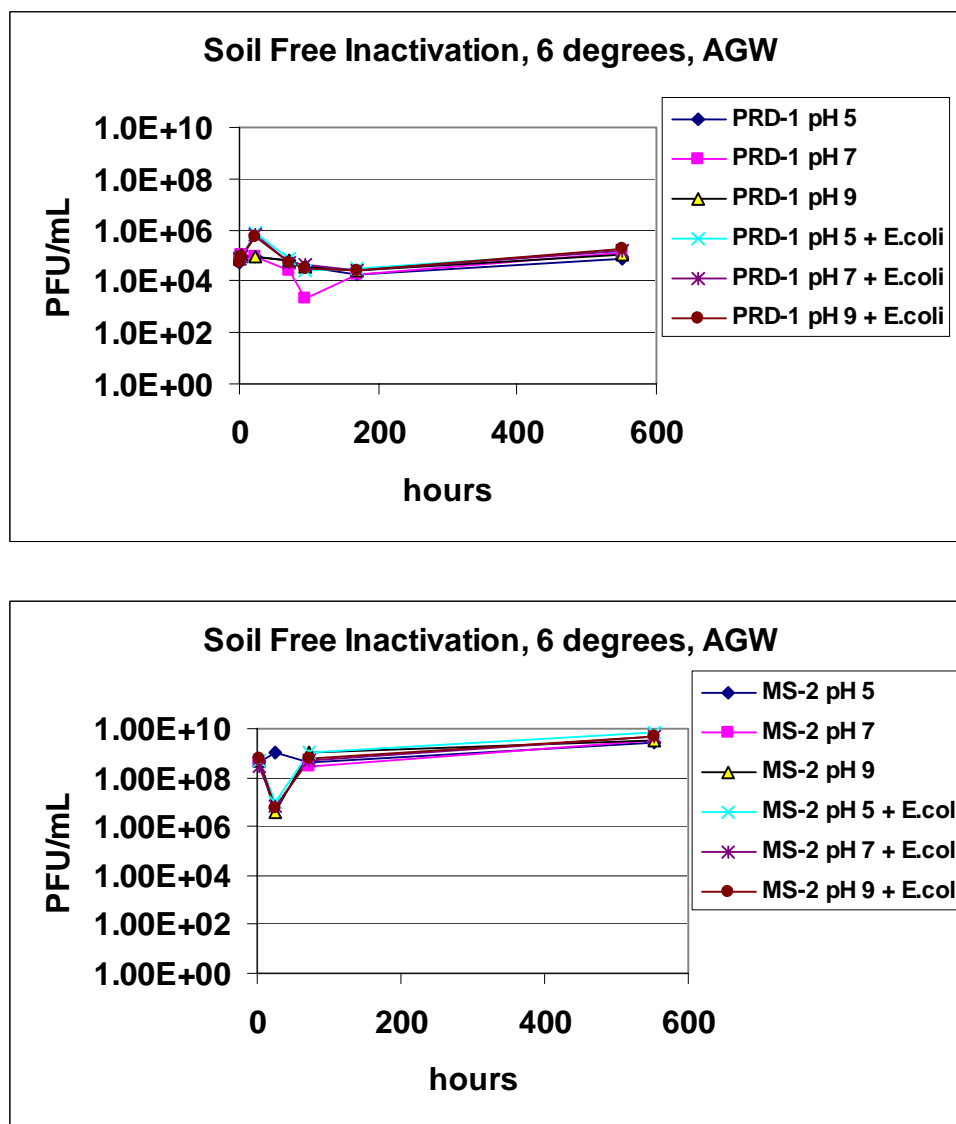
Results and Discussion

This section provides information regarding:

- Virus inactivation rates
- Virus attachment under saturated conditions
- Virus removal at the infiltrative surface
- Characterization of media from the unsaturated columns

Virus Inactivation Rates

Experimental controls in soil-free systems (glass 50-cc syringe columns without soil added) were used to gain an understanding of the inactivation rate of MS-2 and PRD-1 at two temperatures, 6 °C and 23 °C. Results for experiments run at 6 °C are shown in Figure B-16. These experiments were also conducted with the addition of *E. coli*, to determine if the presence of these bacteria (at a concentration of approximately 10⁶ cfu/mL) had any impact on the inactivation or growth of the two viruses. There appears to be no difference in inactivation in the presence of *E. coli*. The results for 23 °C are presented in Figure B-17.



Note:

E. coli was added to some columns to a final concentration of 10^6 cfu/mL.

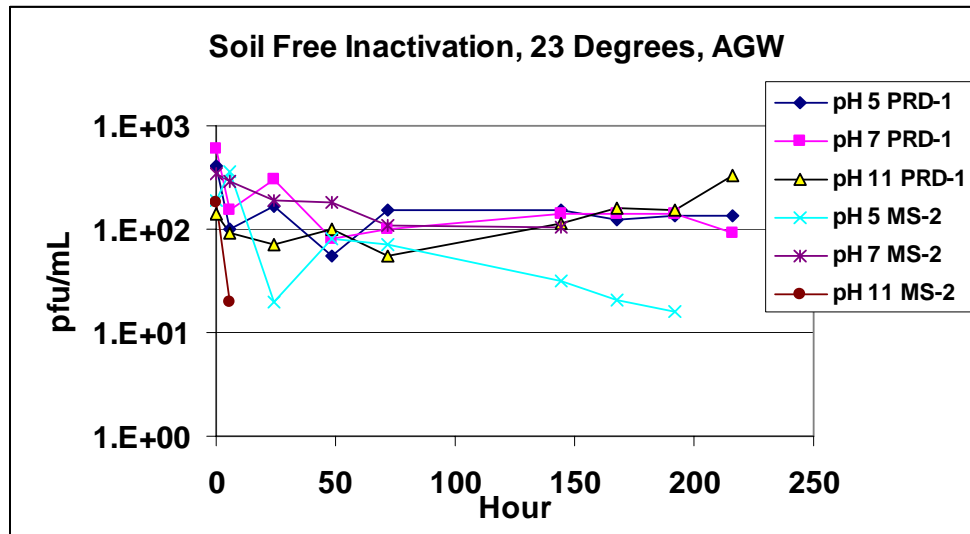
Six columns were run for each condition.

Average values are shown.

Initial concentrations ($t = 0$) ranged from 5.6×10^4 to 7.8×10^4 for PRD-1 and 2.9×10^8 to 6.2×10^8 for MS-2.

Figure B-16

MS-2 and PRD-1 Inactivation in Soil-Free Columns at 6 °C at pH 5, 7, and 9 in Artificial Groundwater



Note: Initial concentrations ($t = 0$) for PRD-1, 1.4×10^2 to 6.0×10^2 and MS-2, 1.8×10^2 to 3.4×10^2

Figure B-17
MS-2 and PRD-1 Inactivation in Soil-Free Columns at 23 °C at pH 5, 7, and 9

The literature suggests that little temperature-induced inactivation will be observed at temperatures below approximately 10 °C. In this study, minimal differences were observed over the course of inactivation rate experiments conducted in soil-free matrices at 6 and 23 °C. Therefore, most subsequent experiments were conducted at 23 °C unless otherwise noted.

As Table B-8 presents, there is a large range of inactivation rates found in the literature. The data collected and calculated inactivation rates from soil-free experiments and in the lysimeter studies are within the range of values found in the literature.

Table B-8
Calculated Inactivation Rates ($-k_i$) for Viruses Observed in This Study and Reported by Other Investigators Under Various Conditions

Researcher	Porous Media?	Temp (C)	Rates ($-k_i$) (day ⁻¹)	Virus	Comments
Reddy <i>et al.</i> 1981	Yes and No		0.04–3.69	many	Compilation of data
Bertucci <i>et al.</i> 1974	No	12	2.21	echovirus 11	Anaerobic digestion
	No	12	2.53	MS-1	Anaerobic digestion
Larkin <i>et al.</i> 1976	Yes	12(?)	0.1	poliovirus	Soil flooded with inoculated, non-chlorinated secondary effluent

Table B-8
Calculated Inactivation Rates (-k_i) for Viruses Observed in This Study and Reported by Other Investigators Under Various Conditions (Cont.)

Researcher	Porous Media?	Temp (C)	Rates (-k _i) (day ⁻¹)	Virus	Comments
Navigato 1999	No	5	0.022	PRD-1	Contaminated groundwater
	No	5	0.056	PRD-1	Radiolabeled phage
	No	5	0.083	MS-2	Contaminated groundwater
	No	5	0.093	MS-2	Radiolabeled phage
Yates 1995	No	4	0.018–0.15	MS-2	Groundwater
Powelson <i>et al.</i> 1990	No	4	0.041	MS-2	Groundwater
Powelson <i>et al.</i> 1993	No	7	0–0.092	MS-2, PRD-1	Groundwater
Schijven <i>et al.</i> 1999	No		0.12	PRD-1	Groundwater
	No		0.030	MS-2	Groundwater
Van Cuyk <i>et al.</i> 2001	Medium sand	18	0.26–1	PRD-1	Wastewater, to little MS-2 Breakthrough to measure
Van Cuyk 2003	No	23	0.0336	PRD-1, pH 5	AGW ^b
	No	23	0.0552	PRD-1 pH 7	AGW
	No	23	~0 ^a	PRD-1, pH 9	AGW
	No	23	0.02688	MS-2, pH 5	AGW
	No	23	~0 ^a	MS-2, pH 7	AGW
	No	23	~0 ^a	MS-2, pH 9	AGW

^a Not enough virus breakthrough to quantify removal rate

^b Artificial groundwater at pH 7

Figure B-18 takes six inactivation rates (10, 1, 0.1, 0.01, and 0.001) and presents the calculated time to 1- or 4-log removal of viruses using these rates. Depending on the rate of inactivation, 4-log removal of viruses by inactivation can be rapid (many hours to days) or may take years. Therefore, gaining an understanding of other mechanisms of virus removal (for example, adsorption) under various environmental conditions is important.

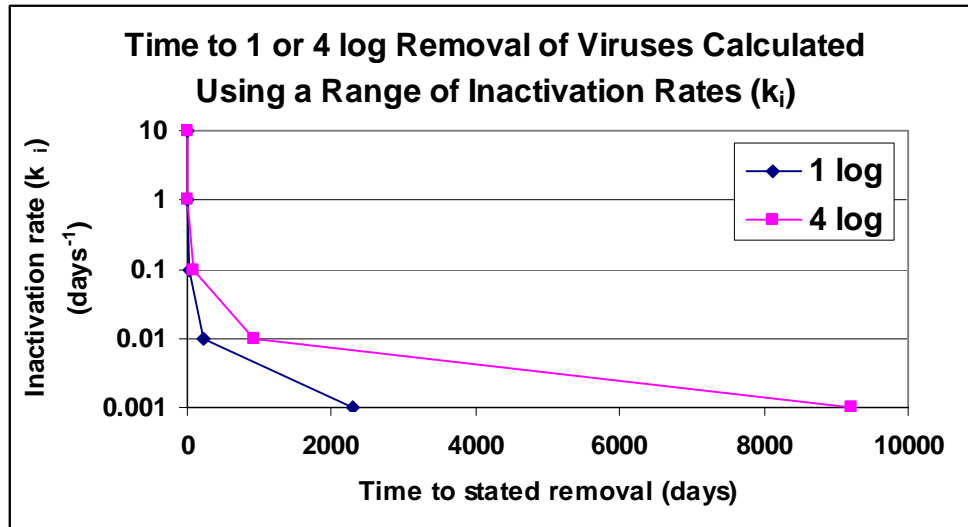
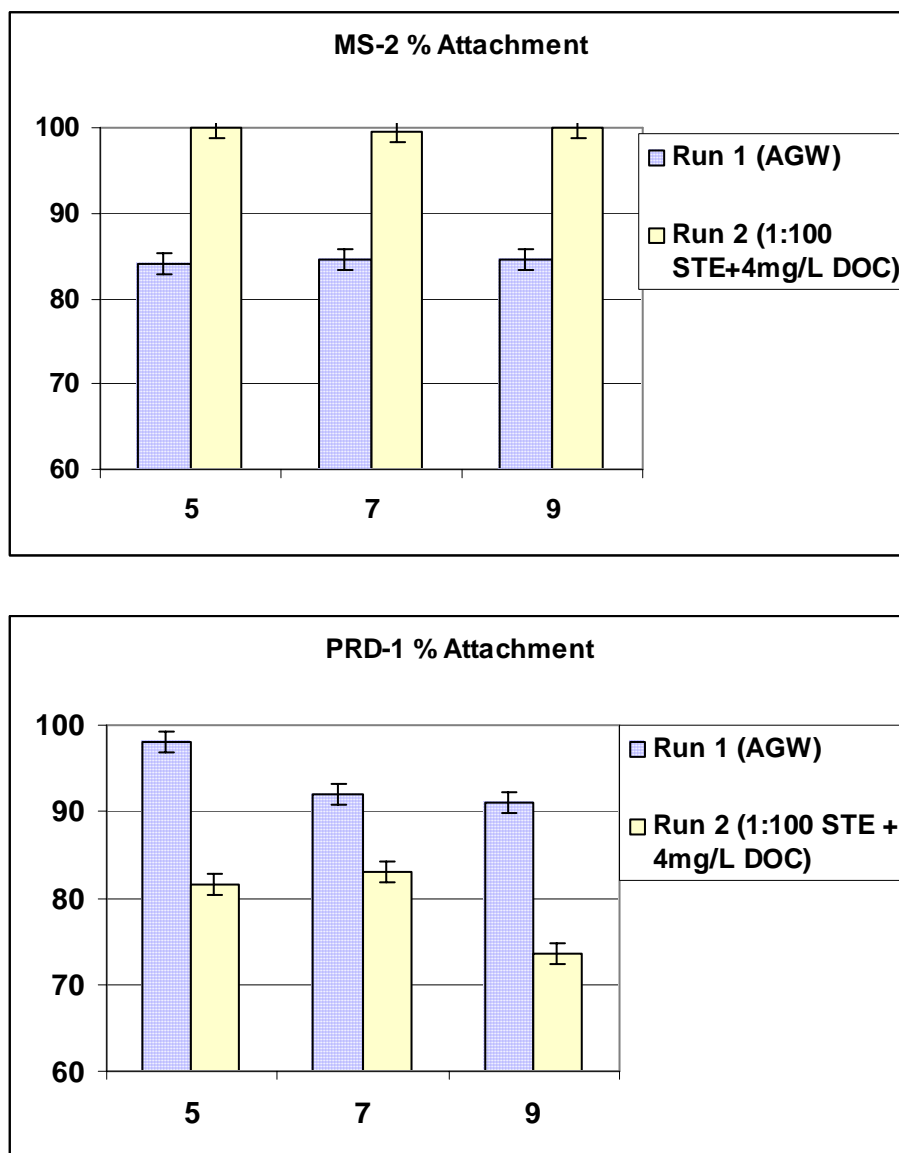


Figure B-18
Time to 1- or 4-Log Removal of Virus Calculated Using a Range of Inactivation Rate (K_i) Values

Virus Attachment Under Saturated Conditions

The pH of groundwater will control the charge on the viruses and the soil surfaces. Most natural waters have pH values that range from pH 5 to pH 9. At these pHs, quartz surfaces will have a negative charge. At pH values above the pH_{iep} for the virus (3.9 for MS-2 and 4.5 for PRD-1), both the virus and the grain surface may be negatively charged and removal of the virus by attachment may be minimal. In some cases, however, the presence of certain minerals (for example, sesquioxides and carbonates) can yield positively charged surfaces in the groundwater pH range and may have a significant impact on the transport of virus (Loveland 1996, Goyal and Gerba 1979). Electrostatic virus attachment may occur when these metal oxides are present and available on soil surfaces (Loveland 1996, Ryan *et al.* 1999).

Figure B-19 presents results for static saturated mini-columns dosed with AGW or dilute STE (1:100 dilution with 4 mg/L DOC) at three different pH values, pH 5, 7, and 9 (each value is the average of six columns). There does not appear to be a significant difference in attachment based on pH. Over the course of this experiment, parallel soil-free column experiments did not show a significant change in virus titer. The increase in removal of virus observed in the soil-filled columns versus soil-free columns is attributed to attachment to soil grains and/or inactivation due to the presence of soil.



Note: Experiments were conducted at 23 °C. Average values shown \pm 1 standard deviation.

Figure B-19
Percent Attachment of MS-2 and PRD-1 in Static Mini-Columns Filled With Medium Sand and Run at pH values 5, 7, and 9

The work of Navigato (1999) using radiolabeled bacteriophages suggests that there may be an increased inactivation of MS-2 and PRD-1 upon passage through a soil column, though no quantification of this process was made. Based on electrostatic interaction, an increase in pH is expected to yield a decrease in virus adsorption to the soil. However, no impact of pH on attachment was seen in this pH range, which is above the pH_{iep} of the viruses and the soil grains. Most of the subsequent experiments presented here were conducted at pH 5–9. This pH range is representative of values found in STE and is within the range of pH values found in most groundwater.

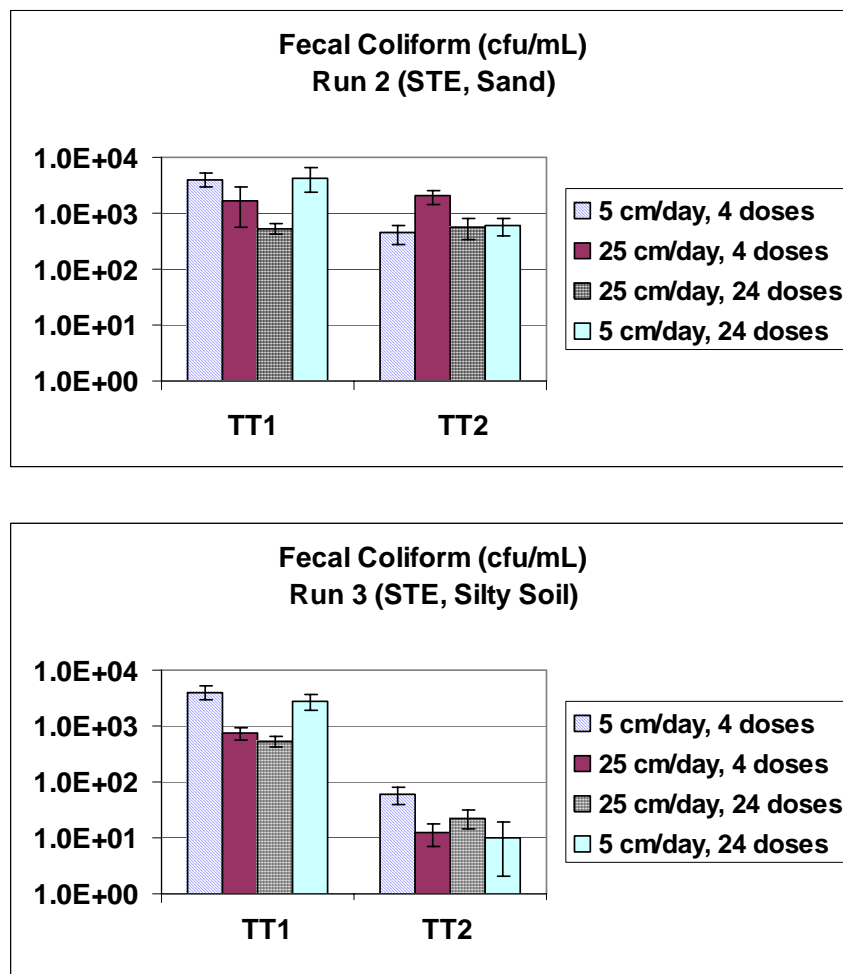
Organic matter may also play an important role in the fate of viruses in the subsurface. Sewage-derived organic matter is an important factor to consider because it is frequently associated with the source of viral contamination. An understanding of the importance of organic matter is vital when considering onsite and other land-based or porous-media wastewater treatment systems. While the interaction of viruses with organic matter is not well understood, studies suggest that organic matter may alter the soil surfaces, adding hydrophobic sites and thereby increasing virus attachment (Bales *et al.* 1993). Other work has shown that organic matter might decrease virus attachment (Sobsey *et al.* 1980, Powelson *et al.* 1991, Pieper *et al.* 1997, Ryan *et al.* 1999) by occupying attachment sites previously available for viruses.

The presence of organic matter may also reverse the surface charge of the soil, which may also yield increased transport. A two-way analysis of variance (ANOVA) was conducted indicating that MS-2 has a statistically significant increase in attachment with change in the carrier fluid (95% confidence level), that is, more MS-2 is removed in the dilute STE with 4 mg/L DOC versus AGW, while the opposite was observed with PRD-1. MS-2 attachment increased with the addition of organic carbon suggesting a beneficial alteration of the soil surfaces due to the presence of this organic carbon. PRD-1 attachment decreased in the dilute STE with DOC columns, perhaps due to DOC-facilitated transport or the “blocking” of virus attachment at the soil surface. Ryan *et al.* 1999 found that PRD-1 attachment sites were blocked by the presence of organic matter.

Virus Removal at the Infiltrative Surface

Unsaturated flow mini-column work was completed to focus on the removal of viruses at the infiltrative surface during early operation of WSASs under various operating conditions (Table B-7). Fecal coliform breakthrough from the columns was measured at the start of each tracer test. Figure B-20 shows the number of fecal coliform bacteria quantified in the percolate of columns dosed with STE (runs 2 and 3) just prior to the addition of virus surrogate tracers to the effluent.

A single-batch sample was collected over a 12-hour interval and the level of fecal coliform was measured in this sample. These results show decrease in fecal coliform breakthrough in the columns that are filled with silty sand with increased time of operation, while little change was observed from tracer test 1 to tracer test 2 in the columns dosed with STE and filled with medium sand. Percent removal of coliform bacteria increased from tracer test 1 to tracer test 2 in both run 2 (98.79% to 99.59%) and run 3 (99.09% to 99.98%).



Notes: Run 2 in medium sand and run 3 in silty sand just before the start of tracer test 1 (TT1) and tracer test 2 (TT2).

Average values for triplicate columns are shown with standard error bars. (Input concentration approximately 2.2×10^5 colony forming unit/mL.)

Percent removal of fecal coliform is presented in the text.

Figure B-20

Concentration of Fecal Coliform Bacteria in Percolate From Columns Dosed With STE

Pore volumes of applied liquid processed by each column regime as of the start of tracer test 1 and tracer test 2 are shown in Figure B-21. At tracer test 1, the 5 cm/day and 25 cm/day columns processed an average of about 60 and 200 pore volumes, respectively. By the time of tracer test 2 the 5 cm/day and 25 cm/day columns processed an average of about 350 and 1,400 pore volumes, respectively.

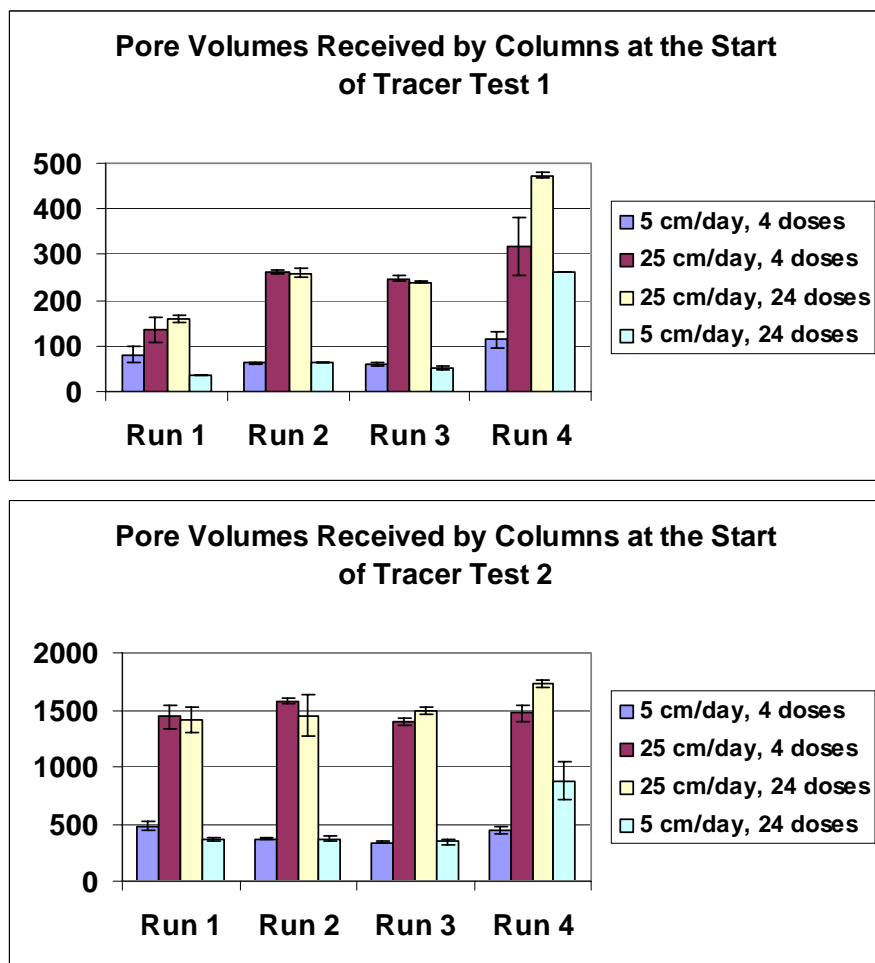
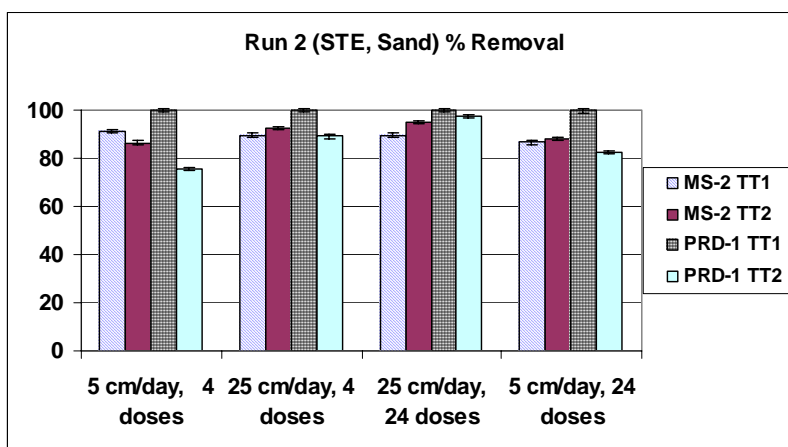


Figure B-21
Pore Volumes of Effluent Received by Each Loading Regime for Each Run

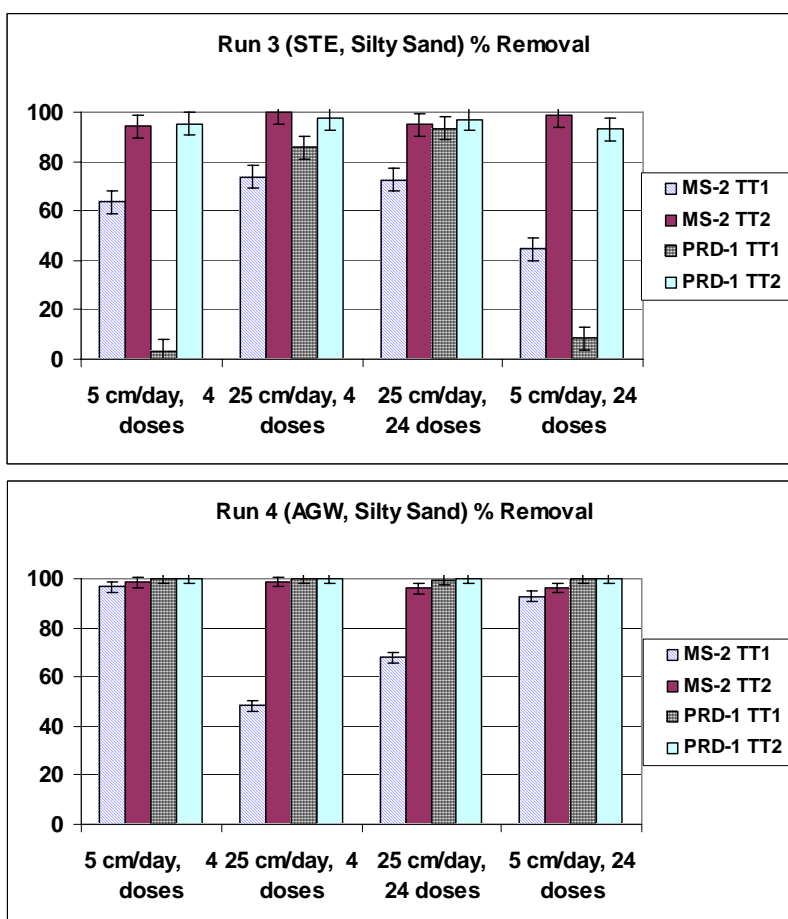
Unsaturated mini-column percent removal of added MS-2 and PRD-1 are shown for all columns in Figure B-22 and Figure B-23. All of the soil percolate volume was collected and analyzed for MS-2 and PRD-1 as were dose pot samples. Runs 1, 3, and 4 show improved removal of added viruses under all conditions with increased time of operation, that is, from tracer test 1 to tracer test 2. The only condition where a decrease in removal was observed with time was in Run 2 (STE, medium sand) where a decrease in the removal of PRD-1 was observed from the first tracer test to the second. No removal of PRD-1 was observed in the columns in Run 1 (AGW, sand) at the first tracer test.

The importance of time of operation in the removal of viruses was discussed previously in the section that described the 1-D column study, with respect to the “conditioning” of the porous media. The addition of AGW to these columns is believed to have been enough to stimulate the microbial community and result in changes in the total biological activity, much like that found in the soil-clogging literature (Gupta and Swartzendruber 1962, Frankenberger *et al.* 1979), even though no visible alteration of the soil was observed. This subject is discussed later in this chapter.



Note: Average values for triplicate columns are shown with pooled standard error. No removal of PRD-1 was observed in these columns during TT1

Figure B-22
Percent Removal of MS-2 and PRD-1 at TT1 and TT2 in All Columns for Run 2



Note: Average values for triplicate columns are shown with pooled standard error.

Figure B-23
Percent Removal From Columns in Runs 3 and 4 for MS-2 and PRD-1 at TT1 and TT2

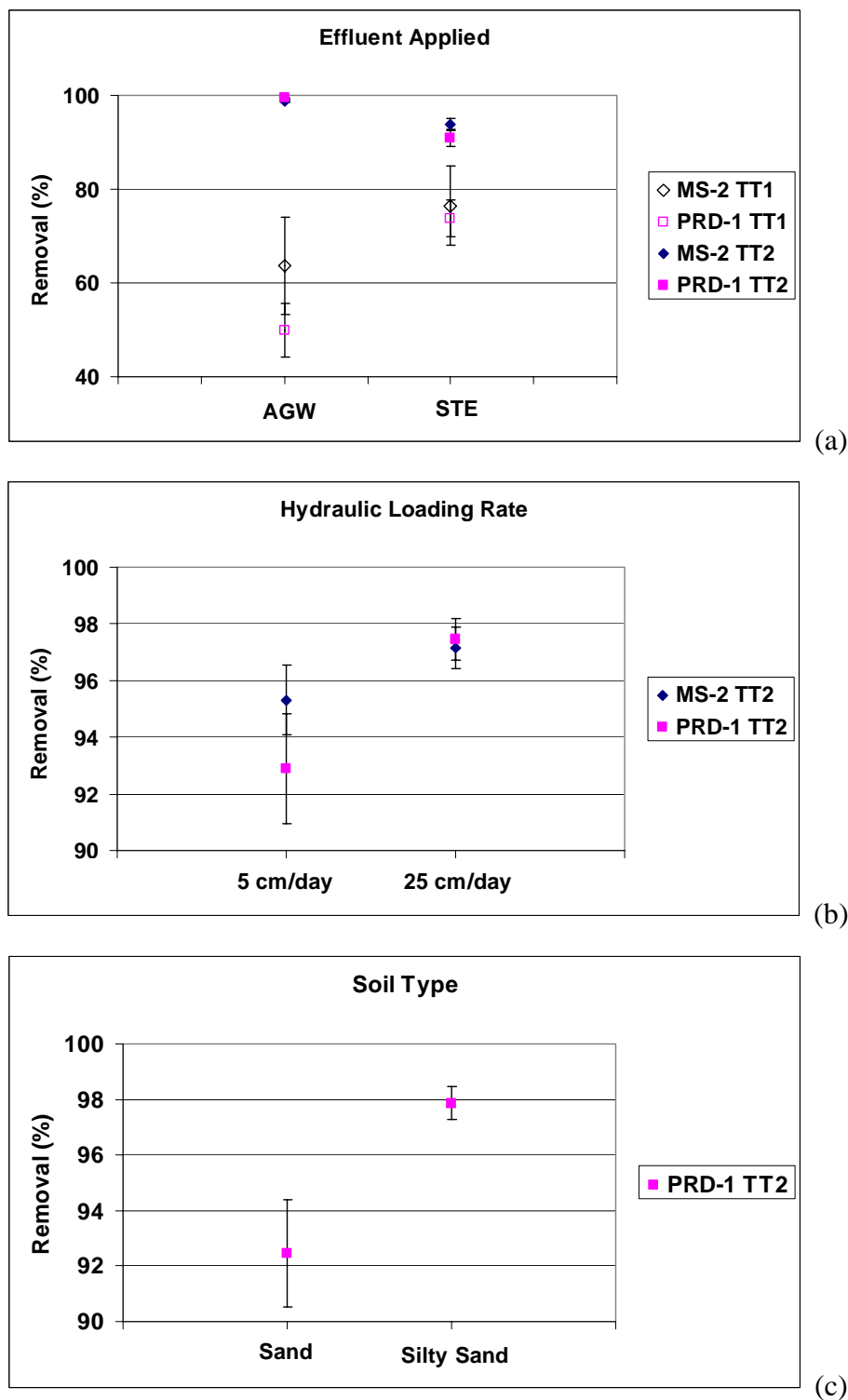
An ANOVA was conducted on the percent removals calculated from these experiments in order to elucidate which factors are important in the removal of viruses. The quality of the effluent applied proved to be important for removal of MS-2 and PRD-1. Figure B-24a shows that when all columns are compared based on effluent applied, there is an increase in the percent of MS-2 and PRD-1 removed from TT1 to TT2. This figure also shows that MS-2 columns at the first tracer test had improved removal when dosed with STE, but by TT2 the MS-2 columns dosed with AGW had significantly higher removal versus those dosed with STE.

Similar results are observed when looking at removal of PRD-1 in these columns. At the first tracer test better PRD-1 removal was observed with STE effluent applied, but by TT2 those dosed with AGW had significantly higher removal of added PRD-1. This change shows an initial benefit (at the time of TT1) of having columns dosed with STE, perhaps by adding hydrophobic sites that result in an increased attachment as suggested by Bales *et al.* (1993). By the second tracer test, the removal is improved in columns dosed with either effluent as compared to the first test, but the removal in AGW-dosed columns is higher. This difference may be due to the stimulation of microbial communities by delivery of effluent or due to the benefit of the presence of salts in the AGW. Previous research has suggested that increasing the concentration of ionic salts and increasing cation valences may enhance virus adsorption (Yates and Yates 1988, Keswick and Gerba 1980, Carlson *et al.* 1968)

Under the conditions studied, hydraulic loading rate also proved to be important in the removal of viruses. While Figure B-24b shows no effect of HLR on removal at the time of the first tracer test, by TT2, columns dosed at the higher HLR (25 cm/day) have improved removal of both MS-2 and PRD-1. The literature suggests the opposite: that an increase in HLR leads to an increase in transport of the viruses (deeper penetration into the porous media). However, a higher HLR may be beneficial to removal of viruses, perhaps due to accelerated soil grain conditioning due to a relatively higher total loading of constituents such as BOD₅.

Soil type impacted the removal of PRD-1 at the time of the second tracer test. Figure B-24c shows that those columns filled with silty sand had higher removal rates for PRD-1 at the time of TT2. The characteristics of the silty sand, such as its higher organic content and higher percentage of hydroxides may be the reasons for the higher PRD-1 removals.

Under the conditions studied there are no apparent difference in removal of virus as a function of dosing, that is, there were no differences observed between columns dosed 4 times daily and those dosed 24 times daily with either bacteriophage at either of the tracer test time points.



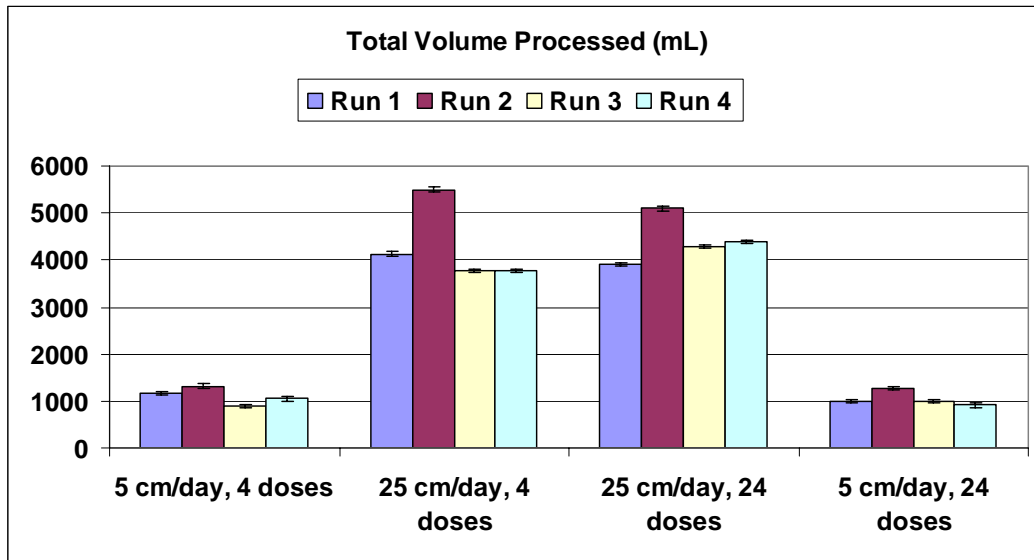
Note: Averages are shown with pooled standard error. $n = 24$. (Note difference in scales.)

Figure B-24

Three Important Factors in the Removal of Viruses in Unsaturated Mini-Columns:
(a) Effluent Applied, (b) Hydraulic Loading Rate, and (c) Soil Type

Characterization of Media From the Unsaturated Columns

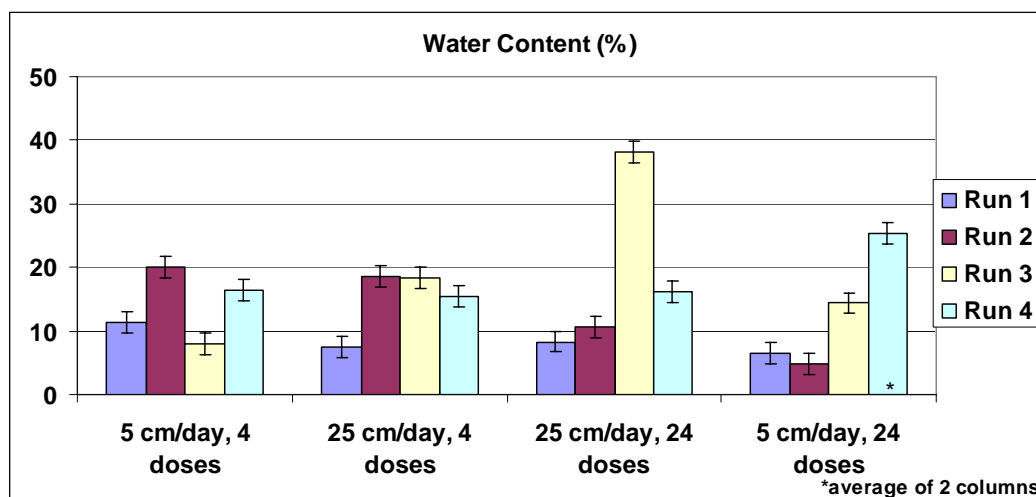
Dismantling of these columns occurred following a time period of dosing representative of 10 weeks of operation. Figure B-25 shows how much effluent was processed by each column over the course of the experiment. As expected, total volumes dosed in Run 2 are slightly higher due to the fact that they were left in operation approximately one week longer than the other columns.



Note: Bars represent average values from triplicate columns with standard error 1 mL processed is equal to a dose of approximately 0.32 cm ($1 \text{ cm}^3/\text{cm}^2 \times (1 \text{ cm})^2$)

Figure B-25
Total Amount of Effluent Applied to Columns in Runs 1–4

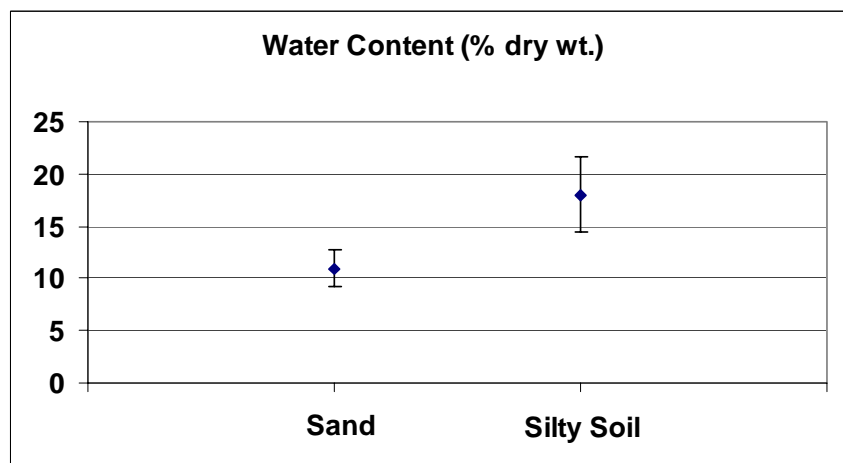
Water content values measured at the time of dismantling are shown in Figure B-26 for all columns. An ANOVA conducted on water content values determined that soil type had the only significant impact on the measured value. Figure B-27 shows higher percentage water content in columns packed with silty sand versus those packed with medium sand ($n = 12$, 95% confidence level). No other factors had a significant impact on the water content of the columns at the time of dismantling.



Note: Averages shown with standard error.

Run 1 = AGW, sand; Run 2 = STE, sand; Run 3 = STE, silty sand; Run 4 = AGW, silty sand

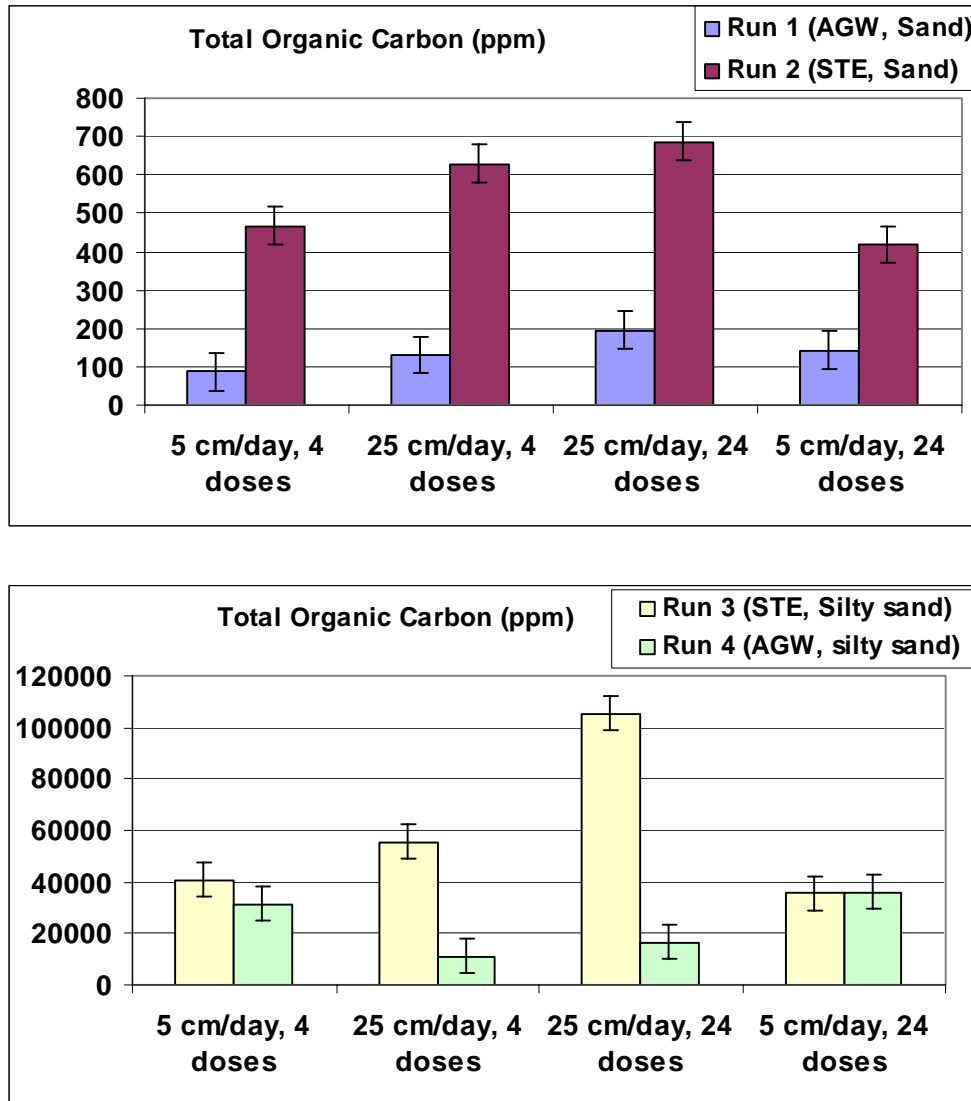
Figure B-26
Water Content (% dry weight) Measured in Columns at Time of Dismantling



Average shown with standard error (n = 12, 95% confidence)

Figure B-27
Importance of Soil Type on Measured Level of Water Content (% dry weight) at the Time of Column Dismantling

TOC levels measured in soil samples are shown in Figure B-28. An ANOVA (n = 12, 95% confidence) conducted on these data shows a significant effect of both soil type and effluent type on the organic carbon in the soil. As expected, higher levels were observed in columns filled with the silty-sand soil and in those columns dosed with STE. Hydraulic loading rate and dosing regime had no statistically significant impact on the TOC values measured at the end of unsaturated mini-column experiments.

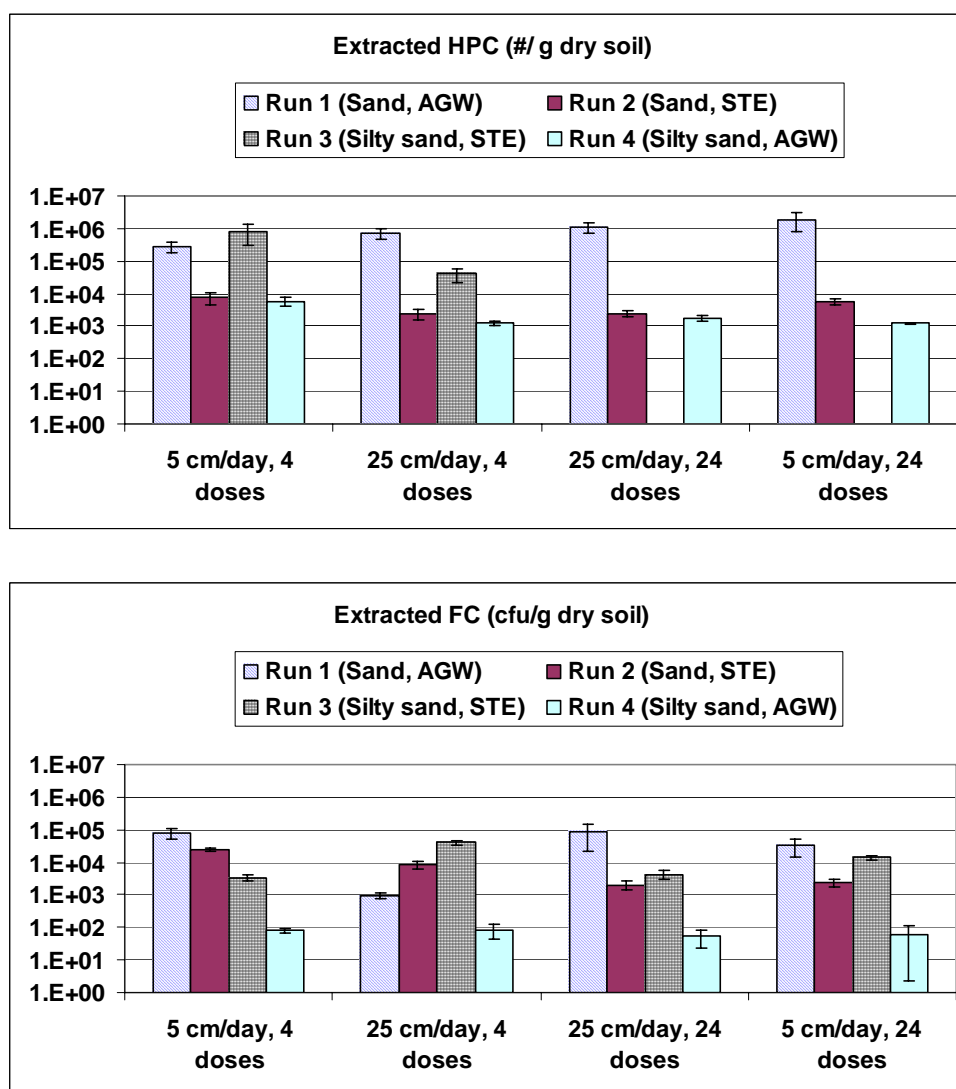


Note: Averages are shown +/- standard error of mean. Note difference in y-axis scales.

Figure B-28

Total Organic Carbon (ppm dry weight) Measured in Soil Samples From Dismantled Columns

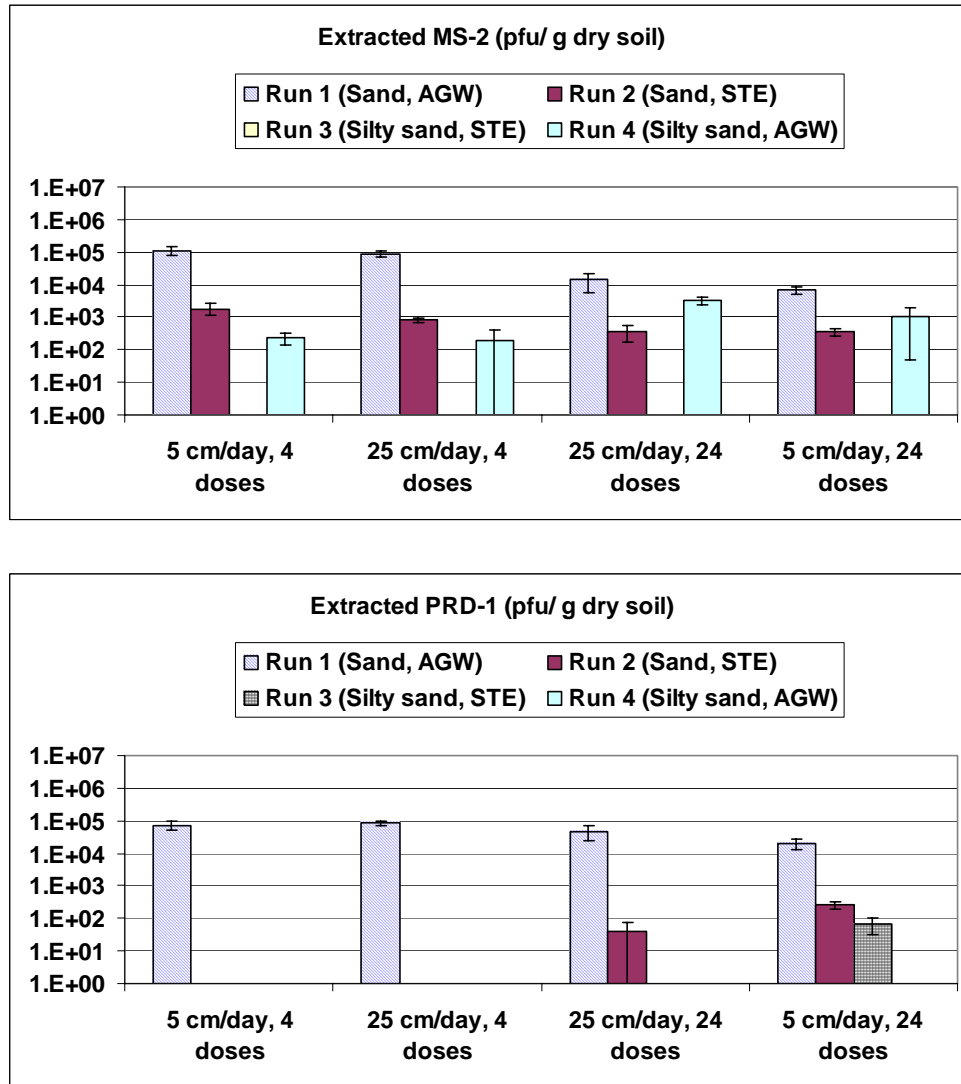
Values of fecal coliform bacteria, heterotrophic bacteria, and MS-2 and PRD-1 extracted from soil columns at the time of dismantling are shown in Figure B-29 and Figure B-30. Consistently, Run 1 columns (sand, AGW) had high levels of extracted HPC and FC bacteria. This result was unexpected and may be due to the stimulation of the bacterial community or due to the efficacy of the method of extraction for recovery of soil-associated bacteria.



Note: Average values shown with standard error.

Figure B-29
Values for FC bacteria and HPC Measured in Soil Sample Extracts

Values of MS-2 and PRD-1 recovered from soil (Figure B-30) represent a small portion of the number of these viruses added to the columns during TT2. The highest values of extracted MS-2 or PRD-1 only represent approximately $1 \times 10^{-4}\%$ of the bacteriophage that was added to the column during the second tracer test alone. Figure B-30 shows little PRD-1 extracted from the columns in Runs 2–4. Run 1 had significantly higher levels of extracted PRD-1.



Note: Average values shown with standard error.

Figure B-30
Values for MS-2 and PRD-1 Measured in Extracted Soil Columns

Comparing the removal of PRD-1 during the tracer tests, initially there was no removal of PRD-1 in the Run 1 columns, then 2-log removal occurred by the second tracer test. This suggests changes in the sand media following continued dosing with AGW. The second tracer test occurred in sand that had been conditioned so that it favored higher adsorption of PRD-1 (as measured by percent removal) and the adsorbed viruses were subsequently removed/extracted via elution with beef extract. The AGW addition may have a two-fold impact on the virus adsorption. The AGW addition may stimulate the microbial community present in the soil leading to increased virus adsorption. Secondly, AGW addition may increase the presence of multivalent cations, altering the electrostatic character of the system, resulting in attachment of the negatively charged virus to the sand. The cations may also link the virus to the porous media by the formation of salt bridges.

Extracted values of MS-2 (Figure B-30) showed that only one run (Run 3, silty sand, STE) had no MS-2 available for extraction via beef extract. Perhaps the presence of organic matter on the soil in combination with that added by STE dosing yielded ineffective extraction of this bacteriophage. Percent removal in these columns did not vary greatly from other column conditions. Run 3 columns extracted for PRD-1 also yield no measurable extracted virus.

Summary and Conclusions

Unsaturated mini-column experiments demonstrated that the removal of viruses within an infiltrative surface zone (of approximately 4 cm) improved over time under conditions studied. The exception occurred in sand-filled columns dosed with STE (Run 2) where the removal of PRD-1 decreased from the first tracer test to the second. These results suggest that under these conditions the presence of dissolved organic matter leads to an increase in the transport of PRD-1.

Statistical analysis conducted on the percent removals calculated from unsaturated column experiments demonstrated that the quality of the effluent applied to the infiltrative surface is important for removal of MS-2 and PRD-1. MS-2 columns at the first tracer test had improved overall removal when dosed with STE, but by the second tracer test the MS-2 columns dosed with AGW had significantly higher removal versus those dosed with STE. Similar results are observed for removal of PRD-1 in these columns, at the first tracer test better PRD-1 removal was observed with STE effluent applied, but by the second tracer test those dosed with AGW had significantly higher removal of added phage. The improved removal viruses when dosing with AGW may be due to the presence of multivalent cations in this matrix. The AGW may stimulate the microbial communities present (as seen in unsaturated column dismantling data) and also beneficially affect the electrostatic character of the system.

Hydraulic loading rate also proved to be important in the removal of viruses. At the time of TT2, columns dosed at the higher HLR (25 cm/day) had higher percent removals for both MS-2 and PRD-1. Soil type altered the removal of PRD-1 at the time of the second tracer test, at which time silty sand had higher removal rates for PRD-1. This result suggests that higher organic matter content of the media may lead to better attachment of viruses to the soil. No significant differences were observed between columns dosed four times daily and those dosed 24 times daily for either bacteriophage at either of the tracer test time points.

These data suggest that over a relatively short period of time (after eight weeks of operation) the infiltrative surface of soil-based wastewater treatment systems can achieve much higher removal than initially measured earlier. Table B-9 shows that TT1 had removals of less than 1-log occur for most conditions (only Run 2 had higher removal, which was 2-log removal for PRD-1). By the time of the second tracer test overall removal had improved in most regimes with 1-log removal most frequently observed in addition to 3- and 4-log average removals. The 3- and 4-log removals were observed for MS-2 in Run 1 (sand, AGW) and for PRD-1 in Run 4 (silty sand, AGW).

One- and 2-log removals were also observed for fecal coliforms in the unsaturated columns at the second tracer test. The low removal of virus under most of the conditions studied at the second tracer test brings forth the importance of the underlying porous media. Removal of viruses in the vadose zone becomes essential if the goal of obtaining at least a 4-log reduction of viruses is to occur in these systems.

Table B-9
Overall Average Removal of MS-2 and PRD-1 in Unsaturated Mini-Column Runs 1–4

	MS-2		PRD-1	
	TT1	TT2	TT1	TT2
Run 1 (Sand, AGW)	50.90 (28.50) ^a	99.99 (0.002)	0	98.71 (1.004)
Run 2 (Sand, STE)	89.28 (2.85)	90.54 (4.22)	99.89 (0.039)	86.22 (9.97)
Run 3 (Silty sand, STE)	63.60 (20.11)	96.94 (5.70)	47.68m (44.99)	95.73 (2.79)
Run 4 (Silty sand, AGW)	76.51 (21.04)	97.46 (1.74)	99.87 (0.43)	99.98 (0.006)

^aValues in parentheses represent 1 standard deviation.

Experimental Data Analysis and Discussion

This section provides information about experimental data analysis and discussion as related to

- Issue of scale
- Modeling virus transport-fate

Issue of Scale

In the three-dimensional (3-D) lysimeter work presented in Van Cuyk *et al.* 2001, after eight weeks of dosing with STE at 5 or 8 cm/d 1-log removal of viruses occurred after travel through either 60 or 90 cm of unsaturated porous media (medium sand). Similar tracer tests conducted in medium sand-filled 1-D columns with 60 cm of unsaturated soil demonstrated much higher removals at the time zero test and even more improved following two weeks of operation with STE loaded at rates of 25 to 50 cm/day.

The reasons for these differences may be due to scale effects. The effect of the fringe, or additional clean infiltrative surface and porous media filter volume on the purification performance should be considered. Higher removal in the 1-D columns may have occurred due to the lack of this “fringe” effect, which is reflected in the volumetric utilization efficiency (VUE) and infiltrative surface utilization (ISU) values being close to one, meaning that all of the infiltrative surface zone and the porous media volume are contacted by applied effluent.

There are always concerns when attempting to scale up from the laboratory scale or even from shorter field scale distances to larger field scales. The removal of viruses in porous media has been suggested to decline with distance. Work conducted by Grant *et al.* (1999) with Norwalk virus particles suggests a fractal model of filtration of virus under saturated conditions that predicts a slow decay in virus concentration with distance. A more resistant population will actually survive and be transported further in theory, which may be due to colloid facilitated transport or virus aggregation. The character of this population may differ greatly from the rest of the population; that is, it may be more resistant to inactivation (at the soil surface and in the pore water) and may have different adsorption characteristics. Therefore, predictions of virus removal at the larger scale may be overestimated if based on these smaller-scale studies. Recognizing this potential for overestimation is important in predicting removals and in calculating set-back distances necessary for protection of groundwater and drinking water supplies.

Modeling Virus Transport-Fate

Using numbers generated from the infiltrative surface column studies (unsaturated mini-columns), a simple model was used to gain an understanding of the importance of the infiltrative surface in the overall removal of viral surrogates in WSASs. This model is a simple spreadsheet model that has been presented previously (Van Cuyk and Siegrist 2001). The model proposes first order removal and divides the WSAS into two sections. The first is the infiltrative zone (IZ), estimated at 4-cm depth and the second is the vadose zone (VZ) at 56 cm (for a total depth from infiltrative surface to groundwater of 60 cm).

Sand was used in these simulations to enable comparison to data collected in the 3-D lysimeters and 1-D column studies. Simulations were run using STE or AGW as the applied effluent with dosing at 5 cm/day and initial virus concentrations of 1×10^7 PFU/100mL.

Equation B-6 was used to calculate k_i values from Run 1 (AGW, sand) and Run 2 (STE, sand) data collected in flow-through unsaturated mini-columns. Calculated k_i values for the infiltrative zone and other input parameters are shown in Table B-10. Initially the IZ was assumed to have removal rates the same as the underlying vadose zone ($k = 0.1 \text{ hr}^{-1}$). Application rate over the design infiltration area (q) was assumed to be 0.208 cm/hr (equal to 5 cm/day), effective porosity (N_e , v/v) was assumed to be 0.2 in both compartments until week 2, where that number was increased to 0.3. The ISU represents the fraction of the infiltrative surface that receives the applied effluent, while VUE represents fraction of the porous media contacted by the applied effluent. The time parameter input for the first order removal equation (Equation B-1) was calculated using the following equation:

$$t = (L * N_e) * (ISU) / (q) \quad \text{Equation B-6}$$

where t is time (hour), L is length of porous media, N_e is effective porosity (v/v), ISU is infiltrative surface utilization (fraction utilized), and q is application rate (cm/hr).

Run 1 (AGW, sand) input parameters (Figure B-31) show the importance of the vadose zone in the early period of operations, but an increase in the importance of the infiltrative zone on the removal of MS-2 and PRD-1 with time of operation. High total removal (4 log and higher) is achieved in these systems by week eight of operation, with most of this removal occurring in the infiltrative zone. Results from Run 2 (STE, Sand) removal rate inputs show that by week eight a 2-log removal of both MS-2 and PRD-1 is achieved, but the importance of the infiltrative zone at this time in the overall removal is less than that of the vadose zone (Figure B-32). These results parallel what was observed in the 3-D lysimeter work (Van Cuyk 2003) where initial breakthrough was observed, followed by 4-log removal of added bacteriophage following a longer period of operation.

Table B-10
Input for Virus Removal Simulation

		Infiltrative zone (0 to 4 cm)		Vadose Zone (4 to 60 cm)	
	Week of operation (at 5 cm/day)	k_1 (hour⁻¹)^a	ISU^b (fraction)	k_2^c (hour⁻¹)	VUE^b (fraction)
MS-2 Run 1 (AGW, Sand)	0.5	0.1	0.05	0.1	0.1
	1	0.3	0.1	0.1	0.2
	2	0.3	0.2	0.1	0.3
	4	40	0.4	0.1	0.6
	8	80	0.6	0.1	0.9
PRD-1 Run 1 (AGW, Sand)	0.5	0.1	0.05	0.1	0.1
	1	0.19	0.1	0.1	0.2
	2	0.19	0.2	0.1	0.3
	4	1.2	0.4	0.1	0.6
	8	2.47	0.6	0.1	0.9
MS-2 Run 2 (STE, Sand)	0.5	0.1	0.05	0.1	0.1
	1	0.57	0.1	0.1	0.2
	2	0.57	0.2	0.1	0.3
	4	0.3	0.4	0.1	0.6
	8	0.13	0.6	0.1	0.9

Table B-10
Input for Virus Removal Simulation (Cont.)

		Infiltrative zone (0 to 4 cm)		Vadose Zone (4 to 60 cm)	
	Week of operation (at 5 cm/day)	k_1 (hour ⁻¹) ^a	ISU^b (fraction)	k_2^c (hour ⁻¹)	VUE^b (fraction)
PRD-1 Run 2 (STE, Sand)	0.5	0.1	0.05	0.1	0.1
	1	1.234	0.1	0.1	0.2
	2	1.234	0.2		0.3
	4	0.6	0.4	0.1	0.6
	8	0.04	0.6	0.1	0.9

^a k_1 values calculated from unsaturated mini-column experiments except week 4 removal rate (k) value, which is the average of weeks 2 and 8 experimentally measured values.

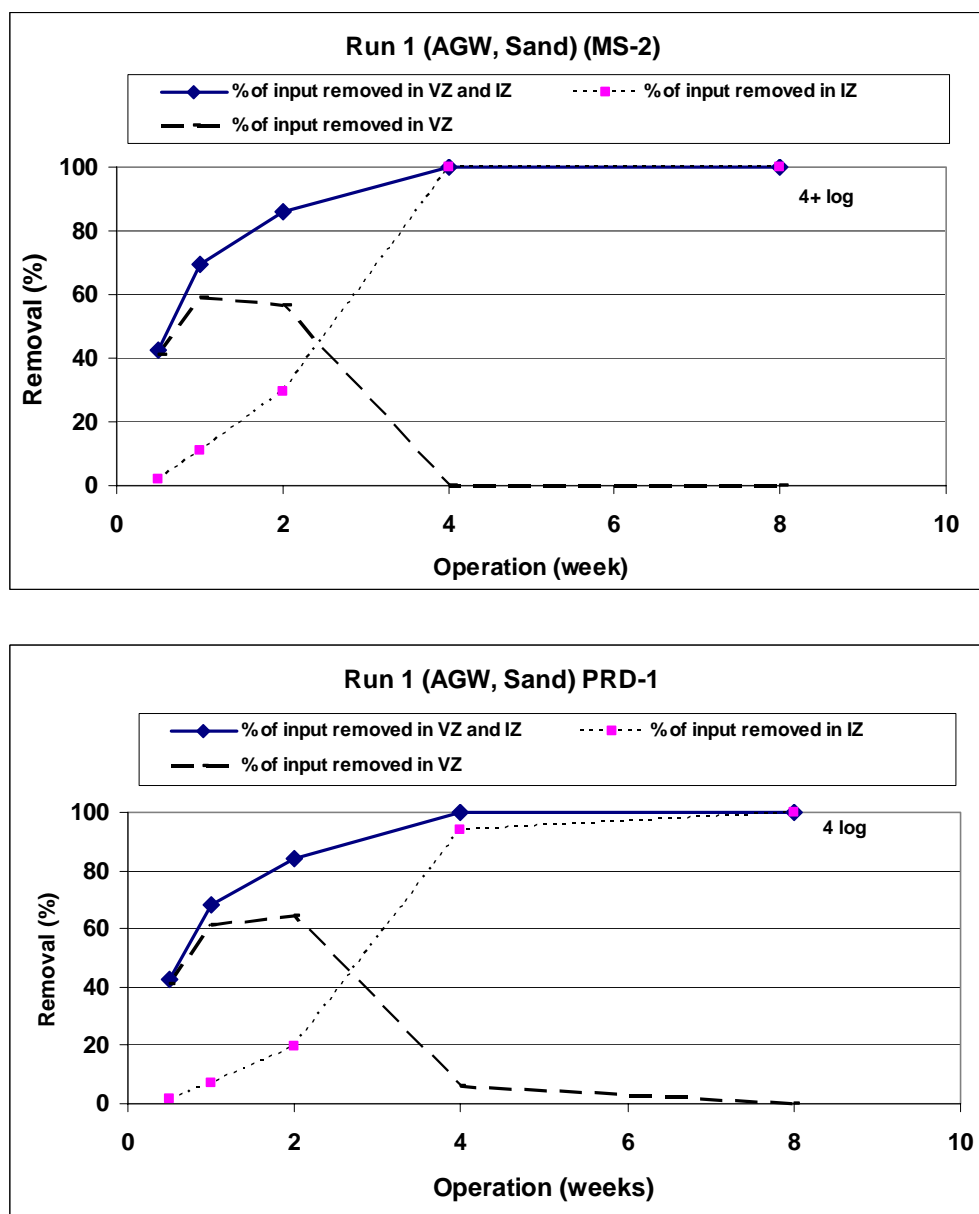
^b ISU and VUE values from observations in lysimeters and literature.

^c Assumed from literature and from Table B-7.

Note: k_i = removal rate

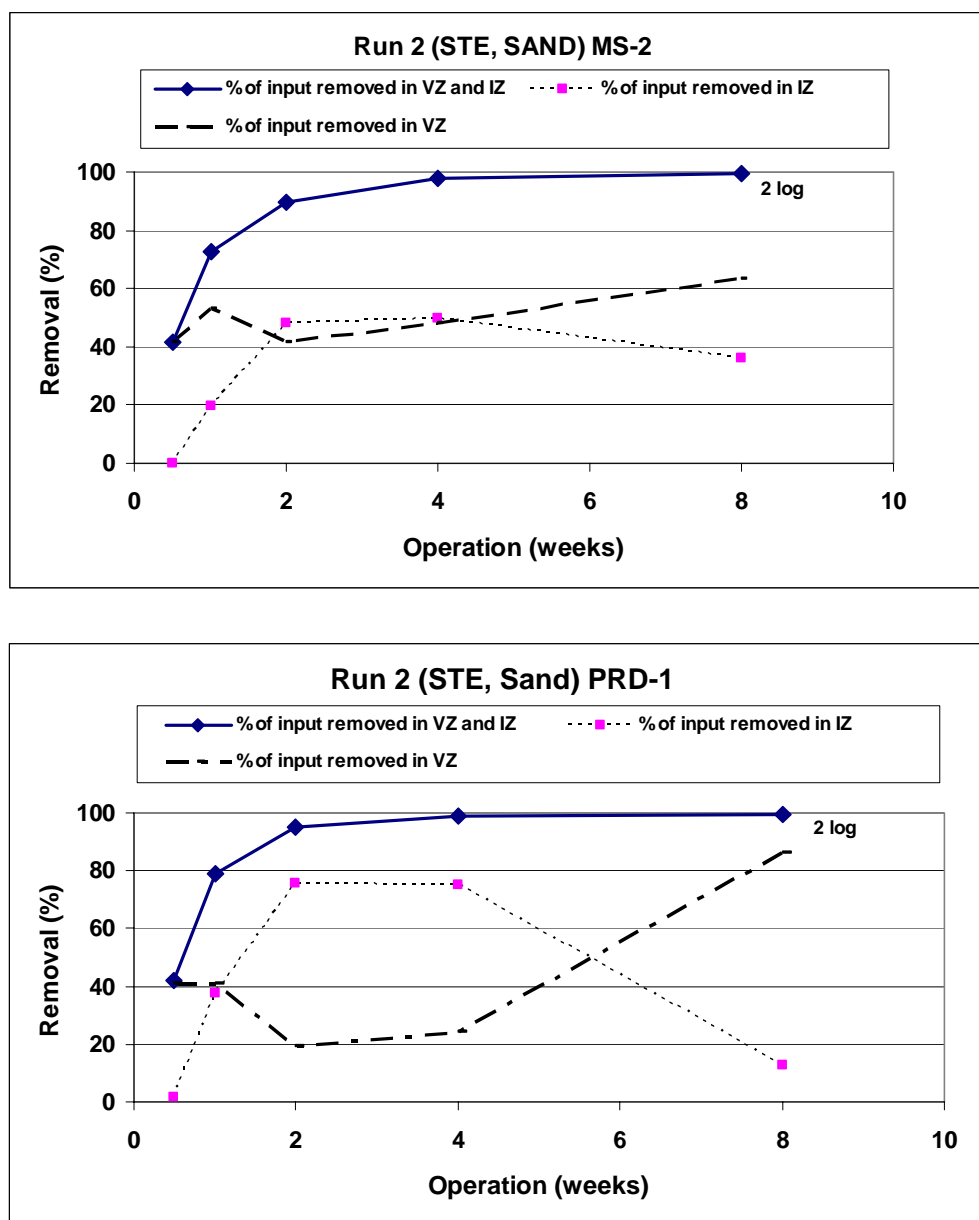
ISU = infiltrative surface utilization, represents the fraction of the infiltrative surface used

VUE = volumetric utilization efficiency, represents fraction of the porous media filter utilized



Notes: Assumes first order removal with respect to concentration.
 1×10^7 PFU/ml of virus added in AGW dosed at 5 cm/day.
 Removal rate numbers obtained from Run 1 mini-column experiments.
 IZ = infiltrative surface zone, first 4 cm of depth; VZ = vadose zone, 4 to 60 cm

Figure B-31
Virus Removal Simulation With Increasing Time of Operation



Notes: Assumes first order removal with respect to concentration.

1×10^7 PFU/ml of virus added in STE dosed at 5 cm/day.

Removal rate numbers obtained from Run 2 mini-column experiments.

IZ = infiltrative surface zone, first 4 cm of depth; VZ = vadose zone, 4 to 60 cm

Figure B-32
Virus Removal Simulation With Increasing Time of Operation

Conclusions

The following conclusions were drawn from the laboratory-scale experiments performed to investigate the fate of bacteria and virus during wastewater treatment in a WSAS:

- One-dimensional columns and unsaturated mini-column work demonstrated that an increased removal of virus may not necessarily be attributed to development of a biozone that alters the flow regime, but that the conditioning of the porous media at the infiltrative surface is important to the removal of viruses. In both experimental systems no noticeable biozone was observed (but biofilms are likely present, as evidenced by HPC bacteria counts in sand-filled unsaturated mini-columns dosed with AGW). In the 1-D column work no changes to hydraulics were measured, yet increased removal of virus was observed following application of higher quality effluent (either AGW or soil percolate effluent).
- Higher levels of soil TOC were found in unsaturated mini-columns that were loaded with STE at a HLR of 5 cm/day versus AGW loaded at 25 cm/day (when comparing in either sand or silty sand). However, higher removal of both MS-2 and PRD-1 was observed at the time of the second tracer test in the columns loaded with AGW at the higher loading rate, versus those in the same soil dosed with STE at 5 cm/day.
- Microdosing, when comparing AGW dosed 24 times/day versus columns dosed with STE four times daily, resulted in higher removal of both MS-2 and PRD-1 in the unsaturated mini-columns at the time of the second tracer test.
- One-dimensional column studies showed that the presence of a clogging zone or visible biozone at the infiltrative surface may not be as important as initial research had suggested. The characteristics of the soil and solution matrix may be more important for conditioning the porous media than forming a visibly developed infiltrative surface. However, 3-D tank lysimeter studies show that the development of a biozone with increased time of operation may be important to the flow regime and the removal of viruses (Van Cuyk *et al.* 2001).
- Mini-columns studies demonstrated that equivalent or even higher removal of viruses may occur at the infiltrative surface when viruses are applied to soil in higher quality effluent as compared to application in STE. The presence of constituents in STE (such as DOC) may be of concern with respect to the removal of viruses in porous media.
- Onsite wastewater systems, including the infiltrative surface and the vadose zone, may be able to achieve high removal of added bacteriophages (from 1 to 4 log, see Figure B-4).

References

- Adams, M. H. 1959. *Bacteriophages*. Interscience Publishers. New York, NY.
- American Public Health Association (APHA). 1998. *Standard Methods for the Examination of Water and Wastewater*. Twentieth Edition. Clesceri, L. S., A. E. Greenberg, and A. D. Eaton (eds.). APHA-American Water Works Association-WPCF, Washington, DC.
- Bales, R. C., S. R. Hinkle, T. W. Kroeger, K. Stocking, and C. P. Gerba. 1991. "Bacteriophage Adsorption During Transport Through Porous Media." *Environ. Sci. Tech.* 25, 2088–2095.

- Bales R. C., S. Li, K. M. Maguire, M. T. Yahya, and C. P. Gerba. 1993. "MS-2 and Poliovirus Transport in Porous Media: Hydrophobic Effects and Chemical Perturbations." *Wat. Res. Research*. 29, 957–963.
- Beach, D. N. 2001. *The Use of One-Dimensional Columns and Unsaturated Flow Modeling to Assess the Hydraulic Processes in Soil-Based Wastewater Treatment Systems*. M.S. Thesis. Department of Geology and Geological Engineering, Colorado School of Mines, Golden, CO.
- Beach, D. N., J. E. McCray, K. S. Lowe, and R. L. Siegrist. 2005. "Temporal Changes in Hydraulic Conductivity of Sandy Porous Media Biofilters during Biomat Development: Experimental Evaluation." *Journal of Hydrology*. In press.
- Bertucci, J., C. Lue-Hing, D. Zene and S. J. Sedita. 1974. *Studies on the Inactivation of Four Enteric Viruses in Anaerobically Digesting Sludge*. Report No. 74-19. Metropolitan Sanitary District Of Greater Chicago, Res. and Dev. Department, Cicero, IL.
- Burge, W. D. and N. K. Enkiri. 1978. "Virus Adsorption by Five Soils." *Journal of Environ. Quality*. 7, 73–76.
- Carlson, G. F., F. E. Woodard, D. F. Wentworth and O. J. Sproul. 1968. "Virus Movement in Groundwater." *J. Water Pollut. Control. Fed.* 40, 57–271.
- Craun, G. F. 1985. "Summary of Waterborne Illness Transmitted Through Contaminated Groundwater." *J. Environ. Health*. 48, 122–127.
- Crites, R. and G. Tchobanoglous. 1998. *Small and Decentralized Wastewater Management Systems*. McGraw-Hill Publishing Company, Boston, MA.
- Frankenberger W. T., F. R. Troeh and L. C. Dumenil. 1979. "Bacterial Effects on Hydraulic Conductivity of Soils." *Soil Sci. Soc. Am. J.* 43, 333–338.
- Gerba, C. P., S. M. Goyal, I. Cech, and G. F. Bagdan. 1981. "Quantitative Assessment of the Adsorptive Behavior of Viruses in Soils." *Environ. Science and Technol.* 15, 940–944.
- Gerba C. P., M. V. Yates, and S. K. Yates. 1991. "Quantitation of Factors Controlling Viral and Bacterial Transport in the Subsurface." *Modeling the Environmental Fate of Microorganisms*. C. J. Hurst (ed.). American Society of Microbiology, Washington, DC. 77–88.
- Grant, S. B., O. Ogunseitan, T. Olson, M. K. Estes. 1999. *Final Report: Norwalk Virus-Like Particles (VLPs) for Studying Natural Groundwater Disinfection*. Grant Number R824775. US EPA, Office of Research and Development.
- Goyal, S. M. and C. P. Gerba. 1979. "Comparative Adsorption of Human Enteroviruses, Simian Rotavirus, and Selected Bacteriophages to Soils." *Applied and Environ. Micro.* 38(2), 241–247.

- Gupta, R. and Swartzendruber. 1962. "Flow-associated Reduction in the Hydraulic Conductivity of Quartz Sand." *Soil Sci. So. Am. Proc.* 26, 6–10.
- Hach. 1998. *Water Analysis Handbook*. Second Edition. Hach Chemical Co., Loveland, CO.
- Harvey, R. W. 1997a. "Microorganisms as Tracers in Groundwater Injection and Recovery Experiments: A Review." *FEMS Microbiology Reviews*. 20, 461–472.
- Harvey, R. W. 1997b. "In Situ and Laboratory Methods to Study Subsurface Microbial Transport." *Manual of Environmental Microbiology*. Hurst, C. J., G. R. Knudsen, M. J. McInerney, L. D. Stetzenback, and M. V. Walter (eds.). ASM Press, Washington, DC. 586–599.
- Jenssen, P. D. and R. L. Siegrist. 1990. "Technology Assessment of Wastewater Treatment by Soil Infiltration Systems." *Water Science & Tech.* 22(3/4), 83–92.
- Keswick, B. H. and C. P. Gerba. 1980. "Viruses in Groundwater." *Environ. Sci. Technol.* 14(11), 1290–1297.
- Larkin, E. P., J. T. Tiernay, and R. Sullivan. 1976. "Persistence of Poliovirus 1 in Soil and on Vegetables Irrigated with Sewage Wastes: Potential Problems." *Virus aspects of Applying Municipal Waste to Land*. L. B. Baldwin *et al.* (ed.). University of Florida, US EPA. 119–130.
- Loveland, J. P., J. N. Ryan, G. L. Amy and R. W. Harvey. 1996. "The reversibility of virus attachment to mineral surfaces." *Colloids and Surfaces*. 107, 205–221.
- Lowe, K. S., D. N. Beach, S. Van Cuyk, R. L. Siegrist, and J. E. McCray. 2005. *Performance Evaluation of Wastewater Renovation by Sandy Porous Media Biofilters*. In preparation.
- Navigato, T. 1999. *Virus Attachment Versus Inactivation in Aquifer Sediments*. M.S. Thesis. University of Colorado, Boulder, CO.
- Nicosia, L. A., J. B. Rose, L. Stark, and M. T. Stewart. 2001. "A Field Study of Virus Removal in Septic Tank Drainfields." *J. Environ. Qual.* 30, 1933–1939.
- Olsen, R. H., J. Siak, and R. Gray. 1974. "Characterization of PRD1, A Plasmid-Dependent Broad Host Range DNA Bacteriophage." *J Virol.* 14, 689–699.
- Pieper, A. P., J. N. Ryan, R. W. Harvey, G. L. Amy, T. H. Illangasekare and D. W. Metge. 1997. "Transport and Recovery of Bacteriophage PRD1 in an Unconfined Sand Aquifer: Effect of Anthropogenic Organic Material." *Environ. Sci. Technol.* 31, 1163–1170.
- Powelson D. K. and C. P. Gerba. 1994. "Virus Removal from Sewage Effluents During Saturated and Unsaturated Flow Through Soil Columns." *Wat. Res.* 28(10), 2175–2181.

Powelson, D. C., J. R. Simpson, and C. P. Gerba. 1990. "Virus Removal from Sewage Effluents During Saturated and Unsaturated Flow Through Soil Columns." *J. Environ. Quality* 19, 396–401.

Powelson, D. K., J. R. Simpson, and C. P. Gerba. 1991. "Effects of Organic Matter on Virus Transport in Unsaturated Flow." *Appl. Environ. Microbiol.* 57, 2192–2196.

Powelson, D. K., C. P. Gerba, and M. T. Yahya. 1993. "Virus Transport and Removal in Wastewater During Aquifer Recharge." *Wat. Res.* 27(4), 583–590.

Reddy, K. R., R. Khaleel, and M. R. Overcash. 1981. "Behavior and Transport of Microbial Pathogens and Indicator Organisms in Soils Treated with Organic Wastes." *J. Environ. Quality.* 10(3), 255–266.

Ryan, J. N., M. Elimelech, R. A. Ard, R. W. Harvey, and P. R. Johnson. 1999. Bacteriophage PRD1 and Silica Colloid Transport and Recovery in an Iron Oxide-Coated Sand Aquifer. *Environ. Sci. Technol.* 33, 63–73.

Schijven, J. F., W. Hoogenboezem, S. M. Hassanizadeh, and J. H. Peters. 1999. "Modeling Removal of Bacteriophages MS2 and PRD1 by Dune Recharge at Castricum, Netherlands." *Water Resour. Research.* 35, 1101–1111.

Sheldon, A. 1999. *Experimental Validation and Reliability Evaluation of Selected Soil VOC Leaching and Volatilization Models Used in Environmental Health Risk Assessment*. Ph.D. Dissertation, Colorado School of Mines, Golden, CO.

Siegrist, R. L. 1987. "Soil Clogging During Subsurface Wastewater Infiltration as Affected by Effluent Composition and Loading Rate." *J. Environ. Quality.* 16, 181–187.

Sobsey, M. D., C. H. Dean, M. E. Knuckles and R. A. Wagner. 1980. "Interactions and Survival of Enteric Viruses in Soil Materials." *Applied and Environ. Microb.* 40, 92–101.

Struse A. M. 1999. *Mass Transport of Potassium Permanganate in Low Permeability Media and Matrix Interactions*. M.S. Thesis. Colorado School of Mines, Golden, CO.

United States Environmental Protection Agency (US EPA). 1978. *Management of Small Waste Flows*. Report of Small Scale Waste Management Project, University of Wisconsin, Madison, WI. EPA-600/2-78-173. US EPA, Municipal Environmental Res. Lab., Cincinnati, OH.

US EPA. 1980. *Design Manual for Onsite Wastewater Treatment and Disposal Systems*. US EPA Municipal Environmental Res. Lab., Cincinnati, OH.

US EPA. 1997. *Response to Congress on Use of Decentralized Wastewater Treatment Systems*. US EPA, Office of Water, Washington, DC.

US EPA. 2000. *National Primary Drinking Water Regulations: Ground Water Rule*. 40CFR Parts 141 and 142.

Van Cuyk, S. M. and R. L. Siegrist. 2004. "Fate of Viruses in the Infiltrative Surface Zone of Systems that Rely on Soil Treatment for Wastewater Renovation." *Proceedings of the Tenth National Symposium on Individual and Small Community Sewage Systems*, American Society of Agricultural Engineers, Sacramento, CA. 387–399.

Van Cuyk, S., R. L. Siegrist, K. Lowe, and R. W. Harvey. 2004. "Evaluating Microbial Purification during Soil Treatment of Wastewater with Multicomponent Tracer and Surrogate Tests." *Journal of Environmental Quality*. 33, 316–329.

Van Cuyk, S. M. 2003. *Fate of Virus During Wastewater Renovation in Porous Media Biofilters*. Ph.D. Dissertation. Environmental Science & Engineering Division, Colorado School of Mines, Golden, Colorado.

Van Cuyk, S. and R. Siegrist. 2001. "Pathogen Fate in Wastewater Soil Absorption Systems as Affected by Effluent Quality and Soil Clogging Genesis." *Proceedings of the Ninth National Symposium on Individual and Small Community Sewage Systems*. Fort Worth, TX.

Van Cuyk, S., R. Siegrist, A. Logan, S. Masson, E. Fischer and L. Figueroa. 2001. "Hydraulic and Purification Behaviors and their Interactions During Wastewater Treatment in Soil Infiltration Systems." *Water Res.* 35 (4), 101–110.

Van Duin, J. 1988. *The Bacteriophages*. First Edition, Calender, R. (ed.). Plenum Press, New York, NY. Vol. 1, 117–167.

Yates, M. V. 1995. "Field Evaluation of the GWDR's Natural Disinfection Criteria." *J. American Water Works Assoc.* 87, 76–85

Yates, M. V. and S. R. Yates. 1988. "A Comparison of Geostatistical Methods for Estimating Virus Inactivation Rates in Ground Water." *Water Res.* 21, 1119–1125.

Zerda, K. S., C. P. Gerba, K. C. Hou and S. M. Goyal. 1985. "Adsorption of Viruses to Charge-Modified Silica." *Applied Environ. Microbiol.* 49, 81–95.



C BIOZONE DEVELOPMENT AND WSAS PERFORMANCE: COLUMN STUDIES

Wastewater treatment for onsite and small community applications commonly relies on infiltration and percolation of primary effluent through soil to achieve purification prior to recharge to groundwater (US EPA 1978, 1980, 1997; Jenssen and Siegrist 1990; Crites and Tchobanoglous 1998). Design of these wastewater soil absorption systems (WSASs) requires delivery and distribution of effluent to the infiltrative surface typically either continuously or intermittently, for a given period of time.

Overview

During operation of the WSAS, development of a biozone has been attributed to the accumulation of suspended soils within the soil pores and microbiological growth (Jones and Taylor 1965; Thomas *et al.* 1966, Bouma 1975; Siegrist 1987; and Tyler *et al.* 1991). As the biozone evolves, the permeability of the infiltrative surface is reduced, and eventually the initial operative loading rate can exceed the capacity of the infiltrative surface zone. The applied effluent spreads laterally due to the increased resistance of the biozone (decreased pore space and decreased hydraulic capacity) until sufficient infiltrative area can absorb the loading. The loading regimes, presented in Table C-1, reveal how the actual hydraulic loading rate (HLR) to an infiltrative surface can be considerably above the design values (Siegrist *et al.* 2001). This departure from the design loading rate is important to recognize as it not only impacts hydraulic performance but also may affect treatment efficiency.

Table C-1
Loading Regimes That Can Occur Within the Space-Time Framework of a WSAS

Design Infiltrative Surface (IS)	Distribution Type	Distribution Features	Distribution and IS Utilization (ISU) During Startup and Maturation Period	HLR @ ISU (actual: design)	Time to HLR = IR and Ponding Ensues ³
Bottom area only ¹	Design	—	Ideally uniform distribution at design rate to design infiltration surface area	2.5 cm/d (0.5:1)	> 3 yr
	Random gravity 1	Distribution box or header to deliver Q between trenches	Each trench receives flow per design but delivery along piping is unequal and only 20% of bottom area receives loading. Daily loading is continuous at 2 to 5 Lpm from a pretreatment tank.	12.5 cm/d (2.5:1)	1 to 2 yr
	Random gravity 2A	Drop-box distribution with flow to only 1 trench at startup	One of four trenches receives flow per design and delivery along piping is unequal and only 10% of the bottom area receives loading. Daily loading is continuous at 2 to 5 Lpm from a pretreatment tank.	100 cm/d (20:1)	< 3 mon
	Random gravity 2B	Drop-box distribution with flow to only 1 trench at startup	One of four trenches receives flow per design and delivery along piping is unequal but due to clogging zone genesis entire bottom area receives loading. Daily loading is continuous at 2 to 5 Lpm from a pretreatment tank.	10 cm/d (2:1)	1 to 2 yr
	Dosed, unequal orifice Q	Distribution via pump and pressure network	All four trenches receive same flow but orifices along piping do not receive equal flow. Assume only 80% of orifices received Q and the orifice spacing yields 50% ISU of bottom IS. Daily loading is dosed 4 times/d.	6.25 cm/d (1.2:1)	> 3 yr
	Dosed, equal orifice Q	Distribution via pump and pressure network	All four trenches receive same flow and all orifices receive equal Q, but the orifice spacing yields 50% ISU of bottom IS. Daily loading is dosed 4 times/d.	5 cm/d (1:1)	> 3 yr

Table C-1
Loading Regimes That Can Occur Within the Space-Time Framework of a WSAS (Cont.)

Design Infiltrative Surface (IS)	Distribution Type	Distribution Features	Distribution and IS Utilization (ISU) During Startup and Maturation Period	HLR @ ISU (actual: design)	Time to HLR = IR and Ponding Ensues ³
Bottom plus sidewall ²	Random gravity 1	Distribution box or header to deliver Q between trenches	Both trenches receive flow per design but delivery along piping is unequal and only 20% of bottom area receives loading. Daily loading is continuous at 2 to 5 Lpm from a pretreatment tank.	37.5 cm/d (7.5:1)	6 to 12 mon
	Random gravity 2A	Drop-box distribution with flow to only 1 trench at startup	One of two trenches receives flow per design and delivery along piping is unequal and only 10% of the bottom area receives loading. Daily loading is continuous at 2 to 5 Lpm from a pretreatment tank.	150 cm/d (30:1)	< 3 mon
	Random gravity 2B	Drop-box distribution with flow to only 1 trench at startup	One of two trenches receives flow per design, and delivery along piping is unequal. Due to clogging zone genesis, entire bottom area receives loading. Continuous daily loading at 2–5 Lpm from a pretreatment tank.	12 cm/d (2.4:1)	1 to 2 yr
	Dosed, unequal orifice Q	Distribution via pump and pressure network	Both trenches receive same flow but orifices along piping do not receive equal flow. Assume only 80% of orifices received Q and the orifice spacing yields 50% ISU of bottom IS. Daily loading is dosed 4 times/d.	30 cm/d (6:1)	6 to 12 mon
	Dosed, equal orifice Q	Distribution via pump and pressure network	Both trenches receive same flow and all orifices receive equal Q, but the orifice spacing yields 50% ISU of bottom IS. Daily loading is dosed 4 times/d	24 cm/d (4.8:1)	6 to 12 mon

¹System is designed to treat 600 gpd using a LTAR of 1.25 gpd/ft² yielding 480 ft² of infiltrative surface needed. Assume actual daily flow is 50% of design flow, or 300 gpd. For bottom area IS design, use 4 trenches, each 40 ft long and 3.0 ft wide, with 1.0 ft of sidewall height (3 ft² per lineal ft and actual HLR = 1.87 gpd per lineal ft).

²System is designed to treat 600 gpd using a LTAR of 1.25 gpd/ft² yielding 480 ft² of infiltrative surface needed. Assume actual daily flow is 50% of design flow, or 300 gpd. Assumes 2 trenches, each 40 ft long and 2.0 ft wide, with 2.0 ft of sidewall height (6 ft² per lineal ft and actual HLR = 3.75 gpd per lineal ft).

³Elapsed computed time for a sand with K_{sat} approximately 800 to 1000 cm/d.

Biozone development can promote unsaturated flow conditions that promote contact between the wastewater constituents and the surface of soil particles, thereby enabling reactions and increasing the time available for treatment process to occur (Schwager and Boller 1997; Van Cuyk *et al.* 2001; Siegrist *et al.* 2001). Furthermore, the biozone is more biogeochemically reactive than the native soil.

The rate of development of the biozone and the loss in hydraulic capacity at the infiltrative surface is dependent on the mass loading rate of effluent onto the infiltrative surface (Siegrist 1987). However, once clogging develops to the point of continuous ponding of the infiltrative surface, the hydraulic resistance of a given type of infiltration zone may be similar even if the historical loading and rate of development is different. That is, systems of a given design in a given soil and climatic setting may yield a similar equilibrium rate after some time of operation. The equilibrium infiltration rate after clogging has evolved, is expected to be affected by several design and environmental factors, including:

- Infiltrative surface architecture
- The orientation of the infiltrative surface
- Soil texture, structure, and hydraulic conductivity properties
- Degree of saturation in the underlying unsaturated zone

The purpose of the research described in this appendix was to explore the biozone genesis and flow and transport process dynamics in a WSAS. To determine the effects of different loading rates on hydraulic and treatment performance, 16 one-dimensional (1-D) columns were established to simulate a vertical column within a WSAS under four loading regimes (Figure C-1).

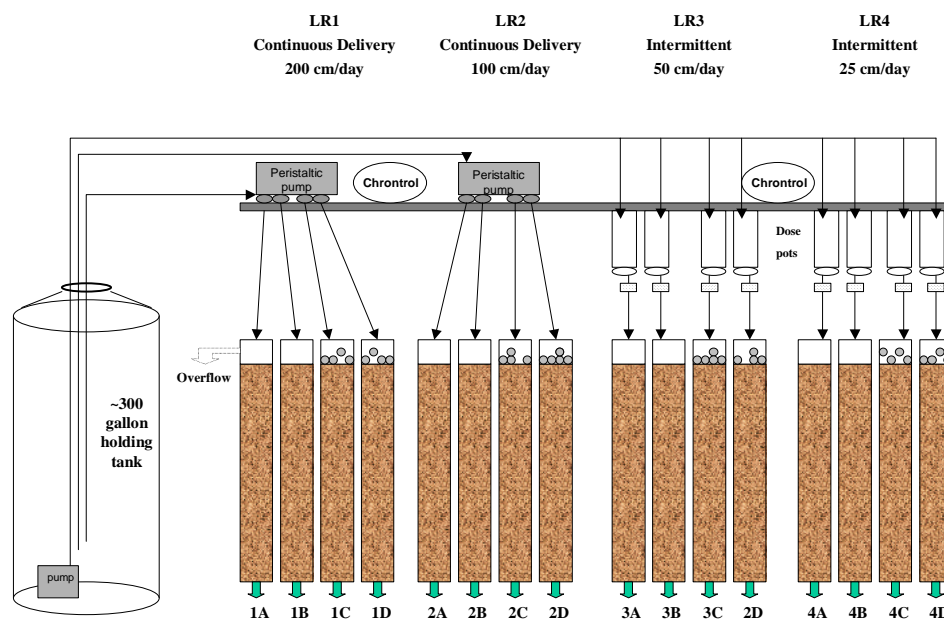


Figure C-1
Schematic of Column Set-Up

The experimental design conditions for each column are described in Table C-2. The concept of accelerated loading was also evaluated to determine if increased application rates (within certain limits) enabled the system to progress through a normal life cycle following a compressed time scale such that shorter-term tests would provide insight into longer-term performance.

Table C-2
Experimental Conditions for the Column Operation

Loading Regime	Column Labels	Infiltrative Surface Character	Exp. Design HLR	Loading Method Features
LR1	1A, 1B	Gravel-Free	200 cm/d 35.36 L/d per column	Continuous delivery at 24.56 mL/min
	1C, 1D	Gravel-Laden		
LR2	2A, 2B	Gravel-Free	100 cm/d 17.68 L/d per column	Continuous delivery at 12.28 mL/min
	2C, 2D	Gravel-Laden		
LR3	3A, 3B	Gravel-Free	50 cm/d 8.84 L/d per column	Dosed 4 times/day (8:00, 12:00, 16:00, and 20:00 hr.) 12.5 cm/dose or 2.20 L/dose 1.10 L/min for 2 min
	3C, 3D	Gravel-Laden		
LR4	4A, 4B	Gravel-Free	25 cm/d 4.42 L/d per column	Dosed 4 times/day (8:00, 12:00, 16:00, and 20:00 hr.) 6.25 cm/dose or 1.10 L/dose 1.10 L/min for 1 min
	4C, 4D	Gravel-Laden		

Notes: Total design loading = 265 L/d (70.1 gpd) at 100% throughput in all 16 columns.

Actual daily loading rates were 65 to 82% of the design rate.

Based on the loading rates applied during this experiment, 20 weeks of operation were expected to reflect periods of operation equivalent to as much as 15.4 yr. of operation compared to a typical design loading rate (5 cm/d) for sandy soils, assuming that all of the applied wastewater was processed through and/or accepted by the columns. Experimental methods, hydraulic performance, and nutrient treatment performance are described in this appendix (see also Beach 2001, Beach *et al.* 2005, Siegrist *et al.* 2002). Additional information on pathogen transport-fate and infiltrative surface characterization is presented in Appendix B, *Pathogen Transport-Fate Studies*.

Methods

This section provides information about the experimental apparatus and monitoring.

Experimental Apparatus

The columns were constructed from clear acrylic pipe, 15 cm in diameter. Outflow and overflow ports were tapped near the bottom and top of each column, with the overflows positioned approximately 20 cm above the infiltrative surface. Prior to packing with sand, the inside walls of the columns were sprayed with an acrylic adhesive and covered with sand. The bonding of sand to the interior wall of the column was intended to roughen the sidewall and minimize preferential sidewall flow. Each column was equipped to monitor both soil moisture tension (SMT) at two locations and water content (time domain reflectometry [TDR]) at three locations (Figure C-2). The columns were selected randomly for construction, packing, and grouping into loading regimes to negate any bias or pattern.

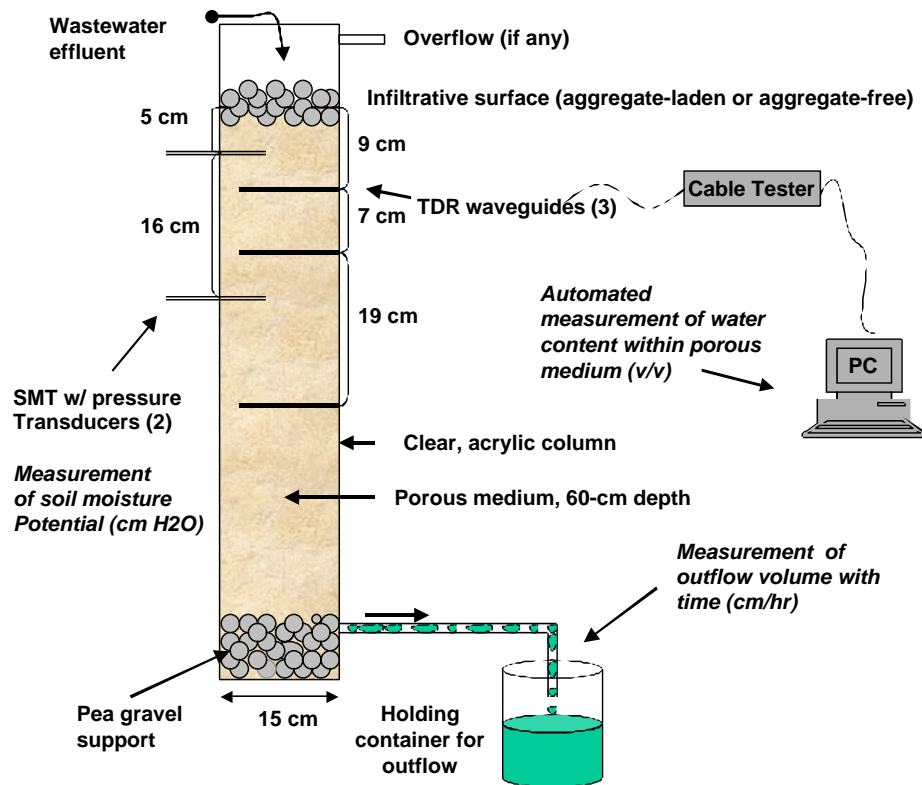


Figure C-2
Schematic of Column Set-Up

A 5-cm deep layer of washed pea gravel (1 to 2 cm in diameter) was placed in the bottom of each column for structural support and to minimize clogging of the outlet port. The gravel was flushed twice with tap water after placement to promote settling and compaction. Each column was then packed with moist sand (approximately 5.5% water by weight, $d_{10}=0.22$ mm, $d_{60}=0.60$ mm) in 5-cm lifts or increments to a total sand depth of 60 cm. Each lift followed the same packing procedure to ensure uniformity within and between columns.

For the gravel-laden columns, after the final lift, a 1-cm layer of sand was removed from the top of the column. The surface was scarified, a layer of washed gravel (nominal 2-cm diameter) was placed on the scarified surface, and dry sand was used to fill in the void spaces. This first gravel-sand lift, used to simulate gravel embedment known to occur in WSASs, was then compacted and gravel then added to a height of 10 cm above the soil surface.

Baseline Characterization

After the columns were fully assembled, baseline characterization including measurement of saturated hydraulic conductivity (K_{sat}), clean-water loading, and a bromide tracer test was completed. To obtain K_{sat} measurements, each column was upflow saturated over a period of eight hours and allowed to sit ponded overnight prior to completion of three falling-head tests. The columns were allowed to drain for a period of three to five days after K_{sat} measurements prior to clean-water loading during which all columns were loaded with tap water for a period of 26 days. All columns were loaded according to the design application method (Table C-2) to consolidate the sand media and establish a steady-state water content distribution. During clean-water loading, tap water containing 500 mg-Br/L was applied to each column to assess mean travel times under each loading regime. Column percolate samples were collected and analyzed using a combination ion-selective electrode for bromide.

Wastewater Loading

Following baseline characterization, wastewater loading was initiated and continued for 138 days. Wastewater (septic tank effluent [STE]) was acquired from a nearby multi-family housing unit at CSM and transported to the laboratory where it was stored in an insulated 300-gallon polyethylene tank. All columns received wastewater from this holding tank. For the continuously loaded columns (LR1 and LR2), wastewater from the holding tank was applied at the design rate via peristaltic pumps (Figure C-1).

For LR3 and LR4, wastewater was pumped from the holding tank to individual dose pots positioned above the column immediately prior to each dosing event. To ensure that each dose pot was filled with the prescribed volume, excess wastewater was pumped to the dose pot and allowed to flow back to the holding tank through an overflow port and tubing. All dosing events were automated using a ChronTrol timer to release the specified volume from the dose pots for a 1- to 2-minute period.

The initial design could not be maintained constantly due to experimental factors such as sediment accumulation in delivering tubing and periodic pump malfunctions. The average hydraulic loading rate prior to ponding for each loading regime was 78% of the design rate for LR1, 82% of the design rate for LR2, 79% of the design rate for LR3, and 65% of the design rate for LR4. In addition, biozone genesis resulted in decreased hydraulic loading rates over time. Throughout this study, the columns remained cloaked with black plastic, except when accessing the columns during monitoring, to prevent algae growth.

Anaerobic conditions developed in LR1 and LR2 after two weeks of operation due to the high STE loading rate and ponding of wastewater at the top of the columns. To alleviate the anaerobic conditions, aeration holes (one-quarter-inch diameter) were drilled through the acrylic column sidewall approximately 10 cm apart along opposing sides of each column and covered with gas permeable tape to allow oxygen transfer through the sidewalls of the columns. Subsequently, continuously ponded conditions to the overflow (20 cm above the infiltrative surface) led to wastewater throughput rates less than the initial loading rates.

Routine Operations

Routine operations continued for 19 weeks (138 days) at which time wastewater loading to the columns was terminated. Routine operations included:

- Application of wastewater to the columns
- Weekly collection of percolate samples for water quality analysis
- Measurement of percolate throughput volumes
- Measurement of soil moisture tension
- Measurement of soil moisture content

In addition, three multicomponent tracer tests (MS-2 and PRD-1 bacteriophages and bromide tracer) were completed during weeks 1, 6, and 15 of column operation. Results of the tracer testing, and moisture content profiles are described in Appendix B, *Pathogen Transport-Fate Studies* with detailed results presented in Beach (2001) and Van Cuyk (2003).

Monitoring

Monitoring activities included:

- Hydraulic performance monitoring
- Treatment performance monitoring
- Multicomponent surrogate and tracer tests
- Terminal monitoring and media characterization

Hydraulic Performance Monitoring

Hydraulic monitoring of the columns included:

- Soil moisture tension
- Soil moisture content
- Falling-head hydraulic conductivity measurements

- Column throughput rates measured by percolate volume
- Ponding heights
- Bromide tracer tests

Soil Moisture Tension

Two soil moisture tensiometers were installed in each column at soil depths of 5 cm and 21 cm. The ceramic cup (SoilMoisture, Inc.) tube assemblies were constructed in the laboratory and equipped with a pressure transducer (Newark Electronics, Inc.). The tensiometers did not provide reasonable or reliable measurements of pressure head in the columns, an outcome thought to be due to the coarse nature of the column media (sand) and the lack of adequate hydraulic continuity between soil solution and the porous cup. Therefore, measurements were ceased during the first week of operation and no pressure-head information was obtained.

Soil Moisture Content

To measure soil moisture content, three TDR sensors (Dynamax, Inc.), 10 cm in length, were installed at soil depths of 9, 16, and 35 cm in each column. TDR measures the travel time of an electric pulse down a wave guide inserted in the soil. The travel time of the pulse depends on the apparent permittivity, or dielectric constant, of the soil media. Since the dielectric constant for water is approximately 70 times greater than of dry soil, the dielectric constant of the soil media depends strongly on the water content of the soil system. All wave guides were connected through multiplexers to a Tektronics 1502C cable tester. The Dynamax TDR system was automated and controlled using a PC and the manufacturer provided the computer software program, TACQ. Prior to installation, the global and individual settings for each wave guide were adjusted according to the manufacturers recommendations (Evet 2000). The software was set up to automatically acquire water content measurements for each TDR wave guide every two hours, starting at 12:00 a.m.

Falling-Head Hydraulic Conductivity Measurements

The effective hydraulic conductivity (K_e) of each column was measured using a falling-head test at the beginning and end of column operation. The term “effective” is used because the column eventually becomes a heterogeneous system, where the hydraulic conductivity is primarily controlled by the biozone. For the measurements prior to wastewater loading, all columns were up-flow saturated over a period of eight hours and allowed to sit ponded overnight to ensure saturation and to reduce air entrapment. Reference locations for initial and final head measurements were specified randomly at each measurement repetition.

At the end of the experiment (138 days), a falling-head test was again performed on all columns. During this falling-head test the change in ponding height (head above the infiltrative surface) was recorded over time as the column was allowed to drain. Up to 29 individual head measurements were recorded per column. Infiltration rates based on the dh/dt for each column were then determined from the average of the individual measurements.

Due to the presence of a biozone, ponded wastewater was present at the infiltrative surface for all LR1 and LR2 tests. However, ponding within the dosed columns, LR3 and LR4, was erratic and unstable throughout the study. Therefore, analysis of falling-head tests was not performed on LR3 and LR4 data.

Column Throughput Rates Measured by Percolate Volume

The percolate from each column was directed into an outflow container, which was calibrated by recording its empty weight prior to system operation. All volume measurements were made by weight using an electric balance. At the beginning of the column study, outflow volume was measured just prior to each dosing event. As conditions moved towards steady-state (continuously ponded), the frequency of monitoring decreased to twice per day and eventually to once every 24 hours, four times per week. Percolate volumes were collected through the day 131 of column operation.

Ponding Heights

In all columns, during some point in operation, the application rate eventually exceeded the infiltration rate and ponding ensued. The level of ponding was periodically monitored throughout the operation of the columns from a reference point made at the top of the infiltrative surface. In LR1 and LR2, and periodically in LR3 and LR4, ponding levels increased to the point of overflow (approximately 20 cm).

Bromide Tracer Tests

Bromide tracer tests were performed as described in the Multicomponent Surrogate and Tracer Tests section.

Treatment Performance Monitoring

Monitoring of water quality included sampling and analysis of the STE applied to the columns as well as the percolate from each column. Sampling and analysis of the applied STE was conducted three separate days each week (Monday, Wednesday, and Friday). Sampling and analysis of the percolate from the columns was conducted at least once every two weeks, with more frequent sample collection and analysis during initial operation of the columns.

Percolate samples were collected from the column outflow containers by pouring percolate from the container into precleaned 250-mL plastic bottles. All samples were labeled and stored at 4 °C until analyses were performed within 24 hours of sample collection. To evaluate laboratory analysis methods, 10% duplicate sample analyses were performed. STE and percolate samples were analyzed for:

- pH—Measured electrometrically following standard methods (Standard Method 2500B) (APHA 1998)

- Alkalinity—Measured using a Hach digital titrator with 1.6N sulfuric acid to a pH 4.8 endpoint (Standard Method 2320B) (APHA 1998).
- Carbonaceous biochemical oxygen demand (cBOD₅)—Measured according to APHA Standard Method 5210B.
- Chemical oxygen demand (COD)—Analysis performed using a Hach reactor digestion, colorimetric method (US EPA-approved) (Hach 1998).
- Total solids (TS)—Measured according to APHA Standard Method 2540B.
- Total suspended solids (TSS)—Measured according to APHA Standard Method 2540D.
- Nutrients (nitrogen and phosphorus)—Total nitrogen (TN) was measured by persulfate digestion, nitrate nitrogen (NO₃⁻) by chromotropic acid method and ammonia nitrogen (NH₄⁺) by salicylate method (US EPA-approved) (Hach 1998). Total phosphorus (TP) was measured according to US EPA acid persulfate method (US EPA Method 365.2).
- Fecal coliform bacteria—Analysis performed by membrane filtration according to APHA method 9222D.

Multicomponent Surrogate and Tracer Tests

Three multicomponent surrogate and tracer tests were completed in each column during the course of the experiment, resulting in a total of 48 individual column tracer tests. Tracer test 1 was completed prior to STE loading, tracer test 2 was completed two weeks after the start of the STE application, and tracer test 3 was completed six weeks after the start of STE application. MS-2 and PRD-1 bacteriophages were added, in addition to bromide (as KBr), to the STE delivered to each column. This multicomponent mixture was applied to the columns for 3 to 14 days with percolate samples collected and monitored, initially four times per day (prior to each dose) and later once every 24 to 48 hours.

The columns were dosed with MS-2 and PRD-1 at a target concentration of 1×10^7 pfu (plaque forming unit)/mL and bromide at 500 mg-Br⁻/L. Results from the bacteriophage tracer tests are described in Appendix B, *Pathogen Transport-Fate Studies*. Levels of bromide were measured in the percolate samples using a combination ion-selective epoxy electrode for bromide (Cole-Parmer 2001) to estimate mean travel times under each loading regime. The concentration-versus-time plots, or breakthrough curves (BTC), provide information about travel times, dispersion within the columns, and heterogeneities that develop due to continued wastewater application.

For each tracer test, a moment analysis was conducted to determine the mean travel time of the center of mass of bromide tracer in each column (Beach *et al.* 2005). Because LR3 and LR4 were dosed four times per day, and thus did not receive a continuous pulse of tracer, the moment analysis was not appropriate for these two loading regimes.

The K_e of the infiltrative surface zone was estimated from bromide tracer test travel times using Darcy's Law (Beach *et al.* 2005). The hydraulic head gradient across a length segment was 9 cm, corresponding to the distance between the top of the biozone and the location of the shallowest TDR probe. The actual thickness of the biozone varied between 2 and 4 cm based on visual observation of soil discoloration, so the measured hydraulic conductivity is termed an "effective" hydraulic conductivity. The difference in head was calculated as the difference between the head at the top of the infiltrative surface and the head at the TDR probe location (9 cm below the infiltrative surface).

After the first few weeks of operation, LR1 and LR2 experienced relatively consistent wastewater ponding at the level of their overflow ports. Ponding within LR3 and LR4 was erratic and unstable throughout the study precluding determination of K_e as described previously (for details see Beach 2001). The stable ponding levels within LR1 and LR2 provided a constant-head boundary condition at the top of each column. Therefore, the distance from the reference point to the top of the ponded water surface equals the hydraulic head at the top of the infiltrative surface (pressure head equals zero at this location). The hydraulic head at the bottom of the infiltrative-surface zone (set to be the location of the 9-cm TDR probe) is equal to the pressure head (elevation head is zero at this location). This bottom pressure-head value was obtained from the TDR-measured water content at this location using water-retention curves measured in the same sand (Ausland 1998 and Beach *et al.* 2005).

The travel time desired for this calculation is the travel time through the 9-cm infiltrative surface zone ($L=9$ cm). This travel time was approximated by subtracting the travel times for tracer test 1 (clean water) from the travel times obtained from tracer tests 2 and 3 to account for only variations caused by changes in the hydraulic properties of the infiltrative surface zone (assuming the zone below did not experience significant hydraulic alteration). Ponding had not occurred in LR2 during tracer test 2 (week two), so the method could not be used. The computed K_e for LR1 is based on an average ponding level (ranging from 1.5 to 20 cm) over three days. Consequently, there is more uncertainty for the values calculated during this tracer test than for those calculated from measurements made during tracer test 3 (week six) for which the ponding levels in LR1 and LR2 columns was relatively constant at the overflow-port level.

Terminal Monitoring and Media Characterization

After 138 days of operation, the columns were shut down and falling-head hydraulic conductivity measurements were made. Once drained, soil samples were taken at depth intervals of 0 to 3 cm, 5 to 8 cm, 10 to 13 cm, and 25 to 28 cm below the infiltrative surface within each column. Samples of the infiltrative surface (0 to 3 cm) were also collected at two locations. Soil samples were not taken from LR1 or columns 2D and 3B (experimentation was continued).

The soil samples were analyzed for water content, TOC, fecal coliform bacteria, and MS-2 and PRD-1 bacteriophages. The results of the terminal soil samples are discussed in Appendix B, *Pathogen Transport-Fate Studies* and Van Cuyk (2003).

Results and Discussion

The following discussion summarizes the results from the 1-D column study. Note that detailed results may be found in several publications including:

- Beach and McCray (2003)
- Beach *et al.* (2005)
- Beach (2001)
- Huntzinger *et al.* (2000, 2001a, 2001b)
- Lowe *et al.* (2005)
- McCray *et al.* (2000)
- Siegrist *et al.* (2002)
- Van Cuyk (2003)
- Van Cuyk *et al.* (2004)

Hydraulic Performance

Hydraulic performance includes:

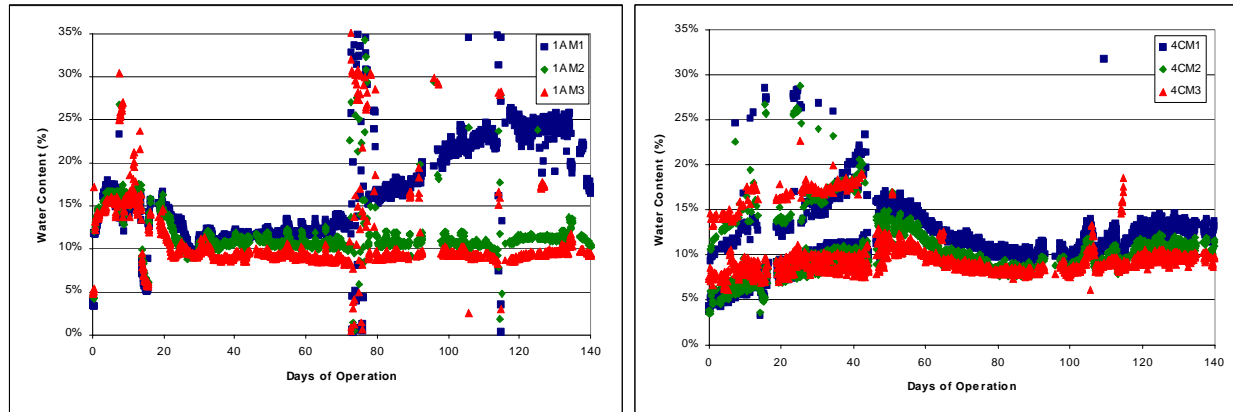
- Soil moisture content
- Falling-head measurements
- Throughput measurements

Soil Moisture Content

Water content measurements obtained from TDR wave guides positioned at three depths (9, 16, and 35 cm) indicated initial volumetric water contents between 5 and 20% (Beach 2001). The increasing water content near the outlet for each column is attributed to capillary effects in the sand media overlying the layer of pea gravel placed in the bottom of each column.

During the course of column operation, TDR measurements were obtained every two hours. Water contents tended to stabilize and approach an equilibrium value as system operation continued. Figure C-3 illustrates this trend for 1A and 4C (all loading regimes have similar trends; see Beach 2001). In several columns, measured water content in the top 16 cm of the column increased to a value near saturation (30–35%) and may be attributed to contact of the TDR with the soil-clogging zone.

In LR3 and LR4, the impact of the intermittent dosing events can be observed early in column operation with the rise of water content during and immediately following a dosing event and the decrease of water content between applications. After clogging-zone development and wastewater ponding, the effects of dosing events were no longer observed because wastewater infiltration no longer occurred only during dosing events, but was continuous and controlled by the permeability of the biozone and height of ponding at the infiltrative surface.



Note: Measurement depths are: M1 = 9 cm; M2 = 16 cm; and M3 = 35 cm

Figure C-3
TDR Derived Volumetric Water Contents for Column 1A and 4C

Falling-Head Measurements

Hydraulic conductivity (K) values were determined using a falling-head test for all 16 columns before wastewater application and at the end of the experiment (mature-biozone tests) from the experimental data (Beach *et al.* 2005). Because the columns were saturated during the clean-water tests, the K values were equal to the saturated hydraulic conductivity (K_{sat}) values for each column.

The clean-water K_{sat} values for all columns varied between 755 and 1,046 cm/day, with a mean value of 910 cm/day, a standard deviation of 84 cm/day, and a coefficient of variation equal to 9%. To determine if there was a statistically significant difference between columns before applying wastewater, a Student t -test was performed on all possible pairs. Results indicated that there was no significant difference (at a 95% confidence level) in initial K_{sat} values between any combination of loading regimes. Therefore, the packing procedure was reproducible and all columns exhibited similar initial hydraulic properties before wastewater application.

The K_e of the biozone at the infiltrative surface for LR1 and LR2 were then calculated from the falling-head measurements (Table C-3). These K_e values were assumed to apply to the biozone infiltrative surface because the low-permeability biozone controls the infiltration rate and overall hydraulic resistance (Beach *et al.* 2005). Because the exact thickness of the biozone was not known, several thicknesses, ranging between 2 and 4 cm, were assumed based on visual observation in the columns. Assuming the 3-cm thick biozone as the most representative case, the K_e values for all columns varied between 0.23 and 1.21 cm/day, with a mean value of 0.66 cm/day, a standard deviation of 0.37 cm/day, and a coefficient of variation equal to 56%.

Table C-3
Calculated Effective Saturated Hydraulic Conductivities of Infiltrative-Surface Zone
Throughout Column Operation

Column	K _e of Infiltrative Surface Zone (cm/day)						
	Initial K _e of Columns	Tracer Tests		Falling Head Prior to Shutdown			
		Week 2	Week 6	Week 20 BZ = 2 cm	Week 20 BZ = 3 cm	Week 20 BZ = 4 cm	Week 20 Average
1A	911	20.07	0.34	0.28	0.39	0.49	0.39
1B	755	4.97	0.45	0.45	0.63	0.79	0.63
1C	869	3.5	0.65	0.51	0.71	0.88	0.70
1D	983	2.5	0.25	0.16	0.23	0.29	0.23
Average	879.5	7.76	0.42	0.35	0.49	0.61	0.49
Coefficient Variation	0.11	1.07	0.41	0.46	0.45	0.44	0.45
2A	935		0.69	0.90	1.22	1.50	1.21
2B	763		0.76	0.84	1.15	1.42	1.14
2C	881		0.36	0.53	0.71	0.85	0.70
2D	929		0.28	0.20	0.27	0.34	0.27
Average	877		0.52	0.62	0.84	1.03	0.83
Coefficient Variation	0.09		0.46	0.52	0.52	0.53	0.52

Note: The lack of measurable ponding in LR2 during the second test precludes calculation of K_e.

The K_e for LR3 and LR4 was not computed using tracer tests.

BZ = Biozone thickness

To provide insight into the source of variability of the falling-head test results, two-way analyses of variance with replication was completed ($\alpha = 0.05$). The total variance of the falling-head data was decomposed into the variance associated with the factors (loading regime and infiltrative surface architecture) and their interactions (loading regime plus infiltrative surface architecture). Results show that while the loading regime had negligible effect on the infiltration rate (3% of the total variance), the infiltrative surface architecture (gravel-free versus gravel-laden) significantly affected the infiltrative rate (64% of the total variance at a 97.6% confidence level). A one-tailed Student *t*-test showed that the two means are different at 98.3% confidence level indicating that the gravel-free infiltration rate exceeds that of the gravel-laden columns (Beach *et al.* 2005).

The biozone formation caused a three-orders of magnitude reduction in K_e during the 20-week experiment, and resulted in increased K_e variability among the columns compared to initial K_{sat} values and K_e at six weeks. Results of a two-way analysis of variance with replication of the K_e data, indicate trends similar to the observed falling-head infiltration rate trends. While the reduction in K_e may be due in part to unsaturated conditions (lowered relative permeability) as well as the reduced conductivity of the biozone (the biozone was at or near saturated throughout the experiment), water content measurements below the biozone were relatively uniform within each column with no apparent relationship between water content and the K_e . Thus, the reduction in K_e is primarily attributed to the low permeability of the biozone material.

Throughput Measurements

Daily volume throughput rates for each column decreased significantly during the course of column operation and appeared to stabilize (Figure C-4).

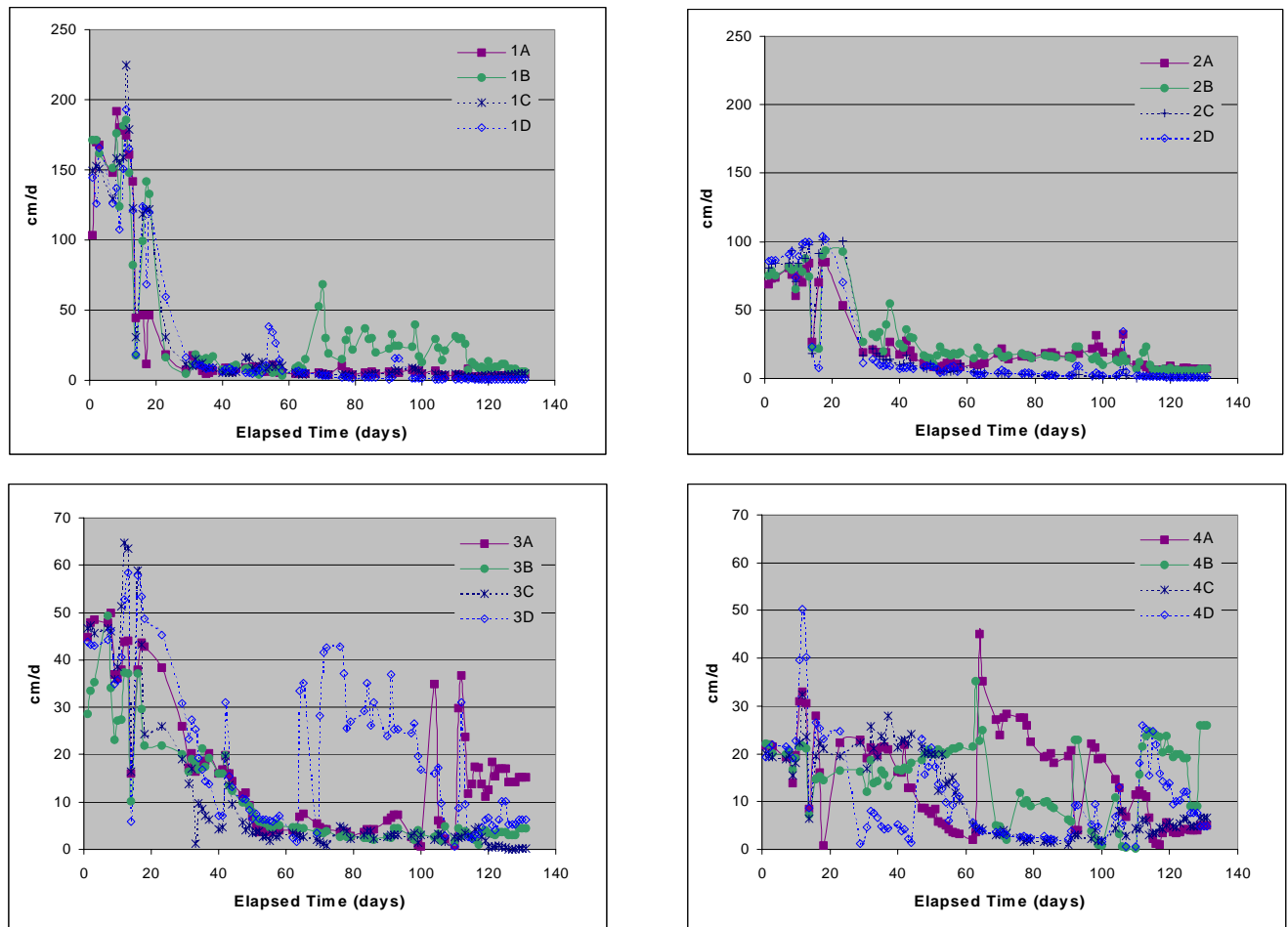


Figure C-4
Daily Throughput Rates for All Loading Regimes

The low point at day 14, appearing in all loading regimes, corresponds to the brief shutdown of the columns to drill aeration holes. In LR1 and LR2, the design application rates were not initially achieved and may be attributed to the pumps set at a rate slightly less than the design rate and/or blockage of the delivery tubing with suspended solids. The average hydraulic loading rate prior to ponding for each loading regime was 78% of the design rate for LR1, 82% of the design rate for LR2, 79% of the design rate for LR3, and 65% of the design rate for LR4. The decrease in throughput rate and ponding is attributed to development of the biozone at the column infiltrative surface. The rate of loss in column throughput is related to the STE loading rate with higher rates of loss observed in columns with higher loading rates of wastewater, which is consistent with biozone phenomena (Siegrist 1987, Siegrist and Boyle 1987).

The variability in column hydraulic performance, as indicated by throughput rate, within a particular loading regime was higher when intermittent dosing methods were used compared to continuous application of wastewater. In these intermittently dosed columns, wastewater was applied at a very high rate (1.1 L/min) for a 1- to 2-minute period, four times per day with resting and/or infiltration occurring between applications. Figure C-4, however, indicates that each column approached a similar steady-state throughput rate in the range of 2 to 10 cm/d, independent of loading method (continuous versus intermittent), design rate (25 to 200 cm/d), or infiltrative surface architecture (aggregate-free versus aggregate-laden).

The throughput data for the last 13 days of operations (days 119 to 131) were analyzed to determine if the rate of change in throughput was negligible, so that each measurement day could be used as a replicate measurement for that column. Visual analysis of the graphical representation of the 13-day period suggested a pseudo-equilibrium steady state (Figure C-4). Linear regressions were conducted on the throughput rates for each column during this 13-day period (Minitab Inc. 2000). A slope of zero indicated that the throughput rates had reached a pseudo-equilibrium steady state. While the throughput rates within each column varied during the 13-day period, this analysis suggested that a pseudo-equilibrium steady-state condition was achieved in most of the columns (11 of 16). Therefore, changes in throughput rates were assumed to be negligible and each day was considered a replicate measurement of throughput during pseudo-equilibrium. Note that the pseudo-equilibrium rates computed for the 13-day period enable direct comparison between the two infiltrative surface types during a comparable period of operation and STE loading.

The mean pseudo-equilibrium throughput rate for all aggregate-free columns was compared to the mean throughput rate for all aggregate-laden columns (average of all throughput rates for each column with the same surface type during the 13-day period) and the standard error of the mean for each surface type was determined (Alder and Roessler 1977, Snedecor and Cochran 1980). The aggregate-free mean pseudo-equilibrium throughput rate was 8.5 cm/d (standard error of the mean = 0.89) compared to the aggregate-laden mean pseudo-equilibrium throughput rate of 3.5 cm/d (standard error of the mean = 0.49). The results indicate that the aggregate-free throughput rate exceeds that of the aggregate-laden columns. Further evaluation of the means using a two-tailed Student *t*-test revealed a significant difference in the mean aggregate-free and aggregate-laden throughput rates at a 95% confidence interval ($\alpha = 0.05$) (Microsoft Corp. 1999).

To provide insight into the source of variability of the throughput rates, two-way analyses of variance with replication was completed ($\alpha = 0.05$). The total variance of the throughput data was decomposed into the variance associated with the factors (loading regime and infiltrative surface) and their interactions (loading regime plus infiltrative surface). The factors and interactions were then ranked based on the magnitude of the mean squares and indicated that the infiltrative surface was the primary factor contributing to the variance in the throughput rate (69.5% of the total variance). There was nearly equal contribution to the variance due to the loading regime and the interaction of the loading regime plus infiltrative surface (17.5% and 12.8%, respectively). There was little contribution to the total variance due to variation within the 13 replicate measurements of the throughput rate for each column (0.2% variance contribution to the total variance).

Treatment Performance

The wastewater applied to the columns was typical of residential wastewater (STE) with average key constituents of:

- $\text{cBOD}_5 = 180 \text{ mg/L}$
- $\text{TSS} = 126 \text{ mg/L}$
- $\text{Total N} = 56 \text{ mg-N/L}$
- $\text{Total P} = 26.5 \text{ mg-P/L}$
- Fecal coliform bacteria range = 2.0×10^2 to $2.20 \times 10^3 \text{ cfu/100mL}$

As expected, a decline in cBOD_5 , TSS, nutrients, and fecal coliform bacteria concentrations were observed in percolate samples (Lowe *et al.* 2005). After 30 days of operation, cBOD_5 in percolate samples from all columns in LR1 and LR2 (continuously dosed) were less than 10 mg/L and remained at this level for the duration of the study. cBOD_5 in percolate samples from LR3 and LR4 (intermittently dosed) were less than 30 mg/L during the entire study. TSS concentrations in percolate samples from all loading regimes were reduced to less than 40 mg/L and remained relatively unchanged.

In general all columns showed nitrification as illustrated by high initial concentrations of NH_4^+ declining over time, corresponding initially low NO_3^- concentrations increasing over time, and decreasing alkalinity. Figure C-5 shows the nitrogen species for columns 2B and 4A, which are representative of both the continuously-dosed and intermittently-dosed columns. Nitrification appears to have started in LR1 and LR2 between 30 and 40 days after startup and in LR3 and LR4 approximately 15 days after startup. The average TP concentration in the wastewater during the study was approximately 26 mg/L. Breakthrough of phosphorous appears to have occurred in LR1 and LR2, which is not surprising based on the high TP application rates in these loading regimes. Fecal coliform bacteria removal rates ranging from 62% to 100% (median removal rate of 99.4%) were observed in all of the columns over the duration of testing, based on 24-hour composite percolate samples.

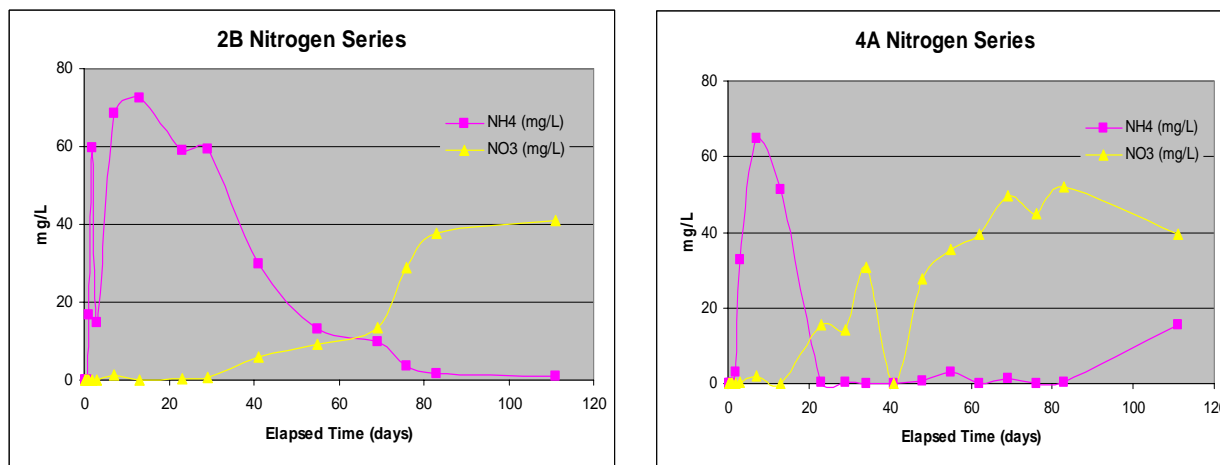


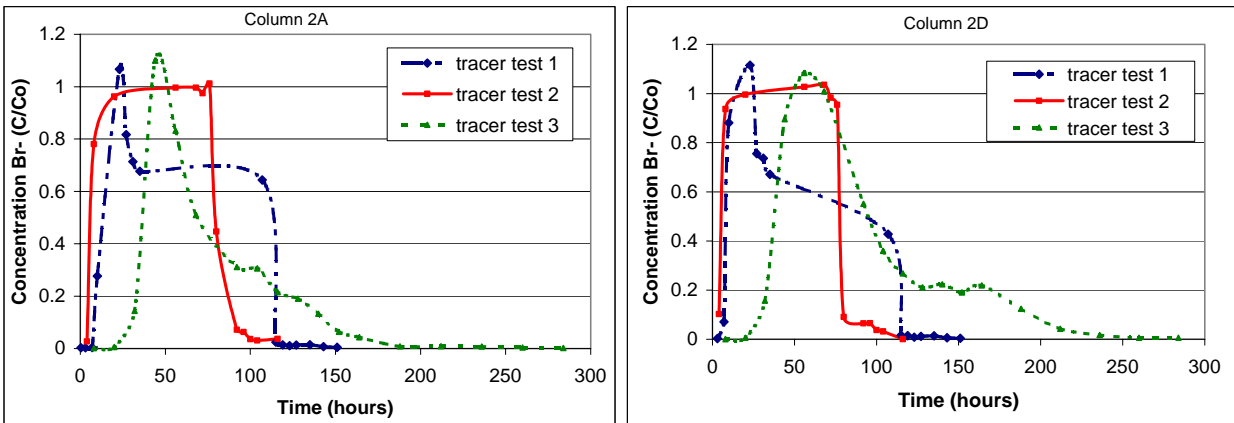
Figure C-5
Representative Nitrogen Series, Columns 2B and 4A

Other constituents of interest include COD, TS, alkalinity, and pH. The average concentration of COD in the wastewater during the study was 457 mg/L. COD concentrations were reduced to less than 100 mg/L in all column percolates during the duration of testing. The average concentration of TS in the applied wastewater was approximately 639 mg/L with TS percolate concentrations remaining relatively unchanged compared to wastewater applied values. Little variation was observed in the alkalinity of the applied wastewater, but percolate samples from all columns showed a decline in alkalinity during the length of the column operation with no significant difference observable between individual columns within each loading regime. While slight depressions (approximately 0.8 to 1.2 pH units) in pH over time were observed in the percolate of several columns, they could not be correlated to alkalinity trends, infiltrative surface, or loading regime.

To evaluate the treatment performance, the ratio of the cumulative mass of constituent applied to the column (M_a) to the cumulative mass of constituent detected in the percolate sample (M_p) was determined (Lowe *et al.* 2005). Observations indicate that while removal efficiencies might be less in systems receiving higher loading rates, ultimately a greater mass of target constituent might be removed prior to the system reaching equilibrium conditions independent of operating history. This suggests that alternative operating methods such as directing all of the flow to one trench for a given time period, then sequentially directing all the flow to a second trench for a given time period, and so forth may be more efficient in terms of mass removal of pollutants in WSASs.

Multicomponent Surrogate and Tracer Tests

Figure C-6 shows representative bromide BTCs from LR2 for one gravel-free and one gravel-laden column. Note that the BTCs for the other loading regimes were similar. Results from the bacteriophage tracer tests are described in Appendix B, *Pathogen Transport-Fate Studies*.



Note: Column 2A is aggregate-free and column 2D is aggregate-laden

Figure C-6
Bromide Breakthrough Curves During Tracer Tests 1, 2, and 3 From LR2

The BTCs from tracer test 1 (clean water) were extremely similar for all columns, indicating that the hydraulic flow regimes prior to wastewater loading were similar. The bromide breakthrough occurs rather quickly (less than 10 hours) with a decrease in concentrations after the peak concentration had occurred. (Note: The drop in breakthrough concentration during tracer addition was due to a change in bromide concentration in the influent holding tank that occurred when refilling the tank.) Also notable is a lack of tailing, which indicates that the porous medium in the columns is relatively homogeneous.

The BTCs for tracer test 2 is similar to that for tracer test 1, because the second tracer test was initiated after only two weeks of wastewater application. In the third tracer test (week six), breakthrough occurs later in all columns and significant tailing is observed. These changes are attributed to the biozone-development at the infiltrative surface with bromide retarded in the low-permeability biozone, increasing the time to observed breakthrough for the bromide pulse center of mass. This phenomenon also creates a heterogeneous system within the columns, wherein a low-permeability zone sits atop high-permeability sand causing additional dispersion of the solute front and increased tailing of the BTC (Brusseau 1994).

The computed mean travel time increased with each successive tracer test. The most significant increase occurred between the second and third tracer tests at which time continuous ponding developed in LR1 and LR2, indicative of biozone development and increased impedance to flow.

The K_e of the infiltrative surface zone in LR1 estimated from bromide tracer test travel times decreased, on average, by two orders of magnitude from week two to week six. For all columns, a reduction of between two to three orders of magnitude occurred between the K_e measured at system startup and the final measurements at week 20. The average K_e values after weeks 6 and 20 are similar for LR1 and LR2 with much of the reduction in K_e occurring over the first several weeks.

The similarities in final K_e values within LR1 and LR2 imply that under continuous application of the same STE and for a given sand media, a similar long-term hydraulic resistance of the infiltrative surface is reached regardless of initial hydraulic loading rate. Based on the results from this study, an exponential equation may be used to relate the effective hydraulic conductivity of the infiltrative surface to the cumulative volume loading of wastewater.

Siegrist (1987) and Siegrist and Boyle (1987) suggested that the rate of biozone development and associated infiltration capacity loss are a function of the mass-loading rate of wastewater pollutants. The results from this 1-D column study support this hypothesis for a given soil type and STE. Once the biozone matures to the point of continuous ponding, the resulting hydraulic conductivity of the infiltrative surface may be somewhat independent of historical loading rates. In other words, two systems of the same soil type loaded under differing design rates may, over time, develop a similar hydraulic resistance at the infiltrative surface. This condition probably occurs because the biozone forms relatively quickly and thereafter controls the long-term infiltration rate. However, the transient values of K_e can be predicted from the cumulative volume of wastewater infiltrated. The relationship between K_e and cumulative volume of effluent wastewater (or volume throughput) was determined for LR1 and for LR2 (Beach *et al.* 2005). Similar exponential functions for LR1, LR2, and LR1 and LR2 combined, indicate that an exponential function can be used to approximate the K_e of the infiltrative surface based on cumulative volume of wastewater applied to the system.

Conclusions

This research was performed to explore the biozone genesis and flow and transport process dynamics in WSASs. The following conclusions are drawn:

- K_e values calculated for the biozone region in the continuously loaded columns reached near steady values after less than three weeks of operation. Loading rate appears to have a negligible effect on K_e while infiltrative surface character has a significant effect on K_e .
- After 20 weeks of wastewater application, the K_e values for the infiltrative surface zone were generally less than 0.1% of the values measured prior to wastewater application for the higher loading regimes (LR1 and LR2), and were less than 1% of the original values for the lower loading regimes (LR3 and LR4).
- In the LR1 and LR2, the computed effective K_e of the infiltrative surface (biozone) for week 20 of operation were very similar. The similarities in K_e for LR1 and LR2 suggest that for a given sand media, STE, and application method, an equivalent long term hydraulic resistance of the biozone may be reached regardless of hydraulic loading history.
- Accelerated loading in the laboratory appears viable as a means of time-scale compression, while still producing infiltration rate responses to wastewater that are meaningful at the field scale.

- Infiltrative surface architecture effects pseudo-equilibrium throughput rates with the aggregate-free throughput rate (8.5 cm/d) over two times greater than that of the aggregate-laden columns (3.5 cm/d). While the pseudo-equilibrium rates computed for the 13-day pseudo-equilibrium period enable direct comparison between the two infiltrative surface types with a comparable period of operation and wastewater loading, these rates may not necessarily be equal to the final long term acceptance rate of the columns had they been operated for years.
- Columns receiving higher loading rates removed a higher total cumulative mass of the target constituents in wastewater prior to loss in throughput rates even though the treatment efficiency may be less at higher loading rates. This factor suggests that alternative operating methods for WSASs such as directing all of the flow to one trench for a given time period, then sequentially directing all the flow to a second trench for a given time period, and so forth may be more efficient in terms of pollutant mass removal.

References

Alder, H. L. and E. B. Roessler. 1977. *Introduction to Probability and Statistics*, Sixth Edition. W. H. Freeman and Company, San Francisco, CA.

American Public Health Association (APHA). 1998. *Standard Methods for the Examination of Water and Wastewater*, Twentieth Edition. Clesceri, L. S., A. E. Greenberg, and A. D. Eaton (eds.). APHA-AWWA-WPCF, Washington, DC.

Ausland, G. 1998. *Hydraulics and Purification in Wastewater*. Doctoral Dissertation. Colorado School of Mines, Golden, CO.

Beach, D. N. 2001. *The Use of One-Dimensional Columns and Unsaturated Flow Modeling to Assess the Hydraulic Processes in Soil-Based Wastewater Treatment Systems*. M.S. Thesis. Department of Geology and Geological Engineering, Colorado School of Mines, Golden, CO.

Beach, D. N. and J. E. McCray. 2003. "Numerical Modeling of Unsaturated Flow in Mature Wastewater Soil Absorption Systems." *Ground Water Monitoring and Remediation*. 23(2), 64–72.

Beach, D. N., J. E. McCray, K. S. Lowe, and R. L. Siegrist. 2005. "Temporal Changes in Hydraulic Conductivity of Sand Porous Media Biofilters During Wastewater Infiltration: Experimental Evaluation." *Journal of Hydrology*. In press.

Bouma, J. 1975. "Unsaturated Flow During Soil Treatment of Septic Tank Effluent." *Journal of Environmental Engineering Division*. ASCE, 101(EE6), 967–983.

Brusseau, M. L. 1994. "Transport of Reactive Contaminants in Heterogeneous Porous Media." *Reviews of Geophysics*. 32(3), 285–313.

Cole-Parmer Instrument Company. 2001. *Operating Instructions for Cole-Parmer 27502-04, -05 Bromide Electrodes*. 1092.

Crites, R. and G. Tchobanoglous. 1998. *Small and Decentralized Wastewater Management Systems*. McGraw-Hill Publishing Company, Boston, MA.

Evett. 2000. *Time Domain Reflectometry (TDR) System Manual*. Dynamac Inc.

Hach. 1998. *Water Analysis Handbook*. Second Edition. Hach Chemical Co., Loveland, CO.

Huntzinger, D. N., J. E. McCray, and S. Van Cuyk. 2000. "Numerical Simulation of Unsaturated Water Flow and Pollutant Transport in Soil-Based Wastewater Treatment Systems." *Geol. Soc. of Amer., Rocky Mountain Section Meeting, Abstracts with Programs*. 29.

Huntzinger, D., J. McCray, R. L. Siegrist, and S. Van Cuyk. 2001a. "Mathematical Modeling of Unsaturated Flow in Wastewater Soil Absorption Systems with Clogging Zones." *Onsite Wastewater Treatment*. Publication No. 701P0101. American Society of Agricultural Engineers, St. Joseph, MI. 106–115.

Huntzinger, D. N., J. E. McCray, R. L. Siegrist, K. Lowe, and S. Van Cuyk. 2001b. "The Use of One-Dimensional Laboratory Experiments to Assess Hydraulic Processes in Wastewater Soil Absorption Systems." *EOS Trans. Amer. Geophys. Union*. 82(20), S196.

Jenssen, P. D. and R. L. Siegrist. 1990. "Technology Assessment of Wastewater Treatment by Soil Infiltration Systems." *Water Science & Tech.* 22(3/4), 83–92.

Jones, J. H. and G. S. Taylor. 1965. "Septic Tank Effluent Percolation Through Sands Under Laboratory Conditions." *Soil Science*. 99(5), 301–309.

Lowe, K. S., D. N. Beach, S. Van Cuyk, R. L. Siegrist, and J. E. McCray. 2005. "Performance Evaluation of Wastewater Renovation by Sandy Porous Media Biofilters." *Journal of Environmental Engineering*. In preparation.

McCray, J. E., D. N. Huntzinger, S. Van Cuyk, and R. Siegrist. 2000. "Mathematical Modeling Of Unsaturated Flow And Transport In Soil-Based Wastewater Treatment Systems." *WEFTEC 2000 Conference Proceedings*, Anaheim, CA. Water Environment Federation, Alexandria, VA.

Microsoft, Corp. 1999. *Excel 2000*.

Minitab, Inc. 2002. *MINITAB Statistical Software*, Release 13. State College, PA. 16801–3008.

Schwager, A. and M. Boller. 1997. "Transport Phenomena in Intermittent Filters." *Water Sciences Technology*. 35(6), 13–20.

Siegrist, R. L. 1987. "Soil Clogging During Subsurface Wastewater Infiltration as Affected by Effluent Composition and Loading Rate." *J. Environmental Quality*. 16, 181–187.

Siegrist, R. L. and W. C. Boyle. 1987. "Wastewater Induced Soil Clogging Development." *J. Environ. Eng.* 113(3), 550–566.

Siegrist, R. L., E. J. Tyler, and P. D. Jenssen. 2001. "Design and Performance of Onsite Soil Absorption Systems." *National Research Needs Conference Proceedings: Risk-Based Decision Making for On-site Wastewater Treatment*, May 19–20, 2000, St. Louis, MO.

Siegrist, R. L., K. S. Lowe, J. McCray, B. Beach, and S. Van Cuyk. 2002. "Accelerated Loading for Evaluation of Long-term Performance of Soil PMBs used for Wastewater Renovation." *Proceedings of the Eleventh Northwest On-Site Wastewater Treatment Short Course*, April 3–4, 2002, Seattle, WA.

Snedecor, G. W. and W. G. Cochran. 1980. *Statistical Methods*, Seventh Edition. Iowa State University Press.

Thomas, R. E., W. A. Schwartz, and T. W. Bendixen. 1966. "Soil Chemical Changes and Infiltration Rate Reduction Under Sewage Spreading." *Soil Science Society of America Proceedings*. 30, 641–646.

Tyler, E. J., M. Milner, and J. C. Converse. 1991. "Wastewater Infiltration from Chamber and Gravel Systems. On-Site Wastewater Treatment." *Proceedings of the Sixth National Symposium on Small Sewage Systems*. Publication 10–91, 214–222. American Society of Agricultural Engineers, St. Joseph, MI.

United States Environmental Protection Agency (US EPA). 1978. *Management of Small Waste Flows*. EPA-600/2-78-173. Report of Small Scale Waste Management Project, University of Wisconsin, Madison, WI. US EPA, Municipal Environmental Res. Lab., Cincinnati, OH.

US EPA. 1980. *Design Manual for Onsite Wastewater Treatment and Disposal Systems*. US EPA, Municipal Environmental Res. Lab., Cincinnati, OH.

US EPA. 1997. *Response to Congress on Use of Decentralized Wastewater Treatment Systems*. US EPA, Office of Water, Washington, DC.

Van Cuyk, S., R. L. Siegrist, A. Logan, S. Masson, E. Fischer, and L. Figueroa. 2001. "Hydraulic and Purification Behaviors and their Interactions During Wastewater Treatment in Soil Infiltration Systems." *Water Research*. 35(4), 953–964.

Van Cuyk, S. 2003. *Fate of Virus During Wastewater Renovation in Soil Porous Media Biofilters*. Ph.D. Dissertation, Colorado School of Mines, Golden, CO.

Van Cuyk, S., R. L. Siegrist, K. Lowe, and R. W. Harvey. 2004. "Evaluating Microbial Purification During Soil Treatment of Wastewater with Multicomponent Tracer and Surrogate Tests." *Journal of Environmental Quality*. 33, 316–329.



D BIOZONE GENESIS AND WSAS PERFORMANCE: FIELD 3-D TEST CELLS

To facilitate onsite wastewater system testing, research, and education through controlled field-scale experimentation, the Mines Park Test Site was installed on the Colorado School of Mines (CSM) campus with support from several entities including private industry, professional organizations, and local, state, and federal government agencies. Field testing was initiated at the Mines Park Test site using three-dimensional (3-D) test cells to evaluate the dynamic and interdependent behavior of biozone genesis and hydraulic and purification processes during wastewater effluent treatment in wastewater soil absorption systems (WSASs). Information gained during this testing will be used for modeling including validation of the Watershed Analysis Risk Management Framework (WARMF) biozone algorithm, HYDRUS 2-D modeling, and refinement of an existing infiltration rate loss model (Siegrist 1987).

The establishment of the Mines Park Test Site southwest of the Mines Park student housing complex near the intersection of Highway 6 and 19th Street in Golden, Colorado was completed in two phases. Phase 1 involved the installation of a wastewater interception and treatment facility to support onsite wastewater systems (OWS) pilot-scale experiments and laboratory research. The Phase 1 wastewater interception and treatment facility includes two 1,500-gallon buried precast concrete tanks, an effluent filter, and a 72-inch diameter concrete chamber for sample collection and pilot-scale treatment unit testing (Figure D-1).

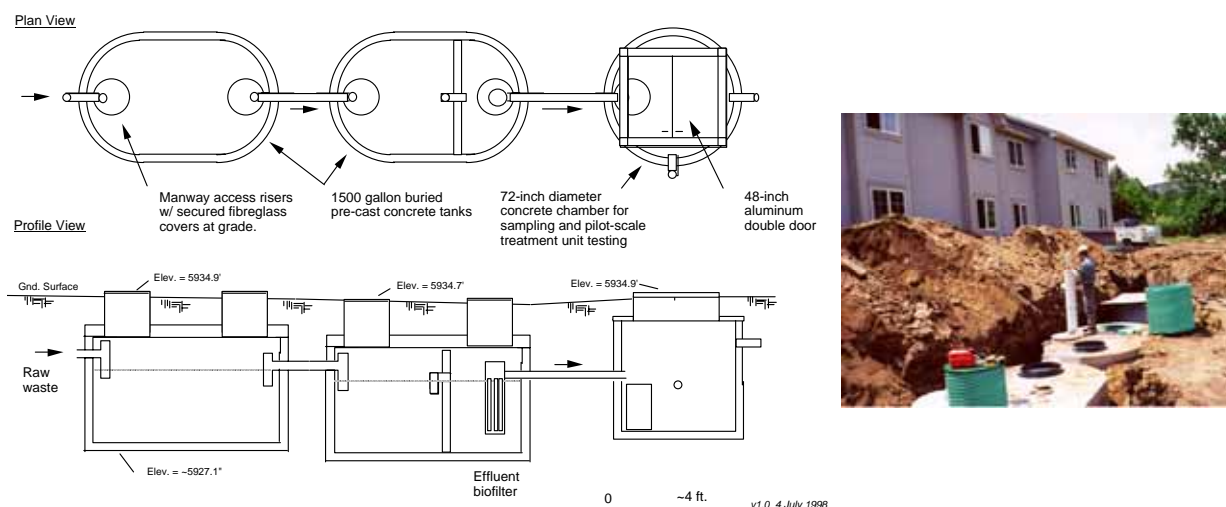


Figure D-1
Phase 1 Septic Tank and Effluent Vault at Mines Park

Routine monitoring indicates that the septic tank effluent (STE) is typical of residential STE containing appreciable concentrations of pollutants (Table D-1).

Table D-1
Effluent Composition of Mines Park Septic Tank Effluent¹

Parameter	Units	Average	No. of Samples	Std. Dev.	Coeff. Var.	Range
pH	–	–	14	–	–	6.19–7.20
Alkalinity	mg CaCO ₃ /L	209	14	17.0	0.081	165–260
TS	mg/L	585	20	54.7	0.093	380–670
TSS	mg/L	60	12	10.9	0.181	0–160
COD	mg/L	504	20	71.7	0.142	400–977
cBOD ₅	mg/L	276	12	22.4	0.081	200–472
Total N	mg-N/L	60.0	14	2.95	0.049	36–78
Nitrate N	mg-N/L	1.62	13	0.317	0.196	<0.05–6
Ammonium N	mg-N/L	53.7	16	5.64	0.105	45.8–62
Total P	mg-P/L	5.37	12	3.012	0.561	0.7–11.0
Fecal coliform bacteria	cfu/100 mL	–	19	–	–	5.1+E4–1.5+E7

¹Based on STE grab samples from the discharge of the second tank, March – September 2001.

Phase 2, initiated during 2002, involved establishment of a field research area to enable controlled field testing of OWS methods and technologies. A site evaluation of the research area was completed during Spring 2002 (Lowe and Siegrist 2002). Field experiments to evaluate the performance of WSASs as affected by infiltrative surface character and loading rate in an Ascalon sandy loam soil were initiated during Fall 2002 with installation of 40 *in situ* test cells representing a pilot-scale soil absorption trench. A set of test cells also received tap water as a control.

Materials and Methods

This section provides information on materials and methods, including:

- Site selection and evaluation
- *In situ* test cell installation and setup
- Monitoring

Site Selection and Evaluation

Initially, a site evaluation was conducted to assess the natural site and soil features critical to the design and performance of onsite wastewater treatment processes (Lowe and Siegrist 2002). This evaluation included:

- Inspecting soil profiles within two backhoe test pits
- Drilling and collecting soil samples from nine soil borings from ground surface to up to 22 feet (6.7 m) below ground surface
- Installing seven shallow groundwater observation wells
- Conducting percolation tests as prescribed by local OWS regulations

In addition, subsurface soil lithology and color were recorded for soil samples collected from the boreholes and analyzed for:

- | | | |
|------------------------|-----------------------|----------------------------|
| • Water content | • Nutrients | • Percent sand/silt/clay |
| • Total organic carbon | – Total nitrogen | • Grain size distribution |
| • Organic matter | – Nitrate-nitrogen | • Cation exchange capacity |
| • pH | – Ammonia-nitrogen | |
| • Potassium | – Available potassium | |

In Situ Test Cell Installation and Setup

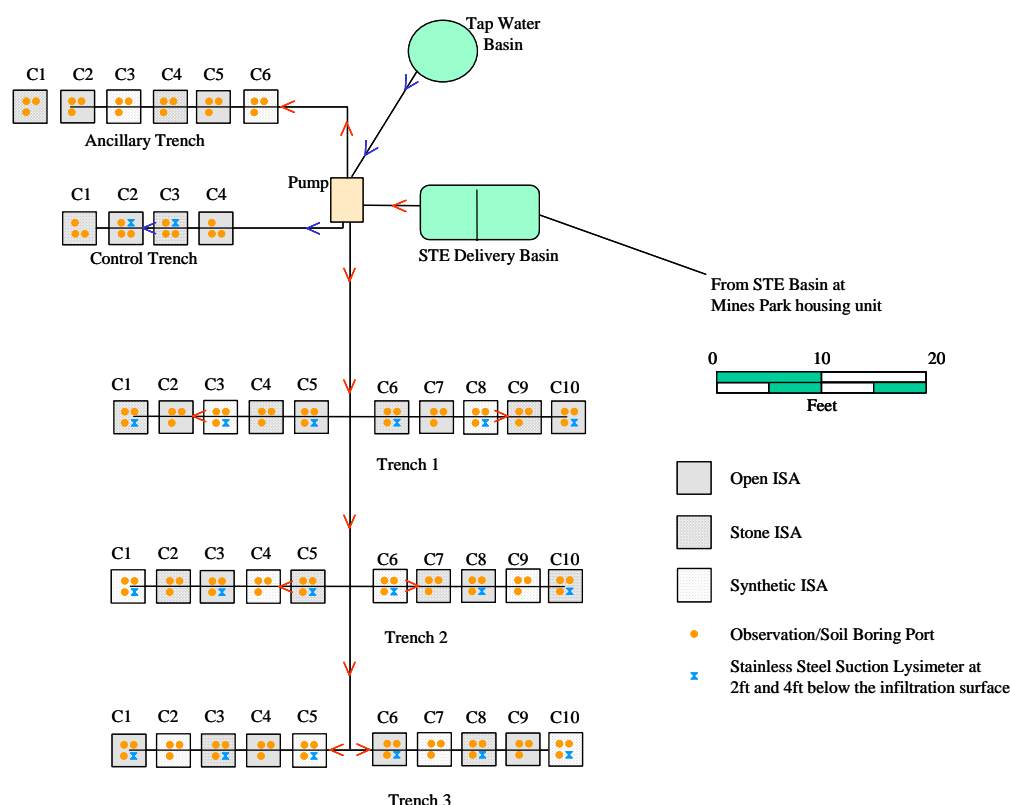
Initial testing at the Mines Park test site was initiated in July 2002 to evaluate under field conditions, the performance of WSASs as affected by infiltrative surface character and hydraulic loading rate in a sandy loam soil. Pilot-scale test cells were installed to mimic a typical OWS comprised of a soil absorption trench used to treat domestic STE. For this study, a replicated factorial design (2^2) was employed to evaluate three infiltrative surface architectures (open, stone, and synthetic) and two loading regimes (LR). Each condition, representative of feasible field conditions, was replicated five times (Table D-2) (3 infiltrative surface architectures \times 2 loading regimes \times 5 replicates = 30 test cells) (Tackett *et al.* 2004).

Table D-2
Experimental Conditions for the Test Cell Operation

Loading Regime	Test Cell ID	Infiltrative Surface Architecture	Exp. Design HLR	Loading Method Features
LR1	T1C1, T1C4, T2C2, T2C5, T3C3	Stone	4 cm/d (12.1 L/d per test cell)	STE with simulated gravity application; continuously dosed over 16 hr at 22 mL/min.
	T1C2, T1C5, T2C3, T3C1, T3C4	Open		
	T1C3, T2C1, T2C4, T3C2, T3C5	Synthetic		
LR2	T1C6, T1C9, T2C7, T2C10, T3C8	Stone	8 cm/d (24.2 L/d per test cell)	STE with simulated gravity application; continuously dosed over 16 hr at 44 mL/min.
	T1C7, T1C10, T2C8, T3C6, T3C9	Open		
	T1C8, T2C6, T2C9, T3C7, T3C10	Synthetic		
Control	TCC1	Stone	4 cm/d (12.1 L/d per test cell)	Tap water with simulated gravity application; continuously dosed over 16 hr at 22 mL/min.
	TCC2	Open		
Control	TCC3	Stone	8 cm/d (24.2 L/d per test cell)	Tap water with simulated gravity application; continuously dosed over 16 hr at 44 mL/min.
	TCC4	Open		

Note: Average loading rates after eight months of operation were 3.8 to 4.6 cm/d for LR1 and 6.3 to 7.7 cm/d for LR2; HLR = hydraulic loading rate

Loading regime 1 (LR1) receives 4 cm/d of STE delivered continuously to the test cell during a 16-hour period each day via a single orifice in the center of the cell. Loading regime 2 (LR2) receives STE in the same fashion but at a design rate of 8 cm/d. By loading the test cells at daily hydraulic loading rates of 4 or 8 cm/d compared to the regulatory prescribed rate of 2 cm/d, six months of daily operation are anticipated to reflect periods of operation equivalent to approximately two and four years, assuming all of the applied STE is processed through the test cell. In addition, six test cells were installed for ancillary testing. Finally, for control purposes, four test cells were installed and loaded with tap water (Table D-2). A total of 40 *in situ* test cells were installed (30 test cells + 6 ancillary cells + 4 controls) (Figure D-2).



Note: ISA = infiltrative surface architecture

Figure D-2
Schematic Detail of Experimental Layout.

Each test cell is approximately 26.5-in. long (approximately 67.3 cm) by 31.5-in. (80.0 cm) wide providing approximately 835 in.² (approximately 5,385 cm²) of bottom area infiltrative surface (Figure D-3). Test cells were installed within a trench with the infiltrative surface (bottom of the trench) located at approximately 30 in. (76 cm) below ground surface. To avoid potential hydraulic cross connection between test cells, each test cell was separated from the adjoining test cell by approximately 12 in. (30.5 cm) as well as end plates that were installed and sealed to the trench bottom and walls using a native soil slurry and bentonite. Stainless-steel suction lysimeters were installed at 2 feet. (61.0 cm) and 4 feet. (122 cm) below the infiltrative surface within a 2-in. diameter borehole in 20 test cells (three replicate conditions plus two control test cells) (Tackett 2004). The lysimeters were nested within the same borehole using a native soil slurry filter pack around the lysimeter and a bentonite seal between the two depths. During lysimeter installation, care was taken to avoid disruption of the infiltrative surface (the drilling rig was not driven on the trench bottom).

Prior to establishment of individual infiltrative surface architectures, the infiltrative surface for each test cell was examined, photographed and prepared in a similar fashion to remove any anomalous features and ensure replicate testing conditions between test cells. The infiltrative surface of the ancillary test cells was not modified and is assumed to be representative of an OWS system installed at a typical residence.

Access ports were installed for inspection of the infiltrative surface and for collection of intact soil cores. Finally, the test cells were backfilled, compacted and the site graded to minimize surface-water ponding due to rainfall and snow.

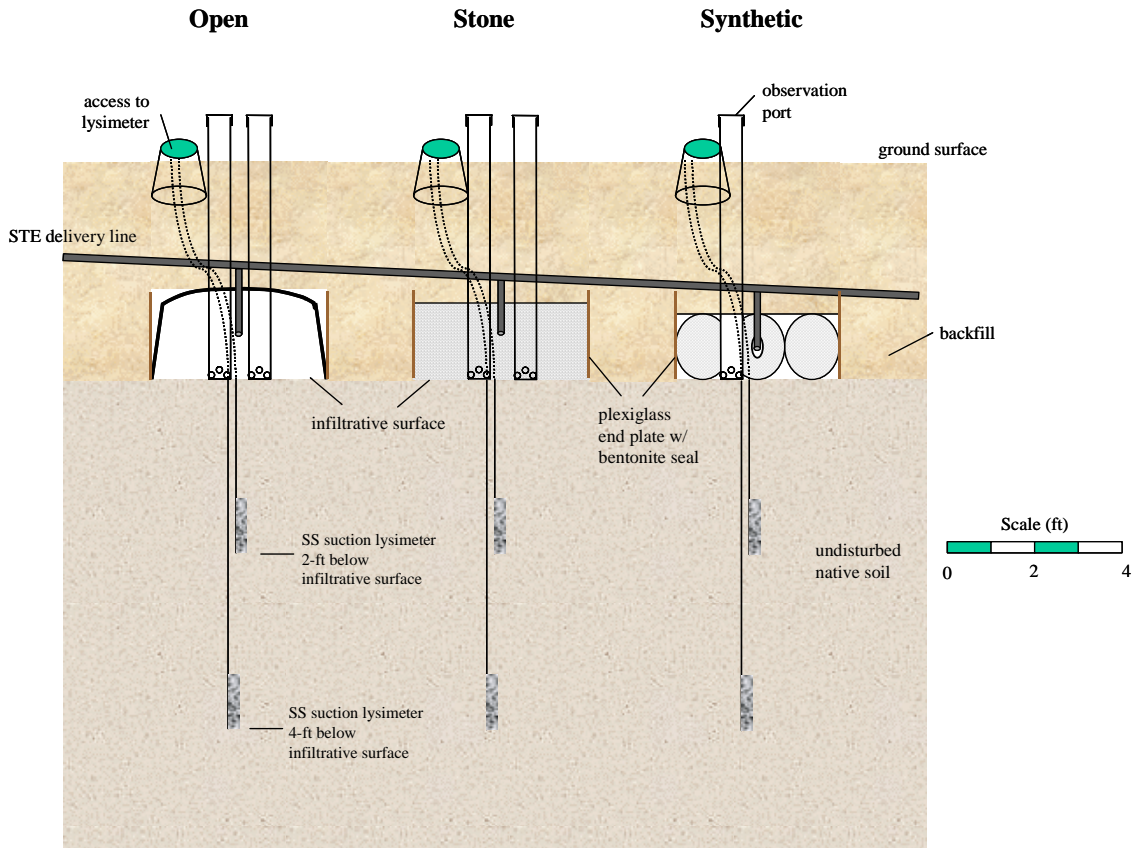


Figure D-3
Cross-Section View of Trench With WSAS Test Cells

Monitoring

Following test cell installation, baseline infiltration rates were measured using a constant-head permeameter (Hargett *et al.* 1982, Siegrist 1987). At least three infiltration rates tests were conducted for each test cell using a 2.5-cm head at the soil infiltrative surface. Test cells were then loaded with clean water for seven weeks to establish equilibrium flow conditions prior to loading with STE. During clean-water loading, a multisurrogate tracer test was conducted (Van Cuyk *et al.* 2001b). During multicomponent tracer and surrogate testing, bromide (approximately 2000 mg-Br/L) and MS-2 and PRD-1 bacteriophages (approximately 10^7 PFU/L) were added to the clean-water delivery basin and applied to the test cells during loading for 14 days. Samples were collected daily (24-hour-composite samples) from each lysimeter within the test area. Bromide samples were analyzed using an ion selective probe and MS-2 and PRD-1 bacteriophage assays were made following the plaque-forming-unit (pfu) technique (*Escherichia coli* and *Salmonella typhimurium* host, respectively) described by Adams (1959).

Loading of the test cells with STE began on May 5, 2003. STE from a nearby multifamily housing unit is being used and is the same STE used in previous research at CSM (Siegrist *et al.* 2002, Van Cuyk *et al.* 2001a). The STE is representative of a medium- to strong-effluent (Table D-1). STE is pumped from the existing interception tank near the housing unit to a delivery basin located at the Mines Park Test Site. From this delivery basin, STE is delivered to individual test cells at the prescribed loading rates of 4 and 8 cm/d (Figure D-1).

Routine field monitoring includes measurement of

- Applied effluent composition
- Applied effluent hydraulic loading rate
- Hydraulic behavior of the soil infiltrative surface (infiltration rate changes, ponding occurrence and magnitude)
- Soil-pore water quality

Grab samples of the STE are collected from the delivery basin approximately weekly and analyzed for a suite of parameters including (APHA 1998, Hach 1998):

- | | |
|--|---------------------------------------|
| • pH | • Total solids |
| • Alkalinity | • Total suspended solids |
| • Carbonaceous biochemical oxygen demand | • Nutrients (nitrogen and phosphorus) |
| • Chemical oxygen demand | • Fecal coliform bacteria |

The volume of STE applied to each test cell is measured every one to two weeks by recording pumping rate and pumping duration. The infiltration rate (cm/d) of the infiltrative surface of each test cell was measured prior to effluent application, after one month of operation, and will be measured after 12 months of operation using a constant-head technique (Hargett *et al.* 1982, Siegrist 1987).

Measurements of the occurrence and magnitude of ponding of the infiltrative surface are made every one to two weeks using an observation port installed in each test cell. Soil-pore water quality in the vadose zone was collected using stainless-steel suction lysimeters after one, two, three, four, five, and nine months of operation. Soil-pore water samples were analyzed for pH, alkalinity, dissolved organic carbon, and nutrients (nitrogen and phosphorus) (APHA 1998, Hach 1998).

During the spring and summer of 2004, a second multicomponent surrogate tracer test will be conducted. Similar to the clean-water tracer test, bromide (approximately 1,500 mg-Br/L) and MS-2 and PRD-1 bacteriophages (approximately 10^7 PFU/L) will be added to the STE delivery basin and applied to the test cells during loading. Samples will be collected daily (24-hr composite samples) from each lysimeter within the test area and analyzed using the methods as described for the clean-water tracer test.

After a period of tracer addition (7 to 10 days), duplicate intact cores may be collected from each test cell and analyzed for the presence of the tracers at selected depths below the infiltrative surface (0 to 4, 13 to 17, 28 to 32, and 58 to 62 cm). Analyses of the soil samples at multiple depths may also be made for morphology and water content, total organic carbon, nutrients, and fecal coliform bacteria.

Data analysis will enable assessment of the time-dependent changes in soil infiltration rates as affected by infiltrative surface architecture and effluent loading (Minitab, Inc. 2002 and Snedecor and Cochran 1980). Analysis of equilibrium infiltration rates achieved after system maturation will be assessed by analysis of variance (ANOVA) and other appropriate statistical tests (Siegrist *et al.* 2002). Analysis of variance and other statistical tests will also be completed to assess any differences or trends observed in soil properties with depth and between the test cells and the different experimental conditions.

Results and Discussion

This section provides results and discussion relevant to:

- Field Site Characteristics
- Baseline Characterization
- Performance

Field Site Characteristics

Based on the site characteristics and soil conditions observed, the site southwest of the Mines Park housing complex was judged to be suitable for wastewater treatment and reclamation research while satisfying the general goal of public health and environmental protection. An important note is that the specific goal of the site evaluation described herein was to ensure that high groundwater or low permeability of the subsurface native material would not diminish the soil treatment efficiency of proposed *in situ* test cells.

The general topography across the site exhibits an easterly aspect with a slope of approximately five to seven percent with the natural soil surface elevation between the elevations of 5,970 and 5,980 feet (1,820 to 1,823 m) above mean sea level. Surface water drainage in the immediate area follows the landscape topography and is generally to the east-southeast toward the small unnamed drainage.

Soil Conditions

General soil characteristics for Mines Park were initially assessed from the US Department of Agriculture (USDA) Soil Conservation Survey (SCS) report (USDA 1983). Soils at Mines Park are reported to be primarily Ascalon sandy loam (mixed, mesic Aridic Argiustolls). The parent materials are generally derived from igneous and metamorphic rocks of the mountains and sedimentary rocks of the foothills.

The typical soil profile includes a neutral, grayish-brown and dark grayish-brown sandy loam surface layer (0 to 7 in., 0 to 18 cm), with a mildly alkaline, brown sandy clay loam (7 to 11 in., 18 to 28 cm) and moderately alkaline, very pale brown sandy loam (11 to 18 in., 28 to 46 cm) subsoil layer, and a substratum of mildly alkaline and moderately alkaline, very pale brown sandy loam and gravelly sandy loam (18 to 60 in., 46 to 152 cm). SCS lists the soil as having moderate permeability and an average depth to bedrock of 60 in. (1.5 m).

Morphologic inspection of the natural soil profiles exposed in two backhoe test pits and nine soil borings was conducted according to accepted procedures (USDA 1981; SSSA 1986; US EPA 1991). Backhoe test pit #1 (BTP1), located in the northwestern portion of the site, revealed soil conditions that are generally dominated by unconsolidated, sandy loam soils with little bedding structure and/or macropores (Figure D-4). Roots were observed as deep as 3 feet (1 m) and a transition zone from sandy loam to highly weathered, friable igneous rock was observed at 5.5 feet (1.7 m) below ground surface (bgs). The soil matrix color of the sandy loam was generally in the 7YR4/4 range with soil mottling absent and of the weathered igneous rock generally in the 2.5YR5/4 range.



Figure D-4
Soil Test Locations

Backhoe test pit #2 (BTP2), located in the southeastern portion of the site, revealed a six-inch layer of sandy loam underlain by highly fractured, weathered siltstone. Observations of subsurface lithology in the nine soil borings revealed similar soil conditions with sandy loam soils ranging from approximately 2 feet (60 cm) thick in the southwestern portion of the site to approximately 6 feet (1.8 m) thick in the northern portions of the site. The transition zone to weathered igneous rock was encountered at each location underlying the sandy loam. Samples of soil materials were collected from soil borings at 2 feet (60 cm) intervals and analyzed for:

- | | | |
|------------------------|-----------------------|----------------------------|
| • Water content | • Nutrients | • Percent sand/silt/clay |
| • Total organic carbon | – Total nitrogen | • Grain size distribution |
| • Organic matter | – Nitrate-nitrogen | • Cation exchange capacity |
| • pH | – Ammonia-nitrogen | |
| • Potassium | – Available potassium | |

Grain size distributions for the sand fraction were determined by sieving dry soil and weighing the various sand fractions. Results indicated that 9 to 52% (average 24%) of the soil was coarse sand to fine gravel (greater than 2 mm), 46 to 85% (average 73%) was medium to fine sand (2 mm to 0.075 mm), and 1.3 to 9% (average 3%) was silt and clay (less than 0.075 mm). The grain size distribution was exceptionally uniform across the site with a general trend of increasing sand particle size with depth. To better define the silt and clay fractions, percent silt/sand/clay analysis was determined by hydrometer analysis. Results from this analysis revealed sandy loam soil texture across the site.

Total percent organic matter in the upper 10 feet of soils ranged from 0.1 to 1.4% (average 0.6%) with a general trend of decreasing organic matter with depth. Cation exchange capacity ranged between 2.5 and 22.1 meq/100 g dry soil (average 8.2 meq/100 g dry soil) and was relatively constant across the site.

As expected, soils with higher clay content had a slightly higher cation exchange capacity. Other properties of interest include pH, total nitrogen (TN), ammonia-nitrogen (NH₄-N), nitrate-nitrogen (NO₃-N), available phosphorus and potassium (avail. P and K), and exchangeable calcium and magnesium (exch. Ca and Mg) (Table D-3).

Table D-3
Summary of Soil Properties

	pH	Org. Mat. (%)	TN (ppm)	NH ₄ -N (ppm)	NO ₃ -N (ppm)	Avail. P (ppm)	Avail. K (ppm)	Exch. Ca (ppm)	Exch. Mg (ppm)	CEC (meq/ 100 g)
High	9.1	1.4	585.7	32.2	1.5	26.0	322.0	3770.0	440.0	22.1
Low	5.2	0.1	6.8	1.9	0.5	1.0	50.0	310.0	70.0	2.5
Average	7.3	0.5	124.0	5.2	0.7	4.4	117.3	1214.8	232.4	8.2
Median	7.4	0.5	77.4	3.7	0.6	2.5	109.0	1005.0	230.0	6.8
Std Dev	1.01	0.33	138.41	4.93	0.19	4.80	46.62	791.94	113.31	4.67
CV	0.14	0.64	1.12	0.94	0.28	1.10	0.40	0.65	0.49	0.57

Subsurface Conditions

No saturated conditions, either perched or continuous, were observed in the two backhoe test pits or eight of nine soils borings. In the southeastern corner of the site located closest to the unnamed surface drainage, continuously saturated conditions were observed at 16.5 feet (5 m) bgs during sampling of soil borings in April 2002. Shallow groundwater observation wells were installed at seven soil boring locations. After installation, groundwater was present at two locations at 9.44 feet (2.88 m) bgs and 14.37 feet (4.38 m) bgs. Soil moisture content, based on dry weight, was determined at each borehole location at 2 feet (60 cm) intervals to approximately 20 feet (6 m) bgs. Results indicated no marked change with depth (excluding the southeastern corner) across the site with most values ranging between 4 and 9%, dry weight basis. While it is acknowledged that these groundwater observation wells were installed during an unusually dry year, mottling indicative of high groundwater was limited across the site. Mottling was observed in three of the nine borings all located in the southeast portion of the site at depths greater than 5 feet (1.5 m) bgs.

Percolation tests were conducted at four locations yielding an average percolation rate of 15.5 minutes per inch. Tests were performed on 4-in. (10-cm) diameter holes at a total depth of 3 feet. (1 m) below ground surface. Each hole was filled with water to at least 14 in. (36 cm) for 20 to 24 hrs, prior to testing. Following saturation of the test hole, the time for the water to drop 1 in. (2.5 cm) within the lower 6 inches (15 cm) of the hole was measured and recorded as the number of minutes per inch drop (min/in). Comparison of the individual rates and the average of all rates together to the boundary range of 5 and 60 min/in, indicates that the site is suitable for conventional soil absorption of STE. While conventional percolation tests are widely recognized as a poor measure of soil hydraulic capacity, tests were completed as required in the Jefferson County Regulations (Jefferson County 1999) and the results provide a relative measure of hydraulic capacity across the site.

Baseline Characterization

Baseline infiltration rates were measured within each test cell using a constant-head permeameter (2.5-cm head at the soil surface). A minimum of three tests were completed for each test cell with more than 800 measurements made across the site. Based on these tests, the infiltration rate of the soil was consistent across the site with an average infiltration rate of 41.8 cm/d (standard deviation of 20.8 cm/d) (Figure D-5).

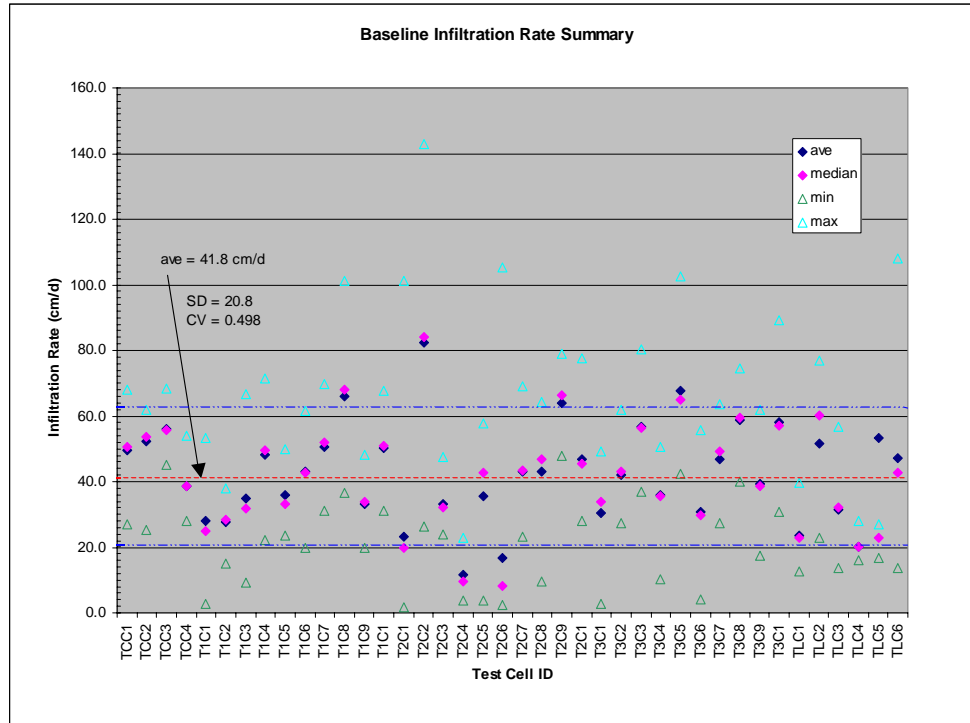


Figure D-5
Baseline Infiltration Rates Measured by Constant-Head Permeameter

Prior to wastewater loading to the test cells, a clean-water multicomponent surrogate and tracer test was conducted to evaluate baseline travel times. Results indicated consistent soil properties across the site with peak bromide tracer concentrations observed at 2 feet below the infiltrative surface at approximately 5 days after tracer/surrogate addition and at approximately 14 days after tracer/surrogate addition at 4 feet below the infiltration surface. In each case the bromide curve showed a similar increasing trend during addition and decreasing trend after tracer addition was terminated. Bacteriophage was sporadically detected in the lysimeter samples indicating a high removal of the bacteriophage by the soil due to either inactivation or adsorption.

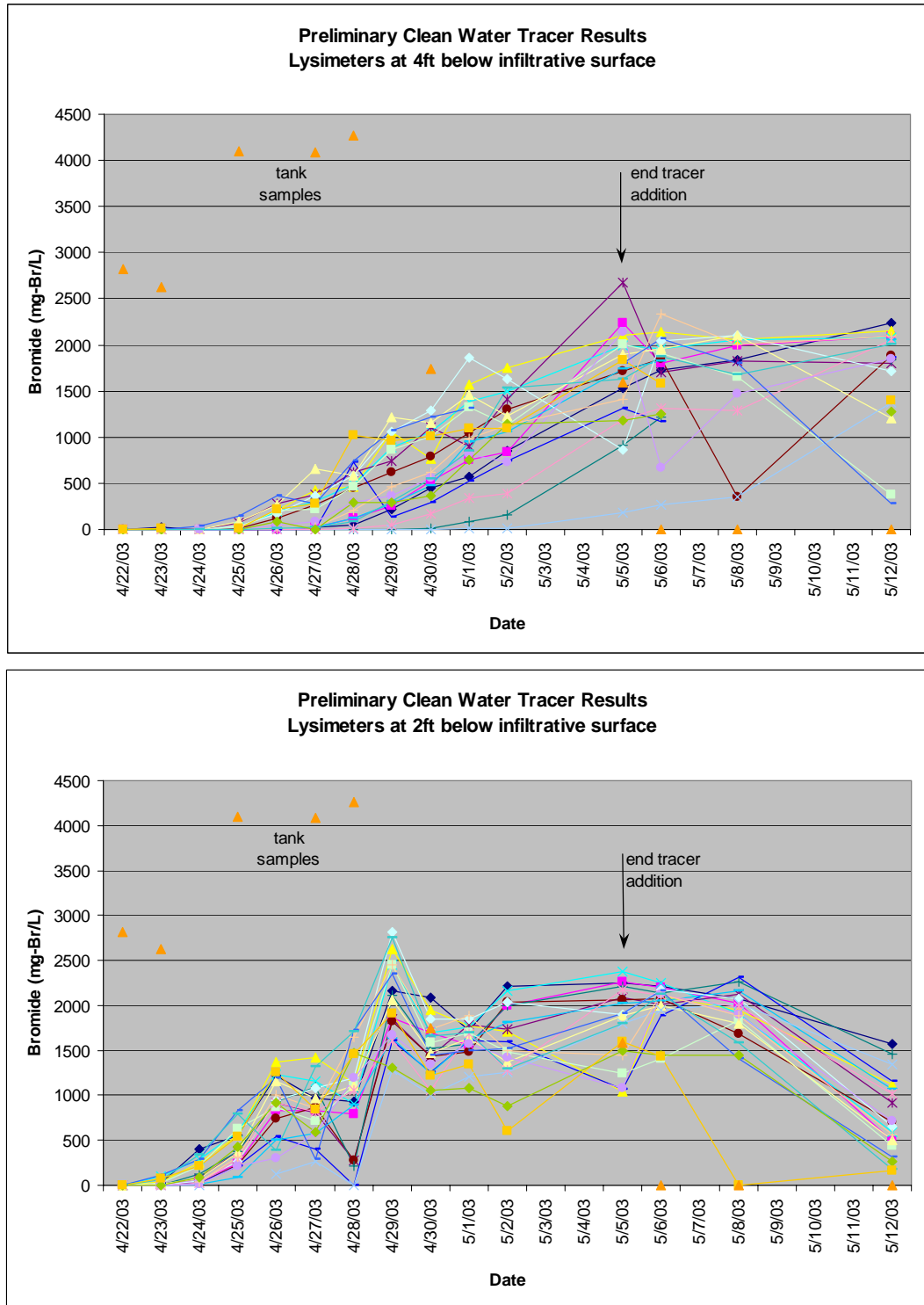


Figure D-6
Clean-Water Bromide Tracer Test

Performance

Within approximately one month of operation with STE design application at 4 or 8 cm/d (2× or 4× times the design rate for this soil type, actual rates ranged from 3.8 to 4.6 cm/d and 6.3 to 7.6 cm/d, respectively), the soil infiltrability had declined and continuous ponding was present indicating the development of a biozone (Siegrist and Boyle 1987). This loss in infiltration rate was consistent with that expected based on *a priori* predictions made using the model of Siegrist (1987), which predicts infiltration rate loss as a function of cumulative mass loading of total BOD and TSS. Based on a STE composition with BOD = 275 mg/L and TSS = 60 mg/L and a hydraulic loading rate of 4 cm/d, model predictions revealed that the loss in infiltration rate would lead to ponding of the infiltrative surface after approximately two months of operation, while at 8 cm/d this was anticipated to occur after one month. Comparison of infiltration rates measured using a constant-head permeameter prior to STE application and after one month of operation revealed a 60 to 85% reduction in infiltration rate (Siegrist *et al.* 2004).

Assessment of the treatment performance as measured by collection and analyses of soil-pore water quality using stainless-steel suction lysimeters at 2 feet and 4 feet below the infiltrative surface is ongoing.

Based on monitoring completed to date, the following behaviors have been observed:

- Phosphorus removal has remained near 100% for both loading rates and all infiltrative surface architectures.
- Near complete nitrogen removal was observed initially, but has declined as there was an increase in NO_3^- concentrations due to nitrification in the shallow vadose zone.
- Samples collected after seven months of operation at the 60-cm depth showed on average approximately 95% removal of DOC for 4 cm/day and approximately 90% for 8 cm/day.
- Test cell infiltrability declined sufficiently that intermittent or continuous ponding of the infiltrative surface evolved after one month or so of operation, but this has had no apparent effect on effluent purification processes.

Results from lysimeter sampling conducted during the first nine months can be found in Tackett 2004 and Tackett *et al.* 2004.

Summary

The Mines Park Test Site was established on the CSM campus in 2002 to facilitate onsite wastewater system testing, research, and education through controlled field-scale experimentation. Site evaluation completed in spring 2002 deemed the area as suitable for wastewater treatment and reclamation research while satisfying the general goal of public health and environmental protection. Installation of the *in situ* test cells was completed in fall 2002 with operation and monitoring of the 40 *in situ* test cells expected to continue through spring/summer 2004. Preliminary results from baseline infiltration rates and the clean-water tracer test indicate that the soil conditions across the site are comparable.

Testing to evaluate wastewater treatment in WSASs as affected by infiltrative surface character and loading rate in a sandy loam soil is ongoing. Preliminary results indicate that within approximately one month of operation, the soil infiltrability had declined and continuous ponding was present. A previously determined infiltration rate loss model (Siegrist 1987) was useful to predict this observed infiltration rate loss in the field. After nine months of operation, high removal rates of nutrients and carbon were observed. Changes to the soil properties, hydraulic behavior of test cells under the design conditions, and treatment performance will continue to be monitored through summer 2004. It is recommended that results from this work be used for biozone genesis modeling (HYDRUS 2-D) and refinement to the WARMF biozone algorithm. Publications describing the testing at the Mines Park Test Site will be forthcoming in conference proceedings and journals.

References

- Adams, M. H. 1959. *Bacteriophages*. Interscience Publishers, New York, NY.
- American Public Health Association (APHA). 1998. *Standard Methods for the Examination of Water and Wastewater*, Twentieth Edition. Clesceri, L. S., A. E. Greenberg, and A. D. Eaton (eds.). APHA-AWWA-WPCF, Washington, DC.
- Hach. 1998. *Water Analysis Handbook*. Second Edition. Hach Chemical Co., Loveland, CO.
- Hargett, D. L., E. J. Tyler, and R. L. Siegrist. 1982. "Soil Infiltration Capacity as Affected by Septic Tank Effluent Application Strategies." *Onsite Sewage Treatment*. ASCE, 1-82, 72-84.
- Jefferson County. 1991. *Individual Sewage Disposal System Regulations*. Adopted by the Board of Health of Jefferson County, Colorado on November 17, 1998. Effective Date, January 1, 1999.
- Lowe, K. S. and R. L. Siegrist. 2002. *Site Evaluation Report for the Wastewater Reclamation Test Site*. Project Report Submitted to Jefferson County Department of Health and Environment. Colorado School of Mines, Golden, CO. June 2002.
- Minitab, Inc. 2002. *MINITAB Statistical Software*, Release 13. State College, PA. 16801-3008.
- Siegrist, R. L., J. E. McCray, and K. S. Lowe. 2004. "Wastewater Infiltration into Soil and the Effects of Infiltrative Surface Architecture." *Small Flows Quarterly*. 5(1), 29-39.
- Siegrist, R. L., K. S. Lowe, J. McCray, B. Beach, and S. Van Cuyk. 2002. "Accelerated Loading for Evaluation of Long-term Performance of Soil PMBs Used for Wastewater Renovation." *Proceedings of the Eleventh Northwest On-Site Wastewater Treatment Short Course*, April 3-4, 2002, Seattle, WA.
- Siegrist, R. L. 1987. "Soil Clogging During Subsurface Wastewater Infiltration as Affected by Effluent Composition and Loading Rate." *J. Environmental Quality*. 16, 181-187.

Siegrist, R. L. and W. C. Boyle. 1987. "Wastewater Induced Soil Clogging Development." *J. Environmental Engineering*. 113(3), 550–566.

Snedecor, G. W. and W. G. Cochran. 1980. *Statistical Methods*, Seventh Edition. Iowa State University Press.

Soil Science Society of America (SSSA). 1986. *Methods of Soil Analysis, Part 1, Physical and Mineralogical Methods*, Second Edition. Arnold Klute (ed.). American Society of Agronomy, Inc. and Soil Science Society of America, Inc., Madison, WI.

Tackett, K. N. 2004. *Vadose Zone Treatment During Effluent Reclamation as Affected by Infiltrative Surface Architecture and Hydraulic Loading Rate*. M.S. Thesis. Environmental Science & Engineering Division, Colorado School of Mines, Golden, CO.

Tackett, K. N., K. S. Lowe, R. L. Siegrist, and S. M. VanCuyk. 2004. "Vadose Zone Treatment During Effluent Reclamation as Affected by Infiltrative Surface Architecture and Hydraulic Loading Rate." *Proceedings of the Tenth National Symposium on Individual and Small Community Sewage Systems*, Sacramento, CA. American Society of Agricultural Engineers, St. Joseph, MI. 655–667.

United States Department of Agriculture (USDA). 1981. *Soil Survey Manual, Chapter 4—Examination and Description of Soils in the Field*. USDA, Soil Conservation Service, Washington, DC.

USDA. 1983. *Soil Survey of Golden Area, Colorado*. USDA, Soil Conservation Service, Washington, DC.

United States Environmental Protection Agency (US EPA). 1991. *Description and Sampling of Contaminated Soils: A Field Pocket Guide*. EPA/625/12-91/002. US EPA, Center for Environmental Research Information, Cincinnati, OH.

Van Cuyk, S., R. L. Siegrist, A. Logan, S. Masson, E. Fischer, and L. Figueroa. 2001a. "Hydraulic and Purification Behaviors and Their Interactions During Wastewater Treatment in Soil Infiltration Systems." *Water Researc*. 35(4), 953–964.

Van Cuyk, S., R. L. Siegrist, and A. J. Logan. 2001b. "Evaluation of Virus and Microbial Purification in Wastewater Soil Absorption Systems Using Multicomponent Surrogate and Tracer Additions." *Onsite Wastewater Treatment*. Publication No. 701P0101. American Society of Agricultural Engineers, St. Joseph, MI. 30–40.



E WATER QUALITY MONITORING

The goals of the water quality monitoring effort described in this appendix are three fold. The first goal was to complete a surface water quality assessment of the Dillon Reservoir study area. This assessment included analysis and interpretation of both spatial and temporal trends and a comparison of the water quality data gathered in the study to surface water quality standards. The second goal was to determine what, if any, are the effects of onsite wastewater systems on surface water quality. The third and final goal was to produce a water quality database that could be used to enable watershed modeling efforts completed as part of this project. This appendix summarizes the water quality monitoring activities completed while further details may be found in Guelfo (2003).

Background

Types of onsite wastewater systems (OWS) vary, but in most cases OWS refers to a septic tank pretreatment unit that disperses effluent to a wastewater soil absorption system (WSAS) (Crites and Tchobanoglous 1998; Siegrist *et al.* 2001; US EPA 1980; US EPA 2002). Some treatment occurs in the tank, but the WSAS must furnish the majority of the wastewater treatment by various processes occurring including filtration, chemical reactions, and biological transformations (Hagedorn *et al.* 1981; Siegrist *et al.* 2001). When installed and maintained correctly, septic systems can provide adequate treatment of domestic wastewater. However, in recent years there has been an increase in septic system densities in some areas (Harman *et al.* 1996). This coupled with systems that are aging, poorly maintained, or poorly designed has caused increased concern over the ability of OWS to protect the underlying groundwater (Canter and Knox 1984; US EPA 1980).

OWS and Watershed Water Quality

In most cases, septic tank effluent (STE) is discharged to a WSAS and not directly to surface waters (Patrick 1988; US EPA 1980). Assuming that this is the case, surface water contamination by OWS will be through discharge of contaminated groundwater to surface water bodies. Jones and Lee (1979) offer several considerations with regards to the potential for contaminated, discharged groundwater to affect the quality of surface water. The first consideration is whether or not there is any interaction between groundwater and surface water that will allow the contaminants to enter the surface water system.

Second, if interactions are present and contaminants are discharged to tributaries, there is some chance that uptake or settling out will occur prior to that stream flowing to a lake where contaminant accumulation could occur.

The third consideration involves the case of contaminants entering a lake through groundwater discharge. If groundwater discharge occurs below stratification in the lake, contaminants may be trapped, for example, in the hypolimnion.

Fourth, is the importance of determining the limiting nutrient because, for example, if nitrogen is the limiting nutrient, then discharge of excess phosphorous will not be of as much concern.

In many cases, nutrient trends observed in surface waters have the potential to be caused by natural processes occurring in and around the stream system (in the riparian zone) (Hill 1996). Such processes may also affect nutrient trends caused by OWS. In order to fully realize what potential forces are present that cause nutrient trends in this study area, it is important to understand some of these processes.

Riparian Zones

A riparian zone is defined as, “the strip of land between the stream channel and hillslope...” (Hill 1996). There has been extensive research done on the ability of riparian zones to reduce the effects of nonpoint source pollution from various activities (such as agriculture, OWS) (Hill 1996). Riparian zones are known most for their ability to remove nitrate-nitrogen, but some research has been done on the removal of sediments and phosphorous as well. Riparian zones can affect the quality of both surface runoff and subsurface waters. Processes discussed in the following sections are meant to be concerned with subsurface flow, though some may extend to the surface runoff as well.

Most literature agrees that the primary removal mechanisms of subsurface nitrate in the riparian zone are vegetation uptake and denitrification (Gilliam 1994; Hill 1996; Vought *et al.* 1994). Hill points out that denitrification results in permanent removal of the nitrate from the riparian zone, while nitrate used by plants will eventually be released back to the soil when the plant decomposes (Hill 1996). In some cases this release could cause an increase in nitrogen levels (US EPA 2000). Other considerations regarding plant uptake of nitrate in the riparian zone include the potential for this mechanism to be seasonal in its magnitude. For example, vegetation may tend to use more nitrate during the summer when peak growing season occurs (Hill 1996). On the other hand, in warm climates seasonal variation may not be an issue. Many experts think that denitrification is the most important removal process of nitrate in the riparian zone subsurface waters (Hill 1996; Vought *et al.* 1994).

The process of denitrification reduces nitrate to nitrite, which is further reduced to gaseous forms of nitrogen (Hill 1996). Denitrification relies on anaerobic soil conditions and a ready supply of nitrate and organic carbon (Hill 1996). One final process that may occur in riparian wetlands is nitrogen fixation (US EPA 2000). This process can occur under both aerobic and anaerobic conditions, and can be a significant sink for nitrogen in wetlands (US EPA 2000).

The removal of phosphorous from groundwater in the riparian zone has not been researched as thoroughly as nitrate. Removal of phosphorous has been documented, but studies have found riparian zones to be much more efficient at nitrate removal (Gilliam 1994; Vought *et al.* 1994). Some studies have found that most of the phosphorous removed in the riparian zones was associated with sediment (Gilliam 1994). Riparian zones tend to be exceptionally efficient at sediment removal (Gilliam 1994), so it naturally follows that phosphorous associated with sediment would be removed as well. Other potential mechanisms for phosphorous removal in the riparian zones are similar to those already discussed for phosphorous removal in a WSAS. Vought *et al.* (1994) pointed out that there could be conflicting conditions necessary for nitrogen and phosphorous removal in the riparian zone. The conditions that are necessary for denitrification to occur may subsequently cause leaching of phosphorous from metal complexes (US EPA 2000; Vought *et al.* 1994). Changes in pH of the riparian zone waters and release of phosphorous from biological decay can also return phosphorous to the water column (US EPA 2000).

Nutrient processes in riparian zones have the potential to be especially complex. However, the literature seems conclusive that nitrate removal is likely. Phosphorous removal may or may not occur depending on riparian zone conditions. The processes discussed previously are concerned mainly with subsurface or groundwater flow; however, Vought *et al.* point out that subsurface flows can extend to water that flows from streams into the riparian zone, and back into the streams (Vought *et al.* 1994). This fact indicates that riparian zone processes may affect nutrient trends seen within the stream as well.

Effects of OWS on Surface Waters

An attempt was made to find other studies that explored the effects of OWS on surface waters through stream monitoring. Only one study was found that incorporated stream monitoring in determining these effects. That study will be summarized in this section. Other studies assessed the potential for surface water contamination by studying groundwater contamination present due to OWS. One such study will also be discussed in this section. Note that there are numerous studies of effects of OWS on groundwater that are not cited in this appendix.

In 1998, Flynn and Barber (2000) conducted a study near Boulder, CO to evaluate whether OWS were impacting surface water or groundwater entering a local reservoir. The reservoir, Barker Reservoir, is of particular concern because it supplies 40% of the drinking water to the city of Boulder. The study monitored a total of 12 drinking water wells and 10 surface water sites situated both north and south of the reservoir in order to meet the objective. Conclusions were drawn based on comparisons between sites situated upgradient of development and those located downgradient. A variety of parameters were analyzed including field parameters (pH and temperature), major ions, boron, nutrients, and bacteria. Results revealed that groundwater north of the reservoir did not demonstrate widespread contamination, but that surface water sites south of the reservoir (groundwater sites were limited in this area so conclusions could not be drawn) had greater concentrations of some wastewater constituents than did other, upgradient surface water sites. The study concluded that this contamination was possibly from OWS, but could also have been generated by runoff, wildlife, or domestic animals (Flynn and Barber 2000).

An older study conducted by Jones and Lee (1979) studied the potential of surface water contamination due to OWS through groundwater monitoring of a newly installed septic system. This study was concerned mainly with the potential for nutrient contamination to a nearby lake in Wisconsin. The purpose of the study was to determine whether or not OWS would be an adequate means of waste disposal for a new development. The study was conducted by placing monitoring wells near a new septic system, not yet in use. These wells were then monitored from a time just before use of the system was initiated to a time four years later. In general, wells were monitored for:

- Alkalinity
- Ammonia
- Calcium
- Chloride
- Magnesium
- Organic nitrogen
- pH
- Potassium
- Sodium
- Soluble orthophosphate
- Specific conductance
- Total phosphorous

After six months of septic system use, only migration of alkalinity and specific conductance were detected; no nutrient migration was found. Samples were collected at various times during the four year sampling period, but never was any migration of nutrients found. Plume migration could be detected, however, through elevated specific conductance and chloride values at progressive distances from the system. Jones and Lee concluded that since no migration of nutrients was measured, OWS posed no threat to nearby surface waters, and therefore, OWS were a viable option for the new development (Jones and Lee 1979).

Description of the Study Area

This study was conducted in the Dillon Reservoir watershed. Dillon Reservoir is a man-made reservoir that was completed in 1963. the reservoir is approximately 3,140 acres in area and 246,777 acre-feet in volume (Summit County Government 1998). There are three major streams that flow into the reservoir: Tenmile Creek, Blue River, and Snake River. This study focuses on portions of Tenmile Creek, Blue River, and the reservoir itself. Further description of these portions of the study area are provided in the following section on a sub-watershed basis.

Watershed Features

In the northern portion of the Dillon Reservoir, watershed geology consists of the Pinedale and Bull Lake glacial drift deposits that are Pleistocene in age. In the northwest portion of the watershed, Precambrian biotite gneiss and migmatite underlies the aforementioned Pleistocene deposits. Near Swan River, there are Tertiary and Cretaceous intrusive porphyries. Closer to Breckenridge, the Pierre Shale, Upper Cretaceous in age, can be found under the soil layer. Finally, along portions of the Blue River there are large deposits of recent stream and outwash gravels (Tweto 1973).

Precipitation varies greatly in the Dillon Reservoir watershed because of the varying degrees of elevation, 7,947 to 14,270 feet, in the study area. This elevation change also causes a high variation in the air temperature of the study area, hence causing varying degrees of snowmelt throughout the study area. Depth to groundwater in the study area ranges from 4 to 70 feet, based on preliminary investigations by Smith (Smith *et al.* 2002). The presence of shallow depths in some areas indicates that there is a high probability of groundwater contributions to base flow in some areas (Smith *et al.* 2002). Furthermore, the presence of flow in the months of January through March, when it is likely that no snowmelt is contributing to flow, indicates that there are other sources of base flow (Lemonds 2003). Therefore flow of OWS effluent through groundwater to surface water is possible.

There are two major areas of development upstream of Dillon Reservoir. These are the towns of Frisco and Breckenridge (see Figure E-1). Rapid development of these towns and others in the area caused Summit County to be the most rapidly growing county in the country from 1970 to 1980. During this time period, there was a 232% increase in population. From 1980 to 1990, there was a 45.6% increase in population. From 1970 to 1998, total number of housing units increased from 2,198 to 23,019 (Summit County Government 1998). Many of these homes use OWS as a primary means of domestic waste disposal. Increases such as those mentioned here have the potential to greatly affect local water quality. The town of Frisco utilizes both surface water and wells as a source of drinking water. Breckenridge utilizes a small reservoir, Goose Pasture Tarn, as well as South Barton Creek for its drinking water.

Smaller focus areas were designated within the study area in order to understand the effects of OWS on a smaller scale. For example Blue River Estates, which is situated along Pennsylvania Creek, uses exclusively OWS as a means of domestic waste disposal. Pennsylvania Creek was therefore chosen as a focus area to determine if these OWS were impacting the creek or the Blue River downstream of its convergence with the creek. Swan River and portions of Tenmile Creek were chosen as focus areas for similar reasons.

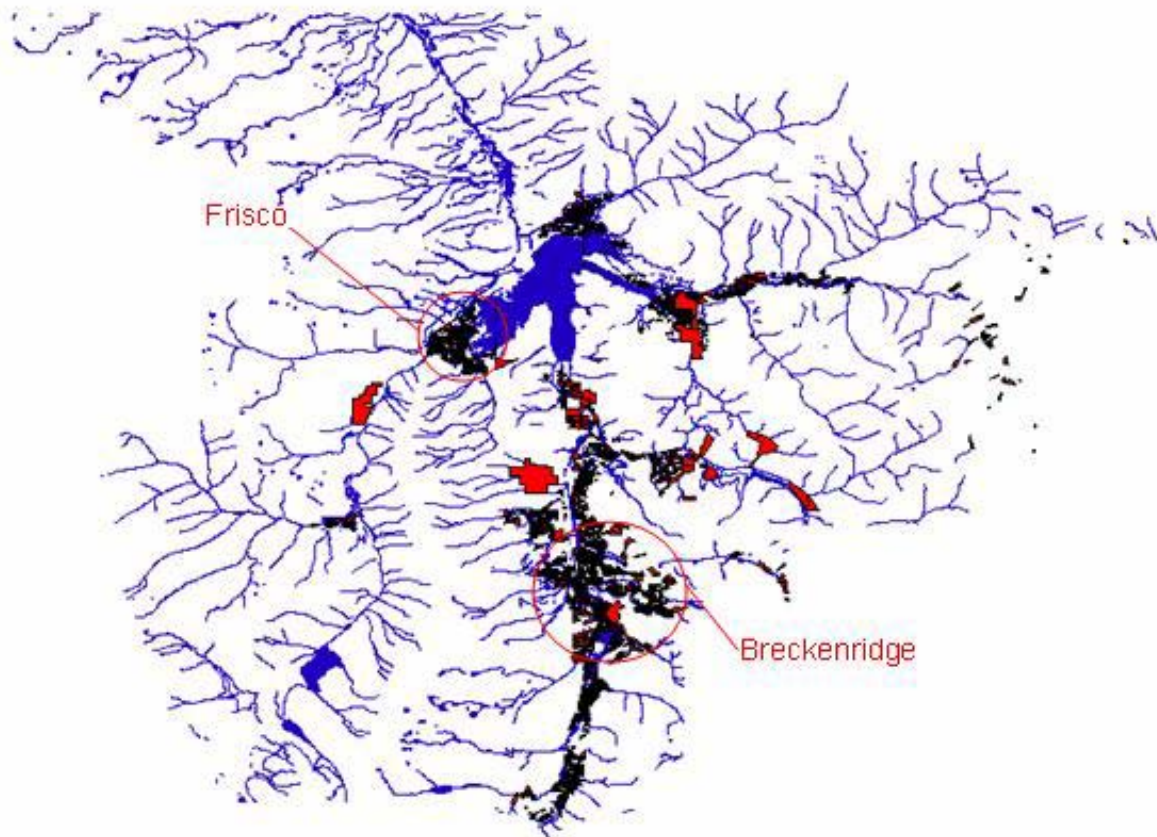


Figure E-1
Location of Frisco and Breckenridge

The Blue River headwaters are located on the Continental Divide south of Dillon Reservoir at an elevation of 12,031 feet. The Blue River is approximately 61.25 miles long. This river ends when it converges with the Colorado River, north of the Dillon Reservoir watershed, at an elevation of approximately 7,333 feet. The portion of the Blue River focused on in this study is a segment that begins approximately 15 miles south of the reservoir and ends where the Blue River flows into Dillon Lake. The town of Breckenridge is located roughly in the middle of this segment (Figure E-1). The mountain lands along this 15-mile stretch of the Blue River have been developed for skiing and recreation as well as mining. Within this 15-mile stretch of the Blue River, there are two tributaries included in this study. These are Pennsylvania Creek and Swan River. Both Pennsylvania Creek and Swan River are home to developments that heavily utilize OWS. In the past, mining activity also took place in areas along Swan River.

Tenmile Creek is located south of Dillon Reservoir. The creek's headwaters are situated near Leadville, Colorado at the Climax molybdenum mine. The river is roughly 18.5 miles long. The headwaters are at an elevation of 11,780 feet. The town of Frisco is located in the bottom portion of the creek, at its input to Dillon Reservoir (Figure E-1). The town of Frisco utilizes both centralized sewage and OWS. Furthermore, areas adjacent to the creek and upstream of Frisco have been the sites of mining activity.

In order to avoid duplicating work that had already been done in the study area, a literature search was done on previous water quality studies conducted in the study area. Only one was sufficiently similar in scope to this project, and that study will be described briefly in the following section. The other studies found are summarized in Table E-1.

Table E-1
Summary of Previous Water Quality Research Done in the Study Area

Study Title	Authors	Year
Eutrophication and Land Use, Lake Dillon, CO	Lewis, W.M.; Saunders, J.F.	1984
Occurrence, transport and fate of trace elements Blue River Basin, Summit County, Colorado- An integrated approach	Apodaca, L.E.; Driver, N.E.; Bails, J.B.	2000
Water quality characteristics and mass balance modeling of the French Gulch drainage, Breckenridge, Colorado	Bails, J.B.	1998
Distribution of trace elements in streambed sediment associated with mining activities in the Upper Colorado River Basin, Colorado, USA	Deacon J.R.; Driver, N.E.	1999
Quantification of metal loading in French Gulch, Summit County, Colorado, using a tracer-injection study, July 1996	Kimball, B.A.; Runkel, R.L.; Gerner, L.J.	1999
Using GIS to investigate septic system sites and nitrate pollution potential	Stark, S.L.; Nuckols, J.R.; Rada, J.R.	1999

Previous Water Quality Studies in the Dillon Reservoir Area

Beginning in January of 1981, field work was conducted in the Dillon Reservoir watershed that included collection and analysis of water samples (Lewis 1984). The goal of this study, part of the Clean Lakes Study and referred to as such, was to create a model that would predict nutrient yields for the lake based on land use and population density (Lewis and Saunders 2002). The model is intended “for the prediction of reservoir responses associated with future growth and various other changes in land use...” (Wyatt 2002). One year of water quality data was collected prior to the development of the Dillon Reservoir Water Quality Model in 1982 (Lewis and Sanders 2002). Water quality data for the initial year of the Clean Lakes Study was collected in three studies (Lewis 1984):

- Time series
- Spatial survey
- Special studies

For the time series study, data were collected at five sites in Dillon Reservoir, 32 times in two years, and eight stream sites, 37 times in two years. Lake sites were situated in the center of the lake in deep water and at each of the four arms of the lake. These four arms are associated with each of the three main inflowing streams, the Blue River, Tenmile Creek, and the Snake River, and with the reservoir outlet. Stream sites were situated at the mouth of each inflowing stream, Blue River, Tenmile Creek, Snake River, Miner’s Creek, and Soda Creek, at the outlet to Dillon Reservoir, and at two WWTP effluent releases.

For the spatial survey, samples were collected at all of the aforementioned Dillon Reservoir sites, plus nine others, and each of the aforementioned surface water stations plus 25 others. Lake sites were monitored a total of 10 times in two years for the spatial survey. Stream sites for this survey were monitored a total of 20 times in two years. Special surveys included diel and enrichment surveys; sites monitored for these surveys varied (Lewis 1984).

The main focus of these studies was to identify sources of phosphorous loading to Dillon Reservoir. However parameters outside of phosphorous species were collected including nitrogen species, field parameters (pH, dissolved oxygen [DO], specific conductance, temperature, and flow), lake transparency, chlorophyll, and phytoplankton (Lewis 1984). Note that many additional wastewater parameters such as sulfur, boron, and oxygen demand were not monitored.

The Clean Lakes Study used field data in conjunction with empirical modeling data to assess phosphorous loading from the study area to Dillon Reservoir. The model was equipped to predict future phosphorous loading and also to show the source of that loading (background, WWTP, or OWS). Modeling results for 1982 showed OWS to be accountable for a higher percentage (12.4%) of phosphorous loading than WWTP effluent (11.1%) (Lewis and Saunders 2002).

Since then, the model has been recalibrated several times incorporating an increased water quality database (Lewis and Saunders 2002). The 1991 simulations still resulted in OWS being accountable for a higher percentage (14.6%) of total phosphorous loading to Dillon Reservoir than local wastewater treatment facilities (13.8%). Simulations for the year 2000, however did not. In this simulation, OWS were accountable for 12.7% of total phosphorous loading in comparison to 16.5% from WWTP effluent. Yet Lewis and Saunders (2002) contend that at full development OWS would be responsible 32.2% of total phosphorous loading to Dillon Reservoir in comparison to 19.8% from WWTP sources. Documents discussing both the original creation of the Dillon Reservoir Water Quality Model in 1982 and its final calibration in 2001 do not mention any studies conducted to use water quality monitoring to further identify and or verify nutrient sources in the Dillon Reservoir watershed.

Note that literature describing in detail development, application, and validation of the Lewis model was difficult to obtain. In particular, documentation is needed to explain the following issues. First, if as contended, OWS are a significant source of phosphorous mass flow in the streams, then some explanation is needed to clarify why phosphorous mass flow increases with increased stream flow (Lewis and Saunders 2002). If the majority of phosphorous loading is from OWS, then mass flow would be contributed through base flow. This would indicate that phosphorous mass flow should decrease as stream flow increases, thereby diluting base flow loading (McCray 2003). Second, in order to further evaluate the model, it would be necessary to know whether or not it accounts for phosphorous that is present in runoff, how it is accounted for, or in the opposite case, why it is not (McCray 2003).

Study Approach

The study approach used in this work involved multiple steps. The first step was to conduct a preliminary assessment of water quality using mass balance calculations in order to predict what levels of nutrients could be expected in the study area. Information from these calculations was then incorporated in the finalization of the monitoring program design. The next step was to begin water quality monitoring, which was done in a two-phase approach that is described in detail in the following section. The final step in the study approach was processing and interpretation of the monitoring results. This section will focus on describing the mass balance calculations, program design, the rationale and differences between Phase I and Phase II sampling, and methods of quality assurance.

Mass Balance Calculations

Water quality assessments can be conducted through means other than water quality monitoring, or observation. Other methods of assessment might include mass balance calculations to predict water quality, or more in-depth types of modeling. Mass balance calculations to make predictions about water quality are described here as a preliminary assessment of the impacts of OWS, where the results helped to finalize the remainder of the study design. Mass balance calculations spotlighted nutrient concentrations in both the focus areas and the Blue River downstream of the focus areas, where applicable.

Approach

Mass balance calculations were focused on nitrate and phosphorous concentrations, due to their importance in answering the questions defined by the objectives of this study. The mass balance calculations were used to answer two questions:

1. If the assumption was made that the background concentrations of nutrients were at or near zero in the streams located in the focus areas (Tenmile Creek, Pennsylvania Creek, and Swan River), then what effects were OWS likely to have on these concentrations?
2. Two of the focus areas, Pennsylvania Creek and Swan River, are tributaries to the Blue River. Therefore, nutrient concentrations in these tributaries will affect concentrations in the Blue River. What sort of effects might be expected?

Theoretical mass balances were applied to a variety of scenarios in order to determine what sort of effects might be expected from the tributaries. Furthermore, these mass balances were conducted with the goal of determining the necessary detection limits for nutrient analysis.

To answer the first question, mass balances were conducted on each of the three focus areas in the study: Pennsylvania Creek, Swan River, and Tenmile Creek. The following formula was used to compute potential concentrations of nitrogen and phosphate:

$$Q_w C_w + Q_s C_s = Q_o C_o$$

Equation E-1

Where, Q_w and Q_s are the flows of the waste stream and stream, respectively, and C_w and C_s are the concentrations of total nitrogen or phosphate in the waste stream and stream, respectively. Q_o is equal to $Q_w + Q_s$. C_o is the concentration of nitrogen or phosphate in Q_o , and C_o was the variable being solved for. Note that in these calculations, the waste stream represents the input of OWS (Figure E-2).

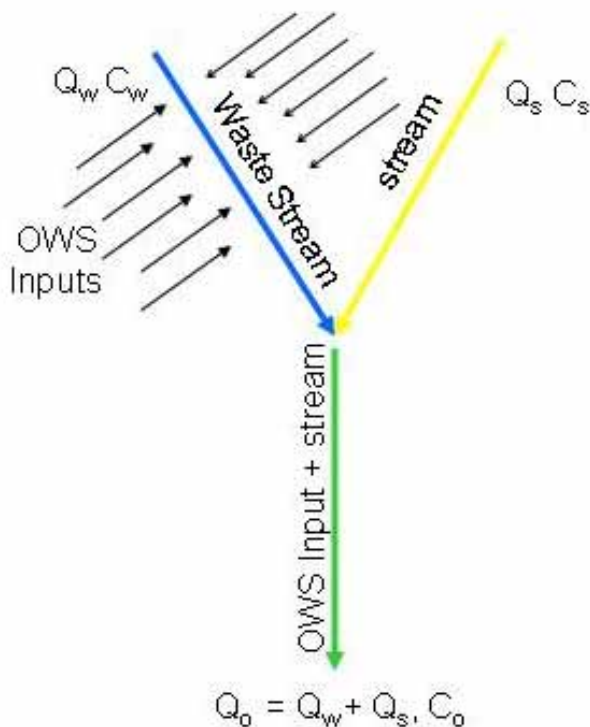


Figure E-2
Schematic of the Mass Balance Used to Predict Nutrient Levels in the Study Area

At this point it would be useful to describe how each variable in the equation was determined, as well as when and how it was varied throughout the calculations. Many calculations were done representing different scenarios and using a spreadsheet model. A portion of this spreadsheet can be found in Table E-2. Reference to this table is useful throughout this discussion. Footnotes below the table describe each column and, when applicable, how that column was calculated.

Table E-2
Example of Spreadsheet Used to Predict Nutrient Levels in the Focus Areas

Pennsylvania Creek														
Nutrient of Concern	Variable being changed	mg/L in OWS effluent	% Removal	# houses	people/hse	# people	L/person/d	Q _w (L/d)	C _w (mg/L)	Q _s (cfs)	Q _s (L/d)	C _s (mg/L)	Q _o (L/d)	C _o (mg/L)
[1]	[2]	[3]	[4]	[5]	[6]	[7]=[5]*[6]	[8]	[9]=[7]*[8]	[10]=[3]-[3]*[4]	[11]	[12]	[13]	[14]=[12]+[9]	(((9)*[10])+([12]*[13]))/[14]
Total N		44	0	254	2.5	635	230	146050	44	2.64	6461643	0	6607693	0.973
Total N	% Removal	44	10	254	2.5	635	230	146050	39.6	2.64	6461643	0	6607693	0.875
Total N	% Removal	44	20	254	2.5	635	230	146050	35.2	2.64	6461643	0	6607693	0.778
Total N	% Removal	44	30	254	2.5	635	230	146050	30.8	2.64	6461643	0	6607693	0.681
Total N	% Removal	44	40	254	2.5	635	230	146050	26.4	2.64	6461643	0	6607693	0.584
Total N	% Removal	44	50	254	2.5	635	230	146050	22	2.64	6461643	0	6607693	0.486
Total N	% Removal	44	60	254	2.5	635	230	146050	17.6	2.64	6461643	0	6607693	0.389
Total N	% Removal	44	70	254	2.5	635	230	146050	13.2	2.64	6461643	0	6607693	0.292
Total N	% Removal	44	80	254	2.5	635	230	146050	8.8	2.64	6461643	0	6607693	0.195
Total N	% Removal	44	90	254	2.5	635	230	146050	4.4	2.64	6461643	0	6607693	0.097
Total N	Q _s	44	0	254	2.5	635	230	146050	44	5.28	12923286	0	13069336	0.492
PO ₄	nutrient	15	0	254	2.5	635	230	146050	15	5.28	12923286	0	13069336	0.168
PO ₄	% Removal	15	10	254	2.5	635	230	146050	13.5	5.28	12923286	0	13069336	0.151
PO ₄	% Removal	15	20	254	2.5	635	230	146050	12	5.28	12923286	0	13069336	0.134
PO ₄	% Removal	15	30	254	2.5	635	230	146050	10.5	5.28	12923286	0	13069336	0.117
PO ₄	% Removal	15	40	254	2.5	635	230	146050	9	5.28	12923286	0	13069336	0.101
PO ₄	% Removal	15	50	254	2.5	635	230	146050	7.5	5.28	12923286	0	13069336	0.084
PO ₄	% Removal	15	60	254	2.5	635	230	146050	6	5.28	12923286	0	13069336	0.067
PO ₄	% Removal	15	70	254	2.5	635	230	146050	4.5	5.28	12923286	0	13069336	0.050
PO ₄	% Removal	15	80	254	2.5	635	230	146050	3	5.28	12923286	0	13069336	0.034
PO ₄	% Removal	15	90	254	2.5	635	230	146050	1.5	5.28	12923286	0	13069336	0.017
PO ₄	Q _s	15	0	254	2.5	635	230	146050	15	1.32	3230822	0	3376872	0.649

[1] Nutrient concentration being predicted in that particular row.

[2] Notes which column is being varied for that particular calculation. For example, the only difference between the second and third rows of calculation is that the percent removal changed from 10 to 20.

(Table E-2 footnotes continued on the next page.)

Table E-2
Example of Spreadsheet Used to Predict Nutrient Levels in the Focus Areas
(Footnotes cont.)

[3] mg/L of [1] found in the OWS effluent.

[4] Percent of column 3 that was removed for the purposes of the calculation in that row to recognize the fact that some of the nutrient is removed before effluent reaches surface waters.

[5] Number of houses surrounding the focus area that could potentially contribute waste flow to surface waters. Aerial photos were used to come up with a number (254), then this number was divided in half and into a third. The purpose of this was to recognize that 100% of the waste flow in the subdivision does not contribute to surface water flow.

[6] The number of persons per household.

[7] Calculated by multiplying columns 5 and 6.

[8] Waste flow in liters that each person contributes in a day.

[9] Waste flow in liters per day calculated by multiplying columns 7 and 8.

[10] Concentration of column 1 in column 9 (the waste flow) calculated by subtracting the percent of the COC removed (column 4) from the original concentration that was in the effluent (column 3).

[11] Flow of the stream, in this case Pennsylvania Creek, in cubic feet per second.

[12] Liters per day converted from Column [11].

[13] Background concentration of column 1 that is in the stream.

[14] Outgoing flow determined by adding the waste flow (column 9) to the stream flow (column 12).

[15] Predicted concentration of column 1 for that particular row calculated by solving equation 1 for C_o .

In order to complete the mass balance it was necessary to determine a reasonable value for Q_w . This is the amount of flow, in liters per day, that OWS contribute to the focus area in question. Values were found in the literature that gave a range for waste flow of 190 to 270 L/person/day (cited from Crites and Tchobanoglous 1998 in Kirkland 2001). The middle of the range, 230 L/person/day, was used for these calculations. However, in order for this value to be useful, it was necessary to determine the value in L/day. To do this, a value for the number of persons in each focus area was needed. Obtaining this value was a two-step process. First, aerial photos were consulted to determine the number of houses in each focus area. Next, an assumption was made about the number of persons residing in each home; a value of 2.5 persons per house was used. The number of houses was multiplied by 2.5 persons per house to determine the number of people in each focus area. The value of 2.5 concurs with census data from the year 2000 that gives a value of 2.48 persons per household in Summit County for that census (US Census Bureau 2002). This number was then multiplied by 230 L/person/day in order to determine Q_w . The assumption was made that 100% of Q_w was contributed to the streams in each focus area. This calculation is associated with columns five through nine in Table E-2. Note that Table E-3 summarizes the homes, number of persons, and waste flow used as a basis for all further calculations and scenarios.

Table E-3
Summary of Base Conditions Used in Mass Balance Calculations

Focus Area	# of Homes	Persons per home	Waste Flow (L/p/day)
Penn. Creek	254	2.5	230
Swan River	200	2.5	230
Tenmile Creek	583	2.5	230

Next it was necessary to find a value for C_w . This value is essentially the concentration of nutrients found in OWS effluent minus the portion that is removed before effluent reaches the surface water. The first step to determining this value was to find typical concentrations of total nitrogen and phosphorous in OWS effluent. These values were found in the literature (Kirkland 2001). Total nitrogen and phosphate values used in these calculations were 44 mg-N/L (reported as median value by Kirkland 2001) and 15 mg-PO₄/L (4.9 mg-P/L, approximately the 25th percentile reported by Kirkland 2001). To determine a value for C_w it was necessary to know how much of the original concentration actually reached the surface water. This information was not available, so varying degrees of removal, from 0 to 90% in intervals of 10% were used in the calculations. For example, using a fractional removal of x and original total nitrogen concentration of 44 mgN/L, C_w was calculated as follows:

$$C_w = 44 \text{ mg-N/L} - 44(x) \quad \text{Equation E-2}$$

Columns three, four, and ten in Table E-2 correspond with this calculation.

Flow of the stream, Q_s , was estimated based on flow measurements made in the streams. For example, in Pennsylvania Creek August flows were measured at 2.64 cfs or 6,461,643 L/day. To simulate high flow, the August flows were doubled; they were divided in half to simulate low flow. Columns 11 and 12 in Table E-2 show these flows in cfs and L/day, respectively.

The final variable that had to be determined in order to solve the mass balance was C_s , which is simply the concentration of the nutrient that would be found in the streams prior to the input of OWS (background concentration). Some preliminary analysis had been done on surface waters in the focus area. In most cases, concentrations of both total nitrogen and phosphate were below the detection limit. So, for this calculation a background concentration of 0 mg/L was assumed for both total nitrogen and phosphate.

For each focus area, several scenarios were created. For example, it seemed unlikely that all houses in each focus area would contribute 100% of their waste flow to the stream. Rather than vary the assumption that 100% of the flow was input to the streams, it was decided to vary the number of houses. The full number of houses counted from the aerial photo in each focus area was divided by two and by three, which had the effect of reducing Q_w .

For each number of houses (full number, one-half, and one-third), three scenarios were set up. The three scenarios are as follows:

1. Calculations were done assuming the flow of the stream, Q_s , was at the August level.

2. The calculations were repeated but altering Q_s to low flow (half of the August value).
3. The calculations were repeated using high flow values (twice the August value).

For each scenario, ten calculations were done, one for each level of percent removal used; 0 to 90% at intervals of 10%.

Once spreadsheets were completed for each focus area, the results were used to generate graphs. Six graphs were generated for each focus area: three for total nitrogen and three for phosphate. Of each set of three, there is one graph that shows results using the full number of houses, one that shows results for one-half the number of houses, and one that shows the results using one-third of the full number of houses. On each graph there are three sets of data: one for high stream flow conditions, one for medium stream flow conditions, and one for low stream flow conditions. All graphs show predicted concentrations of the constituent of concern for 0 to 90% removal. Total nitrogen graphs generated for Pennsylvania Creek are shown in Figure E-3. A complete set of graphs can be found in Appendix B of Guelfo (2003).

These graphs and spreadsheets helped to answer the first question regarding what level of concentrations one might expect as a result of OWS in each focus area. However, the question of how the nutrient levels in these focus areas would affect nutrient levels in the Blue River was yet to be answered. To answer this, a new mass balance was conducted using a mass balance equivalent to that in Equation E-3, but with new variables. This equation is

$$Q_t C_t + Q_s C_s = Q_o C_o \quad \text{Equation E-4}$$

In the second mass balance, Q_t and C_t represent the flow of the tributary and concentration of the nutrients in the tributary (the focus area), respectively. Q_s is the flow of the Blue River and C_s is the background concentration of nutrients in the Blue River. Finally, Q_o is the flow of the Blue River downstream of its convergence with the tributary in question. C_o is the concentration at that point and the variable being solved for in the equation.

Q_o and C_o values from the spreadsheet described and shown in Table E-2 were used as Q_t and C_t in the second calculation. Q_s was measured in the Blue River during the month of August, at a point just upstream of the convergence with each tributary. This value was used as medium stream flow, doubled to simulate high stream flow, and divided in half to simulate low stream flow. C_s was also measured in the Blue River in August. Background concentrations of total nitrogen in the Blue River upstream of Pennsylvania Creek and Swan River were found to be below the detection limit, so 0 mg N/L was used as background for nitrogen in both cases. Phosphate was found in the Blue River upstream of Pennsylvania creek at a value of 0.0215 mg-PO₄/L, so this value was used as background for phosphate upstream of this tributary. Upstream of Swan River, phosphate was below the detection limit so 0 mg/L was used as background upstream of Swan River. Q_o is the sum of Q_t and Q_s . As before, C_o is the variable being solved for. A portion of the spreadsheet used in this part of the calculation is shown in Table E-4.

Table E-4
Example of Spreadsheet Used to Predict Nutrient Levels in the Blue River

Blue River Downstream of Pennsylvania Creek									
Parameter	# houses	% Removal	Q_t (L/d)	C_t (mg/L)	Q_s (cfs)	Q_s (L/d)	C_s (mg/L)	Q_o (L/d)	C_o (mg/L)
[1]	[2]	[3]	[4]	[5]	[6]	[7]	[8]	[9]=[4]+[7]	[10]=((([4]*[5])+([7]*[8]))/[9])
Total N	254	0	6461643	0.973	20	48951841	0	55413484	0.113
Total N	254	10	6461643	0.875	20	48951841	0	55413484	0.102
Total N	254	20	6461643	0.778	20	48951841	0	55413484	0.091
Total N	254	30	6461643	0.681	20	48951841	0	55413484	0.079
Total N	254	40	6461643	0.584	20	48951841	0	55413484	0.068
Total N	254	50	6461643	0.486	20	48951841	0	55413484	0.057
Total N	254	60	6461643	0.389	20	48951841	0	55413484	0.045
Total N	254	70	6461643	0.292	20	48951841	0	55413484	0.034
Total N	254	80	6461643	0.195	20	48951841	0	55413484	0.023
Total N	254	90	6461643	0.097	20	48951841	0	55413484	0.011
PO ₄	254	0	6461643	0.332	20	48951841	0.0215	55413484	0.058
PO ₄	254	10	6461643	0.298	20	48951841	0.0215	55413484	0.054
PO ₄	254	20	6461643	0.265	20	48951841	0.0215	55413484	0.050
PO ₄	254	30	6461643	0.232	20	48951841	0.0215	55413484	0.046
PO ₄	254	40	6461643	0.199	20	48951841	0.0215	55413484	0.042
PO ₄	254	50	6461643	0.166	20	48951841	0.0215	55413484	0.038
PO ₄	254	60	6461643	0.133	20	48951841	0.0215	55413484	0.034
PO ₄	254	70	6461643	0.099	20	48951841	0.0215	55413484	0.031
PO ₄	254	80	6461643	0.066	20	48951841	0.0215	55413484	0.027
PO ₄	254	90	6461643	0.033	20	48951841	0.0215	55413484	0.023

[1] Denotes which nutrient concentration is being predicted in that particular row.

[2] The number of houses shown there refers to the number of houses used to generate column [15] in the Table E-2. Columns [4] and [5] are the same values as columns [14] and [15] in Table E-2.

[3] The percent removal of the original concentration of the nutrient that was removed to calculate C_o in the original calculation (Table E-2), or C_i in this spreadsheet.

[4], [5] These values correspond with columns [14] and [15] from Table E-2, respectively.

[6] Flow of the Blue Rivers measured in August (assumed as medium flow). The August value was doubled to simulate high flow and divided in half to simulate low flow.

[7] Liters per day converted from column [6].

[8] Background concentration of the nutrient in the Blue River.

[9] Columns [4] plus [7].

[10] Variable being solved for in the mass balance. This is the concentration of nutrient in the Blue River downstream of its merge with the tributary in question (i.e. Pennsylvania Creek).

These spreadsheets were used to generate graphs similar to the ones shown in Figure E-3. The purpose of these graphs is to show the predicted concentrations from the variety of scenarios. A set of these graphs is show in Figure E-4.

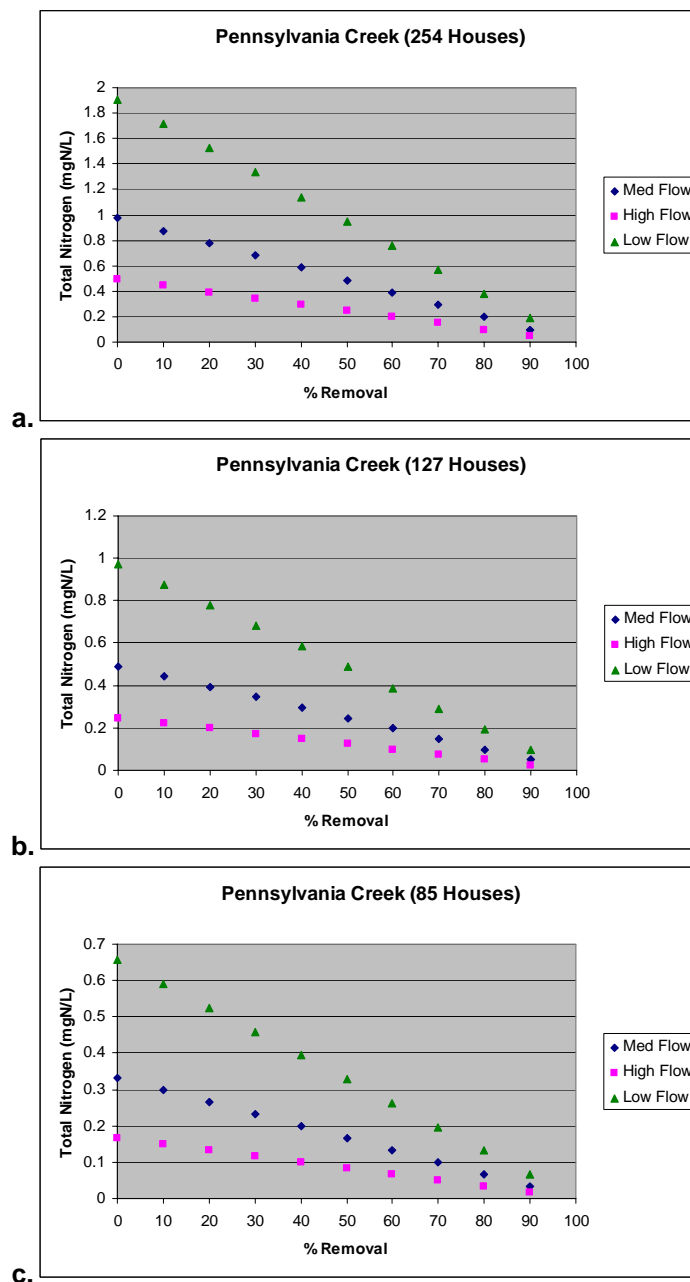


Figure E-3
Predicted Nitrogen Concentrations in Pennsylvania Creek Based on OWS Input Scenarios

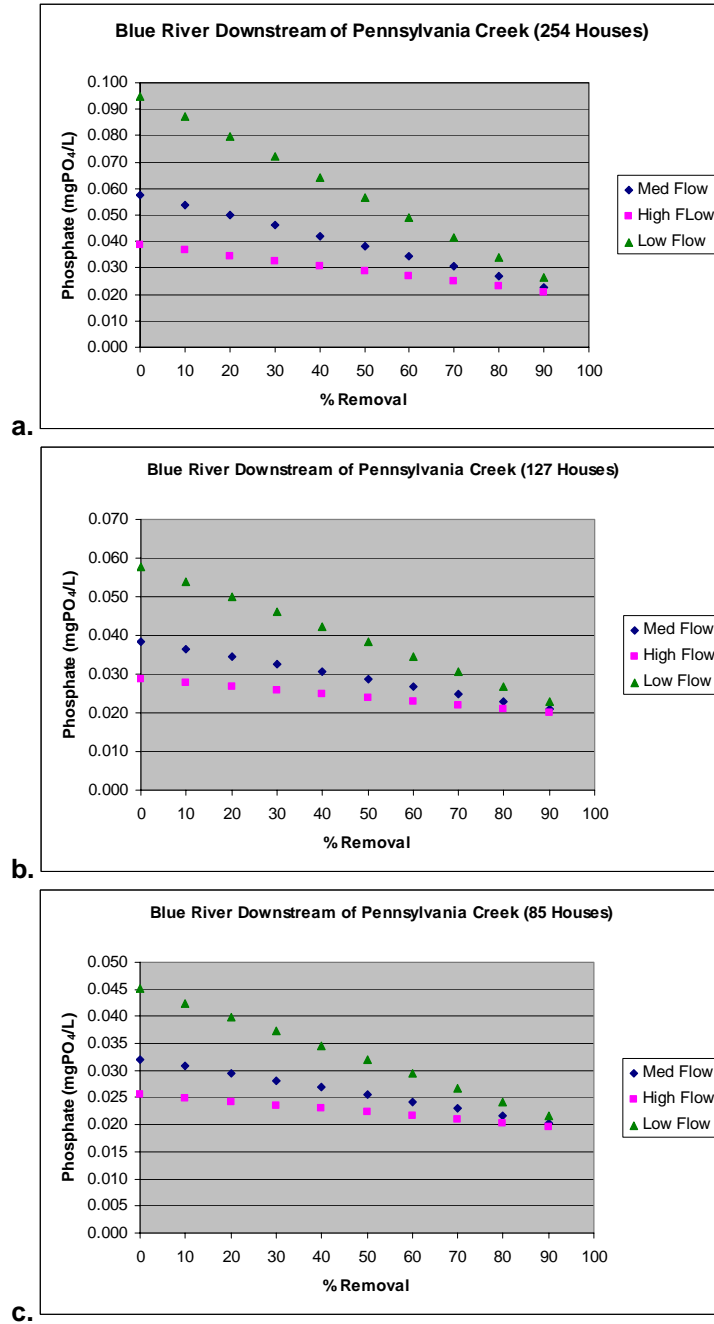


Figure E-4
Predicted Phosphate Levels in the Blue River

Results and Discussion

A summary of the preliminary assessment presented above is presented in Table E-5. From these results it became evident that nutrient levels could be expected to be low (less than 1 mg/L) throughout most of the study area. Knowing this helped to answer questions regarding what kind of analytical detection would be needed. Therefore, these calculations also helped to decide which methods of analysis would be required.

The calculations also made evident that Pennsylvania Creek would be the focus area most likely to exhibit effects of OWS. Furthermore, this focus area was also more likely to have an impact on the Blue River. This knowledge helped to decide which focus area should receive the highest priority for field investigation. Study design is described in further detail in the following section.

Table E-5
Summary of Mass Balance Calculation Results

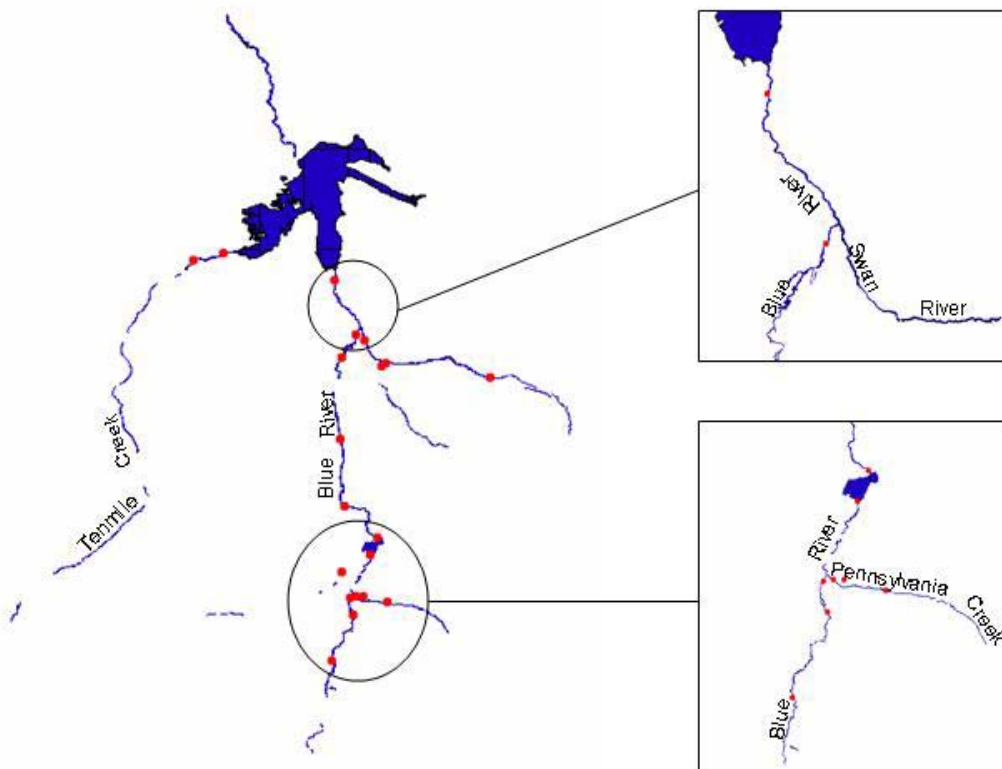
Total Nitrogen	
Location	Range, mgN/L
Pennsylvania Creek	0.017-1.903
Swan River	0.007-1.001
Tenmile Creek	0.002-0.222
Blue River below Pennsylvania Creek	0.001-0.221
Blue River below Swan River	0.001-0.158
Phosphate	
Location	Range, mgPO ₄ /L
Pennsylvania Creek	0.005-0.649
Swan River	0.002-0.344
Tenmile Creek	0.001-0.076
Blue River below Pennsylvania Creek	0.019-0.095
Blue River below Swan River	0.000-0.054

Monitoring Program Design

After the completion of the mass balance calculations described previously, design of the monitoring program was finalized. The following sections describe the main components of this program, and where appropriate, what method or methods were used in the design or selection of that component.

Site Selection and Sampling Frequency

Approximately 20 sites were selected at the initiation of the monitoring program. A map of the sample sites can be found in Figure E-5. Sites were chosen in two ways, the first of which was to meet the objectives of the study. One of the main objectives involves determining the effects of OWS on the streams in the study area. Therefore, sites had to be chosen that targeted the focus areas that, as described in the Background section, were designated to study the effects of OWS on a smaller scale. Specifically, sites were chosen upstream and downstream of each focus area.



Note: Sample sites indicated by a solid circle

Figure E-5
Main Map of Sample Sites and Detailed Maps of the Pennsylvania Creek and Swan River Focus Areas

The remaining sites were selected using the method developed by Sharp (1971). This method provided an even distribution of points throughout the study area and also conveniently situated points upstream and downstream of Breckenridge and at the mouth of the Blue River to Dillon Reservoir.

When monitoring was initiated (Phase I) the decision was made that all sites would be monitored on a monthly basis in order to acquire the background water quality information necessary to evaluate which sites might need more frequent monitoring than others. During the second phase of the study (Phase II) fewer sites were monitored as described in more detail in the following section.

Monitoring Variables and Analytical Methods

Selection of monitoring variables was conducted to meet the objectives of the study. For example, in order to determine the effects of OWS monitoring for the constituents one would expect to see if impacts were occurring (nutrients, chloride, boron) is necessary. Monitoring basic water quality parameters (pH, specific conductance, dissolved oxygen) at each site is also a good idea (Bartram and Ballance 1996; Chapman 1996).

In some cases, the chosen analytical method added additional parameters to the study by default. For example, ion chromatography (IC) was chosen for nitrate and phosphate analysis. The IC automatically analyzes for five constituents: nitrate, phosphate, chloride, fluoride, and sulfate. The same situation occurred with constituents analyzed through inductively coupled plasma (ICP) methods. All analytical methods used in Phase I were chosen to comply with *Standard Methods for the Examination of Water and Wastewater* (APHA 1998) (Table E-6). Phase II analytical methods are the same with the exception of nutrients, which were analyzed at the US Geological Survey (USGS) National Water Quality Laboratory (NWQL). Table E-7 summarizes the methods used by the NWQL for nutrient analysis.

Field Methods and Materials

Field methods for Phase I and II differed. The rationale behind the two-phase sampling will be described later in this section, but the methods used in each phase are documented here.

In Phase I, bottle types were chosen according to *Standard Methods for the Examination of Water and Wastewater* (APHA 1998). In all analytical methods being used, it was appropriate to use water sample collected in either plastic or glass. In one case, amber glass was a requirement. Plastic and glass bottles were washed with tap water and Alconox, and triple rinsed in de-ionized water after each use. In addition, glass bottles were rinsed with 1% hydrochloric acid.

Field parameters in Phase I were collected using a YSI 600R data sonde, or multi-probe. This unit has several probes enabling the collection of pH, DO, specific conductance, and temperature at one time. The sonde comes equipped with a hand-held computer that enables the user to view and store parameter results. The only field measurement that was not made using the YSI 600R was flow. Flow in Phase I was measured using a Price flow meter along with a top-set wading rod and headphones. Two flow meters were available for this project: a Price meter and a pygmy meter.

Water samples in Phase I were collected as grab samples. Prior to collecting the sample, bottles were rinsed twice with native water. Then water samples were collected directly in the bottle from the portion of the stream with the fastest velocity and from the middle of the stream column. Samples were then put directly on ice, returned to the laboratory at the end of each day, and refrigerated at 4 °C. No further preservation was necessary because samples were analyzed within 24 hours.

Table E-6
Summary of Monitoring Parameters and CSM Analytical Methods

Parameter	Method Type	Instrument	Field or Lab Analysis	Method No./Ref.	Detection Limit	Water Volume (mL)
Temp (°C)	thermometric	YSI 600R	field	SM 2550	-5°C	in situ
Flow (cfs)		Price meter	field			in situ
pH	electrometric	YSI 600R	field	SM 4500-H ⁺ B	0	in situ
Dissolved Oxygen (DO) (mg/L)	membrane electrode	YSI 600R	field	SM 4500-O G	0 mg/L	in situ
DO (%Sat)	membrane electrode	YSI 600R	field	SM 4500-O G	0%	in situ
Specific Cond. (mS/cm)	conductance	YSI 600R	field	SM 2510 B	0 mS/cm	in situ
Turbidity (NTU)	nephelometric	Hach 2100A turbidimeter	laboratory	SM 2130 B	0 NTU	fill sample cell
Total Solids (mg/L)	dried at 105°C	n/a	laboratory	SM 2540 B	2.5 mg dried residue	30
Alkalinity (mg/L)	titrimetric	HACH digital titrator	laboratory	SM 2320 B		50
COD (mg/L)	closed reflux, colorimetric method	HACH spectrophotometer	laboratory	SM 5220 D	2 mg/L	2
Total Nitrogen (mg/L)	persulfate method	n/a	laboratory	SM 4500-N C	n/a	2
Ammonia (mg/L)	see comments		laboratory			
Nitrate	ion chromatograph (IC)	Dionex DX600	laboratory	SM 4110 B	0.05 mg/L	1.5
Fluoride (mg/L)	-----	-----	-----	-----	0.01 mg/L	-----
Chloride (mg/L)	-----	-----	-----	-----	0.2 mg/L	-----
Phosphate (mg/L)	-----	-----	-----	-----	0.06 mg/L	-----
Sulfate (mg/L)	-----	-----	-----	-----	0.2 mg/L	-----
Ag (mg/L)	inductively coupled plasma (ICP)	Perkin Elmer Optima 3000	laboratory	SM 3120 B	0.0015mg/L	10
Al (mg/L)	-----	-----	-----	-----	0.0246 mg/L	-----
As (mg/L)	-----	-----	-----	-----	0.0385 mg/L	-----
B (mg/L)	-----	-----	-----	-----	0.0031mg/L	-----
Ba (mg/L)	-----	-----	-----	-----	0.0028 mg/L	-----
Be (mg/L)	-----	-----	-----	-----	0.0004 mg/L	-----
Ca (mg/L)	-----	-----	-----	-----	0.0328mg/L	-----
Cd (mg/L)	-----	-----	-----	-----	0.0024 mg/L	-----
Co (mg/L)	-----	-----	-----	-----	0.0093mg/L	-----

Table E-6
Summary of Monitoring Parameters and CSM Analytical Methods (Cont.)

Parameter	Method Type	Instrument	Field or Lab Analysis	Method No./Ref.	Detection Limit	Water Volume (mL)
Cr (mg/L)	----	----	----	----	0.0061mg/L	----
Cu (mg/L)	----	----	----	----	0.0017mg/L	----
Fe (mg/L)	----	----	----	----	0.0688mg/L	----
K (mg/L)	----	----	----	----	0.0594mg/L	----
Li (mg/L)	----	----	----	----	0.0017mg/L	----
Mg (mg/L)	----	----	----	----	0.0060mg/L	----
Mn (mg/L)	----	----	----	----	0.0008mg/L	----
Mo (mg/L)	----	----	----	----	0.0073 mg/L	----
Na (mg/L)	----	----	----	----	0.048mg/L	----
Ni (mg/L)	----	----	----	----	0.0034mg/L	----
P	----	----	----	----	0.044 mg/L	----
Pb (mg/L)	----	----	----	----	0.0175mg/L	----
S (mg/L)	----	----	----	----	0.1032mg/L	----
Sb (mg/L)	----	----	----	----	0.0222mg/L	----
Se (mg/L)	----	----	----	----	0.0336mg/L	----
Si (mg/L)	----	----	----	----	0.0448mg/L	----
Sn (mg/L)	----	----	----	----	0.0664mg/L	----
Sr (mg/L)	----	----	----	----	0.0009mg/L	----
Ti (mg/L)	----	----	----	----	0.0005mg/L	----
V (mg/L)	----	----	----	----	0.001mg/L	----
Zn (mg/L)	----	----	----	----	0.0014mg/L	----
Fecal Coliform (Count)	fecal coliform membrane filtration	n/a	laboratory	SM 9222 D	n/a	100

SM = Standard Methods for Water and Wastewater Analysis 20th Edition.

---- = Same as above

Table E-7
Methods Used and Detection Limits Obtained by the NWQL for Nutrient Analysis

Parameter	Method	Detection Limit (mg/L)
Nitrogen, ammonia	Colorimetry, salicylate-hypochlorite automated-segmented flow	0.015
Nitrogen, ammonia + organic nitrogen, filtered	Titrimetry, digestion-distillation	0.1
Nitrogen, ammonia + organic nitrogen, whole water	Titrimetry, digestion-distillation	0.1
Nitrogen, nitrite	Colorimetry, diazotization, automated-segmented flow	0.0023
Nitrogen, nitrite + nitrate	Colorimetry, cadmium reduction-diazotization, automated-segmented flow	0.013
Phosphorous, filtered	Colorimetry, phosphomolybdate automated-segmented flow	0.0044
Phosphorous, whole water	Colorimetry, phosphomolybdate automated-segmented flow	0.0037
Phosphorous, phosphate, ortho	Colorimetry, phosphomolybdate automated-segmented flow	0.007

Source: Fishman 1993

Specific conductance, pH, DO, and temperature were all measured directly in the stream during Phase I. Flow was measured by using the meter to determine velocity at each foot across the width of the stream cross section. In some larger sampling sites, where time was an issue, velocity was measured at every other foot across the width of the stream cross section. In all cases, depth was recorded at every foot. Depth and stream velocity measurements were then averaged using a simple, arithmetic average. Average depth was then multiplied by the stream width to get cross-sectional area in square feet. The area was then multiplied by the average stream velocity in feet/s. The result was flow in cubic feet per second. All field equipment was cleaned with de-ionized water after each sampling trip.

Materials and methods (including cleaning methods) in Phase II were altered to adhere to USGS surface water sampling protocol. A complete manual of these methods is available through the USGS (Wilde *et al.* 1999). In order to meet this protocol, it was necessary to acquire many new pieces of field equipment. All equipment was selected according to the guidelines established in the USGS field manual, Chapter A2 (Wilde *et al.* 1999). This chapter describes all possible options for equipment that can be used to accomplish various purposes.

To eliminate confusion regarding which equipment was selected for this project, Table E-8 describes the equipment used and its purpose. Note that this table is a list of equipment that was original to Phase II, not a comprehensive list of equipment used for sampling.

Table E-8
Equipment Original to Phase II Sampling

Equipment Type	Purpose
DH-81 sampler	Surface water collection
Churn splitter	Surface water sample storage and homogenization
Churn carrier	Carries churn splitter and protects from the elements
Processing/preservation chamber and curtain	Protects water sample (i.e. from wind-born contaminants) while sample is being processed and preserved
Peristaltic pump	Used for sample filtration
Disposable 0.45 micron filters	Used for sample filtration
Tygon pump tubing	Used for sample filtration

Sample collection underwent considerable change in Phase II as well. Instead of collecting grab samples, depth and width integrated samples were taken. The method used to accomplish this was the EWI method described in Chapter 2 (Wilde *et al.* 1999). Since samples in Phase II were collected using the EWI method, sample processing had to be added on as an additional step. Processing involves the compositing, subsampling, filtration, and preservation of samples. Complete details on sample processing can be found in Chapter A5 of the USGS field manual (Wilde *et al.* 1999).

During Phase II the same field parameters were collected as in Phase I. However in Phase II, pH and specific conductance were measured in the composite sample rather than being measured directly in the stream, as in Phase I. DO and temperature were still measured directly in the stream. Measurements taken from the composite sample are referred to as subsample measurements. Conversely, those taken directly in the stream are referred to as *in situ* measurements. Step-by-step instructions for both the subsample and *in situ* measurements can be found in the *National Field Manual* in Chapter A6. This chapter also includes sections aimed directly at the specific parameters (pH, DO), including information on maintenance and calibration of probes.

As in Phase I, flow in Phase II was measured using either a Price or pygmy meter. However, the method of computing the flow differed considerably in Phase II. In the second phase, stream velocity was measured so that no increment measured would be equal to or greater than 20% of the total flow. This usually necessitates 20 or more velocity measurements at each sample site. As with the sample collection, the number of measurements needed was determined using prior knowledge of the site and personal opinion and the stream width divided equally into that number of increments.

Stream velocity and depth were measured in the middle of each increment. Stream velocity is determined by counting the number of clicks heard in a given period of time. A chart is used that translates this into stream velocity, based on the clicks and time. The width and depth of each increment were then multiplied to determine the cross-sectional area of that particular increment. This result was then multiplied by the velocity measured in that increment to get the flow for that one increment. Flow values from all of the increments were then totaled to determine total flow for the sample site.

Data Storage and Handling

The results of all flow and water quality analyses were maintained in an Excel spreadsheet. Many of the graphs and statistical analyses used could also be done within the spreadsheet. Results of the monitoring program can be found in the Results section, which is then followed by the Water Quality Assessment section.

Phases I and II Sampling Efforts

Surface water quality monitoring of the Blue River was initiated in September 2001. Phase I of the study lasted until March 2002. This phase served as an initial screening period. The results from this phase helped to decide whether or not the methods being used were appropriate. Phase II was initiated in May 2002 and lasted until September 2002. Phase II involved a more in-depth examination at fewer sites using low-level analytical methods.

Phase I

From the mass balance calculations, it was apparent that nutrient levels could be expected to be low throughout the study area. However, depending on how low, CSM may or may not have had the analytical capability to consistently quantify values that were near trace levels. Having such values is extremely important in determining any trends present in the study area. A decision was made to conduct a few months of sampling using CSM analytical capabilities as a screening for future efforts. It soon became apparent that CSM lab support would suffice for all parameters with the exception of the nutrients. So, in November 2001 efforts were initiated to obtain appropriate low-level nutrient analysis through an outside laboratory. These efforts continued until April 2002 when CSM was able to finalize collaboration with the USGS's NWQL. The NWQL was chosen because it offered the lowest nutrient detection limits. In the meantime, CSM continued to collect and analyze samples. The period from September 2001 to April 2002, shall be referred to as Phase I throughout the remainder of this appendix.

Phase II

In order for an institution outside of the USGS to utilize the NWQL, all surface water samples must be collected using the USGS protocol. Initial protocols used in this study followed generally accepted practices but differed from the USGS protocol. So, before this collaboration could begin, it was necessary for CSM to have personnel trained in the USGS methods.

Due to the time it took to complete this training, CSM did not initiate use of the new methods until May 2002. The period of this study from May 2002 to September 2002 shall be referred to as Phase II.

Several things changed when Phase II of the study began. As mentioned, sample collection methods changed. New protocols, which involved the aforementioned methods of measuring discharge and the EWI method, proved to be more time consuming with respect to time spent at each surface water site. Therefore, the number of sites had to be reduced to ten. These sites were chosen based on data available from Phase I, and were chosen with the goal of targeting the Blue River and Pennsylvania Creek as the focus areas to be monitored with continued frequency. Two sites near the mouth of the Swan River and the Blue River were also included in order to monitor water quality just downstream of the mouth of the Swan River and to monitor water quality entering Dillon Reservoir.

Quality Assurance

During Phase I, attempts were made to collect two blanks and two duplicates, or 10%, during each sampling trip. In Phase II this number was reduced due to the decreased number of sites being monitored. One blank and one duplicate were collected during Phase II sampling trips. In all CSM laboratory analyses, one lab duplicate was analyzed each time an analytical process was run. This usually resulted in two lab duplicates per analysis per sample round.

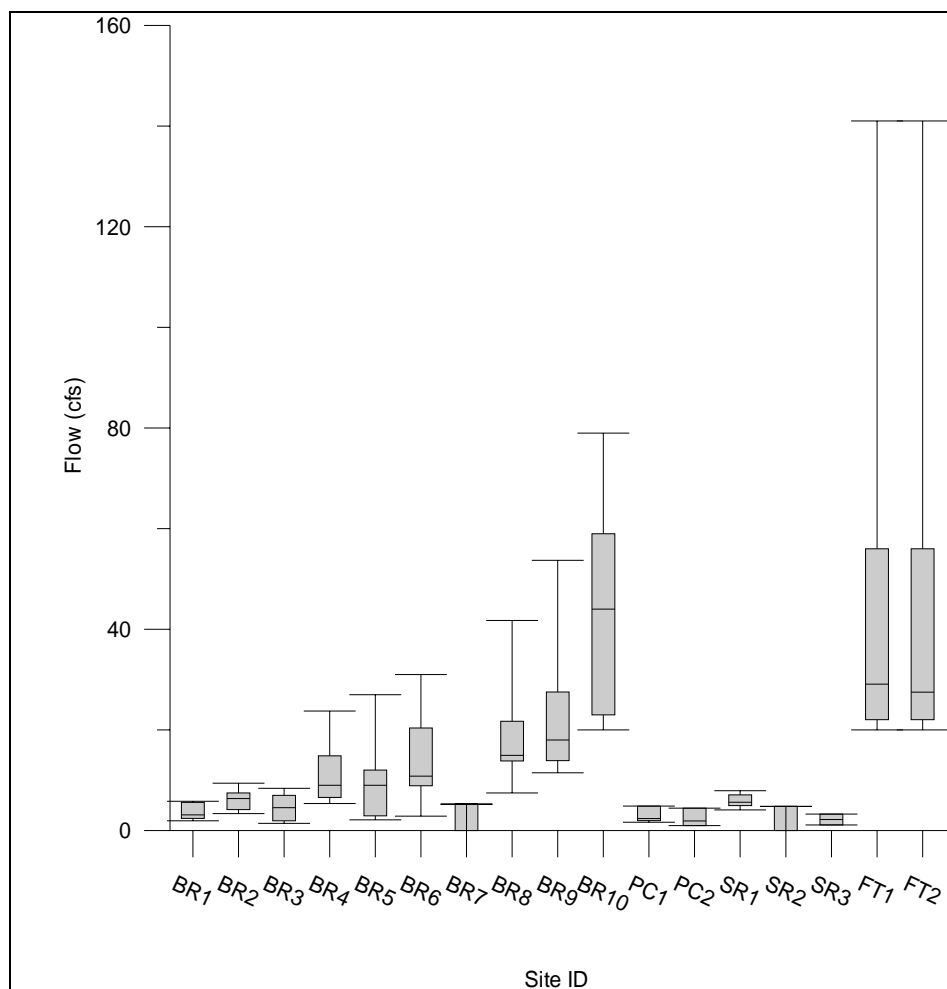
Results

Surface water quality monitoring within the Dillon Reservoir watershed was initiated in September 2001 and continued through September 2002. The results of the Phase I monitoring of the initial 20 sites as well as the four months of Phase II monitoring of 10 of these sites are described in this section.

Flow Measurements

For the period from September 2001 to September 2002, a total of 11 monitoring events were conducted. When possible, a flow measurement was taken at each site visited. During Phase I, this involved measuring flow at as many of the original 20 sites as possible; during Phase II the number of sites was more limited. In the late fall and winter months, which fell during Phase I sampling, two of the 20 sites were completely inaccessible due to snow cover, and ice cover was present at many of those that were accessible. Therefore, discharge measurements were often difficult to obtain. Calculating estimated discharge values for some cases where flow measurements could not be made to calculate mass flux rates was necessary. Discussion of flow in this section is limited strictly to the measured values unless otherwise noted.

Discharge values in this study range from 0.43 to 141 cfs with a median discharge of 10.8 cfs for sites monitored in the entire study area. As these flow values are highly variable, breaking these results down into the individual sites in which they are measured is useful (Figure E-6) (see Figure E-5 for sample locations). Note that a more detailed map with site location is presented later in Figure E-20.



Notes: BR = Blue River, PC = Pennsylvania Creek, SR = Swan River, FT = Tenmile Creek.
 Top and bottom lines represent the minimum and maximum values.
 Top and bottom of box represent the 75th and 25th percentiles, respectively.
 Lines inside of the box represent median values.

Figure E-6
Flow Values for the Majority of Sites in the Study Area

Sites BR1 through BR10 are situated along the Blue River. Discharge values at these ten sites ranged from 1.41 to 79 cfs. Medians at each of these sites vary, but BR1 has a median value of 3.11 cfs. Site BR10 had the largest median value: 44 cfs.

Sites on Pennsylvania Creek posed some of the most difficulty with regards to winter sampling. PC1, the site situated upstream of all development along the creek was completely inaccessible, and PC2 and PC3 were frozen. Furthermore, flow at the latter two sites was so low that even if all the ice were removed, it would be impossible to make a discharge measurement. No flow estimates were made for this stream because there were not enough measured values available to make reasonable estimates. Of the measurements that were taken during this study, flow ranged from 1 to 4.85 cfs, with a median discharge of 2.44 cfs (Figure E-6).

Median flow at site PC2 was slightly higher than PC3. Flows in Pennsylvania Creek were similar to flows in the Blue River in that reach, which indicated that the convergence of Pennsylvania Creek with the Blue River would nearly double flows after site BR3. Median flow increases from BR3 to BR4 confirm this, increasing from 4.54 to 8.98 cfs (Figure E-6).

Flows in Swan River ranged from 1.09 to 7.93 cfs. Median flows appeared in the graph to decrease from upstream to downstream, but this is likely due to the fact that it was possible to obtain only one flow value for site SR3.

Tenmile Creek is different from the other streams discussed here in that it is not a tributary to the Blue River. Like the Blue River, it feeds directly into Dillon Reservoir. Two sites were monitored along Tenmile Creek, situated upstream and downstream of the town of Frisco. Site FT2 is close to the mouth of Tenmile Creek into Dillon Reservoir. This creek is larger and at a lower elevation, so it was not as severely affected by winter conditions. Therefore, obtaining discharge values for each sampling trip was possible. Furthermore, a USGS gauging station is situated at one of the Tenmile Creek sites allowing flow measurements to be obtained for Phase II, though the site was not sampled during this time.

Flow measurements along Tenmile Creek ranged from 20 to 141 cfs with a median value of 29.55 cfs, based on values from September 2001 to September 2002 (Figure E-6). Median values and ranges for the two sites were nearly equal due to the fact that the sites are situated fairly close together with no inputs in between. The highest flows in the study area were observed in Tenmile Creek; however median values at both sites are lower than those observed at the mouth of the Blue River.

Field Parameters

Parameters measured in the field during this study included specific conductance, DO, pH, and water temperature. These parameters were measured during the entirety of both Phases I and II.

Specific Conductance

Specific conductance measurements provide an indicator of the amount of dissolved solids in the water. Specific conductance is proportional to the amount of dissolved solids, increasing as the amount of dissolved solids increases. Measurements of specific conductance in this study area ranged from 1 to 1137 $\mu\text{S}/\text{cm}$.

Some of the lower values were believed to be erroneous either due to error in measurement or data entry. First, values did not fit trends. For example, values of 4 and 2 $\mu\text{S}/\text{cm}$ were entered for sites BR2 and BR3 respectively, in the month of January. However values measured at surrounding sites BR1 and BR5 on the same day were much higher at 157 and 188 $\mu\text{S}/\text{cm}$, respectively. Furthermore, these values fell below average values measured in this study area during previous studies as well as those measured in adjacent areas. A study done in the Blue River found the average specific conductance to be 168 $\mu\text{S}/\text{cm}$ (Lewis *et al.* 1984), and a study in nearby Gore Creek watershed found the average specific conductance to be 145 $\mu\text{S}/\text{cm}$ with the lowest specific conductance measured approximately 100 $\mu\text{S}/\text{cm}$ (Wynn *et al.* 2001).

Based on these studies, the specific conductance dataset was edited to eliminate any values lower than 80 $\mu\text{S}/\text{cm}$. This value was chosen because some streams are located in high mountain areas away from any development where especially low specific conductance measurements might be expected. Once lower values were censored, the specific conductance data set analyzed in this study ranged from 80 to 1,137 $\mu\text{S}/\text{cm}$, with a median value of 171 $\mu\text{S}/\text{cm}$ (Figure E-7).

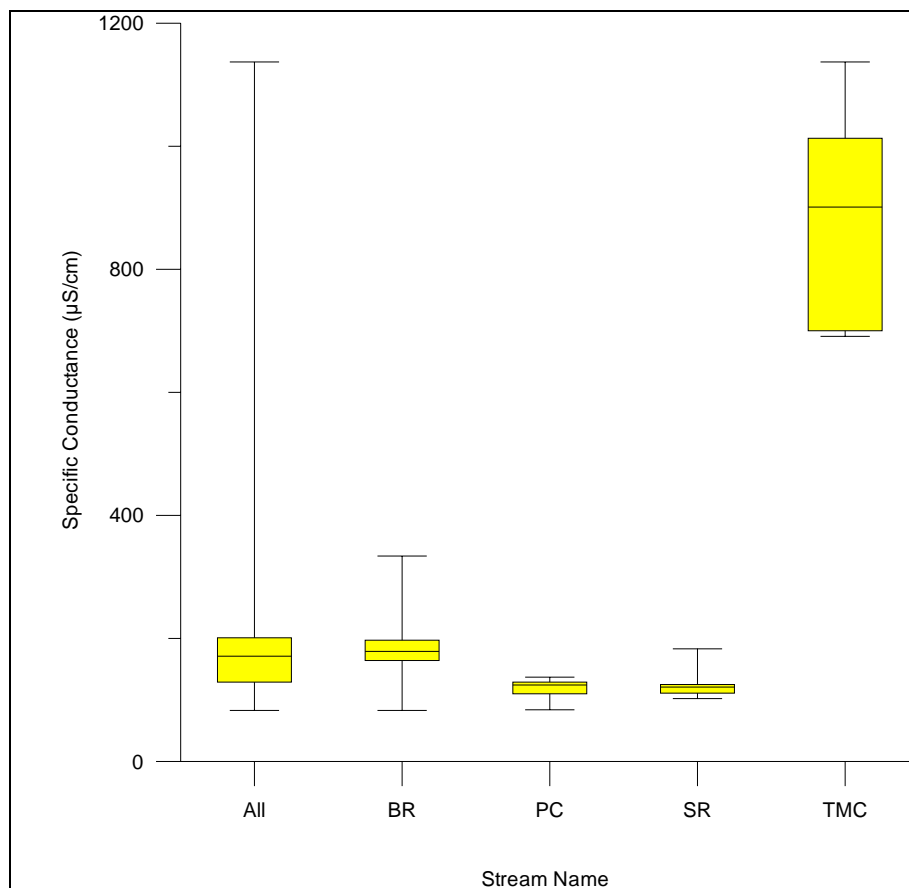


Figure E-7
Specific Conductance Values Measured During This Study

Specific conductance values in different streams in this study area vary considerably (Figure E-7). In the Blue River, values from 83 to 334 $\mu\text{S}/\text{cm}$ have been measured, with a median value of 179 $\mu\text{S}/\text{cm}$. In Pennsylvania Creek, specific conductance ranges were considerably lower; anywhere from 84 to 137 $\mu\text{S}/\text{cm}$ with a median value of 124.3 $\mu\text{S}/\text{cm}$. Similar ranges were seen in Swan River: 102 to 183 $\mu\text{S}/\text{cm}$ and median value of 120.8 $\mu\text{S}/\text{cm}$. In Tenmile Creek, however, ranges were consistently higher than in other areas varying from 691 to 1,137 $\mu\text{S}/\text{cm}$ with a median of 901 $\mu\text{S}/\text{cm}$.

Dissolved Oxygen

DO in the water can vary based on temperature and barometric pressure. DO is a useful indicator of water quality as various pollutants can reduce the amount of oxygen present in a body of water. For example, if water of a high temperature is introduced to a river, the amount of DO will sink because DO is reduced with rising temperature. Furthermore, pollutants such as wastewater may reduce DO levels when they are introduced to a river. This effect occurs because wastewater that is not treated properly can have oxygen demand and will consume oxygen when introduced to a body of water. DO is extremely important to the survival of aquatic life, and so is considered an important parameter to monitor.

During Phase I monitoring, DO values ranged from 5.61 to 11.26 mg/L (Figure E-8). The median of all Phase I measurements was 8.6 mg/L. Though ranges differed slightly, medians of the individual streams did not vary much from the overall median, with the exception of Swan River, which appears to be slightly more oxygenated than other parts of the study area (Figure E-8). Percent saturations could not be calculated for this phase because the exact barometric pressure of each site was not measured.

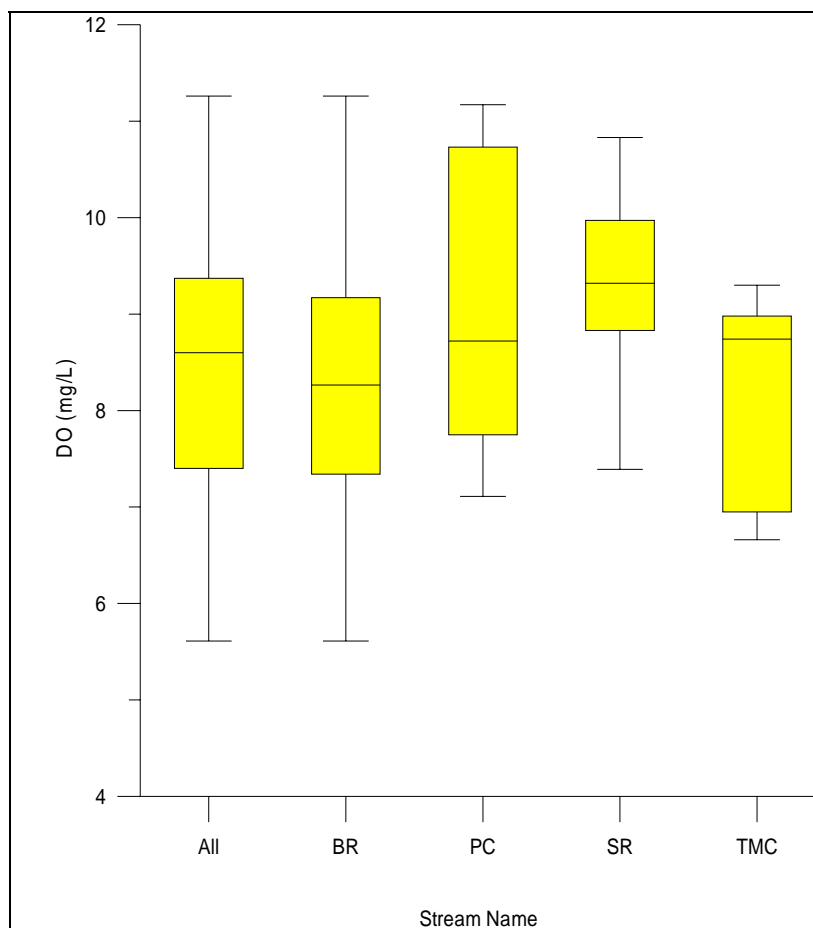


Figure E-8
DO Values Measured During Phase I (September 2001–March 2002) of This Study

During Phase II barometric pressure was measured at each site, so it was possible to calibrate the DO meter at each site according to the precise conditions of saturation based on both temperature and barometric pressure. Therefore, both DO concentration and percent saturation were obtained. However, some malfunction is believed to have occurred in the Phase II sampling because results of the measurements were often times exceptionally supersaturated (for example, 198%). Another factor that caused doubt in the values measured was drift of the DO meter. Oftentimes, it was impossible to get a stable reading. The DO meter is part of a multi-probe that is used frequently to measure other parameters such as water temperature and pH, so it was difficult to have the meter serviced. Yet another concern is the erratic nature of the trends when Phase II DO values are plotted. The lack of consistency seems to indicate that the values are not even valid as an interpretation of upstream to downstream or seasonal trend. Due to these concerns and doubts in the validity of Phase II DO measurements, all Phase II DO readings were eliminated from the data set.

pH

Natural waters usually have a pH of around 7. Maintenance of a relatively neutral pH is important because aquatic life can usually survive only in a pH range of 5 to 9 (Metcalf & Eddy 2003). Significant deviation from this range can indicate addition of pollutants, including wastewaters, which have higher or lower pH. There were more than 150 pH measurements made during this study from September of 2001 to September of 2002.

The values measured ranged from 6.58 to 8.95 standard units. However, 75% of the pH measurements fell in the range of 7.17 to 8.27 standard units. Median of all pH measurements taken was 7.86 standard units. pH did not vary much among the streams monitored in this study (Figure E-9). For example, median pH measured in the Blue River was 7.95. In Pennsylvania Creek, this value was 7.96. In the Swan River and Tenmile Creek, average measured pH was 7.63 and 7.71 respectively. Figure E-9 displays pH values for each stream in the study area.

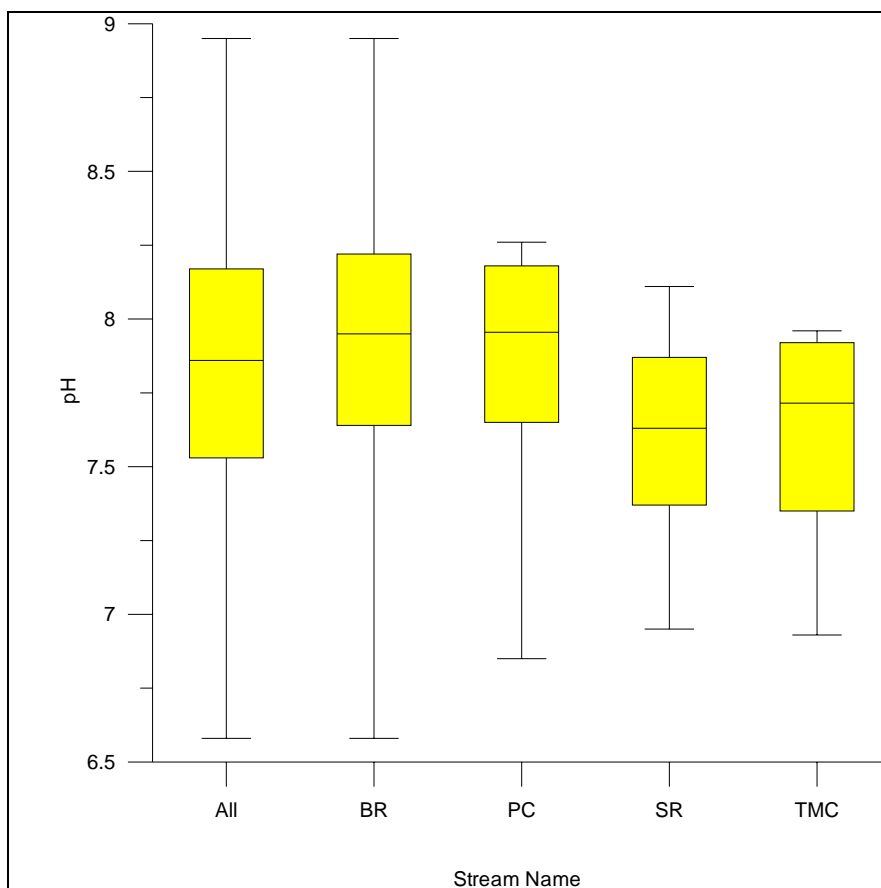


Figure E-9
All pH Values Measured in This Study

Water Temperature

The final field parameter measured for this study is water temperature. Temperature can affect such things as reactions, reaction rates, and aquatic life, so it is important that water temperatures remain within their normal seasonal range. Water temperatures in the Dillon Reservoir watershed were typically low. About 85% of the measurements taken were below 10 °C. During this year of measurements, temperatures ranged from -1.7 °C to 17.35 °C. Median water temperature in the study area was 2.95 °C. Figure E-10 summarizes temperature data from this study. Two of the focus areas, Swan River and Tenmile Creek, were not monitored during the warmer, Phase II months, which should be considered. Hence, overall range and median are likely lower than would have been observed if temperatures were recorded for the spring and summer months.

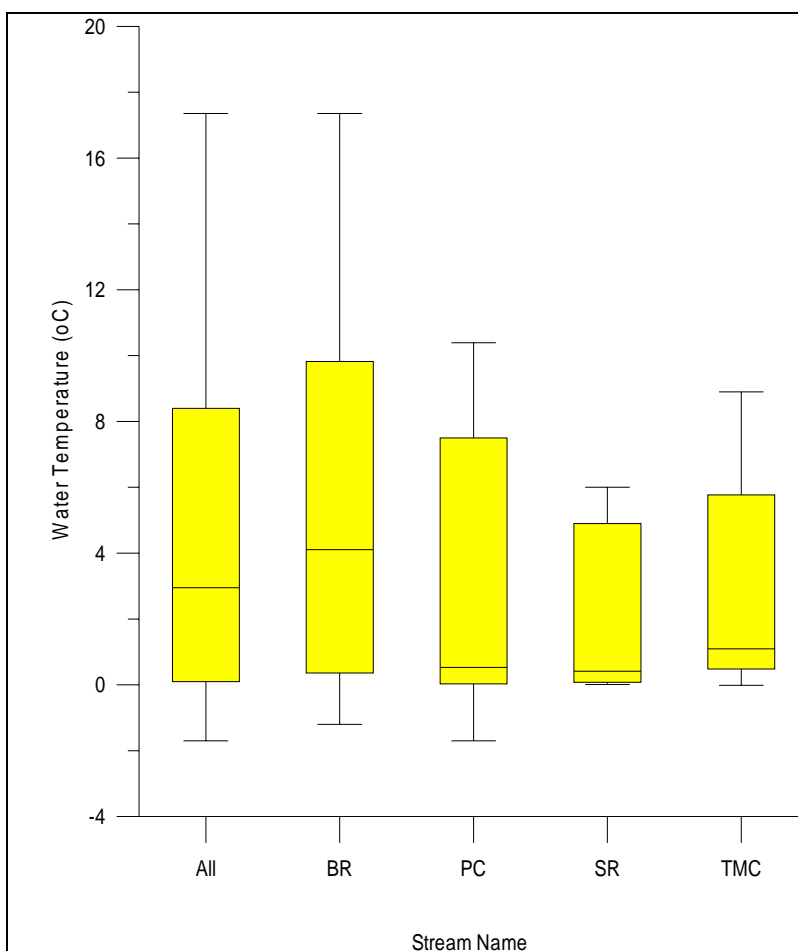


Figure E-10
Temperature Values Measured During Both Phases of This Study

Inorganics

A broad suite of inorganics was measured as a part of this study. Anions, including chloride, fluoride, and sulfate were measured. A broad suite of cations was also measured, including the following metals:

- Aluminum
- Arsenic
- Barium
- Beryllium
- Calcium
- Cadmium
- Chromium
- Cobalt
- Copper
- Iron
- Potassium
- Lithium
- Magnesium
- Manganese
- Molybdenum
- Nickel
- Selenium
- Silica
- Silver
- Sodium
- Lead
- Strontium
- Tin
- Vanadium
- Zinc

Other inorganics that were measured include boron, sulfur, and nutrients. The nutrient parameters include a variety of nitrogen and phosphorous species. A limited set of these parameters will be included in this section. That set will include those for which there is a standard as well as those that are constituents of domestic wastewater.

Major Ions

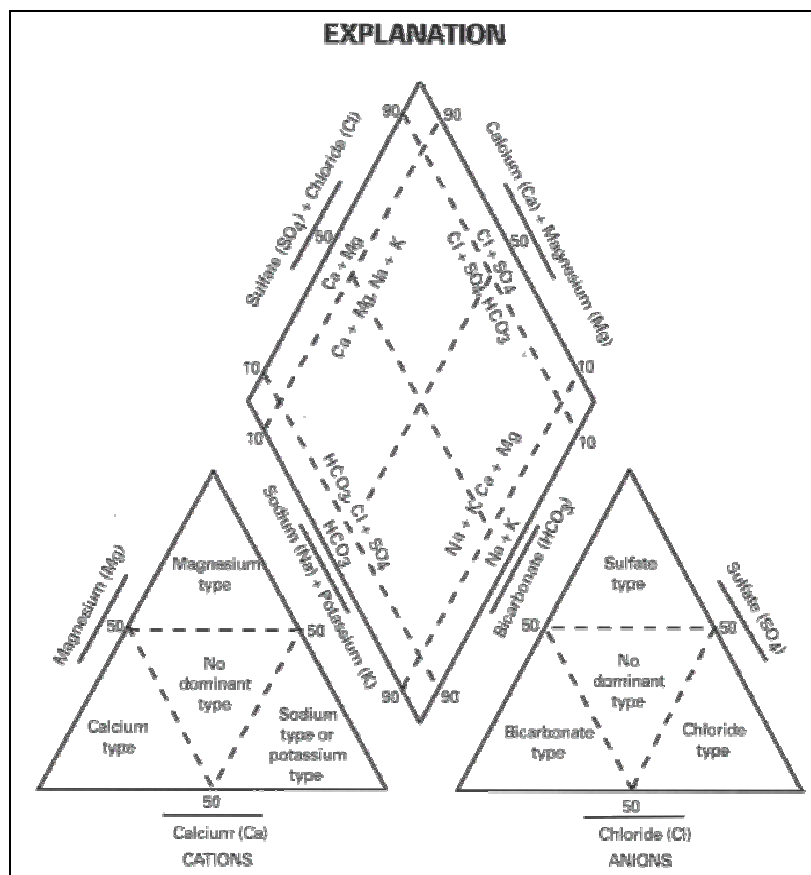
For the purposes of this appendix, major ions include the following cations and anions:

- Bicarbonate
- Carbonate
- Magnesium
- Sodium
- Calcium
- Chloride
- Potassium
- Sulfate

These ions are usually the ones found in the most abundance in natural waters. Other, lesser ions can be grouped in with these major ions according to chemical characteristics (Walton 1970). For example, calcium, barium, strontium, and magnesium all share similar chemical characteristics (+2 charge). In most natural waters, including those in this study area, total concentration of these four ions can be estimated by adding the equivalence of calcium and magnesium, because concentrations of barium and strontium are very small in comparison.

Major ions comprise a large portion of the dissolved constituents in water, and this ionic composition can be represented by a special form of trilinear diagram known as a Piper diagram (Walton 1970). Figure E-11 is an explanation of Piper diagrams. Phases I and II Piper diagrams for this study can be found in Figure E-12 and Figure E-13. These diagrams do not convey concentrations of these ions, but do show relative percentages of the major cations (Ca^{2+} , $\text{Na}^{1+} + \text{K}^{1+}$, and Mg^{2+}) and anions ($\text{HCO}_3^- + \text{CO}_3^{2-}$, SO_4^{2-} , and Cl^-) on two separate trilinear diagrams. The diamond field shown in the middle shows the overall chemical character of the water using a third point that is an intersection of lines projected from the separate cation and anion points.

From the Phase I trilinear diagram, it is apparent that calcium was the dominant cation in nearly all samples. In the Blue and Swan Rivers, calcium usually accounted for 60 to 85% of all cations. This percentage was higher in both Tenmile and Pennsylvania Creeks, where calcium accounted for 80 to 90% of all cations. The anion diagram shows more dramatic differences in streams. In nearly all cases, sulfate is the dominant anion in Tenmile Creek accounting for nearly 75 to 90% of all anions. The majority of the remaining relative percentages are dominated by carbonate. However, in Pennsylvania Creek, carbonate accounts for 100% of all anions. In the Blue and Swan Rivers, carbonate dominates at the lower range of 60 to 90%.



Source: Wynn 2001

Figure E-11
Explanation to Interpret Piper Diagrams Shown in Figure E-12 and Figure E-13

Similar trends were seen in the Piper diagram generated for Phase II; however, during this time, only sites from the Blue River and Pennsylvania Creek were monitored. In the Blue River samples, there were some instances where there was no dominant cation. However, in the majority of cases, calcium dominated accounting for 60 to 95% of all cations. As seen in Phase II, calcium represented 80 to 90% of all cations in Pennsylvania Creek. Carbonate was the dominant anion in all Phase II samples. In the Blue River, carbonate was 60 to 90% of all anions. This number was again higher in Pennsylvania Creek where Carbonate accounts for nearly 100% of all anions.

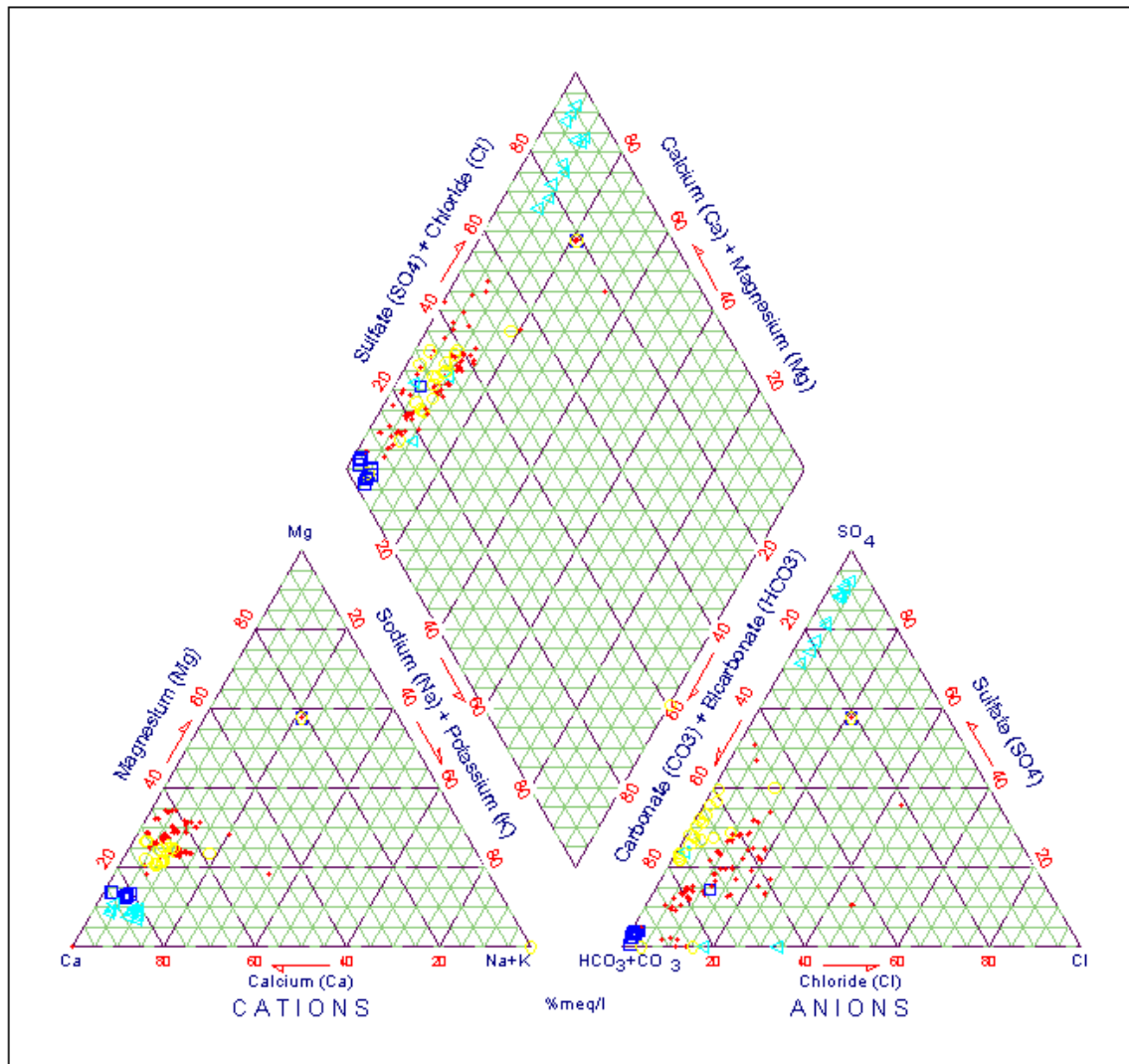


Figure E-12
Piper Diagram for Phase I Major Ions

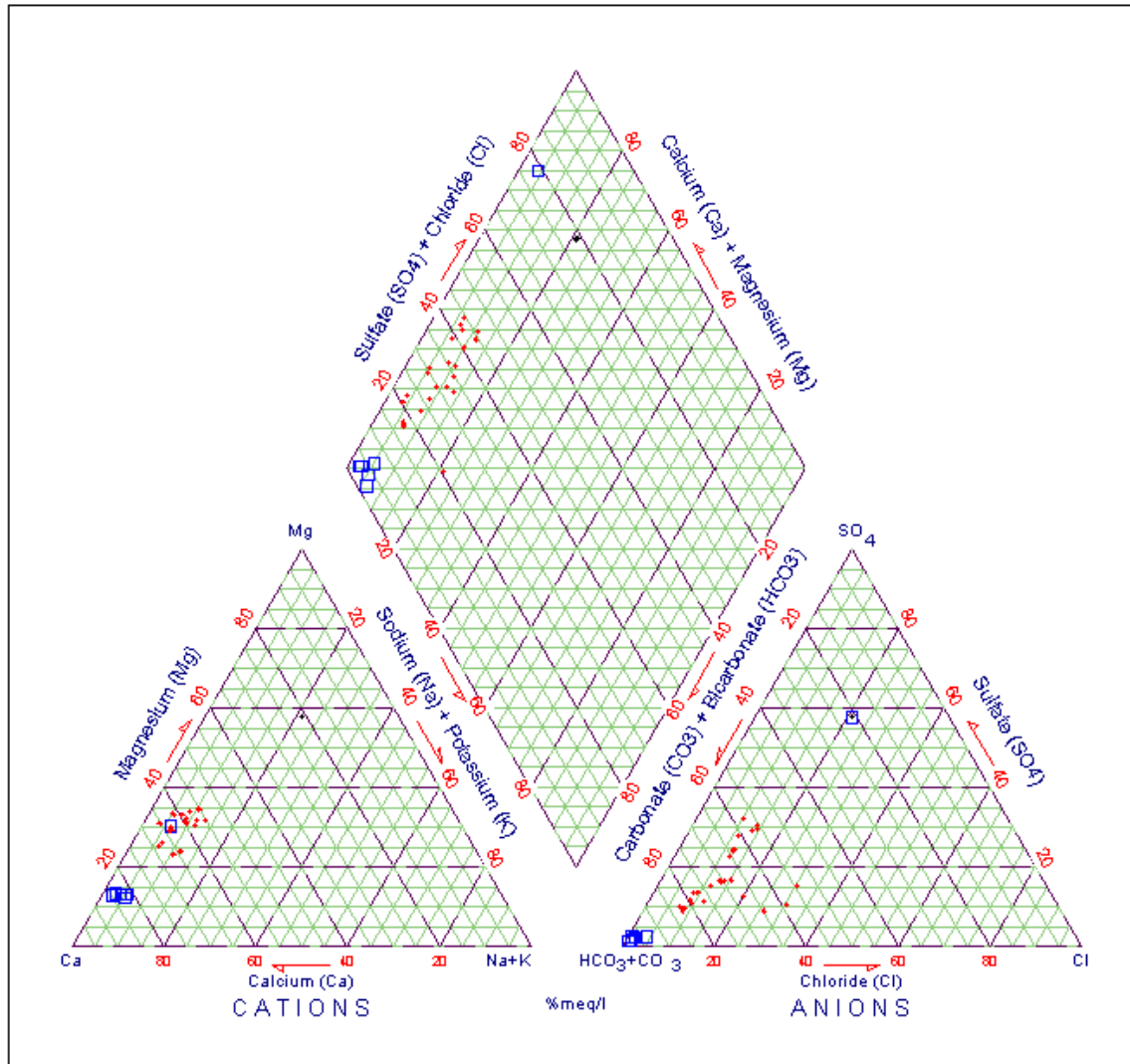


Figure E-13
Piper Diagrams for Phase II Major Ions

Trace Elements

The following trace elements were included in the analyses conducted in this study:

- | | | | |
|-------------|-------------|--------------|-------------|
| • Aluminum | • Chromium | • Molybdenum | • Strontium |
| • Antimony | • Cobalt | • Nickel | • Sulfur |
| • Arsenic | • Copper | • Potassium | • Tin |
| • Barium | • Iron | • Selenium | • Thallium |
| • Beryllium | • Lead | • Silica | • Vanadium |
| • Boron | • Lithium | • Silver | • Zinc |
| • Cadmium | • Manganese | • Sodium | |

Trace elements can be crucial to the health of living organisms, but toxic when present in high amounts. Therefore, oftentimes water quality standards are set for certain trace elements. They will only be discussed in detail for the purposes of this study if there is an applicable water quality standard. In such a case, the Water Quality Assessment section will denote whether or not the surface waters in this study meet the given criteria. Trace elements that were compared to surface water quality standards in this study are as follows:

- Boron
- Cadmium
- Copper
- Iron
- Lead
- Manganese
- Nickel
- Selenium
- Silver
- Zinc

Table E-9 provides a brief synopsis of the results of analyses of these ten trace elements including the range and median value measured in each stream. The table also denotes the number of total measurements made for each parameter, in each river, and how many were found to be below the detection limit. These ranges will include Phase II sampling in the Blue River and Pennsylvania Creek values, but not values from the remaining surface waters, which is important to keep in mind. Further discussion can be found in the Water Quality Assessment section.

Table E-9
Synopsis of Trace Metal Analyses Relevant to This Study

	Blue River	Penn Creek	Swan River	Tenmile Creek
Boron (B)				
Range (mg/L)	0.008-0.129	0.018-0.087	0.001-0.044	0.019-0.028
Median (mg/L)	0.0362	0.0461	0.0182	0.0212
#UR/Total measured	27/88	9/20	8/16	8/14
Detection limit	0.0002	0.0002	0.0002	0.0002
Cadmium (Cd)				
Range (mg/L)	0.003-0.013	---	---	---
Median (mg/L)	0.0069	---	---	---
#UR/Total measured	84/88	---	---	---
Detection limit	0.0045	0.0045	0.0045	0.0045
Copper (Cu)				
Range (mg/L)	0.007-0.007	0.001-0.005	---	---
Median (mg/L)	---	0.0030	---	---
#UR/Total measured	87/88	18/20	---	---
Detection limit	0.1031	0.1031	0.1031	0.1031
Iron (Fe)				
Range (mg/L)	0.002-0.27	0.004-0.316	0.005-0.024	0.005-0.03
Median (mg/L)	0.0219	0.0324	0.0151	0.0082
#UR/Total measured	60/88	14/20	12/26	11/14
Detection limit	0.0008	0.0008	0.0008	0.0008
Lead (Pb)				
Range (mg/L)	0.052-0.052	0.07-0.07	---	---
Median (mg/L)	---	---	---	---
#UR/Total measured	87/88	19/20	---	---
Detection limit	0.0194	0.0194	0.0194	0.0194

Table E-9
Synopsis of Trace Metal Analyses Relevant to This Study (Cont.)

	Blue River	Penn Creek	Swan River	Tenmile Creek
Manganese (Mn)				
Range (mg/L)	0.001-0.303	0.001-0.072	0.001-0.019	0.059-1.439
Median (mg/L)	0.0205	0.0170	0.0088	0.2210
#UR/Total measured	28/88	10/20	6/16	0/14
Detection limit	0.0278	0.0278	0.0278	0.0278
Nickel (Ni)				
Range (mg/L)	0.005-0.136	0.019-0.218	---	---
Median (mg/L)	0.0124	0.1187	---	---
#UR/Total measured	85/88	18/20	---	---
Detection limit	0.0302	0.0302	0.0302	0.0302
Selenium (Se)				
Range (mg/L)	0.037-0.037	---	---	---
Median (mg/L)	---	---	---	---
#UR/Total measured	87/88	---	---	---
Detection limit	0.0445	0.0445	0.0445	0.0445
Silver (Ag)				
Range (mg/L)	0.002-0.002	---	---	---
Median (mg/L)	---	---	---	---
#UR/Total measured	87/88	---	---	---
Detection limit	0.0424	0.0424	0.0424	0.0424
Zinc (Zn)				
Range (mg/L)	0.001-4.825	0.011-0.079	0.008-0.017	0.03-0.096
Median (mg/L)	0.0311	0.0375	0.0134	0.0680
#UR/Total measured	51/88	16/20	11/16	6/14
Detection limit	0.0617	0.0617	0.0617	0.0617

Note: UR = under range (< minimum detection limit)

#UR/Total measured reveals the number of total measurements found to be below detection limits

Nutrients

Nutrient parameters measured in this study were species of both nitrogen and phosphorous. During Phase I, nitrogen species included nitrate, ammonia, and total nitrogen. In Phase II this was expanded to include nitrite and organic nitrogen. During Phase I, phosphorous species included total phosphate and total phosphorous. During Phase II the total phosphorous, dissolved phosphate, and total dissolved phosphorous were analyzed. During Phase I all nutrient analyses were done in laboratories at the CSM. However, during Phase II all nutrient analyses were conducted by the NWQL.

Nutrient parameters were important to this study. As mentioned, a goal of this study is to determine what, if any, are the effects of OWS on the surface waters in the study area. Nutrients can be found in high concentrations in domestic wastewaters and comparatively lower concentrations in pristine surface waters. Therefore, elevated nutrient levels or increasing nutrient trends may be one way to assess if waters are being impacted by OWS effluent. Nutrients are also important to this study area because they are elements critical for biological growth. Elevated nutrient levels can cause increased biological growth and eventually eutrophication of surface waters, which is especially a concern in lakes. Summit County has a special interest in this issue because all surface waters in this study area eventually flow into Dillon Reservoir. If nutrient levels were to become elevated, eutrophication could be a concern for the reservoir.

As mentioned, during Phase I all nutrient analyses were done at CSM. During this time, many of the results were found to be below the detection limits. In fact, nearly all ammonia, total nitrogen, and total phosphorous results for the entire phase were below the detection limits (0.1 mgN/L, 1 mgN/L, and 0.046 mgP/L respectively). As a result the only nutrient parameters that can be presented are those for nitrate and phosphate. Figure E-14 and Figure E-15 are box-whisker plots of all nitrate and phosphate data collected during the Phase I sampling period.

Nitrate concentrations measured in the study area during Phase I ranged from 0.003 mgN/L to 2.722 mgN/L. Figure E-14 shows the ranges of nitrate that were measured in both the entire study area and each individual stream. The lowest nitrate value was measured in Swan River and the highest value was measured in Tenmile Creek. The greatest range of nitrate values was found in Tenmile Creek. Nitrate concentrations in Swan River showed the smallest variability. Median value of nitrate for all nitrate values measured was 0.176 mgN/L. Median values in Blue River and Pennsylvania Creek were close to this at 0.197 and 0.121 mgN/L, respectively. In the Swan River, the median was slightly lower at 0.023 mgN/L. The median value in Tenmile Creek was 0.381 mgN/L, higher than other streams in the study area.

Figure E-15 presents phosphate data that were measured during Phase I of this study. The minimum value measured in this study area was 0.001 mgP/L. This minimum value was the same for all streams. The maximum value in the study area was 0.043 mgP/L, measured in the Blue River. The median of all phosphate concentrations was 0.008 mgP/L, as was the median value for the Blue River.

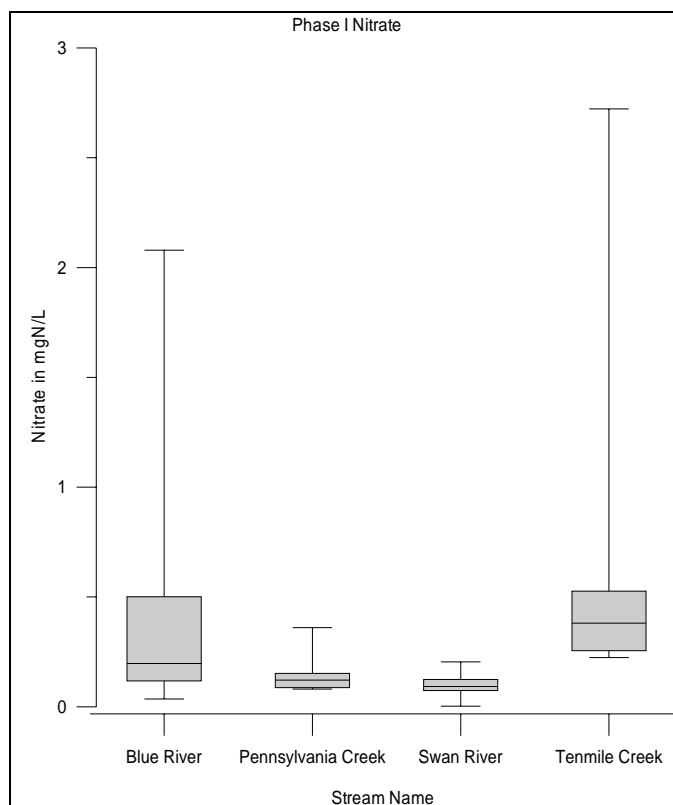


Figure E-14
Box-Whisker Plot of Nitrate Measurements From Phase I

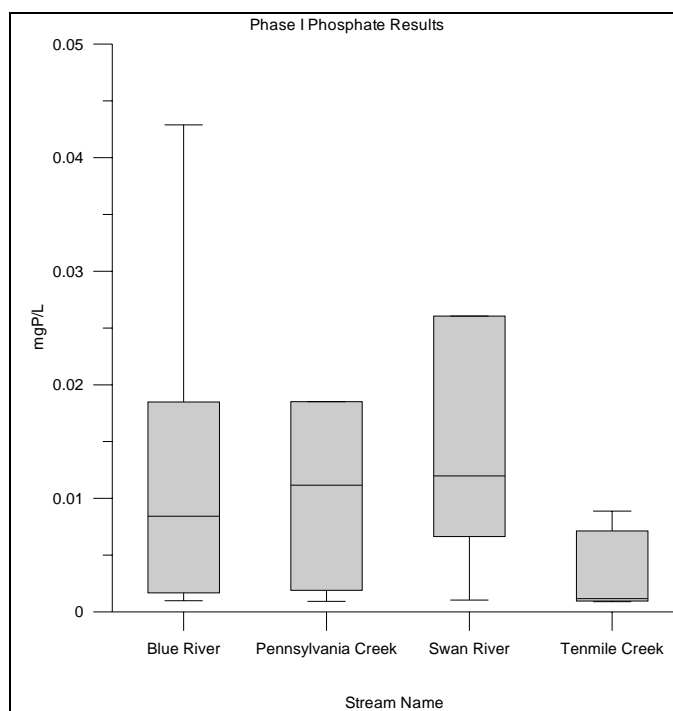


Figure E-15
Box-Whisker Plots of Phosphate Measurements From Phase I

Beginning in June 2002 all nutrient parameters were analyzed at the USGS NWQL to obtain precise, low-level nutrient data. The NWQL can achieve lower detection limits and analyze more parameters (such as organic nitrogen and dissolved phosphorous) than laboratories at CSM. As a result, there is more extensive nutrient data available for Phase II than for Phase I.

Figure E-16, Figure E-17, Figure E-18, and Figure E-19 are box plots that display the results of Phase II nutrient analyses. Results of all nutrient parameters measured in Phase II are included on these plots. These graphs are organized slightly different from Phase I data. Instead of being organized according to parameter, four graphs have been made, two each for the Blue River and Pennsylvania Creek. For each of these streams there is a graph displaying results of all nitrogen species analyses and a graph displaying the results of all phosphorous species analyses. The only two streams analyzed during this phase were the Blue River and Pennsylvania Creek, and no Phase II data is available for the other streams discussed in Phase I.

The following nitrogen parameters were analyzed by the NWQL:

- Dissolved ammonia
- Dissolved ammonia plus organic nitrogen
- Dissolved nitrite plus nitrate
- Dissolved nitrite
- Dissolved nitrogen
- Total nitrogen

Two of these parameters, dissolved ammonia and dissolved nitrite, were below the detection limit in all cases (0.015 mgN/L and 0.0023 mgN/L, respectively). For the purposes of various calculations (calculating total and dissolved nitrogen values) these concentrations were estimated by dividing the detection limit by two, yielding an estimated value for ammonia of 0.0075 mgN/L, and an estimated nitrite value of 0.0012 mgN/L. Occasionally, other parameters were found to be below the detection limit as well. In these cases, the value was again represented as the detection limit divided by two. These values were included in the plots of data found in Figure E-16, Figure E-17, Figure E-18, and Figure E-19. Further presentation of nitrogen parameters will be limited to nitrate plus nitrite results because it is the nitrogen species of most interest to this study.

Phase II nitrate plus nitrite results were lower than Phase I results in both the Blue River and Pennsylvania Creek. In the Blue River, Phase II nitrate plus nitrite concentrations ranged from 0.065 to 0.459 mgN/L (Figure E-16). Please note that for the remainder of this chapter nitrite plus nitrate will be referred to solely as nitrate since nitrite concentrations were all below the detection limit, making nitrite plus nitrate concentrations predominantly nitrate. Median value of nitrate in the Blue River during this phase was 0.067 mgN/L. Pennsylvania Creek nitrate values were measured in the range of 0.02 to 0.07 mgN/L (Figure E-17). The median nitrate measurement for Pennsylvania Creek was 0.0425 mgN/L. During Phase II, the Blue River displayed the most variability in the data set.

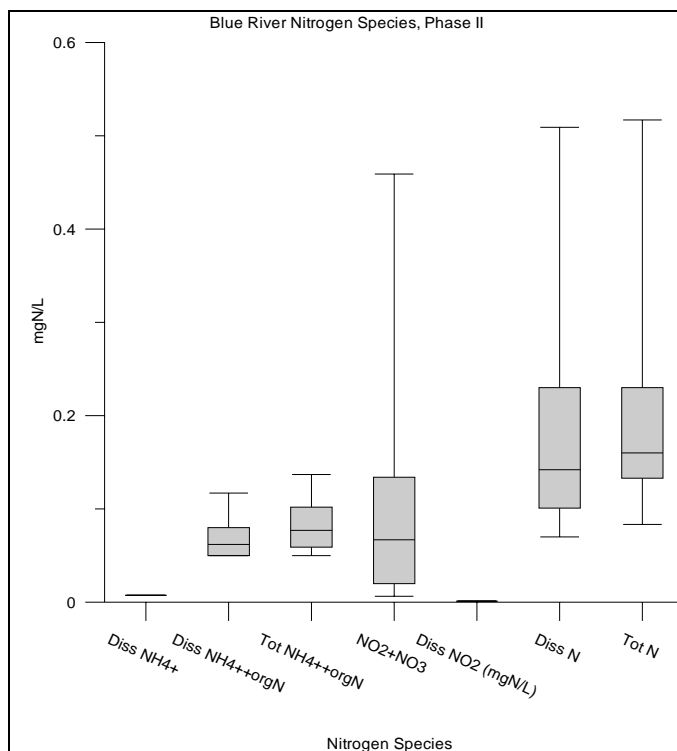


Figure E-16
Box-Whisker Plots of Nitrogen Results for the Blue River During Phase II Analyses

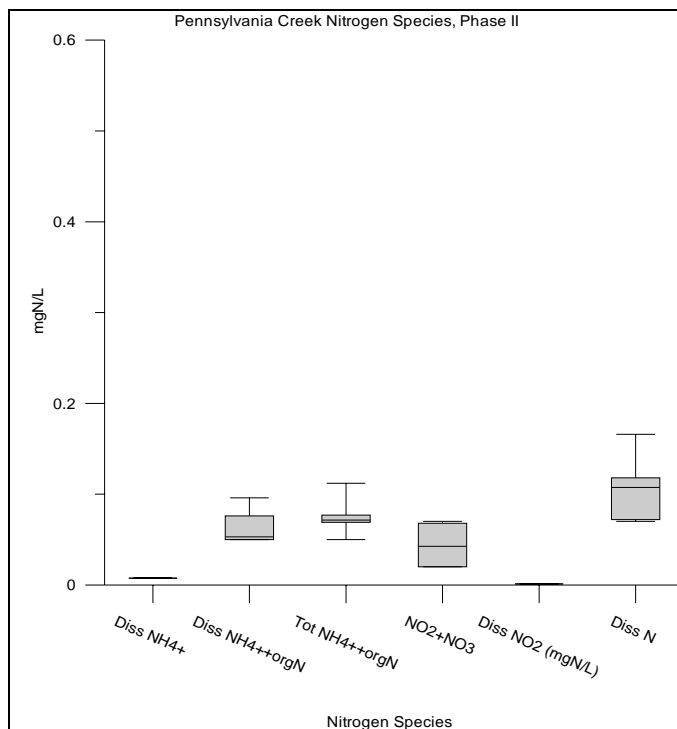


Figure E-17
Box-Whisker Plots of Nitrogen Results for Pennsylvania Creek During Phase II Analyses

Three phosphorous parameters were analyzed by the NWQL for the purposes of this study:

- Dissolved phosphorous
- Total phosphorous
- Dissolved phosphate

As seen with some of the nitrogen species, dissolved phosphate was found to be below the detection limit in all cases and was estimated by dividing the detection limit by two to obtain 0.0035 mgP/L. Dissolved phosphorous was occasionally found to be below the detection limit and in those instances was also estimated as the detection limit divided by two to obtain a value of 0.02 mgP/L. Estimated dissolved phosphorous concentrations were included in the data range presented in the graphs shown in Figure E-18 and Figure E-19. Of the three phosphorous parameters, phosphate is of the most interest to this study. Because it was found to be below the detection limit in all cases, this chapter will instead discuss dissolved phosphorous, which would include any dissolved phosphate present in the analyzed samples. Note that dissolved phosphorous would also include any dissolved organic phosphorous present in the sample.

Dissolved phosphorous in the Blue River ranged from 0.002 to 0.004 mgP/L during Phase II (Figure E-18). The median measurement in this range was 0.0028 mgP/L. Comparing this data to Phase I measurements is not valid because concentrations for Phase I were of phosphate only and not total dissolved phosphorous. Phase II Blue River range was slightly higher than the range measured in Pennsylvania Creek, which was 0.002 to 0.003 mgP/L (Figure E-19). Median values for the two streams, however, were equal. The Blue River again displayed the most variability in concentration range.

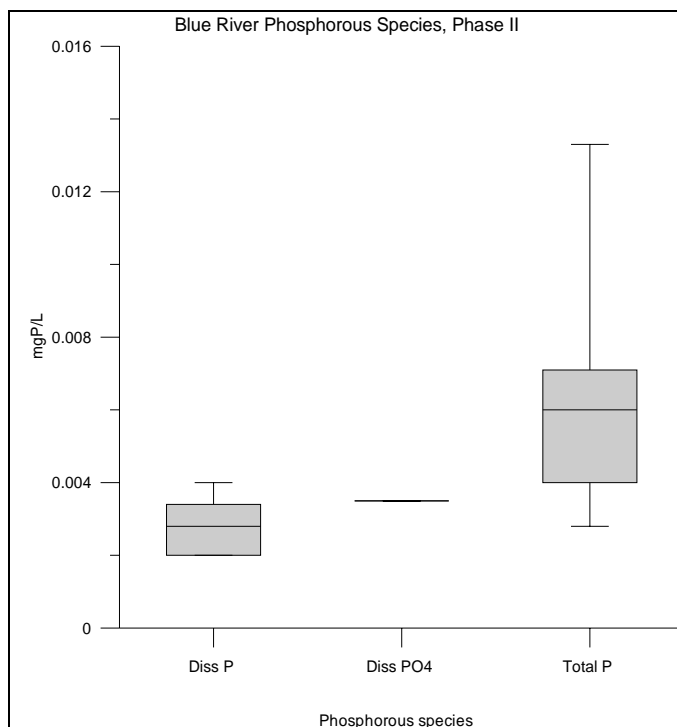


Figure E-18
Box-Whisker Plots of All Blue River Phosphorous Analyses Conducted in Phase II

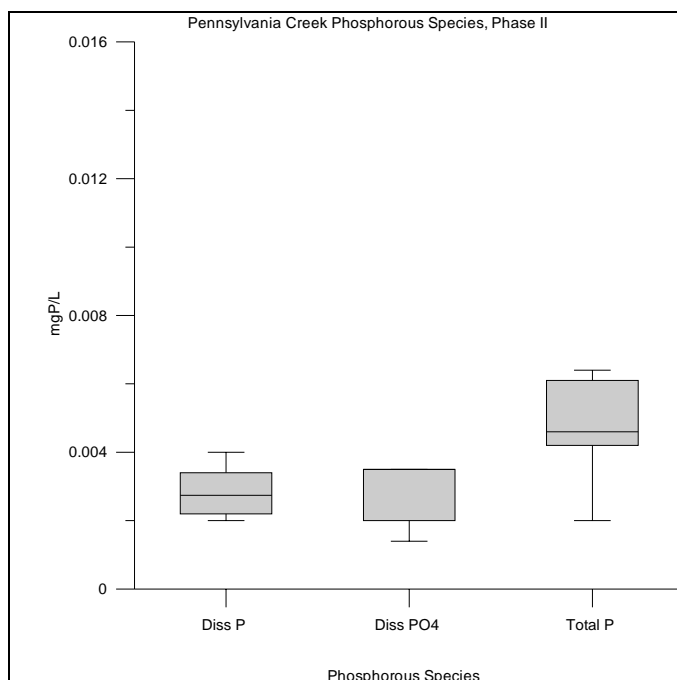


Figure E-19
Box-Whisker Plots of All Pennsylvania Creek Phosphorous Analyses Conducted in Phase II

Other Parameters

Five remaining parameters were analyzed during this study:

- Alkalinity
- Chemical oxygen demand (COD)
- Fecal coliform bacteria
- Total solids
- Turbidity

Table E-10 summarizes the results of these analyses. Note that the ranges of COD are based only on actual values and not those that were found to be below the detection limit. Seventy percent of all COD measurements were below the detection limit (1 mg/L COD). Turbidity was measured at each site during the study. Turbidity is not further discussed because turbidity in this study is primarily an indicator of the levels of solids in the water, and solids analyses were conducted. Alkalinity, though potentially important as a basic water quality indicator, was not needed to support any of the conclusions of this work and will not be further discussed. Finally, fecal coliform bacteria data are especially useful as an indicator of the presence of human and/or animal waste; however, results were found to be zero in approximately 60% of all fecal coliform bacteria analyses and no trend could be detected in the greater-than-zero values.

Table E-10
Summary of Results From Remaining Parameters for the Entire Study Area

Parameter	Entire Study Area	Blue River	Pennsylvania Creek	Swan River	Tenmile Creek
COD (mg/L)					
Range	0.5–79	1–14	0.5–65	1–3	1–4
Median	3	3.6	1	1.5	1
#UR/Total measured	107/150	70/95	16/21	10/16	9/14
Turbidity (NTU)					
Range	0.07–7.5	0.14–7.5	0.07–0.0825	0.15–2.25	0.22–1.5
Median	0.523	0.57	0.21	0.6	0.61
#UR/Total measured	N/A	N/A	N/A	N/A	N/A
Alkalinity (mg/L)					
Range	25–116	25.5–98	35–88	25–58	32–70
Median	54	58	58	36	44
#UR/Total measured	N/A	N/A	N/A	N/A	N/A
Fecal Coliform (#/100mL)					
Range	0–52	0–30	0–15	0–52	0–20
Median	0	0	0	0	2
#UR/Total measured	N/A	N/A	N/A	N/A	N/A

Note: UR = Under Range (less than minimum detection limit); N/A = Not applicable

Water Quality Assessment

Many activities can cause degradation of water quality. Associated with each activity are various parameters that might reveal the cause of the degradation. For example, if wastewater were impacting water quality, it might be apparent in elevated levels of nutrients, oxygen demand, solids, or fecal coliform bacteria. Table E-11 summarizes some of the potential impacts to water quality monitoring variables that might reveal this impact, and whether or not there is the potential to find that impact in this study area.

Table E-11
Example Water Quality Impacts and Associated Monitoring Parameters

Source of Impact	Examples of Parameters to Identify	Potential for Impact in Study Area?
Domestic wastewater	Nutrients (N and P species), solids, oxygen demand, chlorides, boron, sulfur, fecal coliform bacteria, pharmaceuticals, increased alkalinity	Yes
Mining	Depends on type of mining, but some examples are decreased pH, alkalinity, sulfates, and metals—especially iron, lead, copper, and zinc	Yes
Industrial wastewater	Depends on industry, but some variables might include oxygen demand, trihalomethanes, hydrocarbons, benzene, and various metals	No
Agriculture	Nutrients (N and P species), solids, chlorides, fecal coliform bacteria, pesticides, herbicides, boron, selenium, sodium, calcium, magnesium	No
Urban development and runoff	Heavy metals, chlorides, organic compounds, nutrients (N and P species), fecal coliform bacteria	Yes

As previously mentioned, one of the primary goals of this study is to determine what, if any, are the effects of development, and specifically OWS, on the surface waters in the study area. This goal was approached in two ways.

The first approach was to study trends in both space and time, which enables the water quality at each site to be put into context with the water quality at other times of the study and at other sites. Essentially, studying trends in time reveals any times of the year that water quality may be more impacted than others (low flow). Studying trends in space enables the establishment of a land-use gradient. A land-use gradient can be established by sampling sites located in areas upstream of development, in areas of limited development, in areas of maximum development, and downstream of all development. In this way, if constituent levels are observed from upstream to downstream (a trend in space), a gradient may be observed that shows where areas of impact begin and end.

The second approach was to compare in-stream constituent concentrations to state surface water quality standards for the area. This approach enables the water quality of the area to be put in context with the quality of other surface waters.

The Results section introduced some of the water quality results obtained in this study, but made no attempt at interpretation of any trends. These results are further discussed in the information provided in this section in order to assess any potential impacts that are present in the Dillon Reservoir watershed. First, the trends in space and time of some parameters are presented. Second, certain water quality standards are compared to other parameters. Finally, some potential causes of the trends introduced in the first section are discussed.

Figure E-20 illustrates sample stations and Figure E-21 illustrates important features in the study area (focus areas, areas of development, and sources of pollution).

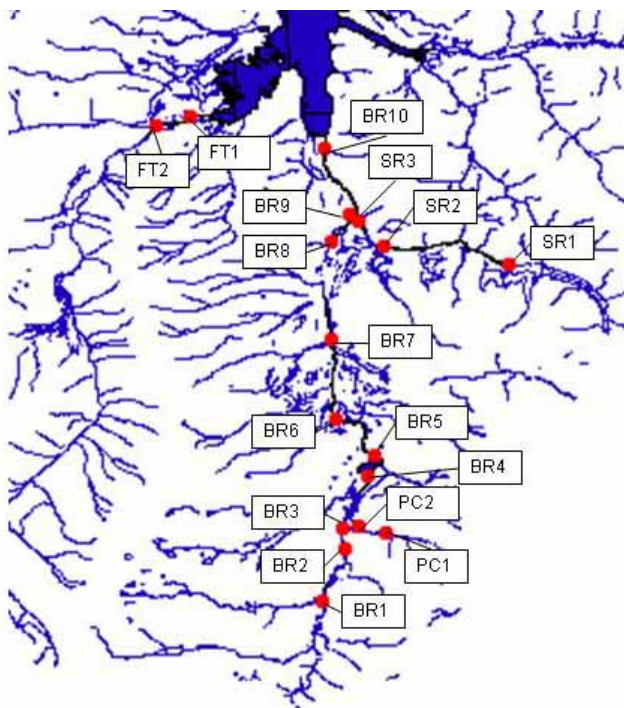


Figure E-20
Map of All Sample Sites Chosen for This Study

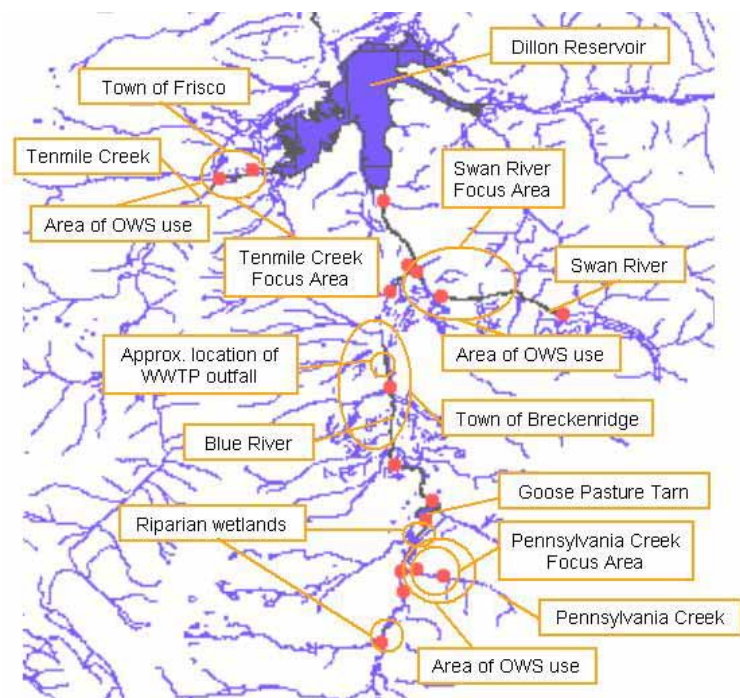


Figure E-21
Important Geographical Features in the Study Area

Trends in Space and Time

The importance of utilizing trends in space and time to answer the questions presented by the goals of this study cannot be understated. This aspect is the key manner in which developmentally impacted areas will be identified. However, not all parameters will be analyzed for trends in space and time. Since the main objective of this study is to identify effects that are developmentally related, only variables that would reveal this relationship will be studied, which will include the following parameters:

- Chemical oxygen demand
- Chlorides
- Field parameters
- Flow
- Nutrients
- Sulfur
- Total solids

These parameters were chosen mainly because they may reveal the effects of domestic and municipal wastewater input.

There is one other main source of impact to this study area, which is mining. Table E-11 addresses some of the variables to be studied in order to determine these impacts. Mining is not a main concern of this study; therefore, trends in space and time of most metals analyzed will not be presented. However, many of the water quality standards used in this study are standards for metals, therefore the comparison to the standards should provide information on any elevated levels of metals, and hence potential mining impacts, in the study area.

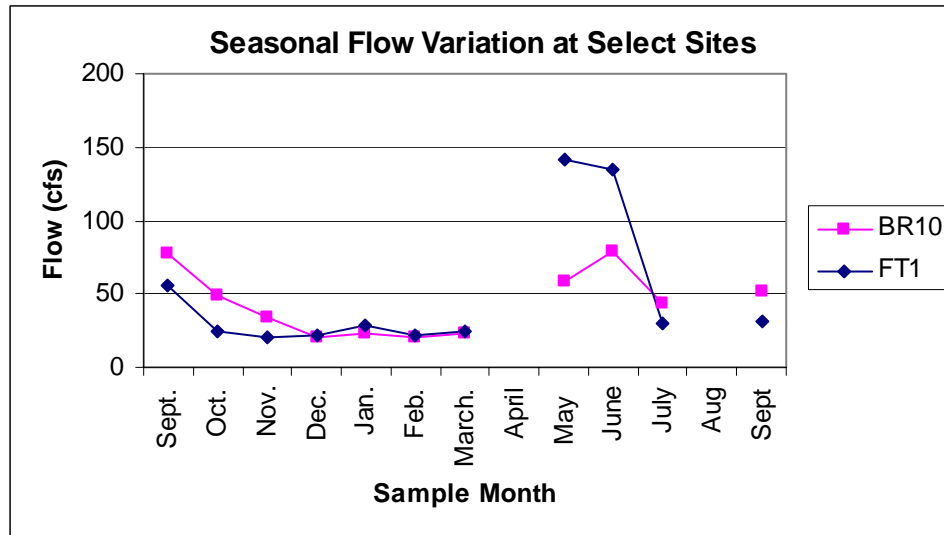
Flow

Flow does not provide a great potential for revealing impacts to water quality. Flow is crucial however to explaining some of the fluctuations seen in other parameters, and in calculating mass flow rates. Therefore both seasonal and upstream to downstream flow trends are discussed here.

As expected, flow measurements demonstrated a clear seasonal flow pattern. From the start of monitoring in September, flow decreased until spring and then began to increase (Figure E-22). This increase lasted until summer. In mid-summer, flow began to decline again.

These flow values are based solely on flows observed during a monthly sampling event, which is important to keep in mind. These values should not be used to indicate when the month of minimum or maximum flow occurred. This determination is made by studying mean monthly flows that can be calculated when flow is measured more frequently than once per month.

Flow is measured on a near-continuous basis (every 15 minutes) at gaging stations that are maintained by the USGS. Several gaging stations were included as monitoring sites in this study. By looking at the data available from select gaging stations in the study area (USGS 2002), it is possible to get a better idea when the months of minimum and maximum flow occurred.



Note: BR10 and FT1 are at the inlets to Dillon Reservoir

Figure E-22
Graph of Seasonal Flow Variation at Two Sites in the Study Area

Mean monthly flow data from three gaging stations in the study area, situated at sites BR5, BR10, and FT1, show that minimum flow occurred during the month of March and maximum flow in the month of June (Figure E-23). Flow at all sample sites likely had similar patterns. Gaging station flows and CSM flows were comparable, which is important to note.

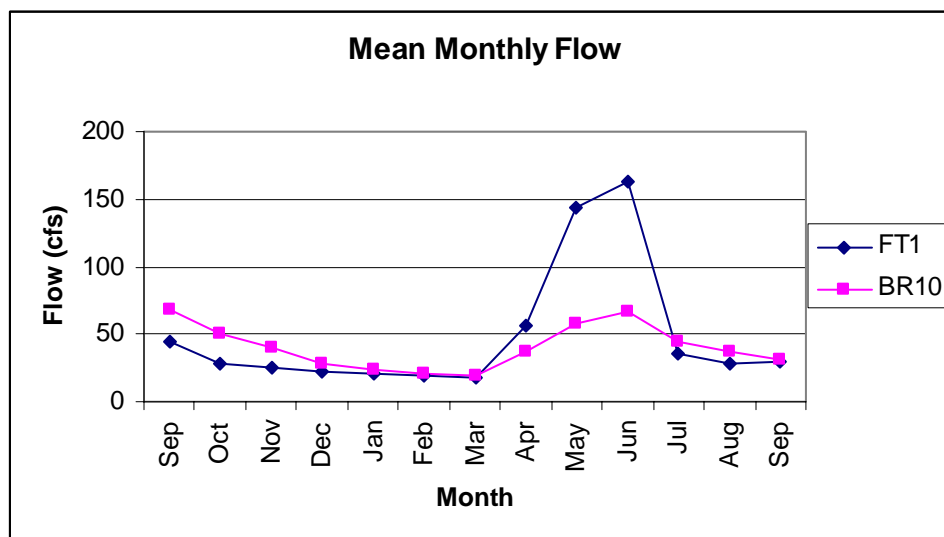
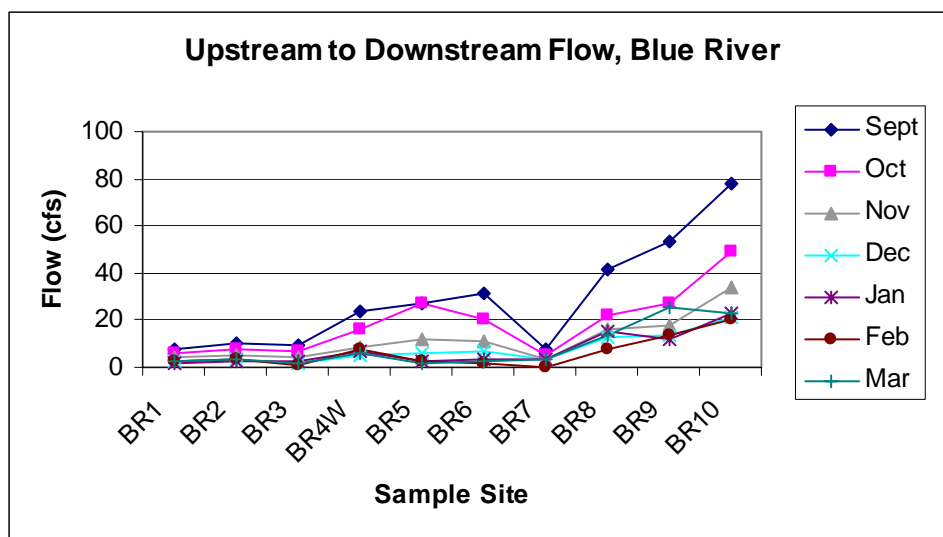


Figure E-23
Mean Monthly Flow Collected at Two Gaging Stations in the Study Area

With the exception of Pennsylvania Creek, which was monitored during Phase II, upstream to downstream trends in the focus area are difficult to determine as there were only two to three sites located along each of these streams. Furthermore, these sites were the most affected by ice cover, limiting the number of times flow was measured. No statements can be made about flow trends in the Swan River. Pennsylvania Creek summer flow measurements indicated that flow between PC1 and PC2 remains fairly constant sometimes showing slight decreases, and other times slight increases. Flow between sites FT1 and FT2 on Tenmile Creek is considered equal based on measurements and on the fact that there are no apparent water inputs between the two sites.

Flow along the Blue River increased from upstream to downstream with the exception of a small stretch through the town of Breckenridge (sites BR6 and BR7). In this stretch flow trends are variable and sometimes decreasing (Figure E-24). After site BR7, flows tended to increase sharply up to the mouth of the Blue River into Dillon Reservoir.



Note: Locations move downstream from left to right on the x-axis

Figure E-24
Flow Values Measured Along the Blue River

Field Parameters

All field parameters measured in this study displayed seasonal variation with the exception of pH, which remained relatively constant through the duration of this study. Water temperature dropped from the beginning of sampling through the winter months, began to warm in March and followed a warming trend through July. No August sample was taken, but by September 2002, temperatures had begun to cool once again (Figure E-25).

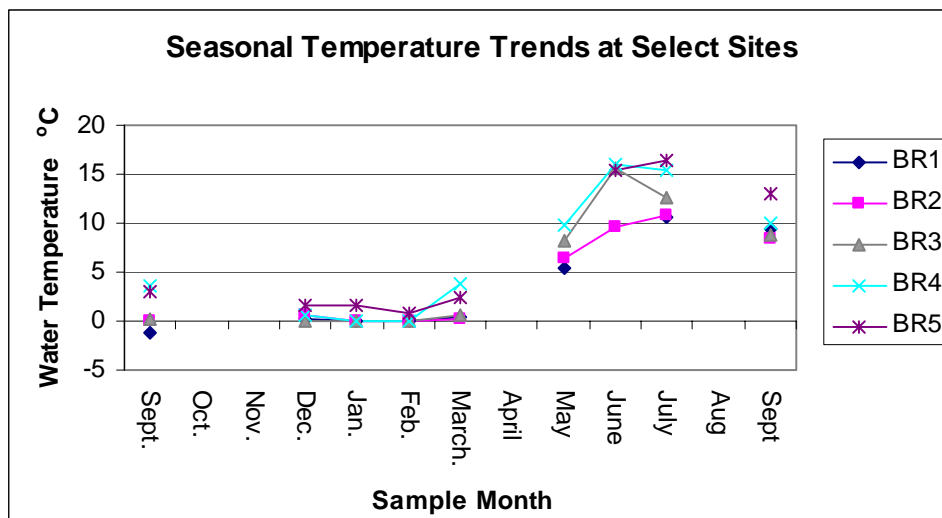


Figure E-25
Seasonal Temperature Trends at Select Blue River Sites

DO measurements increased from October to December and then decreased through February in most cases. A slight increase began in spring months. No DO data is available for the summer months of this study because, as mentioned in the Results section, Phase II DO values were censored. Figure E-26 shows seasonal DO trends representative of what was observed in this study.

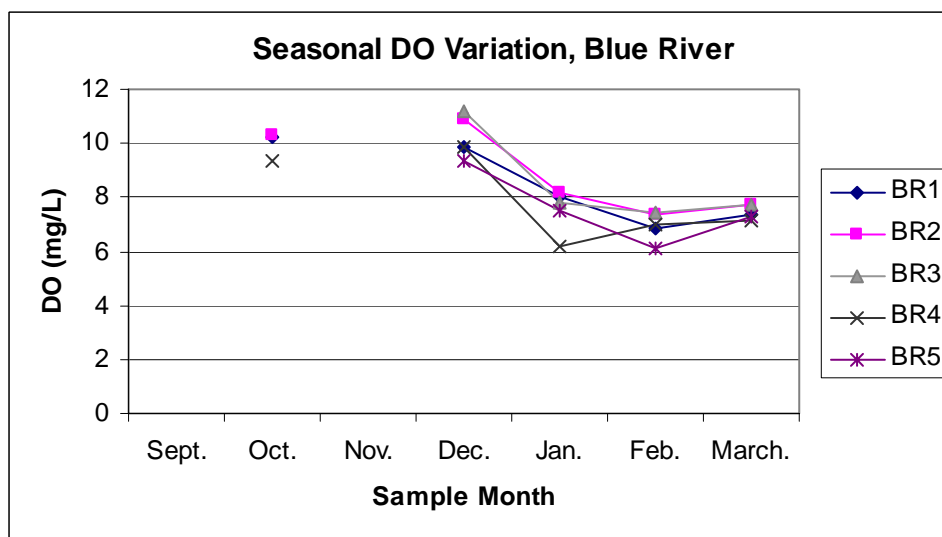
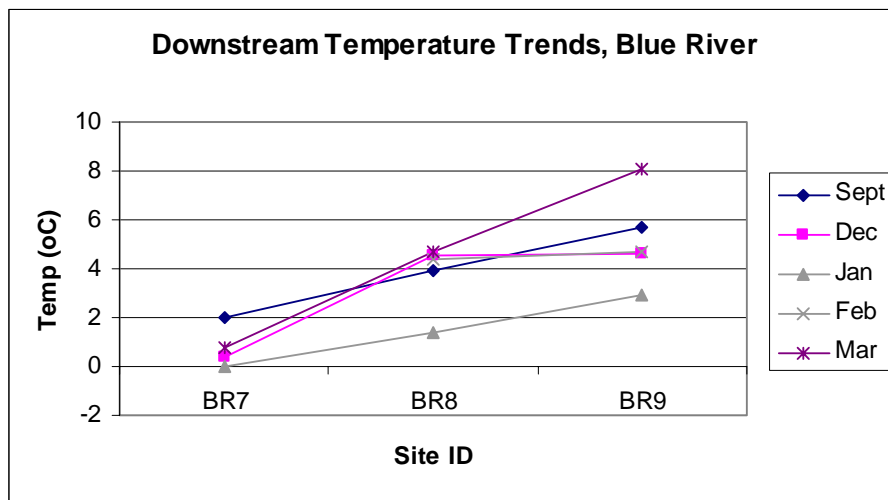


Figure E-26
DO Trends Typical of Sites in the Study Area

Unlike the seasonal trends, upstream to downstream trends in water temperature displayed little regularity in all streams. In other words, some sampling trips displayed a warming trend and others a cooling trend from upstream to downstream sites. There was one consistent occurrence along the Blue River from sites BR7 to BR9. Between these sites a warming trend was usually seen (Figure E-27).

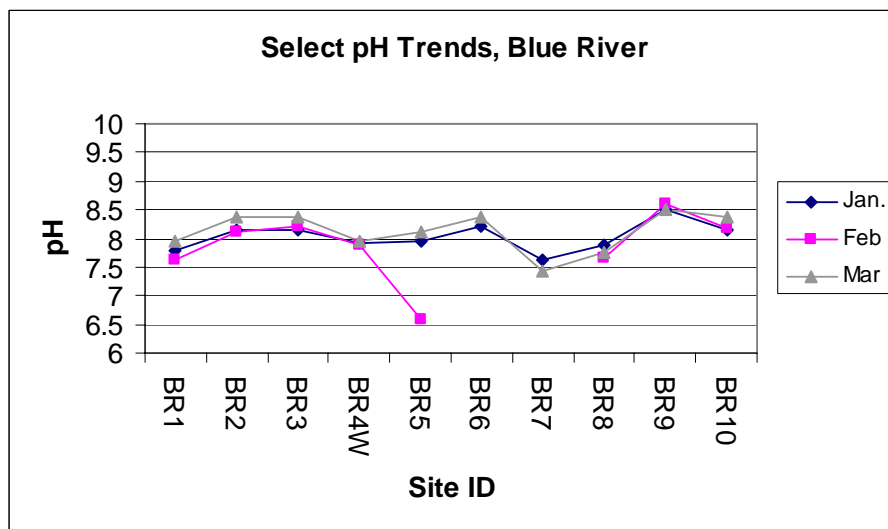


Note: Locations move downstream from left to right on the x-axis

Figure E-27

Graph of Temperature Trends Typical of Those Seen in Sites BR7, BR8, and BR9

Consistency was seen in the upstream to downstream trends in pH of all streams. pH tended to increase in Pennsylvania Creek from PC1 to PC2. pH in Swan River tended to increase from SR1 to SR2, but then decrease from SR2 to SR3 so that overall pH was constant. pH in Tenmile Creek between sites FT1 and FT2 was also constant. More variability was displayed between sites along the Blue River. pH consistently increased from BR1 to BR2 and decreased from sites BR3 to BR4. Beginning around site BR7, an increase in pH was observed until site BR9. Between BR9 and BR10 pH tended to decrease (Figure E-28).

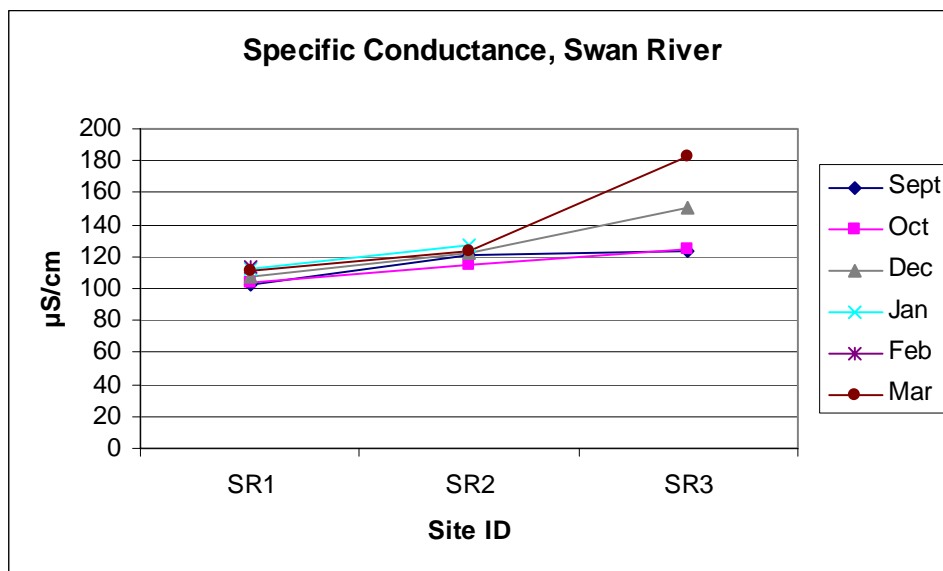


Note: Locations move downstream from left to right on the x-axis

Figure E-28

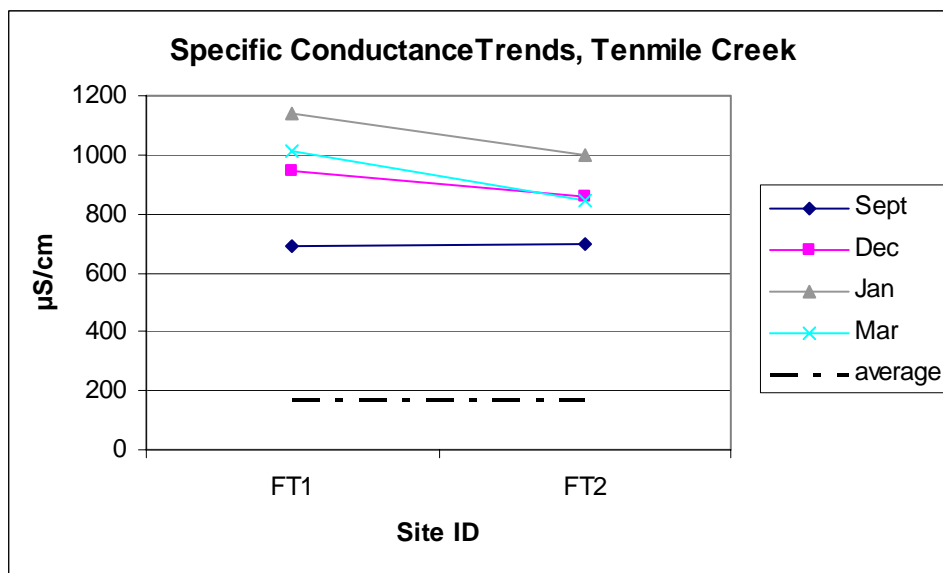
Three months of Upstream to Downstream pH Trends Measured in the Blue River

Upstream to downstream trends in conductivity displayed no regular trends in the Pennsylvania Creek focus area (PC1 to PC2). In the Swan River focus area, however, increasing specific conductance was consistently observed between sites SR1 and SR3 (Figure E-29). In Tenmile Creek, measurements were generally constant from FT1 to FT2. However, these values were always much higher than those seen in the remainder of the study area (Figure E-30).



Note: Locations move downstream from left to right on the x-axis

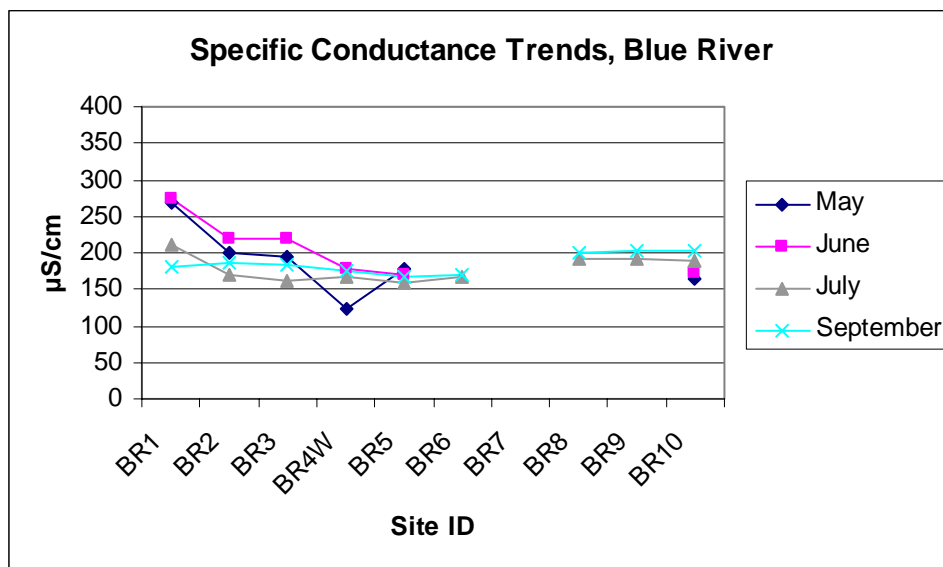
Figure E-29
Specific Conductance Values Measured in Swan River



Note: Locations move downstream from left to right on the x-axis

Figure E-30
Specific Conductance Measurements in Tenmile Creek Compared to the Study Average

With the exception of a decrease from sites BR1 to BR2, specific conductance in the Blue River was relatively constant through the entire study stretch (Figure E-31). In the early months (September through December 2001) of the study a peak was also seen at site BR7.



Note: Locations move downstream from left to right on the x-axis

Figure E-31
Limited Months of Blue River Specific Conductance Data

Upstream to downstream DO trends in both Pennsylvania Creek and Swan River tended to increase moving downstream. In Tenmile Creek, slight decreases between FT1 and FT2 were observed. These decreases were, however, less than 0.5 mg/L in all but one sample month indicating that DO was nearly constant between the two sites. In the Blue River, DO decreases were regularly observed between sites BR3 and BR4 (Figure E-32). In some months decreases also occurred between BR4 and BR5. Note that the minimum DO measurements in the Blue River tended to fall at site BR8. For potential causes of these and any of the other trends discussed in this section refer to the Discussion of Trends and Assessment of Impact section.

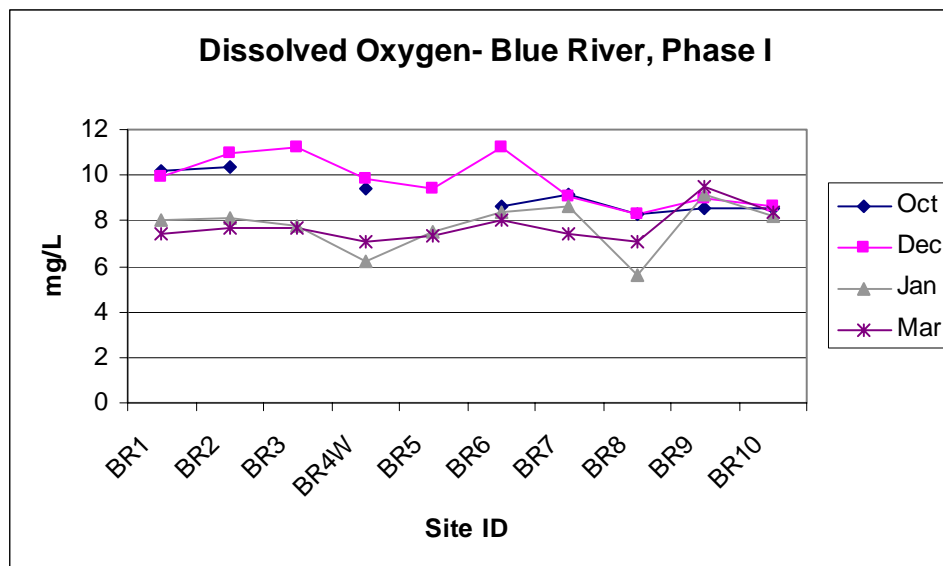


Figure E-32
DO Trends in the Blue River for Select Months

Nutrients

Nutrients in this study include several species of nitrogen and phosphorous. As mentioned, they are particularly important in this study as they can be indicators of wastewater input. For the purposes of this chapter, trends of nutrients will be presented in two sections, one each for nitrogen and phosphorous.

The following nitrogen species were measured during the entirety of this study:

- Ammonia
- Nitrate
- Total nitrogen

During Phase II, nitrogen parameters were expanded to include organic nitrogen and nitrite. Certain nitrogen species (ammonia and nitrite) were found to be below the detection limit in all samples analyzed. These species will not be discussed beyond this point. In Phase I, total nitrogen measurements were also consistently below the detection limit. In Phase II, the total nitrogen parameter was not obtained through analysis but through the addition of the analyses that make up total nitrogen (the total of ammonia, organic nitrogen, nitrate, and nitrite). Of the forms of nitrogen that comprise total nitrogen, two (ammonia and nitrite) have already been stated to be below the detection limit in all cases. This fact indicates that the majority of nitrogen found in this study was in the forms of organic nitrogen and nitrate. Therefore, rather than discuss total nitrogen, these two forms will be discussed individually.

The order of discussion will be as follows:

1. Seasonal nitrate trends in all streams during Phase I and, where possible, Phase II
2. Upstream to downstream trends of nitrate in Tenmile Creek and Swan River focus areas
3. Upstream to downstream trends of both nitrate and organic nitrogen in Pennsylvania Creek and the Blue River

Seasonal variation in organic nitrogen will not be discussed, as there are not enough months of data present.

Nitrate levels in all three focus areas were studied during Phase I. When possible, mass flow rates were calculated for these focus areas. This was not feasible in the Swan River and Pennsylvania Creek focus areas due to lack of flow data during these months; however, concentrations were measured. In the Swan River, even concentration data are too few to discuss seasonal trend; trends in space will be addressed in this section. Seasonal fluctuations in nitrate levels in Pennsylvania Creek were apparent. Nitrate concentrations decreased from mid-fall to early winter and increased slightly from December to January. After January, concentrations decreased until September (Figure E-33). In Tenmile Creek seasonal nitrate trends were studied using mass flow rates because flow values were available for all months. These mass flow rates decreased from September to November, increased slightly from November to January, and displayed a much larger jump from January to February, followed by a decrease from February to March (Figure E-34).

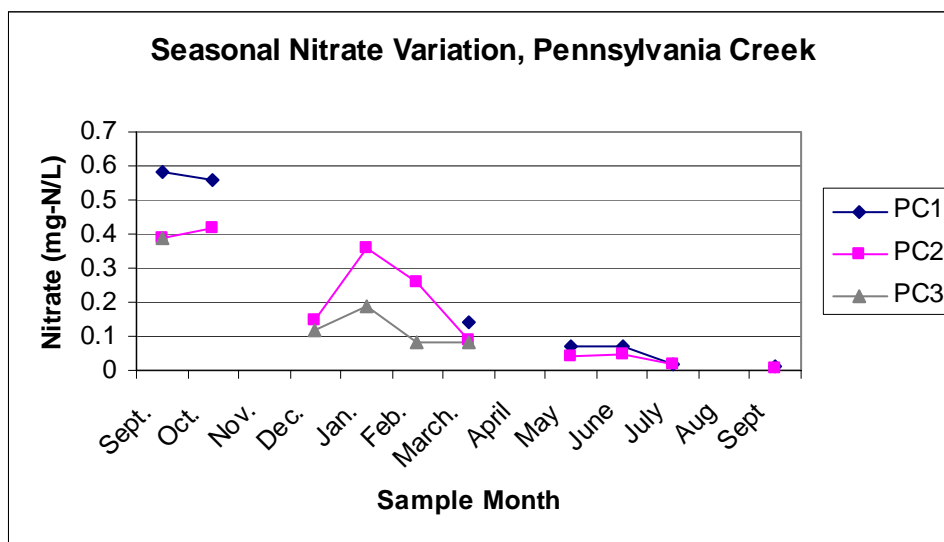


Figure E-33
Seasonal Variations in Nitrate Concentrations Measured in Pennsylvania Creek

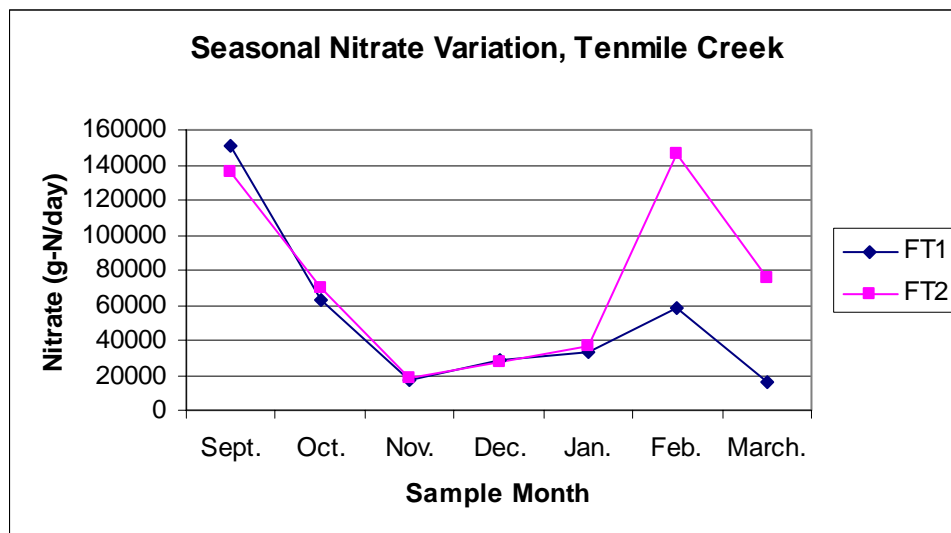


Figure E-34
Nitrate Loading in Tenmile Creek Sites as Measured During Phase I Sampling

There were a variety of important seasonal variations in nitrate loading that were observed in the Blue River. The easiest approach is to split the trends into those observed in the upstream sites, BR1 through BR6, and those observed in the downstream sites BR7 through BR10. In the upstream sites increases in nitrate mass loading were seen from October to November, followed by decreases from November to December. From then until March, levels stayed low. From March to May mass flow rates increased, after which they decreased until the end of sampling in September 2002 (Figure E-35).

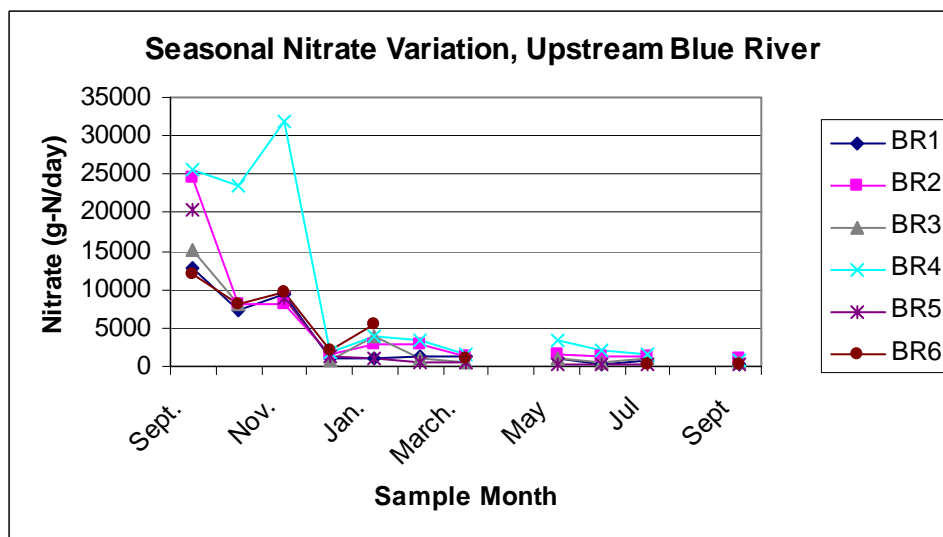


Figure E-35
Seasonal Nitrate Trends in BR1 Through BR6 for the Entire Study Period

Seasonal trends in the downstream sites varied from what was just presented for the upstream sites. The first difference is that there is no increase in mass flow in the fall. Instead, decreases were observed from September until December. After this trends varied, but mass flow remained low through March. By May, mass flow had increased in the one downstream site that was monitored that month: BR10 (Figure E-36). Since increases also occurred by May in the downstream sites and BR10, similar patterns likely were seen at other sites.

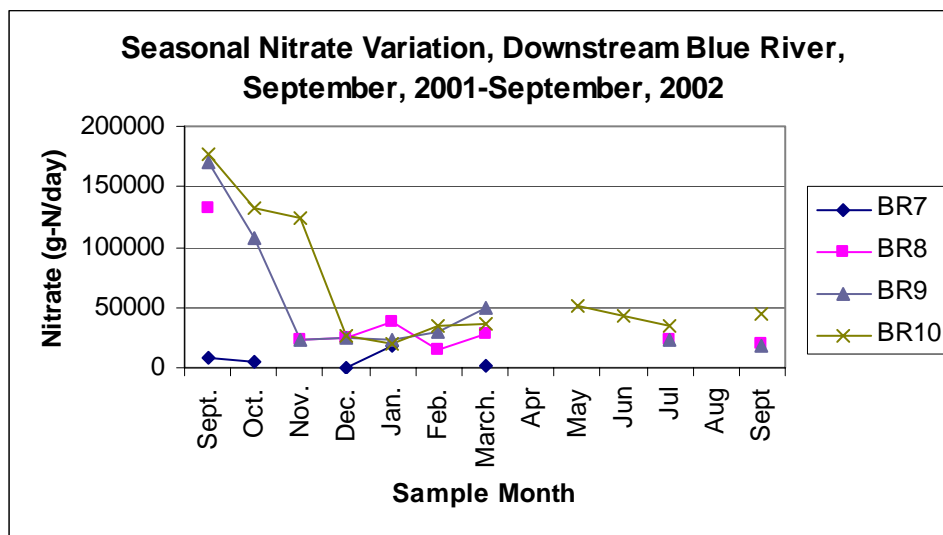
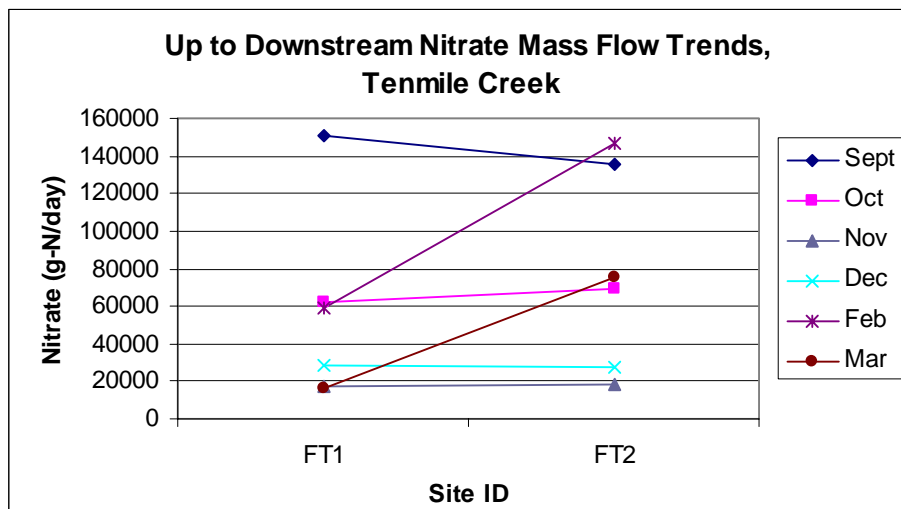


Figure E-36
Seasonal Nitrate Mass Flow Rate Trends in BR7 Through BR10 for the Entire Study Period

As mentioned previously, all Swan River nitrate trends must be discussed with regards to concentration values and not mass flow rates because of the low numbers of flow values available for the area. Upstream to downstream concentration trends in the Swan River were relatively constant, varying less than 0.05 mgN/L.

In Tenmile Creek, upstream to downstream trends were analyzed using mass flow data. Trends here were found to be variable, sometimes increasing and sometimes decreasing from FT1 to FT2 (Figure E-37). One important thing to note is that mass flow from Tenmile Creek into Dillon Reservoir is similar in amount to that of the Blue River. In Tenmile Creek, nitrate mass flow ranged from approximately 16,000 to 151,000 g-N/day. In the Blue River this range was 20,000–178,000 g N/day.

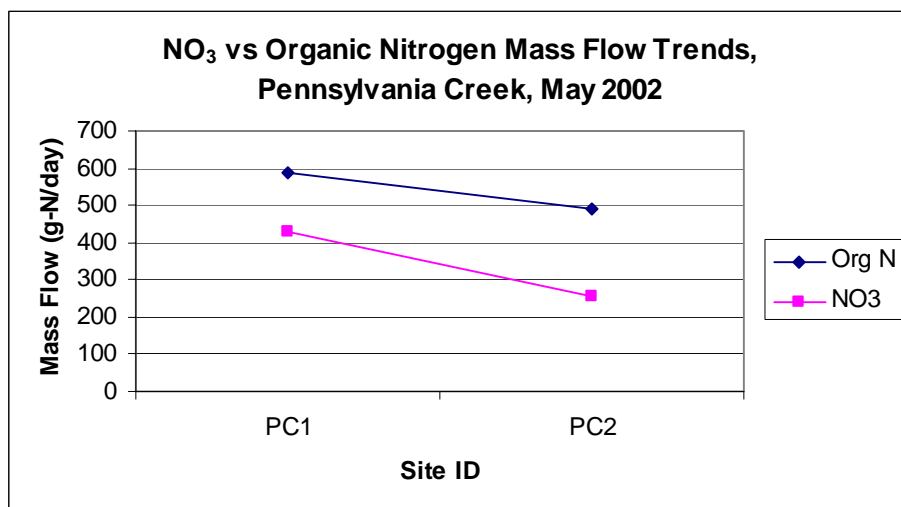
In Pennsylvania Creek, Phase I nitrate concentrations decreased from PC1 to PC2 during all months. Mass flows were not available for Phase I in this focus area because, as mentioned, there were not enough flow data. Phase II nitrate trends from PC1 to PC2 are best presented alongside organic nitrogen data because in most cases the Discussion of Trends and Assessment of Impact section will present potential causes of nitrate and organic nitrogen together.



Note: Locations move downstream from left to right on the x-axis

Figure E-37
Nitrate Mass Flow Rate Trends Observed Between Sites FT1 and FT2.

Organic nitrogen in this study was measured as a part of the Total Kjeldahl Nitrogen (TKN) analysis. TKN analysis measures ammonia nitrogen plus organic nitrogen. A separate analysis was conducted in this study to measure ammonia only. As mentioned, all ammonia results were found to be below the detection limit. Therefore, TKN measurements in this study consist primarily of organic nitrogen and will be referred to as such for the remainder of this appendix. During Phase II, mass flow rates of both organic nitrogen and nitrate in Phase II decreased from PC1 to PC2 in all cases except one. In June, organic nitrogen only demonstrated an increasing trend. Figure E-38 is an example of the typical pattern seen in this area.

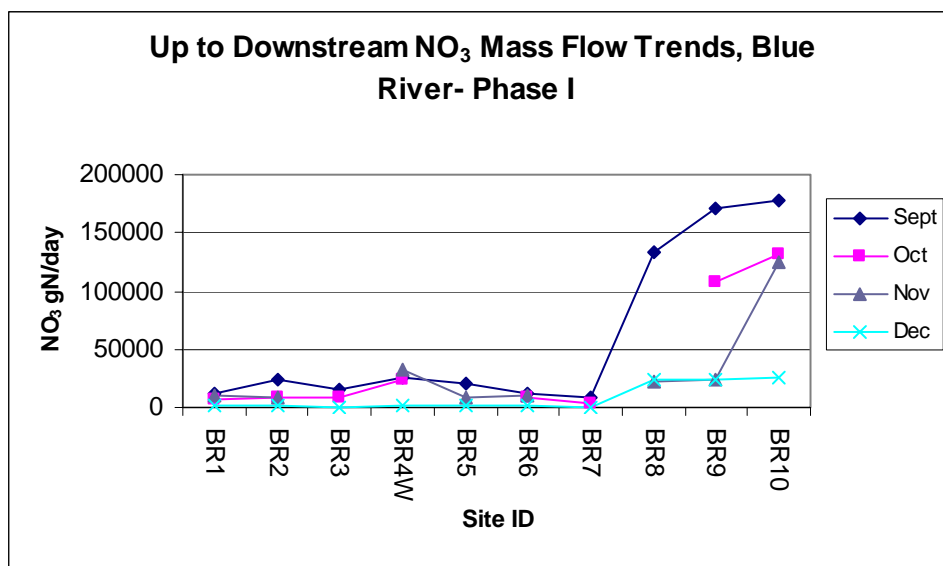


Note: Locations move downstream from left to right on the x-axis

Figure E-38
Nitrate and Organic Mass Flow Trends Typical of Pennsylvania Creek

In the Blue River looking at nitrate and organic nitrogen loading trends together is again useful. However, before doing so, nitrate data from Phase I will be briefly presented as there is no coinciding organic nitrogen data. Nitrate mass flow in the Blue River displays a first look at trends that will be repeated in both Phase I and Phase II data for nitrogen as well as other parameters and that will be a large part of the focus of the Discussion of Trends and Assessment of Impact section.

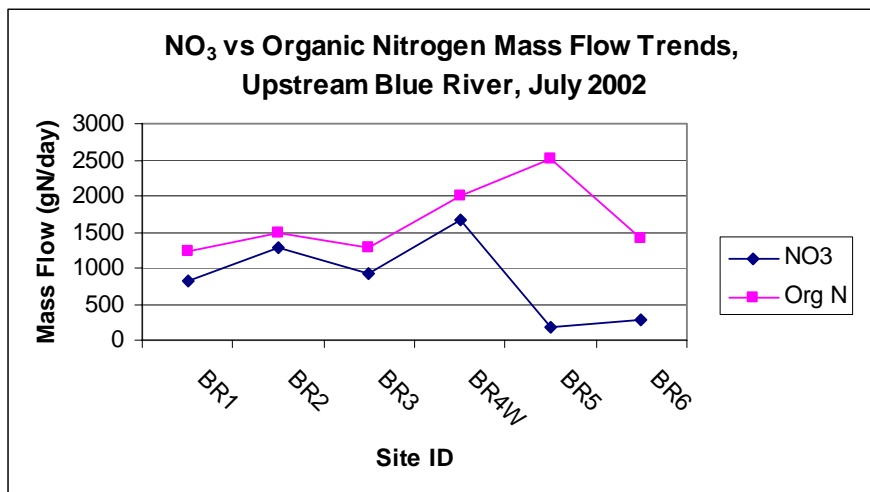
From BR1 to BR2 mass flow rates tended to decrease, followed by an increase from BR2 to BR3 and an increase from BR3 to BR4. Nitrate between sites BR4 to BR5 generally decreased. Beginning at site BR8, large increases were observed in mass flow of nitrate. In most cases, this trend lasted through site BR9 and in some cases it lasted through BR10 (Figure E-39).



Note: Locations move downstream from left to right on the x-axis

Figure E-39
Select Months of Phase I Nitrate Mass Flow Trends in the Blue River

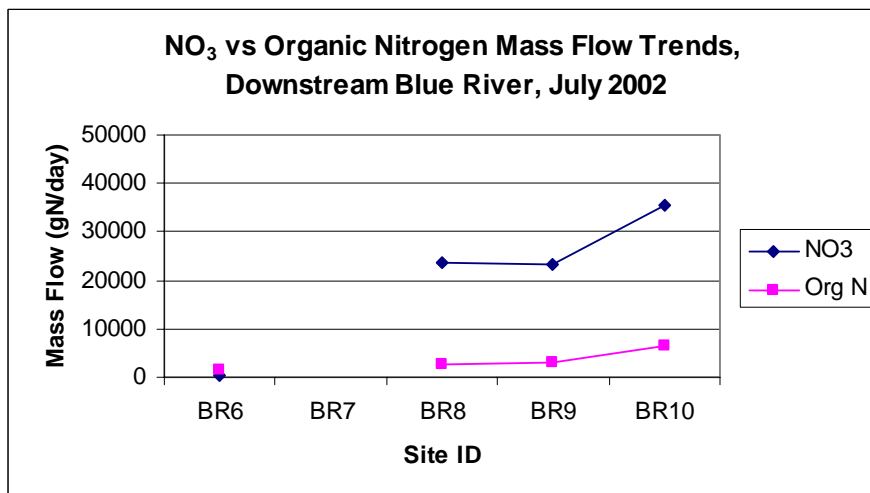
Phase II organic nitrogen and nitrate data in the Blue River display trends such as those just discussed for Phase I. Looking at upstream and downstream sites separately is useful. In the upstream sites (BR1 through BR6), increases from BR1 to BR2, decreases from BR2 to BR3, and increases from BR3 to BR4 were observed in both organic nitrogen and nitrate. However, from BR4 to BR5 trends in the two species vary. Between these sites, nitrogen tended to decrease and organic nitrogen tended to increase. Another interesting observation is that in this stretch of the stream, organic nitrogen was the dominant species. Figure E-40 shows one month of organic nitrogen and nitrate mass flow trends from these sites, which is similar to the trends observed in other months.



Note: Locations move downstream from left to right on the x-axis

Figure E-40
Upstream Organic Nitrogen and Nitrate Trends in the Blue River, July 2002

In the downstream sites (BR8 through BR10 for Phase II; BR7 was not monitored during this phase), trends were again similar to those observed during Phase I. Mass flow increases were seen beginning at site BR8. These increases were not as large in organic nitrogen as they were in nitrate. From BR8 to BR9 this rate remained nearly constant and from BR9 to BR10 slight increases were seen. This situation occurred in both nitrate and organic nitrogen. However, in these downstream sites nitrogen speciation is reversed from what was seen in the upstream sites, and nitrate becomes the dominant nitrogen species. Figure E-41 is an example of trends typically seen in this stretch of the river; BR6 is included in this example to give scale to the increases that were observed between sites BR6 and BR8.



Note: Locations move downstream from left to right on the x-axis

Figure E-41
Downstream Organic Nitrogen and Nitrate Trends in the Blue River, July 2002

During Phase I, the phosphorous species phosphate and total phosphorous were measured. In Phase II, total phosphorous, dissolved phosphate, and dissolved phosphorous were measured. Similar to the nitrogen species, certain phosphorous species were consistently found to be below the detection limit. During Phase I, total phosphorous was below the detection limit (0.046 mgP/L) in all cases. During Phase II, dissolved phosphate was below the detection limit (0.007 mgP/L) in all cases. Therefore, what will be described in this section are total phosphate trends in Phase I as well as the dissolved and total phosphorous results measured in Phase II. Trends of phosphorous in space and time will be presented. As with nitrogen, trends will continue to be discussed in terms of mass flow rates when possible.

As mentioned, phosphate is the only phosphorous species that was detected during Phase I. However, even this data is below the detection limit in many cases, which makes it difficult to determine the presence of any seasonal trends in the focus areas or the downstream Blue River sites. Determination of seasonal trends was possible, however, in the upstream sites. These sites show that there were large decreases in phosphate mass flow from the fall to the winter months. After this, trends vary (Figure E-42).

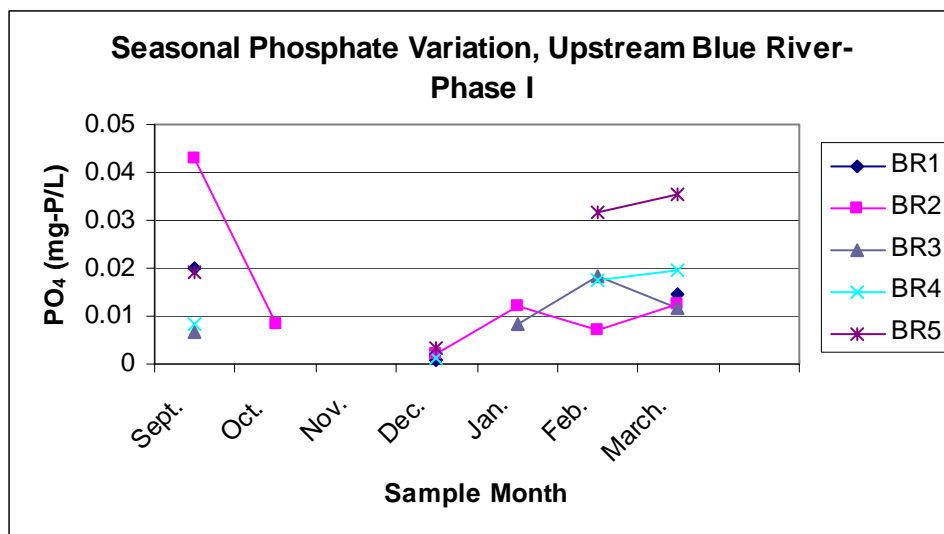
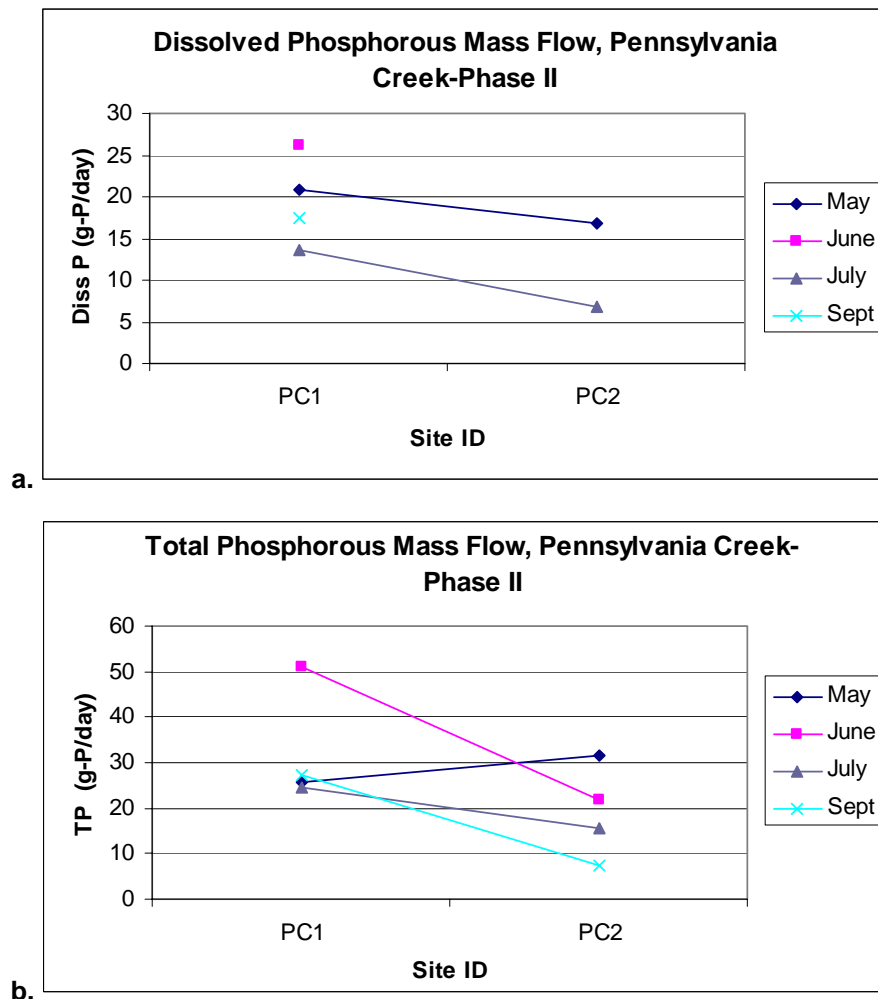


Figure E-42
Seasonal Phosphate Trends Observed in Sites BR1 Through BR5

Unfortunately, no other seasonal trends are available for phosphorous. All other Phase I phosphorous data were found to be below the detection limit. Data from Phase II cannot be compared with Phase I phosphate data because Phase II data are for total and dissolved phosphorous. Phase II data cannot stand alone to determine seasonal trends because there are only four months of data. Therefore, further discussion of phosphorous data will be limited to trends in space.

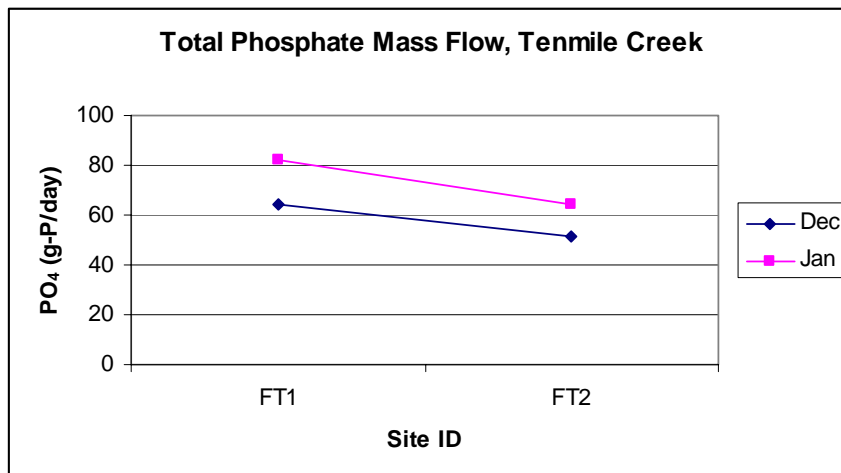
In Pennsylvania Creek, total phosphate concentrations were available for one month during Phase I, and during this month concentrations decreased from PC1 to PC2. During Phase II mass flow rates of both total and dissolved phosphorous also decreased from PC1 to PC2 as can be seen in Figure E-43.



Note: Locations move downstream from left to right on the x-axis

Figure E-43
Upstream to Downstream Mass Flow Trends for (a) Dissolved and (b) Total Phosphorous in Pennsylvania Creek, Phase II

Data from Swan River total phosphate analyses in Phase I were below the detection limit too frequently to determine upstream to downstream trend. Tenmile Creek data showed decreases between FT1 and FT2 in the two months of total phosphate data that were available (Figure E-44).

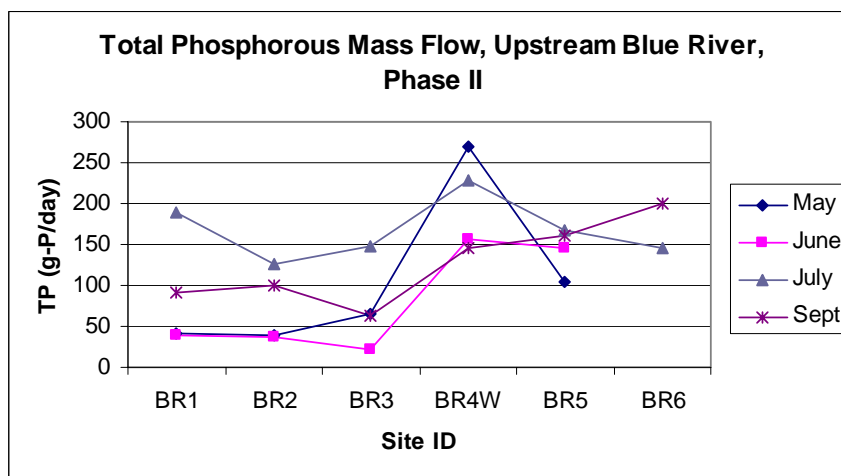


Note: Locations move downstream from left to right on the x-axis

Figure E-44

Total Phosphate Mass Flow Rate Trends Observed in Tenmile Creek, Phase I

In the upstream Blue River sites, trends seen in Phase I phosphate, along with those seen in Phase II total and dissolved phosphorous data, were similar to those seen in the nitrogen data. All three data sets showed trends of increases from BR3 to BR4 and decreases from BR4 to BR5. Total phosphorous trends are shown in Figure E-45 as an example. Unlike nitrogen, there is a lack of consistent trend from BR1 to BR3.

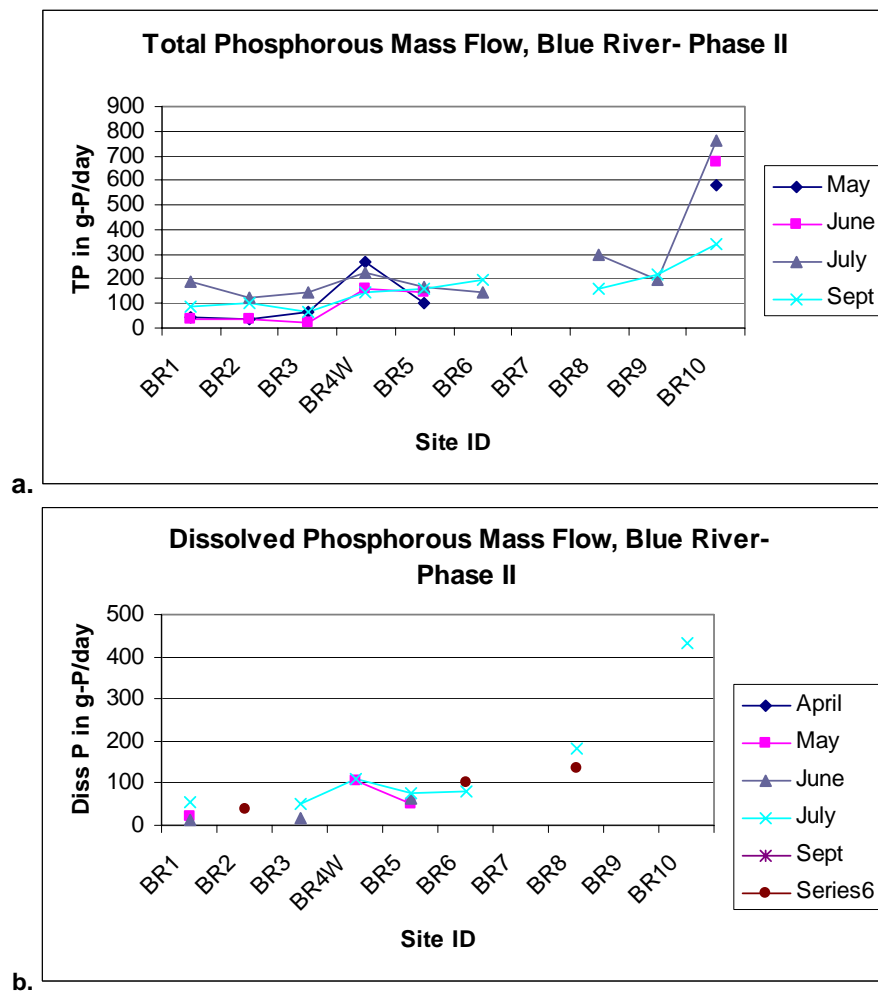


Note: Locations move downstream from left to right on the x-axis

Figure E-45

Upstream Total Phosphorous Trends in Space

Downstream Blue River trends in phosphorous were slightly different from those seen in nitrogen. Phase I total phosphate data is rather limited, but data that are present do not show the large downstream increases as seen in nitrogen. In Phase II, only two months (July and September) of data were collected in the downstream sites, with the exception of site BR10, which was monitored throughout the phase. In these two months, total phosphorous shows increases between BR6 and BR8 in one month and decreases in the other (Figure E-46a). Dissolved phosphorous shows slight increases between BR6 and BR8 in both months (Figure E-46b). Much larger increases were seen between BR8 or BR9 and BR10 in both Phases I and II data.



Note: Locations move downstream from left to right on the x-axis

Figure E-46

Total (a) and Dissolved (b) Phosphorous Mass Flow Trends Observed in the Blue River, Phase II

Supporting Parameters

Thus far this appendix has focused mainly on field parameters and nutrients to enable a water quality assessment. In the Discussion of Trends and Assessment of Impact section, when potential causes of these trends are discussed it will be useful to incorporate other parameters that may support or disprove some of the theories presented. Most of the parameters discussed in the following information were chosen because they would help to determine if domestic or municipal wastewaters are impacting the study area. Solids, oxygen demand, sulfur, chlorides (Metcalf & Eddy 2003) and boron (Flynn and Barber 2000) are all parameters that have the potential to help determine wastewater impact. As will be discussed in the Discussion of Trends and Assessment of Impact section, little or no impact related to development is thought to be present in the focus areas of this study. Therefore, trends in the supplemental parameters will be discussed for the Blue River only.

Seasonal variation of total solids in the Blue River was observed. Mass flow appears to have decreased from the fall through the winter and then increased by the May sampling trip (Figure E-47).

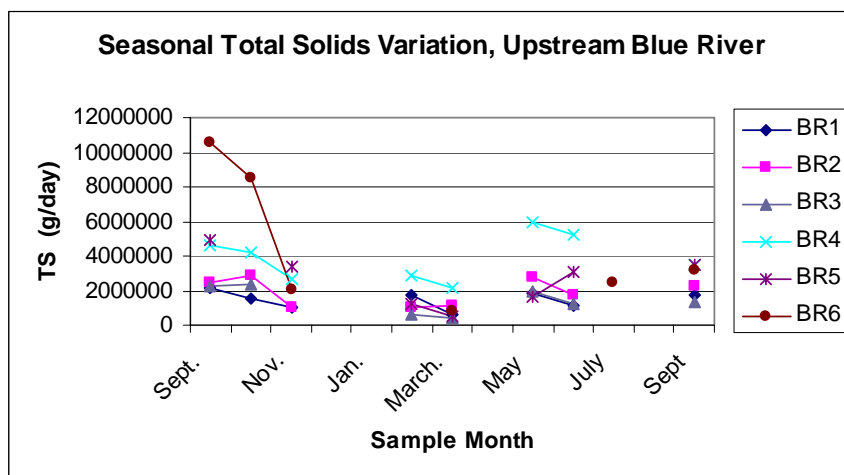
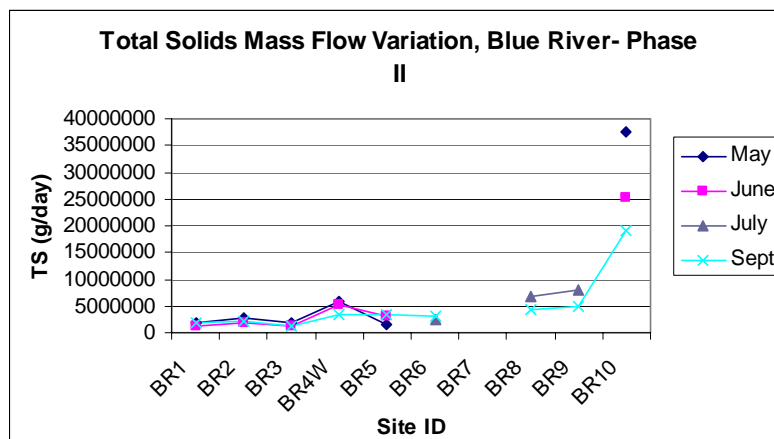


Figure E-47
Seasonal Total Solids Mass Flow Rate Trends Measured in the Blue River

Upstream to downstream trends in total solids measurements from both phases are similar to what was exhibited in the nutrients. To review what those trends are, there are slight increases from BR1 to BR2, decreases from BR2 to BR3, increases from BR3 to BR4 and decreases from BR4 to BR5. Figure E-48 shows solids data from Phase II as an example. In the upstream sites, mass flow trends show increases occurring between sites BR6 and BR10.

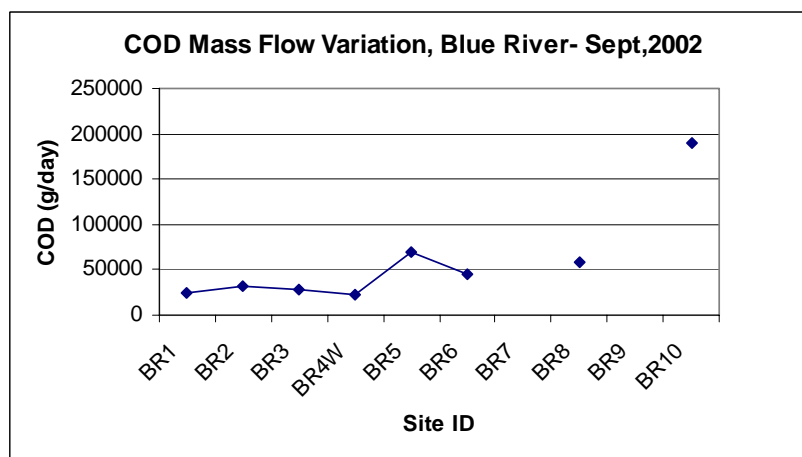


Note: Locations move downstream from left to right on the x-axis

Figure E-48
Upstream to Downstream Solids Mass Flow Measured in the Blue River

In this study, oxygen demand was measured in the form of COD as opposed to biological oxygen demand (BOD) for two main reasons. First, preliminary BOD tests on waters from the study area found BOD to be at or near zero. COD tends to be higher than BOD due to the fact that some things can be oxidized chemically that cannot be oxidized biologically (Metcalf & Eddy 2003). The second reason is that most BOD tests are run for five days, whereas a COD test can be completed in approximately three hours. Unfortunately, COD results were also found to be below the detection limit (1 mg/L) in the majority of samples collected during the study.

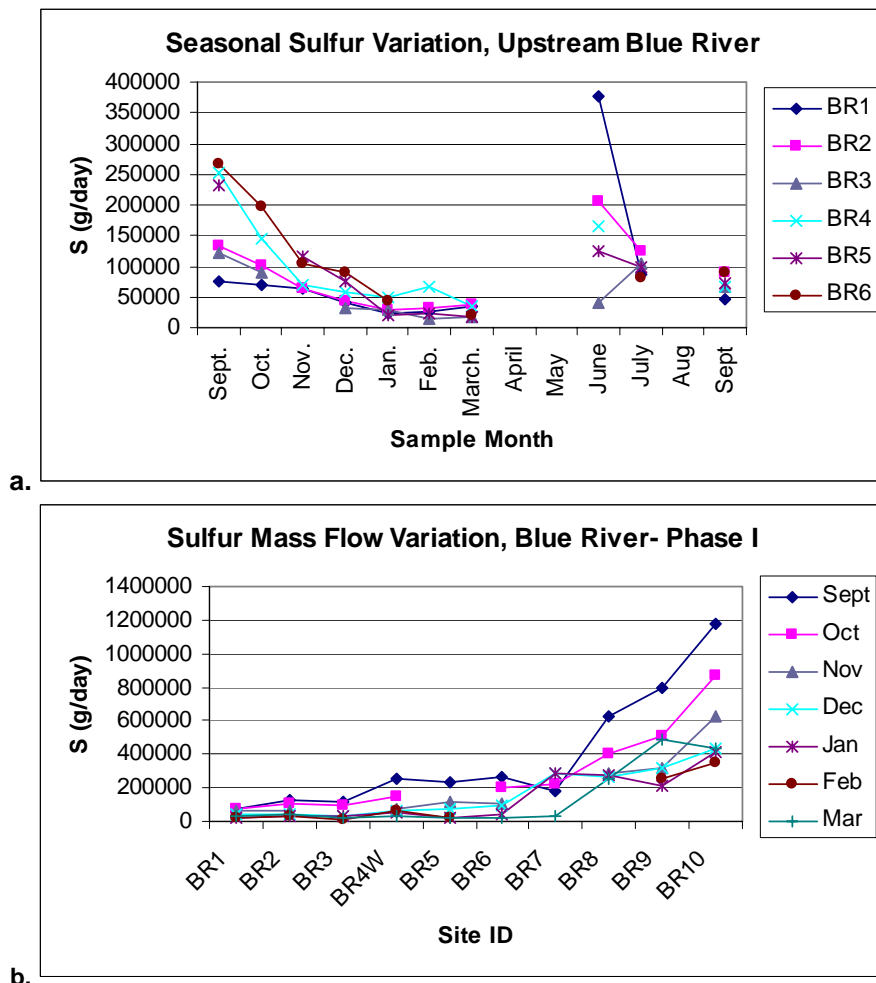
Making any conclusions about water quality impact with only one month of COD data would be difficult; however, the data are presented to help support conclusions based on other water quality data. COD data collected in September of 2002 are shown in Figure E-49. In the upstream sites, COD remains low until an increase between sites BR4 and BR5. From BR5 to BR8, COD appears to remain constant. COD increases dramatically from BR8 to BR10.



Note: Locations move downstream from left to right on the x-axis

Figure E-49
COD Mass Flow Trends for September 2002 in the Blue River

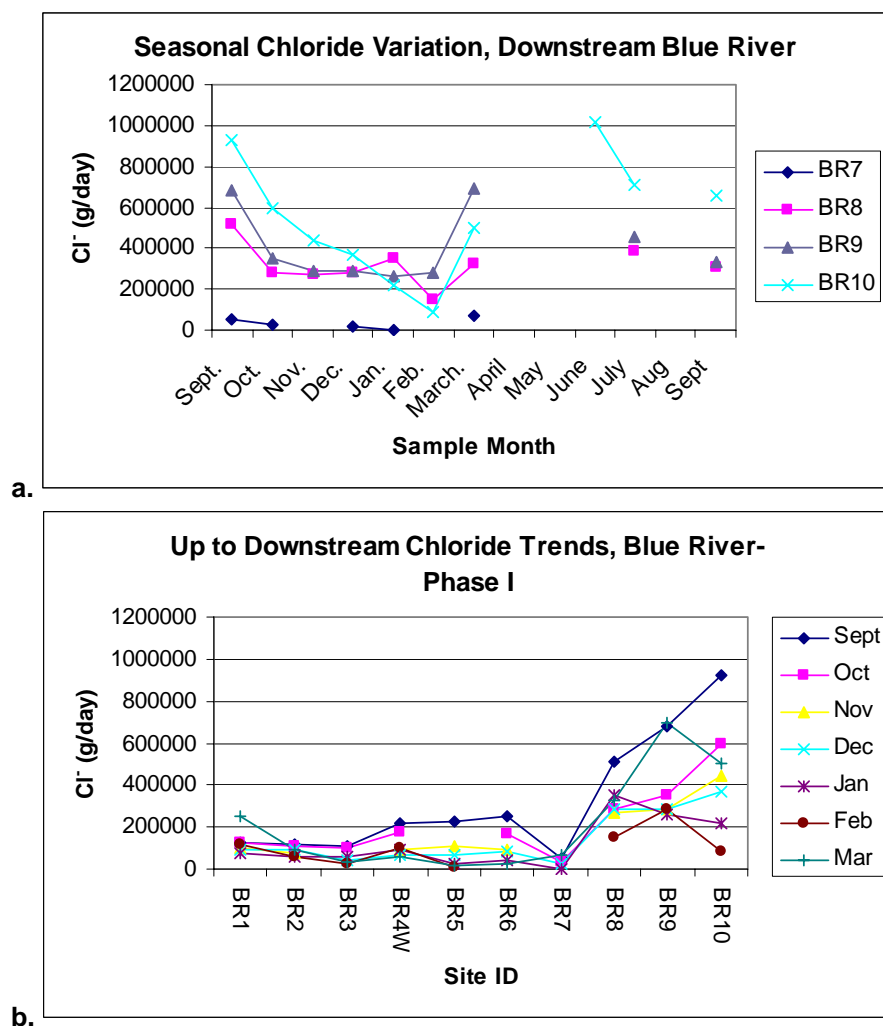
Seasonally, sulfur trends were similar to those observed in total solids. Mass loading rates decreased from September 2001 through the winter. In the May sampling trips, increases in sulfur loading were seen. This trend was the same for all sites along the Blue River. Figure E-50a uses the upstream Blue River sites as an example. In both phases, mass flow trends from upstream to downstream are also similar to those observed in other parameters. Increases were observed from BR3 to BR4; trends from BR1 to BR3 and BR4 to BR5 vary. In the upstream sites, most months displayed an increase beginning at site BR8 (Figure E-50b).



Note: Locations move downstream from left to right on the x-axis

Figure E-50
Sulfur Mass Flow Trends for the Blue River: (a) Seasonal and (b) Upstream to Downstream

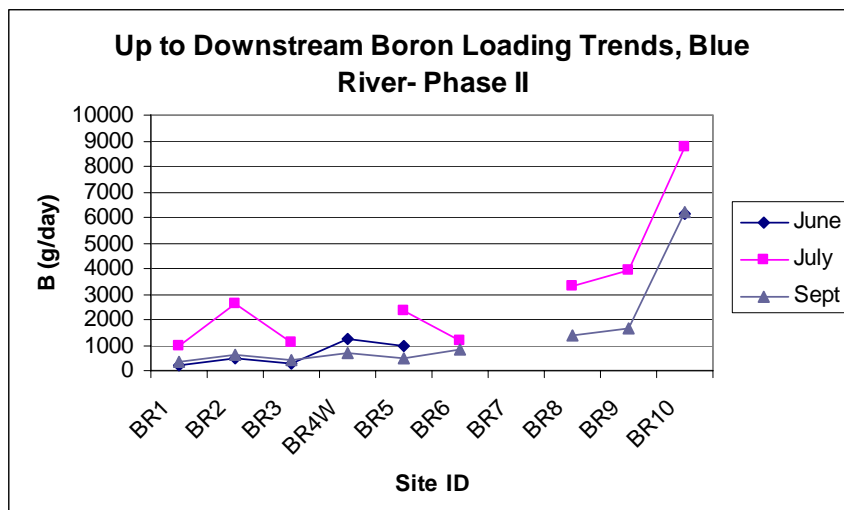
Seasonal fluctuations in mass flow rates of chlorides were again the same as those observed in total solids (and in sulfur). Figure E-51a uses a limited number of the Blue River sites to demonstrate that chloride mass flows decreased from the fall to the winter and began to increase in spring. Chloride appears to have peaked some time during the summer (which month is not known due to missing data points) and then began to decline through the end of the study. Figure E-51b shows chloride mass flow data from upstream to downstream in Phase I to show that again trends are similar to what has been observed in other parameters. Chloride increases were regularly observed between sites BR3 and BR4. Mass flow trends then vary some from BR4 to BR6, but in most months decrease from BR6 to BR7. Following site BR7, chloride mass flows begin a sharp increase. Trends from BR9 to BR10 vary, but seem to continue to increase in the majority of months.



Note: Locations move downstream from left to right on the x-axis

Figure E-51
Chloride Mass Flow Trends for the Blue River: (a) Seasonal and (b) Upstream to Downstream

Because of the number of months that boron data is missing, it is not possible to discuss seasonal trends in boron. However, upstream to downstream trends can be observed. In the upstream sites along the Blue River, mass flow trends in boron again display an increase between sites BR3 and BR4. The increase in the upstream sites near BR 8 is also present. Figure E-52 presents the Phase II boron data as an example.



Note: Locations move downstream from left to right on the x-axis

Figure E-52
Boron Mass Flow Trends for the Blue River

Comparison to Criteria and Standards

Another means of evaluating water quality is through comparison of monitoring results to water quality standards. The state of Colorado has standards for various surface water constituents. Two sets of state standards were found that contained regulations potentially applicable to this study: Colorado Regulation No. 31 and Colorado Regulation No. 33. Regulation No. 31 is a set of basic water quality standards and methods for surface waters in Colorado. Regulation No. 33 is specific to the upper Colorado River basin, of which the Dillon Reservoir watershed is a part.

Standards in this document were specific to certain reaches of streams, and in some cases provided equations that enabled them to be site specific. When possible, site-specific standards were used preferentially followed by stream- or reach-specific standards. There were no parameters measured in this study for which a statewide standard could be applied. In instances where no site or stream specific standard could be found, the state standard usually applied to total recoverable metals, which were not measured as part of this study.

For any given parameter there might be several numerical limits. Oftentimes these are acute (one-day) and chronic (30-day) values. For example, iron has both an acute and a chronic standard for each site in this study. In order to know if a parameter meets the chronic standard, water quality must be monitored more frequently than once per month. Therefore, only acute values were used as a basis of comparison in this study.

Acute values are those that are not to be exceeded more than once in 30 days, which is important to note. In this study, measurements were made roughly once per month. If an acute value was exceeded during this one measurement, this fact will be denoted in this section; however, one-time measurements higher than the acute values cannot be considered a violation of the standard. The information presented here should be used only to gain a general impression of water quality in the study area as compared to standards, not to gauge magnitude or number of violations.

Table E-12 is a summary of parameters monitored in this study for which an applicable standard was either found or calculated and the number of times that standard was exceeded. A complete list of standards can be found in Appendix C of Guelfo (2003). This appendix also includes a more detailed explanation of how calculated standards were determined. As can be seen in the table, there were a total of 52 instances where one of the standards was exceeded.

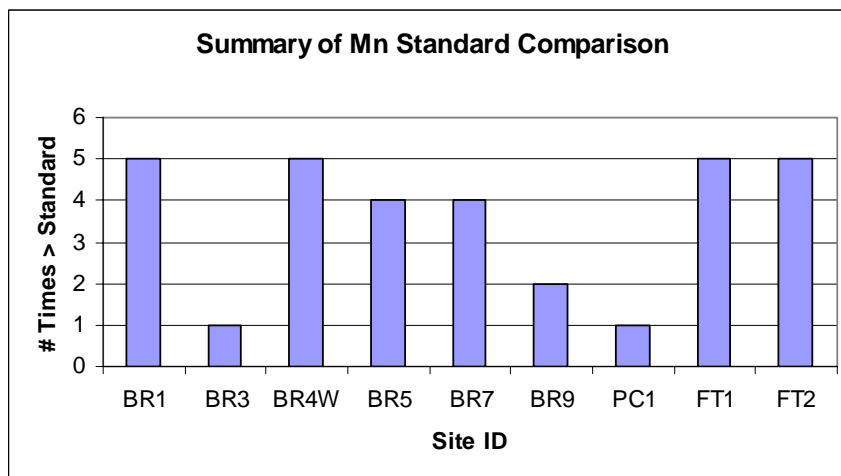
Table E-12
Summary of Results of Water Quality Monitoring Results to Colorado Standards

Parameter	No. of Times Exceeded	Parameter	No. of Times Exceeded
Dissolved Oxygen (DO)	1	Silver (Ag)	0
pH	0	Cadmium (Cd)	3
Fecal Coliform	0	Copper (Cu)	0
Ammonia (NH ₃)	0	Iron (Fe)	0
Boron (B)	0	Manganese (Mn)	32
Nitrite (NO ₂)	0	Lead (Pb)	2
Nitrate (NO ₃)	0	Nickel (Ni)	0
Chloride (Cl)	0	Selenium (Se)	1
Sulfate (SO ₄)	8	Zinc (Zn)	10

Thirty-two of the instances where a standard was exceeded were with respect to the manganese (Mn) standard. In the Blue River, the standard for manganese is 50 µg/L. In Tenmile Creek the standard is higher at 180 µg/L. The graph in Figure E-53 shows which sites exceed the standard along with the number of times it was exceeded at each site.

The majority of occurrences in Figure E-53 occurred in the Blue River and Tenmile Creek. The sites along Tenmile Creek were not monitored in Phase II, so not as many samples were taken for those sites during the study. This factor is important to consider because it effectively decreases the number of “chances” these sites had to exceed the standard in comparison to most Blue River sites and the Pennsylvania Creek sites. Other exceedances likely would have been seen if Tenmile Creek had been monitored in Phase II.

Manganese (Mn) is a metal that at certain levels is crucial to the health of aquatic environments, but at higher concentrations can be toxic to humans and aquatic life (Chapman 1996). Instances where manganese is exceeded could be indicative of a problem; however, these concentrations were measured during a low flow year, which is important to keep in mind. During years of higher flow it is possible that no manganese concentrations higher than the standard would be observed.



Note: Locations move downstream from left to right on the x-axis

Figure E-53
Sites that Exceeded the Manganese Standard and the Number of Times It Was Exceeded

Zinc (Zn) was also found in concentrations higher than the standard in 10 measurements. All 10 measurements were in waters from the Blue River. They were limited to sites BR7 to BR10, indicating that the source of zinc may be situated downstream of Breckenridge. As with manganese, zinc is crucial to the health of aquatic life, but can be toxic at higher levels (Chapman 1996). The Blue River standards are aimed at preserving water quality that will protect cold-water aquatic life. If zinc concentrations persist at these levels in years with normal flow, it may be necessary to consider remedial actions.

Another parameter in which concentrations higher than the standard were observed a number of times was sulfate in Tenmile Creek. These sulfate levels are not surprising considering Piper diagrams shown in the Results section revealed this creek to be sulfate dominated. This sulfate likely originates in mine drainages that are released near the headwaters of Tenmile Creek. Sulfate is not harmful, but can lend an unpleasant taste to water (Chapman 1996).

Outside of the standards already discussed there were some isolated occurrences where other standards were exceeded. These can be found in Table E-12. These were thought to be likely isolated instances that do not represent potential problems. Overall comparison of stream water quality data to available standards seems to indicate that water quality in the study area is relatively high and that the only potential problem areas are with respect to manganese, zinc, and sulfate.

Discussion of Trends and Assessment of Impact

Thus far in this section, seasonal and upstream to downstream trends of parameters in both the focus areas and along the Blue River have been presented. However, no attempt has been made at explaining these trends. This section will revisit the parameters in the same order as presented in Trends in Space and Time section in an attempt to present what could be the causes of these trends. The final portion of this section will summarize impacted areas.

Flow

Seasonal variations in flow were of the type to be expected in mountain streams. The decrease in flow from fall to winter is a natural result of the onset of colder temperatures causing landscape water to be frozen and stationary for the season. Spring increases in flow are due to the annual thaw. This thaw is usually over by summer when flows begin to decline once more. Note that flows in September 2002 were, on average, 47% lower than those measured in September 2001. This difference is to be expected due to the drought that Colorado experienced in 2002.

The Blue River proved to be a gaining stream with the exception of a small stretch through the town of Breckenridge (BR6 to BR8) (see Figure E-24), probably due to the effects of past mining activity on the area. Dredge boat mining left large stretches of alluvial deposits in the river plain that eliminated the regular stream channel. As a result, flows often move downstream beneath the deposits, especially during times of low flow. In periods of higher flow, the deposits become saturated and some of the flow moves as surface water. Usually flow returns to the surface at the beginning of spring runoff; however, this year is an exception due to drought conditions.

Field Parameters

Trends in water temperature are directly related to the season. Temperatures are expected to be colder during the winter and warmer during the summer.

Seasonal specific conductance trends appear related to flow. Specific conductance is lower in waters that originate in snowmelt than in base-flow contributors such as groundwater. In the winter when most flow is contributed by base flow, specific conductance will be higher. In the spring when snowmelt starts to dominate the flow in streams, specific conductance is lower. Thus, specific conductance trends are usually opposite that of flow (Figure E-54).

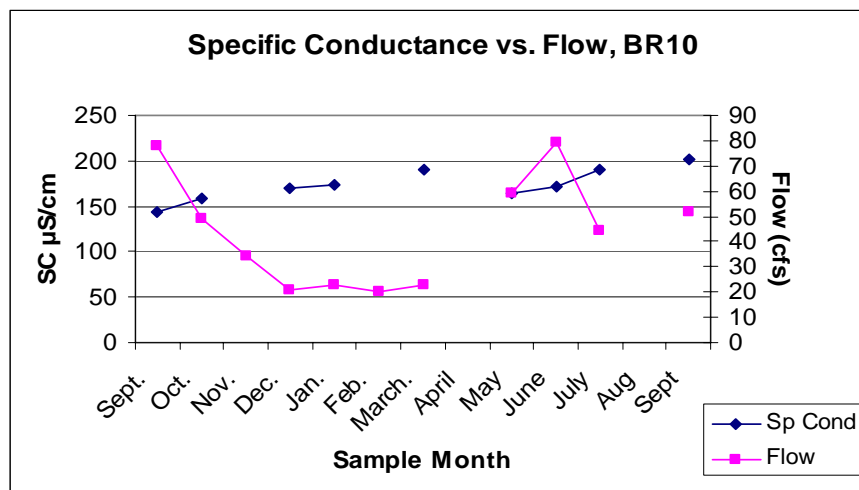


Figure E-54
Specific Conductance Values Plotted Versus Flow for Site BR10

DO measurements increased during the fall and then decreased in the winter months (see Figure E-26). A slight increase began in spring months. Increased ice cover from December to March, caused by dropping temperatures is thought to have limited exchange of oxygen with the atmosphere, causing DO values to drop. When streams began to thaw in the early spring, DO began to increase again. Therefore, DO was indirectly dependant on water temperature.

Upstream to downstream trends of field parameters appear to be due to a mix of natural and developmentally related causes. As mentioned, temperature trends varied with the exception of a warming trend from BR7 to BR9 (seen in Figure E-27). This trend could possibly be due to the input of effluent from a wastewater treatment plant (WWTP) in Breckenridge, situated in between the two sites (see Figure E-21). In order to better determine whether or not the WWTP could be the cause of this temperature trend, mass balance calculations were conducted using the following equation:

$$Q_E T_E + Q_S T_S = Q_O T_O$$

Equation E-4

where Q_E and T_E are flow and temperature of the WWTP effluent (obtained from plant records), Q_S and T_S are the flow and temperature of the stream at site BR6 just upstream of the WWTP input (obtained from study data), and Q_O and T_O are the flow and temperature of the Blue River just upstream of the WWTP input. T_O was the variable being solved for.

Computed values of T_O were then compared to measured water temperature at site BR8 just downstream of the WWTP. If computed values were greater than or equal to the measured values, that was taken as an indication that the WWTP could be responsible for the observed increase. Computed and measured values are shown side-by-side in Table E-13. As can be seen by the table, it is possible that the WWTP is fully responsible for the observed increase in some months and partially responsible in others. Note that site BR8 is not immediately downstream of the WWTP outfall and in between the outfall some further warming may occur due to some ponding that occurs in the river between the two points.

Table E-13**Computed Versus Measured Temperature Values for the Blue River Downstream of the Iowa Hill WWTP**

Computed Temp Value °C	Measured Temp Value °C	Could WWTP have caused increase?
3.70	3.9	Partially
2.51	4.51	Partially
4.75	1.36	Yes
6.76	4.66	Yes

The cause of the increasing pH trend seen in Pennsylvania Creek is not known, and pH values in the other two focus areas were described as constant. pH trends in the Blue River may be, in part, developmentally related. Domestic wastewaters tend to have a higher pH than surface waters and could cause an increase in pH when added to receiving waters. Domestic wastewater input from the WWTP could have caused the pH increase beginning at site BR7 (see Figure E-26). Other pH trends in the Blue River are thought to be due to natural causes. The decrease from BR3 to BR5 could be attributed to dilution effects of the input of Pennsylvania Creek between these two sites. Finally, the pH decrease seen between BR9 and BR10 may be due to the input of Swan River.

Conductivity trends in Swan River may be developmentally related. There is a subdivision, Ten Mile Vista, as well as a golf course, situated along the Swan River between the upstream and downstream sites (see Figure E-21). There has been new construction in this area during the study period, which could result in increasing the amounts of dissolved constituents in the water thereby increasing specific conductance. The elevated specific conductance levels in Tenmile creek (see Figure E-30) are likely mining related. The headwaters of Tenmile Creek are situated near heavily mined lands close to Leadville, CO. This mine drainage has a much higher specific conductance than other waters due to high amounts of dissolved constituents, and likely causes the increased levels in Tenmile Creek. No regular trend, and thus no potential causes, is present in the Pennsylvania Creek focus area.

In the Blue River the decrease in specific conductance in the upstream sites (see Figure E-31) is likely due to dilution that occurs with the input of pristine stream waters from tributaries situated between the two sites (McCullough Gulch) (see Figure E-20). The peak observed at BR7 was likely caused by construction of a kayak park that was being completed in the river bed upstream of the site.

Pennsylvania Creek and Swan River DO trends exhibited increasing DO, and Tenmile Creek was nearly constant. DO in the Blue River in the BR3 to BR4 reach was decreasing and could have been caused by use of oxygen in the decay of organic matter present in the wetlands. The decreases mentioned between BR4 and BR5 may be related to the presence of a lake in the area. This lake, Goose Pasture Tarn, is situated in between these sites (see Figure E-21) and DO levels in the lake are likely lower since calmer waters naturally have less oxygen exchange with the atmosphere. Like temperature and pH trends, the lower DO measurements observed at site BR8 may be caused by the WWTP input mentioned previously.

From the field parameters analyzed in this study potential areas of impact begin to become evident. The most prominent of these areas is the Blue River downstream of the Breckenridge wastewater treatment facility. There is some evidence that the Blue River near the Pennsylvania Creek focus area (near sites BR3 and BR4) is impacted as well. As trends of other parameters (nutrients) are discussed, field parameters will come back into play to help support further conclusions regarding areas that do and do not show evidence of water quality impact.

Nutrients

Due to the natural cycling of nutrients in the environment, some nutrient trends in the study area are highly likely to be due to natural causes. On the other hand, elevated nutrient levels are one of the key indicators of developmental impact. In this way, causes of nutrient trends can be difficult to describe and pinpoint. The following information in this section will describe in detail potential causes of nutrient trends in this study area.

Seasonal trends could only be assessed for the Pennsylvania Creek and Tenmile Creek focus areas. As mentioned, decreases in mass flow were observed in the fall months in both areas. The cause of this decrease is not known. The decreased mass flow is possibly directly related to a decrease in flow during this time. Winter increases were also seen in both areas. Again, no cause can be identified, but one possibility is that the increase is associated with an increase in winter population during ski season.

In the Blue River, especially in the upstream sites, seasonal trends are thought to be influenced by the natural cycling of nitrogen in nearby riparian wetlands. Potential mechanisms occurring in riparian zones were described in the Background section of this appendix. They will only be summarized here.

Sites BR1 through BR6 are situated near two riparian wetland zones (see Figure E-21). In these sites, a nitrate increase was observed from October to November (see Figure E-35). This increase is thought to be caused by a fall release of nitrogen from decaying plants in the wetlands. After such a release, nitrogen levels in riparian wetlands could be expected to remain low until the spring thaw allowed more decaying plants to release another pulse of nitrogen into the environment. In the upstream sites, nitrogen levels did remain low until the spring thaw, when they increased. This spring increase likely also has another cause—spring runoff, which increases flow and is often associated with large loading increases.

The spring increase observed in the Blue River sites was not very big, which is important to note. Mass flow rates increased in the spring but to levels approximately 93% lower than those seen just the previous fall (Figure E-55). This difference is likely because the drought Colorado experienced in 2002 did not bring the normal spring increase in flows. After the spring increase, nitrate loading in the Blue River began to decrease once again. This decrease could be due to a combination of causes. The first is the decreasing flows in the summer season. The second moves back to riparian processes. Increased nitrogen uptake often occurs during the growing season, causing decreased nitrogen levels.

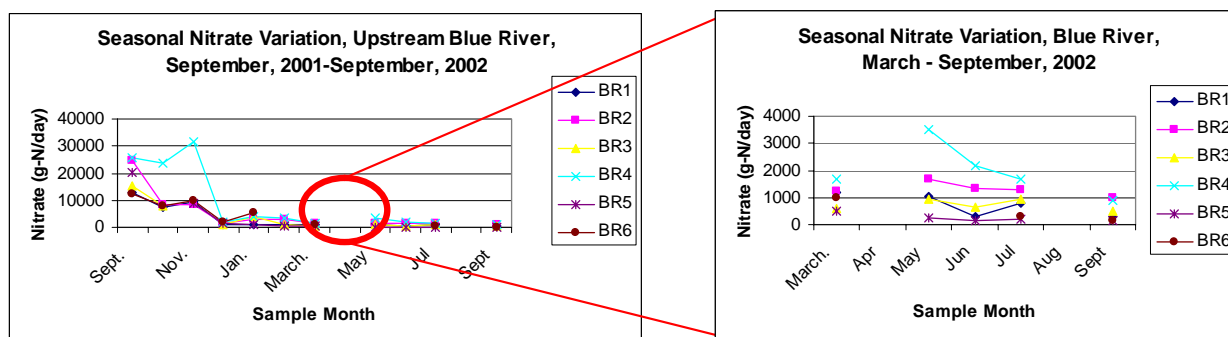


Figure E-55
Upstream Site Nitrate Levels in the Blue River From the Entire Study Period and From Spring Through Summer Only

In the upstream sites, no increases in nitrate mass flows were observed in the fall months, likely because these sites are not near a riparian zone. Spring loading increases were observed and are likely flow related as described previously. Similar to those observed in the upstream sites, these increases are not as large as might be expected during a normal flow year. As seen in the upstream sites, nitrogen levels began to decline through the summer months. This decline is likely due to flow decreases, but could be due in part to plant uptake, though this reach of the stream is not heavily vegetated.

Upstream to downstream trends of nitrate in the Swan River focus area were stated to be constant from SR1 to SR3. Trends were variable in the Tenmile Creek area and no potential causes are offered. That leaves only the Pennsylvania Creek focus area. When trends were presented, organic nitrogen and nitrogen trends were presented together. Trends in the two nitrogen species have the potential to be extremely closely linked due to the nature of the nitrogen cycle. In Pennsylvania Creek both nitrate and organic nitrogen trends were decreasing. This decrease could be due to plant uptake of nitrogen in riparian zones associated with this focus area.

Nitrate and organic nitrogen trends in the Blue River also proved to follow similar patterns from upstream to downstream. In the upstream sites, increases were observed in both species from BR1 to BR2 and BR3 to BR4. Note that organic nitrogen is the dominant nitrogen species in this stretch of the stream. Several factors may be responsible for these increases. With regards to both increases, natural causes may be responsible. As mentioned, the Blue River near these sites includes multiple riparian wetlands. Nitrogen cycling in the wetlands is thought to potentially produce nitrate and organic nitrogen increases in the following manner:

1. Nitrogen flowing into the wetlands may be taken up by vegetation
2. Vegetation could then die, releasing organic nitrogen
3. Released organic nitrogen would eventually be converted to nitrate in the process of nitrification

If these processes were happening concurrently in the area, seeing the described increases in both nitrate and organic nitrogen would be possible. This scenario may also support organic nitrogen as the dominant species during this stretch. Organic nitrogen is readily converted to nitrate in the environment. Though reaction times are not known, organic nitrogen likely would only be dominant if water samples were being taken close to the source. If this scenario were occurring, these sites would be close to the source of nitrogen present in the riparian wetlands.

The second potential cause of these trends is developmentally related and would likely only apply to the increases seen from BR3 to BR4. Beginning near site BR2, there are many homes situated near the Blue River. In this area, homes use OWS. If effluent from these systems were to reach groundwater and eventually flow into the Blue River, it could cause increases in nitrate. However, OWS effluent is not thought to be the cause of the observed increase in organic nitrogen. Most organic nitrogen in OWS effluent is converted to other forms before even leaving the common septic tank, and then ammonia is converted to nitrate in the soil. Pets and use of fertilizer could also be contributing nutrients to the river, which could potentially increase both nitrate and organic nitrogen.

A third potential cause of the observed increase between sites BR3 and BR4 is the input of Pennsylvania Creek. Mass flow rates measured near the mouth of Pennsylvania Creek at site PC2 should provide the information necessary to determine if that could be the sole cause of the increase. Comparison of mass flow rates measured at this site to increases seen between sites BR3 and BR4 showed that Pennsylvania Creek could not be solely responsible for the increases seen in either nitrate or organic nitrogen. Mass flows measured at site PC2 might have been responsible for only about 16% and 27% of the increases seen in nitrate and organic nitrogen, respectively.

The fourth and final scenario to consider is that a combination of the processes just described is causing the nitrate trends observed in these sites. Natural processes are entirely likely to be occurring in this portion of the study area that involve nutrient cycling and would impact nutrient trends. Pennsylvania Creek is also extremely likely to be partially responsible for trends seen between BR3 and BR4. However, developmentally related causes could possibly be present too.

Nitrate and organic nitrogen trends between sites BR4 and BR5 differed. Nitrate decreased while organic nitrogen increased. These two sites are located on the inlet and outlet sides of a small, man-made reservoir known as Goose Pasture Tarn (see Figure E-21). The wetlands between BR3 and BR4 are situated just upstream of this reservoir. Processes in Goose Pasture Tarn are thought to be the cause of the observed loading trends.

Nitrogen speciation reversed in the downstream sites, which is likely due to a combination of causes. First, previously generated organic nitrogen would be moving further away from the source at this point in the stream. The more time organic nitrogen is in the water, the more likely that enough time has passed for it to undergo nitrification.

Second, at this location in the stream, the river has passed through Breckenridge. That municipality has the potential to contribute nitrate in various ways, including discharge from the Iowa Hill WWTP situated in the area and urban runoff. To determine whether or not the WWTP could be responsible for the entire increase, comparisons were made between loading increases in the area (BR7 to BR8) and loading from the WWTP.

Permitted facilities such as the Iowa Hill facility must submit monthly reports to both the State of Colorado and the United States Environmental Protection Agency (US EPA) (CDPHE 2002a). These reports include mass flow information for various parameters (ammonia, temperature, fecal coliform bacteria, BOD, and phosphate), and also flow information. Results of these reports were obtained for the purpose of this study, but were found to have limited use. For example, the Iowa Hill WWTP facility is an advanced wastewater treatment facility and has a nitrification unit process (CDPHE 2002b). Therefore, the majority of the nitrogen loading from that facility is in the form of nitrate. Nitrate, however, is not monitored because the permitted release is concerned mainly with ammonia. Ammonia is monitored, but as this study found ammonia to be below the detection limit in all cases, this could not be used for comparison. To overcome this data gap, the outfall of the WWTP was monitored in February 2003.

Nitrate loading from the treatment facility to the Blue River was estimated in the following manner. In February 2003, a sample of the WWTP outfall was monitored. Analysis revealed nitrate concentrations of 11.6 mgN/L. Flow information from the WWTP is available for the first day of each month from September 2001 until June 2002. Each flow value was multiplied by the measured concentration to provide a mass flow estimate for the first day of each month. Sampling dates, however, did not tend to correspond with the first day of the month. So, first-day mass flow estimates of nitrate from the WWTP were compared to nitrate mass flow increases observed between sites BR7 and BR8 in the same month. So for example, the BR7 to BR8 increase in the month of September 2001 was compared to the estimate calculated for September 1, 2001. In most cases, observed nitrate mass flow increases were extremely close to the estimated mass flows from the WWTP (Table E-14). These calculations are believed to show that the WWTP could potentially be responsible for the entire nitrate loading increase seen in the adjacent stretch of the Blue River.

Table E-14
Estimated N Mass Flow From Iowa Hill WWTP Versus Nitrate Mass Flow Increases Seen in the Blue River

	WWTP NO3 Mass Flow gN/day	BR7-BR8 NO3 Increase gN/day
Sept, 2001	21500	123815
Nov, 2001	21300	23024
Dec, 2001	27500	23788
Jan, 2002	32400	19394
Feb, 2002	32400	14814
Mar, 2002	32600	25504

The only seasonal trend discussed with relation to phosphorous was phosphate trends seen in site BR1 through BR5 during Phase I. The trends were large decreases in mass flow from the fall to the winter months. These decreases were likely caused by a seasonal decrease in the flow rate.

No upstream to downstream phosphorous trends were available for Swan River, and trends were decreasing in both Pennsylvania Creek and Tenmile Creek. One potential cause of this decrease may be plant uptake, but this does not explain a phosphorous uptake during the winter. Other potential causes for the decrease are not known.

In the Blue River, phosphate from Phase I and total and dissolved phosphorous from Phase II all demonstrated increasing mass flow trends from BR3 to BR4 and decreases from BR4 to BR5. Here it is useful to note that dissolved phosphorous consists of two dissolved factions: phosphate P and organic P. Due to the fact that Phase II dissolved phosphate concentrations were below detection, the assumption can be made that the majority of dissolved phosphorous is organic. This factor has implications for the source since, like organic nitrogen, organic phosphorous is likely to be generated by natural processes such as the decay of plant material. In that light, potential causes of the phosphorous trends are essentially the same as those discussed for nitrogen. Nearby riparian zones could be fully or partially responsible for phosphorous increases. Input of development, including domestic wastewaters, could also be partially responsible; however, organic P from OWS is extremely unlikely. Furthermore, input of Pennsylvania Creek could cause the increase. Comparisons between mass flow rates in phosphorous measured at site PC2 were compared to the BR3 to BR4 increase observed in phosphorous to try and determine if this was true. As was the case with nitrogen, mass flow comparisons showed that Pennsylvania Creek could only be partially responsible for the increases. In the case of phosphorous, Pennsylvania Creek could be responsible for as much as 12% of the dissolved portion and 15% of the total portion.

Phase I phosphate data from the upstream Blue River sites were limited and data did not show any increases in these sites as was observed with nitrogen. In Phase II only two months of data were available for these upstream sites, and in one month there is an increasing trend, in the other a slight decreasing trend.

As with nitrogen, the natural question to ask is whether or not the WWTP could be responsible for any increases present. Comparisons of phosphorous data to estimated mass flows from the WWTP were not as readily conducted as they were with nitrate because loading numbers from the WWTP to the US EPA provided only phosphate mass flows. Total phosphate measured during Phase I of this study was below detection limit in the sites near the WWTP. Another possibility would be to compare total phosphorous mass flow increases in the downstream sites to phosphate mass flows. However, WWTP information stops in June 2002 and Phase II did not measure the downstream sites until July 2002; therefore, matching months of data were not available.

The WWTP effluent was monitored, but found to be below detection for both phosphate and total phosphorous. However, these samples were analyzed at CSM as opposed to NWQL. Therefore, detection limits were not as low as would be desired. So, the approach that was taken was that all phosphate mass flow data from the WWTP was averaged to come up with one mass flow value representing total phosphate input by the plant per day. This approach is justified in part due to the fact that nitrogen loading from the plant appeared relatively constant based on data shown in Table E-14. Estimated phosphate loading from the plant was 440 g-P/day. In the one month where total phosphorous increased from BR7 to BR8, this level would have been more than enough phosphorous to account for the 150 g-P/day increase in the Blue River.

Increases in total phosphorous during Phase II were observed between BR9 and BR10 in both months where total phosphorous was monitored at these sites. This increase is probably caused by the input of Swan River to the Blue River. No loading information is available from Swan River for comparison, but no other causes of phosphorous input between the two sites is known.

Supporting Parameters

Most of the supporting parameters were chosen because they are domestic wastewater constituents that have the potential to help further determine which causes discussed are occurring. For example, if a site displays increased levels of nutrients as well as all wastewater parameters, it would support the statement that that site is being impacted by domestic wastewater.

Total Solids

Though wastewaters are high in total solids, presence of elevated solids in surface waters could also be reasonable to expect in riparian wetlands (US EPA 2002). Solids were still included in this section, however, because their presence in a stream reach combined with other wastewater parameters, or their presence in an area not situated near such a riparian ecosystem would act as evidence of domestic wastewater influence. Even treated effluent from a WWTP can have more elevated amounts of solids than the receiving waters, especially in surface waters where background solids are extremely low (less than 50 mg/L). In the case of OWS effluent input, many solids are removed as that effluent moves through the soil column, but this does not necessarily affect dissolved solids levels, meaning that total solids could still be elevated.

The seasonal variations seen in solids in the Blue River were probably due in their entirety to flow. Mass flow decreased from the fall through the winter and increased in spring. These are identical to flow patterns seen in the area. Upstream to downstream trends in total solids were similar to many other parameters. Increases that were seen from BR1 to BR2 and BR3 to BR4 could be due to solids generated by the riparian wetlands. Furthermore, the solids increase from BR3 to BR4 could be a result of development and OWS present in the area, as already described. This increase could also be due in part to the input of Pennsylvania Creek; comparisons done as those described above showed it could be responsible for 16% of the increase. The decrease from BR4 to BR5 is most likely a direct result of the removal of solids in Goose Pasture Tarn.

Increases in total solids were also seen in the upstream sites. In this stretch of the stream, these solids are more likely from anthropogenic sources such as the town of Breckenridge and/or the wastewater treatment facility. The town itself could affect solids mass flows through activities such as the sanding of roads in the winter and runoff.

COD

Only one month of COD data was available, so no seasonal trends were available. The only trend to note in the upstream sites is that COD decreased between BR4 and BR5. As with other trends seen in that reach of the stream, this decrease could be due to Goose Pasture Tarn. Release of organic matter in the tarn could be causing this trend. There was a small increase in COD from BR6 to BR8, which may be due to oxygen demand loading from urban causes. A much larger increase in COD was seen between BR8 and BR10, which could be caused by the convergence of the Swan River with the Blue River.

Sulfur

Sulfur is a naturally occurring component in surface waters, but it is also a wastewater constituent. Sulfur is required in the synthesis of proteins and so is subsequently released when those proteins degrade (Metcalf & Eddy 2003). As seen in the total solids data, seasonal sulfur trends appeared to be directly caused by flow. In the upstream to downstream trends prior to site BR3, trends vary, but there were consistent increases from BR3 to BR4. Natural processes in this area are not likely to release sulfur and cause this increase, and Pennsylvania Creek was estimated to be responsible for 6% of the increase at best. So, this increase is perhaps evidence of the input of OWS in the area to this stretch of the Blue River. Large jumps in loading were also observed upstream of site BR7, which may further support municipal impact on water quality in the Blue River.

Chloride

Chlorides are also naturally occurring in water due to processes such as weathering of rocks. However, they are found in wastewaters because they are present in human excreta and in things such as water softeners (Metcalf & Eddy 2003). Conventional waste treatment methods do not remove chlorides, so higher than usually chloride levels can be indicative of the presence of wastewater (Metcalf & Eddy 2003); chloride acts as a natural tracer.

Seasonal chloride trends, like those seen in solids and sulfur, were probably attributable to fluctuations in flow. Upstream to downstream trends in chloride also repeat trends described before. Increases were observed from BR3 to BR4, which could either be due to development and OWS input, to de-icing of the roads in the area, and/or the input of Pennsylvania Creek. Pennsylvania Creek is estimated to be responsible for approximately 2% of this increase.

Chloride levels remained constant through the remainder of the upstream sites. This may indicate that increases seen from BR3 to BR4 are not due to de-icing of the roads, because roads near the BR4 to BR6 stretch of the Blue River are also near the stream. If de-icing were affecting water quality, mass flow increases past BR4 would be expected. Mass flow remains constant, however, until the BR6 to BR8 area when it begins to increase. Again, this increase is possibly due to de-icing of the roads, but not likely as these impacts would be expected to produce a more constant mass flow increase from upstream to downstream. These chlorides are more likely contributed from other urban sources. In the case of chlorides, comparisons were done to mass loading information from the WWTP as was done for nitrate and phosphorous.

Concentration of chloride in the WWTP was found to be 31 mg-Cl/L. Using this concentration along with the flow data from the Iowa Hill WWTP, estimated chloride mass flow rates were calculated for each month. Estimated mass flow of chloride from the WWTP was then compared to the BR7 to BR8 observed increase for each month. Comparisons showed that in most cases loading from the treatment plant could not account for all of the chloride mass flow increase between site BR7 and BR8 (Table E-15). Based on these estimates, the WWTP could account for approximately 60% of the mass flow increases observed.

Table E-15
Estimated Chloride Mass Flow From the Iowa Hill WWTP Versus Chloride Mass Flow
Increases Seen in the Blue River

Date	WWTP Cl g/day	BR7-BR8 Cl g/day
Sept, 2001	57300	464007
Oct, 2001	53000	251262
Nov, 2001	57000	270240
Dec, 2001	73400	262628
Jan, 2002	86500	354447
Feb, 2002	86500	149567
Mar, 2002	87000	258112

Boron

Like chloride, boron is a natural tracer that is found in domestic wastewater as a product of the breakdown of some fruits and in certain cleaning materials (Flynn and Barber 2000). Natural processes in the environment would not likely produce boron increases or decreases in streams. No seasonal trends were presented for boron because of a lack of data. Upstream to downstream trends showed increases from BR3 to BR4 and after BR7. In the upstream sites this increase could be due to OWS impact, but 43% of the increase may be due to Pennsylvania Creek. The only potential cause known for these trends in the downstream sites is municipal wastewater effluent input from the WWTP.

Assessment of Impact

The previous sections describe the recurrence of several trends in the study area. From BR1 to BR2, increases were seen in nitrate, organic nitrogen, and solids. No increases were seen in phosphorous or in the other parameters that would be expected if anthropogenic impacts were occurring in this area. Therefore, trends seen in this stretch of the river are thought to be from natural causes.

Increases were seen from BR3 to BR4 in nitrate, organic nitrogen, total phosphorous, dissolved phosphorous, total solids, sulfur, chloride, and boron. Decreases in DO were observed in this same stretch. Due to the presence of the riparian wetlands in this area, it is likely that natural processes are occurring that possibly affect nutrients, solids, and DO. Pennsylvania Creek surface water can be at least partially responsible for these increases. Table E-16 summarizes how much of each increase Pennsylvania Creek can be held accountable for. Since increases were seen in this stretch in all of the wastewater parameters discussed in this chapter it is likely that at least part of the increases might be attributable to the impacts of housing development and use of OWS in the area.

Table E-16
Summary of Comparison Results Quantifying the Portion of the BR3 to BR4 Increase for Which Pennsylvania Creek Could Be Responsible

Parameter	Average BR3-BR4 increase in g/day	Average PC2 loading in g/day	% of increase attributable to Penn Creek
Total solids	3367949	538660	16
Nitrate	1315	204	16
Organic N	1412	380	27
Total P	125	19	15
Dissolved P	59	7	12
Boron	625	270	43
Chloride	40808	760	2
Sulfur	62789	3920	6

From BR4 to BR5, DO decreases were observed along with nitrate decreases, organic nitrogen increases, phosphorous decreases, solids decreases, and COD increases. This mixture of trends is thought to be entirely attributable to processes in Goose Pasture Tarn. These processes include natural cycling of organic matter and sedimentation processes that occur in still waters.

The stretch of the Blue River after BR6 and up until BR9 displayed increases in temperature, solids, nitrate, organic nitrogen, phosphorous, sulfur, chloride, and boron. This combination of trends is thought to be evidence of the impact of urban causes including the Iowa Hill WWTP, which discharges effluent in this stretch of the Blue River.

Finally, various trends were observed in parameters from BR9 to BR10. Any trends seen in this stretch of the river are considered attributable to the input of Swan River to the Blue River.

The final point for consideration is to compare impacts of rural development and OWS to those attributable to urban development and the WWTP. The main concern with any of these impacts is how they might affect Dillon Reservoir. If all of the increases from BR3 to BR4 are assumed to be attributable to rural development and OWS, and all the increases from BR6 to BR8 are attributable to urban development and the WWTP, one can estimate percentages of the mass flow to Dillon Reservoir that each is responsible for. Comparisons were made based on the average increases in each wastewater parameter from BR3 to BR4 and from BR6 to BR8 to the mass flows of each parameter into Dillon Reservoir as measured at site BR10 (Table E-17).

These calculations were done under the assumption that 100% of the loading from each of these areas makes it to Dillon Reservoir. This assumption is important to note, especially in the case of mass flow from the upstream sites, where 100% of the loading probably does not make it to Dillon Reservoir. Before reaching Dillon Reservoir, water from this stretch must pass through several lakes and ponds.

As can be seen from Table E-17, urban development and the WWTP are likely responsible for higher percentages of nitrate, dissolved phosphorous, boron, chloride and sulfur to Dillon Reservoir. Rural development and OWS may be responsible for relatively higher total solids, organic nitrogen and total phosphorous mass flow to the reservoir.

Table E-17
Summary of Results Comparing Rural and Urban Development and Wastewater
Constituent Mass Flow to Dillon Reservoir

Parameter	Average BR3 - BR4 increase in g/day ¹	Average BR6 - BR8 Increase in g/day ¹	Average Mass Flow to Lake Dillon, g/day ²	Maximum % attributable to rural development	Maximum % attributable to urban development
Tot solids	3368000	1315929	15445517	22	9
Nitrate	1315	34037	65974	2	52
Org N	1412	451	8013	18	6
Total P	125	55	590	21	9
Diss P	59	103	430	14	24
Boron	625	689	3887	16	18
Chloride	40808	219161	551188	7	40
Sulfur	62789	257604	738122	9	35

¹ Assumption was made that 100% of this mass flow was contributed to Dillon Reservoir.

² Calculated using mass flow rates measured near the mouth of Dillon Reservoir at site BR10.

Summary and Conclusions

Water quality monitoring efforts can be conducted with a variety of objectives that greatly influence program design. Objectives of this study were to:

- Determine what if any are the effects of OWS on the surface waters of the study area
- Conduct a water quality assessment to determine impact, including a comparison to surface water quality standards
- Produce a water quality database that can be used in the calibration of a watershed scale model

Based on the literature, relatively few studies have been done assessing the impacts of OWS on surface waters, though much work is available on the effects to groundwater. In addition, riparian zone processes have the potential to affect nutrient levels in both stream and subsurface waters.

The mass balance calculations predicted low nutrient levels throughout the study area, which is consistent with monitoring data and these calculations predicted that Pennsylvania Creek was the area most likely to demonstrate OWS impacts. While analysis of data did not reveal seasonal trends in water quality, both urban and rural development types are affecting water quality in the Blue River; however, rural effects (including OWS) are not a relatively more important source. Even though two areas of impact have been identified, impacts are still small and water quality in the study area appears suitable for designated uses.

Specific conclusions include:

- Upstream to downstream trends and interpretation in the focus areas show that Tenmile Creek, Swan River, and Pennsylvania Creek do not demonstrate any impact due to OWS.
- Upstream to downstream trends and interpretation in sites BR1 through BR6 show the effects of processes occurring in adjacent riparian wetlands. Within this area, the stretch of the Blue River from BR3 to BR4 may be impacted to a limited extent by rural development including use of OWS in the Pennsylvania Creek focus area. This same stretch is also influenced in part by inputs from Pennsylvania Creek.
- Upstream to downstream trends and interpretation in sites BR7 through BR10 show the potential impacts of urban development including the Iowa Hill WWTP.
- Trends between BR9 and BR10 are likely caused by development in the Blue River and inputs of Swan River.
- Based on the comparison to State of Colorado standards, numerous exceedances of surface water quality standards were observed only for manganese, zinc, and sulfate. These standard exceedances may be the product of drought conditions. Furthermore, Tenmile Creek is the only potential problem area with exceedances in both manganese and sulfate.

The results of this research have led to new questions that would require further work in this area. Namely:

- Exactly which riparian zone processes are at work in the upstream Blue River area?
- What is the nature of the groundwater surface water interactions in the area?
- Do other parameters support impact of OWS and the WWTP in the areas mentioned?

Some of the work that could be done to answer these questions is as follows:

- Conduct monitoring of the final 10 sites with the addition of sites on the Blue River that may help to pinpoint pollutant sources (additional sites within the city of Breckenridge).
- Complete a detailed study of nutrients in one or more of the riparian wetlands in the area to determine which cycling mechanisms are present.
- Quantify the groundwater/surface water interactions present in this study area (Note Smith *et al.* 2002 indicates yes) to reveal subsurface flow and transport processes affecting the study area. This study could be done through more detailed monitoring and the use of tracer tests.
- Sample surface waters for additional parameters, such as caffeine, ethylenediamine tetraacetate (EDTA), and emerging and organic compounds that would further reveal anthropogenic factors and water quality relationships.

References

American Public Health Association (APHA). 1998. *Standard Methods for the Examination of Water and Wastewater*, Twentieth Edition. Clesceri, L. S., A. E. Greenberg, and A. D. Eaton (eds.). APHA-AWWA-WPCF, Washington, DC.

Bartram, J. and R. Balance (eds.). 1996. *Water Quality Monitoring: A Practical Guide to the Design and Implementation of Freshwater Quality Studies and Monitoring Programmes*. Chapman and Hall, London.

Canter, L. W. and R. C. Knox. 1984. *Evaluation of Septic Tank System Effects on Ground Water Quality*. EPA-600/S2-84-107. United States Environmental Protection Agency (US EPA), Research and Development.

Chapman, D. (ed.). 1996. *Water Quality Assessments: A Guide to the Use of Biota, Sediments and Water in Environmental Monitoring*. Chapman and Hall, London.

Colorado Department of Public Health and Environment (CDPHE). 2002a. Authorization to Discharge Under the Colorado Discharge Permit System, Permit No. CO-0045420. Water Quality Control Division. Accessed on November 5, 2002.

CDPHE. 2002b. Summary of Rationale, Permit No. CO-0045420. Water Quality Control Division. Accessed on November 5, 2002.

Crites, R. and G. Tchobanoglous. 1998. *Small and Decentralized Wastewater Management Systems*. McGraw-Hill Publishing Company, Boston, MA.

- Fishman, M. J. 1993. *Methods of Analysis by the US Geological Survey National Water Quality Laboratory—Determination of Inorganic and Organic Constituents in Water and Fluvial Sediments*. US Geological Survey Open File Report 93-125.
- Flynn, J. L. and L. B. Barber. 2000. *Quality of Ground Water and Surface Water in an Area of Individual Sewage Disposal System Use Near Barker Reservoir, Nederland, Colorado August to September 1998*. US Geological Survey Open File Report 00-214.
- Gilliam, J. W. 1994. “Riparian Wetlands and Water Quality.” *Journal of Environmental Quality*. 23, 896–900.
- Guelfo, J. L. 2003. *Water Quality Monitoring in the Lake Dillon Watershed, Colorado to Enable Assessment of Development Impacts*. M.S. Thesis. Environmental Science & Engineering Division, Colorado School of Mines, Golden, CO.
- Hagedorn, C., E. L. McCoy, *et al.* 1981. “The Potential for Ground Water Contamination from Septic Effluents.” *Journal of Environmental Quality*. 10(1), 1–8.
- Harman, J., W. D. Robertson, J. A. Cherry, and L. Zanini. 1996. “Impacts on a Sand Aquifer from an Old Septic System: Nitrate and Phosphate.” *Ground Water*. 34(6), 1105–1114.
- Hill, A. R. 1996. “Nitrate Removal in Stream Riparian Zones.” *Journal of Environmental Quality*. 25, 743–755.
- Jones, R. A. and F. G. Lee. 1979. “Septic Tank Wastewater Disposal Systems as Phosphorous Sources for Surface Waters.” *Water Pollution Control Federation Journal*. 51(11), 2764–2775.
- Kirkland, S. L. 2001. *Coupling Site-Scale Fate and Transport with Watershed-Scale Modeling to Assess the Cumulative Effects of Nutrients from Decentralized Wastewater Systems*. M.S. Thesis. Department of Geology and Geological Engineering, Colorado School of Mines, Golden, CO.
- Lemons, P. J. 2003. *Modeling Pollution Transport and Fate to Assess the Effects of Onsite Wastewater Systems on the Lake Dillon Watershed, Colorado*. M.S. Thesis. Department of Geology and Geological Engineering, Colorado School of Mines, Golden, CO.
- Lewis, W. M., J. F. Saunders, *et al.* 1984. *Eutrophication and Land Use Dillon Reservoir, CO*. Springer-Verlag, New York, NY.
- Lewis, W. M. and J. F. Saunders. 2002. *Dillon Reservoir Water Quality Model Revision and Recalibration for 2001*. Dillon Reservoir Clean Lakes Study.
- McCray, J. 2003. E-mail regarding Lewis model. J. Guelfo, Golden, CO.
- Metcalf & Eddy, Inc. 2003. *Wastewater Engineering: Treatment, Disposal, and Reuse*. McGraw-Hill Companies Inc., Boston, MA.

Patrick, S. T. 1988. "Septic Tanks as Sources of Phosphorous to Lough Erne, Ireland." *Journal of Environmental Management*. 26, 239–248.

Sanders, T. G., R. C. Ward, *et al.* 1983. *Design of Networks for Monitoring Water Quality*. Water Resources Publications, Littleton..

Siegrist, R. L., E. J. Tyler, and P. D. Jenssen. 2001. "Design and Performance of Onsite Wastewater Soil Absorption Systems." *National Research Needs Conference Proceedings: Risk-Based Decision Making for On-site Wastewater Treatment*. Project No. 1001446. EPRI, Palo Alto, CA, US EPA and National Decentralized Water Resources Capacity Development Project. March 15, 2001.

Sharp, W. E. 1971. "A Topologically Optimum Water-Sampling Plan for Rivers and Streams." *Water Resources Research*. 7(6), 1641–1646.

Smith, H., J. E. McCray, *et al.* 2002. *Use of Uncertain or Low Cost Data to Characterize the Subsurface Hydrology of the Blue River Watershed, Colorado*. Annual GSA Meeting, Denver, CO.

State of Colorado. 2001. The Basic Standards and Methodologies for Surface Water, Colorado Regulation No. 31. 5 CCR 1002–31.

State of Colorado. 2002. Classifications and Numeric Standards for Upper Colorado River Basin and North Platte River (Planning Region 12), Regulation No. 33.

Summit County Government. 1998. Population and Housing Data 1970–1998.
<http://www.co.summit.co.us/>

Tweto, O. 1973. *Reconnaissance Geologic Map of the Dillon 15-Minute Quadrangle, Summit, Eagle, and Grand Counties, Colorado*. USGS Open File Report 73-285.

US Census Bureau. 2002. US Census Bureau State and County Quickfacts.
<http://quickfacts.census.gov/qfd/>

United States Environmental Protection Agency (US EPA). 1980. *Design Manual for Onsite Wastewater Treatment and Disposal Systems*. US EPA Municipal Environmental Research Laboratory, Cincinnati, OH.

US EPA. 2000. *Constructed Wetlands Treatment of Municipal Wastewaters*. EPA/625/R-99/010. US EPA, Office of Research and Development.

US EPA. 2002. *Onsite Wastewater Treatment Systems Manual*. EPA 625/R-00/008. Office of Water, US EPA, Washington, DC.

United States Geological Survey (USGS). 2002. Surface-Water Data for the Nation.
<http://waterdata.usgs.gov/usa/nwis/sw>

Vought, L. B. M., J. Dahl, *et al.* 1994. "Nutrient Retention in Riparian Ecotones." *Ambio*. 23(6), 342–348.

Walton, W. C. 1970. *Groundwater Resource Evaluation*. McGraw-Hill Book Company, New York, NY.

Wilde, F. D., D. B. Radtke, *et al.*, (eds.). 1999. *National Field Manual for the Collection of Water-Quality Data*. USGS, Denver, CO.

Wyatt, L. 2002. *Ramifications of Recalibration: Issues Discussion Paper*, DRAFT. Summit Water Quality Committee.

Wynn, K. H., N. J. Bauch, *et al.* 2001. *Gore Creek Watershed, Colorado—Assessment of Historical and Current Water Quantity, Water Quality, and Aquatic Ecology, 1968–1998*. US Geological Survey, Water Resources Investigations 99-4270.



F SITE-SCALE MODELING USING HYDRUS 2-D

Wastewater soil absorption systems (WSAS) are used nationwide in mountain and rural communities for treatment of household wastewater. Currently, few rigorous non-empirical quantitative tools are available for assessing water flow, wastewater-pollutant transformation, and contaminant transport processes in WSAS. Development and use of rigorous mathematical models would provide a better understanding of the important physicochemical processes relevant to contaminant treatment in these systems and would be of great benefit to system design and regulation. A quantitative assessment may also provide valuable information relevant for optimizing system operation such that the groundwater-contamination risk is minimized and to maximize system life.

Background

WSAS commonly employed for onsite and small wastewater applications are designed for application of primary-treated wastewater into a subsurface trench that is installed in natural soil. Wastewater in the trench infiltrates through the underlying soil media toward the groundwater table. Wastewater is typically applied to the trench with a cumulative daily loading of 1 to 5 cm/d (Jenssen and Siegrist 1990). In the early stages of WSAS operation, these loadings may often result in rapid, nearly saturated flow near the point(s) of effluent delivery. However, soil clogging will evolve at the infiltrative base and sidewall surfaces of the trench (Jones and Taylor 1965; Siegrist 1987) and lead to reduced permeability and porosity. This biozone can cause ponding of septic tank effluent (STE) on the infiltrative surface, typically by 9 months of age (Bouma 1975). Soil clogging may have a beneficial impact on purification (Siegrist and Boyle 1987). However, if clogging is too extensive it can cause hydraulic failure by causing “back-up” of STE into the dwelling or to the ground surface.

This appendix presents a modeling study of flow and pollutant transport and transformation in a WSAS for a new system that has not yet developed an infiltrative surface biozone, and for a mature system with an established biozone. For the new system, two types of wastewater application are investigated: uniform application over the entire trench and focused application over a smaller subarea of the trench. The unsaturated flow behavior, which is controlled in part by biozone development, plays a critical role in wastewater pollutant treatment.

Orthophosphate (PO_4) and ammonium (NH_4) were chosen as the pollutants of interest because of their environmental importance and because of the reactive nature of these chemicals in the vadose zone. However, the mathematical processes described are generally relevant to a wide variety of pollutants present in wastewater (such as BOD, TSS, virus, and other pollutants). Further details regarding the modeling described in this appendix may be found in McCray *et al.* (2000) and Beach and McCray (2003).

Methodology

This section describes the methodology used for OWS site-scale modeling using HYDRUS 2-D.

Conceptual Model

The physical system is a subsurface trench that is open (i.e., does not contain aggregate on the infiltrative surface) (Figure F-1). Flow and transport in the system is modeled at various stages of operation at a realistic loading rate for a single-family system.

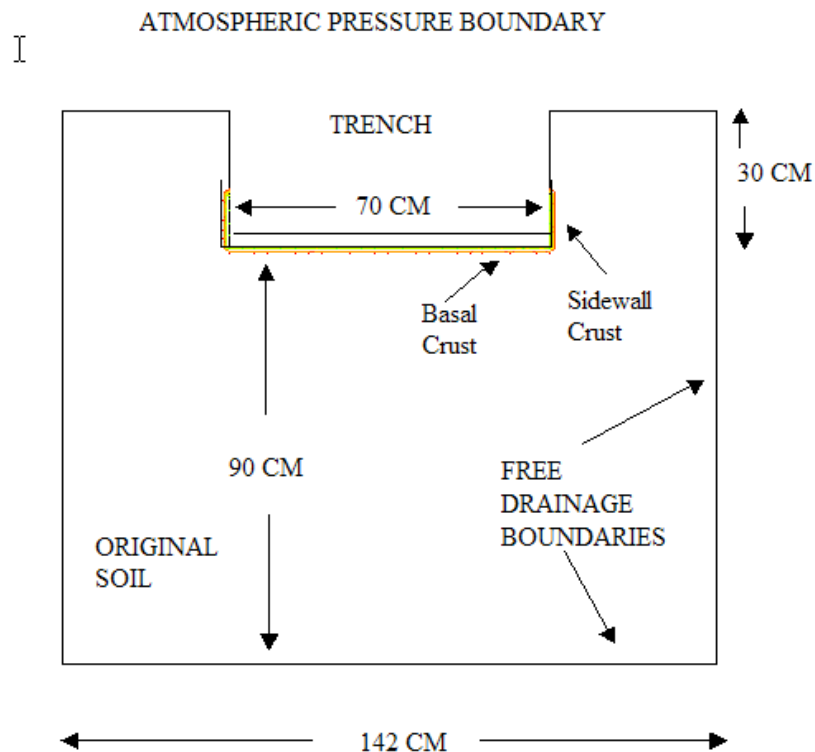


Figure F-1
Conceptual Model of a WSAS

Two cases are considered in this appendix: a new startup system where the soil-infiltrative surface does not have a biozone; and a mature system where basal and sidewall biozones are fully developed. In the new system, the wastewater is assumed to infiltrate at a uniform daily rate. For the mature system, wastewater is assumed to be permanently ponded at the infiltrative surface. The surface application rate for the new system and the ponded depth for the mature system are selected such that the volumes of wastewater leaving the model domain are equal for the two systems. This method ensures that the two systems are simulated with equal loading rates. This analysis assumes that a given family would produce the same amount of wastewater regardless of the condition of the infiltrative surface.

Mathematical Model

The mathematical model involves:

- Mathematical formulation
- Model boundary condition definition
- Hydraulic parameter selection
- Solute-transport parameter selection

Mathematical Formulation

Unsaturated flow and multi-species reactive contaminant transport behavior in a typical WSAS are simulated using HYDRUS 2-D, a two-dimensional, finite-element numerical model (Simunek *et al.* 1996). The model utilizes the well-known mixed form of Richards' equation (Richards 1931, Celia *et al.* 1990) wherein both pressure head and moisture content are variables in a governing partial differential equation for unsaturated flow. Input parameters to the model include saturated hydraulic conductivity and capillary pressure-moisture content parameters. The van Genuchten (1980) relationship for capillary-pressure head vs. moisture content is used in conjunction with the transform technique of Mualem (1976) to obtain the relationship for unsaturated hydraulic conductivity required for model input. The van Genuchten equation is given by:

$$\theta(h) = \theta_r + (\theta_s - \theta_r)[1 + |\alpha h|^n]^{-m}, \quad m = 1 - 1/n \quad \text{Equation F-1}$$

where θ is the unitless moisture content (volume of water per bulk volume of soil), θ_r is the residual water content, and θ_s is the water content of the soil when fully saturated (assumed equal to the porosity), h is the pressure head [L], α is a parameter that is inversely related to the magnitude of capillary head [L⁻¹], and m and n are empirical parameters related to structural characteristics of the soil. The unsaturated hydraulic conductivity function is given by:

$$K(\theta, h) = S_e [1 - (1 - S_e^{1/m})^m]^2 \quad \text{Equation F-2}$$

$$S_e = [\theta(h) - \theta_r] / (\theta_s - \theta_r) \quad \text{Equation F-3}$$

Pollutant transport is simulated by solving the well-known advection-dispersion equation (ADE) including the processes of zero- or first-order transformations, and contaminant sorption to solids (reversible and irreversible, linear and nonlinear, and dual-domain). The average linear water velocity (v) required for input into the model is calculated at each time step for every finite element by solution of Richards' equation. For these simulations, the molecular diffusion is assumed negligible compared to mechanical dispersion, and therefore that the hydrodynamic dispersion (D) [L²/T] is linearly related to the water velocity (v) [L/T]. Both longitudinal (along the flow path) and transverse dispersion coefficients are considered in the two-dimensional modeling presented here.

The proportionality constant relating velocity to D is known as the dispersivity (α_L for longitudinal dispersivity, α_T for transverse dispersivity) [L]:

$$D_L = \alpha_L v \quad D_T = \alpha_T v \quad \text{Equation F-4}$$

First-order, instantaneous, linear sorption of pollutants to soil is described by the following relation:

$$C_{\text{soil}} = K_D C \quad \text{Equation F-5a}$$

Where C_{soil} is the concentration of chemical on the soil phase [M/M], C is the concentration in the aqueous phase [M/L³], and K_D is the equilibrium soil water partition (or distribution) coefficient [L³/M]. Sorption causes the contaminant velocity to be regarded by a factor known as the retardation coefficient (R):

$$R = 1 + \rho_B K_D \theta^{-1} \quad \text{Equation F-5b}$$

Where ρ_B is the dry bulk density of the soil [M/L³]. Thus, the velocity of the pollutant can be expressed by v/R . Sorption according to a non-linear isotherm is described here by the Langmuir isotherm:

$$C_{\text{soil}} = K_L C / (1 + aC) = a C_{\text{soil}}^{\text{MAX}} C / (1 + aC) \quad \text{Equation F-6a}$$

Where K_L is the Langmuir constant ($K_L = a C_{\text{soil}}^{\text{MAX}}$, [L³M]), “ a ” is an adsorption constant related to binding energy (L³/M), and $C_{\text{soil}}^{\text{MAX}}$ is the maximum sorption capacity of the soil (M/M). The Langmuir isotherm is appropriate for modeling sorption of many pollutants because it reduces to a linear adsorption isotherm for relatively small soil and aqueous concentrations, while accounting for a maximum soil sorptive capacity at relatively higher soil and aqueous concentrations. The retardation factor for this case is given by:

$$R = 1 + \rho_B K_L \theta^{-1} [(1 + aC)^2]^{-1} \quad \text{Equation F-6b}$$

Many researchers use Freundlich isotherms to model non-linear sorption:

$$C_{\text{soil}} = K_F C^N \quad \text{Equation F-7}$$

where K_F is the Freundlich constant and N is an exponent that determines the shape of the curve. Values for N are commonly less than one for environmental applications, but may be greater than one. When $N = 1$, equation F-7 simplifies to a linear isotherm. For $N < 1$, the Freundlich equation can also be used to simulate a maximum soil sorptive capacity.

Biochemical decay (or first-order losses from the aqueous phase in general) is described by a first-order model using a first-order decay constant, k (T⁻¹):

$$dC/dt = -kC \quad \text{Equation F-8}$$

Equation F-8 is solved simultaneously with the ADE. Boundary and initial conditions for the model are described below.

Model Boundary Condition Definition

The wastewater in the simulations is applied to the center of the trench depicted in Figure F-1. For new systems, it is possible that the wastewater will infiltrate faster than it can spread over the entire trench (Appendix C, *Biozone Development and WSAS Performance: Column Studies*). Thus, for new systems, two cases are assumed: one where the wastewater infiltrates over an area equal to half the trench basal area (“focused” application, Case A), and one where the wastewater is distributed uniformly over the entire trench basal surface (Case B). For the uniform application scenario, a loading rate of 1.5 cm/day is assumed, which is in the range reported by other researchers (discussed previously). In the simulated focused system, the wastewater is applied to an area in the center of the trench that is half the total trench area, but at twice the loading rate (3 cm/day), resulting in the same total wastewater loading as for the uniform application. For the mature system, the biozone is fully developed at the sidewall and base, and it is assumed that all the ponded wastewater must infiltrate through the basal and sidewall biozone (Case C). The ponding depth is 5 cm and is chosen such that net STE infiltration is the same as for Cases A and B ($\pm 5\%$).

These flow rates are applied as a boundary condition at the appropriate location within the trench assuming the daily average flow rate is applied at a uniform constant rate during the simulation. Other areas of the trench not achieving flow are assigned no-flow conditions. The outer boundaries of the WSAS are assigned free-drainage boundary conditions (unit hydraulic-head gradient, or zero matric-pressure-head gradient). Constant chemical concentrations are assigned to the infiltrating STE water (values used for influent concentrations discussed below). Other areas of the trench are assigned a zero-concentration boundary condition, while the bottom and sides of the WSAS are assigned zero concentration-gradient conditions. The simulations are run until steady-state concentrations are reached throughout the WSAS to represent long-term conditions for each case.

It is assumed that a pressure head of -40 cm of water exists uniformly at the start of the simulations. However, because the simulations are run to steady-state chemical and hydraulic conditions for the analysis reported here, the initial condition has essentially no impact on the final results.

Hydraulic Parameter Selection

Table F-1 summarizes all the hydraulic parameters used in the simulations. Hydraulic properties of the sub-biozone soil are chosen to represent a loamy sand. The thicknesses, saturated hydraulic conductivity values, and porosity values of the basal and sidewall biozones were chosen from the experimental range reported in the literature (Jones and Taylor 1965; Bouma 1975; Siegrist 1987; Tyler *et al.* 1991; Schwager and Boller 1997; Amoozegar and Niewoehner 1998; Keys *et al.* 1998).

Table F-1
Hydraulic Parameters

Parameter	Sub-Biozone Soil	Basal Biozone	Sidewall Biozone
K_{sat} (cm/day)	350	0.1	0.5
θ_s	0.41	0.35	0.39
α (cm ⁻¹)	0.124	0.145	0.145
n	2.3	2.7	2.7
θ_r	0.057	0.045	0.045

Capillary-pressure parameters for a WSAS biozone have not been reported in the literature. Thus, it was assumed that the capillarity of the biozone was similar to that of fine silt. This is realistic because biozones have been observed to behave similar to capillary barriers as well as lower-permeability barriers (Van Cuyk *et al.* 2000).

Solute-Transport Parameter Selection

Solute-transport parameters used in these simulations are reported in Table F-2. An STE ammonium (NH_4) concentration of 50 mg/L is used (or about 39 mg $\text{NH}_4\text{-N/L}$). This value is based on the measured values and on values reported in the literature (McCray *et al.* 2003). For examples, STE collected from a Colorado School of Mines family apartment building and from a condominium complex by Breckinridge, Colorado over several months exhibited concentrations of 28–60 mg $\text{NH}_4\text{-N/L}$. In addition, Otis *et al.* (1973) reported values of 20–46 mg $\text{NH}_4\text{-N/L}$ for six septic systems. Robertson *et al.* (1998) measured concentrations between about 17 and 135 mg $\text{NH}_4\text{-N/L}$ from 10 septic systems. Finally, Crites and Tchobanoglous (1998) reported between 30–50 mg $\text{NH}_4\text{-N/L}$. Note that NH_4 concentrations (and not $\text{NH}_4\text{-N}$) are used for the simulations because reaction and sorption parameters reported in the literature are usually applicable for NH_4 transport.

For ammonium, the processes of instantaneous-linear-reversible sorption and first-order biochemical transformation of NH_4 to nitrate is included. Volatilization is neglected. The measured transformation reaction rates and measured sorption coefficients are realistic values obtained from the ranges reported in the literature for K_D (0 to 3.5 cm³/g) and for k (0.11 to 24 day⁻¹) (Cho 1971; Geng *et al.* 1996; Yamaguchi *et al.* 1996; Ling and El-Kadi 1998; DeSimone and Howes 1998; Fischer 1999). The values varied between 0.11 to 0.6 day⁻¹ in most of the reviewed studies although Yamaguchi *et al.* (1996) reported much higher values between 9.6 and 24 day⁻¹.

A STE phosphate (PO_4) concentration of 10 mg-P/L was selected for model input because it is representative of actual systems. This value is based on measured values for PO_4 in STE reported in the literature. For examples, STE collected from a Colorado School of Mines family apartment building and from a condominium complex by Breckinridge, Colorado over several months exhibited concentrations of about 2–24 mg- $\text{PO}_4\text{/L}$.

Otis *et al.* (1973) reported values of 10–14 mg-PO₄/L for PO₄ for six septic systems. Robertson *et al.* (1998) measured concentrations between about 2 and 12 mg-PO₄/L in STE from 10 septic systems. However, assuming that about 85% of total phosphorus (TP) are comprised of orthophosphate (Corell 1998), the chosen PO₄ concentration of 10 mg-P/L represents a TP that is somewhat lower than the range for TP (12–20 mg-P/L) reported by Crites and Tchobanoglous (1998).

The phosphate sorption parameters used in the simulations are also given in Table F-2.

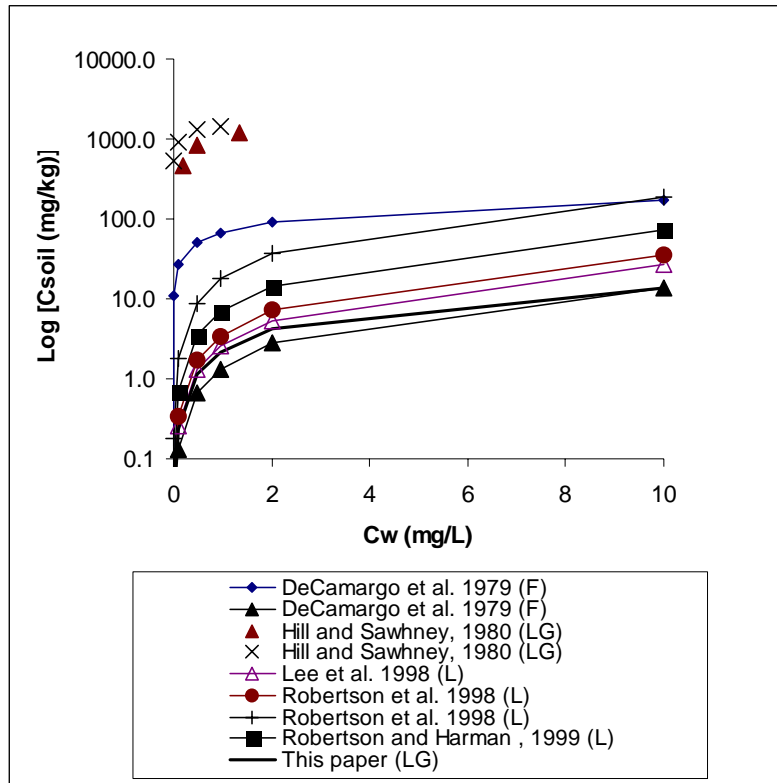
Table F-2
Solute-Transport Parameters

Parameter	Sub-Biozone Soil	Biozones ¹
	General	
α_L (cm)	1.0	1.0
α_L (cm)	0.1	0.1
ρ_B (g/cm ³)	1.60	1.60
	Ammonium	
K_D (cm ³ /g)	0.52	0.52
² k (day ⁻¹)	0.25 day ⁻¹	0.25 day ⁻¹
	Phosphate	
K_L (cm ³ /g)	2.5	2.5
a (cm ³ /mg)	83	83
C_{soil}^{MAX} (mg/g)	30	30
³ k (day ⁻¹)	0.0013	0.0013

¹For both basal and sidewall biozones. ²For transformation to nitrate. ³For precipitation with metals.

Phosphate reaction is highly variable and depends on the type of soil below the infiltration trench. It is generally known that phosphate will both sorb to soil and precipitate from solution after complexing with metal cations. For these simulations, both processes are included. Sorption is thought to occur relatively rapidly relative to typical transport velocities in soil (Harman *et al.* 1996). Thus, instantaneous sorption is assumed for the simulations. Several laboratory and field studies have concluded that soils have a limited sorption capacity (Magdoff *et al.* 1974; Campbell and Racz 1975; De Camargo *et al.* 1979; Hill and Sawhney 1981; Harman *et al.* 1996). Langmuir sorption isotherms are often used when incorporating a maximum soil-sorption capacity in modeling efforts. Freundlich curves can also provide a limiting soil concentration (De Camargo *et al.* 1979).

For these modeling efforts, a hypothetical Langmuir-type sorption curve that yields sorption isotherms that are within the range of sorption isotherms reported in the literature is used. Figure F-2 illustrates sorption data collected from various literature sources. Note that the curve falls within the range of nearly all the literature data in the low-concentration “linear” stage. However, the high-concentration part of the isotherm is in the lower ranges of the reported data. This occurs because a soil sorptive capacity of 30 mg/kg, a value that lies within the range of values (15–50 mg/kg) reported by Harman *et al.* (1996) for field conditions is used.



Notes: L = linear isotherm, F = Freundlich isotherm, LG = Langmuir isotherm.
 “Symbols only” indicate actual data [from Hill and Sawhney 1981],
 “Lines plus symbols” show isotherms that were reported only by providing K_D or
 Freundlich isotherm parameters.

Figure F-2
Sorption Isotherms From the Literature

Note that the most of the curves in Figure F-2 are based on single measured K_D values, which cannot model a maximum soil concentration. Thus, most of these single- K_D curves probably overestimate sorption capacity at relatively high values for C and C_{soil} . Precipitation is known to be an important mechanism for phosphate reaction in soil water systems. Sorption surfaces for phosphates are primarily calcium carbonate, metal hydroxide soil coatings, and solid organic carbon (Harman *et al.* 1996). According to Harmon *et al.* (1996), precipitation is more likely to be a rate-limited process than sorption, but is not significantly affected by wastewater-loading history. In addition, precipitation may provide an unlimited capacity to fix phosphate, providing the soil water chemistry is appropriate (Jones and Lee 1979). However, most researchers agree that it is very difficult to separate the mechanisms of sorption and precipitation.

Generally, authors who attempt to quantify phosphate sorption and precipitation lump it into the sorption isotherm, where precipitation would contribute to the maximum sorption capacity of the soil (Hill and Sawhney 1981; De Camargo *et al.* 1979; Robertson and Harman 1999; Robertson *et al.* 1998). Lee *et al.* (1998) used an analytical model for vadose zone and groundwater transport that included the process of linear, reversible sorption, but could not explicitly account for precipitation. Thus, these researchers used a first-order mass loss term (similar to that given in Equation F-8) to account for precipitation-loss of phosphate from the soil water. This approach is sensible because the amount of phosphate that can precipitate is dependent on the aqueous-phase concentration. The authors obtained a value of 0.0013 day^{-1} by calibrating a simple transport model to field data. For simplicity, the first-order loss-term of PO_4 reported by these authors to simulate phosphate precipitation is used. The value used by Lee *et al.* (1998) is undoubtedly site-specific. This value is used in simulations as a realistic estimate for precipitation, and not because it is believed to be a globally applicable value.

Many of the authors referenced previously have documented that soil-phase phosphate concentrations are highest in the zone of 15 centimeters to one meter below the infiltrative surface. Because the modeling domain here includes 90 centimeters of soil, the assumption has been made that reaction and sorption parameters are uniform within the modeling domain. However, even for uniform sorption and precipitation parameters, one would expect more phosphate to be retained in the upper portions of the soil because the aqueous concentrations of all constituents are larger closer to the source, and will decrease with depth as the chemical reacts with the soil. This behavior is illustrated by the model-simulation results and is described in more detail later.

Results and Discussion

The results and discussion presented in this section include:

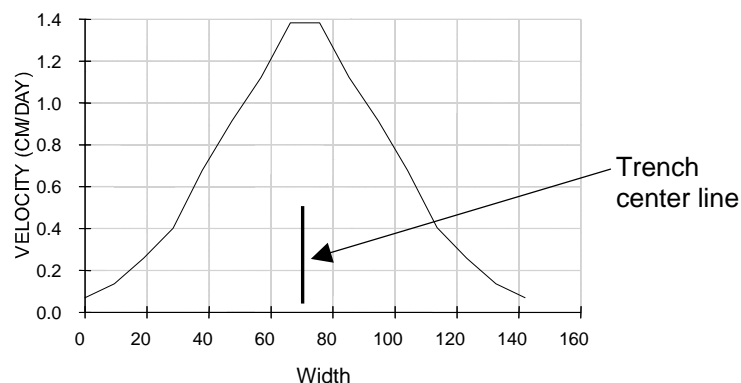
- Unsaturated water flow
- Ammonium transport
- Phosphate transport

Unsaturated Water Flow

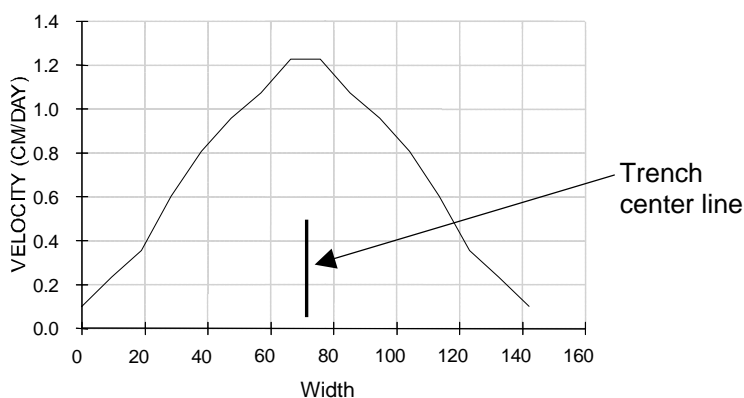
Simulated velocity profiles at the 90-cm depth of the modeled WSAS represent the magnitude and spatial variability of the hydraulic residence times in the three systems (Figure F-3). Similar trends are apparent at other depths. The figure illustrates that the hydraulic residence time is spatially variable and may vary significantly as a function of the infiltrative-surface conditions and application method. For Cases A and B, the flow of water is primarily vertical with lateral removal due to capillarity. For the biozone case, a lower and somewhat more uniform water-content distribution develops because a portion of the water is infiltrated laterally through the sidewall biozone. Some additional lateral movement may possibly occur due to the increased capillarity at the lower overall water content.

The impact of the biozone on hydraulic residence time can be easily observed from this figure. The biozone causes slower water velocities, which could allow more time for first-order reactions to occur, thus enhancing pollutant removal. The slower velocities are particularly beneficial with regard to phosphate treatment because precipitation of PO_4 is typically assumed to be rate-limited (Harman *et al.* 1996), and sorption may also be somewhat rate-limited (De Camargo *et al.* 1979).

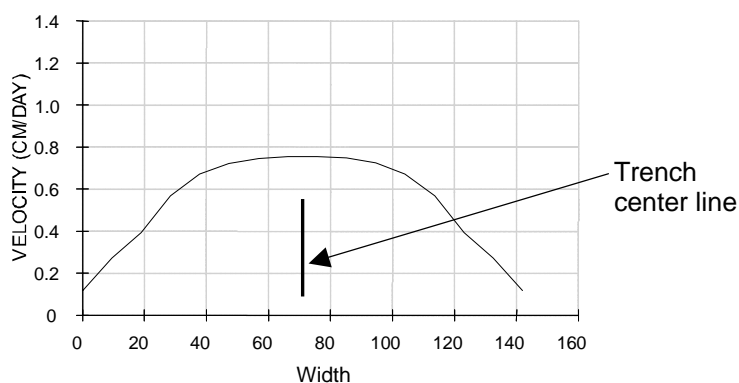
A.



B.



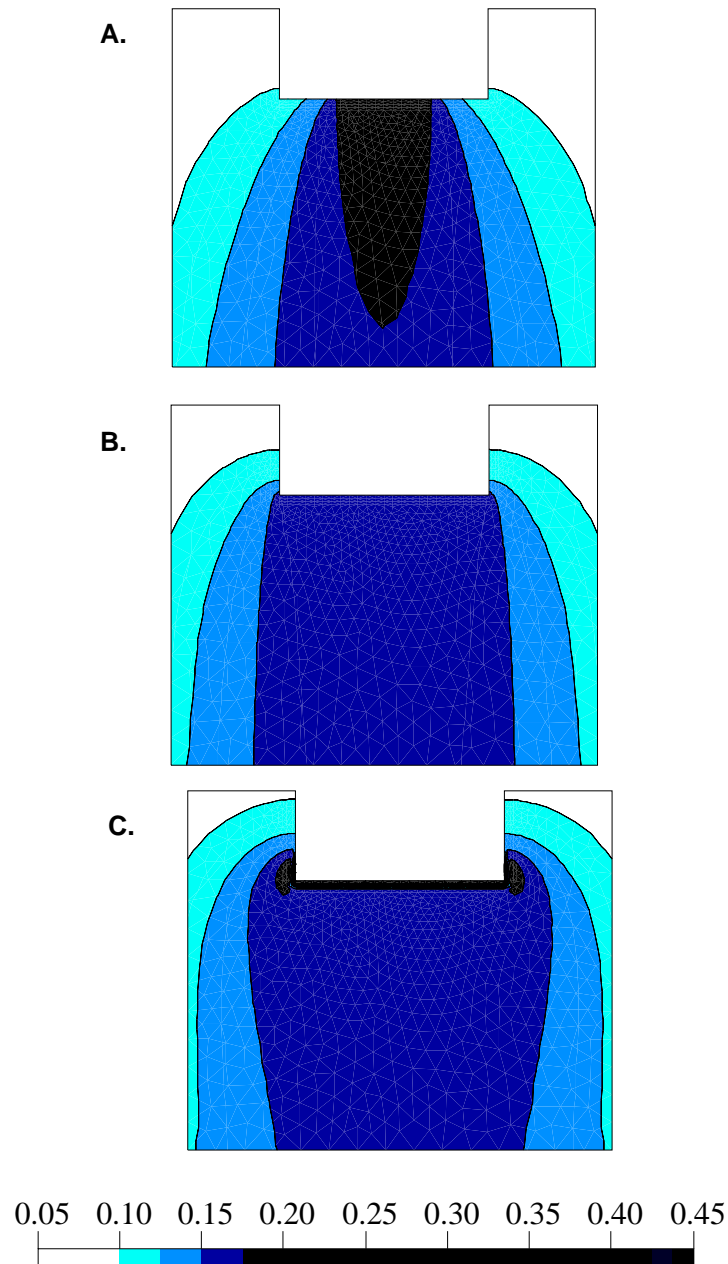
C.



Notes: Steady-state water velocities (cm/day) at the 90-cm depth for a WSAS system that is: (A) new (no biozone) with focused application of wastewater in center of trench; (B) new (no biozone) with uniform application of wastewater over trench; (C) mature (biozone).

Figure F-3
Steady-State Water Velocities

Analysis of the simulated water content distribution throughout the WSAS is also informative (Figure F-4).



Notes: Steady-state water contents for a WSAS system that is: (A) new (no biozone) with focused application of wastewater in center of trench; (B) new (no biozone) with uniform application of wastewater over trench; (C) mature (biozone present).

Figure F-4
Steady-State Water Contents

The focused application (Case A) results in higher water saturations below the application point. This explains the higher water velocities below the center of the trench (recall Figure F-3). When wastewater is distributed evenly over the width of the trench, the water content is more uniform across the WSAS.

The mature system (Case C) exhibits somewhat lower water contents in the soil below the biozone with a noticeably larger hydraulic volume. The increased hydraulic volume results mainly from infiltration through the sidewall, which does not occur for the systems with no biozone. In addition, the biozone exhibits nearly saturated conditions due to its higher capillarity and lower hydraulic conductivity. This phenomena is typical during infiltration into a layered soil. Although not explored here, the higher water contents may have a significant effect on biological treatment within the biozone zone. Based on these simulations, it is clear that the nature of the infiltrative surface and the effluent distribution impact the volume of soil exposed to advancing wastewater. The mature system provides a larger soil volume for precipitation and sorption reactions.

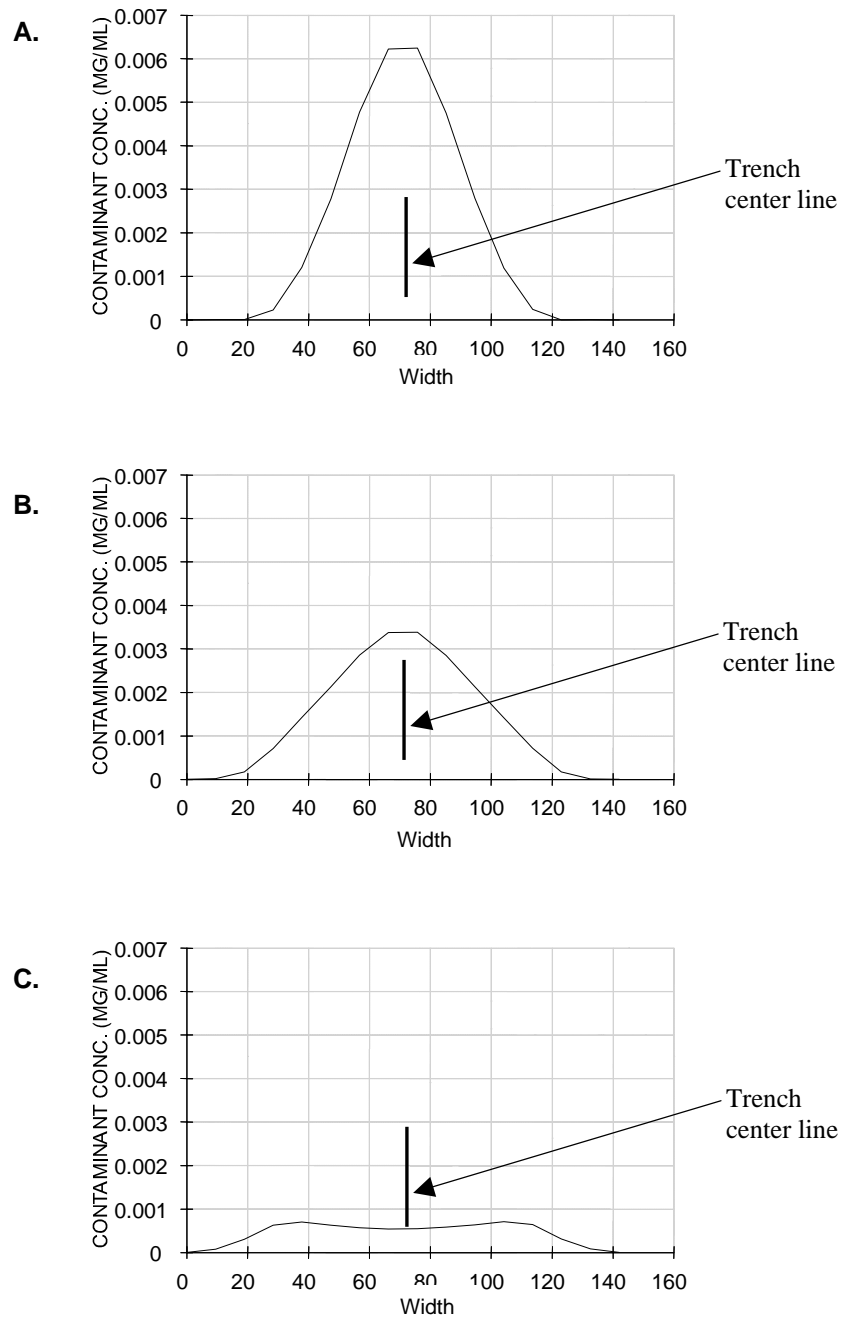
Ammonium Transport

The transport and transformation of NH_4 is illustrated in Figure F-5, which depicts steady-state concentration profiles across the horizontal section of the WSAS at a depth of 90 cm. These steady-state profiles are representative of the long-term concentrations within the soil and flowing water below an infiltrative surface. Recall that the input STE concentration of NH_4 is 0.050 mg/ml (50 mg/L). The figure shows that the concentration exiting the bottom boundary is significantly impacted by both effluent distribution and biozone development.

The focused application (Case A) results in higher ammonium concentrations at depth because of the higher water velocities and larger water contents in the center of the system. The larger overall water contents, particularly near the infiltrative surface, cause larger unsaturated hydraulic conductivities, faster advective transport, and less time for degradation reactions. The more-uniform application (Case B) exhibits a significant improvement in pollutant reduction for the selected depth.

The biozone in the mature system (Case C) significantly alters the hydraulic regime (as described previously), results in slower transport, and enables increased transformation of ammonium. Specifically, the NH_4 concentrations are smaller in the zones of smaller water velocities because more time has elapsed to enable transformation to nitrate. In addition to the impact of water velocity on transformation, the larger soil zone may allow for additional sorption, which further slows the domain-average velocities and increases the amount of NH_4 that can biochemically degrade before reaching a selected depth.

The mass fluxes exiting the bottom boundary (which could represent fluxes input to groundwater) for the three cases (A, B, C) are 45, 28, and 6 mg/day, respectively. The concentrations exiting the 90-cm depth are 12%, 6%, and 2% of the ammonium concentrations in the applied STE for cases A, B, and C, respectively. The presence of a mature biozone significantly enhances the treatment capacity of the system.



Notes: Steady-state ammonium concentrations (mg/mL) at the 90-cm depth for a WSAS system that is: (A) new (no biozone) with focused application of wastewater in center of trench; (B) new (no biozone) with uniform application of wastewater over trench; (C) mature (biozone present).

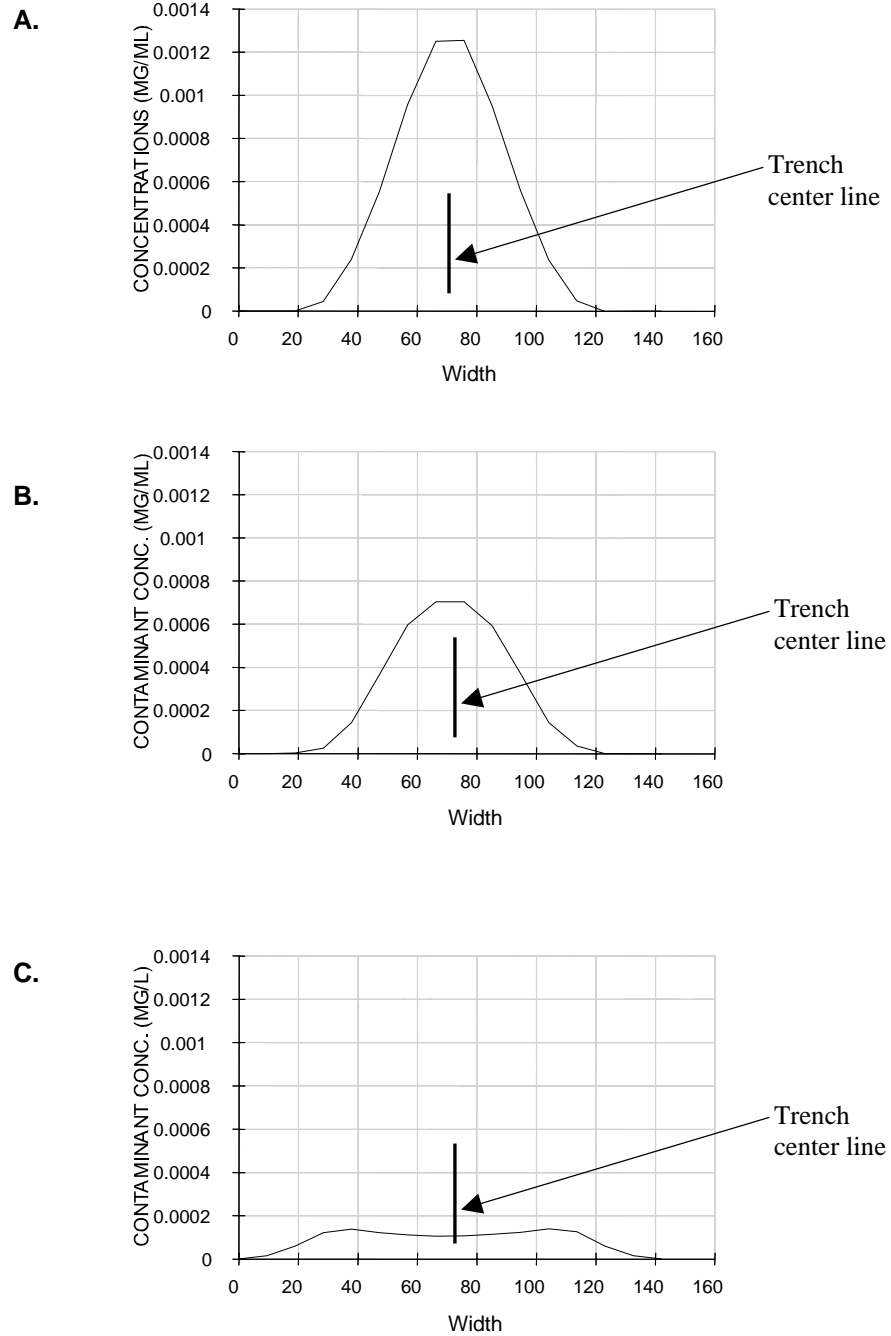
Figure F-5
Steady-State Ammonium Concentrations

Of course, the amount of ammonium transformed depends greatly on the first-order decay rate. However, the relative differences in mass reduction for the three cases are similar. These simulations show the importance of the infiltrative surface character and effluent distribution on pollutant transformations.

Phosphate Transport

Phosphate transport experiences the same behaviors as exhibited for ammonium transport described above (Figure F-6). Recall that the concentration of phosphate in the applied STE was 0.01 mg/mL (10 mg/L). Coincidentally, the reductions in simulated concentrations at the 90-cm depth are similar to those exhibited by ammonium. Compared to ammonium, the sorption of phosphate is much higher, while the “reaction rate” of precipitation is much lower than the reaction rate of ammonium transformation. The increased sorption for phosphate causes slower overall velocities, and thus allows more time for precipitation. However, the first-order precipitation rate for phosphate is much lower than the first-order transformation rate for ammonium, resulting in similar concentration reductions. This behavior suggests that both sorption and precipitation/transformation will play a significant role in the degree of treatment. This is true even for reversible sorption, where the contaminant is not sorbed permanently to the soil, but merely experiences “retarded transport.”

Note that the steady-state concentrations will vary with depth. For example, the steady-state phosphate concentrations in the mature system are significantly greater at shallower depths (Figure F-7). Steady-state conditions depend on sorption and reaction rates, as well as on soil water velocities and water-content distributions. Thus, the shape and extent of the contaminant “plume” in the vadose zone may differ greatly for pollutants with different transformation rates or sorption characteristics. The soil type will also play a significant role in determining the shape and extent of the contaminant plume because hydraulic properties impact the velocity of the soil water, and because metal-cation concentrations in the soil may control precipitation. Given the variability in hydraulic, transport, and reaction parameters, the depth to groundwater required to adequately treat wastewater pollutants is likely to be highly site and pollutant specific.



Notes: Steady-state phosphate concentrations (mg/mL) at the 90-cm depth for a WSAS system that is: (A) new (no biozone) with focused application of wastewater in center of trench; (B) new (no biozone) with uniform application of wastewater over trench; (C) mature (biozone present).

Figure F-6
Steady-State Phosphate Concentrations

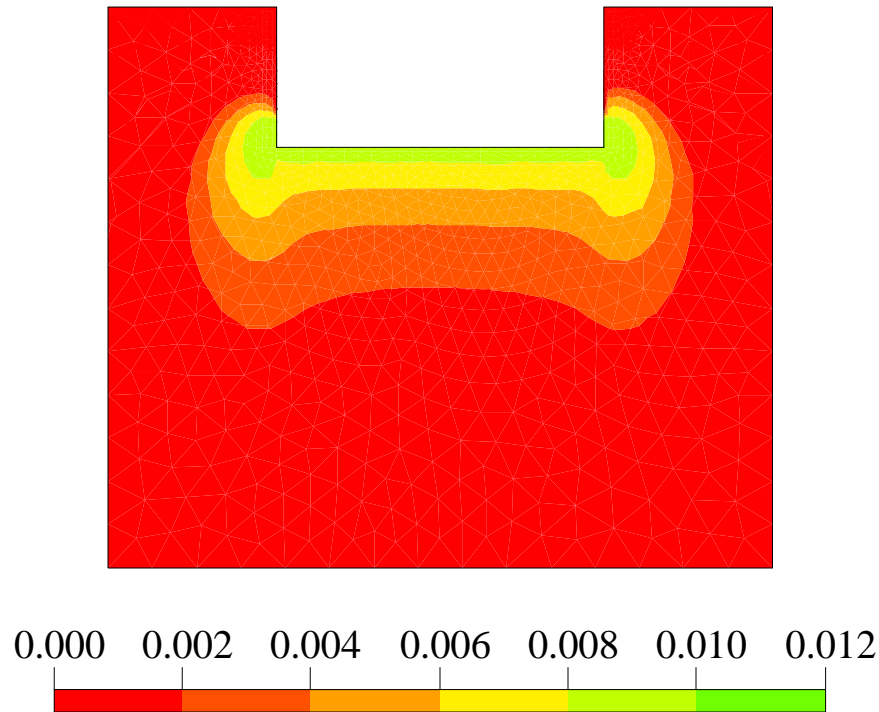


Figure F-7
Steady-State Phosphate Concentrations in the WSAS (mg/mL) for a Mature (Biozone Present) System

Figure F-7 illustrates that, even for a homogeneous sorption and transformation domain, the field-observed phenomena of higher soil phosphate concentrations below the infiltrative surface can be simulated using instantaneous, reversible sorption isotherms. As the aqueous concentrations available to the soil decrease, so will the amount of chemical partitioned to the soil (recall Equations F-5 through F-7). Thus, the higher steady-state soil water concentrations near the infiltrative surface will result in larger steady-state soil concentrations (recall Equations F-5 through F-7). These simulations illustrate that the increased soil phosphate concentrations typically observed below the infiltrative surface can be explained by sorption and transformation mechanisms as well as by the existence of special chemical conditions that are conducive to precipitation.

Conclusions

This research illustrates that the impact of biozone formation on pollutant treatment depends on several factors:

- Chemical transformation rates
- Contaminant sorption capacity of the soil
- Infiltration capacity (hydraulic conductivity) of the native soil and biozones

Given the wide variety of pollutants in wastewater, the large range of transformation rates possible for a given pollutant, and the variations in local soil type, biozone development is likely to play a significant role in controlling treatment for certain pollutants at a given site, but may impart little impact for others. Because the biozone has a great potential to impact treatment efficiency, it is important to better understand the evolution of biozone hydraulic properties as well as mechanisms that control biozone growth and permeability. The implications of these various factors on treatment of specific wastewater pollutants (nitrogen species, phosphates, and selected pathogens) remain to be rigorously evaluated. The use of multidimensional, numerical, unsaturated flow and transport models can be a valuable tool in elucidating these factors.

References

- Amoozegar, A. and C. P. Niewoehner. 1998. "Soil Hydraulic Properties Affected by Various Components of Domestic Wastewater." *Proceedings of the Eighth National Symposium on Individual and Small Community Sewage Systems*. Publication 3-98, 155–166. American Society of Agricultural Engineers, St. Joseph, MI.
- Beach, D. N. and J. E. McCray. 2003. "Numerical Modeling of Unsaturated Flow in Wastewater Soil Absorption Systems." *Ground Water Monitoring and Remediation*. 23(2), 64–72.
- Bouma, J. 1975. "Unsaturated Flow During Soil Treatment of Septic Tank Effluent." *J. Environmental Engineering*. ASCE. 101, 967–983.
- Campbell, L. B. and G. J. Racz. 1975. "Organic and Inorganic P Content, Movement and Mineralization of P in Soil Beneath a Feedlot." *Can. J. Soil Sci.* 55, 457–466.
- Celia, M. A., E. T. Bouloutas, and R. L. Zarba. 1990. "A General Mass-Conservative Numerical Solution for the Unsaturated Flow Equation." *Water Resour. Res.* 26, 1483–1496.
- Corell, D. L. 1998. "The Role of Phosphorus in the Eutrophication of Receiving Waters: A Review." *J. Environ. Qual.* 27, 261–266.
- Cho, C. M. 1971. "Convective Transport of Ammonium with Nitrification in Soil." *Can. J. Soil Sci.* 51(3), 339–350.
- Crites, R. C. and C. Tchobanoglous. 1998. *Small and Decentralized Wastewater Systems*. McGraw-Hill Publishing Company, Boston, MA.
- De Camargo, O. A., J. W. Biggar, and D. Nielsen. 1979. "Transport of Inorganic Phosphorus in an Alfisol." *Soil Sci. Soc. Am. J.* 43, 884–890.
- DeSimone, L. A. and B. L. Howes. 1998. "Nitrogen Transport and Transformations in a Shallow Aquifer Receiving Wastewater Discharge: A Mass Balance Approach." *Water Resour. Res.* 34(2), 271–285.

- Fischer, E. A. 1999. *Nutrient Transformation and Fate During Intermittent Sand Infiltration of Wastewater*. M.S. Thesis, Colorado School of Mines, Golden CO.
- Geng, Q. Z., G. Girard, and E. Ledoux. 1996. "Modeling of Nitrogen Cycle and Nitrate Transfer in Regional Hydrogeologic Systems." *Ground Water*. 34(2), 293–304.
- Harman, J., W. D. Robertson, J. A. Cherry, and L. Zanini. 1996. "Impacts on a Sand Aquifer from an Old Septic System: Nitrate and phosphate." *Ground Water*. 34(6), 1105–1114.
- Hill, D. E. and B. L. Sawhney. 1981. "Removal of Phosphorus from Waste Water by Soil Under Aerobic and Anaerobic Conditions." *J. Environ. Qual.* 19(3), 401–405.
- Jenssen, P. D. and R. L. Siegrist. 1990. "Technology Assessment of Wastewater Treatment by Soil Infiltration Systems." *Water Sci. Tech.* 22(3/4), 83–92.
- Jones, J. H. and G. S. Taylor. 1965. "Septic Tank Effluent Percolation Through Sands Under Laboratory Conditions." *Soil Science*. 99(5), 301–309.
- Jones, R. A. and G. F. Lee. 1979. "Septic Tank Wastewater Disposal Systems as Phosphorus Sources for Surface Waters." *J. Water Pollut. Control Fed.* 51, 2764–2775.
- Keys, J. R., E. J. Tyler, and J. C. Converse. 1998. *Predicting Life for Waste Water Absorption Systems*. ASAE Publication 03-98, 167–176. American Society of Agricultural Engineers, St. Joseph, MI.
- Lee, S., D. C. McAvoy, J. Szydluk, and J. L. Schnoor. 1998. "Modeling the Fate and Transport of Household Chemicals in Septic Systems." *Ground Water*. 36(1), 123–132.
- Ling, G., and A.I. El-Kadi (1998). A Lumped Parameter Model for Nitrogen Transformation in the Unsaturated Zone, *Water Resour. Res.*, 34(2), 203–212.
- McCray, J. E., D. Huntzinger, S. Van Cuyk, and R. Siegrist. 2000. *Mathematical Modeling of Unsaturated Flow and Transport in Soil-based Wastewater Treatment Systems*. WEFTEC 2000 Symposium. Water Environment Federation, Anaheim, CA.
- McCray, J. E., S. L. Kirkland, R. L., Siegrist, and G. D. Thyne. 2003. "Hydrologic Modeling of Nutrients from Onsite Wastewater Systems: Review of Input Parameters." submitted to *Ground Water*.
- Magdoff, F. R., D. R. Keeney, J. Bouma, and W. A. Ziebell. 1974. "Columns Representing Mound-type Disposal Systems for Septic Tank Effluent: II., Nutrient Transformations and Bacterial Populations." *J. Environ. Qual.* 3, 228–234.
- Mualem, Y. 1976. "A New Model for Predicting the Hydraulic Conductivity of Unsaturated Porous Media." *Water Resour. Res.* 12, 513–522.

- Otis, R. J., W. C. Boyle, and D. K. Sauer. 1973. *Small-Scale Waste Management Program*. U. Wisconsin.
- Richards, L. A. 1931. "Capillary Conduction of Liquid Through Porous Media." *Physics*. 1, 318–333.
- Robertson, W. D. and J. Harman. 1999. "Phosphate Plume Persistence at Two Decommissioned Septic System Sites." *Ground Water*. 37(2), 228–236.
- Robertson, W. D., S. L. Schiff, and C. J. Ptacek. 1998. "Review of Phosphate Mobility and Persistence in 10 Septic System Plumes." *Ground Water*. 36(6), 1000–1010.
- Schwager, A. and M. Boller. 1997. "Transport Phenomena in Intermittent Filters." *Water Sci. Technol.* 35(6), 13–20.
- Siegrist, R. L. 1987. "Soil Clogging During Subsurface Wastewater Infiltration as Affected by Effluent Composition and Loading Rate." *J. Environ. Qual.* 16(2), 181–187.
- Siegrist, R. L. and W. C. Boyle. 1987. "Wastewater Induced Soil Clogging Development." *J. Environ. Engineering*. 113(3), 550–566.
- Simunek, J., M. Sejna, and M. T. van Genuchten. 1996. *HYDRUS-2D for Simulating Water Flow and Solute Transport in Two-dimensional Variably Saturated Media*. International Ground Water Modeling Center, Colorado School of Mines, Golden, CO.
- Tyler, E. J., M. Milner, and J. C. Converse. 1991. *Wastewater Infiltration from Chamber and Gravel Systems*. ASAE Publication 10-91. 214–222. American Society of Agricultural Engineers, St. Joseph, MI.
- Van Cuyk, S., R. Siegrist, A. Logan, S. Masson, E. Fischer, and L. Figueroa. 2000. "Hydraulic and Purification Behaviors and Their Interactions During Wastewater Treatment in Soil Infiltration Systems." *Water Research*. (in press).
- van Genuchten, M. T. 1980. "A Closed-form Equation for Predicting the Hydraulic Conductivity of Unsaturated Soils." *Soil Sci. Soc. Amer. J.* 44, 892–898.
- Yamaguchi, T., P. Moldrup, D. E. Rolston, S. Ito, and S. Teranish. 1996. "Nitrification in Porous Media During Rapid, Unsaturated Water Flow." *Water Research*. 30(3), 531–540.



G WATERSHED MODELING USING BASINS/SWAT

The mountainous regions of Colorado have experienced development and considerable population growth in the past years. From 1970 to 1980, Summit County, located in the middle of the Colorado Rocky Mountains, was the fastest growing county in the US, with over 200% population growth (Summit County 2002). However, in many areas of these mountainous regions, centralized sewer systems have not been constructed. Consequently, residents rely on onsite wastewater systems (OWS) for treatment and disposal of their wastewater. Most homes that utilize these systems for wastewater disposal also use private groundwater wells for drinking water. In the Dillon Reservoir watershed (Figure G-1), located in southern Summit County, watershed water quality management issues related to OWS effluent are more prominent due to population growth, thin soils, and potential nutrient and pathogen transport to surface water and groundwater supplies in the montane environment. The Dillon Reservoir watershed includes Upper Blue River, Tenmile Creek, and Snake River.

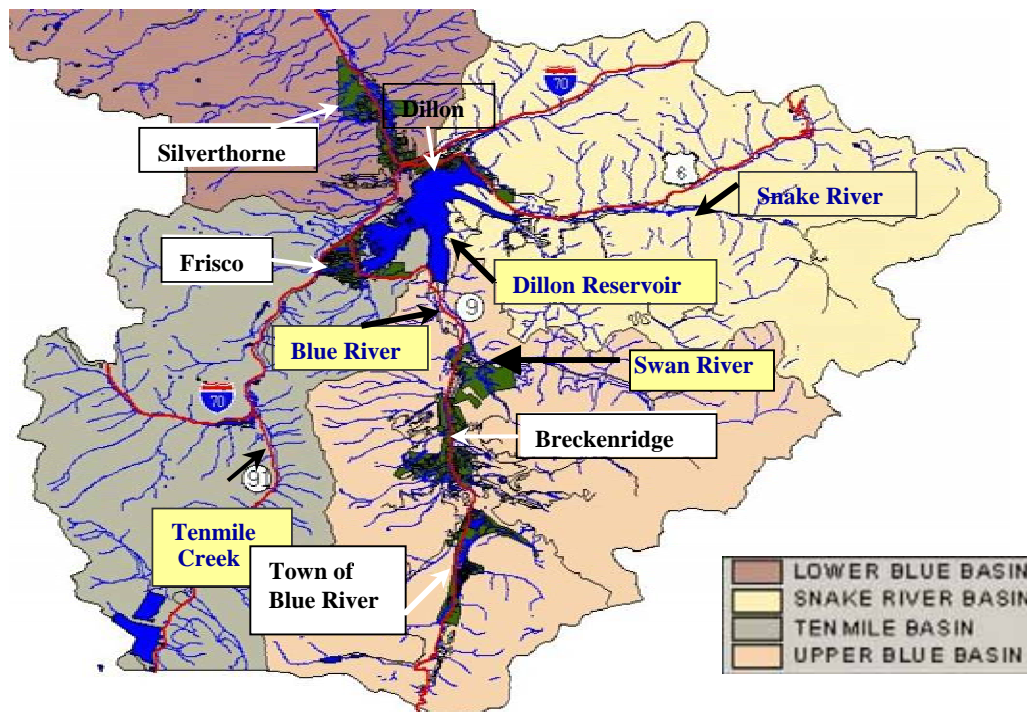


Figure G-1
The Dillon Reservoir Watershed

Introduction

The objective of the work presented in this appendix was to model the effects of wastewater pollutants, specifically phosphorus, on surface water in the Dillon Reservoir watershed using a geographical information system (GIS)-linked watershed-scale water quality model. The goal was to use a free, public-domain model to maximize the practical benefits of the research. Soil and Water Assessment Tool (SWAT), which is incorporated in the Better Assessment Science Integrating Point and Nonpoint Sources (BASINS) modeling package available from the United States Environmental Protection Agency (US EPA), was used for the study (Neitsch *et al.* 2001a). SWAT utilizes primarily physically-based data, simulates land-use and management scenarios, and takes into account process interactions through a GIS environment. This appendix summarizes the work completed, while additional details can be found in Lemonds (2003).

Phosphorus (P) concentrations in Dillon Reservoir have long been a concern. One major concern of elevated concentrations of phosphorus in reservoirs is eutrophication. Brady and Weil (1999) define eutrophication as the nutrient enrichment of water bodies that stimulates growth of aquatic organisms, which leads to a deficiency of oxygen. This process is accelerated by human-related contributions of point and nonpoint sources of phosphorus. Ongoing studies to quantify sources of phosphorus in the watershed have been completed by Lewis and Saunders (1998, 1999, 2002), and regulations for input of phosphorus into Dillon Reservoir have been implemented. Municipal or domestic wastewater treatment plants treating more than 2,000 gallons per day in the Dillon Reservoir watershed cannot legally discharge effluent with a total phosphorus concentration of 0.5 mg L^{-1} or greater (CDPHE 2001). Also, total phosphorus discharged in the watershed by point sources may not exceed $1,621 \text{ lb year}^{-1}$, except under certain conditions.

The Water Quality Control Division of the Colorado Department of Public Health and Environment is authorized to approve point source/nonpoint source tradeoffs in the watershed (CDPHE 2001). The tradeoffs in the Dillon Reservoir watershed were the nation's first point/nonpoint trading program (US EPA 1999). By controlling nonpoint sources, point source dischargers receive a credit toward their allocation. However, credit is only given for the control of nonpoint sources in existence since July 30, 1984, and is assigned based on site-specific data or a specific water quality modeling approach (CDPHE 2001). Regulations also maintain that a state-local partnership will provide the means for maintaining the quality of Dillon Reservoir to the level it was in 1982 (CDPHE 2001). Although regulations for the control of phosphorus have been developed, a better understanding of the contributions from each important source in the watershed, including naturally occurring phosphorus, is necessary.

As part of this project, numerous models were reviewed (Lemonds 2003). An evaluation of the selected models demonstrated that each can predict distinct aspects of watershed water quality and hydrology in different ways. Table G-1 shows the models reviewed and the capabilities of each. Watershed Analysis Risk Management Framework (WARMF), BASINS, and Water Quality Analysis Simulation Program (WASP4) modify and link several less comprehensive models to accomplish simulation of the watershed hydrology.

MODular three-dimensional finite-difference ground-water FLOW model (MODFLOW) and the MIKE SHE modeling system utilize various modules and packages to integrate surface-water and groundwater components. SWATMOD (a comprehensive basin model that links SWAT and MODFLOW) and MODBRANCH (combined groundwater-surface-water model that links BRANCH [Branch-Network Dynamic Flow Model] and MODFLOW) link MODFLOW, which is best at simulating groundwater flow, with two models that better model the surface water component.

Table G-1
Summary of Models Reviewed and Their Capabilities

Model	Surface Water	Ground Water	Vadose Zone	Transport and Transformation of N and P	Virus and Pathogen Transport
SWAT	○	○	○	○	~
HSPF	○	○	○	○	~
WARMF	○	○	○	○	○
MODFLOW-MT3D	○	○	○	○	~
SWATMOD	○	○	○	○	~
MODBRANCH	○	○	○	○	~
MANAGE	○	○	○	○	~
MIKESHE	○	○	○	○	~
WASP4	○	○	○	○	~
PLOAD	○	~	○	○	~
IDRISI-AgriFlux	○	~	○	○	~

Note: Relative thoroughness in simulating each component by the models is represented as more robust by large circles, less robust by small circles, and not capable of simulating component if no circle is present.

All of the models have some weaknesses and would not be expected to flawlessly describe the Dillon Reservoir watershed. Although WARMF has the practical Consensus model, which can be used for TMDL development, the model's simulation of groundwater flow is not the most accurate representation possible when compared to MODFLOW's simulation of groundwater flow. The Lasserre *et al.* (1999) GIS-linked model is specialized to model nitrate contamination, but more elements related to water supply must also be quantified. Donigian *et al.* (1996) contend that the water quality routines in Hydrological Simulation Program—Fortran (HSPF) are best for calculating detailed soil processes, like nutrient transformation, attenuation, leaching, and sorption, and the ability to incorporate changing land use and pollutant loads is an advantage compared to similar models. However, like the Lasserre *et al.* (1999) model, HSPF lacks the capability of groundwater quantity assessment. Similarly, SWAT's groundwater routines are simplistic, but it has strong capability in simulating surface-water hydrology and nutrient transport.

Watershed-Scale Modeling Methodology

This section provides information about watershed-scale modeling methodology, including:

- Approach
- Description of BASINS
- SWAT setup
- Simulation setup

Approach

Comprehensive and accurate watershed-scale modeling is an arduous task, which SWAT helps to simplify through several methods. First, SWAT was employed in a GIS environment to subdivide the Dillon Reservoir watershed into smaller, spatially-linked subwatersheds with grid-based information (Digital Elevation Model). Then, GIS coverages of land use, management practices, and soil type were employed to further divide each subwatershed into hydrologic response units (HRUs). An HRU is not a spatial subdivision but is a total area within a subwatershed that possesses similar land uses and soils. The HRUs simplify model simulations by combining together land uses and soil types that overlie each other in the GIS environment so that loadings from each HRU may be calculated efficiently and then summed for each subwatershed. The pollutant loadings from each subwatershed were then routed downstream through each subwatershed's outlet.

Free, public-domain data from government agencies were used for initial model development and for calibration. After initial development of the model, results were evaluated against observed values. Typically, SWAT models do not need rigorous calibration (Arnold *et al.* 1999; Arnold and Allen 1996; Fontaine *et al.* 2002; Manguerra and Engel 1998; Santhi *et al.* 2001; Srinivasan *et al.* 1998), but in this case, snowmelt parameters and variables accounting for orographic, or rain shadow, effects were adjusted.

In the application of the model, point-source discharges were incorporated. In addition, OWS in the watershed were included by methods described in the following sections. To fulfill the objectives of the study, a sensitivity study was performed to determine the influence of several parameters' effects on phosphorus loading into the Blue River.

Description of BASINS

BASINS was developed by the US EPA to solve watershed management and water quality issues (Lahlou *et al.* 1998). The three main objectives of BASINS are to (US EPA 2001):

- Support the examination of environmental data
- Assist in analysis of dynamic environmental systems
- Supply a structure for investigating different management scenarios

BASINS is not a model but a Windows-based front-end interface that allows input of common data to several different hydrologic models and provides a post-processor that can be used with the models. An important attribute of BASINS is its ability to simulate conditions using a whole-watershed approach. To simulate and predict water quality in a watershed, BASINS incorporates several features (US EPA 2001):

- National databases that include information on parameters such as cartographic, soil, and climate information
- Tools that allow for large- or small-scale assessment of an area
- Data evaluation and organization tools
- Watershed characterization reports
- Surface-water quality models
- Watershed models and postprocessors

A GIS provides the user environment through which BASINS incorporates a wide array of data. The GIS organizes spatial data and displays them in a logical format for the user. A benefit of the GIS integration is the ability of BASINS to carry out studies from the regional-scale to the reach-scale.

Through the GIS, BASINS incorporates several data extensions that assist in data management. The data extensions included are:

- Theme Manager—Enables coverages other than the default themes to be loaded into a BASINS view.
- Import BASINS Data—Gives users the option to import supplementary data sets in the form of shape or grid themes and then prepares them to work correctly with BASINS GIS operations.
- National Hydrographic Dataset (NHD) Download Tool—Enables users to download the NHD reach files for the specific study area directly from the US Geological Survey (USGS) NHD website and import the files into the BASINS view.
- Grid Projector—Converts ArcView/ArcInfo grid data between map projections and can project maps to and from latitude-longitude and different Cartesian coordinates. US EPA (2001) lists the projections that the Grid Projector is capable of completing.
- GenScn—Displays and interprets output from model applications, including HSPF and SWAT.
- WDMUtil—Assists with the management of Watershed Data Management (WDM) files, which HSPF (Bicknell *et al.* 1996) uses in modeling watersheds.

Through an extension, GenScn and WDMUtil can be opened directly from the BASINS interface.

The BASINS system also includes two watershed delineation tools to facilitate the analysis of smaller basins. The Manual Delineation Tool enables the user to manually delineate a watershed into subwatersheds by his knowledge of the basin topography and with the use of a mouse. The Automatic Delineation Tool uses the Digital Elevation Model (DEM) for the area and user-specified limits for the size and number of subwatersheds to calculate subwatersheds.

BASINS 3.0 includes interfaces with four models for watershed management:

- QUAL2E (Brown and Barnwell 1987)—An instream water quality and eutrophication model. The model can simulate the fate and transport of chemical constituents in streams with a given flow condition (US EPA 2001).
- HSPF (Bicknell *et al.* 1996)—A model linked to BASINS through the WinHSPF interface. HSPF can simulate point and nonpoint sources, flow, and water quality.
- SWAT—A physically-based model developed to simulate varying land management practices, land uses, and agricultural chemical yields (Arnold *et al.* 1998) developed by the Agricultural Research Service (ARS), a branch of the US Department of Agriculture (USDA). With data available in BASINS, SWAT can support long-term studies of flow and water quality predictions.
- PLOAD—A GIS-based model designed by CH2M Hill. For any user-defined pollutant, PLOAD predicts nonpoint-source loadings on an average annual basis (US EPA 2001). PLOAD is the simplest of the four models included in BASINS. PLOAD was developed as a simple model that could be customized for a broad range of applications, including storm water permitting, watershed management, and reservoir protection (US EPA 2001).

Included in the BASINS analysis system are other important features. One of these is a package of several data assessment tools. TARGET, ASSESS, and Data Mining are geographically-based tools that enable the user to gain perspective and form preliminary relationships between water quality data and potential causes of impaired waters (US EPA 2001).

TARGET performs broad water quality assessments of the entire area extracted from the BASINS data set for the study at a state or regional level. Based on the water quality parameters and thresholds selected by the user, TARGET is able to rank watersheds and give the results in a report format.

Capabilities of ASSESS include water quality and point-source discharge evaluation for a grouping of watersheds or a single watershed. In water quality assessment, the water quality statistical summaries database is used, and the Permit Compliance System (PCS) stations' data are used for point-source discharge assessment. ASSESS can be useful to study watersheds of concern after preliminary evaluations using TARGET have identified specific areas of water quality decline.

The Data Mining tool helps users to obtain and visualize water quality and point-source loading information available through the BASINS data sets. Of the three assessment tools, Data Mining enables the greatest large-scale examination of an area and is able to identify endangered stream reaches. Data Mining supplies summaries of water quality for six four-year periods from 1970 to 1997, supports analyses of monitoring programs, and identifies geographic, time period, and chemical constituent data gaps.

The four models included in BASINS (SWAT, QUAL2E, HSPF, and PLOAD) each provide solutions to different modeling questions. After review of the four models, it was determined that the two models most applicable to the research objectives were HSPF and SWAT because of their ability to simulate detailed watershed processes. The capabilities of HSPF and SWAT are described in the following two sections.

HSPF

HSPF (Bicknell *et al.* 1996) was redeveloped from the early 1960s Stanford Watershed Model (Crawford and Linsley 1966). HSPF can model many parameters, including surface runoff, groundwater recharge, and transport processes for fecal coliform, nitrogen species, and organic-phosphorus on both pervious and impervious surfaces. Simulation results show time histories of runoff, flow rate, water quantity, and water quality (solute concentrations) at any point in a watershed (Donigian and Huber 1991). Extensive data are needed for input into the model. According to Lohani *et al.* (2002), the strength of HSPF is its comprehensive nature and ability to simulate years of hourly rainfall, soil moisture, and evaporation data.

HSPF has three main modeling components, including modules that simulate hydrologic processes for pervious land, impervious land, and routing through reservoirs and stream reaches. HSPF can simulate spatial variability by dividing the watershed into homogeneous land segments based on land use, soil properties, and stream reach uniformity (Chen *et al.* 1995). Only the sections that model the water budget for pervious and impervious land segments and hydraulic behavior are needed for basic simulations with HSPF (Engelmann *et al.* 2002). Equations from the LANDS module of the Stanford Watershed Model IV were used in HSPF to simulate surface runoff from pervious areas, surface runoff from impervious areas, interflow from pervious areas, and groundwater flow. Algorithms for production and removal of sediment in HSPF were taken from the ARM and NPS model (Bicknell *et al.* 1996), and equations were then added to HSPF to simulate soil scour.

For simulation of each land segment, HSPF uses conceptual and physical parameters. Some of the physical parameters needed for modeling include:

- Total watershed area
- Stream lengths
- Surface area of streams and reservoirs
- Land slope
- Manning roughness
- Infiltration rate
- Interception capacities of vegetation

Conceptual parameters required include:

- Soil storage capacity
- Evapotranspiration rate
- Groundwater recession parameter

Lohani *et al.* (2002) find three major limitations in the usage of HSPF. First, they cite the complexity of the model. HSPF requires large amounts of time to prepare time-series inputs, and since the model contains so many parameters, trial-and-error calibration and validation also demand a great deal of time. To expedite the calibration process, HSPFParm (Donigian *et al.* 1999) and HSPEXP (Lumb *et al.* 1994) were created, but Lohani *et al.* (2002) suggest that the process still remains laborious.

The second limitation of HSPF is the user interface. Land-use and watershed parameters are kept in the User Control File (UCI), which is in FORTRAN format. To change land uses for different growth and development scenarios, the UCI file must be recalculated for each new scenario, which can be a difficult task. Manual formatting and constant alterations can also lead to errors in the FORTRAN format, which may not necessarily be detected by HSPF (Lohani *et al.* 2002).

The third weakness of HSPF is its output interface. Lohani *et al.* (2002) describe that land use changes that affect the hydrology of a watershed are evaluated quantitatively with statistics and qualitatively with visual examination of hydrographs. However, HSPF output is located in the WDM file, which is in binary format. The US Geological Survey (USGS) and EPA's DOS-based ANNIE program can graph and show results, but the process is arduous according to Lohani *et al.* (2002). In addition, graphics are not easily imported into other applications.

SWAT

SWAT was developed to predict the effect of management practices on water, sediment, nutrient, and pesticide yields at the watershed scale. SWAT was originally developed to simulate hydrology and surface-water quality in agricultural basins. SWAT incorporates physical data and can simulate processes including (Neitsch *et al.* 2001b):

- Surface runoff
- Return flow
- Percolation
- Evapotranspiration
- Crop growth
- Nutrient and pesticide loading
- Water transfer
- Snowmelt
- Anthropogenic effects

Supplemental information on the data requirements and theoretical basis of SWAT is presented in the Supplemental Information: Theoretical Formulation of SWAT section, which follows the References section in this appendix.

Since SWAT is primarily a surface-water model with limited groundwater simulation capabilities, SWATMOD (Sophocleous *et al.* 1999) was developed to evaluate long-term water management scenarios by integrating the surface water and groundwater components of a watershed into one model. The existing models SWAT (Arnold *et al.* 1993) and MODFLOW (McDonald and Harbaugh 1988) were linked, and a GUI and decision-support system were developed to address issues related to water rights and management of the watershed. SWATMOD is not publicly available. SWAT was developed by the USDA, Agricultural Research Service (USDA-ARS) as an expansion of the Simulator for Water Resources in Rural Basins (SWRBB) model (Arnold and Williams 1994) from the subwatershed scale to the basin scale. SWAT includes algorithms for simulating contaminant transport, stream and lake water quality, weather generation, and interfacing with GIS primarily for simulation of surface water hydrology (Deliman *et al.* 1999).

SWATMOD was applied to a basin in south-central Kansas in order to specifically simulate water-shortage periods when water-supply issues might be most significant (Sophocleous *et al.* 1999). With the use of a decision support system, the user is able to test several unique management scenarios by changing model conditions, performing simulations, and viewing the new results and impact of the changes graphically. Part of the application of SWATMOD also included the calibration of the model by trial-and-error and parameter-estimation methods (PEST) (Doherty *et al.* 1994) using historical stream flow and water levels from 1955 to 1980. A sensitivity analysis concluded that surface yield and total recharge are most sensitive to the hydraulic conductivity of the pond bottoms and water-storage properties of the soil (Sophocleous *et al.* 1999).

SWAT Setup

The following section describes the application of the SWAT model applied to the Dillon Reservoir watershed. Data were obtained from several different sources. Most of the data sources were public-domain databases, which were available through government agencies. Factors involved in model setup include:

- Watershed delineation
- Development of hydrologic response units
- Weather attributes
- Input adaptation
 - Point-source discharge attributes
 - Reservoir attributes
 - Subbasin attributes (attributes specific to each subwatershed, which include management practices that incorporate phosphorus from OWS into the subsurface)

Watershed Delineation

The SWAT ArcView interface contains a Watershed Delineation tool. This tool is used to subdivide the watershed of interest into smaller subwatersheds that are hydrologically related. The watershed delineation process requires ArcView GIS 3.x and the Spatial Analyst extension. If the model is implemented through the BASINS interface, then a manual delineation option is available. Using this option, the Spatial Analyst extension is not required.

In order to delineate subwatersheds in SWAT, a DEM is required. For the application to the Dillon Reservoir watershed, a USGS 300-meter resolution, 1-degree DEM was employed. Information extracted and calculated from the DEM and used in the model includes overland slope and slope length.

Development of Hydrologic Response Units (HRUs)

An HRU is based on land-use and soil information incorporated into SWAT. An HRU is defined as a unique land-use/soil combination within a subwatershed. HRUs are smaller divisions of the subwatershed that are not spatially related to each other (Neitsch *et al.* 2001b). SWAT uses topography, land use, and soils information to calculate the area and hydrologic parameters of each HRU.

The land-use information, which was available through BASINS, is a 1:250,000-scale quadrangle of Landuse/Landcover Geographic Information Retrieval Analysis System (GIRAS) spatial data. The land use/land cover digital data were collected by the USGS and converted to ARC/INFO by the US EPA.

The soil attributes utilized are part of the State Soil Geographic (STATSGO) Database, which was developed by the National Cooperative Soil Survey (USDA-NRCS Soil Survey 2002). The soil maps were compiled from more detailed soil survey maps, and where soil survey maps were not available, data on geology, topography, vegetation, climate, and Land Remote Sensing Satellite (LANDSAT) images were integrated into one unit. Each soil map unit is linked to attributes in the Map Unit Interpretations Record relational database, which provides the proportionate extent of the component soils and their properties (US EPA 2002a).

In the STATSGO database, soil attributes are stored in polygon format. Each polygon includes multiple soil series with information on its areal percentage of the polygon. In the SWAT ArcView Interface, the dominant soil series is selected, and the interface extracts properties for the model from a relational database. A relational database is a type of database that associates objects with complex relationships into a more efficient and easily retrievable form than traditional databases, which only link repeated fields within several separate databases. Examples of the properties extracted include soil texture, bulk density, hydraulic conductivity, available water capacity, organic carbon, and total depth of soil.

After the land-use and soil data were imported into the model, HRUs were determined. Only the percentages of soils and land uses within each subbasin are known. The HRU represents a total area in the subbasin with the same soil/land-use characteristics. No interaction between HRUs in a subwatershed is assumed. Loadings from each HRU within a subbasin associated with runoff (such as nutrients and sediment) are calculated individually. Then, using hydraulic properties of the HRUs, one total loading for the subwatershed is calculated by summing weighted averages of the loadings for each HRU based on the total area defined for each HRU in the subwatershed.

Multiple HRUs were assigned to each subwatershed in the model. Threshold levels may be set to eliminate minor soil and land uses. Neitsch *et al.* (2001b) recommend a land-use threshold of 20% and a soil threshold of 10%. These threshold values were used for the application to the Dillon Reservoir watershed. The land-use threshold indicates that if a land use covers less than 20% of the area of the subbasin, the land use is eliminated and its area is then reallocated to the remaining land uses. The soil threshold restricts the number of HRUs by eliminating minor soils within each land use that is above the land-use threshold.

DiLuzio *et al.* (2001) suggest one to ten HRUs per subwatershed. In the setup of the model, seven land uses and three soil types were demarcated for the watershed. For each subwatershed there were one to five HRUs defined. The HRUs lend increased accuracy to the calculation of loadings within a subwatershed and provide a more accurate physical description of the water balance. For example, different land uses and soil combinations support different plant species, which can affect residue cover and runoff quantity and quality. Accounting for plant diversity within a subwatershed allows for greater accuracy in the calculation of runoff that enters the main stream reach (Neitsch *et al.* 2001b). In addition, by representing areas with different soils and land uses with HRUs, the model is more capable of accounting for the differences in evapotranspiration and other hydrologic conditions of different land covers (DiLuzio *et al.* 2001).

Weather Attributes

After delineation of the subwatersheds and HRUs, weather data for the watershed was defined. Weather information incorporated into the model includes precipitation, air temperature, solar radiation, and wind. Figure G-2 shows the distribution of weather stations within the watershed. The availability and acquisition of the different types of weather data is described in the following subsections.

Precipitation data were available from the National Climatic Data Center (NCDC) and the Natural Resources Conservation Service's (NRCS) National Water and Climate Center SNOTEL Data Network. Six stations were obtainable within the Dillon Reservoir watershed (Figure G-2). Daily precipitation values were incorporated into the model.

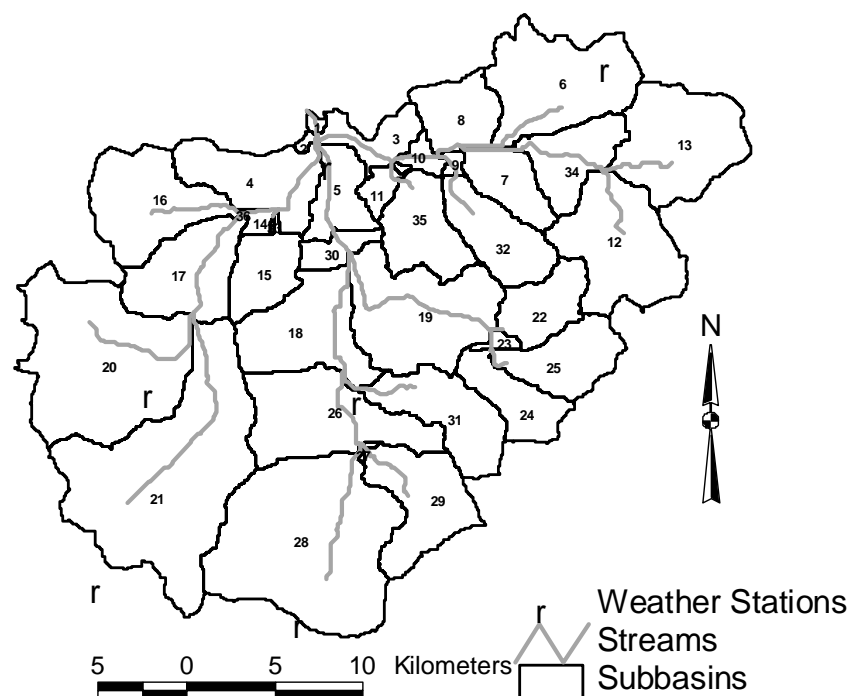


Figure G-2
Distribution of Weather Stations Within the Dillon Reservoir Watershed

Temperature data were available from the NCDC and the NRCS National Water and Climate Center SNOTEL Data Network. Six stations were accessible within the Dillon Reservoir watershed (Figure G-2). Daily minimum and maximum temperature values were incorporated into the model.

Wind data were not as readily available as temperature and precipitation data. Wind speeds were acquired from Eagle County Airport in Gypsum, Colorado. The airport is about 20 miles (32 km) from the center of the Dillon Reservoir watershed. Wind speed information is only required if the Penman-Monteith evapotranspiration method is used in the model. For the Dillon Reservoir watershed model application, wind data were not incorporated.

Solar radiation data were obtained from the US Database feature that is incorporated into SWAT (US EPA 2002a). The station from which data were extracted is about 15.5 miles (25 km) from the center of the Dillon Reservoir watershed. Daily radiation values were incorporated into the model.

Input Adaptation

Input adaptation for the application to the Dillon Reservoir watershed included definition of point-source discharges into Blue River and its tributaries, Dillon Reservoir levels, reservoir outflow, and information specific to particular subwatersheds.

Examples of information specific to each subwatershed include:

- Soil properties
- Stream-water chemical properties
- Groundwater properties
- Stream-routing parameters
- Consumptive water use
- Management practices

Point-Source Discharge Attributes

Point-source discharges incorporated into the model include:

- Alpine Rock Company McCain Pit
- Arapahoe Basin Ski Area WWTP
- Breckenridge Sanitation District McDill Placer WWTP
- Breckenridge Sanitation District South Blue River WWTP
- Breckenridge Sanitation District Valley of the Blue WWTP
- Breckenridge WWTP
- Copper Mountain WWTP
- Frisco Wastewater Treatment Plant (WWTP)
- Iowa Hill Water Reclamation
- Ralston Resorts—Keystone WWTP
- Snake River WWTP
- Vail Pass Rest Area
- Wayne Bristol Water Supply

The Breckenridge WWTP is the largest of the point-source discharges. Figure G-3 shows the location of the point source discharges incorporated into the model. Since daily loadings were not available for some sites, monthly averages of daily loadings were employed in the model. When point sources are added in the model, the loading data are incorporated directly into the stream channel network. Examples of information included in the point-source discharge data are mass loading per day of nitrate (NO_3^-), phosphate as P ($\text{PO}_4\text{-P}$), and ammonia (NH_3), and total outflow per day.

Point-source data were obtained from the US EPA, Office of Water Permit Compliance System (US EPA 2002a), which is a national computerized management information system. Data from the National Pollutant Discharge Elimination System (NPDES) is managed by the automated permit compliance system. The permitting program through NPDES regulates discharges from wastewater treatment facilities.

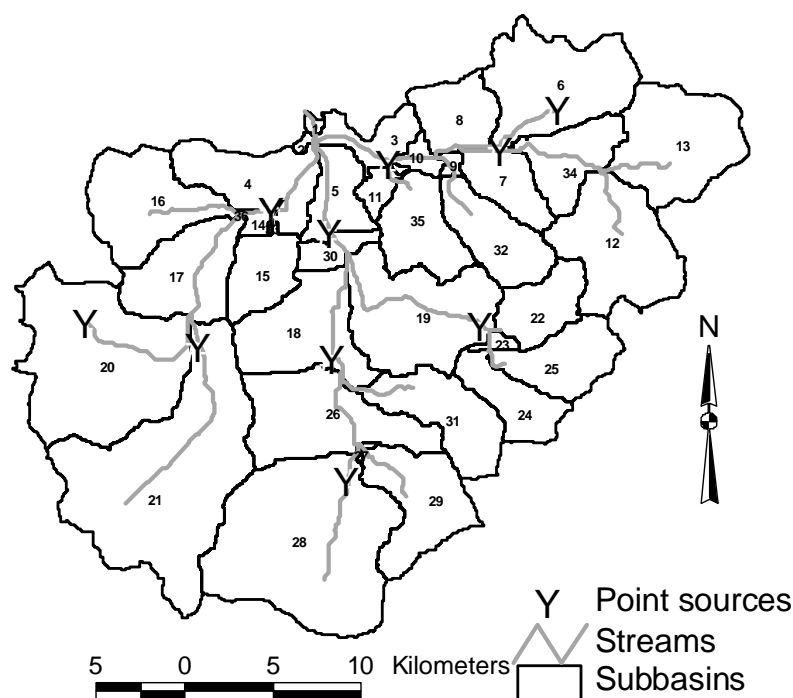


Figure G-3
Location of Point-Source Discharges Incorporated Into the SWAT Model

Reservoir Attributes

SWAT enables the definition of several reservoir parameters. Examples include the reservoir surface area when the reservoir is filled to the principal spillway, volume of water needed to fill the reservoir to the principal spillway, and initial reservoir volume for the start of the simulation. In addition, the amount of water removed from the reservoir for use outside the watershed is taken into account. This aspect is especially significant in the application to the Dillon Reservoir watershed since the City of Denver, Colorado, removes water from the reservoir for consumptive use. Measured daily outflow at Dillon Dam also was incorporated into the model. The outflow data from the dam were obtained from the USGS, and Denver Water (Denver Water 2002) provided consumptive use information. Initial concentrations of nutrients in the reservoir may also be assigned in the reservoir input file, but in the model construction only physical parameters of the reservoir were incorporated.

Subbasin Attributes

For the input files specific to subwatersheds, the soil properties, stream-water chemical properties, groundwater properties, stream-routing parameters, consumptive water use, and management practices may be refined to better represent the watershed. To alter these properties in SWAT, the user chooses the subbasin, land use, and soil for which modifications are to be made. For initial development of the model, only consumptive water use and management practices were customized.

In SWAT, consumptive water use represents water removed from the basin. Water may be removed from the shallow aquifer, deep aquifer, reach, pond, or reservoir. As previously described, the City of Denver removes water from the Dillon Reservoir watershed through the Roberts Tunnel. There are several diversions (water removal from the basin) besides Roberts Tunnel. Bemrose-Hoosier, McCullough-SP, and Monte Cristo are three agricultural diversions near Hoosier Pass that transport water south out of the watershed. Data for the flow of these diversions were obtained from the USGS. In the model, the water was removed directly from the reach. Monthly average values of flow were incorporated into SWAT for this type of diversion. This approach worked well when considering the diversions transport water primarily during the summer months.

To incorporate OWS into the model, a fertilizer management practice was used. Jeff Arnold, one of the authors of SWAT, suggested that this would be the most practical way to implement OWS into the model because there are currently no algorithms in SWAT to rigorously simulate injection of water below the ground surface, as occurs in OWS (personal communication, Jeff Arnold, Agricultural Research Service 2002).

To complete this task, the mass input rate of OWS pollutants of concern must equal the mass of nutrient input by fertilizer. Thus, a summary of OWS effluent flow rates and water quality parameters was compiled. Then, fertilizer application input parameters were adjusted in SWAT to achieve the appropriate nutrient mass input rate to the subsurface.

Several authors have published that typical loading rate values for OWS range from 1 to 8.4 cm day⁻¹ (Kirkland 2001; McCray *et al.* 2000; Siegrist and Boyle 1987; Van Cuyk *et al.* 2001). Kirkland (2001) completed an extensive review of published information concerning OWS effluent composition. She found the median concentration of total N to be 44 mg N L⁻¹, the median concentration of organic N to be 14 mg N L⁻¹, the median concentration of ammonium (NH₄⁺) to be 60 mg N L⁻¹, and the median concentration of nitrate (NO₃⁻) to be 0.20 mg N L⁻¹. For phosphorus as P (PO₄-P), Kirkland (2001) found the median concentration in OWS effluent to be 10 mg P L⁻¹. For the relatively large population associated with a watershed, median values for OWS parameters are appropriate.

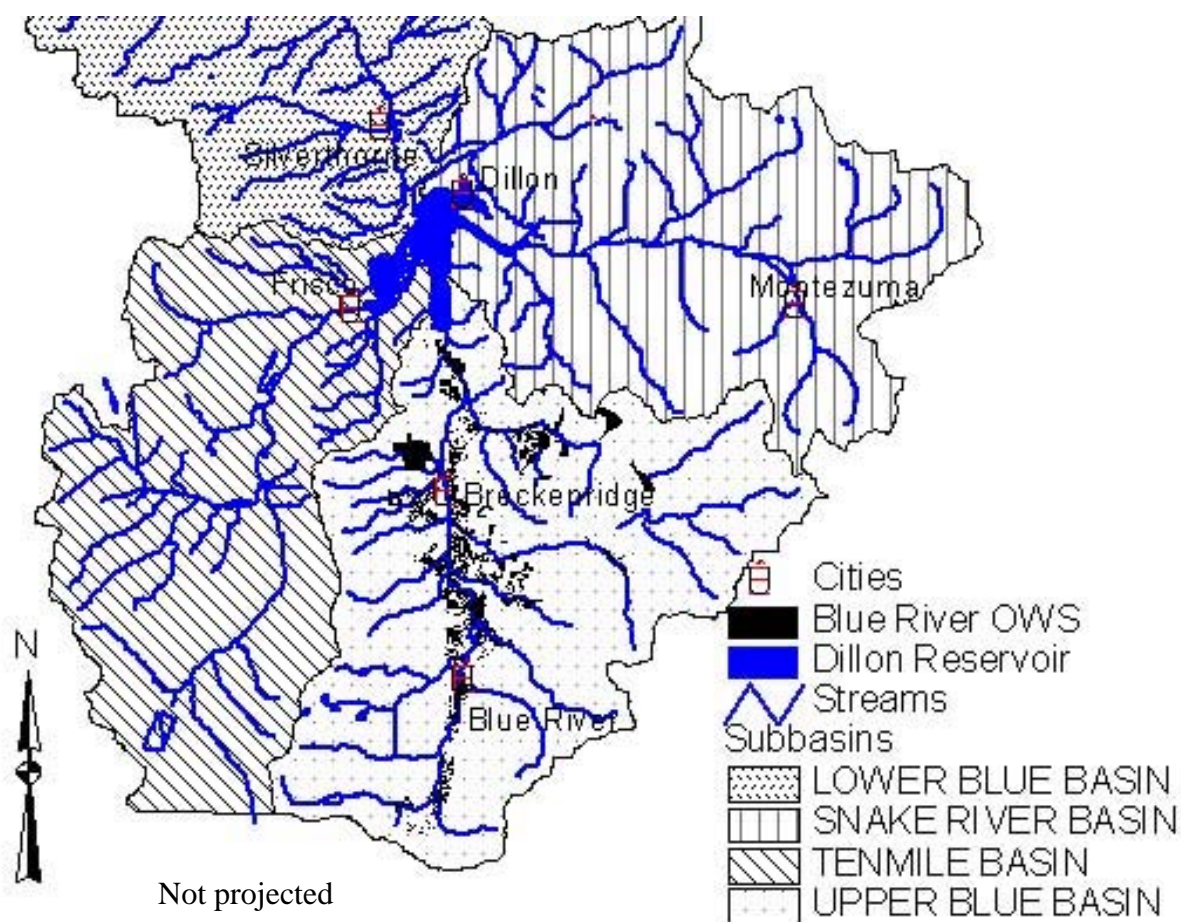
The nutrient phosphorus was used in this research as an example OWS pollutant. To determine the mass of phosphorus per hectare that is loaded per day by OWS for each subwatershed, the following calculation, using subwatershed 28 as an example, was completed using the median value of OWS loading and phosphorus concentration:

$$\left(\frac{10 \text{ mgP}}{\text{L}}\right) \cdot \left(\frac{165 \text{ L}}{\text{cap} \cdot \text{day}}\right) \cdot \left(\frac{1455 \text{ cap}}{\text{subwatershed 28 area}}\right) \cdot \left(\frac{\text{subwatershed 28 area}}{1695 \text{ ha}}\right) \cdot \left(\frac{1 \text{ kg P}}{10^6 \text{ mg P}}\right) = \frac{0.00142 \text{ kgP}}{\text{ha} \cdot \text{day}}$$

Equation G-1

The result is 0.00142 kg P ha⁻¹ day⁻¹. Implementing the fertilizer management practice in seven-day intervals was assumed to adequately represent OWS effluent processes, so the result from Equation G-1 is multiplied by seven. The product is 0.01 kg P ha⁻¹ 7 days⁻¹. This calculation was performed for all subwatersheds where OWS application was simulated.

The areal distribution of the applied manure was determined based on the distribution of OWS along the Blue River (Figure G-4). Manure was applied to HRUs that represented land uses and soils where OWS were located in each subwatershed. Lemonds (2003) describes in detail the areal distribution of the fertilizer application.



Note: Small dots show the location of OWS.

Figure G-4
Distribution of OWS Along the Blue River

Figure G-5 shows the subwatersheds where manure was applied, but note that since HRUs do not represent spatial areas, these areas can not be shown on a map.

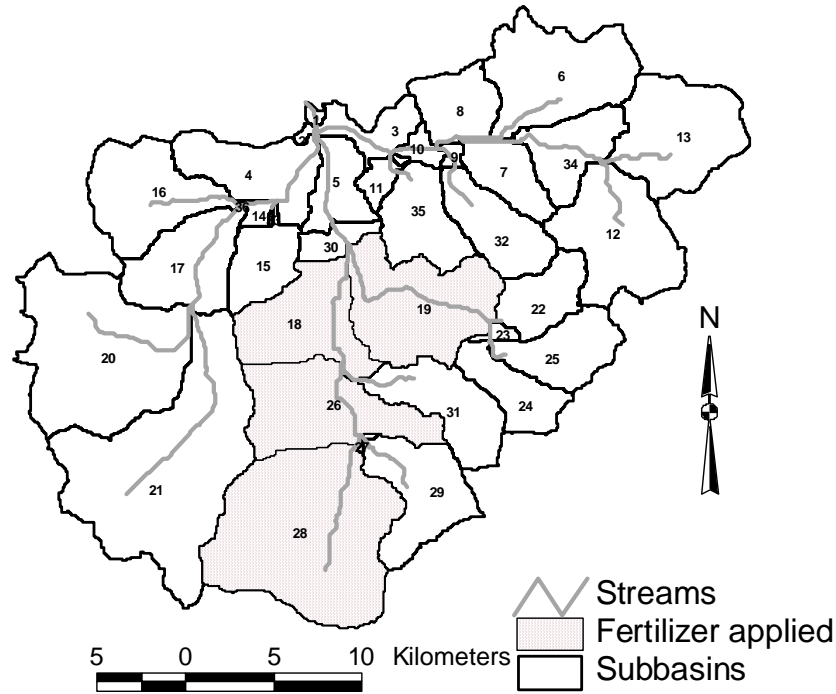


Figure G-5
Subbasins Where Fertilizer Application Was Used to Simulate OWS Inputs for SWAT Modeling

SWAT enables the user to define the type of fertilizer or manure applied in the watershed. Of the options available, swine manure most closely matches that of human waste (personal communication, Robert Siegrist, Colorado School of Mines 2002). Therefore, swine manure was applied. Quality parameters defined for the swine manure in SWAT were $0.015 \text{ kg mineral P (kg fertilizer)}^{-1}$ and $0.001 \text{ kg organic P (kg fertilizer)}^{-1}$. OWS effluent occurs as the mineral form of P (Kirkland 2001). By applying $0.620 \text{ kg manure per hectare every seven days}$, the correct amount of P is applied:

$$\left(\frac{0.016 \text{ kg total P}}{\text{kg fertilizer}} \right) \cdot \left(\frac{0.620 \text{ kg fertilizer}}{\text{ha} \cdot 7 \text{ days}} \right) = \frac{0.01 \text{ kg P}}{\text{ha} \cdot 7 \text{ days}} \quad \text{Equation G-2}$$

SWAT enables manure to be applied below the top 10 mm of soil so that it has minimal interaction with surface runoff, which is desired for OWS application. Manure is applied in the solid phase. OWS is normally applied in the liquid phase. However, SWAT assumes equilibrium mass transfer between the solid and aqueous phases in the active mineral pool of P (see the Supplemental Information: Theoretical Formulation of SWAT section, which follows the References section in this appendix), so the application methods yield the same result. Note that SWAT lacks the ability to simulate pathogen transport, including bacteria and viruses, which occur in OWS effluent (personal communication, Susan Neitsch, Spatial Sciences Laboratory-Texas A&M University 2002)

OWS pollutants are potentially transported to the groundwater by infiltrating water. The manure application does not incorporate this component. Irrigation water is not a good method to simulate OWS water input because this irrigation water can runoff the surface (unlike OWS in the study area) and would also adversely influence the water budget. Note that in these simulations, domestic pumping was assumed to equal OWS input. However, recharge of water due to OWS input is insignificant compared to precipitation at the subwatershed scale. Thus, the water added from precipitation is assumed to infiltrate the wastewater pollutants. The justification for this assumption is provided as follows.

Kirkland (2001) found that the median household wastewater flow rate is 165 L cap⁻¹ day⁻¹ and that this value is similar to the value reported in the *Design Manual for Onsite Wastewater Treatment and Disposal Systems* (US EPA 1980). Information on the number of persons serviced by OWS in the watershed was also available from the Summit County Environmental Health Department. For example, the amount of water that would have to be applied over subbasin 28 if water were incorporated into the OWS simulation in SWAT is

$$\left(\frac{165 \text{ L}}{\text{cap} \cdot \text{day}} \right) \cdot \left(\frac{1 \times 10^{-3} \text{ m}^3}{1 \text{ L}} \right) \cdot \left(\frac{1455 \text{ people}}{1695 \text{ ha}} \right) \cdot \left(\frac{1 \text{ ha}}{1 \times 10^4 \text{ m}^2} \right) \cdot \left(\frac{1000 \text{ mm}}{1 \text{ m}} \right) = \frac{0.014 \text{ mm}}{\text{day}}$$

Equation G-3

where 165 L cap⁻¹ day⁻¹ is the median household wastewater flow rate, 1,455 people is the number of people in the subwatershed serviced by OWS, 1,695 ha is the area of the HRU where manure was applied, and 0.014 mm is the amount of water per day that would need to be applied if water from OWS were incorporated into SWAT.

The average daily precipitation at the Breckenridge climate station, where precipitation values are most representative of the precipitation received where OWS are located along Blue River, is 1.5 mm. The average value from 1990 to 2002 of precipitation minus runoff and evapotranspiration simulated by SWAT for this area (Figure G-5) is 0.32 mm H₂O day⁻¹. At the subwatershed scale, OWS input is less than 5% of the recharge due to precipitation. For this reason, combined with the fact that SWAT cannot currently simulate a subsurface input of infiltrating wastewater, the effect of infiltrating wastewater in the watershed-scale simulations was neglected. However, focused application of wastewater is an important mechanism for vadose-zone transport of wastewater and wastewater pollutants at the site scale. For watershed scale simulations, however, this assumption is considered appropriate.

Simulation Setup

The final step in model application is setup of the simulation. The input for this part of SWAT enables users to define information regarding the channel water-routing method, the method used for calculating PET, print-out frequency, and parameters that affect the entire watershed (such as snowmelt parameters). The period of simulation is also defined in this final step.

Annual print-out frequency was initially used to assess simulation results, although monthly print-out frequency was used in the calibration stage. The variable storage stream-water routing method was incorporated and is described in more detail in Lemonds (2003). For the initial simulation, watershed parameters, including those that affect snowmelt, snow formation, and nutrient enrichment, were left unaltered from the default value assigned by SWAT.

Brady and Weil (1999) define evapotranspiration as the combined loss of water from a given area, and during a specified period of time, by evaporation from the soil surface and by transpiration from plants. The PET describes how fast water vapor would be lost from a densely vegetated plant-soil system if soil water content were continuously maintained at an optimal level (Brady and Weil 1999)

Three methods for calculating PET are available in SWAT. The Penman-Monteith calculates the most accurate estimates of evapotranspiration when PET is calculated on an hourly basis and then summed to attain daily values (Neitsch *et al.* 2001a). However, using mean daily input values for the Penman-Monteith method can create large errors due to diurnal distributions of wind speed, humidity, and net radiation (Neitsch *et al.* 2001a). The Priestly-Taylor equation will underestimate PET in semiarid or arid environments because the advection component of the energy balance is significant in these areas (Neitsch *et al.* 2001a). For the application to the Dillon Reservoir watershed, the Hargreaves method was chosen. This is the simplest of the three methods, but since sub-daily wind, solar radiation, and relative humidity data were not available, it provided the best simulation of PET in the Dillon Reservoir watershed.

SWAT Calibration to Streamflow

This section describes the calibration approach utilized for the SWAT model applied to the Dillon Reservoir watershed and the changes made to initial parameters during calibration. SWAT is based primarily on physical parameters; that is, the parameters that can be measured in the field. Several authors have stated that because SWAT uses mostly measured parameters and selects input from readily available GIS databases, it does not require arbitrary or tedious calibration procedures (Arnold *et al.* 1999; Arnold and Allen 1996; Fontaine *et al.* 2002; Manguerra and Engel 1998; Santhi *et al.* 2001; Srinivasan *et al.* 1998). In addition, Santhi *et al.* (2001) write, “It is important to understand that SWAT is not a “parametric model” with a formal optimization procedure (as part of the calibration process) to fit any data.” Instead, variables incorporated in SWAT that are not physically-based, but are based on empirical equations from physical data, (such as runoff curve number) may be adjusted. However, adjustments may be made to other physically-based input parameters assuming that the adjustments remain within the range of measured values of each specific parameter.

For the application of SWAT to the Dillon Reservoir watershed, parameter adjustment was necessary to obtain a reasonable match of simulation results to observed streamflow at several gaging stations, a necessity for assessing pollution transport at the watershed scale. This section describes the parameters that were modified and the procedures used to determine the new values. After calibration to streamflow, the model was used as a base case for a sensitivity study to assess the importance of the hydrologic and phosphorus input parameters for which few measured data exist.

Calibration Procedure

To calibrate the model's streamflow simulation, measured streamflow from two USGS gaging stations were used. The stations are located on the Blue River. One is in the town of the Blue River near the headwaters, and the other is located approximately one-half mile upstream of Dillon Reservoir (Figure G-6). The model simulation was executed for 11 years (1990–2000). The first two years were not examined in order to reduce the inaccuracies in preliminary calculation of state variables on the calibration parameter values, such as soil water content and residue cover as suggested by Fontaine *et al.* (2002) and Santhi *et al.* (2001). Streamflow was the most important element calibrated in the model because transport of nutrients to Dillon Reservoir is extremely dependent on streamflow.

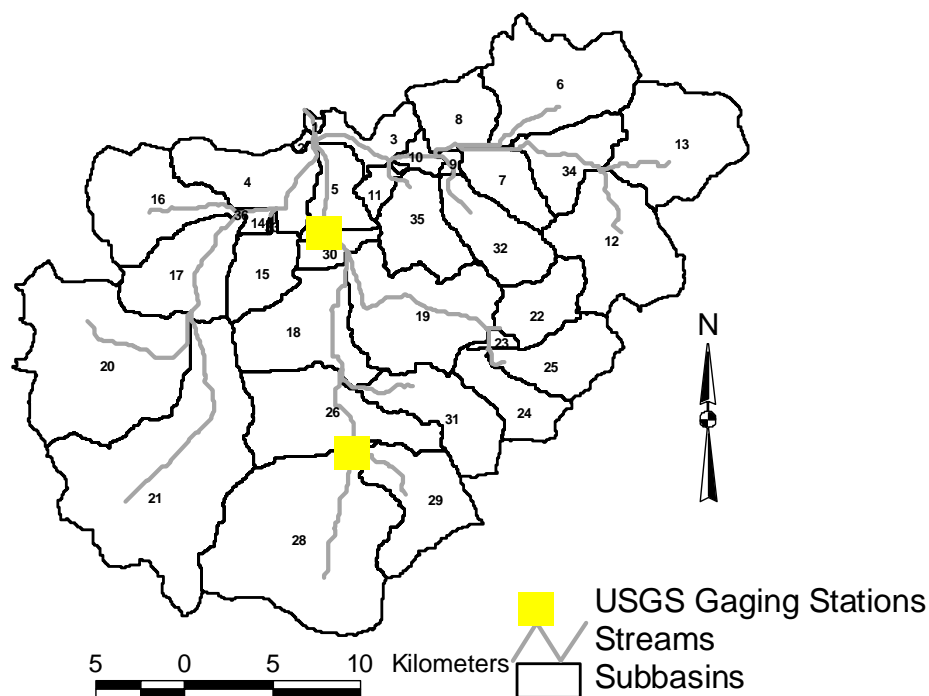


Figure G-6
Location of the Two USGS Gaging Stations Used in the Streamflow Calibration of the Model

Initial Parameter Adjustments

As Neitsch *et al.* (2001b) suggest in the SWAT User's Manual, annual streamflow (rather than daily or monthly) data were analyzed first. The model simulation was conducted using the watershed input data described in the Supplemental Information: Theoretical Formulation of SWAT section. Visual comparison of annually averaged streamflow data versus simulated values revealed an initial under prediction of flow (Figure G-7).

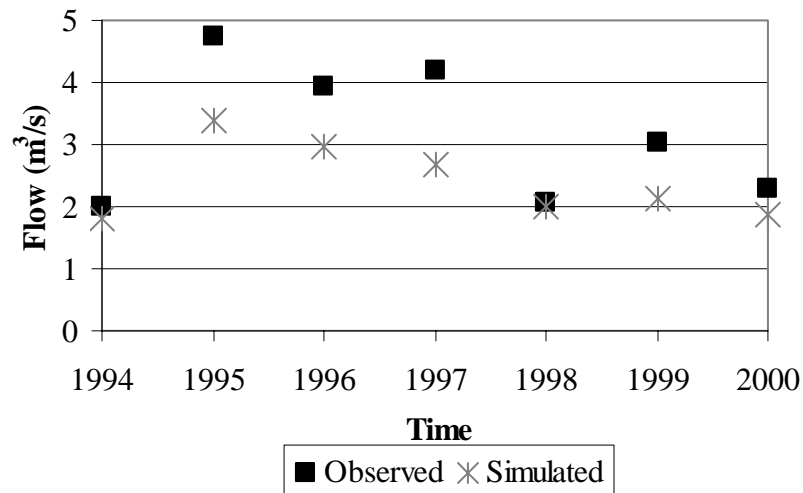


Figure G-7
Annually Averaged Streamflow Data for the Blue River Just Upstream of Dillon Reservoir
Versus Simulated Values

The runoff curve number, groundwater variables, and soil properties were varied. Groundwater parameters include:

- Groundwater revap (water movement from the shallow aquifer to the unsaturated zone) coefficient
- Threshold depth of water in the shallow aquifer for revap to occur
- Baseflow recession constant
- Deep aquifer percolation factor
- Specific yield of the shallow aquifer
- Groundwater delay time for the shallow aquifer
- Initial groundwater height

Soil properties include:

- Available water capacity
- Saturated hydraulic conductivity
- Soil depth
- Soil bulk density

Table G-2 shows the soil properties, groundwater parameters, and runoff curve numbers that are employed and the values used in the model. Ultimately, the aforementioned variables were kept at their initial values, except for the runoff curve number, which was increased by 8% for each land use/soil type.

In the absence of measured data, the initial values were reasonable and similar to values measured by Smith *et al.* (2002) and values reported by Fetter (1994). The curve number uses three hydrologic conditions (good, fair, and poor), and four distinct Hydrologic Soil Groups (A, B, C, and D). The majority of soils in the Dillon Reservoir watershed are characterized as Hydrologic Soil Group B, and their condition is “good.” Despite altering several of the variables that have improved SWAT models in the past (Arnold and Allen 1996; Santhi *et al.* 2001; Srinivasan *et al.* 1998), the timing and magnitude of flow did not improve.

Table G-2
Soil Properties and Groundwater Parameters That Are Used by SWAT

Parameter	Units	Parameter Value	
Soil Bulk Density ^a	g cm ⁻³	Soil Layer 1	1.42
		Soil Layer 2	1.50
		Soil Layer 3	1.45
		Soil Layer 4	1.50
Saturated Hydraulic Conductivity ^a	mm hr ⁻¹	Soil Layer 1	30.0
		Soil Layer 2	14.0
		Soil Layer 3	4.10
		Soil Layer 4	28.0
Available Water Capacity ^a	mm mm ⁻¹	Soil Layer 1	0.12
		Soil Layer 2	0.09
		Soil Layer 3	0.06
		Soil Layer 4	0.04
Soil Depth ^a	mm	Soil Layer 1	406.4
		Soil Layer 2	660.4
		Soil Layer 3	1524.0
		Soil Layer 4	1778.0
Groundwater “Revap” Coefficient: Controls movement of water from shallow aquifer up to unsaturated zone	dimensionless	0.02	
Threshold depth of water in shallow aquifer for revap to occur	mm	1.0	
Baseflow Recession Constant	dimensionless	0.048	

Table G-2
Soil Properties and Groundwater Parameters That Are Used by SWAT (Cont.)

Parameter	Units	Parameter Value
Deep Aquifer Percolation Factor: Fraction of percolation from the root zone that reaches the deep aquifer	dimensionless	0.05
Specific Yield of Shallow Aquifer ^b	dimensionless	0.03
Groundwater delay time for shallow aquifer	days	31.0
Initial groundwater height ^b	m	5
Runoff curve number ^c	dimensionless	63–91, depending on land use and soil type

^aParameter value extracted from STATSGO Database (USDA-NRCS Soil Survey 2002)

^bParameter value within reasonable range of values in Fetter (1999) or Smith *et al.* (2002)

^cParameter value based on SCS runoff equation (Soil Conservation Service 1972)

Temperature and Precipitation Corrections

SWAT was originally developed for basins with an agricultural influence. Unlike most study areas where SWAT has been applied, the Dillon Reservoir watershed is in a mountainous area. Similar to the findings of Fontaine *et al.* (2002), who applied SWAT to the mountainous Wind River Basin in Wyoming, SWAT did not initially simulate processes dependent on temperature or precipitation accurately in the Dillon Reservoir watershed. Processes that were affected include evapotranspiration and precipitation and snowmelt/snow formation processes.

In initial simulations, SWAT identified the closest defined meteorological station for each subwatershed by its proximity to the centroid of the subwatershed. The data, including temperature and precipitation, from this station then were assigned throughout the subwatershed. However, this approach was not the most accurate representation of climate conditions in the watershed because both temperature and precipitation generally vary with elevation. Under or over predictions of streamflow will result depending on the elevation of the gage.

Elevation in the Dillon Reservoir watershed ranges from 7,947 to 14,272 feet (2,422 m to 4,350 m). To account for the topographic relief and orographic effects on temperature and precipitation in the basin, elevation bands and lapse rates were incorporated into the model. The algorithms for elevation bands and lapse rates previously existed in SWAT but were not used during initial simulations. In addition, several parameters related to snowmelt and snow formation were adjusted. These modifications are discussed in the following sections.

To better represent temperature variations in the watershed due to elevation, a temperature lapse rate was applied to the entire watershed. The lapse rate is computed by relating elevation to mean annual temperature at seven meteorological stations in the basin. Figure G-8 shows this relationship.

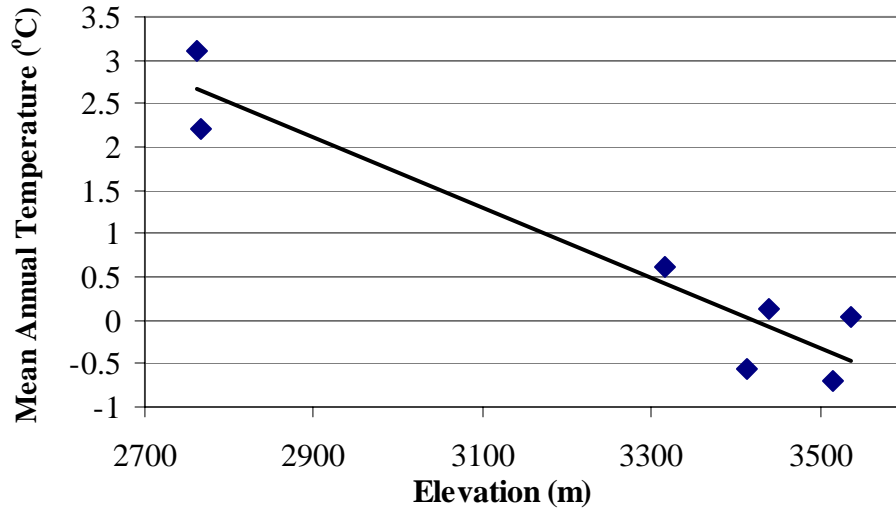


Figure G-8
Dillon Reservoir Watershed Mean Annual Temperature Versus Elevation

The trend line yields a slope of $-0.004\text{ }^{\circ}\text{C}/\text{m}$. This translates into an average watershed lapse rate (dT/dZ) of $-4\text{ }^{\circ}\text{C}/1,000\text{ m}$. The calculated temperature lapse rate compares favorably to the lapse rate of $-5\text{ }^{\circ}\text{C}/1,000\text{ m}$ that Fontaine *et al.* (2002) calculated for the Upper Wind River Basin, a mountainous watershed in Wyoming with elevations ranging from 1,865 to 4,207 meters.

When a temperature lapse rate is defined in SWAT, subbasin temperatures are adjusted for each elevation band in a subbasin as a function of the lapse rate and the difference between elevation of the meteorological gaging station and the average elevation specified for the band (Neitsch *et al.* 2000a). For temperature,

$$T_{mx,band} = T_{mx} + (EL_{band} - EL_{gage}) \cdot \frac{tlaps}{1000} \quad \text{Equation G-4}$$

$$T_{mn,band} = T_{mn} + (EL_{band} - EL_{gage}) \cdot \frac{tlaps}{1000} \quad \text{Equation G-5}$$

$$\bar{T}_{av,band} = \bar{T}_{av} + (EL_{band} - EL_{gage}) \cdot \frac{tlaps}{1000} \quad \text{Equation G-6}$$

where $T_{mx,band}$ is the maximum daily temperature in the elevation band ($^{\circ}\text{C}$), $T_{mn,band}$ is the minimum daily temperature in the elevation band ($^{\circ}\text{C}$), $\bar{T}_{av,band}$ is the mean daily temperature in the elevation band ($^{\circ}\text{C}$), T_{mx} is the maximum daily temperature recorded at the gage ($^{\circ}\text{C}$), T_{mn} is the minimum daily temperature recorded at the gage, \bar{T}_{av} is the mean daily temperature recorded at the gage, EL_{band} is the mean elevation in the elevation band (m), EL_{gage} is the elevation at the recording gage (m), $tlaps$ is the temperature lapse rate ($^{\circ}\text{C km}^{-1}$), and 1000 is the factor needed to convert meters to kilometers (Neitsch *et al.* 2000a).

Generally, precipitation varies directly with elevation, especially in areas of large topographic relief that are influenced by orographic effects. For example, Hjernstad (1970) found that precipitation at an elevation of 3,200m in Colorado is almost six times the precipitation that occurs at the base of the western slopes at 1,750m. A precipitation lapse rate is applied to the model to account for the variation in precipitation with elevation.

The lapse rate for precipitation is determined by relating elevation to mean annual precipitation at six gages in the basin (Figure G-9). The trend line yields a slope of 0.5 mm/m.

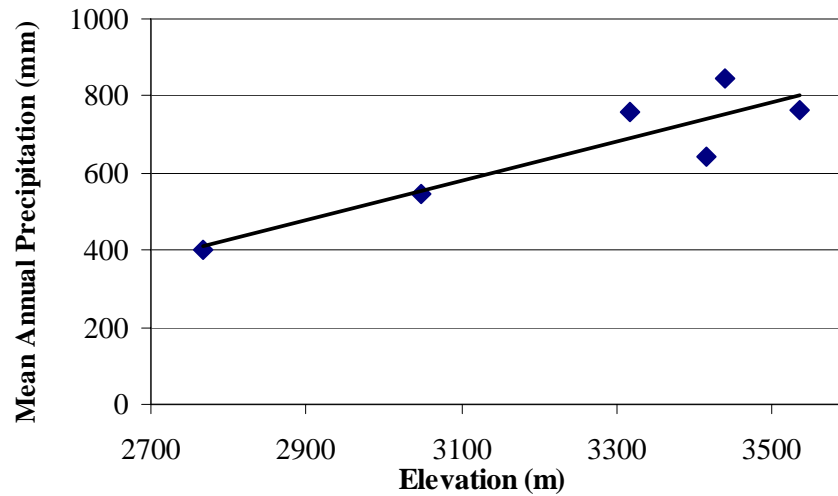


Figure G-9
Dillon Reservoir Watershed Mean Annual Precipitation Versus Elevation

Using the methods of Fontaine *et al.* (2002), the precipitation lapse rate was derived for use in the model. SWAT operates on a daily time step and defines precipitation events as precipitation volume within a 24-hour period. The lapse rate was calculated by distributing the annual precipitation lapse rate of 0.5 mm/m throughout all of the precipitation events that occurred in one year. This method generates an average watershed basin precipitation lapse rate (dP/dZ) of +5.0 mm/km derived from information from six available meteorological stations in the basin.

When a precipitation lapse rate is defined in SWAT, subbasin precipitation values are adjusted for each elevation band in a subbasin as a function of the lapse rate and the difference between elevation of the meteorological gaging station and the average elevation specified for the band (Neitsch *et al.* 2000a). A linear function is used to model precipitation,

$$R_{band} = R_{day} + (EL_{band} - EL_{gage}) \cdot \frac{plaps}{1000} \quad \text{when } R_{day} > 0.01 \quad \text{Equation G-7}$$

where R_{band} is the precipitation falling in the elevation band (mm H₂O), R_{day} is the precipitation recorded at the gage (mm H₂O), EL_{band} is the mean elevation in the elevation band (m), EL_{gage} is the elevation at the recording gage (m), $plaps$ is the precipitation lapse rate (mm H₂O/km), and 1000 is the factor needed to convert meters to kilometers (Neitsch *et al.* 2000a).

Orographic effects are a substantial concern in modeling the Dillon Reservoir watershed because elevation in the watershed varies greatly. To address this issue, SWAT allows up to 10 elevation bands to be defined. For each band, precipitation and maximum and minimum temperature are adjusted based on a defined lapse rate and the elevation difference between a meteorological station and the average elevation specified for each band (Neitsch *et al.* 2000a).

Six elevation bands were defined in the model. Their elevations and the average elevation of each band are shown in Table G-3.

Table G-3
Elevation Bands Used in the SWAT Model of the Dillon Reservoir Watershed

Elevation Band	Elevation Range (m)	Average Elevation (m)
1	2,500–2,800	2,650
2	2,801–3,100	2,950
3	3,101–3,400	3,250
4	3,401–3,700	3,550
5	3,701–4,000	3,850
6	4,001–4,400	4,150

After precipitation and temperature values are redefined for each band based on the lapse rate equations above, new average subbasin values must be calculated. For precipitation,

$$R_{day} = \sum_{bnd=1}^b R_{band} \cdot fr_{bnd} \quad \text{Equation G-8}$$

where R_{day} is the daily average precipitation adjusted for orographic effects (mm H₂O), R_{band} is the precipitation falling in the elevation band bnd (mm H₂O), fr_{bnd} is the fraction of subbasin area within the elevation band, and b is the total number of elevation bands in the subbasin (Neitsch *et al.* 2000a). For temperature,

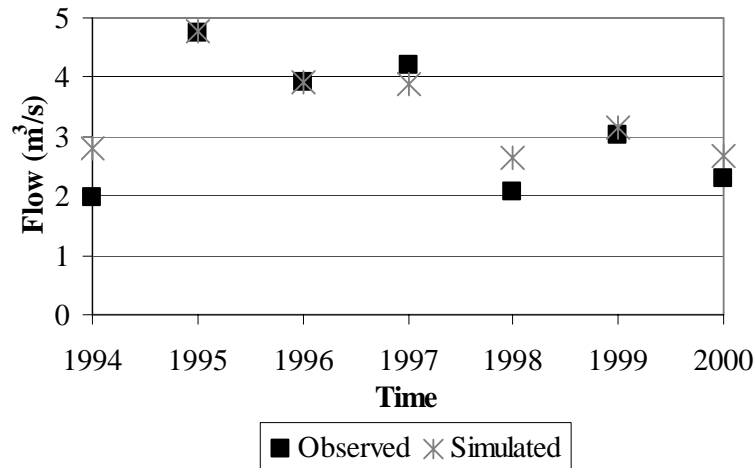
$$T_{mx} = \sum_{bnd=1}^b T_{mx,band} \cdot fr_{bnd} \quad \text{Equation G-9}$$

$$T_{mn} = \sum_{bnd=1}^b T_{mn,band} \cdot fr_{bnd} \quad \text{Equation G-10}$$

$$\bar{T}_{av} = \sum_{bnd=1}^b \bar{T}_{av,band} \cdot fr_{bnd} \quad \text{Equation G-11}$$

where T_{mx} is the daily maximum temperature adjusted for orographic effects ($^{\circ}\text{C}$), T_{mn} is the daily minimum temperature adjusted for orographic effects ($^{\circ}\text{C}$), \bar{T}_{av} is the daily mean temperature adjusted for orographic effects ($^{\circ}\text{C}$), $T_{mx,bnd}$ is the maximum daily temperature in the elevation band bnd ($^{\circ}\text{C}$), $T_{mn,bnd}$ is the minimum daily temperature in the elevation band bnd ($^{\circ}\text{C}$), $\bar{T}_{av,bnd}$ is the mean daily temperature in the elevation band bnd ($^{\circ}\text{C}$), fr_{bnd} is the fraction of subbasin area within the elevation band, and b is the total number of elevation bands in the subbasin.

The improvement in average annual streamflow simulation after the incorporation of the elevation bands and lapse rates was considerable (Figure G-10). Average monthly streamflow simulation was also examined for improvement. Not only do the monthly average streamflow results show magnitude of flow, but they also show seasonal variation of flow, which is especially important in the Dillon Reservoir watershed, where snowmelt is a governing watershed hydrologic process.



Note: Initial simulation revealed an under prediction of flow (refer to Figure G-7).

Figure G-10

Annually Averaged Streamflow Data for the Blue River Just Upstream of Dillon Reservoir Versus Simulated Values After Incorporation of Lapse Rates and Elevation Bands

Figure G-11 shows the monthly streamflow results for Blue River just upstream of Dillon Reservoir before and after incorporation of elevation bands. Figure G-11 illustrates that the seasonal flow patterns in the SWAT model outcome can be improved. Similar to Fontaine *et al.* (2002) SWAT model applied to the Wind River Basin, several problems are evident. First, the rising limb of each yearly hydrograph begins too early. Second, in some years numerous discharge peaks are present when there should only be one. Third, the recession limb of the yearly hydrograph begins too early. Finally, for two to three months of the year, streamflow approaches $0.0 \text{ m}^3\text{s}^{-1}$. These problems may all be attributed to the incorrect simulation of snowmelt and other properties of snow in the watershed. To correct these problems, three parameters in SWAT were adjusted, as described in the next section.

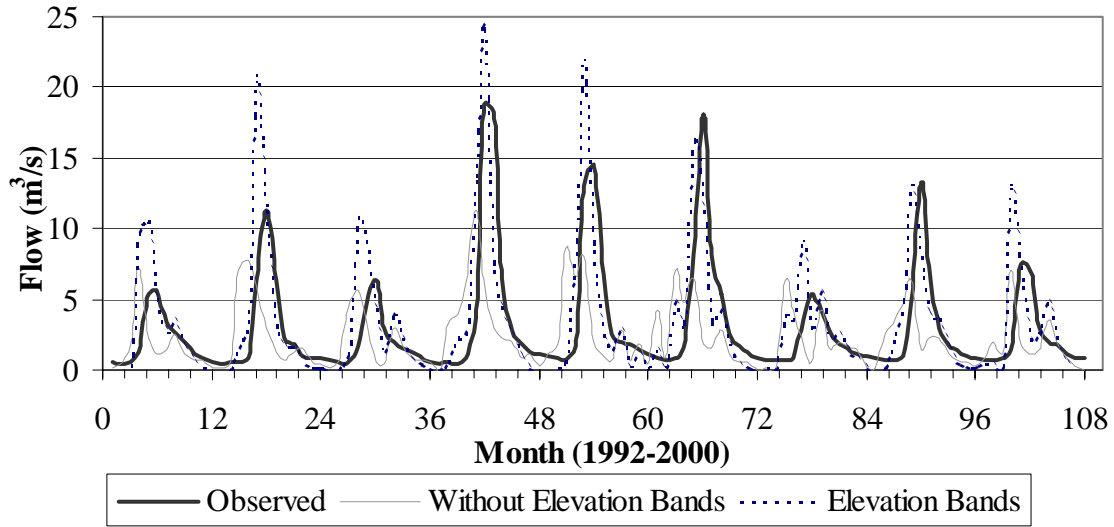


Figure G-11
Monthly Streamflow Results for Blue River Just Upstream of Dillon Reservoir Before and After Incorporation of Elevation Bands

Parameters in SWAT that simulate snowmelt processes and control the formation of snow were adjusted to create a better match to observed streamflow data. The parameters that were modified include a factor that accounts for snowpack characteristics and two factors that account for the melting rate of snow.

The temperature of the snowpack is a function of the mean daily temperature during the preceding days and varies as a dampened function of air temperature, according to Anderson (1976). A lagging factor controls the influence of the previous day's temperature on the current day's snowpack temperature. The lagging factor accounts for snowpack density, snowpack depth, exposure, and other factors affecting snowpack temperature, according to Neitsch *et al.* (2001a) in the SWAT Theoretical Documentation (2001). The snowpack temperature is calculated by:

$$T_{snow(dn)} = T_{snow(dn-1)} \cdot (1 - \ell_{sno}) + \bar{T}_{av} \cdot \ell_{sno} \quad \text{Equation G-12}$$

where $T_{snow(dn)}$ is the snowpack temperature on a given day ($^{\circ}\text{C}$), $T_{snow(dn-1)}$ is the snowpack temperature on the previous day ($^{\circ}\text{C}$), ℓ_{sno} is the snow temperature lag factor, and \bar{T}_{av} is the mean air temperature on the current day ($^{\circ}\text{C}$). As the lagging factor, ℓ_{sno} , approaches 1.0, the mean air temperature on the current day exerts an increasingly greater influence on the snowpack temperature, and the snowpack temperature from the previous day exerts less and less influence (Neitsch *et al.* 2001a). In SWAT, the default value is 1.0. In the model of the Dillon Reservoir watershed, the value was adjusted to 0.035. This value, which produced the best fit to observed data, is consistent with the findings of Fontaine *et al.* (2002) who observed that values of ℓ_{sno} will range from 0.0 to 0.5 for areas characterized by deep snowpack.

Snowmelt in SWAT is calculated as a linear function of the difference between the threshold temperature for snowmelt and the average snowpack maximum air temperature by:

$$SNO_{mlt} = b_{mlt} \cdot sno_{cov} \cdot \left[\frac{T_{snow} + T_x}{2} - T_{mlt} \right] \quad \text{Equation G-13}$$

where SNO_{mlt} is the amount of snowmelt on a given day (mm H₂O), b_{mlt} is the melt factor for the day (mm H₂O/day-°C), sno_{cov} is the fraction of the HRU area covered by snow, T_{snow} is the snowpack temperature on a given day (°C), T_x is the maximum air temperature on a given day (°C), and T_{mlt} is the base temperature above which snowmelt is allowed (°C). The melt factor, b_{mlt} (mm H₂O/day-°C), is calculated by

$$b_{mlt} = \frac{(b_{mlt6} + b_{mlt12})}{2} + \frac{(b_{mlt6} - b_{mlt12})}{2} \cdot \sin\left(\frac{2\pi}{365} \cdot (d_n - 81)\right) \quad \text{Equation G-14}$$

where b_{mlt6} is the melt factor for June 21 (mm H₂O/day-°C), b_{mlt12} is the melt factor for December 21 (mm H₂O/day-°C), and d_n is the day number of the year. The parameters b_{mlt6} and b_{mlt12} represent maximum and minimum melting values that occur on the summer and winter solstices, respectively. In the model, default values for these parameters are both 4.5 mm H₂O/day-°C. For the application of SWAT to the Dillon Reservoir watershed, these values were adjusted to 3.0 for b_{mlt6} and 2.0 for b_{mlt12} .

Other parameters were not changed from their default values in SWAT. The mean air temperature at which precipitation is equally likely to be rain as it is to be snow or freezing rain was left unchanged at 1.0 °C. Also, the temperature at which snow will begin to melt was unaltered from the assigned value of 0.5 °C. The areal snow coverage threshold at 100% snow cover and at 50% were left unadjusted from the default values in SWAT of 1 mm H₂O and 0.5 mm H₂O. The default value of 1 mm H₂O for the areal snow coverage threshold means that the impact of the areal depletion curve (snow volume versus fraction of areal coverage of snow) is minimal. A summary of the snowmelt parameters incorporated in SWAT, and the values used in the model are shown in Table G-4.

Table G-4
Snowmelt/Snow Formation Parameters Used in Model Calibration

Input Parameters	Units	Default Value	Value Used
Lag Factor, ℓ_{sno}	dimensionless	1.0	0.035
Maximum melt factor, b_{mlt6}	mm (day-°C) ⁻¹	4.5	3.0
Minimum melt factor, b_{mlt12}	mm (day-°C) ⁻¹	4.5	2.0

Table G-4
Snowmelt/Snow Formation Parameters Used in Model Calibration (Cont.)

Input Parameters	Units	Default Value	Value Used
Snow/rain threshold	°C	1.0	1.0
Snowpack melt temperature threshold	°C	0.5	0.5
Areal snow coverage threshold at 100%	mm	1.0	1.0
Areal snow coverage threshold at 50%	mm	0.5	0.5

The adjustment of the snowmelt and snow formation parameters made a substantial improvement in the simulation of streamflow. Figure G-12 shows simulated streamflow with the modifications made to the snowmelt and snow formation variables in SWAT and including the previously described adjustments to precipitation and temperature.

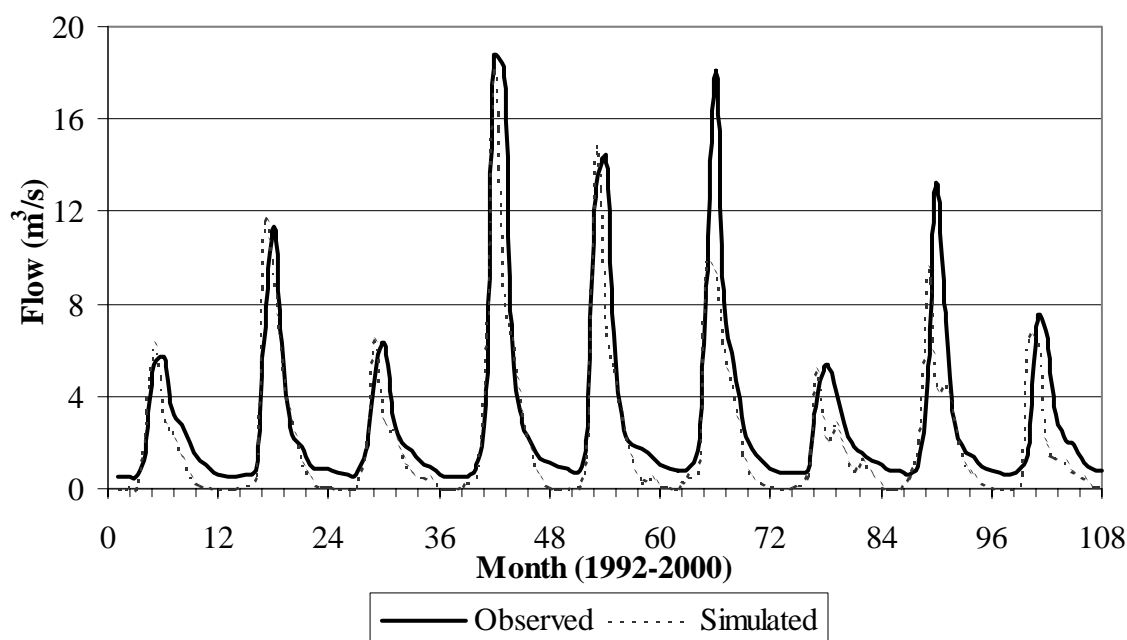


Figure G-12
Final Monthly Streamflow Results for the Blue River Just Upstream of Dillon Reservoir After Model Adjustment

The four streamflow simulation problems that were apparent after the implementation of elevation bands and lapse rates essentially were resolved. The rising limb of each yearly hydrograph begins at the correct time. In most of the years simulated, there is only one discharge peak per year. In 1998 and 1999 small subpeaks are visible; however, these are only minor peaks that when averaged with surrounding points do not make a great deal of difference in flow simulation.

The recession limb of each yearly hydrograph begins at nearly the correct time. The years of higher discharge particularly show improvement in the timing of the recession limb of the hydrograph (Figure G-12, months 18, 46, 70, and 92). The only problem that was not completely resolved was the streamflow approaching $0.0 \text{ m}^3 \text{ s}^{-1}$ for two to three months of the year. However, improvement was made. In the best-fit scenario, monthly streamflow approaches $0.0 \text{ m}^3 \text{ s}^{-1}$ at least one month of each simulated year. Comparison of Figure G-11 and Figure G-12 show that the simulated hydrograph was smoothed considerably and better corresponds to the observed values of streamflow.

Statistics show the numeric improvement made in streamflow simulation. The R^2 value of monthly-averaged streamflow after elevation band and lapse rate implementation was 0.45. After modification of the additional snowmelt parameters, the R^2 value was increased to 0.70. R^2 values of 0.65 to 0.70 for monthly-averaged streamflow are appropriate considering the numerous potential measurement errors in data collection (personal communication, Susan Neitsch, Spatial Sciences Laboratory, Texas A&M University 2002). For example, spatial variability in rainfall, soils, and land use, errors in measuring streamflow, and errors caused by sampling strategies are all potential causes of inaccurate observed values (Santhi *et al.* 2001).

Sensitivity Study

This section provides information about the sensitivity study, including

- Approach
- Sensitivity study results
- Model performance

Approach

Streamflow was calibrated to produce a more accurate representation of hydrology in the basin. Nutrient loadings are dependent upon streamflow, so it was important to have the most accurate model of streamflow possible. The runoff curve number was increased by 8% from initial values input during model development. Due to the mountainous characteristics of the basin, the most significant parameters affecting streamflow were related to orographic effects and snowmelt. Elevation bands and lapse rates accounted for the orographic effects in the watershed. Snowmelt parameters that were adjusted include a snowmelt lag factor and minimum and maximum snowmelt factors. All variables that were adjusted fell within reasonable ranges of accepted values. Final simulation of monthly-averaged streamflow indicated a close match to observed values with an R^2 value of 0.70.

As just described, SWAT was applied such that it produced an extremely good match to observed streamflow data. This match is a critical first step for a pollutant-transport model. To simulate pollutant transport, it is necessary to know the values for many input parameters that influence the reaction, transformation, and interphase partitioning of the pollutants.

Unfortunately, the available input data on these parameters, as well as all the observed data required to calibrate a model, is insufficient in the Dillon Reservoir watershed to develop a rigorous calibrated model, which is true in most watersheds. However, a sensitivity study can be done to understand the relative importance of these parameters on model output. This study is accomplished by varying the input parameters over a reasonable range (based on the literature and common hydrologic knowledge) and evaluating the influence on model output. The next step is to use the parameters that are deemed most important (in terms of the influence on the model) to evaluate the performance of the model in simulating actual data. This exercise can also lend insight into designing a data-collection plan that would improve model performance. For this effort, phosphorus is chosen as an example OWS pollutant. The procedure described herein could also be used for other pollutants, although the type and values of fate and transport parameters may differ considerably from those for phosphorus.

For the sensitivity study, modeling was completed for a 10-year period. Observed phosphorus concentration data for seven of the ten years were available at the Blue River approximately one-half mile upstream from Dillon Reservoir (the same location of the measured streamflow data presented in the SWAT Calibration to Streamflow section). The observed phosphorus data are from the US EPA Storage and Retrieval (STORET) database (US EPA 2002b) and from data collected by Summit County, Colorado, officials. The first two years were not examined in order to reduce inaccuracies in preliminary calculation of state variables, such as soil water content and residue cover as suggested by Fontaine *et al.* (2002) and Santhi *et al.* (2001).

Table G-5 summarizes the SWAT variables that were tested in the sensitivity analysis and the initial values assigned by SWAT. In the following section, descriptions of those SWAT input parameters that were found to have a 40% change or greater in P loading for the simulated scenarios are discussed. These parameters are P soil partitioning coefficient, P availability index, soil bulk density, initial soluble P soil concentration, and soil organic carbon content. In addition, the concentration of P in the simulated OWS effluent is discussed; although it was not found to cause a 40% change in P loading.

Table G-5
SWAT Parameters Tested in the Sensitivity Study

Parameter	Units	Initial Value in SWAT model
P Soil Partitioning Coefficient	$\text{m}^3 \text{Mg}^{-1}$	175
P Enrichment Ratio	dimensionless	Model calculates for each storm event
P Percolation Coefficient	$\text{m}^3 \text{Mg}^{-1}$	10
P Availability Index	dimensionless	0.4
Residue Decomposition Coefficient	dimensionless	0.05

Table G-5
SWAT Parameters Tested in the Sensitivity Study (Cont.)

Parameter	Units	Initial Value in SWAT model	
Soil Bulk Density	g cm ⁻³	Soil Layer 1	1.42
		Soil Layer 2	1.50
		Soil Layer 3	1.45
		Soil Layer 4	1.50
Surface Runoff Lag Coefficient	days	4	
Lateral Flow Travel Time	days	Model calculates dependent on hydraulic properties	
Initial Residue Cover	kg ha ⁻¹	0.0	
Soil Organic Carbon Content	% soil weight	Soil Layer 1	0.87
		Soil Layer 2	0.29
		Soil Layer 3	0.1
		Soil Layer 4	0.05
Initial Soluble P Soil Concentration	mg P kg soil ⁻¹	Soil Layer 1	5
		Soil Layer 2	5
		Soil Layer 3	5
		Soil Layer 4	5
P Uptake Distribution	dimensionless	20	
Michaelis-Menton Half-Saturation Constant	mg P L ⁻¹	0.025	
Concentration of P in OWS Effluent*	kg P	0.011 kg mineral P	
	kg fertilizer ⁻¹	0.005 kg organic P	

*P was applied as manure 10 mm below the soil surface, as described in the text of the SWAT Setup section.

The base-case scenario is composed primarily of initial values generated by SWAT or selected from GIS databases by SWAT during model development. Reasonable ranges for several of the variables were found in Kirkland (2001), Brady and Weil (1999), and the Soil Survey of Summit County Area, Colorado (1980). Before the sensitivity study, no parameters dealing with phosphorus transport and fate were adjusted.

Research was completed to ensure that all base-case values fell within reasonable ranges for each variable. Table G-6 summarizes the base-case scenario for the SWAT input parameters tested in the sensitivity study.

Table G-6
Sensitivity Study Base-Case Values, Values Tested, and Justification of Values

Parameter	Units	Base-Case Value		Values Tested		Justification for Range
				Min	Max	
P Soil Partitioning Coefficient	$\text{m}^3 \text{Mg}^{-1}$	15		2	175	Kirkland (2001)
P Enrichment Ratio	dimensionless	Model calculates for each storm event		10^{-3}	5	Brady and Weil (1999); Neitsch <i>et al.</i> (2001a)
P Percolation Coefficient	$10 \text{ m}^3 \text{Mg}^{-1}$	13.5		10	17.5	Neitsch <i>et al.</i> (2001a)
P Availability Index	dimensionless	0.4		0.01	0.7	Neitsch <i>et al.</i> (2001a)
Residue Decomposition Coefficient	dimensionless	0.05		0.02	0.1	Neitsch <i>et al.</i> (2001a)
Soil Bulk Density	g cm^{-3}	Soil Layer 1	1.42	0.8	1.90	Brady and Weil (1999)
		Soil Layer 2	1.50	0.9	2.00	
		Soil Layer 3	1.45	0.85	1.95	
		Soil Layer 4	1.50	0.9	2.00	
Surface Runoff Lag Coefficient	days	4		1	10	Neitsch <i>et al.</i> (2001a)
Lateral Flow Travel Time	days	Model calculates dependent on hydraulic properties		1	180	Neitsch <i>et al.</i> (2001a)
Initial Residue Cover	kg ha^{-1}	1.0		10^{-3}	10^4	Neitsch <i>et al.</i> (2001a)
Soil Organic Carbon Content	% soil weight	Soil Layer 1	0.87	0.5	1.5	Brady and Weil (1999); Soil Survey of Summit County Area (1980)
		Soil Layer 2	0.29	0.1	0.4	
		Soil Layer 3	0.10	0.05	0.2	
		Soil Layer 4	0.03	0.05	0.1	

Table G-6
Sensitivity Study Base-Case Values, Values Tested, and Justification of Values (Cont.)

Parameter	Units	Base-Case Value		Values Tested		Justification for Range
				Min	Max	
Initial Soluble P Soil Concentration	mg P kg soil ⁻¹	Soil Layer 1	5	5	20	Brady and Weil (1999)
		Soil Layer 2	5	2	7	
		Soil Layer 3	5	2	5	
		Soil Layer 4	5	2	5	
P Uptake Distribution	dimensionless	20		1	100	Neitsch <i>et al.</i> (2001a)
Michaelis-Menton Half-Saturation Constant	mg P L ⁻¹	0.025		10 ⁻³	0.05	Neitsch <i>et al.</i> (2001a)

Sensitivity Study Results

Sensitivity study results presented in this section pertain to:

- P Soil Partitioning Coefficient
- P Availability Index
- Soil Bulk Density
- The Amount of Organic Carbon in the Soil
- Initial Concentration of Mineral P in the Soil
- Concentration of P in Simulated OWS Effluent

A summary of sensitivity study results is also provided.

Sensitivity to P Soil Partitioning Coefficient

The first parameter examined in the study was the P soil partitioning coefficient, $k_{d,surf}$. The parameter is the ratio of the soil concentration of P to the aqueous concentration of P at equilibrium. This parameter was assigned a base-case value of 15 m³Mg⁻¹, which was the median value based on a cumulative frequency distribution (CFD) compiled by Kirkland (2001). While holding all other parameters constant, $k_{d,surf}$ was varied to determine the sensitivity of the model to this variable.

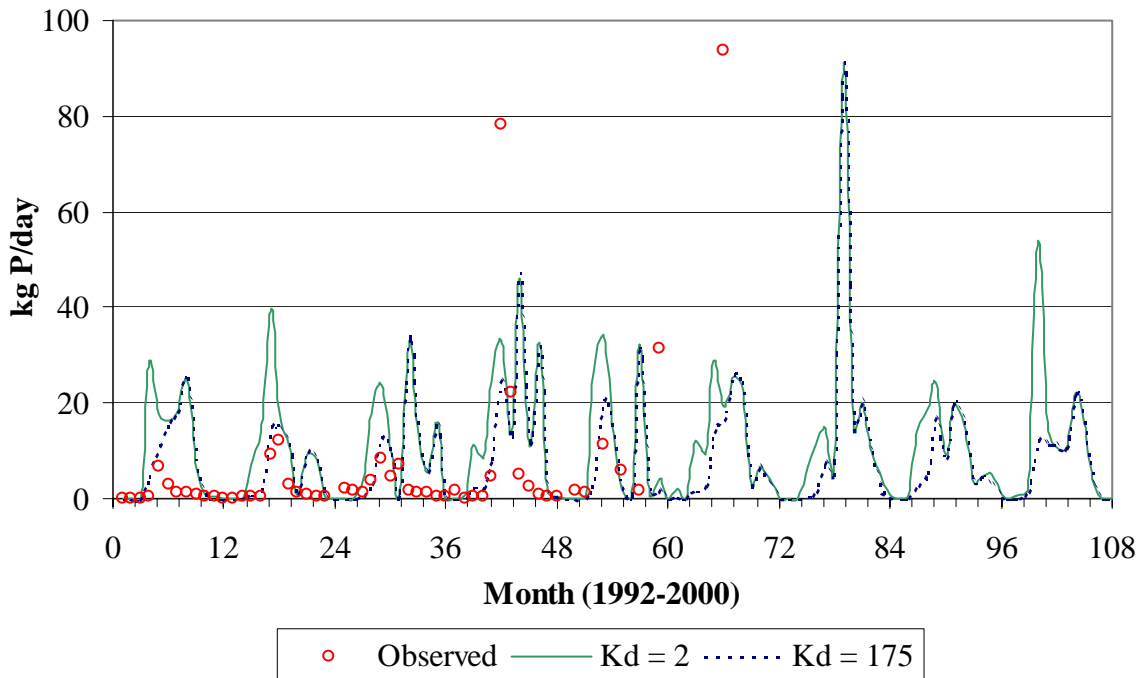
In an extensive literature review, Kirkland (2001) found from 18 sources that the range of values of $k_{d,surf}$ varied from 1.4 to 478 m³Mg⁻¹. For the sensitivity study, the 10th, 50th, and 90th percentile values, 2, 15, and 175, respectively, from the CFD were selected (Kirkland 2001).

Table G-7 summarizes the average daily mass loading of P by varying values of $k_{d,surf}$. As expected, decreasing $k_{d,surf}$ allowed less P to partition to the soil, which increased P loading. However, the increase in sorption of P by increasing $k_{d,surf}$ appears to have a non-linear relationship, noting the small difference in average daily loading of P between $k_{d,surf}$ values of 15 and 175. Figure G-13 shows the sensitivity of P loading with the adjustments made to $k_{d,surf}$.

Table G-7
Summary of Average Daily Loading of P by Varying P Soil Partitioning Coefficient, $k_{d,surf}$

	Initial Value ($\text{m}^3 \text{mg}^{-1}$)	Case 1	Case 2
$k_{d,surf}$	15	2	175
Average Daily Loading of P (mineral and organic) (kg)	28.0	36.4	21.0

Note: Loading is simulated for the Blue River about 0.5 miles upstream of Dillon Reservoir.



Note: Loading is simulated for the Blue River about 0.5 miles upstream of Dillon Reservoir.

Figure G-13
Sensitivity to P Soil Partitioning Coefficient, $k_{d,surf}$

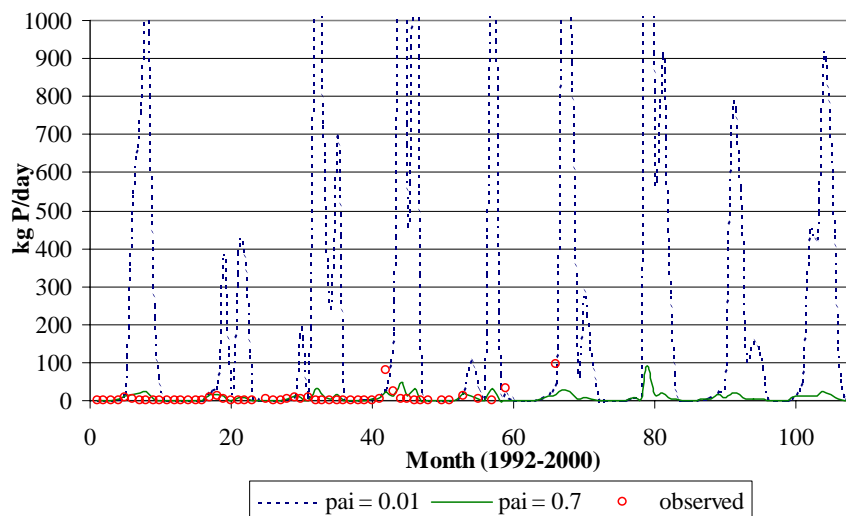
Sensitivity to the P Availability Index

The effect of the P availability index, *pai*, on model results was also tested. The *pai* specifies the fraction of fertilizer P that is in solution after a period of rapid reaction with the soil (Neitsch *et al.* 2001a) (also see Equation G-29 in the Supplemental Information: Theoretical Formulation of SWAT section, which follows the References section in this appendix.). The default value in SWAT for *pai* is 0.40. The user may set the value of *pai* inside the range of 0.01 to 0.7. By lowering the *pai*, loading of P increases because the *pai* affects the concentration of P in the active and stable solution P pools (also see Equation G-17 and Equation G-18 in the Supplemental Information: Theoretical Formulation of SWAT section, which follows the References section in this appendix). Table G-8 summarizes the average daily mass loading of P by varying values of *pai*, and Figure G-14 shows the sensitivity of P loading with the adjustments made to *pai*. The increase in P loading sensitivity to *pai* appears to have a non-linear relationship, noting the large difference in average daily loading of P between *pai* values of 0.4 and 0.01.

Table G-8
Summary of Average Daily Loading of P by Varying P Availability Index

	SWAT Initial Value	Case 1	Case 2
<i>pai</i>	0.40	0.01	0.7
Average Daily Loading of P (mineral and organic) (kg)	28.0	384.1	20.7

Note: Loading is simulated for the Blue River about 0.5 miles upstream of Dillon Reservoir.



Note: For the value of *pai* = 0.01, the peaks were truncated to better show the sensitivity of all *pai* values tested. Loading is simulated for the Blue River about 0.5 miles upstream of Dillon Reservoir.

Figure G-14
Sensitivity to P Availability Index, *pai*

Sensitivity to the Soil Bulk Density

Another factor that was tested in the sensitivity study was the bulk density of the soil, ρ_b . Soil bulk density can significantly affect P transport because of its relationship to the amount of soluble P lost in runoff. This is shown in Equation G-15 and can also be defined by the linear retardation factor, r_f , as

$$r_f = 1 + \frac{\rho_b}{\theta} k_{d,surf} \quad \text{Equation G-15}$$

where ρ_b is the bulk density of the soil (Mg m^{-3}), θ is the volumetric moisture content, and k_d is the soil water partitioning coefficient for P ($\text{m}^3 \text{Mg}^{-1}$) (Fetter 1999). Also, bulk density is a factor that affects the amount of P moving from the top 10 mm of soil into the first soil layer (also see Equation G-41 in the Supplemental Information: Theoretical Formulation of SWAT section, which follows the References section in this appendix). In converting input nutrient-level concentrations to mass units, ρ_b is used. The input soil concentration is multiplied by ρ_b and the depth of the soil to calculate the equivalent initial mass of P.

The value of ρ_b may vary from 0.8 to 2.5 g cm^{-3} in SWAT. Brady and Weil (1999) suggest values ranging from 0.8 to 1.2 g cm^{-3} for loamy A (surface) soil horizons and between 1.9 and 2.2 g cm^{-3} for compacted glacial tills, both of which are common in the Dillon Reservoir watershed. Table G-9 summarizes the average daily mass loading of P by varying values of ρ_b . Case 1 in Table G-9 shows that a decrease in ρ_b results in a decrease in P loading to the stream and that an increase in ρ_b (Case 2) results in an increase in P loading to the stream.

Table G-9
Summary of Average Daily Loading of P by Varying the Soil Bulk Density, ρ_b .

	SWAT Initial Value (g cm^{-3})	Case 1	Case 2
Soil Layer 1	1.42	0.80	1.90
Soil Layer 2	1.50	0.90	2.00
Soil Layer 3	1.45	0.85	1.95
Soil Layer 4	1.50	0.90	2.00
Average Daily Loading of P (mineral and organic) (kg)	28.0	15.5	33.5

Note: Loading is simulated for the Blue River about 0.5 miles upstream of Dillon Reservoir.

Sensitivity to the Amount of Organic Carbon in the Soil

The amount of soil organic carbon, $orgC_{ly}$, also was tested in the sensitivity study. This variable affects SWAT's calculation of the concentration of humic organic P (also see Equation G-19 and Equation G-20 in the Supplemental Information: Theoretical Formulation of SWAT section, which follows the References section in this appendix).

By increasing the $orgC_{ly}$ values, P loading is increased as a result of the relationship defined in SWAT that associates carbon levels to organic N levels by the ratio of 14:1 and organic N levels to P levels by the ratio of 8:1.

Two scenarios of $orgC_{ly}$ were completed for the sensitivity study. The majority of soils in the Dillon Reservoir watershed are alfisols and inceptisols, with a small portion of mollisols (Soil Survey of Summit County Area, Colorado 1980). Descriptions of these soil orders and typical values of organic carbon content in the top 15 cm of each soil order are shown in Table G-10. Representative values based on Table G-10 and the default values in the model were chosen for the scenarios tested.

Table G-10
The Dillon Reservoir Watershed Soil Order Descriptions and Typical Values of Organic Carbon Content, $orgC_{ly}$, in the Upper 15 cm for Each Soil Order

Soil Order	Soil Characteristics ¹	Typical Organic Carbon Content ¹
Alfisol	Illuvial clay assemblage; medium to high supply of bases; typically formed under forest vegetation in climates with seasonal moisture deficit	0.5–3.8
Inceptisol	Moist; horizons of parent material alteration but not from illuviation; weak soil horizon development	0.06–6.0
Mollisol	Nearly black, organic-rich surface horizon; high supply of bases; >50% base saturation	0.6–4.0

¹ Adapted from Brady and Weil (1999).

Note: Loading is simulated for the Blue River about 0.5 miles upstream of Dillon Reservoir.

Table G-11 summarizes the average daily mass loading of P by varying values of $orgC_{ly}$.

Table G-11
Summary of Average Daily Loading of P by Varying the Amount of Soil Organic Carbon, $orgC_{ly}$

	SWAT Initial Value (%soil weight)	Case 1	Case 2
Soil Layer 1	0.87	1.50	0.50
Soil Layer 2	0.29	0.40	0.10
Soil Layer 3	0.10	0.20	0.05
Soil Layer 4	0.03	0.10	0.05
Average Daily Loading of P (mineral and organic) (kg)	28.0	36.0	23.3

Note: Loading is simulated for the Blue River about 0.5 miles upstream of Dillon Reservoir.

Sensitivity to Initial Concentration of Mineral P in the Soil

Initial solution P concentrations in the soil were examined in the sensitivity study. The default value in SWAT is to initialize all layers with 5 mg P kg soil⁻¹. The active and stable mineral P pool values also are dependent on the value of the soluble P concentration. According to Brady and Weil (1999), a reasonable range for organic P is 200 to 350 mg P kg soil⁻¹, and a reasonable range for inorganic P is 100 to 650 mg P kg soil⁻¹ for the majority of soils similar to those found in the Dillon Reservoir watershed. With the value set at 5 mg P kg soil⁻¹, the total inorganic P in the soil is 150 mg P kg soil⁻¹. When the values for Case 1 (Table G-12) are used, the total inorganic P is 278 mg P kg soil⁻¹, and for Case 2, total inorganic P equals 83 mg P kg soil⁻¹. Table G-12 summarizes the average daily mass loading of P by varying values of initial soluble P concentrations in the soil. As shown in Table G-12, all scenarios provide reasonable ranges of mineral and organic P loading, but there is a considerable increase in the loading of P with increased initial values of soluble P soil concentrations.

Table G-12
Summary of Average Daily Loading of P by Varying the Initial Soluble P Soil Concentrations

	SWAT Initial Value (mg kg ⁻¹)	Case 1	Case 2
Soil Layer 1	5	20	5
Soil Layer 2	5	7	2
Soil Layer 3	5	5	2
Soil Layer 4	5	5	2
Average Daily Loading of P (mineral and organic) (kg)	28.0	81.1	28.0

Note: Loading is simulated for the Blue River about 0.5 miles upstream of Dillon Reservoir.

Sensitivity to Concentration of P in Simulated OWS Effluent

In addition to the SWAT P input parameters that were adjusted in the sensitivity study, the concentration of P in the OWS effluent was varied. Kirkland (2001) compiled information from 56 sources describing the concentration of P in OWS effluent and constructed a CFD. From this diagram the 10th, 50th, and 90th percentile values, 2.0 mg P L⁻¹, 10.0 mg P L⁻¹, and 18.8 mg P L⁻¹, respectively, were used. Increasing and decreasing the concentration of P in the manure applied had little effect on P loading, as Table G-13 shows.

Table G-13
Summary of Average Daily Loading of P by Varying the Concentration of P in the OWS Effluent

	50 th Percentile (mg P L ⁻¹)	10 th Percentile	90 th Percentile
Concentration of P	10.0	2.0	18.8
Average Daily Loading of P (mineral and organic) (kg)	28.0	28.007	27.997

Note: Loading is simulated for the Blue River about 0.5 miles upstream of Dillon Reservoir.

Summary of Sensitivity Study Results

The study that was performed elucidated the relative sensitivity that parameters affecting P transport and fate have on the SWAT model of the Dillon Reservoir watershed. The most sensitive parameters of the 13 tested, in order of greatest sensitivity, are the:

- P availability index, pai
- Initial concentration of mineral P in the soil
- Bulk density of the soil, ρ_b
- P soil partitioning coefficient, $k_{d,surf}$
- Organic carbon content of the soil, $orgC_{ly}$

Table G-14 shows the percent change in daily P loading using the ranges shown in Table G-6 and Table G-13 for each of the 13 parameters.

Table G-14
Percent Change in P Loading Using Parameter Ranges Shown in Table G-6 and Table G-13

Parameter	Percent Change
P availability index	179.6
Initial concentration of mineral P in the soil	97.4
Bulk density of the soil	73.3
P soil partitioning coefficient	53.7
Organic carbon content of the soil	42.7
Plant uptake	28.1
Initial residue cover	21.3
P enrichment ratio	20.4

Table G-14
Percent Change in P Loading Using Parameter Ranges Shown in Table G-6 and Table G-13
(Cont.)

Parameter	Percent Change
Surface runoff lag time	4.7
Michaelis-Menton Half saturation constant	3.0
P percolation coefficient	2.6
Lateral flow lag time	1.2
P concentration in OWS effluent	0.036
Residue decomposition coefficient	0.0

Note: Loading is simulated for the Blue River about 0.5 miles upstream of Dillon Reservoir.

Model Performance

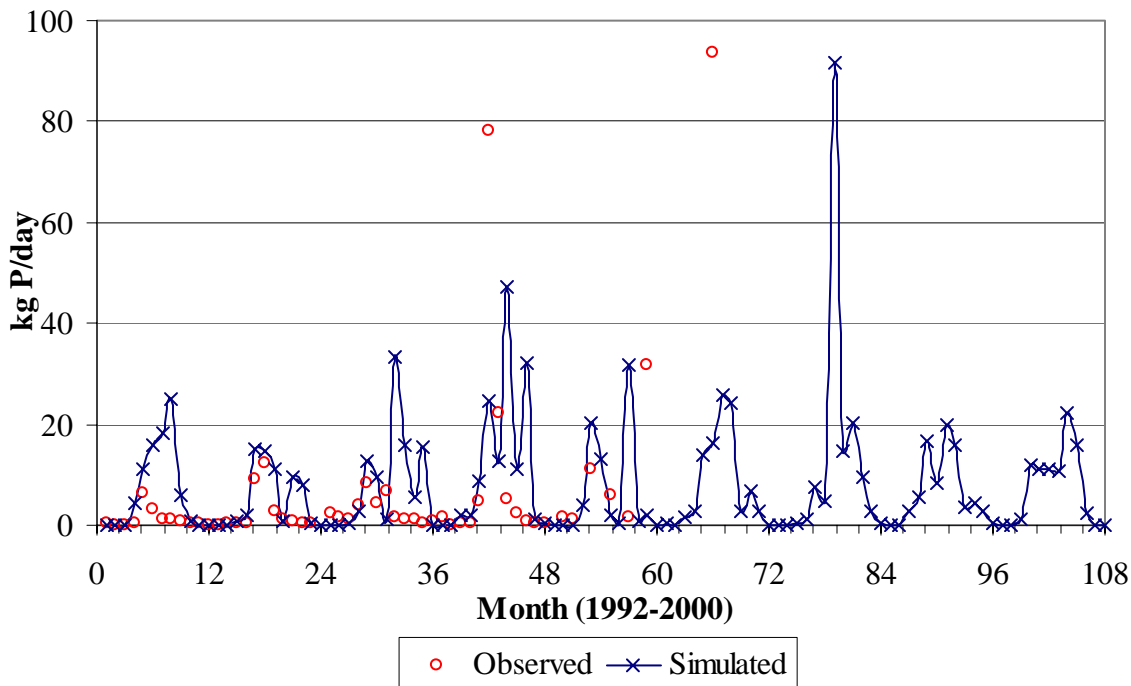
After the sensitivity study, parameters were adjusted within their reasonable ranges and a best-fit model to observed values was produced. Table G-15 shows the values of the parameters that created the best visual match to the limited observed P data. Figure G-15 shows the observed P values plotted versus the best-fit model.

Table G-15
SWAT Parameter Value Changes That Produced the Best-Fit Model to Observed Data

Parameter, Units	Initial SWAT Values	Value of Parameter for Best-Fit Model	
P Availability Index, <i>pai</i> , dimensionless	0.4	0.7	
Soil Bulk Density, ρ_b , g cm ⁻³	1.42	Soil Layer 1	0.80
	1.50	Soil Layer 2	0.90
	1.45	Soil Layer 3	0.85
	1.50	Soil Layer 4	0.9
Soil Organic Carbon Content, <i>orgC_{ly}</i> , % soil weight	0.87	Soil Layer 1	0.5
	0.29	Soil Layer 2	0.1
	0.10	Soil Layer 3	0.05
	0.05	Soil Layer 4	0.05

Table G-15
SWAT Parameter Value Changes That Produced the Best-Fit Model to Observed Data
(Cont.)

Parameter, Units	Initial SWAT Values	Value of Parameter for Best-Fit Model	
Initial Soluble P Soil Concentration, mg P kg soil ⁻¹	5	Soil Layer 1	5
	5	Soil Layer 2	2
	5	Soil Layer 3	2
	5	Soil Layer 4	2



Note: Loading is simulated for the Blue River about 0.5 miles upstream of Dillon Reservoir

Figure G-15
Observed P Values and the Best-Fitting Model to Observed P Data Plotted Versus Time

For the best-fitting model to observed data, as shown in Table G-15, the values of $orgC_{ly}$ for each layer were decreased slightly to better reflect the values reported for the soils in the watershed (Soil Survey of Summit County Area, Colorado 1980). The values of the initial soluble P concentration for each soil layer were decreased slightly because, according to Brady and Weil (1999), the reasonable range for inorganic P concentration in soils similar to those found in the Dillon Reservoir watershed is 100 to 650 mg P kg soil⁻¹.

The bulk density was also decreased somewhat based on information presented by Brady and Weil (1999). The P availability index was increased to 0.7, which is the upper limit of the parameter's range in SWAT. The resulting simulation produced P loading values generally within a factor of 10 of measured data and often within a factor of 2.

At this stage of the research, the model performs reasonably well given the large number of uncertain P transport parameters. The model could be used to evaluate the potential influence of different watershed-scale management practices. However, the model is not recommended for detailed planning. The excellent performance of the streamflow model suggests that a better model could be developed with more P stream data and more certainty on the value of P input parameters.

Summary and Conclusions

The SWAT model, one of the four models interfaced through the US EPA's watershed management tool BASINS, was applied to the Dillon Reservoir watershed. SWAT incorporates physically-based parameters to simulate hydrology and water quality at the watershed scale. After incorporation of input data from GIS into the model, reasonable values were chosen for several subsurface hydraulic parameters, for which no appropriate measured data were available. Calibration to nine years of measured streamflow data (1992–2000) resulted in an excellent match between measured streamflow data and model output (an R^2 value of 0.70 for average monthly flow).

Next, OWS pollutant flow and transport was assessed using SWAT. The nutrient phosphorous was chosen for this implementation. To simulate OWS pollutant input in the Dillon Reservoir watershed, a fertilizer operation was defined and developed in SWAT. SWAT allows for several different management practices within the model, including fertilization, tillage, irrigation, and urban processes. Fertilizer was added to HRUs within subwatersheds along the Blue River, where the highest densities of OWS are located. From an extensive review of septic tank effluent composition completed by Kirkland (2001), values of the loading rate and nutrient concentrations were compiled. Then, calculations to determine the amount of fertilizer to be added to each HRU were completed based on the chemical composition of the fertilizer applied.

A sensitivity study was conducted on parameters affecting the transport and fate of P. A sensitivity study was performed because there were insufficient measured data for the many P transport and fate parameters required by SWAT. Fourteen input parameters were tested for their influence on the model results. To ensure model accuracy, parameters were tested within reasonable ranges of published values. Five parameters were found to cause changes of 40% or greater in simulated results of P loading to the Blue River (about 0.5 miles upstream of Dillon Reservoir), one of three major tributaries of Dillon Reservoir. Parameters sensitive to variation were the P availability index, the soil organic carbon content, the initial concentration of mineral P in the soil, the P soil partitioning coefficient, and the soil bulk density. Some parameters that were not sensitive to modifications included the P percolation coefficient, the concentration of P in simulated OWS effluent, and lateral flow lag time.

Based on the results of the modeling effort, the following conclusions were made:

- SWAT accurately simulated the watershed hydrologic processes using public data that can easily be incorporated using the SWAT ArcView interface or BASINS. Variables associated with elevation-dependent temperature and precipitation (orographic) effects and snowmelt were adjusted to achieve this result, along with an 8% increase in the runoff curve number. The orographic and snowmelt factors are particularly significant in the Dillon Reservoir watershed, where the elevation varies approximately 2,000 m. Because pollutant transport to Dillon Reservoir depends largely on an accurate simulation of streamflow, a precise fit of streamflow results to observed values was imperative.
- SWAT can be modified to simulate a mountainous watershed. Although the model was originally created to predict chemical yields in agriculture-dominated watersheds, adjustments made to account for the effects of topography and snowmelt in the alpine watershed resulted in a model that can accurately simulate streamflow hydrographs of the watershed.
- To achieve the best-fit pollutant transport model, several model input parameters were adjusted (initial soluble P concentration in the soil, soil bulk density, soil organic carbon content, and P availability index). The resulting simulation produced P loading values within a factor of 10 and usually within a factor of 2 of measured P mass loadings. Initially, the model over predicted soil P loading. Therefore, the changes reflect that soil-retention processes effectively attenuate P from OWS prior to reaching the streams. However, longer simulations may be required to understand the influence of these processes over a time frame of many decades.
- The uncertainty associated with the assignment of some chemical and hydrologic parameters indicates that additional information on the actual values and variability of pollutant-transport input variables is necessary. This option is feasible, considering that most of the parameters containing approximated values (soil organic carbon content, P soil-partitioning coefficient, mineral P concentration in the soil, and soil bulk density) may be quantified with additional collection and analysis of field data from the Dillon Reservoir watershed. However, whether or not additional measurement would benefit these particular simulations is not clear. For example, if parameter values varied greatly over the watershed, collecting enough measurements to obtain accurate values of input parameters might be impractical. In such cases, sensitivity studies that use the reasonable range of parameters to assess a range in possible model outcomes still can be useful and may be the only option.
- Despite the uncertainties related to model inputs, the model performs reasonably well. Thus, the model could be used to evaluate the effects of various watershed-scale management options related to OWS (such as the effects of population growth or the influence of implementing advanced-treatment systems for septic tank effluent). However, the model is not recommended for making detailed decisions related to regulation of P concentrations in streams in the watershed.

Recommendations for future work include improvement of variable certainty with field measurement of chemical and hydrologic SWAT parameters, simulation of increased densities of OWS in the watershed due to development, and comparison of SWAT with another watershed-scale water quality model that is applied to the Dillon Reservoir watershed.

Four of the most sensitive parameters, the initial concentration of mineral P in the soil, the initial soil organic carbon content, the P soil-partitioning coefficient, and the soil bulk density can be measured from soil core samples. These measurements are viable from two perspectives. First, the measurement of these parameters is relatively inexpensive and, second, the laboratory procedures required for measurement of the parameters is reasonably straightforward. However, while measurements may be relatively easy to obtain, they may have little effect on model output (as described in the Approach section). Therefore, additional measurement of parameters is not necessarily desirable. More research in this area is recommended. Rather, a better understanding of the range and variability of parameter values in the watershed, and the effect on model output and management-practice implementation could be obtained with limited additional measurement.

The P availability index, the parameter that affects P loading the most, can also be measured from soil core samples. However, the procedures for measuring the P availability index as described by Sharpley *et al.* (1984) are extremely detailed and can take more than six months to complete. In addition, measurement of the P enrichment ratio requires meticulous research of the soils and laboratory procedures. These variables are of substantial importance to model results; thus, an effort should be made to obtain narrower reasonable ranges for the variables in the Dillon Reservoir watershed. However, obtaining accurate spatially dependent values for these parameters in the watershed is not feasible. Consequently, these parameters will likely remain as fitting parameters in a rigorous model-calibration effort.

Another source of soil parameter data is the Soil Survey of Summit County Area, Colorado (1980). Information that can be obtained from the soil survey includes soil bulk density, clay content, hydrologic soil group, available water capacity, and grain particle size. Soil surveys are available in digital format as the Soil Survey Geographic (SSURGO) Data Base (1995). The SSURGO database provides more detailed information than the STATSGO database, which is incorporated into SWAT. According to the *SSURGO Data Use Information Manual*, SSURGO was developed for use at the county, parish, and township level. The SSURGO database is not available for the entire portion of Summit County; however, a GIS expert could incorporate data from the SSURGO database where it is available in the Dillon Reservoir watershed into the SWAT model. The current model interfaces included in SWAT and BASINS do not allow for ready incorporation of SSURGO data.

Finally, continued measurement of surface-water quality data and groundwater data will be critical for developing rigorous calibration of watershed-scale pollutant-transport models. The current water quality data for most OWS pollutants is sparse or nonexistent after 1997. In the near term, surface-water quality data collected by Guelfo (2003) and groundwater data collected by Smith *et al.* (2002) can be used to improve model simulations. However, a continued monitoring program would be necessary to develop truly reliable pollutant-transport models.

Development in the Dillon Reservoir watershed is a certainty. From 1970 to 1980, Summit County, Colorado, which encompasses the entire watershed, had the fastest growing population in the US with a growth rate of 232%. From 1980 to 1990 the growth rate was 45.6% (Summit County 2002). Due to the heavy emphasis on tourism in the watershed, population will continue to increase. When population increases, the number of OWS will also rise. Therefore, the model must be able to simulate these changes. With the present formulation of OWS input, the model can accommodate these changes; however, information regarding more recent population growth rates and the number of OWS installed per year in the watershed should be collected. Then, supplementary scenarios with the SWAT model can be created.

The SWAT model is capable of accurately simulating OWS-pollutant transport at the watershed scale. However, as described in the SWAT Setup section, the limitation of applying OWS nutrients as fertilizer has serious restrictions. Modification of SWAT to allow injection of wastewater of a specified quality in the subsurface soil layers would significantly reduce the number of assumptions and uncertainty associated with OWS application.

References

- Allen, R. G. 1986. "A Penman For All Seasons." In: *Soil and Water Assessment Tool Theoretical Documentation, Version 2000*. S. L. Neitsch, J. G. Arnold, J. R. Kiniry, and J. R. Williams.
- Allen, R. G., M. E. Jensen, J. L. Wright, and R. D. Burman. 1989. "Operational Estimates of Evapotranspiration." In: *Soil and Water Assessment Tool Theoretical Documentation, Version 2000*. S. L. Neitsch, J. G. Arnold, J. R. Kiniry, and J. R. Williams.
- Anderson, E. A. 1976. "A Point Energy and Mass Balance Model of Snow Cover." In: *Development of Snowfall-Snowmelt Routine for Mountainous Terrain for the Soil Water Assessment Tool (SWAT)*. T. A. Fontaine, T. S. Cruickshank, J. G. Arnold, and R. H. Hotchkiss. 2002.
- Arnold, J. G., P. M. Allen, G. Bernhardt. 1993. "A Comprehensive Surface-Groundwater Flow Model." *Journal of Hydrology*. 142(1-4), 47–69.
- Arnold, J. G. and J. R. Williams. 1994. *SWRRB – A Watershed Scale Model for Soil and Water Resources Management*. United States Department of Agriculture, Agriculture Research Service, Grassland Soil and Water Research Laboratory, Temple, TX.
- Arnold J. G. and P. M. Allen. 1996. "Estimating Hydrologic Budgets for Three Illinois Watersheds." *Journal of Hydrology*. 176, 57–77.
- Arnold, J. G., R. Srinivasan, R. S. Muttiah, J. R. Williams. 1998. "Large Area Hydrologic Modeling and Assessment – Part I: Model Development." *Journal of American Water Resources Association*. 34(1), 73–78.

Arnold, J. G., R. Srinivasan, R. S. Muttiah, and P. M. Allen. 1999. "Continental Scale Simulation of the Hydrologic Balance." *Journal of the American Water Resources Association*. 35(5), 1037–1051.

Anderson, E. A. 1976. "A Point Energy and Mass Balance Model of Snow Cover." In: *Development of a Snowfall-Snowmelt Routine for Mountainous Terrain for the Soil Water Assessment Tool (SWAT)*. T. A. Fontaine, T. S. Cruickshank, J. G. Arnold, and R. H. Hotchkiss. 2002.

Barrow, N. J. and T. C. Shaw. 1975. "The Slow Reactions Between Soil and Anions. 2. Effect of Time and Temperature on the Decrease in Phosphate Concentration in Soil Solution." In: *Soil and Water Assessment Tool Theoretical Documentation, Version 2000*. S. L. Neitsch, J. G. Arnold, J. R. Kiniry, and J. R. Williams.

Bicknell, B. R., J. C. Imhoff, J. L. Kittle, Jr. A. S. Donigian, Jr., and R. C. Johanson. 1996. *Hydrological Simulation Program – Fortran User's Manual for Release 11*. EPA/600/R-93/174. US EPA, Athens, GA.

Boswell, V. G. 1926. "The Influence of Temperature Upon the Growth and Yield of Garden Peas." In: *Soil and Water Assessment Tool Theoretical Documentation, Version 2000*. S. L. Neitsch, J. G. Arnold, J. R. Kiniry, and J. R. Williams.

Brady, N. C. and R. R. Weil. 1999. *The Nature and Properties of Soils*. Prentice Hall, Inc., Upper Saddle River, NJ.

Brown, L. C. and T. O. Barnwell, Jr. 1987. "The Enhanced Water Quality Models QUAL2E and QUAL2E-UNCAS Documentation and User Manual." In: *Soil and Water Assessment Tool Theoretical Documentation, Version 2000*. S. L. Neitsch, J. G. Arnold, J. R. Kiniry, and J. R. Williams.

Chapra, S. C. 1997. "Surface Water-Quality Modeling." In: *Soil and Water Assessment Tool Theoretical Documentation, Version 2000*. S. L. Neitsch, J. G. Arnold, J. R. Kiniry, and J. R. Williams.

Chen, Y. D., S. C. McCutcheon, R. F. Carsel, A. S. Donigian, J. R. Cannell, and J. P. Craig. 1995. "Validation of HSPF for the Water Balance Simulation of the Upper Grande Ronde Watershed, Oregon, USA." *Proceedings of the Boulder Symposium on Man's Influence on Freshwater Ecosystems and Water Use*. IAHS Publication 230, 3–13.

Colorado Department of Public Health and Environment (CDPHE). 2001. Water Quality Control Commission. March 2, 2001. November 27, 2002.
<http://www.cdphe.state.co.us/op/regs/waterregs>

Crawford, N. H. and R. K. Linsley. 1966. *Digital Simulation in Hydrology: Stanford Watershed Model IV*. Technical Report 39. Civil Engineering Department, Stanford University, Stanford, CA.

Danish Hydraulic Institute. 1999a. *MIKE SHE Pre- and Post-Processing User Manual*. DHI Software, Denmark.

Danish Hydraulic Institute. 1999b. *MIKE SHE Water Movement User Manual*. DHI Software, Denmark.

Deliman, P. N., R. H. Glick, and C. E. Ruiz. 1999. *Review of Watershed Water Quality Models*. Technical Report W-99-1. US Army Corps of Engineers, Waterways Experiment Station, Vicksburg, MI.

Denver Water. 2002. November 27, 2002. <http://www.denverwater.org/>

DiLuzio, M., R. Srinivasan, and J. G. Arnold. 2001. *Soil And Water Assessment Tool Arcview Interface Manual, Version 2000*.

Doherty, J., L. Brebber, and P. Whyte. 1994. *PEST: Model-Independent Parameter Estimation*. Watermark Computing.

Donigian Jr., A. S. and W. C. Huber. 1991. *Modeling Of Nonpoint Source Water Quality In Urban and Non-Urban Areas*. EPA 600/3-91/039. Environmental Research Laboratory, Office of Research and Development, US EPA, Athens, GA.

Donigian Jr., A. S., W. C. Huber, and T. O. Barnwell, Jr. 1996. "Models of Nonpoint Source Water Quality for Watershed Assessment and Management." *Proceedings of Watershed '96*. June 8–12, 1996, Baltimore, MD.

Donigian, Jr., A. S., J. C. Imhoff, and J. L. Kittle, Jr. 1999. *HSPF-Parm: An Interactive Database of HSPF Model Parameters, Version 1.0*. AQUA TERRA Consultants, Mountain View, CA.

Engelmann, C. J. K., A. D. Ward, A. D. Christy, and E. S. Bair. 2002. "Application of the BASINS Database and NPSM Model on a Small Ohio Watershed." *Journal of the American Water Resources Association*. 38(1), 289–300.

Fetter, C. W. 1994. *Applied Hydrogeology, Third Edition*. Prentice Hall Publishers, Upper Saddle River, NJ.

Fetter, C. W. 1999. *Contaminant Hydrogeology, Second Edition*. Prentice Hall Publishers, Upper Saddle River, NJ.

Fontaine, T. A., T. S. Cruickshank, J. G. Arnold, and R. H. Hotchkiss. 2002. "Development of a Snowfall-Snowmelt Routine for Mountainous Terrain for the Soil Water Assessment Tool (SWAT)." *Journal of Hydrology*. 262, 209–223.

Green, W. H. and G. A. Ampt. 1911. "Studies On Soil Physics, 1. The Flow of Air and Water Through Soils,." In: *Soil and Water Assessment Tool Theoretical Documentation, Version 2000*. S. L. Neitsch, J. G. Arnold, J. R. Kiniry, and J. R. Williams.

Guelfo, J. L. 2003. *Water Quality Monitoring in the Dillon Reservoir Watershed, Colorado, to Enable Assessment of Development Impacts*. Thesis, Colorado School of Mines, Golden, CO.

Hargreaves, G. H. and Z. A. Samani. 1982. "Estimating Potential Evapotranspiration." In: *Soil and Water Assessment Tool Theoretical Documentation, Version 2000*. S. L. Neitsch, J. G. Arnold, J. R. Kiniry, and J. R. Williams.

Hargreaves, G. H. and Z. A. Samani. 1985. "Reference Crop Evapotranspiration from Temperature." In: *Soil and Water Assessment Tool Theoretical Documentation, Version 2000*. S. L. Neitsch, J. G. Arnold, J. R. Kiniry, and J. R. Williams.

Hargreaves, G. L., G. H. Hargreaves, and J. P. Riley. 1985. "Agricultural Benefits for Senegal River Basin." In: *Soil and Water Assessment Tool Theoretical Documentation, Version 2000*. S. L. Neitsch, J. G. Arnold, J. R. Kiniry, and J. R. Williams.

Hjermstad, L. M. 1970. *The Influence of Meteorological Parameters on the Distribution of Precipitation Across Central Colorado Mountains*. Atmospheric Science Paper, No. 163. Colorado State University, Fort Collins, CO.

Jones, C. A, C. V. Cole, A. N. Sharpley, and J. R. Williams. 1984. "A Simplified Soil and Plant Phosphorus Model. I. Documentation." In: *Soil and Water Assessment Tool Theoretical Documentation, Version 2000*. S. L. Neitsch, J. G. Arnold, J. R. Kiniry, and J. R. Williams.

Kirkland, S. L. 2001. *Coupling Site-Scale Fate and Transport with Watershed-Scale Modeling to Assess the Cumulative Effects Of Nutrients From Decentralized Onsite Wastewater Systems*. Thesis, Colorado School of Mines, Golden, CO.

Knisel, W. G. 1980. "CREAMS, A Field Scale Model for Chemicals, Runoff and Erosion from Agricultural Management Systems." In: *Soil and Water Assessment Tool Theoretical Documentation, Version 2000*. S. L. Neitsch, J. G. Arnold, J. R. Kiniry, and J. R. Williams.

Lahlou, M., L. Shoemaker, S. Choudhury, R. Elmer, A. Hu, H. Manguerra, and A. Parker. 1998. *Better Assessment Science Integrating Point and Nonpoint Sources: BASINS Version 2.0 User's Manual*. EPA 823/B/98/006. US EPA, Office of Water.

Larson, L. L. and E. L. Peck. 1974. "Accuracy of Precipitation Measurements for Hydrologic Modeling." In: *Soil and Water Assessment Tool Theoretical Documentation, Version 2000*. S. L. Neitsch, J. G. Arnold, J. R. Kiniry, and J. R. Williams.

Lasserre, F., M. Razack, and O. Banton. 1999. "A GIS-linked Model for the Assessment of Nitrate Contamination in Groundwater." *Journal of Hydrology*. 224, 81–90.

- Lemons, P. J. 2003 *Modeling Pollution Transport and Fate to Assess the Effects of Onsite Wastewater Systems on the Lake Dillon Watershed, Colorado*. M.S. Thesis. Department of Geology and Geological Engineering, Colorado School of Mines, Golden, CO.
- Leonard, R. A., W. G. Knisel, and D. A. Still. 1987. "GLEAMS: Groundwater Loading Effects on Agricultural Management Systems." In: *Soil and Water Assessment Tool Theoretical Documentation, Version 2000*. S. L. Neitsch, J. G. Arnold, J. R. Kiniry, and J. R. Williams.
- Lewis, W. M, Jr. and J. F. Saunders, III. 1998. *Studies of Phosphorus Yields from South Barton Gulch 1997 Final Report*. Prepared for the Summit Water Quality Committee.
- Lewis, W. M, Jr. and J. F. Saunders, III. 1999. *A Quantitative Evaluation of Factors Controlling Transparency in Dillon Reservoir, Colorado*. Prepared for the Summit Water Quality Committee.
- Lewis, W. M, Jr. and J. F. Saunders, III. 2002. *Dillon Reservoir Water Quality Model Revision and Recalibration for 2001*. Prepared for the Summit Water Quality Committee.
- Lohani, V, D. F. Kibler, and J. Chanat. 2002. "Constructing a Problem Solving Environment Tool for Hydrologic Assessment of Land Use Change." *Journal of the American Water Resources Association*. 38(2), 439–452.
- Lumb, A. M., R. B. McCammon, and J. L. Kittle, Jr. 1994. *Users Manual for an Expert System (HSPEXP) for Calibration of the Hydrological Simulation Program – Fortran*. USGS Water Investigations Report 94-4168.
- Magoon, C. A. and C. W. Culpepper. 1932. "Response of Sweet Corn to Varying Temperatures from Time of Planting to Canning Maturity." In: *Soil and Water Assessment Tool Theoretical Documentation, Version 2000*. S. L. Neitsch, J. G. Arnold, J. R. Kiniry, and J. R. Williams.
- Manguerra, H. B. and B. A. Engel. 1998. "Hydrologic Parameterization of Watersheds for Runoff Prediction Using SWAT." *Journal of the American Water Resources Association*. 34(5), 1149-1162.
- McCray, J. E., D. N. Huntzinger, S. Van Cuyk, and R. L. Siegrist. 2000. "Mathematical Modeling of Unsaturated Flow and Transport in Soil-Based Wastewater Treatment Systems." *WEFTEC 2000 Symposium*. Water Environment Federation, Anaheim, CA.
- McDonald, M. G, and A. W. Harbaugh. 1988. "A Modular Three-Dimensional Finite-Difference Ground-Water Flow Model." *Techniques of Water-Resources Investigations*. United States Geological Survey. Book 6, Chapter A1.
- McElroy, A. D., S. Y. Chiu, J. W. Nebgen, A. Aleti, and F. W. Bennett. 1976. "Loading Functions for Assessment of Water Pollution from Nonpoint Sources." In: *Soil and Water Assessment Tool Theoretical Documentation, Version 2000*. S. L. Neitsch, J. G. Arnold, J. R. Kiniry, and J. R. Williams.

- Mein, R. G. and C. L. Larson. 1973. "Modeling Infiltration During a Steady Rain." In: *Soil and Water Assessment Tool Theoretical Documentation, Version 2000*. S. L. Neitsch, J. G. Arnold, J. R. Kiniry, and J. R. Williams.
- Menzel. 1980. "Enrichment Ratios for Water Quality Modeling." In: *Soil and Water Assessment Tool Theoretical Documentation, Version 2000*. S. L. Neitsch, J. G. Arnold, J. R. Kiniry, and J. R. Williams.
- Monteith, J. L.. 1965. "Evaporation and the Environment." In: *Soil and Water Assessment Tool Theoretical Documentation, Version 2000*. S. L. Neitsch, J. G. Arnold, J. R. Kiniry, and J. R. Williams.
- Munns, D. N. and R. L. Fox. 1976. "The Slow Reaction Which Continues After Phosphate Adsorption: Kinetics and Equilibrium in Some Tropical Soils." In: *Soil and Water Assessment Tool Theoretical Documentation, Version 2000*. S. L. Neitsch, J. G. Arnold, J. R. Kiniry, and J. R. Williams.
- Neitsch, S. L., J. G. Arnold, J. R. Kiniry, and J. R. Williams. 2001a. *Soil and Water Assessment Tool Theoretical Documentation, Version 2000*.
- Neitsch, S. L., J. G. Arnold, J. R. Kiniry, and J. R. Williams. 2001b. *Soil and Water Assessment Tool User's Manual, Version 2000*.
- Priestly, C. H. B. and R. J. Taylor. 1972. "On the Assessment of Surface Heat Flux and Evaporation using Large-Scale Parameters." In: *Soil and Water Assessment Tool Theoretical Documentation, Version 2000*. S. L. Neitsch, J. G. Arnold, J. R. Kiniry, and J. R. Williams.
- Rajan, S. S. S. and R. L. Fox. 1972. "Phosphate Adsorption by Soils. 1. Influence of Time and Ionic Environment on Phosphate Adsorption." In: *Soil and Water Assessment Tool Theoretical Documentation, Version 2000*. S. L. Neitsch, J. G. Arnold, J. R. Kiniry, and J. R. Williams.
- Santhi, C., J. G. Arnold, J. R. Williams, W. A. Dugas, R. Srinivasan, and L. M. Hauck. 2001. "Validation of the SWAT Model on a Large River Basin with Point and Nonpoint Sources." *Journal of the American Water Resources Association*. 37(5), 1169–1188.
- Sharpley, A. N. 1982. "A Prediction of the Water Extractable Phosphorus Content of Soil Following Phosphorus Addition." In: *Soil and Water Assessment Tool Theoretical Documentation, Version 2000*. S. L. Neitsch, J. G. Arnold, J. R. Kiniry, and J. R. Williams.
- Sharpley, A. N., C. Gray, C. A. Jones, and C. V. Cole. 1984. "A Simplified Soil and Plant Phosphorus Model. II. Prediction of Labile, Organic, and Sorbed P Amounts." In: *Soil and Water Assessment Tool Theoretical Documentation, Version 2000*. S. L. Neitsch, J. G. Arnold, J. R. Kiniry, and J. R. Williams.

- Sharpley, A. N. and J. R. Williams (eds.). 1990. "EPIC – Erosion Productivity Impact Calculator, 1. Model Documentation." In: *Soil and Water Assessment Tool Theoretical Documentation, Version 2000*. S. L. Neitsch, J. G. Arnold, J. R. Kiniry, and J. R. Williams.
- Siegrist, R. L. and W. C. Boyle. 1987. "Wastewater-Induced Soil Clogging Development." *Journal of Environmental Engineering*. 113(3), 550–565.
- Smith, H. L., J. E. McCray, K. S. Lowe, and R. L. Siegrist. 2002. *Use of Uncertain or Low Cost Data to Characterize the Subsurface Hydrology of the Blue River Watershed, Colorado*. Geological Society of America, Annual Meeting, October 27–30, 2002, Denver, CO.
- Soil Conservation Service. 1972. "Section 4: Hydrology." In: *National Engineering Handbook*. In: *Soil and Water Assessment Tool Theoretical Documentation, Version 2000*. S. L. Neitsch, J. G. Arnold, J. R. Kiniry, and J. R. Williams.
- Soil Survey Geographic (SSURGO) Data Base, Data Use Information. 1995. Miscellaneous Publication No. 1527. USDA, Natural Resources Conservation Service, National Soil Survey Center.
- Soil Survey of Summit County Area, Colorado. 1980. US Government Printing Office.
- Sophocleous, M. A., J. K. Koelliker, R. S. Govindaraju, T. Birdie, S. R. Ramireddygar, and S. P. Perkins. 1999. "Integrated Numerical Modeling for Basin-Wide Water Management: The Case of the Rattlesnake Creek Basin in South-Central Kansas." *Journal of Hydrology*. 214, 179–196.
- Srinivasan R., T. S. Ramanarayanan, J. G. Arnold, and S. T. Bednarz. 1998. "Large Area Hydrologic Modeling and Assessment Part II: Model Application." *Journal of the American Water Resources Association*. 34(1), 91–101.
- Summit County. 2002. Colorado County Government. Accessed November 27, 2002. <http://www.co.summit.co.us/>
- United States Department of Agriculture (USDA)-NRCS Soil Survey. 2002. Accessed December 5, 2002 and December 27, 2002. http://soils.usda.gov/soil_survey/main.html
- United States Environmental Protection Agency (US EPA). 1980. "Design Manual: Onsite Wastewater Treatment and Disposal Systems." In: *Coupling Site-Scale Fate and Transport with Watershed-Scale Modeling to Assess the Cumulative Effects of Nutrients From Decentralized Onsite Wastewater Systems*. S. L. Kirkland. 2001. Thesis, Colorado School of Mines, Golden, CO.
- US EPA. 1999. A Summary of US Effluent Trading and Offset Projects. November 1999. November 27, 2002. <http://www.epa.gov/owow/watershed/trading/traenvrn.pdf>
- US EPA. 2001. *Better Assessment Science Integrating Point and Nonpoint Sources (BASINS) Version 3.0*. EPA 823/B/01/001. US EPA, Office of Water, Washington, DC.

US EPA. 2002a. *BASINS Metadata*. Accessed October 10, 2002 and November 27, 2002. <http://www.epa.gov/OST/BASINS/metadata.htm>

US EPA. 2002b. *STORET*. Accessed September 24, 2002. <http://www.epa.gov/STORET>

Van Cuyk, S., R. Siegrist, A. Logan, S. Masson, E. Fischer, and L. Figueroa. 2001. "Hydraulic and Purification Behaviors and Their Interactions During Wastewater Treatment in Soil Infiltration Systems." *Water Resources*. 35(4), 953–964.

Williams, J. R. and R. W. Hann. 1973. "HYMO, A Problem-Oriented Computer Language for Building Hydrologic Models." In: *Soil and Water Assessment Tool Theoretical Documentation, Version 2000*. S. L. Neitsch, J. G. Arnold, J. R. Kiniry, and J. R. Williams.

Williams, J. R. 1975. "Sediment Routing for Agricultural Watersheds." In: *Soil and Water Assessment Tool Theoretical Documentation, Version 2000*. S. L. Neitsch, J. G. Arnold, J. R. Kiniry, and J. R. Williams.

Williams, J. R. and R. W. Hann. 1978. "Optimal Operation of Large Agricultural Watershed with Water Quality Constraints." In: *Soil and Water Assessment Tool Theoretical Documentation, Version 2000*. S. L. Neitsch, J. G. Arnold, J. R. Kiniry, and J. R. Williams.

Williams, J. R., C. A. Jones, and P. T. Dyke. 1984. "A Modeling Approach to Determining the Relationship Between Erosion and Soil Productivity." In: *Soil and Water Assessment Tool Theoretical Documentation, Version 2000*. S. L. Neitsch, J. G. Arnold, J. R. Kiniry, and J. R. Williams.

Williams, J. R., A. D. Nicks, and J. G. Arnold. 1985. "Simulator for Water Resources in Rural Basins." In: *Soil and Water Assessment Tool Theoretical Documentation, Version 2000*. S. L. Neitsch, J. G. Arnold, J. R. Kiniry, and J. R. Williams.

Supplemental Information: Theoretical Formulation of SWAT

This section describes the theoretical formulation of SWAT, while Appendix A in Lemonds, 2003 provides further details related to the theoretical concepts in SWAT.

SWAT is a watershed-scale model developed by the USDA, ARS to predict the impact of management practices on water, sediment, and agricultural chemical yields in watersheds that possess different soils, land uses, and management conditions over long durations (Neitsch *et al.* 2001a). SWAT primarily uses physically-based data; that is, instead of using regression equations, SWAT utilizes theory-based hydrologic and climate equations. Data from the watershed are used as input to these equations (Neitsch *et al.* 2001a).

SWAT simulates water movement, sediment movement, crop growth, and nutrient cycling (Neitsch *et al.* 2001a). Other important attributes of SWAT include its:

- Computational efficiency that enables complex watersheds to be modeled in a straightforward manner
- Incorporation of easily accessible data from government agencies, which is available for most watersheds
- Ability to simulate long-term impacts of pollutant buildup and downstream impact.

SWAT was developed from the Simulator for Water Resources in Rural Basins (SWRRB) model (Williams *et al.* 1985; Arnold *et al.* 1990). Other models important in the creation of SWAT include Chemicals, Runoff, and Erosion from Agricultural Management Systems (CREAMS) (Knisel 1980), Groundwater Loading Effects on Agricultural Management Systems (GLEAMS) (Leonard *et al.* 1987), and Erosion-Productivity Impact Calculator (EPIC) (Williams *et al.* 1984).

Model Formulation for Hydrology

SWAT can simulate many different physical processes. In preparation for modeling a watershed, the basin is divided into subwatersheds. Subwatersheds are valuable if land uses and soils vary greatly and impact hydrology in different ways and to simulate minor tributaries to the main river in the watershed. Data for each subwatershed are grouped into the following types (Neitsch *et al.* 2001a):

- Climate
- HRUs
- Ponds/wetlands
- Groundwater
- Main stream reaches that drain the subwatershed

SWAT simulations are based on water balance in the subwatersheds, the entire watershed, and the two major parts of the hydrologic cycle, the land phase and the water routing phase. To simulate the hydrologic cycle, SWAT uses the following water balance equation for a specified spatial region:

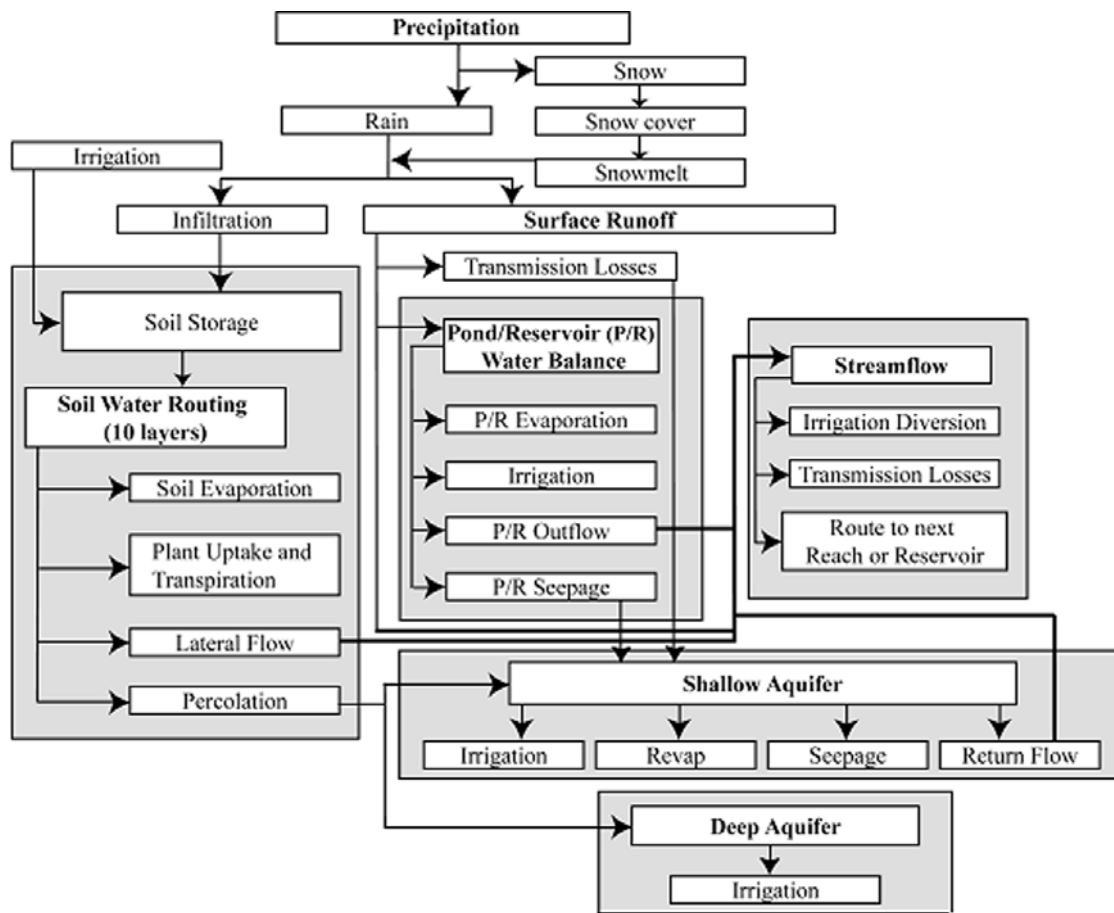
$$SW_t = SW_0 + \sum_{i=1}^t (R_{day} - Q_{surf} - E_a - w_{seep} - Q_{gw}) \quad \text{Equation G-16}$$

where SW_t is the final soil water content (mm H₂O), SW_0 is the initial soil water content on day i (mm H₂O), t is the time (days), R_{day} is the amount of precipitation on day i (mm H₂O), Q_{surf} is the amount of surface runoff on day i (mm H₂O), E_a is the amount of evapotranspiration on day i (mm H₂O), w_{seep} is the amount of water entering the vadose zone from the soil profile on day i (mm H₂O), and Q_{gw} is the amount of return flow on day i (mm H₂O). Return flow is the water that is lost from the shallow aquifer to the stream.

Figure G-16 summarizes the physical processes in the hydrologic cycle that SWAT is able to simulate. The major groupings are:

- Soil storage
- Streamflow
- Shallow aquifer
- Deep aquifer
- Pond/reservoir water balance
- Surface runoff
- Precipitation

Precipitation provides input of water into the model, and streamflow out of the watershed, evapotranspiration, and losses to the deep aquifer provide the means for water to leave the watershed.



Source: Neitsch *et al.* 2001a

Figure G-16
Schematic Diagram Showing the Physical Processes in the Hydrologic Cycle That SWAT Can Simulate

Land Phase of the Hydrologic Cycle

Information needed for the land phase of the hydrologic cycle include:

- Climate
- Hydrology
- Land cover and plant growth
- Erosion
- Nutrients
- Pesticides
- Land management

The climate inputs provide the moisture and energy to the simulated watershed. The climate information that SWAT requires includes daily precipitation, maximum and minimum air temperature, solar radiation, wind speed, and relative humidity (Neitsch *et al.* 2001a). Values for these variables may be derived from observed data or can be generated using a weather generator, an option in SWAT. The WXGEN weather generator (Sharpley and Williams 1990) is incorporated into SWAT. SWAT calculates snow cover based on average-daily temperature. Soil temperature is calculated at the soil surface and at the center of each soil layer. A soil layer is a specific stratum of soil that has similar properties related to its structure and water-holding capacity. SWAT can simulate up to ten soil layers. In addition to the soil layers, SWAT also simulates shallow aquifer and deep aquifer systems.

SWAT simulates the hydrology of the watershed using several different physical processes. Canopy storage accounts for the water that is intercepted by vegetation and is subsequently evaporated. SWAT's hydrologic algorithms also simulate infiltration and redistribution. Infiltration is the entry of water into the soil, and redistribution is the movement of water through the soil profile after the precipitation event has ended (Neitsch *et al.* 2001a).

Evapotranspiration includes evaporation from rivers and lakes, bare soil, vegetative surfaces, transpiration by plants, and sublimation of snow and ice (Neitsch *et al.* 2001a). SWAT uses rainfall amounts to calculate surface runoff volume, infiltration, and peak runoff rate for each HRU. In SWAT, ponds and reservoirs are distinctly different. Ponds act as holding structures for runoff and are assumed to be located off the main channel, which means they never receive water from upstream subwatersheds (Neitsch *et al.* 2001a).

In SWAT precipitation data may be read from an input file or generated by the model. However, Neitsch *et al.* (2001a) suggest that measured precipitation be used in the model whenever available due to the increased accuracy in SWAT's ability to simulate streamflow hydrographs when observed information is provided. Although measured precipitation data is better than randomly generated information, uncertainties still exist. Neitsch *et al.* (2001a) discuss the inherent variability of using observed data.

Gage measurements of precipitation may only catch a fraction of the total precipitation due to wind eddies caused by the gage. Larson and Peck (1974) relate that deficits of 10% for rain and 30% for snow are typical discrepancies for gages that protrude above the ground surface and are not specifically designed to shield against the effects of wind.

Brady and Weil (1999) define evapotranspiration as the combined loss of water from a given area, and during a specified period of time, by evaporation from the soil surface and by transpiration from plants. The potential evapotranspiration rate (PET) describes how fast water vapor would be lost from a densely vegetated plant-soil system if soil water content were continuously maintained at an optimal level (Brady and Weil 1999).

In SWAT there are three options for estimating PET: the Penman-Monteith method (Monteith 1965; Allen 1986; Allen *et al.* 1989), the Priestly-Taylor method (Priestly and Taylor 1972), and the Hargreaves method (Hargreaves *et al.* 1985). In addition, SWAT can also read daily PET values if another method is preferred or measurements are available. Table G-16 shows the data requirements of the three PET methods.

Table G-16

Data Requirements of the Three Methods Available in SWAT for Computing PET

	Air Temperature	Wind Speed	Relative Humidity	Solar Radiation
Penman-Monteith	X	X	X	X
Priestly-Taylor	X		X	X
Hargreaves	X			

The original Hargreaves method was developed from a study of cool-season Alta fescue grass lysimeter data from Davis, California (Hargreaves and Samani 1982). Hargreaves and Samani (1985) then improved the equation. This form of the Hargreaves method (Hargreaves and Samani 1985) is employed in SWAT as

$$\lambda E_o = 0.0023 \cdot H_o \cdot (T_{mx} - T_{mn})^{0.5} \cdot (\bar{T}_{av} + 17.8) \quad \text{Equation G-17}$$

where λ is the latent heat of vaporization (MJ kg^{-1}), E_o is the potential evapotranspiration (mm d^{-1}), H_o is the extraterrestrial radiation ($\text{MJ m}^{-2} \text{d}^{-1}$), T_{mx} is the maximum air temperature for a given day ($^{\circ}\text{C}$), T_{mn} is the minimum air temperature for a given day ($^{\circ}\text{C}$), and \bar{T}_{av} is the mean air temperature for a given day ($^{\circ}\text{C}$).

Up to ten soil layers may be simulated by SWAT. Soil parameters used in the calculation of percolation through the soil include the bulk density of the soil, the percent clay content of the soil, saturated hydraulic conductivity, and the available water capacity. Available water capacity is the water available for plant extraction and is the difference between field capacity and the permanent wilting point. Field capacity is the amount of water held in the soil at a tension of 0.033 MPa and usually represents the soil water remaining after allowing a thoroughly wetted soil to drain for about two days (Neitsch *et al.* 2001a). The permanent wilting point is the amount of water held in the soil at a tension of 1.5 MPa and typically is the soil water content when plants growing in the soil wilt and do not recover if their leaves are kept in a humid atmosphere overnight (Neitsch *et al.* 2001a).

Saturated and unsaturated flow in the soil are simulated by SWAT. For saturated soils, flow is gravity driven and primarily occurs in the downward direction (Neitsch *et al.* 2001). This movement is characterized with a storage routing method by

$$w_{perc,ly} = SW_{ly,excess} \cdot \left(1 - \exp \left[\frac{-\Delta t}{TT_{perc}} \right] \right) \quad \text{Equation G-18}$$

where $w_{perc,ly}$ is the amount of water percolating to the underlying soil layer on a given day (mm H₂O), $SW_{ly,excess}$ is the drainable volume of water in the soil layer on a given day (mm H₂O), Δt is the length of the time step (hrs), and TT_{perc} is the travel time for percolation (hrs). The travel time for percolation is defined by

$$TT_{perc} = \frac{SAT_{ly} - FC_{ly}}{K_{sat}} \quad \text{Equation G-19}$$

where TT_{perc} is the travel time for percolation (hrs), SAT_{ly} is the amount of water in the soil layer when completely saturated (mm H₂O), FC_{ly} is the water content of the soil layer at field capacity (mm H₂O), and K_{sat} is the saturated hydraulic conductivity for the layer (mm hr⁻¹). When the soil water content of a soil layer exceeds field capacity, saturated flow occurs.

Unsaturated flow in the soil may take place in any direction due to gradients occurring between high and low water contents. Unsaturated flow is indirectly modeled as a function of the depth distribution of plant water uptake and the depth distribution of soil water evaporation.

Two options for simulating infiltration and runoff are available in SWAT: the Soil Conservation Service (SCS) Curve Number method (Soil Conservation Service 1972) and the Green-Ampt Mein-Larson method (Green and Ampt 1911; Mein and Larson 1973). The SCS Curve Number method is an empirical model based on rainfall-runoff relationships. The equation is a function of the soil's permeability, land use, and antecedent soil water conditions (Neitsch *et al.* 2001). The SCS curve number equation is

$$Q_{surf} = \frac{(R_{day} - I_a)^2}{(R_{day} - I_a + S)} \quad \text{Equation G-20}$$

where Q_{surf} is the accumulated runoff or rainfall excess (mm H₂O), R_{day} is the rainfall depth for the day (mm H₂O), I_a is the initial abstractions, which includes surface storage, canopy interception, and infiltration prior to runoff (mm H₂O), and S is the retention parameter (mm H₂O).

The retention parameter is a function of the spatial variability of soils, land uses, management practices, and slope, and it changes through time as a function of soil water content. The retention parameter, S , is defined by

$$S = 25.4 \left(\frac{1000}{CN} - 10 \right) \quad \text{Equation G-21}$$

where CN is the curve number for the day. The initial abstractions, I_a , are commonly estimated as $0.2S$ so that the accumulated runoff or rainfall excess, Q_{surf} , equals

$$Q_{surf} = \frac{(R_{day} - 0.2S)^2}{(R_{day} + 0.8S)} \quad \text{Equation G-22}$$

Runoff will occur only if $R_{day} > I_a$.

The other infiltration/runoff method incorporated into SWAT is the Green-Ampt Mein-Larson (Green and Ampt 1911; Mein and Larson 1973) excess rainfall method to determine infiltration. This method requires sub-daily precipitation data provided by the user. The infiltration rate equation for this method is

$$f_{inf,t} = K_e \cdot \left(1 + \frac{\Psi_{wf} \cdot \Delta\theta_v}{F_{inf,t}} \right) \quad \text{Equation G-23}$$

where $f_{inf,t}$ is the infiltration rate at time t (mm hr^{-1}), K_e is the effective hydraulic conductivity (mm hr^{-1}), Ψ_{wf} is the wetting front matric potential (mm), $\Delta\theta_v$ is the change in volumetric moisture content across the wetting front (mm mm^{-1}) and $F_{inf,t}$ is the cumulative infiltration at time t ($\text{mm H}_2\text{O}$).

SWAT simulates two aquifers: a shallow aquifer and a deep aquifer. The unconfined, shallow aquifer contributes flow to the stream reach in each subwatershed. The deep aquifer is confined and transports water to regional aquifers outside of the watershed (Neitsch *et al.* 2001a). The water balance for the shallow aquifer is

$$aq_{sh,i} = aq_{sh,i-1} + w_{rchrg} - Q_{gw} - w_{revap} - w_{deep} - w_{pump,sh} \quad \text{Equation G-24}$$

where $aq_{sh,i}$ is the amount of water stored in the shallow aquifer on day i (mm H₂O), $aq_{sh,i-1}$ is the amount of water stored in the shallow aquifer on day $i-1$ (mm H₂O), w_{rchrg} is the amount of recharge entering the aquifer on day i (mm H₂O), Q_{gw} is the groundwater flow, or base flow, into the main channel on day i (mm H₂O), w_{revap} is the amount of water moving into the soil zone in response to water deficiencies on day i (mm H₂O), w_{deep} is the amount of water percolating from the shallow aquifer into the deep aquifer on day i (mm H₂O), and $w_{pump,sh}$ is the amount of water removed from the shallow aquifer by pumping on day i (mm H₂O).

Water that percolates through the vadose zone becomes shallow aquifer recharge. The shallow, unconfined aquifer contributes base flow to the main stream within each subwatershed only if the amount of water stored in the shallow aquifer surpasses a threshold value specified by the user. Water also may move from the shallow aquifer into the soil profile. In the SWAT Theoretical Documentation Manual (Neitsch *et al.* 2001a), the term for this movement is “revap.” Percolation to the deep aquifer occurs only if a user-specified threshold value is exceeded (Neitsch *et al.* 2001a).

The water balance for the deep aquifer is

$$aq_{dp,i} = aq_{dp,i-1} + w_{deep} - w_{pump,dp} \quad \text{Equation G-25}$$

where $aq_{dp,i}$ is the amount of water stored in the deep aquifer on day i (mm H₂O), $aq_{dp,i-1}$ is the amount of water stored in the deep aquifer on day $i-1$ (mm H₂O), w_{deep} is the amount of water percolating from the shallow aquifer into the deep aquifer on day i (mm H₂O), and $w_{pump,dp}$ is the amount of water removed from the deep aquifer by pumping on day i (mm H₂O).

If the deep aquifer is the source of pumping for irrigation or for consumptive use, then the model will allow the total volume of water in the deep aquifer to be removed on a given day. Water that enters the deep aquifer is not considered in further water budget calculations and is considered lost from the watershed system (Neitsch *et al.* 2001a).

The current version of SWAT does not print groundwater table heights to an output file, but the value is updated daily by the model (Neitsch *et al.* 2001a). In addition, while chemical constituents may be transported to and through the groundwater, SWAT cannot track chemical mass in the groundwater nor does it provide concentration information in an output file.

One plant growth model is used to simulate every type of plant and land cover in SWAT. Separation between perennial and annual plants is possible, as is the assessment of water and nutrient removal from the root zone, transpiration, and biomass production. Annual plants grow from the date of planting to the date of harvest or until the total accumulated heat units equal potential heat units for the plant (Neitsch *et al.* 2001a).

The heat unit theory (Boswell 1926; Magoon and Culpepper 1932) is based on the concept that plants have heat requirements that must be met for the plant to reach maturity. Perennials live continuously, becoming dormant in the winter. Growth of perennials occurs during periods when the average daily temperature exceeds the base temperature that is specified by the user.

SWAT incorporates the Modified Universal Soil Loss Equation (MUSLE) (Williams 1975) to simulate erosion and sediment yield in each HRU. The MUSLE uses the amount of runoff, while the Universal Soil Loss Equation (USLE) uses rainfall as an erosive energy indicator (Neitsch *et al.* 2001a). Benefits of using the amount of runoff instead of rainfall include increased prediction accuracy, elimination of a delivery ratio, and ability to calculate single-storm sediment yields (Neitsch *et al.* 2001a). The hydrology model provides the amount of runoff, which is needed for the MUSLE evaluation.

Nutrient processes may be simulated with SWAT. SWAT uses the basic nitrogen cycle to simulate the transformation of nitrogen. Plant use of nitrogen is approximated using the plant growth algorithms in SWAT. Removal of nitrate and organic N by water flow serves as a means of removing nitrogen from the soil. Runoff, lateral flow, and percolation may contain nitrate as well. Transport of organic N with sediment is simulated using a loading function developed by McElroy *et al.* (1976) and modified by Williams and Hann (1978) to include applications of individual runoff events. The loading function estimates daily organic N runoff loss based on the organic N concentration in the uppermost layer of soil, the sediment yield, and the enrichment ratio, which is the concentration of organic N in the sediment divided by the concentration in the soil (Neitsch *et al.* 2001a).

Plant growth algorithms in SWAT are incorporated to simulate the uptake of P by plants. Similar to the nitrogen processes, soluble P and organic P may be removed from the soil by water movement. Sediment transport of P is estimated with the McElroy *et al.* (1976) loading function. Soluble P removed with runoff is calculated using solution P concentration in the top 10 mm of soil, the runoff volume, and a soil-partitioning factor (Neitsch *et al.* 2001a).

SWAT is capable of predicting several different agriculture-related processes and different land management practices. Fertilization of crops including application of N and P, irrigation applications, tillage operations, and crop and management rotations can all be simulated with SWAT. One of these practices accounts for the application, movement, degradation, and adsorption of pesticides. The algorithms for pesticide transport and fate were adapted from GLEAMS (Leonard *et al.* 1987). In addition to irrigation practices, SWAT can model the transfer of water between reservoirs, reaches, and subwatersheds, and model the export of water from the watershed. While SWAT does not allow for OWS inputs directly, OWS are simulated in the application to the Dillon Reservoir, as is described in the Simulation Results section located in Chapter 4, *Biozone Algorithm*.

Routing Phase of the Hydrologic Cycle

After the land-phase processes have been modeled, the loadings that SWAT has calculated are routed through the stream network. Using a command structure similar to the hydrologic model HYMO (Williams and Hann 1973), SWAT determines mass flow and fate of chemicals in the stream and streambed. The routing processes may be split into two types: routing in the main channel and routing in the lake.

Four components help route streams through the main channel: flood, sediment, nutrient, and channel pesticide routing. In flood routing, water evaporation, transmission through the channel bed, and water removal for irrigation or human use are modeled. Flow can be increased with direct precipitation onto the channel or through the addition of point-source discharges. Sediment transport is controlled by peak channel velocity. Excess stream energy can reentrain settled material and cause streambed degradation. Stream routing parameters such as Manning's "n" coefficient for overland flow and streamflow, slope steepness, channel width, and channel depth may be adjusted. Nutrient routing equations were adapted from QUAL2E (Brown and Barnwell 1987). SWAT can track nutrients in the aqueous phase and those adsorbed to bed sediment. Pesticide transformations are controlled by first-order decay relationships. Settling, burial, resuspension, volatilization, diffusion, and transformation are modeled by the channel pesticide equations.

Reservoir routing is made up of the following components:

- Inflow
- Outflow
- Rainfall on the surface
- Evaporation
- Seepage from the reservoir bottom
- Diversions

Three options exist for outflow from the reservoir. One is user-specified outflow. The second is designed predominantly for small, uncontrolled reservoirs and calls for a specific water release rate. The third is intended for managed reservoirs and requires the user to specify a monthly target volume for the reservoir (Neitsch *et al.* 2001a).

Inflow of sediment may be derived from streams or direct flow into the reservoir from the subwatershed. Sediment settling is controlled by equilibrium sediment concentration, and median particle size. The volume of outflow and the suspended sediment concentration at the time of outflow directs the amount of sediment exiting the reservoir as outflow.

Chapra's (1997) nitrogen and phosphorus mass balance model is used to simulate reservoir nutrients. The model assumes that the reservoir is well mixed (no stratification), P is the limiting nutrient, and total P is a measure of the lake's trophic status (Neitsch *et al.* 2001a).

The second assumption is usually valid when the lake is dominated by nonpoint sources, and the third assumption indicates that there is a relationship between total P and biomass. Chapra's (1997) model is also used to simulate pesticides in the reservoir. One pesticide may be partitioned into dissolved and particulate phases in the water and sediment layers (Neitsch *et al.* 2001a).

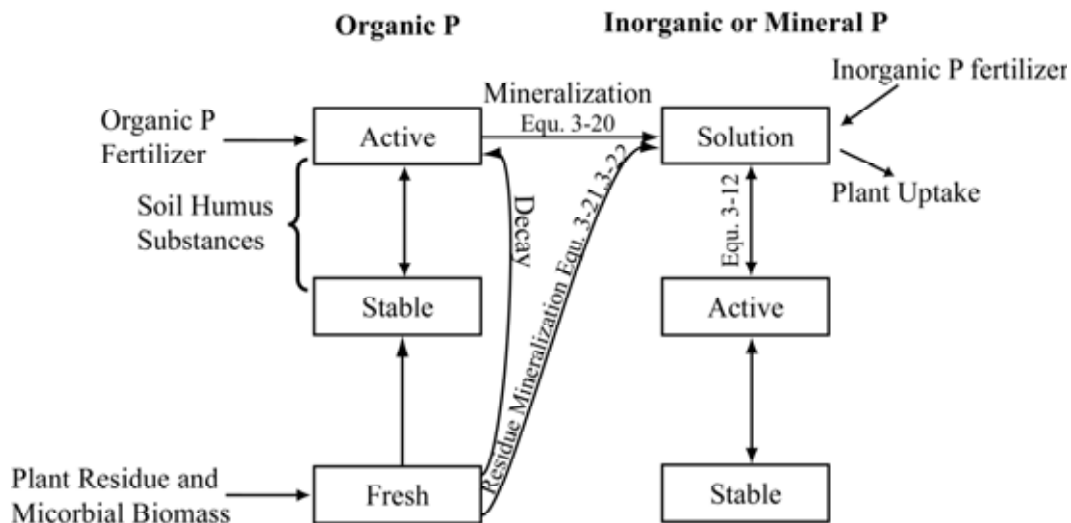
Model Formulation for Phosphorus Transport and Fate

SWAT simulates six different forms of phosphorus in the soil (Neitsch *et al.* 2001a):

- Active organic P
- Stable organic P
- Fresh organic P
- Stable inorganic P
- Active inorganic P
- Solution inorganic P

In SWAT the term “stable” means that these forms of P move slowly to the labile form, and the term “active” means that these forms of P move quickly to the labile form of P, where labile P is the P available for plant uptake (personal communication, Jeff Arnold, Agricultural Research Service 2002). The *SWAT Theoretical Documentation Manual* (Neitsch *et al.* 2001a) refers to the six forms of P as “pools” and inorganic P as “mineral P;” therefore, this appendix will also refer to these constituents as “pools” and “mineral P,” respectively, from this point forward.

Figure G-17 shows the relationship between the P pools simulated in SWAT. To simplify the description of the model formulation for P in this section, a table of the SWAT input variables and a short description of the variable follows each subsection.



Note: See Lemonds 2003 for reference to equations. Source: Neitsch *et al.* 2001a.

Figure G-17
SWAT Soil Phosphorus Forms (Pools) and the Processes That Contribute to the Movement and Fate of Phosphorus

Initialization of Soil Phosphorus Levels

Users may define the amount of solution inorganic P and the total amount of active and stable organic P in the soil layers. An assumption in SWAT is that only inorganic P may occur in a soluble form. If the user chooses not to define specific values for these parameters, SWAT will initialize values as follows.

The concentration of solution inorganic P in all soil layers is assigned a value of 5 mg (kg soil)⁻¹ initially, which is representative of unmanaged land under native vegetation (Neitsch *et al.* 2001a). The concentration of P in the active mineral pool as defined by Jones *et al.* (1984) is

$$\min P_{act,ly} = P_{solution,ly} \cdot \frac{1 - pai}{pai} \quad \text{Equation G-26}$$

where $\min P_{act,ly}$ is the concentration of P in the active mineral pool in soil layer ly (mg kg⁻¹), $P_{solution,ly}$ is the concentration of P in solution in soil layer ly (mg kg⁻¹), and pai is the P availability index. The pai is described in further detail in Lemonds (2003) (see Section 3.2.4 in Lemonds 2003) and is defined by

$$pai = \frac{P_{solution,f} - P_{solution,i}}{fert_{min P}} \quad \text{Equation G-27}$$

where $P_{solution,f}$ is the amount of P in solution after fertilization and incubation, $P_{solution,i}$ is the amount of P in solution before fertilization, and $fert_{min P}$ is the amount of soluble P fertilizer added to the sample. The concentration in the stable mineral pool as defined by Jones *et al.* (1984) is

$$\min P_{sta,ly} = 4 \cdot \min P_{act,ly} \quad \text{Equation G-28}$$

where $\min P_{sta,ly}$ is the concentration of P in the stable mineral pool in soil layer ly (mg kg⁻¹) and $\min P_{act,ly}$ is the concentration of P in the active mineral pool in soil layer ly (mg kg⁻¹).

Levels of organic P are given values based on the assumption that the N:P ratio for humic materials is 8:1. The concentration of humic organic P in a soil layer, $orgP_{hum,ly}$, is

$$orgP_{hum,ly} = 0.125 \cdot orgN_{hum,ly} \quad \text{Equation G-29}$$

where $orgN_{hum,ly}$ is the concentration of humic organic N in the soil layer (mg kg⁻¹).

The value for $orgN_{hum,ly}$ is calculated based on the assumption that the C:N ratio for humic materials is 14:1 and is calculated by

$$orgN_{hum,ly} = 10^4 \cdot \left(\frac{orgC_{ly}}{14} \right) \quad \text{Equation G-30}$$

where $orgC_{ly}$ is the amount of organic carbon in the layer (%).

Values of P in the fresh organic pool are set to zero for all soil layers except for the top 10 mm of soil (Neitsch *et al.* 2001). In the top 10 mm, the fresh organic P pool value, $orgP_{frsh,surf}$, is calculated by

$$orgP_{frsh,surf} = 0.0003 \cdot rsd_{surf} \quad \text{Equation G-31}$$

where rsd_{surf} is the residue material (i.e. decaying plants) in the top 10 mm of soil (kg ha^{-1}).

Calculations in SWAT are performed on a mass basis. Nutrient levels may be input as concentrations; however, SWAT converts these to masses by

$$\frac{conc_P \cdot \rho_b \cdot depth_{ly}}{100} = \frac{\text{kg P}}{\text{ha}} \quad \text{Equation G-32}$$

where $conc_P$ is the concentration of P in a layer (mg kg^{-1}), ρ_b is the bulk density (Mg m^{-3}), and $depth_{ly}$ is the depth of the soil layer ly (mm). The SWAT input variables from this section are shown in Table G-17. In summary, the usual case in SWAT is either to let SWAT use default values for all the initialization parameters or to specifically define the variables listed in Table G-17 from measured data.

Table G-17
SWAT Input Variables for Initialization of Soil P Levels

Input Variable	Definition
$P_{solution,ly}$	Concentration of P in solution in soil layer ly (mg kg^{-1})
$orgP_{hum,ly}$	Concentration of humic organic (stable and active) P in a soil layer (mg kg^{-1})
pai	P availability index
rsd_{surf}	Residue material (i.e. decaying plants) in the top 10 mm of soil (kg ha^{-1})
ρ_b	Bulk density of soil layer (Mg m^{-3})

Phosphorus Mineralization of Humus

Formulations by Jones *et al.* (1984) are used to model phosphorus mineralization. Two of the six pools of phosphorus incorporated into SWAT that are considered for mineralization are: fresh organic P, including crop residue and microbial biomass, and active organic P related to soil humus. Decomposition and mineralization may only occur if the soil layer temperature is above 0 °C (Neitsch *et al.* 2001a). The two mechanisms are dependent on water availability and temperature. The temperature factor for nutrient cycling is

$$\gamma_{tmp,ly} = 0.9 \cdot \frac{T_{soil,ly}}{T_{soil,ly} + \exp[9.93 - 0.312 \cdot T_{soil,ly}]} + 0.1 \quad \text{Equation G-33}$$

where $\gamma_{tmp,ly}$ is the nutrient cycling temperature factor for layer ly , and $T_{soil,ly}$ is the temperature of layer ly (°C). The water factor for nutrient cycling is

$$\gamma_{sw,ly} = \frac{SW_{ly}}{FC_{ly}} \quad \text{Equation G-34}$$

where $\gamma_{sw,ly}$ is the nutrient cycling water factor for layer ly , SW_{ly} is the water content of layer ly on a given day (mm H₂O), and FC_{ly} is the water content of layer ly at field capacity (mm H₂O).

In the humic fraction of soil (the active and stable forms of organic P), phosphorus is divided between the active and stable organic pools by using the ratio of humus active organic N to stable organic N. Mineralization is calculated for the humus active organic P pool by

$$P_{min a,ly} = 1.4 \cdot \beta_{min} \cdot (\gamma_{tmp,ly} \cdot \gamma_{sw,ly})^{1/2} \cdot orgP_{act,ly} \quad \text{Equation G-35}$$

where $P_{min a,ly}$ is the phosphorus mineralized from the humus active organic P pool (kg P ha⁻¹), β_{min} is the rate coefficient for mineralization of the humus active organic nutrients, $\gamma_{tmp,ly}$ is the nutrient cycling temperature factor for layer ly , $\gamma_{sw,ly}$ is the nutrient cycling water factor for layer ly , and $orgP_{act,ly}$ is the amount of phosphorus in the active organic pool (kg P ha⁻¹). The calculated mineralized phosphorus is then added to the solution P in the soil layer. The SWAT input variable from this section is shown in Table G-18.

Table G-18
SWAT Input Variable for P Mineralization of Humus

Input Variable	Definition
β_{min}	Rate coefficient for mineralization of the humus active organic nutrients

Decomposition and Mineralization of Residue

Fresh organic phosphorus decomposition and mineralization is only allowed in the first soil layer. Decomposition is defined as the breakdown of fresh organic residue into simpler organic compounds, and mineralization is the microbial conversion of organic, plant-unavailable P to inorganic, plant-available P. Both processes are controlled by a decay rate constant that is updated daily and calculated as a function of the C:N ratio and C:P ratio of the residue, temperature, and soil water content. Mineralization of residue in the fresh organic P pool is calculated by

$$P_{minf,ly} = 0.8 \cdot \delta_{ntr,ly} \cdot orgP_{frsh,ly} \quad \text{Equation G-36}$$

where $P_{minf,ly}$ is the phosphorus mineralized from the fresh organic P pool (kg P ha⁻¹), $\delta_{ntr,ly}$ is the residue decay rate constant, and $orgP_{frsh,ly}$ is the phosphorus in the fresh organic pool in layer ly (kg P ha⁻¹). The mineralized phosphorus is added to the solution P pool in the soil layer.

Decomposition of residue in the fresh organic P pool is calculated by

$$P_{dec,ly} = 0.2 \cdot \delta_{ntr,ly} \cdot orgP_{frsh,ly} \quad \text{Equation G-37}$$

where $P_{dec,ly}$ is the phosphorus decomposed from the fresh organic P pool (kg P ha⁻¹), $\delta_{ntr,ly}$ is the residue decay rate constant, and $orgP_{frsh,ly}$ is the phosphorus in the fresh organic pool in layer ly (kg P ha⁻¹). The decomposed phosphorus is added to the humus organic pool in the soil layer.

The decay rate constant that governs organic phosphorus decomposition and mineralization is defined by

$$\delta_{ntr,ly} = \beta_{rsd} \cdot \gamma_{ntr,ly} \cdot (\gamma_{tmp,ly} \cdot \gamma_{sw,ly})^{1/2} \quad \text{Equation G-38}$$

where $\delta_{ntr,ly}$ is the residue decay rate constant, β_{rsd} is the rate coefficient for mineralization of the residue fresh organic nutrients, $\gamma_{ntr,ly}$ is the nutrient cycling residue composition factor for layer ly , $\gamma_{tmp,ly}$ is the nutrient cycling temperature factor for layer ly , and $\gamma_{sw,ly}$ is the nutrient cycling water factor for layer ly .

The nutrient cycling residue composition factor for layer ly , $\gamma_{ntr,ly}$, is

$$\gamma_{ntr,ly} = \min \left\{ \begin{array}{l} \exp \left[-0.693 \cdot \frac{(\varepsilon_{C:N} - 25)}{25} \right] \\ \exp \left[-0.693 \cdot \frac{(\varepsilon_{C:P} - 25)}{25} \right] \end{array} \right. \quad \text{Equation G-39}$$

1.0

where $\varepsilon_{C:N}$ is the C:N ratio on the residue in the soil layer, and $\varepsilon_{C:P}$ is the C:P ratio on the residue in the soil layer. The SWAT input variable from this section is shown in Table G-19.

Table G-19
SWAT Input Variable for Decomposition and Mineralization of Residue

Input Variable	Definition
β_{rsd}	Rate coefficient for mineralization of the residue fresh organic nutrients

Sorption of Inorganic P

As a result of the reaction with the soil, solution P concentration decreases quickly after application of soluble P fertilizer (Neitsch *et al.* 2001a). The initial rapid reaction is followed by significantly slower reduction in solution P that can continue for many years (Barrow and Shaw 1975; Munns and Fox 1976; Rajan and Fox 1972; Sharpley 1982). To model the quick depletion of solution P, SWAT assumes rapid equilibration takes place between solution P and the active mineral pool with equations taken from Jones *et al.* (1984) (Neitsch *et al.* 2001a). The resulting slow equilibration process between the “active” and “stable” mineral pools is simulated by equations from Jones *et al.* (1984).

The phosphorus availability index controls the equilibration between the solution and active mineral pools. The index is defined by the fraction of fertilizer P in solution after a certain time period characterized by the rapid reaction stage. To measure the index, soil is saturated and dried over six months and solution P is extracted with anion exchange resin (Neitsch *et al.* 2001a). The phosphorus availability index, pai , is described by Equation G-27.

In the rapid reaction process between solution and active mineral pools, the rate of flow from the solution to the active mineral pool is ten times the rate from the active mineral pool to solution. For slow phosphorus sorption, SWAT assumes that the active mineral phosphorus pool has a slow equilibration process with the stable mineral phosphorus pool. When the system is at equilibrium, the active mineral pool is one-quarter the size of the stable mineral pool. When not in equilibrium, the rate of flow from the solution to the active mineral pool is ten times the rate from the active mineral pool to solution. The SWAT input variable from this section is shown in Table G-20.

Table G-20
SWAT Input Variable for Sorption of Inorganic P

Input Variable	Definition
pai	Phosphorus availability index

Leaching

SWAT simulates leaching as the movement of P in response to a concentration gradient that is created when plant roots remove soluble P from the soil solution in the root zone. SWAT only allows soluble P from the top 10 mm of soil to leach into the first soil layer by

$$P_{perc} = \frac{P_{solution,surf} \cdot w_{perc,surf}}{10 \cdot \rho_b \cdot depth_{surf} \cdot k_{d,perc}} \quad \text{Equation G-40}$$

where P_{perc} is the amount of P moving from the top 10 mm of soil into the first soil layer (kg P ha⁻¹), $P_{solution,surf}$ is the amount of P in solution in the top 10 mm (kg P ha⁻¹), $w_{perc,surf}$ is the amount of water percolating to the first soil layer from the top 10 mm on a given day (mm H₂O), ρ_b is the bulk density of the top 10 mm (Mg m⁻³), which is assumed to be equal to the bulk density of the first soil layer, and $depth_{surf}$ is the depth of the surface layer (10 mm). $k_{d,perc}$ is the phosphorus percolation coefficient (m³ Mg⁻¹), which is defined as the ratio of phosphorus concentration in the surface 10 mm of soil to the concentration of phosphorus in the percolate (Neitsch *et al.* 2001a). In this equation the subscript *perc* refers to the agriculture-related term percolation that is used to describe water movement in unsaturated soils.

The SWAT input variables from this section are shown in Table G-21.

Table G-21
SWAT Input Variables for Leaching

Input Variable	Definition
ρ_b	Bulk density of the soil (Mg m ⁻³)
$k_{d,perc}$	P percolation coefficient (m ³ Mg ⁻¹)

Phosphorus Transport Mechanisms

The transfer of nutrients, particularly P, from the soil to streams and lakes is a common occurrence in the erosion process and can lead to dangerous nutrient enrichment of surface water bodies. Particles become sorbed to sediment, which then becomes mobile in overland water flow during a precipitation or snowmelt event. The following section describes the processes by which P is transported from land areas to the stream network.

Due to the low mobility of solution P in the soil, surface runoff will interact only partly with the solution P that is stored in the top 10 mm of soil (Neitsch *et al.* 2001a). The amount of soluble phosphorus lost in runoff, P_{surf} (kg P ha⁻¹), is

$$P_{surf} = \frac{P_{solution,surf} \cdot Q_{surf}}{\rho_b \cdot depth_{surf} \cdot k_{d,surf}} \quad \text{Equation G-41}$$

where $P_{solution,surf}$ is the amount of P in solution in the top 10 mm (kg P ha⁻¹), Q_{surf} is the amount of surface runoff on a given day (mm H₂O), ρ_b is the bulk density of the top 10 mm (Mg m⁻³) (assumed to be equivalent to the bulk density of the first soil layer), $depth_{surf}$ is the depth of the “surface” layer (10 mm), and $k_{d,surf}$ is the P soil water partitioning coefficient (m³ Mg⁻¹). The $k_{d,surf}$ parameter is the ratio of the soluble P concentration in the surface 10 mm of soil to the concentration of soluble P in surface runoff. This parameter is also called the distribution coefficient and is obtained from a measured linear isotherm fit to soil water sorption experimental data.

The SWAT input variables from this section are shown in Table G-22.

Table G-22
SWAT Input Variables for Movement of Soluble P

Input Variable	Definition
$k_{d,surf}$	P soil water partitioning coefficient (m ³ Mg ⁻¹)
ρ_b	Bulk density of the soil (Mg m ⁻³)

Organic and mineral P are carried with sediment in surface runoff. These two forms of P are strongly associated with sediment loading from each HRU. Therefore, changes in sediment loading will affect the amount of organic and mineral P transported. An equation developed by McElroy *et al.* (1976) and modified by Williams and Hann (1978) is utilized to calculate the amount of P transported with sediment:

$$sed_{Psurf} = 0.001 \cdot conc_{sedP} \cdot \frac{sed}{area_{hru}} \cdot \varepsilon_{P:sed} \quad \text{Equation G-42}$$

where sed_{Psurf} is the amount of phosphorus transported with sediment to the main channel in surface runoff (kg P ha⁻¹), $conc_{sedP}$ is the concentration of P attached to sediment in the top 10 mm (g P (metric ton soil)⁻¹), sed is the sediment yield on a given day (metric tons), $area_{hru}$ is the HRU area (ha), and $\varepsilon_{P:sed}$ is the P enrichment ratio.

The concentration of P attached to sediment in the 10-mm soil surface layer, $conc_{sedP}$ (g P (metric ton soil)⁻¹), is

$$conc_{sedP} = 100 \cdot \frac{(\min P_{act,surf} + \min P_{sta,surf} + orgP_{hum,surf} + orgP_{frsh,surf})}{\rho_b \cdot depth_{surf}} \quad \text{Equation G-43}$$

where $\min P_{act,surf}$ is the amount of P in the active mineral pool in the top 10 mm (kg P ha⁻¹), $\min P_{sta,surf}$ is the amount of P in the stable mineral pool in the top 10 mm (kg P ha⁻¹), $orgP_{hum,surf}$ is the amount of P in the humic organic pool in the top 10 mm (kg P ha⁻¹), $orgP_{frsh,surf}$ is the amount of P in the fresh organic pool in the top 10 mm (kg P ha⁻¹), ρ_b is the bulk density of the first soil layer (Mg m⁻³), and $depth_{surf}$ is the depth of the soil surface layer (10 mm).

The SWAT input variables from this section are shown in Table G-23.

Table G-23
SWAT Input Variables for Organic and Mineral P Attached to Sediment in Surface Runoff

Input Variable	Definition
ρ_b	Bulk density of the soil (Mg m ⁻³)
$\mathcal{E}_{P:sed}$	P enrichment ratio

The P enrichment ratio is defined as the ratio of the concentration of P transported with the sediment to the concentration of P in the soil surface layer (Neitsch *et al.* 2001a). The P enrichment ratio as defined by Menzel (1980) is

$$\mathcal{E}_{P:sed} = 0.78 \cdot (conc_{sed,surf})^{-0.2468} \quad \text{Equation G-44}$$

where $conc_{sed,surf}$ is the concentration of sediment in surface runoff (Mg sed (m H₂O)⁻³). SWAT calculates $\mathcal{E}_{P:sed}$ for each storm event or allows the user to define one value to be used for all events. If the user allows SWAT to calculate an enrichment ratio for each storm event, then the enrichment ratio is a function of the concentration of sediment in surface runoff, $conc_{sed,surf}$, which is calculated by

$$conc_{sed,surf} = \frac{sed}{10 \cdot area_{hru} \cdot Q_{surf}} \quad \text{Equation G-45}$$

where sed is the sediment yield on a given day (metric tons), $area_{hru}$ is the HRU area (ha), and Q_{surf} is the amount of surface runoff on a given day (mm H₂O).

Phosphorus Lag in Surface Runoff and Lateral Flow

SWAT incorporates two storage functions that lag a portion of the surface runoff and lateral flow release to the main channel. In large subbasins with a time of concentration greater than one day, only a fraction of the runoff and lateral flow will arrive at the reach on the day that each is generated. Nutrients in the runoff and lateral flow are lagged as well. After the loading of P in surface runoff and lateral flow is calculated, the amount of P reaching the main channel reach is calculated as

$$P_{surf} = (P'_{surf} + P_{stor,i-1}) \cdot \left(1 - \exp \left[\frac{-surlag}{t_{conc}} \right] \right) \quad \text{Equation G-46}$$

$$sedP_{surf} = (sedP'_{surf} + sedP_{stor,i-1}) \cdot \left(1 - \exp \left[\frac{-surlag}{t_{conc}} \right] \right) \quad \text{Equation G-47}$$

where P_{surf} is the amount of solution P discharged to the main channel in surface runoff on a given day (kg P ha^{-1}), P'_{surf} is the amount of solution P loading generated in the HRU on a given day (kg P ha^{-1}), $P_{stor,i-1}$ is the solution P loading stored or lagged from the previous day (kg P ha^{-1}), $sedP_{surf}$ is the amount of sediment-attached P discharged to the main channel in surface runoff on a given day (kg P ha^{-1}), $sedP'_{surf}$ is the amount of sediment attached P loading generated in the HRU on a given day (kg P ha^{-1}), $sedP_{stor,i-1}$ is the amount of sediment-attached P loading stored or lagged from the previous day (kg P ha^{-1}), $surlag$ is the surface runoff lag coefficient, and t_{conc} is the time of concentration for the HRU (hrs).

The SWAT input variables from this section are shown in Table G-24.

Table G-24
SWAT Input Variables for P Lag in Surface Runoff and Lateral Flow

Input Variable	Definition
$surlag$	Surface runoff lag coefficient
$\mathcal{E}_{P:sed}$	P enrichment ratio

Summary of Phosphorus Fate and Transport Processes

The transport and fate of P is important to understand so that better predictions of nutrient enrichment to surface-water bodies may be made. Phosphorus can undergo several *in situ* processes, including mineralization, decomposition, and sorption. Movement with surface runoff, either dissolved in the water or sorbed to sediment that is in the runoff, characterizes the movement of P into the stream network and eventually into large surface-water bodies.

Table G-25 summarizes the hydrologic phase in which each form of P is transported in the SWAT formulation.

Table G-25
Summary of the Transport Pathways Available to Each of the Six Pools of P in SWAT

Form of P	Transport Pathway
Active organic P	Overland flow of sediment (P attached to sediment entrained in surface runoff)
Stable organic P	Overland flow of sediment (P attached to sediment entrained in surface runoff)
Fresh organic P	Overland flow of sediment (P attached to sediment entrained in surface runoff)
Stable inorganic P	Overland flow of sediment (P attached to sediment entrained in surface runoff)
Active inorganic P	Overland flow of sediment (P attached to sediment entrained in surface runoff)
Solution inorganic P	Overland flow of water (P in solution with surface runoff)



H WATERSHED MODELING USING MANAGE

Use of modeling as an environmental assessment tool can range from simple, low-cost mass balance modeling to more complex, costly numerical modeling with various levels in between. One of the objectives of this project was to apply various levels of models in order to provide a range of options for those attempting to select an appropriate model for their own watershed.

This appendix focuses on the use of an assessment tool called Method for Assessment, Nutrient-loading, and Geographic Evaluation (MANAGE) of watersheds and aquifers. MANAGE was implemented with the intent of exploring a simpler, low-cost, and less time-intensive option for watershed assessment.

Different models are appropriate to different situations dependent upon the needs of the user. There are a few considerations to keep in mind when considering simple versus complex models (Joubert and Lucht 2000):

- Results of all models, simple or complex, are only as good as the input values, and all results are estimates.
- Oftentimes results of more complex models are used with overconfidence.
- More complex models are not always a better solution, especially in situations where qualitative comparisons may suffice.

In cases where qualitative comparisons meet the objectives of a study, simpler models have the advantage of requiring less input data, less resources, and less time. However, cases may arise when a complex model is necessary. Examples of such situations include instances when results are to be compared with monitored water quality data and when attempting to model the movement of an effluent plume in groundwater (Joubert and Lucht 2000). MANAGE can be categorized as a simple model, requiring only input values that can be determined from geographic data available for free in most areas.

Background

MANAGE was created for and initially applied in the Wickford Harbor watershed in Rhode Island. MANAGE was applied in Wickford Harbor to address the observed decline in water quality of the harbor. A full report of this application of MANAGE can be found online at <http://www.uri.edu/ce/wq/mtp/wick/report.html>. Besides describing the results of the Wickford Harbor watershed assessment, this report also provides documentation that is extremely useful for those wishing to apply MANAGE to their own watershed.

Results of the Wickford Harbor assessment are not presented here, but it is important to note that this initial application, for which MANAGE was created, was in a coastal watershed environment, which is in contrast to the alpine watershed studied during this project. Other than the study presented here, Wickford Harbor is the only other application of MANAGE that the authors of this report are aware of.

Description of MANAGE

MANAGE was created by the University of Rhode Island (URI) Cooperative Extension to be applied in communities of Rhode Island to aid in assessment and management of nonpoint pollution sources and management of water resources (Joubert and Lucht 2000). MANAGE has been referred to as a “screening-level pollution risk assessment method” (Joubert and Lucht 2000). MANAGE involves three main components:

- Use of watershed characteristics as “indicators” to assess the risk that pollutant inputs and other factors will lead to an adverse water quality impact
- Nutrient loading estimates via mass balance calculations
- Use of geographical information system (GIS) to create maps for use in analysis and identification of pollutant hotspots

The first two components are completed in an Excel spreadsheet set up for MANAGE. The third component is completed using GIS software. In this case, ArcView 3.2 was used. MANAGE is intended to be a low-cost assessment method using data that is typically available at no cost. The three components of MANAGE enable a user to combine qualitative, quantitative, and visual methods to evaluate the water quality threats to a study area. Each component is described in more detail in the sections that follow. Note that MANAGE is designed to run one study area at a time. If a user wishes to run, for example, an entire study area followed by sub-watersheds of the entire study area, each area must be run separately and the results compared by the user.

Water Quality Indicator Analysis

Expressing pollutant risks in a quantitative manner is often difficult. For example identifying and quantifying the pollution present at a site or sites in a watershed may be difficult and expensive. In such cases, qualitative methods that utilize comparison can be more useful. An example utilized in MANAGE is demonstrated in watershed indicators. Indicators do not quantify pollution effects and do not identify the location of contaminated sites. Rather indicators are used in an attempt to denote the risk of pollutant input or physical stresses that may adversely affect water quality in a watershed (Joubert and Lucht 2000). One example of an indicator is the percentage of total land use that is commercial or industrial. This type of land use has the potential to negatively impact water quality. The larger the amount of such land uses, the greater the chance that a water quality impact will occur.

MANAGE calculates the percentage of total land use that is comprised of these high-intensity categories and then compares this percentage to a scale that indicates that if watershed land uses are greater than 25% high-intensity categories, there is a high risk that these land uses are (or will, if the scenario is being run for future situations) negatively impact water quality. This knowledge is useful when considering such factors as potential sites to monitor or future development plans.

In this appendix, watershed indicators used in MANAGE are split into two categories. The first category is land-use indicators. In addition to the indicators example described previously, MANAGE also evaluates land-use indicators including the amount of:

- Impervious surface
- Forest and wetland
- High-intensity land use in the riparian zone
- Impervious surface in the riparian zone
- Forest and wetland in the riparian zone

Evaluating the presence of various land uses can be important when considering water quality. For example, impervious surfaces may increase the amount of runoff that alters hydrology and has the potential to carry pollutants. This condition is even more pronounced in the riparian zone due to its proximity to surface waters. This proximity reduces the chance that pollutants will be filtered out before reaching surface waters. Furthermore, ecosystems present in undeveloped riparian zones typically have the ability to buffer the impact of pollutants through such processes as filtration and plant uptake. Therefore, preservation of this zone is important. Each land-use indicator is evaluated as a percent of total land use or total riparian land use and given a ranking based on a scale that is individual to the land use. Indicators and their ranking scale can be found in Table H-1. Note that all scales used in MANAGE to rank water quality impact risk associated with the various indicators are based on the literature (Joubert and Lucht 2000).

The second category of indicators is natural resource indicators. These indicators are focused on different aspects of soils, including the presence of excessively permeable soils and presence of excessively restrictive soils. For example, in MANAGE soils are categorized into four hydrologic soil groups, A, B, C, and D. Hydrologic group A is the highest permeability; D the lowest. MANAGE evaluates the presence of hydrologic soil group A, or excessively permeable soils, as a percent of the total soil coverage and ranks it on a scale similar to that used with land use indicators (see Table H-1). If the amount of permeable soils exceeds 60% MANAGE gives a rank of high risk that there will be pollution impact. This high-risk rank is given because high-permeability soils tend to be situated in areas of recharge and high permeability has the potential to allow pollutants to pass through quickly to the groundwater aquifer. Restrictive soils are important for the opposite reason. The permeability of restrictive soils is extremely low indicating that water would move through extremely slow. In such cases, water may not infiltrate at all and instead become runoff. In cases where this runoff carries pollution, pollutants could be contributed directly to surface waters.

Table H-1
A List of Indicators and Their Associated Rating Scales Used by MANAGE

Land Use Indicators	Rating Scale			
	Low	Medium	High	Very High
High intensity land use	<10%			> 25%
Impervious surface	< 10%			> 25%
Forest and wetland	> 80%			< 20%
Riparian high intensity land use	<5%			> 15%
Riparian impervious surface	< 5%			> 15%
Riparian forest and wetland	> 95%			< 60%
Soil Indicators	Rating Scale			
	Low	Medium	High	Very High
High permeability soils	< 10%			>60%
Restrictive layer	< 2%			> 10%

Nutrient Loading Analysis

The second component of MANAGE is a nutrient-loading component that provides estimates of nitrogen and phosphorous loading in the study area. These estimates are calculated using a mass balance approach. The first step in the mass balance approach is to calculate an estimated water budget. Results of the water budget are then used to aid in nutrient loading estimates of both nitrogen and phosphorous. Note that this is a simplified mass balance that does not take into account situations where the per acre nutrient loading may be higher than the average, the effects of storm events, other pollutants, and nutrient uptake through natural processes (Joubert and Lucht 2000). The mass balance is an estimate of nutrients at the source; therefore, numbers are best used as a basis of comparison to each other and not to actual nutrient loading values derived from monitoring data.

The water budget is calculated by MANAGE using precipitation and evapotranspiration (ET) values entered by the user. Both values are typically available from data generated at local weather stations and are entered into MANAGE as inches per year. MANAGE subtracts the ET from the average annual precipitation to estimate the amount of precipitation that is available to form either recharge or runoff. Other components of the water budget, such as depression storage and interflow, are assumed to be negligible. The amount of precipitation that becomes recharge is assumed to be the amount that is left after runoff is subtracted from the available precipitation. A runoff value is calculated for each land use and then the individual values summed to estimate a total runoff. Runoff for each land use is calculated by multiplying the area of that land use by the runoff coefficient for that land use and total precipitation. This yields a volume of runoff for each land use. Once these volumes are summed they can be divided by the area to get runoff in inches per year. Results are shown in MANAGE as both volumetric and normalized values.

The water budget is useful in and of itself; however, volumetric values for recharge and runoff are utilized further in the nutrient loading estimates. Note that the area of each land use and runoff coefficients are values input into MANAGE by the user, which is discussed further in the MANAGE Setup section.

As with available precipitation, nutrient loading in MANAGE is split into two parts: that which is the result of groundwater recharge loading and that which is the result of surface runoff loading. The two parts are summed to provide numbers estimating the total amount of nutrient loading in the watershed. The process for calculating nutrient loading estimates for nitrogen and phosphorous is identical. In MANAGE, nutrient loading to groundwater is assumed to originate from five sources:

- Septic systems
- Fertilized lawns
- Fertilized agricultural areas
- Pet waste
- Unfertilized pervious areas

The process for calculating nutrient loading from each of the five sources differs slightly in each case; however, there are two main methods. For the first four sources, loading is estimated by multiplying the amount of that source (for example, the area of fertilized lawns) by the amount of nutrient loading typically found in that source (for example, lb/acre/year) to yield loading in pounds per year. The method for unfertilized pervious areas differs slightly.

Pervious areas consist of the following:

- Pasture
- Forest
- Orchards
- Unfertilized lawns

The area of each of these land uses is summed then multiplied by a typical loading factor for pervious areas. The loading values from the five sources are then summed to estimate total nutrient loading to groundwater. Dividing this value by the volume of recharge results in an estimated concentration of the nutrients in groundwater recharge.

Other nutrient loading occurs as a result of surface runoff. This loading is calculated by estimating a runoff nutrient loading value for each land use and then summing the individual values to obtain a total value. The amount of loading from each individual land use is calculated by multiplying the area of the land use by the loading factor for that land use. The total loading due to surface water runoff in pounds per year can be divided by runoff volume to obtain concentration or area of the study area to obtain a value in pounds per acre per year. Runoff and recharge loading are summed to estimate total loading in the study area. These values can then be manipulated to gain information about the various sources of the loading, which may help in management practices and source identification.

GIS Analysis

The third and final component of a MANAGE analysis is the GIS analysis. The GIS analysis provides geographic locations of potential pollution sources through both hotspot mapping and location identification of some of the watershed indicators, as well as a means with which to view natural resources. These supplement the other components of MANAGE that do not provide site-specific information.

Hotspot mapping is a means of locating areas that are at a high risk for pollutant impacts. The term nonpoint source pollution often gives the impression that the pollution in question is diffuse or cannot be located (Joubert and Lucht 2000). However, looking at watershed characteristics can often give some idea of where this pollution is likely to occur. For example, nonpoint pollution can be traced to certain types of intense land use (for example, high-density residential), or to natural features such as soil type that may allow for easier transport of pollutants to either surface or groundwaters (for example, high-permeability soils) (Joubert and Lucht 2000). In general, maps of these watershed characteristics are widely available, so the maps can be used to overlay different characteristics (for example, high-density residential areas and high-permeability soils) in order to display the hotspots that are at the highest risk of nonpoint pollution impacts.

GIS can also be used to identify the location of certain indicators. One example is to use GIS to identify the location of high- and very-high-risk land uses. Finally, GIS can be used to create natural resource maps such as soil and land use maps.

Summary

The three components of this tool combine to form MANAGE, a simple assessment method with several advantages (Joubert and Lucht 2000):

- MANAGE is rapid and low-cost, which is beneficial in situations where resources are limited.
- The results of MANAGE can aid in identifying the most serious problems, which can then be targeted for further study.
- Products of MANAGE, such as the map database, can be useful in other town planning efforts.
- The results can be documented when composing town plans or zoning in order to bookmark the need for improvement.
- MANAGE can be used to identify potential impacts before they occur so that pollution can be prevented.

MANAGE Setup

The *Wickford Harbor Watershed Assessment* report (see the Background section at the beginning of this appendix for the web address) (Joubert and Lucht 2000) contains several appendices that document how to set up and utilize MANAGE. Appendix D, Technical Documentation, contains step-by-step instructions detailing which GIS coverages are needed, what GIS functions need to be performed on that data, and how to use the data to complete the MANAGE assessment. Information contained in that document will not be repeated here; however, this section will provide clarification when needed, and when applicable how this project used steps that differ from those used in the original application of MANAGE.

GIS Setup

Setting up a GIS database for the study area was the initial task completed when applying MANAGE in the Dillon Reservoir watershed. A list of the original GIS coverages obtained for this study, the location where this data was accessed, and a description of the file can be found below in Table H-2. Note that the bolded entries are those that are crucial to the eventual completion of the MANAGE nutrient-loading input tables. Others are useful for generating maps and completing qualitative evaluation, but if not obtained, they will not prevent application of MANAGE.

Table H-2
GIS Coverages Obtained for This Project

File	Source Location	Description
STATSGO Spatial Files	http://www.ftw.nrcs.usda.gov/statsgo_ftp.html	STATSGO soil database and spatial coverage
SSURGO Spatial Files	http://lighthouse.nrcs.usda.gov/gateway	SSURGO soil database and spatial coverage
lroads.shp	http://www.dot.state.co.us	Local roads in Summit County
froads.shp	http://www.dot.state.co.us	Major roads in Summit County
Highways.shp	http://www.dot.state.co.us	Highways in Summit County
div5_lakes.shp	http://cdss.state.co.us	Lakes in Division 5 (includes Summit County)
div5_rivers.shp	http://cdss.state.co.us	Rivers in Division 5
div5_counties.shp	http://cdss.state.co.us	Counties in Division 5
l_leadco.shp*	http://lighthouse.nrcs.usda.gov/gateway	Land use map which includes part of Summit County
l_denvc0.shp*	http://lighthouse.nrcs.usda.gov/gateway	Land use map which includes part of Summit County
warmft.shp	N/A	Parcel map including OWS location
Basins.shp	N/A	Study area boundaries (including sub-watersheds)
Cities.shp	http://www.dot.state.co.us	Cities in the study area

* These two land use maps each include a portion of Summit County and needed to be merged in order to obtain an appropriate coverage.

As mentioned, Appendix D of the report on Wickford Harbor contains step-by-step instructions on how to set up MANAGE. These instructions include a list of steps that should be taken to manipulate or create the necessary coverages using the base list provided in Table H-2. However, in some cases coverage comparable to that used in the Wickford Harbor project could not be obtained for this project, and therefore compromises had to be made.

Rhode Island utilized both a SSURGO soil map and a sewer line map in their GIS work; comparable maps could not be found for the Dillon Reservoir watershed. Some manipulation of the land-use coverages was also necessary; the steps necessary to do this were not outlined in the Wickford Harbor project.

With the exception of these situations, GIS setup followed the steps outlined in Appendix D of the Wickford Harbor report for all GIS setup. The process was completed a total of four times: once for the entire watershed and once for each of three focus areas analyzed in this project. Note that Rhode Island recommends use of Arc/Info GIS software to complete all GIS work. This software facilitates input of data into the MANAGE Excel spreadsheet. Arc/Info was neither available nor conducive to this project, so all work was done using ArcView GIS 3.2.

Setup of MANAGE Excel File

Two of the three MANAGE components, land use indicator analysis and nutrient loading analysis, are completed in an Excel file designed by the University of Rhode Island. This Excel file is set up so that values can be entered, either manually or automatically, into input tables. These values are then used to calculate water budget, nutrient loading estimates, and watershed indicator results. Outside of the main input tables other opportunities for user input into this spreadsheet include best management practices (BMPs) and assumptions. Input BMPs can be used for evaluation of current or future potential BMPs. Assumptions made in the model can be evaluated and altered when appropriate. For this project, the MANAGE spreadsheet was obtained from the University of Rhode Island.

The first step taken in setting up the MANAGE Excel file was to complete the input tables. There are five input tables available in MANAGE. The first three are used if the user wishes to complete a surface water and groundwater watershed assessment. The last two are used if the user wishes to complete a groundwater assessment only. Table 1 through Table 3 are entitled “Surface Watershed Land Use/Hydrologic Soil Group Distribution,” “Land Use Distribution in the Unsewered Portion of the Surface Watershed,” and “Land Use Distribution in the Riparian Areas of the Surface Watershed,” respectively. Input Table 1 is shown in Table H-3.

Table H-3
Input Table 1 From MANAGE

INPUT TABLE 1:							
Surface Watershed Land Use/Hydrologic Soil Group Distribution:							
LAND USE	Total Area (acres)	Hydrologic Soil Group					% of Total Land Use
		A	B	C	D	Unknown	
[1] HD Res.(>8 /ac)	0.0	0.0	0.0	0.0	0.0	0.0	0.0%
[2] MHD Res.(4-7.9/ac)	0.0	0.0	0.0	0.0	0.0	0.0	0.0%
[3] MD Res.(1-3.9/ac)	0.0	0.0	0.0	0.0	0.0	0.0	0.0%
[4] MLD Res.(0.5-0.9/ac)	2,509.9	135.9	1,633.6	326.4	414.0	0.0	1.2%
[5] LD Res.(<0.5/ac)	2,509.9	135.9	1,633.6	326.4	414.0	0.0	1.2%
[6] Commercial	1,552.0	161.0	822.0	253.0	316.0	0.0	0.7%
[7] Industrial	159.2	15.3	93.0	36.7	14.3	0.0	0.1%
[8] Roads	559.8	0.0	401.0	5.0	153.7	0.0	0.3%
[9] Airports	0.0	0.0	0.0	0.0	0.0	0.0	0.0%
[10] Railroads	0.0	0.0	0.0	0.0	0.0	0.0	0.0%
[11] Junkyards	0.0	0.0	0.0	0.0	0.0	0.0	0.0%
[12] Recreation	4,481.6	0.0	3,511.4	954.7	15.5	0.0	2.1%
[13] Institution	0.0	0.0	0.0	0.0	0.0	0.0	0.0%
[14] Pasture	254.5	103.5	24.6	0.0	126.5	0.0	0.1%
[15] Cropland	15.4	0.0	5.5	9.9	0.0	0.0	0.0%
[16] Orchards	0.0	0.0	0.0	0.0	0.0	0.0	0.0%
[17] Brush	63,356.0	206.4	56,821.1	2,124.0	4,204.5	0.0	30.1%
[18] Forest	114,286.4	747.6	83,273.3	25,749.0	4,516.6	0.0	54.3%
[19] Barren	16,864.8	567.4	15,160.4	888.2	248.8	0.0	8.0%
[20] Wetland	546.2	27.3	109.8	110.4	298.8	0.0	0.3%
[21] Water	3,419.4	0.0	0.0	0.0	0.0	3,419.4	1.6%
[22] Transitional	0.0	0.0	0.0	0.0	0.0	0.0	0.0%
Total (acres)	210,515.1	2,100.1	163,489.1	30,783.7	10,722.8	3,419.4	100%
		1.0%	77.7%	14.6%	5.1%	1.6%	

Values for the input tables can be obtained in three ways. A command file for MANAGE has been written for use with Arc/Info GIS software. This command file facilitates gathering of input table values from the land-use, soils, sewers, and riparian area coverages. However, this file does not work with ArcView GIS software. Creation of a command file that does work with ArcView is in progress by the creators of MANAGE but was not completed at the time of this study. The second way in which input data values can be obtained is manually. In this case values are estimated from hard-copy maps or other sources and input by hand into the tables. The third manner in which values can be obtained is a combination (hybrid) of the first two methods. This means that work is done and values obtained through use of GIS, but rather than have the command file gather and enter the values into the tables, the values are entered by hand. This method was used in this study.

The hybrid method of data input involves querying various GIS coverages once the GIS setup is completed. All three tables involve entering the acreage of a certain land use divided amongst the various soil types. For example, in Table H-3 total forested acres are approximately 114,287 acres. To get input values for the table, ArcView was used to determine the amount of total forested acres situated on hydrologic group A, the amount situated on group B, and so on.

The remaining tables are similar but utilize modified hydrologic groups A+B, C, D, and restrictive. Restrictive soils are those that have a permeability of less than 0.2 in./hr at depths of 20 to 60 in. (Joubert and Lucht 2000).

Once the input tables are complete, the user can evaluate and/or change other values used in the model. For example, there is a place in the spreadsheet where one can implement best management practices (BMPs). If BMPs are in place in the study area then they should be accounted for in the original implementation of the model provided the intent of the original run is to represent current conditions. Otherwise, BMPs may be evaluated in future scenarios in order to determine which ones might be most effective in improving the water quality of a study area.

Other values that can be altered include some of the assumptions made in MANAGE, including:

- Assumptions about precipitation and ET
- Surface runoff coefficients
- Nutrient loading coefficients
- The number of malfunctioning septic systems

The creators of MANAGE carried out an extensive literature search to ensure that appropriate values were used for the surface runoff and nutrient loading coefficients. As a result, these values should only be changed if users have ensured that they have more appropriate values. Precipitation and ET data are usually readily available for most regions, so users should find values specific to their study area.

Once the spreadsheet is finalized, results can be evaluated. The MANAGE spreadsheet automatically generates some of these results, which is important to note. For example, MANAGE automatically calculates and summarizes the watershed water quality indicators. They are summarized in the worksheet entitled “Risk.” Results of the nutrient loading are summarized in the “Best Easy Out” worksheet. This worksheet summarizes factors such as nitrate loading to groundwater in lb/acre/yr. Inspection of the MANAGE worksheet entitled “MANAGE” provides information about how these results are generated. This worksheet is the heart of the model where all calculations originate. Furthermore, this worksheet can be useful in finding the values necessary to create statistics not automatically generated by the spreadsheet.

Fine Tuning MANAGE

To date, this Dillon Reservoir study appears to be only the second application of MANAGE. Consequently, situations that were not encountered in the original Wickford Harbor application are expected. This section describes some of the obstacles that had to be overcome in applying MANAGE to the Dillon Reservoir watershed.

As mentioned in the GIS Setup section, there were some instances where GIS coverages that were available for the Wickford Harbor watershed were not available in the Dillon Reservoir watershed. All GIS directions in the Wickford Harbor report are given under the assumption that the user has coverages that are identical in nature, so some steps had to be modified. Specifically, extra or modified steps had to be taken to get appropriate soils and land-use maps. Furthermore, Rhode Island used a map of sewer lines to estimate the locations of the sewered areas of the watershed. No such map was available for the Dillon Reservoir watershed, so a parcel map denoting which parcels utilized OWS was used instead.

Wickford Harbor watershed, for which MANAGE was designed, is located in the coastal region of Rhode Island. There is obviously a great deal of difference in the environment of this watershed and the Dillon Reservoir watershed. Therefore, there were some concerns about the applicability of various model parameters to regions outside of and dissimilar to the Wickford Harbor watershed. Specifically, concerns were raised about surface runoff and nutrient loading coefficients, number of septic systems, and percentage of malfunctioning septic systems.

When precipitation occurs, some will be intercepted through processes such as uptake by vegetation, depression storage or ponding, infiltration into soils, evaporation, and transpiration (Novotny 2003). The portion left over has the potential to become surface runoff. Surface runoff is important because it can generate the highest loads of particulate pollutants (Novotny 2003). One means of estimating the volume of surface runoff is through use of surface runoff coefficients. For example, MANAGE calculates surface runoff by calculating a runoff amount for each land use and then summing these values to obtain a total runoff. To calculate a runoff value for each land use, MANAGE employs the following equation:

$$\text{Volume of runoff} = [\text{amount of precipitation (in length/time)}] \times [\text{area of land use type (in Length}^2\text{)}] \times [\text{runoff coefficient}]$$

Equation H-1

In Equation H-1 the runoff coefficient is a value that attempts to estimate the portion of the total precipitation that becomes runoff.

Novotny (2003) indicates that coefficients can differ for flat versus sloped watersheds with larger coefficients being necessary for sloped catchments. The Wickford Harbor watershed, for which the current MANAGE runoff coefficients were selected, is flat in comparison to the topography of Colorado. Therefore, it may be appropriate to select different coefficients. However, for this report, time constraints prohibited the research necessary to select different values and the original values were kept in place.

There was also concern about the applicability of the nutrient loading factors utilized in MANAGE. These nutrient loading factors, sometimes referred to as export coefficients, are values that express pollutant generation per unit area and time for each land use (Novotny 2003). In MANAGE, nutrient loading factors are expressed as lb/acre/yr. Multiplied by the area, in acres, of each land use, these factors provide a means of estimating nutrient loading from each land use in surface runoff.

Novotny (2003) points out that unit loads are highly site-specific and depend on a number of factors including demography, geography, and hydrology. Furthermore values that are developed for various land uses are often based on averages from a wide range of measured values. As with the surface runoff coefficients, the validity of the nutrient loading factors used in MANAGE was questioned due to the differences in the geography and hydrology of Colorado versus Rhode Island. However, unlike surface runoff coefficients, unit loads of nutrients for the study area were available.

As described in Appendix G, *Watershed Modeling Using BASINS/SWAT*, the watershed model Better Assessment Science Integrating Point and Nonpoint Sources (BASINS)/ Soil and Water Assessment Tool (SWAT) was also applied to the study area. This model utilized data specific to the study area to develop unit loading factors for nutrients. These nutrient loading factors were adapted to MANAGE through simple spreadsheet manipulation. The majority of the manipulation involved combining daily loading values into annual loading factors for a period of eight years and then using the lowest and highest annual values as the input range necessary for MANAGE. Some additional manipulation of the data had to be done in order to combine species of nitrogen and phosphorous to get values for total nitrogen and total phosphorous.

Like MANAGE, BASINS/SWAT separated unit loads by land use; however, values were only available for some of the MANAGE land uses. The land use categories for which new values were obtained are brush, pasture, barren, and forest. This situation was determined acceptable because these land uses make up the majority of the study area. Once setup of MANAGE was complete for the entire watershed, as well as each focus area, results could be evaluated.

Results of MANAGE Applied to the Dillon Reservoir Watershed

MANAGE was successfully applied to the Dillon Reservoir watershed. MANAGE was initially applied to the entire study area, and then to each of the three major sub-watersheds: Tenmile Creek, Blue River, and Snake River sub-watersheds. The following sections describe and compare the results of each of the four major model runs.

Watershed Features

Besides providing a means to assess the potential water quality impacts of a watershed, MANAGE provides many statistics that describe the watershed in question. At this point a discussion of these statistics is useful as well as a summarization of some other existing information about the watershed.

This project was conducted in the Dillon Reservoir watershed situated in the southern portion of Summit County, Colorado. Summit County is located in the southeast corner of the northwest quadrant of the state, and spans an elevation range of 7,947 to 14,270 feet. The Dillon Reservoir watershed was created with the completion of the reservoir in 1963. Since that time, the area has undergone many changes, including a rapid increase in population, that have led to increased concern about the preservation of water quality.

One specific concern regards the number of OWS in the watershed. Increased population has led to new development, and much of this development utilizes OWS as a primary means of wastewater disposal. Though OWS can be a safe and viable means of waste disposal, some cases of OWS impact on the environment have been documented. Tools such as MANAGE can be a step towards understanding how OWS might impact water quality in the study area environment.

MANAGE calculates the total acreage of the Dillon Reservoir watershed to be 210,510 acres. The predominant land use in this watershed is forest, which comprises approximately 54%. Forest is also the predominant land use in the riparian zones of the watershed (the areas within 150 feet of a surface water body), occupying approximately 62% of these areas. Soils in MANAGE are mapped according to hydrologic soil groups A, B, C, and D. The most predominant soil group in the Dillon Reservoir watershed is soil group B. B-group soils have low to moderate surface runoff potential with moderate infiltration rates and moderately-fine to moderately-coarse texture (Novotny 2003). Table H-4 summarizes these overall study area features as well as those for each sub-watershed assessed using MANAGE.

Table H-4
Study Area Characteristics by Watershed and by Sub-Watershed

Feature	Entire Study Area	Tenmile Creek Basin	Blue River Basin	Snake River Basin
Total Acres	210515	68248	79932	61222
Predominant Land Use	Forest (54.3%)	Forest (48.9)	Forest (58.8)	Forest (55.2%)
Predominant Riparian Land Use	Forest (60.1%)	Forest (55.1)	Forest (62.7%)	Forest (63.7%)
Predominant Hydrologic Soil Group	B (77.7%)	B (94%)	B (78.6%)	B (58.9%)

Watershed Indicators

As mentioned, MANAGE utilizes watershed indicators as one means of assessing the health of a watershed. Indicators are watershed characteristics that can be used in conjunction with a rating scale from the literature to denote the risk of pollution from that characteristic. An example would be the percent of total land use that is forest or wetland. In order to maintain a low risk of pollution transport due to lack of forest and wetland areas, a watershed should have greater than 80% forest and wetland. All indicators and their associated rating scales are shown in Table H-1. Note that all indicators can be split into two categories: land-use indicators and soil indicators. As the names imply, land-use indicators are concerned mainly with certain types and amount of land uses in the study area, and soil indicators investigate the presence of certain types of soil. These two groups of indicators are discussed in the following section; all indicator results are summarized in Table H-5.

Table H-5
Summary of Results of Watershed Indicator Analysis

Indicator	Value/Risk Entire Study Area	Value/Risk Blue River Basin	Value/Risk Snake River Basin	Value/Risk Tenmile Creek Basin
High and High Risk Land Uses (%)	1.1 / Low	0.9 / Low	1.1 / Low	1.3 / Low
Estimated Impervious Surface (%)	1.2 / Low	1.3 / Low	1.0 / Low	1.3 / Low
Forest and Wetland (%)	54.6 / Medium	59.2 / Medium	55.4 / Medium	49.1 / Medium-High
Riparian High and High Risk Land Uses (%)	3.1 / Low	2.4 / Low	3.8 / Low	3.3 / Low
Riparian Estimated Impervious Surface (%)	2.7 / Low	2.8 / Low	2.7 / Low	2.6 / Low
Riparian Forest and Wetland (%)	60.4 / Medium-High	63.1 / High	63.9 / High	55.3 / Extreme
Excessively permeable soils (%)	1.0 / Low	2.5 / Low	0.2 / Low	0.0 / Low
Restrictive soils (%)	3.2 / Medium	5.0 / Medium	2.0 / Low-Medium	2.4 / Medium

Land-Use Indicators

Land uses are an important consideration because some can generate pollutants (such as land uses that have impervious surfaces) and alter hydrology. Land-use factors considered by MANAGE include the presence of high- and very-high-risk land uses and then the specific presence of impervious surfaces and the amount of forest and wetland. Each of these factors is considered twice for each run of MANAGE, once for the entire area of consideration and a second time in the riparian zone only (for an entire sub-watershed and then just for the riparian zone of that sub-watershed). The riparian zone is considered separately because it is especially important as a buffer zone and as an area of natural treatment.

MANAGE considers the presence of high- and very-high-risk land use as a watershed health indicator. High-risk land uses include high- and medium-high-density residential (greater than four units/acre); schools, hospitals, and other institutional uses; and actively tilled cropland. Very-high-risk land uses include commercial and industrial; highways, railroads, and airports; and junkyards. In the entire watershed, 1.1% of the land use is high- and very-high-risk. This number varies only slightly between the different sub-watersheds analyzed with MANAGE. The Blue River basin had the least amount of such land uses at 0.9%; the Tenmile Creek basin had the greatest at 1.3%. In MANAGE, 0 to 10% presence of high- and very-high-risk land uses is associated with a low risk of water quality impacts from these land uses. Therefore the entire watershed, along with each sub-watershed, falls in the low-risk range.

In the riparian zone, the entire watershed contains approximately 3.1% high- and very-high-risk land uses. The number varies among the three sub-watersheds analyzed: from 2.8% in the Blue River basin to 3.8% in the Tenmile Creek basin. In the riparian zone, MANAGE considers the presence of less than 5% high- and very-high-risk land uses to be a low risk to water quality. However, MANAGE suggests that the presence of any such land uses warrants a site inspection because there is a high potential for contamination hot spots and pollution movement. This aspect will be addressed in the GIS Analysis section.

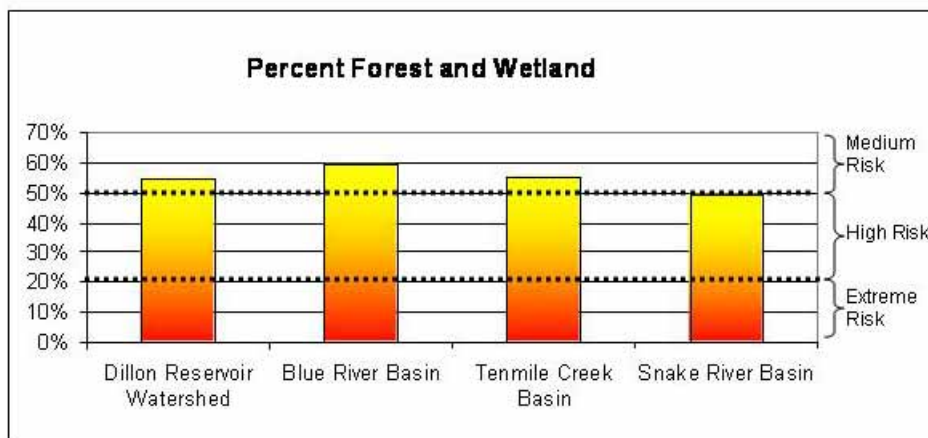
Impervious surfaces (such as pavement and roofs) prevent water from seeping into the ground, thereby increasing runoff and decreasing groundwater recharge. Furthermore, runoff from impervious surfaces has the potential to carry with it pollutants from such surfaces as parking lots and roofs. The greater the amount of impervious surface, the higher the risk that such surfaces will cause detriment to water quality. MANAGE estimates the amount of impervious surface based on the type and amount of land use entered into the MANAGE spreadsheet. MANAGE estimates that the Dillon Reservoir watershed is approximately 1.2% covered by impervious surfaces. This represents a low risk of water quality impact due to the presence of impervious surfaces. In each sub-watershed studied with MANAGE, results were similar, ranging from 1.0 to 1.3% impervious surface.

As with high- and very-high-risk land uses, the amount of impervious surface in the riparian zones is higher than that seen in the entire watershed. For riparian zones in the entire watershed, there is an estimated 2.7% impervious surface. For riparian zones in each of the sub-watersheds, there is little variation; a range of 2.6% to 2.8%. These values represent a low risk of impact to water quality from impervious surfaces in the riparian zones.

Forest and wetland areas can be crucial to watershed health for several reasons. Forests aid in the interception and infiltration of rainfall thereby reducing runoff, which helps to maintain stream flow, reduce erosion, and cycle nutrients. Similarly, wetlands can filter, intercept, and take up pollutants. In addition, they provide important habitat and hydrologic control in riparian environments. Because of these benefits, the relationship between forest and wetland areas and watershed health is inverse: the more forest and wetland a watershed has, the less likelihood that there is any impact due to lack of forested areas.

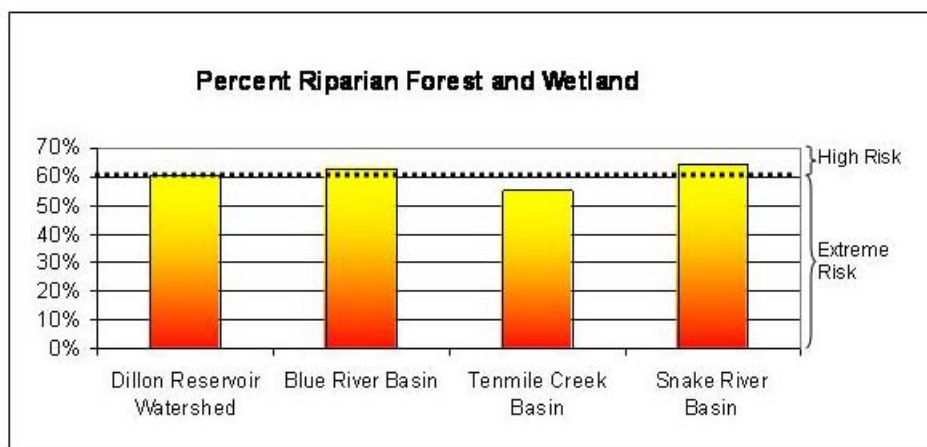
MANAGE considers a watershed with 80% or greater forested and wetland areas as having a low risk of water quality impact. The Dillon Reservoir watershed is approximately 55% forest and wetland, meaning that there is a medium risk of water quality impacts due to lack of forest and wetland areas (see Figure H-1). In the sub-watersheds, this number varies. The Tenmile Creek basin has the lowest amount of forest and wetland areas at approximately 49%, which means that this sub-watershed has a medium-high risk of water quality impacts due to lack of forest and wetland. The Blue River has the greatest amount of forest and wetland: 59%. The Snake River basin is in the middle; 55% is covered by forest and wetland.

In the riparian zone, forest and wetland areas are even greater. However, in order to maintain a low risk of pollution due to lack of forest and wetland in the riparian zone, MANAGE has a rating of 95% or greater of such areas. Sixty percent of the riparian zones within the entire watershed are either forest or wetland, representing a high risk of impact due to lack of forest and wetland (see Figure H-2). Riparian zones in the Tenmile Creek basin contain slightly less forest (55%), which represents an extreme risk to water quality. The Snake River basin has the most forested riparian zones, approximately 64%. However, this level is still a high risk of impact.



Note: Data shown for the entire Dillon Reservoir watershed and each sub-watershed analyzed using MANAGE

Figure H-1
Percent of Land Use That Is Forest and Wetland and Indicator Ranking Scale



Note: Data shown for the entire Dillon Reservoir watershed and each sub-watershed analyzed using MANAGE

Figure H-2
Percent of Riparian Forest and Wetland and Indicator Ranking

Soil Indicators

In addition to using land-use features as watershed indicators, MANAGE looks at soil features that might indicate some risk of pollutant movement in the study area. Soil characteristics that are considered for watershed indicators are the presence of excessively permeable soils in the entire area of consideration and the presence of restrictive layers of soil within unsewered areas.

Excessively permeable soils are an important consideration in watershed health because they represent potential groundwater recharge zones in which pollutants might be carried through the unsaturated zone to the groundwater. MANAGE categorizes all soils into one of the four hydrologic soil groups. These groups, A, B, C, and D, are indicative of soil permeability, with Group A being the most permeable and D the least. In MANAGE, watersheds with greater than 60% high-permeability soils (hydrologic soil group A) are at a high risk of water quality impact due the possibility of quick pollutant transport through the unsaturated zone. Soils in the Dillon Reservoir watershed are only 1% hydrologic group A, which represents a low risk of impact. These numbers vary in the individual sub-watersheds. In the Snake River and Tenmile Creek Basins, there are significantly less amounts of high-permeability soils at 0.2 and 0%, respectively. In the Blue River basin, on the other hand, soils are more permeable with 2.5% high-permeability soils. Potential reasons for this difference among the sub-watersheds are discussed in the Discussion section. All sub-watersheds fall in to the low-risk category of water pollution impact.

In contrast to excessively permeable soils that allow pollutants to move quickly into deeper groundwater zones, excessively low-permeability soils can be a problem because they will not allow water (and possibly pollutants) to infiltrate into the subsurface. In these situations, water may remain on or near the surface and become runoff. This condition is significant primarily in unsewered zones where runoff, and any pollutants it carries, will quickly converge with nearby surface water bodies without the benefit of potential treatment processes that may occur in the vadose zone. In sewerred zones, such runoff would likely be intercepted by storm water systems. In MANAGE, soils are categorized according to hydrologic soil groups A, B, C, and D, but they are also re-categorized in a slightly modified manner that allows for classification of restrictive soils. In this classification system, soils are either hydrologic group A+B, group C, group D, or restrictive. Restrictive soils are those with a permeability of less than 0.2 in./hr at shallow depths of about 20 to 60 in. Presence of this type of permeability at shallow depths is what prevents infiltration.

In unsewered areas of the Dillon Reservoir watershed, soils are 3.2% restrictive. MANAGE considers between 2 and 10% restrictive soils to represent a medium- to medium-high-risk of water quality impact. Therefore, the entire study area is at a medium risk due to the presence of restrictive soils in the unsewered portions of the watershed. This level varies somewhat among individual sub-watersheds. The Blue River basin has the greatest amount of restrictive soils at 5.0%, which is still a medium-risk of water quality impact. The Snake River and Tenmile Creek basins were slightly lower with 2 and 2.4% restrictive soils, respectively, still representing a medium-risk of water quality impact.

Nutrient Loading

MANAGE utilizes mass balances to predict the amount of nutrient loading that might occur in the study area. This prediction is accomplished using an estimated water budget and nutrient loading factors. Nutrient estimates represent sources of the nutrients at the point of origin and not the amount that might reach a groundwater aquifer or stream. Hence the generated estimates are best used as a means to compare nutrient loading among geographic areas and/or land uses and not as values that might be found through monitoring. Results of the mass balance are discussed in the sections that follow; however, because nutrient loading is calculated using the estimated water budget, first describing the results of this budget is beneficial.

Water Budget

A water budget is an evaluation of the sources of water input and discharges in a watershed (Fetter 2001). MANAGE creates an estimated water budget based on the amount of available input (such as precipitation) in the study area as specified by the user. The water budget is created in the manner described in the Nutrient Loading Analysis section. The Dillon Reservoir watershed receives approximately 26 inches of precipitation annually. This value was input by the authors based on data from several local weather stations. Approximately 15 of the 26 inches is output in the form of ET estimated by the Watershed Analysis Risk Management Framework (WARMF). This characteristic means that there are approximately 11 in./year of available precipitation. This value does not change in the sub-watersheds.

In MANAGE, available precipitation becomes either surface water runoff or groundwater recharge. MANAGE estimates that 2.4 (or 22%) of the 11 available inches of precipitation becomes surface water runoff. The remaining 8.6 inches/year (or 78%) becomes groundwater recharge. These numbers vary slightly in the three sub-watersheds analyzed in MANAGE due to the fact that surface runoff volume is estimated using Equation H-1. The land-use area in this equation will change for each sub-watershed as each one has, for example, a different amount of residential area. However, to obtain inches/year of runoff, the volume of runoff must be divided by the area of the sub-watershed. In this study, the ratio of the runoff volume to the sub-watershed area was fairly consistent between all sub-watersheds as well as the entire study area. For this reason, runoff varied from 2.2 to 2.5 in./year. Recharge is merely the available precipitation less the runoff, so recharge also varied little: 8.5 to 8.7 in./year. The results of the water budget are summarized in Table H-6 including values in both in./year and gallons for the entire watershed and each sub-watershed.

Table H-6
Summary of Water Budget Estimates Generated by MANAGE

Watershed	Precip (in/yr)	Precip (Mgal/yr)	ET (in/yr)	ET (Mgal/yr)	Avail. Precip (in/yr)	Avail. Precip (Mgal/yr)	Runoff (in/yr)	Runoff (Mgal/yr)	Recharge (in/yr)	Recharge (Mgal/yr)	OWS Recharge (Mgal/yr)	Tot. Recharge (Mgal/yr)
Entire	26	148616	15	85740	11	62876	2.4	13561	8.6	49315	66	49381
Blue River	26	56432	15	32557	11	23875	2.2	4687	8.8	19187	57	19244
Tennile Creek	26	48181	15	27796	11	20384	2.5	4716	8.5	15668	6	15674
Snake River	26	43220	15	24935	11	18286	2.3	3795	8.7	14491	2	14493

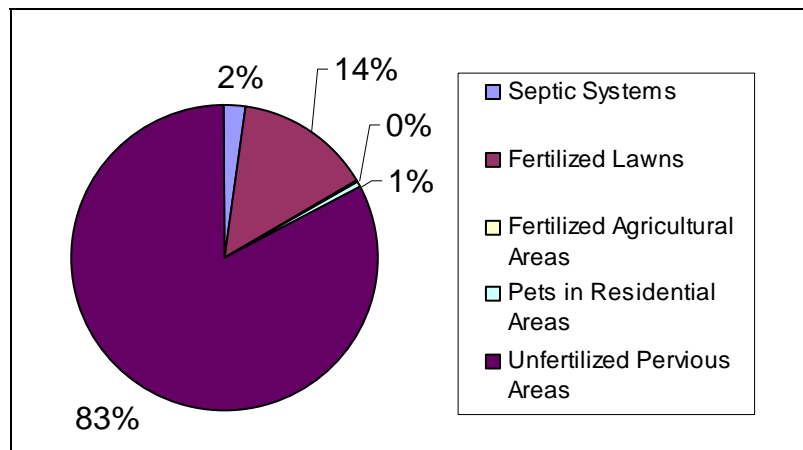
Nitrogen Loading

Nitrogen loading in MANAGE occurs in two main components. In the water budget all available precipitation was contributed to the groundwater as recharge or to the surface water as runoff. Nitrogen input occurs using the same mechanisms: nitrogen contributed to groundwater through recharge or nitrogen contributed to surface water through runoff. A comparatively smaller, additional loading in MANAGE is contributed through direct atmospheric deposition to surface waters.

Total nitrogen loading in the Dillon Reservoir watershed is estimated by MANAGE to be 680,505 lb/N/yr or 3.2 lb/ac/yr. Of the total nitrogen loading, 58% is contributed as surface runoff, 38% as groundwater recharge, and 4% as direct atmospheric deposition to surface waters. MANAGE assumes that nitrogen in groundwater recharge comes from five sources:

- Septic systems
- Fertilized lawns
- Fertilized agricultural areas
- Pets
- Unfertilized pervious areas

Figure H-3 shows the relative contribution of each of these sources to nitrogen in groundwater recharge.



Note: Data shown for the Dillon Reservoir watershed based on analysis using MANAGE

Figure H-3
Source of Nitrogen in Groundwater Recharge

As the figure shows, the largest source of nitrogen to groundwater recharge is unfertilized pervious areas. These areas include: pasture, brush, forest, and unfertilized lawns. Most nitrogen in these areas will be generated by natural processes. While the results vary in the sub-watersheds, in all cases, unfertilized pervious areas make up the majority of nitrogen loading to groundwater (Table H-7).

Table H-7
Summary of Nitrogen Contributions to Surface Water and Groundwater

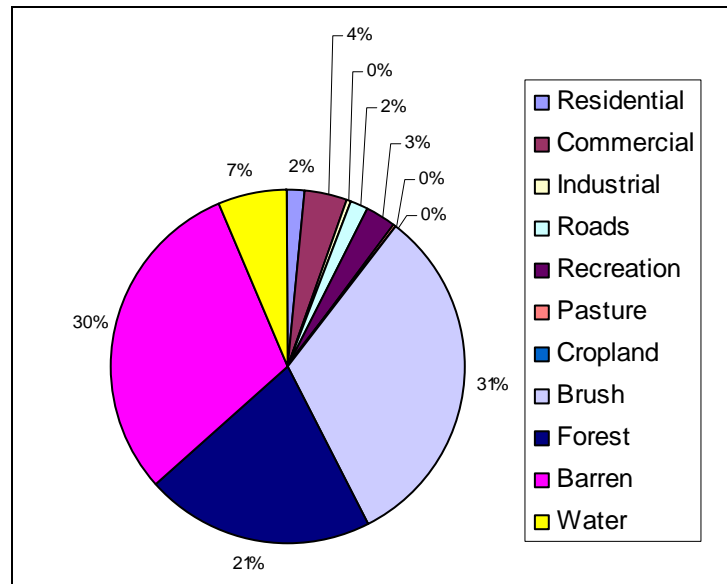
Watershed	Entire	Blue River	Tenmile Creek	Snake River
Surface Water N Loading				
Total N (lb/yr)	419628	149818	149306	118966
Residential (%)	1.7	3.8	4.6	0.7
Commercial (%)	4	4.3	2	6.1
Industrial (%)	0.3	0.2	0	0.8
Roads (%)	1.5	0	4.3	0
Recreation (%)	2.7	2	3.3	2.8
Pasture (%)	0.3	0.9	0	0
Cropland (%)	0.1	0	0	0.4
Brush (%)	31.8	27.4	30.3	39.2
Forest (%)	21	23.3	14.5	26.6
Barren (%)	30.1	35.7	32.7	15.8
Water (%)	6.5	2.5	8.4	7.6
Groundwater N Loading				
Total N (lb/yr)	260878	117611	82831	75584
Septic Systems (%)	2.3	16.8	1.9	0.4
Fertilized Lawns (%)	14.3	14.4	15.3	10.2
Fertilized Agricultural Areas (%)	0.4	0	0	1.3
Pets (%)	0.6	1.2	0.2	0.3
Unfertilized Pervious Areas (%)	82.4	67.6	82.6	87.9

Note: Data shown for the entire Dillon Reservoir watershed and each sub-watershed analyzed using MANAGE

Nitrogen that is input to surface waters via runoff has its origin in the various land uses in MANAGE. All MANAGE land-use categories could potentially contribute to nitrogen in runoff; however, only certain land uses were present in this study area. Those land uses are:

- Residential • Industrial • Recreation • Cropland • Forest
- Commercial • Roads • Pasture • Brush • Barren

Nitrogen is also contributed through direct atmospheric deposition to surface waters (See the “Water” category in Table H-7). Figure H-4 shows the relative contribution of each of these sources to nitrogen loading in surface runoff and atmospheric deposition. In surface runoff, the largest contributors to the nitrogen load are the land uses brush and barren. As with groundwater recharge, the largest sources of nitrogen in surface waters are likely to be generated by natural causes. Again, results varied in the sub-watersheds (Table H-7). In the Blue River and Tenmile Creek basins, brush and barren land uses were still the largest contributors of nitrogen to surface waters. In the Snake River basin, brush and forest land uses were responsible for the majority of nitrogen loading to surface waters; however, brush and forest land uses still represent natural sources of nitrogen.



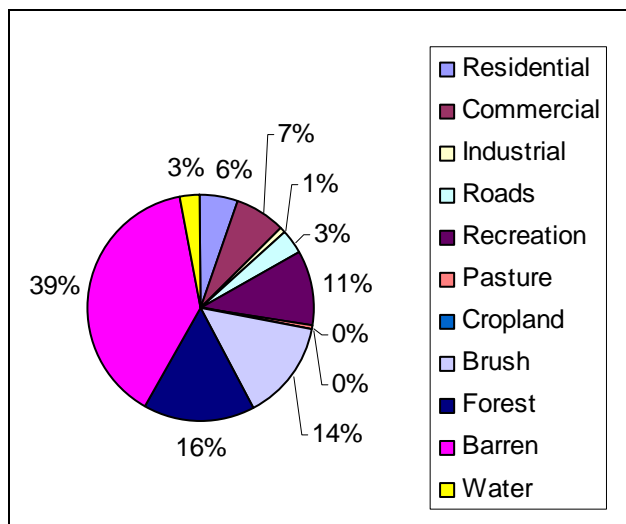
Note: Data shown for the Dillon Reservoir watershed based on analysis using MANAGE

Figure H-4
Sources of Nitrogen Loading to Surface Runoff

Phosphorous Loading

Phosphorous loading in MANAGE is considered only as surface runoff and direct atmospheric deposition to surface waters. MANAGE does not consider phosphorous loading to groundwater under the assumption that the majority of phosphorous is sorbed to soil during infiltration (Joubert and Lucht 2000). Therefore, the only phosphorous considered in MANAGE is that contributed by each of the land-use categories. They are the same as those listed for nitrogen in the Nitrogen Loading section.

Total phosphorous loading in the Dillon Reservoir watershed is estimated by MANAGE to be 38090 lb/N/yr or 0.2 lb/ac/yr. Phosphorous loading to groundwater is not considered, so nearly all of this phosphorous is contributed through surface runoff, excluding the small portion, (approximately 3%) contributed through direct atmospheric deposition to surface water. Relative sources of phosphorous loading in the Dillon Reservoir watershed are shown in Figure H-5.



Note: Data shown for the Dillon Reservoir watershed based on analysis using MANAGE

Figure H-5
Relative Sources of Phosphorous Loading to Surface Waters

As observed with nitrogen, the majority of phosphorous loading is contributed from natural sources (such as barren, forest, and brush). Similar results are observed in the sub-watersheds (Table H-8). Note that though the majority of phosphorous in the Blue River sub-watershed is contributed by natural causes, residential contributions play a fairly large role as well. This situation is addressed in the Discussion section.

Table H-8
Summary of Phosphorous Loading to Surface Water

Watershed	Entire	Blue River	Tennmile Creek	Snake River
Total N (lb/yr)	38090	14622	13316	9442
Residential (%)	5.7	11.8	1.4	2.7
Commercial (%)	7.1	7.3	4.1	11.4
Industrial (%)	0.9	0.6	0.0	2.6
Roads (%)	3.4	0.0	9.7	0.0
Recreation (%)	10.7	7.4	13.1	13.0
Pasture (%)	0.4	1.0	0.0	0.0
Cropland (%)	0.1	0.0	0.0	0.4
Brush (%)	14	11.2	13.7	19.7
Forest (%)	15.9	16.4	11.2	22.9
Barren (%)	39.2	43.3	43.4	23.6
Water (%)	2.7	1.0	3.5	3.6

Note: Data shown for the Dillon Reservoir watershed based on analysis using MANAGE

GIS Analysis

The final component of a MANAGE assessment is use of GIS to show locations of surface and groundwater pollution hotspots as well as some watershed indicators. This section will focus on presentation of the following maps created for GIS analysis of this study area:

- Natural resources
- Watershed indicators
- Hotspots

Note that maps are briefly described and presented, but not discussed. Discussion of all results can be found in the Discussion section that follows.

Natural Resources Maps

GIS analysis in MANAGE can provide a tool for mapping natural resources of a watershed. This tool can be especially useful, if maintained over time, to monitor changes in the watershed. Many natural resources maps can be created. For example, GIS can be used to create land-use maps, soil maps, and maps of surface water bodies. Two natural resources maps are shown for land use and soils (see Figure H-6 and Figure H-7). Other natural resources maps are not shown due to their size and detail.

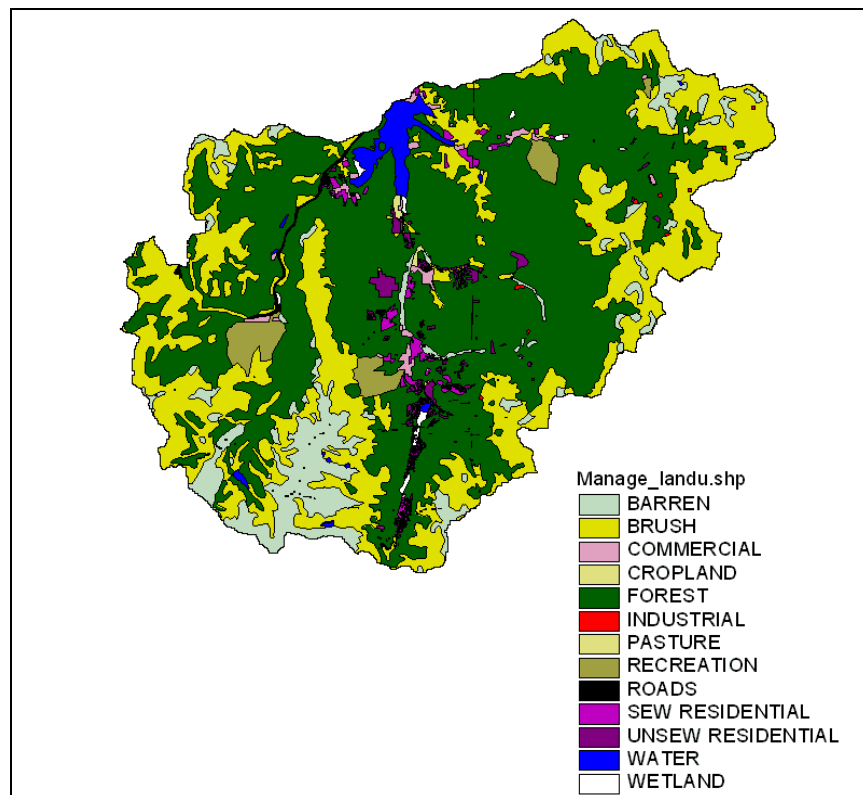
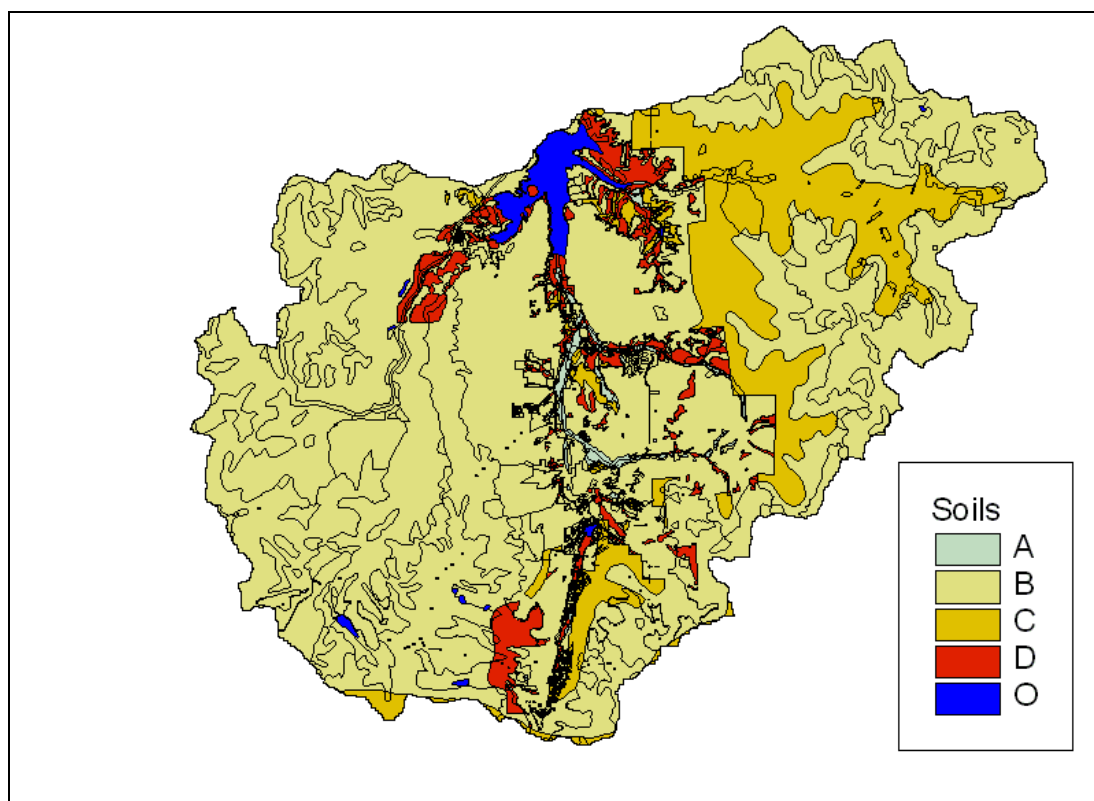


Figure H-6
Land-Use Map of the Dillon Reservoir Watershed Generated by MANAGE



Note that O indicates “Other.” In most cases O is water.

Figure H-7
Soil Map of the Dillon Reservoir Watershed Generated by MANAGE

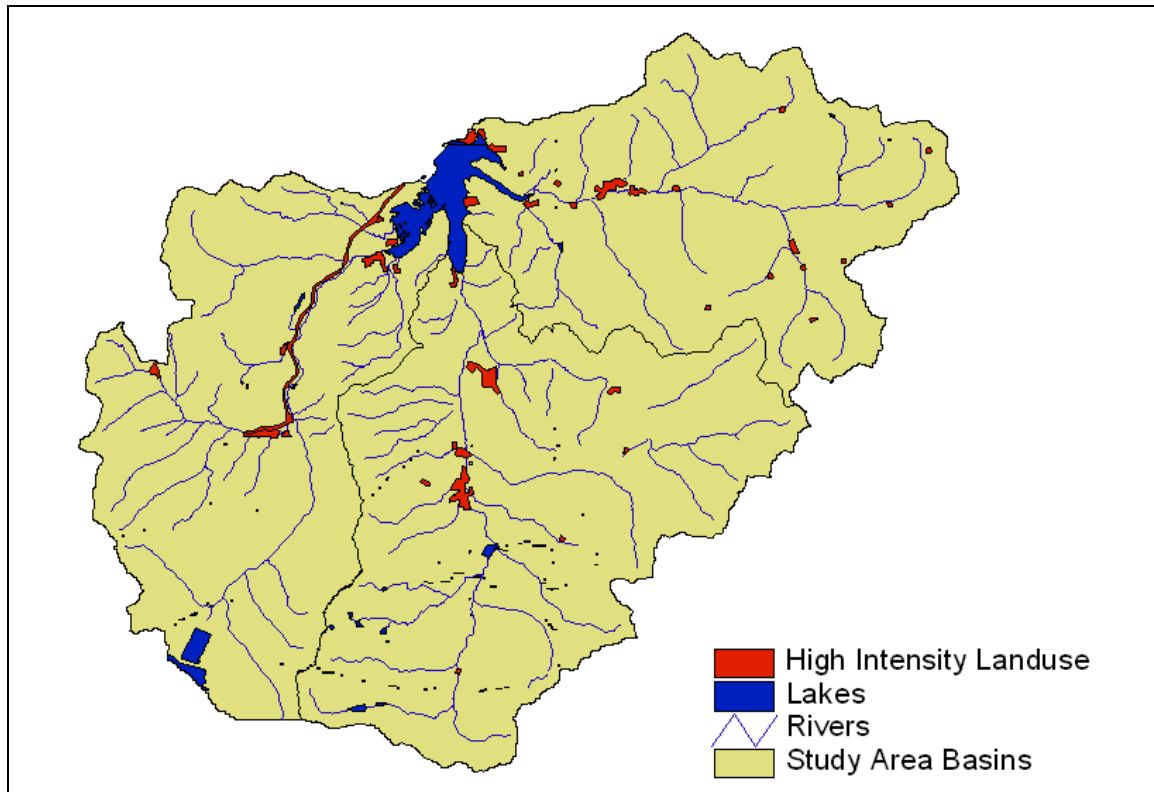
Watershed Indicators Maps

Mapping the presence of some of the watershed indicators is possible using GIS. Mapping the following watershed indicators was possible in this study:

- High- and very-high-risk land uses
- Riparian high- and very-high-risk land uses
- Forest and wetland
- Riparian forest and wetland
- Excessively permeable soils
- Restrictive soils

Forest and wetland areas as well as excessively permeable soils (hydrologic group A) can be seen on the natural resource maps in Figure H-6 and Figure H-7.

Restrictive soils were limited. Therefore, the only watershed indicator map shown (Figure H-8) shows the location of high- and very-high-risk land uses. High- and very-high-risk land uses found in this watershed are commercial, industrial, and roads. Note that though the location of these land uses can be observed, it was not possible to identify each site (with a business or site name).

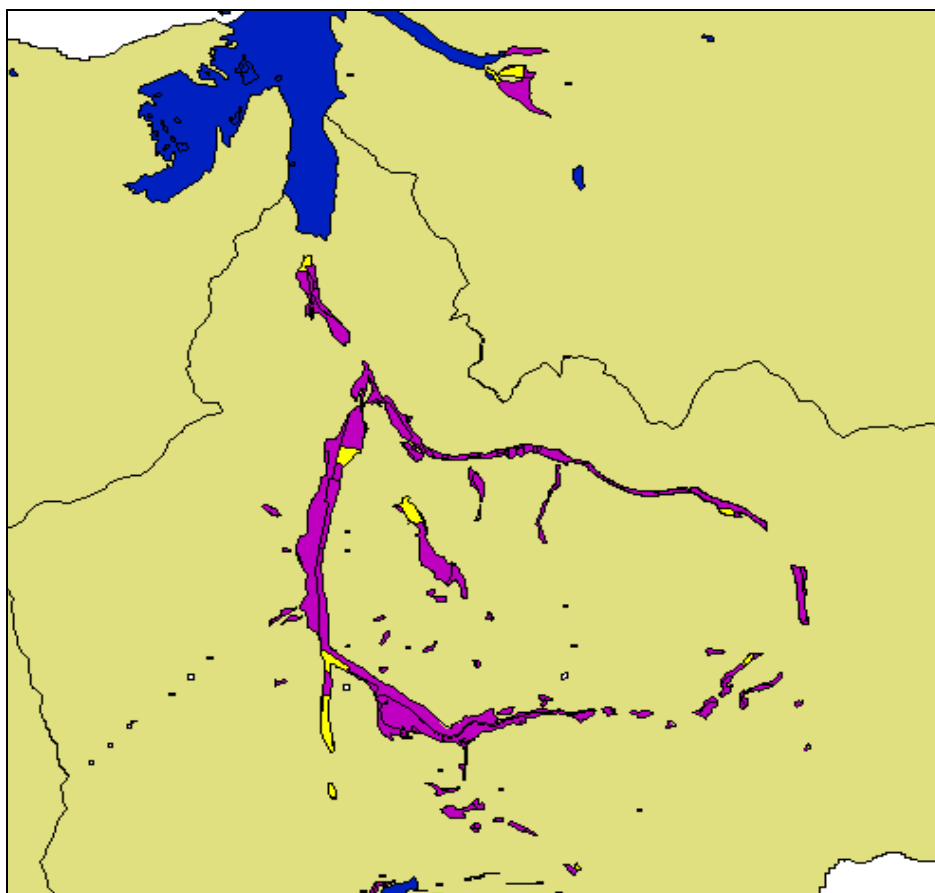


Note: Data shown for the Dillon Reservoir watershed based on analysis using MANAGE

Figure H-8
Locations of High- and Very-High-Risk Land Uses

Hotspots Maps

In this study, several hotspots maps were created to show locations where MANAGE estimated pollution would have potential of occurring. The first hotspots map shown (Figure H-9) is a groundwater hotspots map. This map shows the locations where pollution to groundwater might occur. A risk of pollution is believed to be at these hotspots because they are locations where high- and very-high-risk land uses, which have potential to generate pollution, overly high-permeability soils, where pollutants might travel quickly to the groundwater. Note that this map is focused on the portion that shows the groundwater hotspots; lakes in the study area are shown for reference.



Note: Purple areas are hydrologic group A soils while yellow areas are locations where high- and very-high-risk land uses overly those soils. Lakes are shown for location reference.

Figure H-9
Groundwater Hotspots in the Dillon Reservoir Watershed as Generated by MANAGE

The second hotspots map (Figure H-10) is a surface water hotspots map. For this map several factors were considered. The key to all surface water hotspots presented in this map is that they are situated on restrictive soils. Restrictive soils have extremely low permeability at shallow depths; therefore, there is the risk that they will not allow runoff and/or pollutants to infiltrate the surface. This condition would cause overland flow of runoff and pollutants to flow into nearby surface waters. However, restrictive soils alone are not a threat. A pollution source must be present in order for restrictive soils to have a negative impact. Consequently, the presence of the following characteristics situated on top of restrictive soils was considered: OWS and high- and very-high-intensity land uses.

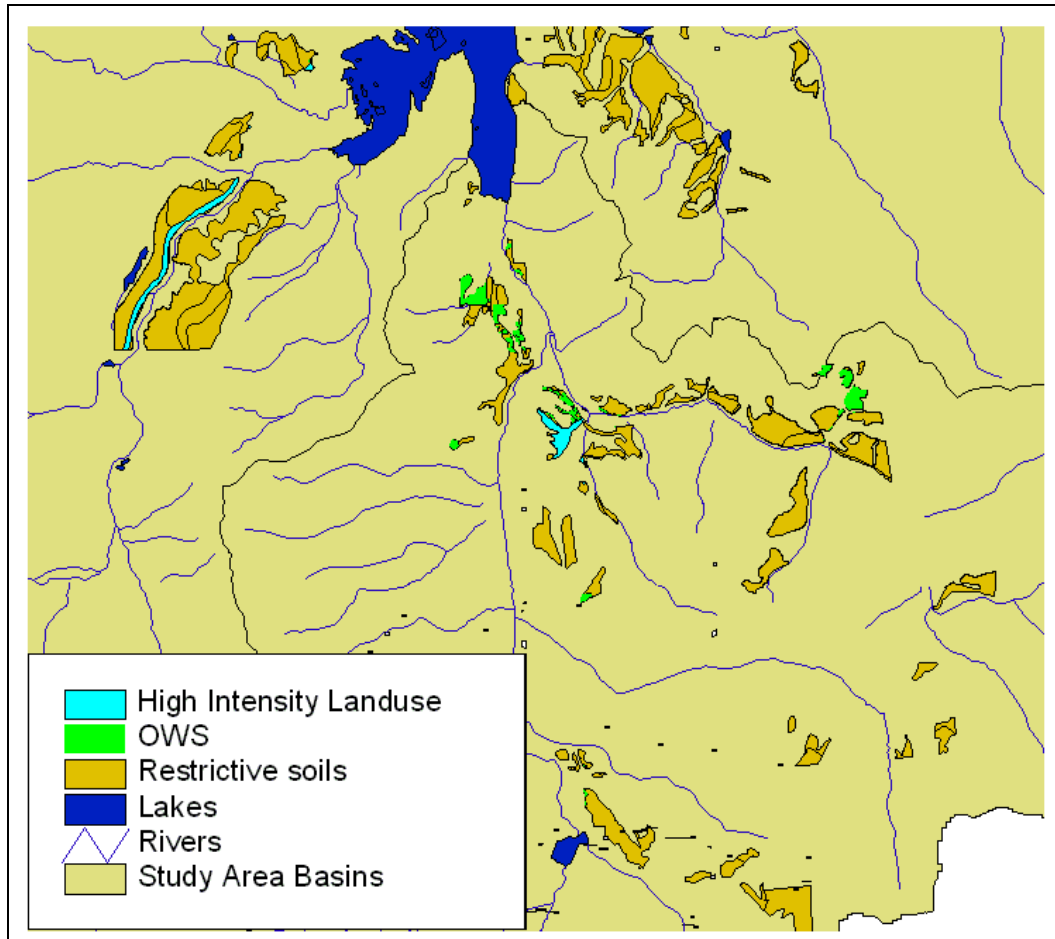


Figure H-10
Surface Water Hotspots in the Dillon Reservoir Watershed as Generated by MANAGE

The final hotspots map presented (Figure H-11) is a riparian zone hotspots map. This map investigates the presence of OWS and high- and very-high-intensity land uses in the riparian zone. These conditions would be a concern for pollution transport because their presence within the riparian zone essentially means that they are situated in extremely close proximity to streams. Regardless of what type of soil is present in the riparian zone, there is the potential for a particularly short pathway from pollution input to groundwater to stream. Due to the small nature of the riparian zone, details of the map when viewed for the entire watershed are impossible to see. Therefore, the map shows just one region of riparian zone as an example. The map shows portions of the Blue River basin and Tenmile Creek basin where both OWS and high- and very-high-risk land uses can be found in the riparian zone.

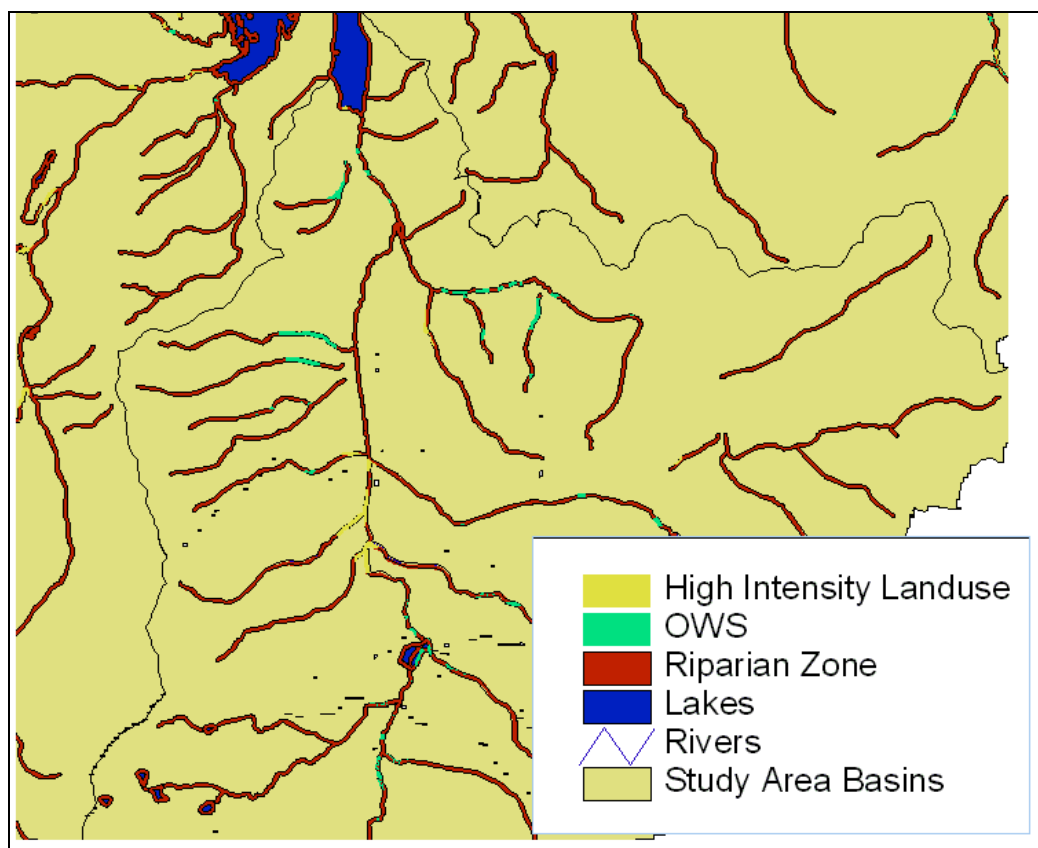


Figure H-11
Riparian Zone Hotspots in a Portion of the Dillon Reservoir Watershed as Generated by MANAGE

Discussion

MANAGE results present

- Potential pollution risks through qualitative analysis
- Pollution sources through nutrient loading estimates
- Potential geographical locations of pollution through GIS analysis

The objective of this project was to determine what, if any, are the impacts of OWS on the environment of the Dillon Reservoir watershed. This section discusses this further and provides further clarification and insight into the MANAGE results presented previously.

Watershed Indicators

In this study area, many of the watershed indicators utilized by MANAGE indicated a low risk of negative water quality impact. However, there are some important considerations to note when interpreting these results. Consideration of these results in conjunction with what is known about both the watershed in question and the watershed in which MANAGE was developed is important.

The majority of watershed indicators in MANAGE indicated a low risk of negative water quality impact. However, this situation was not the case when considering the amount of forest and wetland present in each basin analyzed and its respective riparian zone. In the basins and the watershed as a whole, the risk of water quality impact due to lack of forest and wetland areas ranged from medium to high. In the riparian zones, risk of water quality impact due to the same factor ranged from high to extreme. In the basin areas, MANAGE considers less than 80% forest/wetland areas to present a medium risk of water quality impact. MANAGE was developed in a coastal region where 80% or greater of forest or wetland may be the natural condition of land use. This condition may be unrealistic in the Dillon Reservoir watershed. Alpine regions have naturally thinner forests, which is especially true in this watershed where much of the land is situated above tree line. Furthermore, wetlands are not as prevalent in this type of ecosystem. Therefore, the risk due to lack of forest/wetland in the basins is possibly overstated by MANAGE.

There are some separate considerations for forest/wetland areas in the riparian zone that may indicate risk in these areas is not as overstated as in the basins. First, the watershed has a history of dredge-boat mining, which has impacted riparian zones of many of the streams in this watershed (such as the Blue River and Swan River). Potentially, both riparian forest and wetland areas have been reduced. Furthermore, development in the Dillon Reservoir watershed tends towards the flat valley bottoms. While the development seems to avoid the wetland areas, the amount of forest in these areas may have been reduced. Therefore, some restoration of riparian zones in this watershed may be beneficial because risk to water quality impact in these zones is present.

MANAGE indicated that the Dillon Reservoir watershed is at a low risk of water quality impact due to the presence of a large amount of high-permeability soils. This evaluation is most likely correct; however, some factors should be noted. As described in the Fine Tuning MANAGE section, modifications had to be made in order to create a soil coverage that could be utilized in this evaluation. These modifications led to soil coverage with a higher resolution in the Blue River basin than in other basins studied. In general, the small regions of group A soils were apparent only in this high-resolution portion. Therefore, the amount of these soils present in the study area has possibly been underestimated.

The same situation is also applicable to evaluation of the amount of restrictive soils in the watershed. Risk due to the presence of these soils is already medium in the Dillon Reservoir watershed; therefore, there is some chance that the risk could be higher. However, restrictive soils do not pose a risk unless there is some pollution present, which is important to remember. The majority of development in the study area is in the Blue River sub-watershed, so increased amounts of restrictive soils may not necessarily cause increased amounts of water pollution.

This section attempts to combine the watershed indicator analysis completed using MANAGE with knowledge about this study area and the original application of MANAGE in order to make a better evaluation of the potential risks to water quality in the Dillon Reservoir watershed. Whether or not a MANAGE user chooses to complete a similar exercise, remembering that the watershed indicators only represent risk of pollution problems, not actual pollution problems is important. This evaluation is useful in helping to identify areas where pollution prevention and mitigation might occur before a problem is present. In the Dillon Reservoir watershed, indicator analysis suggests restoration of natural habitat in the riparian zones might be a beneficial consideration. Furthermore, consulting further soil records or conducting field evaluations to verify the amount of restrictive soils in the area might also be useful.

Nutrient Loading

MANAGE creates an estimated water budget for use in the nutrient loading estimates. However this water budget can also be used to look at some of the impacts of development on a watershed. Development tends to increase the amount of surface runoff in a watershed due to increases in factors, such as impervious surfaces, which do not allow precipitation to percolate into the ground. Because of this, MANAGE calculates an estimate of the amount of runoff that would occur if a watershed were 100% forested. The Dillon Reservoir watershed would not be 100% forested in its natural state, which is recognized, but this evaluation does provide some estimate of the impact of development on surface runoff.

In the entire watershed, MANAGE estimates that there has been a 38% increase in surface runoff due to development in the area (see Table H-9). This number varies in the sub-watersheds. In the Blue River basin, runoff has increased 44%; similarly, runoff has increased 41% in the Tenmile Creek basin. Runoff has increased only 25% in the Snake River basin. These increases verify that most of the development in the study area is situated in the Tenmile Creek and Blue River basins and that this development is affecting the hydrology of the watershed.

Table H-9
Estimated Runoff Increase Due to Development in the Study Area

Watershed	Surface Runoff	Runoff if 100%	
	Mgal/yr	Forest Mgal/yr	% Increase
Entire	13561	8467	38
Blue River	4687	2630	44
Tenmile Creek	4716	2791	41
Snake River	3795	2837	25

Nitrogen loading in MANAGE occurs through two pathways: surface runoff and groundwater recharge. Nitrogen in surface runoff in the entire watershed was predominantly generated by barren, forest, and brush land uses. There was no case in the entire watershed or in the sub-watersheds analyzed that any developmentally-related land use generated greater than 5% of the nitrogen in the surface runoff of that watershed. This fact indicates that the majority of nitrogen in surface runoff is naturally generated (though the amount of runoff may be developmentally impacted), and therefore not likely a concern.

Natural causes, specifically unfertilized pervious areas, also generate the majority of nitrogen found in groundwater recharge in the entire watershed and in each sub-watershed. Effects of OWS are accounted for in nitrogen sources to groundwater recharge. In the entire watershed, only 2.3% of nitrogen is estimated to be generated by OWS. However, this number is considerably higher in the Blue River basin, where 16.8% of nitrogen is generated by OWS. This information does not provide a good indication that OWS should be converted to a central wastewater treatment plant (CWTP). MANAGE provides no means of estimating and comparing the amount of nitrogen that would be generated by a CWTP to that being generated by OWS. Therefore, using MANAGE to know if conversion to CWTP would truly provide any benefits is impossible.

Unlike nitrogen, phosphorous loading in MANAGE is only considered in surface runoff. The assumption is made that 100% of phosphorous in groundwater recharge undergoes sorption to soil in the vadose zone. Therefore, MANAGE assumes that OWS do not contribute any phosphorous that has the potential to negatively impact water quality. Like nitrogen, the majority of phosphorous in surface runoff is generated by natural causes and is therefore not a likely concern. In summary, nutrient loading in the Dillon Reservoir watershed seems to be due predominantly to natural causes. Natural sources of nutrients do not require mitigation; however, further investigation of OWS contributions to nitrogen in the Blue River Basin might be useful.

GIS Analysis

The GIS hotspot analysis provides physical locations where pollution is likely to occur and that might be useful sites for pollution mitigation. To a large extent the maps speak for themselves and do not need to be discussed. However, there are some things to consider. In all of the hotspots maps presented noting the proximity of the hotspots to streams is useful. For example, high-intensity land uses are located to a large extent along surface water bodies. The same holds true for both surface and groundwater hotspots. This characteristic confirms a need to investigate and possibly mitigate pollution in the riparian zones of this study area.

When utilizing hotspot analysis the fact that these maps can be used to archive current hotspots for use in comparison to future situations should be remembered. Tracking changes will help to monitor and/or prevent expansion of potential problem areas. Hotspots maps can also be utilized as a tool to map proposed development to provide a screening-level evaluation of whether or not this development will have a negative impact.

Summary and Conclusions

A watershed assessment using the screening level assessment method known as MANAGE was completed as part of this project in order to assess a low-cost and less resource intensive, watershed-scale modeling option. Consideration, of the conclusions of the assessment made utilizing MANAGE is important, in addition to providing some general conclusions about the assessment tool itself for those who may consider using the tool in the future.

MANAGE, a watershed assessment tool developed by the University of Rhode Island Cooperative Extension, has three main components: watershed indicator analysis, nutrient loading estimates, and GIS analysis. The results of these three components are utilized together to evaluate the overall health of a watershed. Through utilizing MANAGE in the Dillon Reservoir watershed several advantages and disadvantages of MANAGE have become apparent. Regarding implementation of MANAGE, there are several advantages: MANAGE is available at no cost and requires fewer resources than many models. MANAGE has fewer input data requirements, and those that are required are typically available for free (such as GIS coverages). On the other hand, MANAGE was originally created for and implemented in Rhode Island, so implementation in areas outside of Rhode Island may require a substantial amount of time to research and modify the model as appropriate (such as nutrient loading factors). Furthermore, implementation of MANAGE in numerous sub-watersheds may be cumbersome because each sub-watershed requires a separate MANAGE file.

There are also advantages and disadvantages to the results produced by a MANAGE assessment. Results are relatively quick to obtain and provide an easy means to complete a screening level assessment that may be used to guide future watershed plans and evaluations. In other words, it is a useful tool for identifying potential problem areas. However, results of MANAGE nutrient loading estimates are point-of-origin estimates and cannot be used as realistic estimates of the magnitude of nutrient loading to groundwater or surface water. In addition, the estimates do not consider known point sources and therefore comparing the impacts of point versus nonpoint sources (such as CWTP versus OWS) is impossible. Finally, the estimates assume 100% of phosphorous in groundwater recharge undergoes sorption in the subsurface, which eliminates consideration of groundwater sources of phosphorous-to-phosphorous loading.

Conclusions from this Dillon Reservoir watershed assessment using MANAGE include:

- All areas analyzed using MANAGE showed limited potential impact due to development. This result is because analysis of watershed indicators involving development were low and nutrient loading tended to be from natural, and not developmentally related, causes. MANAGE does not show OWS to be a major cause of nutrient loading in any areas considered. Levels of OWS contribution were higher, however, in the Blue River sub-watershed.
- In the riparian zone, the situation differs. Watershed indicator analysis revealed that lack of forest and wetland areas may be impacting these zones. Hotspots maps showed that in many cases both surface and groundwater hotspots were situated alongside streams. This information is supported by historical documentation of mining in these zones. This evidence supports a need to better investigate and evaluate the risk to water quality due to detriment of these areas.


References

Fetter, C. W. 2001. *Applied Hydrology, Fourth Edition*. Prentice Hall Inc., Upper Saddle River, NJ.

Joubert, L. and J. Lucht. 2000. *Wickford Harbor Watershed Assessment*. College of Environment and Life Sciences Report #00-03, Contribution #3847. University of Rhode Island.

Novotny, V. 2003. *Water Quality Diffuse Pollution and Watershed Management, Second Edition*. John Wiley & Sons, Inc.

Copyright ©2005 Colorado School of Mines, Golden, CO.
All rights reserved.

 Printed on recycled paper in the United States of America.

WU-HT-00-27

NDWRCDP

Washington University, Campus Box 1150, One Brookings Drive, Cupples 2, Rm. 11, St. Louis, Missouri 63130-4899 • USA

*This report is available online at www.ndwrcdp.org. This report is also available through the
National Small Flows Clearinghouse • West Virginia University/NRCCE, P.O. Box 6064, Morgantown, WV 26506-6064 • USA
Tel: (800) 624-8301 • WWCDRE45*

